UNCLASSIFIED

AD NUMBER

AD474377

LIMITATION CHANGES

TO:

Approved for public release; distribution is unlimited.

FROM:

**Distribution authorized to U.S. Gov't. agencies and their contractors;
Administrative/Operational Use; 30 JUN 1965.
Other requests shall be referred to U. S. Army Electronics Command, Fort Monmouth, NJ.**

AUTHORITY

USAEC ltr 14 Mar 1969

THIS PAGE IS UNCLASSIFIED

SECURITY MARKING

The classified or limited status of this report applies to each page, unless otherwise marked.

Separate page printouts MUST be marked accordingly.

THIS DOCUMENT CONTAINS INFORMATION AFFECTING THE NATIONAL DEFENSE OF THE UNITED STATES WITHIN THE MEANING OF THE ESPIONAGE LAWS, TITLE 18, U.S.C., SECTIONS 793 AND 794. THE TRANSMISSION OR THE REVELATION OF ITS CONTENTS IN ANY MANNER TO AN UNAUTHORIZED PERSON IS PROHIBITED BY LAW.

NOTICE: When government or other drawings, specifications or other data are used for any purpose other than in connection with a definitely related government procurement operation, the U. S. Government thereby incurs no responsibility, nor any obligation whatsoever; and the fact that the Government may have formulated, furnished, or in any way supplied the said drawings, specifications, or other data is not to be regarded by implication or otherwise as in any manner licensing the holder or any other person or corporation, or conveying any rights or permission to manufacture, use or sell any patented invention that may in any way be related thereto.

JANSKY & BAILEY RESEARCH and ENGINEERING DIVISION

474377

TROPICAL PROPAGATION RESEARCH

Semiannual Report Number 6

1 January 1965 - 30 June 1965

Prepared for

U. S. ARMY ELECTRONICS COMMAND

Fort Monmouth, New Jersey

Signal Corps Contract

DA 36-039 SC-90889

Sponsored by

ADVANCED RESEARCH PROJECTS AGENCY

Office of Secretary of Defense

ATLANTIC RESEARCH

DISCLAIMER NOTICE

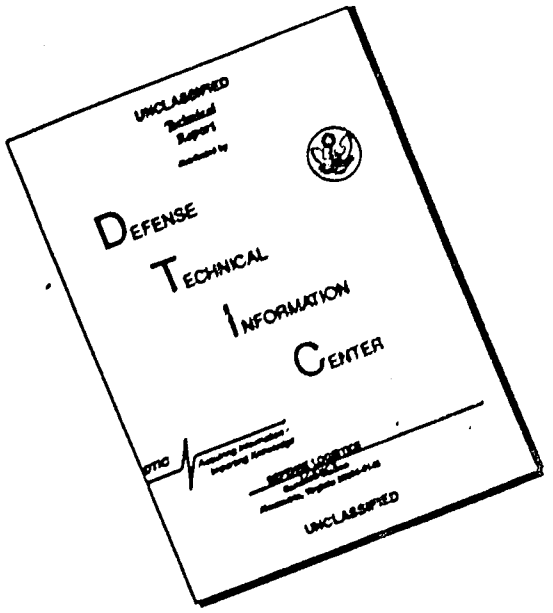

THIS DOCUMENT IS BEST QUALITY AVAILABLE. THE COPY FURNISHED TO DTIC CONTAINED A SIGNIFICANT NUMBER OF PAGES WHICH DO NOT REPRODUCE LEGIBLY.

TROPICAL PROPAGATION RESEARCH

Semiannual Report Number 6

1 January 1965 - 30 June 1965

Jansky & Bailey
Research and Engineering Division
of
Atlantic Research Corporation
Alexandria, Virginia

Prepared for

U. S. ARMY ELECTRONICS COMMAND

Sponsored by

ADVANCED RESEARCH PROJECTS AGENCY
Office of Secretary of Defense

ARPA Order Number: 371
Program Code Number: 2860
Contract Number: DA 36-039 SC-90889

Approved by

Frank T. Mitchell, Jr.
Division Director

L. G. Sturgill
Project Director

ABSTRACT

This sixth semiannual report presents results of work accomplished during the period 1 January 1965 to 30 June 1965 under a program on radio propagation research in tropical vegetated environments. The objectives of this program are to collect and analyze basic propagation data, together with basic environmental data, needed to improve the design and operation of radio communications in such environments.

The field measurements on this program are being carried out in Thailand in a specially selected area of tropical vegetated terrain about 30 miles in diameter. Measurements of transmission loss are conducted in the frequency range of 100 kc to 10 gc, with antenna heights, polarizations, and transmission ranges as the primary measurement variables. Basic environmental data, such as terrain profiles, vegetation characteristics, and weather data are also collected and, through the technique of statistical correlation, are used to identify the quantitative effects of the environment on propagation path loss.

This report continues, as has been the case with previous reports, with the reporting of new data reduced directly from the field measurements. This data is presented in graphic form in terms of basic transmission loss. However, the major portion of this report is devoted to the detailed analysis of a relatively large quantity of the field data. The block of measured data selected for analysis consists of all the data thus far obtained from one sector of the test area, designated as Radial A, and includes an analysis of data presented in Semiannual Reports 4 and 5 as well.

The data is analyzed mainly from the statistical point of view. Several families of curves are presented which display the trends of the measured path loss data in relation to the various measurement parameters. The continuously recorded field data generally exhibits wide variations and some of this data has been analyzed by means of a 10-level totalizer to obtain the statistical distributions of the measured data.

Ultimately, a simple model is sought by which the path loss can be predicted for tropical vegetated terrains. Toward this end, this report compares some measured results with a rough-earth model developed by Egli in 1957, the model being modified by a "foliage" factor.

CONTENTS

		Page
Abstract		i
1.	Introduction	1-1
2.	General Discussion	2-1
3.	Results of Field Measurements	3-1
3.1	Summary of Measurements	3-1
3.2	Basic Data Format	3-1
3.3	Propagation Path Profiles	3-2
3.4	L_b vs Antenna Height	3-6
4.	Data Analysis	4-1
4.1	Introduction	4-1
4.2	Analysis of Field Point Medians	4-4
4.2.1	Summary of Measured Data	4-5
4.2.2	Theoretical Models	4-44
4.2.2.1	NBS Model	4-44
4.2.2.2	Computer-Induced Statistical Terrain Model	4-56
4.2.2.3	Smooth-Earth Model	4-61
4.2.2.4	Egli's Rough-Earth Model	4-74
4.3	Time and Spatial Variations of L_b	4-90
4.3.1	Time Variability	4-90
4.3.2	Variation with Antenna Height	4-107
4.3.2.1	Fine-Grain Variability	4-107
4.3.2.2	Variability of Field Point Medians with Antenna Height	4-126
4.3.2.2.1	Comparison of L_b vs Distance for Various Receiving Antenna Heights	4-126
4.3.2.2.2	Comparison of Height Variation with Smooth-Earth Model	4-162
4.3.2.2.3	Comparison of Height Variation with NBS Model	4-203
4.3.2.2.4	Comparison Between Height Variation for $d < 2$ miles and $d \geq 2$ miles	4-214
4.3.3	Variability of L_b with Range	4-244
4.3.3.1	Data Analysis	4-250
4.3.3.2	Summary of Vehicular Data Analysis Results	4-252
4.4	Other Factors Affecting L_b	4-365
4.4.1	Climatology	4-365
4.4.1.1	Analysis of Climatological Data	4-365
4.4.1.2	Nomographs for Computation of N_s and k from Psychrometric Data	4-365
4.4.2	Tropical Vegetation	4-371
4.4.2.1	Vegetation Measurements	4-374
4.4.3	Polarization	4-407
4.5	Radio Noise Measurements	4-413
4.5.1	Results of Noise Measurements	4-416
4.5.2	Noise Measuring Instrumentation	4-419
4.6	Use of Propagation Data for Communication Calculations	4-423

CONTENTS, continued

		Page
5.	Measurements Above 425 Mc	5-1
5.1	Measurement Site Selection	5-2
5.2	Field Measurements	5-2
6.	Technical Film Report	6-1
7.	Meetings and Conferences	7-1
8.	Project Personnel	8-1
Appendix A	Smooth-Earth Height Functions	A-1
Appendix B	Field Measurement Notes	B-1
References		
Document Control Data, DD Form 1473		
Distribution List		

ILLUSTRATIONS

Figure		Page
3.1	Radial Points and Field Points Along Trail B	3-8
3.2	Terrain Profile Between Transmitter and Field Points FPB-1, FPB-2, and FPB-3. . . .	3-9
3.3	Terrain Profile Between Transmitter and Field Points FPB-4 and FPB-5.	3-10
3.4	Terrain Profile Between Transmitter and Field Points FPB-5.5 and FPB-6.	3-11
3.5	Terrain Profile Between Transmitter and Field Point FPB-7	3-12
3.6	Terrain Profile Between Transmitter and Field Point FPB-8	3-13
3.7	Terrain Profile Between Transmitter and Field Point FPB-8.5	3-14
3.8	Terrain Profile Between Transmitter and Field Point FPB-9	3-15
3.9	Terrain Profile Between Transmitter and Field Point FPB-10.	3-16
3.10	Variation of Basic Transmission Loss with Receiving Antenna Height $L_b = F_A(25.5, 21, V, d, H_r)$	3-17
3.11	Variation of Basic Transmission Loss with Receiving Antenna Height $L_b = F_A(25.5, 40, V, d, H_r)$	3-18
3.12	Variation of Basic Transmission Loss with Receiving Antenna Height $L_b = F_A(25.5, 13, H, d, H_r)$	3-19
3.13	Variation of Basic Transmission Loss with Receiving Antenna Height $L_b = F_A(50, 13, V, d, H_r)$	3-20
3.14	Variation of Basic Transmission Loss with Receiving Antenna Height $L_b = F_A(50, 13, H, d, H_r)$	3-21

ILLUSTRATIONS, continued

Figure		Page
3.15	Variation of Basic Transmission Loss with Receiving Antenna Height $L_b = F_A(50, 80, H, d, H_r)$	3-22
3.16	Variation of Basic Transmission Loss with Receiving Antenna Height $L_b = F_A(100, 13, H, d, H_r)$.	3-23
3.17	Variation of Basic Transmission Loss with Receiving Antenna Height $L_b = F_A(250, 13, V, d, H_r)$.	3-24
3.18	Variation of Basic Transmission Loss with Receiving Antenna Height $L_b = F_A(250, 40, V, d, H_r)$.	3-25
3.19	Variation of Basic Transmission Loss with Receiving Antenna Height $L_b = F_A(250, 40, H, d, H_r)$.	3-26
3.20	Variation of Basic Transmission Loss with Receiving Antenna Height $L_b = F_A(250, 80, H, d, H_r)$.	3-27
3.21	Variation of Basic Transmission Loss with Receiving Antenna Height $L_b = F_A(400, 13, V, d, H_r)$.	3-28
3.22	Variation of Basic Transmission Loss with Receiving Antenna Height $L_b = F_A(400, 80, V, d, H_r)$.	3-29
3.23	Variation of Basic Transmission Loss with Receiving Antenna Height $L_b = F_A(400, 13, H, d, H_r)$.	3-30
3.24	Variation of Basic Transmission Loss with Receiving Antenna Height $L_b = F_A(400, 40, H, d, H_r)$.	3-31
3.25	Variation of Basic Transmission Loss with Receiving Antenna Height $L_b = F_A(400, 80, H, d, H_r)$.	3 32

ILLUSTRATIONS, continued

Figure		Page
3.26	Variation of Basic Transmission Loss with Receiving Antenna Height $L_b = F_B(25.5, 21, V, d, H_r)$	3-33
3.27	Variation of Basic Transmission Loss with Receiving Antenna Height $L_b = F_B(25.5, 40, V, d, H_r)$	3-34
3.28	Variation of Basic Transmission Loss with Receiving Antenna Height $L_b = F_B(25.5, 80, V, d, H_r)$	3-35
3.29	Variation of Basic Transmission Loss with Receiving Antenna Height $L_b = F_B(25.5, 13, H, d, H_r)$	3-36
3.30	Variation of Basic Transmission Loss with Receiving Antenna Height $L_b = F_B(25.5, 40, H, d, H_r)$	3-37
3.31	Variation of Basic Transmission Loss with Receiving Antenna Height $L_b = F_B(25.5, 80, H, d, H_r)$	3-38
3.32	Variation of Basic Transmission Loss with Receiving Antenna Height $L_b = F_B(50, 13, V, d, H_r)$	3-39
3.33	Variation of Basic Transmission Loss with Receiving Antenna Height $L_b = F_B(50, 40, V, d, H_r)$	3-40
3.34	Variation of Basic Transmission Loss with Receiving Antenna Height $L_b = F_B(50, 80, V, d, H_r)$	3-41
3.35	Variation of Basic Transmission Loss with Receiving Antenna Height $L_b = F_B(50, 13, H, d, H_r)$	3-42
3.36	Variation of Basic Transmission Loss with Receiving Antenna Height $L_b = F_B(50, 40, H, d, H_r)$	3-43

ILLUSTRATIONS, continued

Figure		Page
3.37	Variation of Basic Transmission Loss with Receiving Antenna Height $L_b = F_B(50, 80, H, d, H_r)$	3-44
3.38	Variation of Basic Transmission Loss with Receiving Antenna Height $L_b = F_B(100, 13, V, d, H_r)$	3-45
3.39	Variation of Basic Transmission Loss with Receiving Antenna Height $L_b = F_B(100, 40, V, d, H_r)$	3-46
3.40	Variation of Basic Transmission Loss with Receiving Antenna Height $L_b = F_B(100, 80, V, d, H_r)$	3-47
3.41	Variation of Basic Transmission Loss with Receiving Antenna Height $L_b = F_B(100, 13, H, d, H_r)$	3-48
3.42	Variation of Basic Transmission Loss with Receiving Antenna Height $L_b = F_B(100, 40, H, d, H_r)$	3-49
3.43	Variation of Basic Transmission Loss with Receiving Antenna Height $L_b = F_B(100, 80, H, d, H_r)$	3-50
3.44	Variation of Basic Transmission Loss with Receiving Antenna Height $L_b = F_B(250, 13, V, d, H_r)$	3-51
3.45	Variation of Basic Transmission Loss with Receiving Antenna Height $L_b = F_B(250, 40, V, d, H_r)$	3-52
3.46	Variation of Basic Transmission Loss with Receiving Antenna Height $L_b = F_B(250, 80, V, d, H_r)$	3-53
3.47	Variation of Basic Transmission Loss with Receiving Antenna Height $L_b = F_B(250, 13, H, d, H_r)$	3-54

ILLUSTRATIONS, continued

Figure		Page
3.48	Variation of Basic Transmission Loss with Receiving Antenna Height $L_b = F_B(250, 40, H, d, H_r)$.	3-55
3.49	Variation of Basic Transmission Loss with Receiving Antenna Height $L_b = F_B(250, 80, H, d, H_r)$.	3-56
3.50	Variation of Basic Transmission Loss with Receiving Antenna Height $L_b = F_B(400, 13, V, d, H_r)$.	3-57
3.51	Variation of Basic Transmission Loss with Receiving Antenna Height $L_b = F_B(400, 40, V, d, H_r)$.	3-58
3.52	Variation of Basic Transmission Loss with Receiving Antenna Height $L_b = F_B(400, 80, V, d, H_r)$.	3-59
3.53	Variation of Basic Transmission Loss with Receiving Antenna Height $L_b = F_B(400, 13, H, d, H_r)$.	3-60
3.54	Variation of Basic Transmission Loss with Receiving Antenna Height $L_b = F_B(400, 40, H, d, H_r)$.	3-61
3.55	Variation of Basic Transmission Loss with Receiving Antenna Height $L_b = F_B(400, 80, H, d, H_r)$.	3-62
4.1	Measured Results, L_b Vs Distance	
4.1A	$L_b = F_A(f, 13, V, d, 20)$.	4-8
4.1B	$L_b = F_A(f, 13, V, d, 40)$.	4-9
4.1C	$L_b = F_A(f, 13, V, d, 80)$.	4-10
4.1D	$L_b = F_A(f, 40, V, d, 20)$.	4-11
4.1E	$L_b = F_A(f, 40, V, d, 40)$.	4-12

ILLUSTRATIONS, continued

Figure		Page
4.1F	$L_b = F_A(f, 40, V, d, 80)$	4-13
4.1G	$L_b = F_A(f, 80, V, d, 20)$	4-14
4.1H	$L_b = F_A(f, 80, V, d, 40)$	4-15
4.1I	$L_b = F_A(f, 80, V, d, 80)$	4-16
4.1J	$L_b = F_A(f, 13, H, d, 20)$	4-17
4.1K	$L_b = F_A(f, 13, H, d, 40)$	4-18
4.1L	$L_b = F_A(f, 13, H, d, 80)$	4-19
4.1M	$L_b = F_A(f, 40, H, d, 20)$	4-20
4.1N	$L_b = F_A(f, 40, H, d, 40)$	4-21
4.1O	$L_b = F_A(f, 40, H, d. 80)$	4-22
4.1P	$L_b = F_A(f, 80, H, d, 20)$	4-23
4.1Q	$L_b = F_A(f, 80, H, d, 40)$	4-24
4.1R	$L_b = F_A(f, 80, H, d, 80)$	4-25
4.2	Measured Results, L_b Vs Frequency	
4.2A	$L_b = F_A(f, 13, V, d, 20)$	4-26
4.2B	$L_b = F_A(f, 13, V, d, 40)$	4-27
4.2C	$L_b = F_A(f, 13, V, d, 80)$	4-28
4.2D	$L_b = F_A(f, 40, V, d, 20)$	4-29
4.2E	$L_b = F_A(f, 40, V, d, 40)$	4-30
4.2F	$L_b = F_A(f, 40, V, d, 80)$	4-31
4.2G	$L_b = F_A(f, 80, V, d, 20)$	4-32
4.2H	$L_b = F_A(f, 80, V, d, 40)$	4-33

ILLUSTRATIONS, continued

Figure		Page
4.2I	$L_b = F_A(f, 80, V, d, 80)$	4-34
4.2J	$L_b = F_A(f, 13, H, d, 20)$	4-35
4.2K	$L_b = F_A(f, 13, H, d, 40)$	4-36
4.2L	$L_b = F_A(f, 13, H, d, 80)$	4-37
4.2M	$L_b = F_A(f, 40, H, d, 20)$	4-38
4.2N	$L_b = F_A(f, 40, H, d, 40)$	4-39
4.2O	$L_b = F_A(f, 40, H, d, 80)$	4-40
4.2P	$L_b = F_A(f, 80, H, d, 20)$	4-41
4.2Q	$L_b = F_A(f, 80, H, d, 40)$	4-42
4.2R	$L_b = F_A(f, 80, H, d, 80)$	4-43
4.3	Comparison Between Measured Results and NBS Model Including $G(\bar{H})$ Functions $L_b = F_A(25.5, 80, V, d, 80)$	4-48
4.4	Comparison Between Measured Results and NBS Model Without $G(\bar{H})$ Functions $L_b = F_A(25.5, 80, V, d, 80)$	4-49
4.5	Comparison Between Measured Results and NBS Model Including $G(\bar{H})$ Functions $L_b = F_A(100, 80, V, d, 80)$	4-50
4.6	Comparison Between Measured Results and NBS Model Without $G(\bar{H})$ Functions $L_b = F_A(100, 80, V, d, 80)$	4-51
4.7	Best Fit to Measured Results $L_b = F_A(25.5, 80, V, d, 80)$	4-52
4.8	Best Fit to Measured Results $L_b = F_A(100, 80, V, d, 80)$	4-53
4.9	Best Fit 10 db Below Measured Results $L_b = F_A(25.5, 80, V, d, 80)$	4-54

ILLUSTRATIONS, continued

Figure		Page
4.10	Best Fit 10 db Below Measured Results $L_b = F_A(100, 80, V, d, 80)$	4-55
4.11	Radials Used to Obtain Computer-Induced Statistic	4-57
4.12	Composite of L_b Along Ten Radials $L_b = F_A(25.5, 80, V, d, 80)$	4-58
4.13	Comparison Between Measured Results and Computer-Induced Terrain Statistics $L_b = F_A(25.5, 80, V, d, 80)$	4-59
4.14	Comparison Between Measured Results and Computer-Induced Terrain Statistics $L_b = F_A(100, 80, V, d, 80)$	4-60
4.15	Smooth-Earth Model $L_b = F_A(f, 80, V, d, 20)$	4-62
4.16	Comparison Between Measured Results and Smooth-Earth Model	
4.16A	$L_b = F_A(0.105, 80, V, d, 20)$	4-63
4.16B	$L_b = F_A(0.300, 80, V, d, 20)$	4-64
4.16C	$L_b = F_A(0.880, 80, V, d, 20)$	4-65
4.16D	$L_b = F_A(2.0, 80, V, d, 20)$	4-66
4.16E	$L_b = F_A(6.0, 40, V, d, 20)$	4-67
4.16F	$L_b = F_A(12.0, 80, V, d, 20)$	4-68
4.16G	$L_b = F_A(25.5, 80, V, d, 20)$	4-69
4.16H	$L_b = F_A(50.0, 80, V, d, 20)$	4-70
4.16I	$L_b = F_A(100, 80, V, d, 20)$	4-71
4.16J	$L_b = F_A(250, 80, V, d, 20)$	4-72
4.16K	$L_b = F_A(400, 80, V, d, 20)$	4-73

ILLUSTRATIONS, continued

Figure		Page
4.17	Foliage Factor (F.F.)	4-78
4.18	Sample Composite of Measured Results Normalized to Egli Model	4-79
4.19	Comparison Between Measured Results and Egli Model	
4.19A	$L_b = F_A(25.5, 13\text{-}80, V, d, 20\text{-}80)$	4-80
4.19B	$L_b = F_A(50, 13\text{-}80, V, d, 20\text{-}80)$	4-81
4.19C	$L_b = F_A(100, 13\text{-}80, V, d, 20\text{-}80)$.	4-82
4.19D	$L_b = F_A(250, 13\text{-}80, V, d, 20\text{-}80)$.	4-83
4.19E	$L_b = F_A(400, 13\text{-}80, V, d, 20\text{-}80)$.	4-84
4.19F	$L_b = F_A(25.5, 13\text{-}80, H, d, 20\text{-}80)$	4-85
4.19G	$L_b = F_A(40, 13\text{-}80, H, d, 20\text{-}80)$	4-86
4.19H	$L_b = F_A(100, 13\text{-}80, H, d, 20\text{-}80)$.	4-87
4.19I	$L_b = F_A(250, 13\text{-}80, H, d, 20\text{-}80)$.	4-88
4.19J	$L_b = F_A(400, 13\text{-}80, H, d, 20\text{-}80)$.	4-89
4.20	Fine-Grain Variability as a Function of Receiving Antenna Height	
4.20A	$L_b = F_A(0.880, 80, V, d, H_r)$.	4-109
4.20B	$L_b = F_A(12, 21, V, 1.0, H_r)$	4-110
4.20C	$L_b = F_A(100, 13, V, 1.0, H_r)$.	4-111
4.20D	$L_b = F_A(100, 80, V, d, H_r)$.	4-112
4.20E	$L_b = F_A(100, 13, H, d, H_r)$.	4-113
4.20F	$L_b = F_A(100, 80, H, d, H_r)$.	4-114
4.20G	$L_b = F_A(250, 13, V, 0.2, H_r)$.	4-115

ILLUSTRATIONS, continued

Figure		Page
4.20H	$L_b = F_A(250, 13, V, 0.45, H_r)$	4-116
4.20I	$L_b = F_A(250, 80, V, 0.2, H_r)$	4-117
4.20J	$L_b = F_A(250, 80, V, 0.45, H_r)$	4-118
4.20K	$L_b = F_A(250, 80, H, 0.2, H_r)$	4-119
4.20L	$L_b = F_A(250, 80, H, 0.45, H_r)$	4-120
4.20M	$L_b = F_A(400, 13, V, 1.0, H_r)$	4-121
4.20N	$L_b = F_A(400, 80, V, 1.0, H_r)$	4-122
4.20O	$L_b = F_A(400, 13, H, 1.0, H_r)$	4-123
4.20P	$L_b = F_A(400, 80, H, 1.0, H_r)$	4-124
4.21	Comparison of L_b vs Distance for Various Receiving Antenna Heights	
4.21A	$L_b = F_A(f, H_t, V, d, H_r)$	4-128
4.21B	$L_b = F_A(25.5, 80, V, d, H_r)$	4-129
4.21C	$L_b = F_A(50, 80, V, d, H_r)$	4-130
4.21D	$L_b = F_A(100, 80, V, d, H_r)$	4-131
4.21E	$L_b = F_A(250, 80, V, d, H_r)$	4-132
4.21F	$L_b = F_A(400, 80, V, d, H_r)$	4-133
4.21G	$L_b = F_A(25.5, 40, V, d, H_r)$	4-134
4.21H	$L_b = F_A(50.0, 40, V, d, H_r)$	4-135
4.21I	$L_b = F_A(100, 40, V, d, H_r)$	4-136
4.21J	$L_b = F_A(250, 40, V, d, H_r)$	4-137
4.21K	$L_b = F_A(400, 40, V, d, H_r)$	4-138
4.21L	$L_b = F_A(25.5, 13, V, d, H_r)$	4-139

ILLUSTRATIONS, continued

Figure		Page
4.21M	$L_b = F_A(50, 13, V, d, H_r)$	4-140
4.21N	$L_b = F_A(100, 13, V, d, H_r)$	4-141
4.21O	$L_b = F_A(250, 13, V, d, H_r)$	4-142
4.21P	$L_b = F_A(400, 13, V, d, H_r)$	4-143
4.21Q	$L_b = F_A(2.0, 80, H, d, H_r)$	4-144
4.21R	$L_b = F_A(12.0, 80, H, d, H_r)$	4-145
4.21S	$L_b = F_A(25.5, 80, H, d, H_r)$	4-146
4.21T	$L_b = F_A(50, 80, H, d, H_r)$	4-147
4.21U	$L_b = F_A(100, 80, H, d, H_r)$	4-148
4.21V	$L_b = F_A(250, 80, H, d, H_r)$	4-149
4.21W	$L_b = F_A(400, 80, H, d, H_r)$	4-150
4.21X	$L_b = F_A(6.0, 40. H, d, H_r)$	4-151
4.21Y	$L_b = F_A(12.0, 40, H, d, H_r)$	4-152
4.21Z	$L_b = F_A(25.5, 40, H, d, H_r)$	4-153
4.21AA	$L_b = F_A(50, 40, H, d, H_r)$	4-154
4.21BB	$L_b = F_A(100, 40, H, d, H_r)$	4-155
4.21CC	$L_b = F_A(250, 40, H, d, H_r)$	4-156
4.21DD	$L_b = F_A(400, 40, H, d, H_r)$	4-157
4.21EE	$L_b = F_A(25.5, 13, H, d, H_r)$	4-158
4.21FF	$L_b = F_A(50, 13, H, d, H_r)$	4-159
4.21GG	$L_b = F_A(100, 13, H, d, H_r)$	4-160
4.21HH	$L_b = F_A(400, 13, H, d, H_r)$	4-161
4.22	Sample Composite of Measured Antenna Height Functions $L_b = F_A(50, 80, V, d, H_r)$	4-164

ILLUSTRATIONS, continued

Figure		Page
4.23	Comparison Between Measured and Theoretical Smooth-Earth Functions	
4.23A	$L_b = F_A(400, 80, H, \geq 2, H_r)$	4-165
4.23B	$L_b = F_A(400, 40, H, \geq 2, H_r)$	4-166
4.23C	$L_b = F_A(400, 13, H, \geq 2, H_r)$	4-167
4.23D	$L_b = F_A(250, 80, H, \geq 2, H_r)$	4-168
4.23E	$L_b = F_A(250, 40, H, \geq 2, H_r)$	4-169
4.23F	$L_b = F_A(100, 80, H, \geq 2, H_r)$	4-170
4.23G	$L_b = F_A(100, 40, H, \geq 2, H_r)$	4-171
4.23H	$L_b = F_A(100, 13, H, \geq 2, H_r)$	4-172
4.23I	$L_b = F_A(50, 80, H, \geq 2, H_r)$	4-173
4.23J	$L_b = F_A(50, 40, H, \geq 2, H_r)$	4-174
4.23K	$L_b = F_A(50, 13, H, \geq 2, H_r)$	4-175
4.23L	$L_b = F_A(25.5, 80, H, \geq 2, H_r)$	4-176
4.23M	$L_b = F_A(25.5, 40, H, \geq 2, H_r)$	4-177
4.23N	$L_b = F_A(25.5, 13, H, \geq 2, H_r)$	4-178
4.23O	$L_b = F_A(12.0, 40, H, \geq 2, H_r)$	4-179
4.23P	$L_b = F_A(60, 40, H, \geq 2, H_r)$	4-180
4.23Q	$L_b = F_A(2.0, 40, H, \geq 2, H_r)$	4-181
4.23R	$L_b = F_A(400, 80, V, \geq 2, H_r)$	4-182
4.23S	$L_b = F_A(400, 40, V, \geq 2, H_r)$	4-183
4.23T	$L_b = F_A(400, 13, V, \geq 2, H_r)$	4-184
4.23U	$L_b = F_A(250, 80, V, \geq 2, H_r)$	4-185

ILLUSTRATIONS, continued

Figure		Page
4.23V	$L_b = F_A(250, 40, V, \geq 2, H_r)$	4-186
4.23W	$L_b = F_A(250, 13, V, \geq 2, H_r)$	4-187
4.23X	$L_b = F_A(100, 80, V, \geq 2, H_r)$	4-188
4.23Y	$L_b = F_A(100, 40, V, \geq 2, H_r)$	4-189
4.23Z	$L_b = F_A(100, 13, V, \geq 2, H_r)$	4-190
4.23AA	$L_b = F_A(50, 80, V, \geq 2, H_r)$	4-191
4.23BB	$L_b = F_A(50, 40, V, \geq 2, H_r)$	4-192
4.23CC	$L_b = F_A(50, 13, V, \geq 2, H_r)$	4-193
4.23DD	$L_b = F_A(25.5, 80, V, \geq 2, H_r)$	4-194
4.23EE	$L_b = F_A(25.5, 40, V, \geq 2, H_r)$	4-195
4.23FF	$L_b = F_A(25.5, 13, V, \geq 2, H_r)$	4-196
4.23GG	$L_b = F_A(12.0, 21, V, \geq 2, H_r)$	4-197
4.23HH	$L_b = F_A(6.0, 40, V, \geq 2, H_r)$	4-198
4.23II	$L_b = F_A(2.0, 80, V, \geq 2, H_r)$	4-199
4.23JJ	$L_b = F_A(0.880, 80, V, \geq 2, H_r)$	4-200
4.23KK	$L_b = F_A(0.300, 80, V, \geq 2, H_r)$	4-201
4.23LL	$L_b = F_A(0.105, 80, V, \geq 2, H_r)$	4-202
4.24	Comparison Between Measured and Theoretical Rough-Earth Height Functions	
4.24A	$L_b = F_A(25.5, 80. H, d, H_r)$	4-204
4.24B	$L_b = F_A(50, 80, H, d, H_r)$	4-205
4.24C	$L_b = F_A(100, 80, H, d, H_r)$	4-206
4.24D	$L_b = F_A(250, 80, H, d, H_r)$	4-207
4.24E	$L_b = F_A(400, 80, H, d, H_r)$	4-208

ILLUSTRATIONS, continued

Figure		Page
4.24F	$L_b = F_A(25.5, 80, V, d, H_r)$	4-209
4.24G	$L_b = F_A(50, 80, V, d, H_r)$	4-210
4.24H	$L_b = F_A(100, 80, V, d, H_r)$.	4-211
4.24I	$L_b = F_A(250, 80, V, d, H_r)$.	4-212
4.24J	$L_b = F_A(400, 80, V, d, H_r)$.	4-213
4.25	Comparison Between Measured Height Functions for $d < 2$ Miles and $d \geq 2$ Miles	
4.25A	$L_b = F_A(25.5, 80, H, d, H_r)$	4-215
4.25B	$L_b = F_A(25.5, 40, H, d, H_r)$	4-216
4.25C	$L_b = F_A(25.5, 13, H, d, H_r)$	4-217
4.25D	$L_b = F_A(50.0, 80, H, d, H_r)$	4-218
4.25E	$L_b = F_A(50.0, 40, H, d, H_r)$	4-219
4.25F	$L_b = F_A(50.0, 13, H, d, H_r)$	4-220
4.25G	$L_b = F_A(100, 80, H, d, H$).	4-221
4.25H	$L_b = F_A(100, 40, H, d, H_r)$.	4-222
4.25I	$L_b = F_A(100, 13, H, d, H_r)$.	4-223
4.25J	$L_b = F_A(250, 80, H, d, H_r)$.	4-224
4.25K	$L_b = F_A(250, 40, H, d, H_r)$.	4-225
4.25L	$L_b = F_A(400, 80, H, d, H_r)$.	4-226
4.25M	$L_b = F_A(400, 40, H, d, H_r)$.	4-227
4.25N	$L_b = F_A(400, 13, H, d, H_r)$.	4-228
4.25O	$L_b = F_A(25.5, 80, V, d, H_r)$	4-229
4.25P	$L_b = F_A(25.5, 40, V, d, H_r)$	4-230
4.25Q	$L_b = F_A(25.5, 13, V, d, H_r)$	4-231

ILLUSTRATIONS, continued

Figure		Page
4.25R	$L_b = F_A(50, 80, V, d, H_r)$	4-232
4.25S	$L_b = F_A(50, 40, V, d, H_r)$	4-233
4.25T	$L_b = F_A(50, 13, V, d, H_r)$	4-234
4.25U	$L_b = F_A(100, 80, V, d, H_r)$	4-235
4.25V	$L_b = F_A(100, 40, V, d, H_r)$	4-236
4.25W	$L_b = F_A(100, 13, V, d, H_r)$	4-237
4.25X	$L_b = F_A(250, 80, V, d, H_r)$	4-238
4.25Y	$L_b = F_A(250, 40, V, d, H_r)$	4-239
4.25Z	$L_b = F_A(250, 13, V, d, H_r)$	4-240
4.25AA	$L_b = F_A(400, 80, V, d, H_r)$	4-241
4.25BB	$L_b = F_A(400, 40, V, d, H_r)$	4-242
4.25CC	$L_b = F_A(400, 13, V, d, H_r)$	4-243
4.26	Example of Vehicular Raw Data	
4.26A	$F_A(25.5, 40, V, 1.0\text{-}1.2, 7)$	4-245
4.26B	$F_A(50.0, 80, H, 1.0\text{-}1.2, 7)$	4-246
4.26C	$F_A(100, 40, H, 1.0\text{-}1.2, 7)$	4-247
4.26D	$F_A(250, 80, V, 0.8\text{-}1.0, 7)$	4-248
4.26E	$F_A(400, 40, H, 0.8\text{-}1.0, 7)$	4-249
4.27	A Sample Strip Chart Analysis	4-250
4.28	Totalizer Diagram	4-252
4.29	Statistical Distribution of L_b	
4.29A	$L_b = F_A(0.880, 80, V, 0.2\text{-}0.4, 7)$	4-256

ILLUSTRATIONS, continued

Figure		Page
4.29B	$L_b = F_A(0.880, 80, V, 3.5\text{-}4.0, 7)$	4-257
4.29C	$L_b = F_A(6.0, 40, V, 0.4\text{-}0.6, 7)$	4-258
4.29D	$L_b = F_A(6.0, 40, V, 3.0\text{-}3.2, 7)$	4-259
4.29E	$L_b = F_A(12.1, 21, V, 0.8\text{-}1.0, 7)$	4-260
4.29F	$L_b = F_A(12.1, 21, V, 2.8\text{-}3.0, 7)$	4-261
4.29G	$L_b = F_A(25.5, 80, V, 0.4\text{-}0.6, 7)$	4-262
4.29H	$L_b = F_A(25.5, 80, V, 9.0\text{-}9.5, 7)$	4-263
4.29I	$L_b = F_A(50, 80, V, 0.0\text{-}0.2, 7)$	4-264
4.29J	$L_b = F_A(50, 80, V, 4.0\text{-}4.5, 7)$	4-265
4.29K	$L_b = F_A(100, 80, V, 0.6\text{-}0.8, 7)$	4-266
4.29L	$L_b = F_A(100, 80, V, 2.8\text{-}3.0, 7)$	4-267
4.29M	$L_b = F_A(250, 80, V, 0.6\text{-}0.8, 7)$	4-268
4.29N	$L_b = F_A(250, 80, V, 2.6\text{-}2.8, 7)$	4-269
4.30	Reduced Vehicular Data $L_b = F_A(0.880, 80, V, d, 7)$	4-270
4.31	Standard Deviation of Vehicular Data $L_b = F_A(0.880, 80, V, d, 7)$	4-271
4.32	Comparison Between Vehicular Data and Measured F.P. Data $L_b = F_A(0.880, 80, V, d, 7)$	4-272
4.33	Comparison Between Vehicular Data and Theoretical Smooth-Earth Model $L_b = F_A(0.880, 80, V, d, 7)$	4-273
4.34	Comparison Between Vehicular Data and Theoretical Smooth-Earth Model Plus 9 db $L_b = F_A(0.880, 80, V, d, 7)$	4-274

ILLUSTRATIONS, continued

Figure		Page
4.35	Reduced Vehicular Data $L_b = F_A(6.0, 40, V, d, 7)$	4-275
4.36	Standard Deviation of Vehicular Data $L_b = F_A(6.0, 40, V, d, 7)$	4-276
4.37	Comparison Between Vehicular Data and Measured F.P. Data $L_b = F_A(6.0, 40, V, d, 7)$	4-277
4.38	Comparison Between Vehicular Data and Theoretical Smooth-Earth Model $L_b = F_A(6.0, 40, V, d, 7)$	4-278
4.39	Comparison Between Vehicular Data and Theoretical Smooth-Earth Model Plus 30 db $L_b = F_A(6.0, 40, V, d, 7)$	4-279
4.40	Reduced Vehicular Data $L_b = F_A(12.1, 21, V, d, 7)$	4-280
4.41	Standard Deviation of Vehicular Data $L_b = F_A(12.1, 21, V, d, 7)$	4-281
4.42	Comparison Between Vehicular Data and Measured F.P. Data $L_b = F_A(12.1, 21, V, d, 7)$	4-282
4.43	Comparison Between Vehicular Data and Theoretical Smooth-Earth Model $L_b = F_A(12.1, 21, V, d, 7)$	4-283
4.44	Comparison Between Vehicular Data and Theoretical Smooth-Earth Model Plus 17 db $L_b = F_A(12.1, 21, V, d, 7)$	4-284
4.45	Reduced Vehicular Data $L_b = F_A(25.5, 40, V, d, 7)$	4-285
4.46	Standard Deviation of Vehicular Data $L_b = F_A(25.5, 40, V, d, 7)$	4-286
4.47	Comparison Between Vehicular Data and Measured F.P. Data $L_b = F_A(25.5, 40, V, d, 7)$	4-287

ILLUSTRATIONS, continued

Figure		Page
4.48	Comparison Between Vehicular Data and Egli Model $L_b = F_A(25.5, 40, V, d, 7)$.	4-288
4.49	Reduced Vehicular Data $L_b = F_A(25.5, 80, V, d, 7)$.	4-289
4.50	Standard Deviation of Vehicular Data $L_b = F_A(25.5, 80, V, d, 7)$.	4-290
4.51	Comparison Between Vehicular Data and Measured F.P. Data $L_b = F_A(25.5, 80, V, d, 7)$.	4-291
4.52	Comparison Between Vehicular Data and Theoretical Smooth-Earth Model $L_b = F_A(25.5, 80, V, d, 7)$.	4-292
4.53	Comparison Between Vehicular Data and Theoretical Smooth-Earth Model Plus 25 db $L_b = F_A(25.5, 80, V, d, 7)$.	4-293
4.54	Comparison Between Vehicular Data and Egli Model $L_b = F_A(25.5, 80, V, d, 7)$.	4-294
4.55	Comparison Between Vehicular Data and Median of Computer-Induced Statistic Including $G(\bar{H})$ Functions $L_b = F_A(25.5, 80, V, d, 7)$.	4-295
4.56	Comparison Between Vehicular Data and Median of Computer-Induced Statistic Without $G(\bar{H})$ Functions $L_b = F_A(25.5, 80, V, d, 7)$.	4-296
4.57	Comparison Between Vehicular Data and N.B.S. Model Including $G(\bar{H})$ Functions $L_b = F_A(25.5, 80, V, d, 7)$.	4-297
4.58	Comparison Between Vehicular Data and N.B.S. Model Without $G(\bar{H})$ Functions $L_b = F_A(25.5, 80, V, d, 7)$.	4-298
4.59	Reduced Vehicular Data $L_b = F_A(25.5, 13, H, d, 7)$.	4-299

ILLUSTRATIONS, continued

Figure		Page
4.60	Standard Deviation of Vehicular Data $L_b = F_A(25.5, 13, V, H, 7)$	4-300
4.61	Comparison Between Vehicular Data and Measured F.P. Data $L_b = F_A(25.5, 13, H, d, 7)$	4-301
4.62	Comparison Between Vehicular Data and Egli Model $L_b = F_A(25.5, 13, H, d, 7)$	4-302
4.63	Reduced Vehicular Data $L_b = F_A(25.5, 40, H, d, 7)$	4-303
4.64	Standard Deviation of Vehicular Data $L_b = F_A(25.5, 40, H, d, 7)$	4-304
4.65	Comparison Between Vehicular Data and Measured F.P. Data $L_b = F_A(25.5, 40, H, d, 7)$	4-305
4.66	Comparison Between Vehicular Data and Egli Model $L_b = F_A(25.5, 40, H, d, 7)$	4-306
4.67	Reduced Vehicular Data $L_b = F_A(25.5, 80, H, d, 7)$	4-307
4.68	Standard Deviation of Vehicular Data $L_b = F_A(25.5, 80, H, d, 7)$	4-308
4.69	Comparison Between Vehicular Data and Measured F.P. Data $L_b = F_A(25.5, 80, H, d, 7)$	4-309
4.70	Comparison Between Vehicular Data and Egli Model $L_b = F_A(25.5, 80, H, d, H_r)$	4-310
4.71	Reduced Vehicular Data $L_b = F_A(50, 80, V, d, H_r)$	4-311
4.72	Standard Deviation of Vehicular Data $L_b = F_A(50, 80, V, d, H_r)$	4-312

ILLUSTRATIONS, continued

Figure		Page
4.73	Comparison Between Vehicular Data and Measured F.P. Data $L_b = F_A(50, 80, V, d, H_r)$	4-313
4.74	Comparison of Vehicular Data and Theoretical Smooth-Earth Model $L_b = F_A(50, 80, V, d, H_r)$	4-314
4.75	Comparison Between Vehicular Data and Theoretical Smooth Earth Model Plus 28 db $L_b = F_A(50, 80, V, d, H_r)$	4-315
4.76	Comparison Between Vehicular Data and Egli Model $L_b = F_A(50, 80, V, d, H_r)$	4-316
4.77	Comparison Between Vehicular Data and Median of Computer-Induced Statistic Including $G(\bar{H})$ Functions $L_b = F_A(50, 80, V, d, H_r)$	4-317
4.78	Comparison Between Vehicular Data and Median of Computer-Induced Statistic Without $G(\bar{H})$ Functions $L_b = F_A(50, 80, V, d, H_r)$	4-318
4.79	Comparison Between Vehicular Data and N.B.S. Model Including $G(\bar{H})$ Functions $L_b = F_A(50, 80, V, d, H_r)$	4-319
4.80	Comparison Between Vehicular Data and N.B.S. Model Without $G(\bar{H})$ Functions $L_b = F_A(50, 80, V, d, H_r)$	4-320
4.81	Reduced Vehicular Data $L_b = F_A(100, 13, V, d, H_r)$	4-321
4.82	Standard Deviation of Vehicular Data $L_b = F_A(100, 13, V, d, H_r)$	4-322
4.83	Comparison Between Vehicular Data and Measured F.P. Data $L_b = F_A(100, 13, V, d, H_r)$	4-323
4.84	Comparison Between Vehicular Data and Egli Model $L_b = F_A(100, 13, V, d, H_r)$	4-324

ILLUSTRATIONS, continued

Figure		Page
4.85	Reduced Vehicular Data $L_b = F_A(100, 40, V, d, H_r)$.	4-325
4.86	Standard Deviation of Vehicular Data $L_b = F_A(100, 40, V, d, H_r)$.	4-326
4.87	Comparison Between Vehicular Data and Measured F.P. Data $L_b = F_A(100, 40, V, d, H_r)$.	4-327
4.88	Comparison Between Vehicular Data and Egli Model $L_b = F_A(100, 40, V, d, H_r)$.	4-328
4.89	Reduced Vehicular Data $L_b = F_A(100, 80, V, d, H_r)$.	4-329
4.90	Standard Deviation of Vehicular Data $L_b = F_A(100, 80, V, d, H_r)$.	4-330
4.91	Comparison Between Vehicular Data and Measured F.P. Data $L_b = F_A(100, 80, V, d, H_r)$.	4-331
4.92	Comparison Between Vehicular Data and Theoretical Smooth-Earth Model $L_b = F_A(100, 80, V, d, H_r)$.	4-332
4.93	Comparison Between Vehicular Data and Theoretical Smooth-Earth Model Plus 30 db $L_b = F_A(100, 80, V, d, H_r)$.	4-333
4.94	Comparison Between Vehicular Data and Egli Model $L_b = F_A(100, 80, V, d, H_r)$.	4-334
4.95	Comparison Between Vehicular Data and Median of Computer-Induced Statistic Including $G(\bar{H})$ Functions $L_b = F_A(100, 80, V, d, H_r)$.	4-335
4.96	Comparison Between Vehicular Data and Median of Computer-Induced Statistic Without $G(\bar{H})$ Functions $L_b = F_A(100, 80, V, d, H_r)$.	4-336

ILLUSTRATIONS, continued

Figure		Page
4.97	Comparison Between Vehicular Data and N.B.S. Model Including $G(\bar{H})$ Functions $L_b = F_A(100, 80, V, d, H_r)$	4-337
4.98	Comparison Between Vehicular Data and N.B.S. Model Without $G(\bar{H})$ Functions $L_b = F_A(100, 80, V, d, H_r)$	4-338
4.99	Reduced Vehicular Data $L_b = F_A(100, 13, H, d, H_r)$	4-339
4.100	Standard Deviation of Vehicular Data $L_b = F_A(100, 13, H, d, H_r)$	4-340
4.101	Comparison Between Vehicular Data and Measured F.P. Data $L_b = F_A(100, 13, H, d, H_r)$	4-341
4.102	Comparison Between Vehicular Data and Egli Model $L_b = F_A(100, 13, H, d, H_r)$	4-342
4.103	Reduced Vehicular Data $L_b = F_A(100, 40, H, d, H_r)$	4-343
4.104	Standard Deviation of Vehicular Data $L_b = F_A(100, 40, V, d, H_r)$	4-344
4.105	Comparison Between Vehicular Data and Measured F.P. Data $L_b = F_A(100, 40, H, d, H_r)$	4-345
4.106	Comparison Between Vehicular Data and Egli Model $L_b = F_A(100, 40, H, d, H_r)$	4-346
4.107	Reduced Vehicular Data $L_b = F_A(100, 80, H, d, H_r)$	4-347
4.108	Standard Deviation of Vehicular Data $L_b = F_A(100, 80, H, d, H_r)$	4-348
4.109	Comparison Between Vehicular Data and Measured F.P. Data $L_b = F_A(100, 80, H, d, H_r)$	4-349

ILLUSTRATIONS, continued

Figure		Page
4.110	Comparison Between Vehicular Data and Egli Model $L_b = F_A(100, 80, H, d, H_r)$	4-350
4.111	Comparison Between Vehicular Data and Computer-Induced Statistic Including $G(\bar{H})$ Functions $L_b = F_A(100, 80, H, d, H_r)$	4-351
4.112	Comparison Between Vehicular Data and Computer-Induced Statistic Without $G(\bar{H})$ Functions $L_b = F_A(100, 80, H, d, H_r)$	4-352
4.113	Comparison Between Vehicular Data and N.B.S. Model Including $G(\bar{H})$ Functions $L_b = F_A(100, 80, H, d, H_r)$	4-353
4.114	Comparison Between Vehicular Data and N.B.S. Model Without $G(\bar{H})$ Functions $L_b = F_A(100, 80, H, d, H_r)$	4-354
4.115	Reduced Vehicular Data $L_b = F_A(250, 80, V, d, H_r)$	4-355
4.116	Standard Deviation of Vehicular Data $L_b = F_A(250, 80, V, d, H_r)$	4-356
4.117	Comparison Between Vehicular Data and Measured F.P. Data $L_b = F_A(250, 80, V, d, H_r)$	4-357
4.118	Comparison Between Vehicular Data and Theoretical Smooth-Earth Model $L_b = F_A(250, 80, V, d, H_r)$	4-358
4.119	Comparison Between Vehicular Data and Theoretical Smooth-Earth Model Plus 50 db $L_b = F_A(250, 80, V, d, H_r)$	4-359
4.120	Comparison Between Vehicular Data and Egli Model $L_b = F_A(250, 80, V, d, H_r)$	4-360

ILLUSTRATIONS, continued

Figure		Page
4.121	Comparison Between Vehicular Data and Median of Computer-Induced Statistic Including $G(\overline{H})$ Functions $L_b = F_A(250, 80, V, d, H_r)$	4-361
4.122	Comparison Between Vehicular Data and Median of Computer-Induced Statistic Without $G(\overline{H})$ Functions $L_b = F_A(250, 80, V, d, H_r)$	4-362
4.123	Comparison Between Vehicular Data and N.B.S. Model Including $G(\overline{H})$ Functions $L_b = F_A(250, 80, V, d, H_r)$	4-363
4.124	Comparison Between Vehicular Data and N.B.S. Model Without $G(\overline{H})$ Functions $L_b = F_A(250, 80, V, d, H_r)$	4-364
4.125	Climatological Data Summary	4-366
4.126	Nomograph 1. Computation of Partial Pressure of Water Vapor, e, from Psychrometric Data.	4-368
4.127	Nomograph 2. Computation of N_s and X from Partial Vapor Pressure, e, (mm Hg)	4-369
4.128	Frequency Distribution of Tree Heights in Plot #1	4-377
4.129	Frequency Distribution of Tree Heights in Plot #2	4-378
4.130	Frequency Distribution of Tree Heights in Plot #3	4-379
4.131	Frequency Distribution of Tree Heights in Plot #5	4-380
4.132	Frequency Distribution of Tree Heights in Plot #5.5	4-381
4.133	Frequency Distribution of Tree Heights in Plot #6	4-382
4.134	Frequency Distribution of Tree Heights in Plot #7	4-383

ILLUSTRATIONS, continued

Figure		Page
4.135	Frequency Distribution Of Tree Heights In Plot #8	4-384
4.136	Frequency Distribution Of Tree Heights In Plot #9	4-385
4.137	Basal Area vs Tree Height In Plot #1	4-386
4.138	Basal Area vs Tree Height In Plot #2	4-387
4.139	Basal Area vs Tree Height In Plot #3	4-388
4.140	Basal Area vs Tree Height In Plot #5	4-389
4.141	Basal Area vs Tree Height In Plot #5.5 . . .	4-390
4.142	Basal Area vs Tree Height In Plot #6	4-391
4.143	Basal Area vs Tree Height In Plot #7	4-392
4.144	Basal Area vs Tree Height In Plot #8	4-393
4.145	Basal Area vs Tree Height In Plot #9	4-394
4.146	Distribution Of Tree Heights In Plot #1 . . .	4-395
4.147	Distribution Of Tree Heights In Plot #2 . . .	4-396
4.148	Distribution Of Tree Heights In Plot #3 . . .	4-397
4.149	Distribution Of Tree Heights In Plot #5 . . .	4-398
4.150	Distribution Of Tree Heights In Plot #5.5 . .	4-399
4.151	Distribution Of Tree Heights In Plot #6 . . .	4-400
4.152	Distribution Of Tree Heights In Plot #7 . . .	4-401
4.153	Distribution Of Tree Heights In Plot #8 . . .	4-402
4.154	Distribution Of Tree Heights In Plot #9 . . .	4-403
4.155	Composite Distribution Of Tree Heights From All Plots	4-404
4.156	Floristic Profile for Plot #9	4-405

ILLUSTRATIONS, continued

Figure		Page
4.157	Floristic Profile, Plan View, Plot #9	4-406
4.158	L_b for Vertical Polarization Minus L_b for Horizontal Polarization at 25.5 mc. . .	4-408
4.159	L_b for Vertical Polarization Minus L_b for Horizontal Polarization at 50 mc. . . .	4-409
4.160	L_b for Vertical Polarization Minus L_b for Horizontal Polarization at 100 mc . . .	4-410
4.161	L_b for Vertical Polarization Minus L_b for Horizontal Polarization at 250 mc . . .	4-411
4.162	L_b for Vertical Polarization Minus L_b for Horizontal Polarization at 400 mc . . .	4-412
4.163	Variation of Recorded Noise Level With Antenna Height	4-418
4.164	Combined Median Noise Levels for Nov., Dec., and Jan. For Horizontal Polarization	4-420
4.165	Combined Median Noise Levels for Nov., Dec., and Jan. for Vertical Polarization	4-421
4.166	Communication Margin as a Function of Confidence Level	4-430
4.167	Factor to Convert M (Median) to M (P%). . . .	4-432
4.168	Communication Range as a Function of Confidence Level	4-433
5.1	Test Areas for Measurements Above 425 Mc . .	5-5
5.2	Area A for Measurements Above 425 Mc Line-of-Sight Test Path	5-6
5.3	Area B for Measurements Above 425 Mc Line-of-Sight Test Path	5-7

ILLUSTRATIONS, continued

Figure		Page
A.1	Theoretical Smooth-Earth Height Functions, Vertical Polarization	A-4
A.2	Theoretical Smooth-Earth Height Functions, Horizontal Polarization	A-5

1. INTRODUCTION

This sixth semiannual report presents results of a program devoted to theoretical and experimental studies of radio propagation in tropical vegetated environments. This program is sponsored by the Advanced Research Projects Agency, Department of Defense, as a part of Project SEACORE, and is directed by the U. S. Army Electronics Command, Fort Monmouth, New Jersey. The main objectives of this program are to collect and analyze basic data on radio propagation in a tropical vegetated environment, and to develop prediction techniques so that a broad spectrum of improvements in the design and operation of tactical communications equipments for such environments can be obtained.

The experimental portion of this program is being carried out in Thailand in cooperation with the Military Research and Development Center in that country. The frequency range of the measurements extends from 100 kc to 10 gc. The major portion of the work is devoted to the range between 100 kc and 400 mc. In this lower range the acquisition of data and other information that can be applied to the design and operation of vehicular and short-range man-pack equipment is emphasized.

2. GENERAL DISCUSSION

Those who are concerned with the planning and implementation of warfare communications in tropical vegetated environments soon encounter many problems in attempting to evaluate the effects of the environment on the performance of the equipment they intend to use. This is particularly true of land mobile and man-pack equipment. The same kind of problems arise when attempting to design and specify new equipments to obtain better performance, or to meet new requirements in such environments. In either case, the problems frequently stem from the lack of a workable model to predict the quantitative influence on equipment performance of such environmental elements as terrain, climate, vegetation, and ambient radio noise. Furthermore, the predictions should be expressible in quantitative terms of performance, or effectiveness, to permit an intelligent selection from among the various alternatives that are generally available.

For example, it would be most useful to be able to confidently predict the effects upon the operating range of an existing man-pack set when it is to be operated in some specific tropical vegetated area where a military operation is to be carried out. Or it would be useful to know how much improvement could be obtained under these conditions by altering some parameter of the radio set, such as its antenna height, or antenna orientation, or frequency. The predictions necessary to resolve such alternatives must be obtainable through simple, direct means if they are to be effectively used in the planning and management of tactical communications for the highly mobile situations characteristic of limited warfare.

The prediction techniques necessary to these

objectives cannot be obtained through purely theoretical means. The number of variables involved is far too great to manage analytically. Therefore, the task must be approached through empirical methods, using data from experimental measurements within the environment to obtain the needed prediction models. Such an approach is statistical in nature and the analysis naturally must proceed through statistical concepts and methods. Because of the statistical nature of the investigation, the answers obtained cannot be regarded as certain, but at least it is generally possible to measure the amount of uncertainty involved along the way.

The design and operation of radio systems require a prediction of power loss between the transmitter and receiver. The power radiated from an antenna diverges and spreads over a large area. As a result, the power available at the receiving antenna is only a small fraction of the radiated power. The ratio of received power to radiated power has been defined as radio transmission loss and this quantity determines whether the received signal will be useful. The magnitude of this ratio is primarily a function of propagation distance and can vary over a very large range, in some cases as much as 10^{20}, or 200 decibels. Among the many factors that must be considered in radio systems engineering, transmission loss probably is the most significant.

The total array of factors affecting communications performance falls into two broad categories: those associated with equipment performance, and those associated with the influence of the environment on the propagation mechanism. Since transmission loss includes the power gain of the transmitting and receiving antennas, it cannot be identified exclusively with either of the above categories. But if transmission loss is

converted to basic transmission loss by adding the antenna power gains referred to isotropic antennas, and if the antenna gains are regarded as equipment performance factors, basic transmission loss then becomes identified exclusively with the environmental category of factors. A reasonable hypothesis, therefore, is that the influence of the physical environment on radio communication performance from antenna to antenna is related entirely through the parameter of basic transmission loss.

In a tropical vegetated area practically all of the above factors come into play. The experimental program in Thailand was carefully designed to isolate and study these factors, as well as their interrelationships, by means of experimental measurements of radio transmission loss. The basic experimental variables are frequency, height of the transmitting antenna, height of the receiving antenna, transmitting antenna polarization, terrain characteristics, climate and ambient radio noise. The basic approach being taken involves measurement and analysis of the natural environmental elements just as carefully as the measurement and analysis of the propagation data.

However, because the experiments in Thailand are being conducted entirely in one type of tropical region, the vegetation parameters in these measurements cannot be regarded as an experimental variable in relation to basic transmission loss. Rather, they should be regarded in the sense of a constant. To introduce variations into the vegetation parameters the experiments must be moved and conducted in a different vegetation environment. In this regard, the present program plan anticipates carrying out these experiments next in a tropical rain forest region, in contrast with the wet-dry tropical region prevailing in Thailand.

Previous reports have described the experimental procedures employed in Thailand, and have presented a considerable amount of data resulting directly from the field measurements prior to the application of a more detailed data analysis. The purpose of doing this was to provide this data to interested government agencies that are currently involved in a variety of communication problems related to similar environments. The data evidently has been quite helpful in this respect, and interest in the data has been expressed from several different points of view. However, much of this interest appears to be concerned more with the analysis of the data than with the direct application of the data as first reduced from field measurements.

During the current reporting period, a sufficiently large quantity of field data was accumulated, and appropriately reduced, to permit the beginning of a comprehensive analysis. Consequently, a large portion of this report is devoted to the presentation of this analysis in considerable detail and it is hoped that the results in this report will be interesting and useful. However, the techniques and results presented here should not be regarded as the program end objectives. They are only a step toward these objectives — a means to the end, so to speak. The end objectives require that much of the complexity that is characteristic of radio propagation predictions be removed, and that the prediction techniques utlimately developed will be easily applicable to the problems at hand. Much work remains to be done to reach these ends.

The purpose of Section 3 of this report is to present new field data that has been reduced during this reporting period. Section 4 is devoted to analysis of a larger block of field data, including field data that has been presented in previous semiannual reports. For reasons which will

become clear in the discussions, some of the new data obtained during this period has been included in Section 4. Section 4 also includes a comparison of the results from the experimental data with those obtained with existing propagation models for unvegetated terrain. Markedly good agreement was obtained with a foliated rough-earth model whose rough-earth statistics were given by Egli in 1957.

In Section 4.6 an example is presented to demonstrate one method of applying the results of this report to a practical communications problem. The operating characteristics of an AN/PRC-10 are selected as a set of equipment parameters and the "communication margin" at various per cent confidence levels is calculated for a tropical vegetated terrain.

The frequency range of the measurement program in Thailand has been extended to 10 gc, the measurements consisting chiefly of line-of-sight transmissions over obstacle, refractive index measurements along the -of-sight path, and measurements of short-range transmissions directly through foliage. Discussion of progress in this phase of the program is presented in Section 5. Sections 6, 7, and 8 deal with technical film reports, meetings and conferences, and project personnel, respectively.

3. RESULTS OF FIELD MEASUREMENTS

3.1 Summary of Measurements

The raw data being obtained in Thailand can be classified under five general categories: (1) field point data, (2) vehicular data, (3) background noise, (4) climatological data, and (5) terrain and tropical vegetation characteristics.

The field point data consists of those propagation measurements which are made at fixed points within the vegetation. For any one field point measurement, the frequency, polarization, distance and transmitting antenna height are held constant while receiving antenna height is varied. The vehicular data consists of continuously recorded field strength as a function of distance within the radial sectors. The transmitting systems used for field point measurements and vehicular measurements are identical.

New field point data is presented in Section 3.4 of this report. Terrain data pertinent to Radial B is presented in Section 3.3. Since presentation of the other categories of data requires a significant amount of data analysis, they more appropriately are included in Section 4. Vehicular data is presented and discussed in Section 4.3.3, climatology data in Section 4.4.1, tropical vegetation data in Section 4.4.2, and noise data in Section 4.5.

3.2 Basic Data Format

Following the practice used in past reports, this report presents measured field strength data in the form of basic transmission loss. A detailed discussion of basic transmission loss and the derivation of a general equation used for converting measured field strength values to basic

transmission loss appears in Semiannual Report Number 4. The equation used to carry out the conversion is repeated below.

$$L_b = 36.57 + 20 \log f + 20 \log E_1 - 20 \log E_{(meas)} \quad (1)$$

where

L_b = Basic transmission loss in db.

f = Frequency in megacycles.

E_1 = Unattenuated field strength in μv/m expected from the transmitting system at one mile.

$E_{(meas)}$ = Any measured value of field strength produced at a distant point as a result of radiation from the transmitting system used to determine E_1 above.

The transmitting antennas which have been used in the measurement program are summarized in Table I. Table I provides a brief description of the antenna and a statement of the expression used to determine 20 log E_1 for use in equation 1.

3.3 Propagation Path Profiles

Field strength measurements are currently being made along two trail systems. The two trails have been designated Radial A and Radial B. A detailed map and profiles of the Radial A system are presented in Semiannual Report Number 4. The Radial B trail system, which runs generally in a southwesterly direction from the base camp, is shown in Figure 3.1 of this report. The profile contours indicated on Figure 3.1 are in meters. Also shown in Figure 3.1 are the locations of field points and radial points. Field points are defined as those fixed locations at which measurements are made as a function of receiving antenna heights; radial points are used as reference distances from the transmitter when making vehicular trail measurements. The radial distance to each of

Table I

TRANSMITTING ANTENNAS

Frequency (mc)	Pol.	Nominal Height (feet)	Description	20 log E_1 (db/μv/m)
0.105 0.300 0.880	V	80	Ground-based vertical radiator with capacative top loading and wire radial ground system.	77.4 + 20 Log I + 20 Log f where I = base current in amps f = frequency in megacycles
2	V	80	Ground-based vertical, tuned with BC 939B tuning unit.	86.4 + 20 Log I where I = base current in amps
6	V	40	Ground-based, quarter-wave vertical tuned with modified BC 939B tuning unit.	91.4 + 20 Log I where I = base current in amps
12	V	21	Ground-based vertical antenna cut to $\lambda/4$.	91.4 + 20 Log I where I = base current in amps
25.5	V	10	Ground-based vertical antenna cut to $\lambda/4$.	72.8 + 10 Log P where P = power delivered to antenna in watts

Table I (Continued)

Frequency (mc)	Pol.	Nominal Height (feet)	Description	20 Log E_c (db/μv/m)
25.5	V	40 80	Elevated λ/2 vertical skirted dipole.	72.8 + 10 Log P where P = power delivered to antenna in watts
50 100 250 400	V	13 40 80	Elevated vertical skirted λ/2 dipole.	72.8 + 10 Log P where P = power delivered to antenna in watts
2 6 12	H	40 80	Horizontal λ/2 dipole consisting of wire strung between two towers with jumpers to allow change in frequency. Center feed with tuned section of 72-ohm twin lead.	91.4 + 20 Log I + 20 Log D where I = input current in amps $D = \frac{\text{Cos } (\frac{\pi}{2} \text{ Cos } \theta)}{\text{Sin } \theta}$ θ = angle between dipole axis and ray to receiving point
25.5 50 100 250 400	H	13 40 80	λ/2 horizontal dipole mounted on vertical tower.	72.8 + 10 Log P + 20 Log D where P = power delivered to antenna in watts $D = \frac{\text{Cos } (\frac{\pi}{2} \text{ Cos } \theta)}{\text{Sin } \theta}$ θ = angle between dipole axis and ray to receiving point

the field points and their terrain elevations are given below.

Field Point	Distance (Miles)	Height (Meters)
FPB-1	0.2	450
FPB-2	0.45	450
FPB-3	0.7	450
FPB-4	1.0	470
FPB-5	2.0	480
FPB-5.5	3.0	500
FPB-6	4.3	450
FPB-7	6.7	350
FPB-8	10.5	380
FPB-9	14.2	365
FPB-10	19.0	760

In addition to the field points listed above, there are four other field points, designated FPB-8.5, FPB-9.5, FPB-11, and FPB-12, which are not accessible by trail and require the use of a helicopter to transport measuring equipment. These points lie at radial distances of 11.4, 15.3, 21.6, and 28.9 miles, respectively, from base camp.

Figures 3.2 through 3.9 show the terrain elevation profiles between the transmitter and each field point. These profiles indicate that field points that lie within 1 mile of the transmitter (FPB-1 through FPB-4) would constitute line-of-sight paths in the absence of vegetation and field points beyond 1 mile (FPB-5 through FPB-12) constitute beyond-the-horizon paths. The Radial A system, described in Semiannual Report Number 4, has a line-of-sight "cut-off" point

approximately 1.5 miles from the transmitter, again assuming the absence of vegetation.

3.4 L_b Vs Antenna Height

Figures 3.10 through 3.55 represent new field-point data which has been reduced during the current reporting period. The information contained in these figures coupled with similar information presented in Semiannual Reports 4 and 5 form a basic set of measured data. This type of data is continuously recorded as the receiving antenna is raised from an elevation of about 13 feet to 80 feet above ground level. Since the fine-grain variation of the signal with elevation is generally small, the continuous recording is broken down into equal increments of antenna height and then the median signal level for each increment is plotted. The increment chosen corresponds to about 6 feet of tower height and provides roughly 12 to 13 median signal levels for each curve. The fine-grain variability in field strength obtained from this data is presented in Section 4.3.2.1

It has been found convenient to use a systematic method of identifying the various sets and families of curves similar to the ones shown in Figures 3.10 through 3.55. The following identification has been adopted and is used universally throughout this report in identifying specific curves.

$$L_b = F(f, H_t, P, d, H_r)$$

The above format, which is used to identify each L_b graph, relates the basic transmission loss derived from measurements to five basic variables: frequency, in megacycles (f); transmitting antenna height, in feet, (H_t); polarization, horizontal or vertical, (P); distance, in

miles, (d); and receiving antenna height, in feet, (H_r). An example is the identification found in Figure 3.10, $L_b = F_A(25.5, 21, V, d, H_r)$. This identification denotes that the receiving antenna height and distance were varied while the other three variables remained fixed at the values indicated.

Although d, the separation distance between transmitter and receiver, remains constant for a given measurement in height, the family of curves shown in each graph is generated by a variation of d. For this reason no specific value of d is used in the identification in Figures 3.10 through 3.55. Instead, the value is specified on the applicable curve itself.

The subscript "A" denotes that the data pertains to Radial A. A subscript "B" denotes data pertaining to Radial B.

In order to assist in the correlation of the data given in Section 3.1 to weather conditions or to time of year, each curve given in Figures 3.10 through 3.55 is identified in more detail in Appendix B. In addition to the information given on the curves, the exact date of measurement and the measurement number is given in Appendix B.

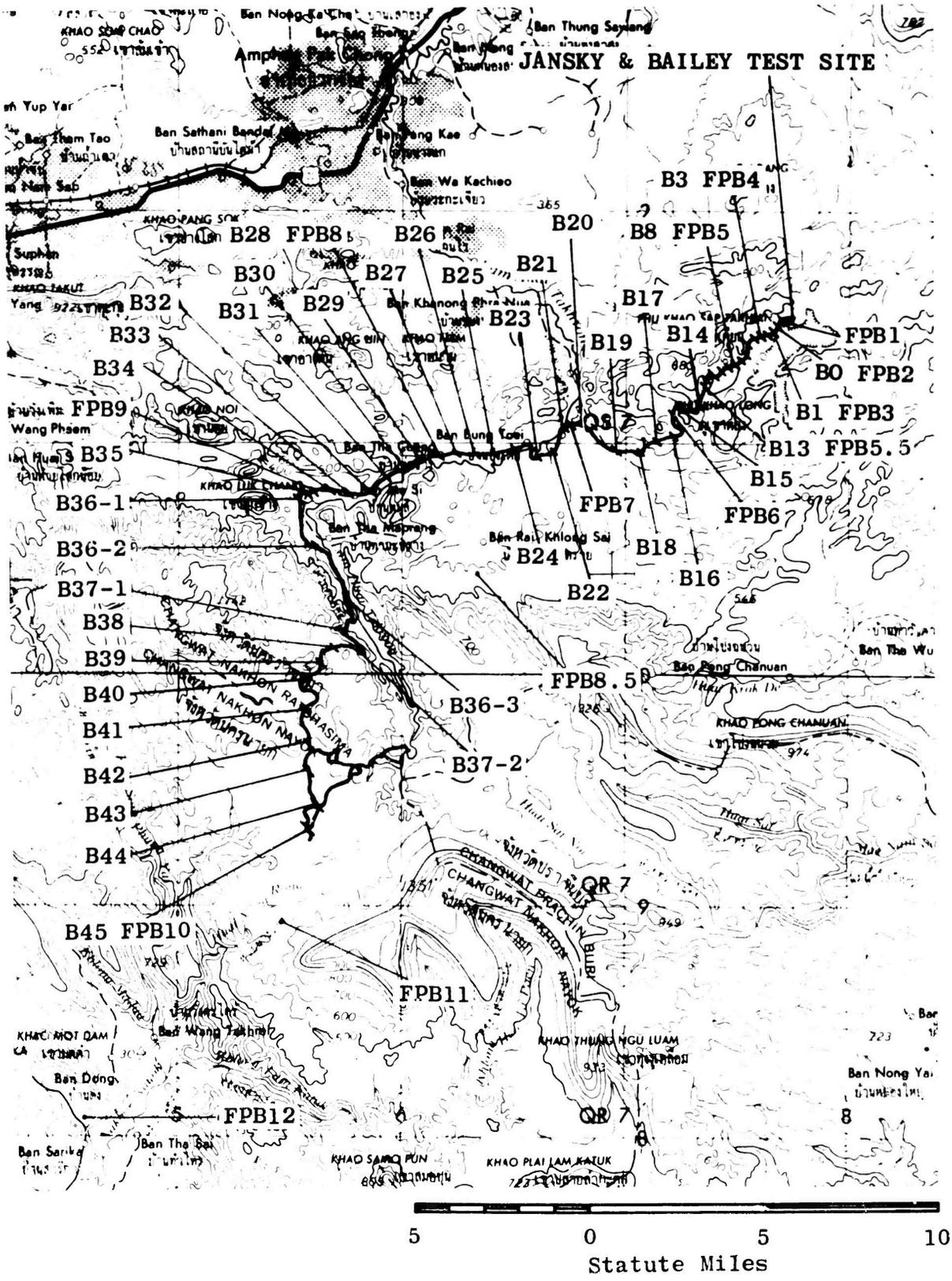

Figure 3.1 Radial Points and Field Points Along Trail B

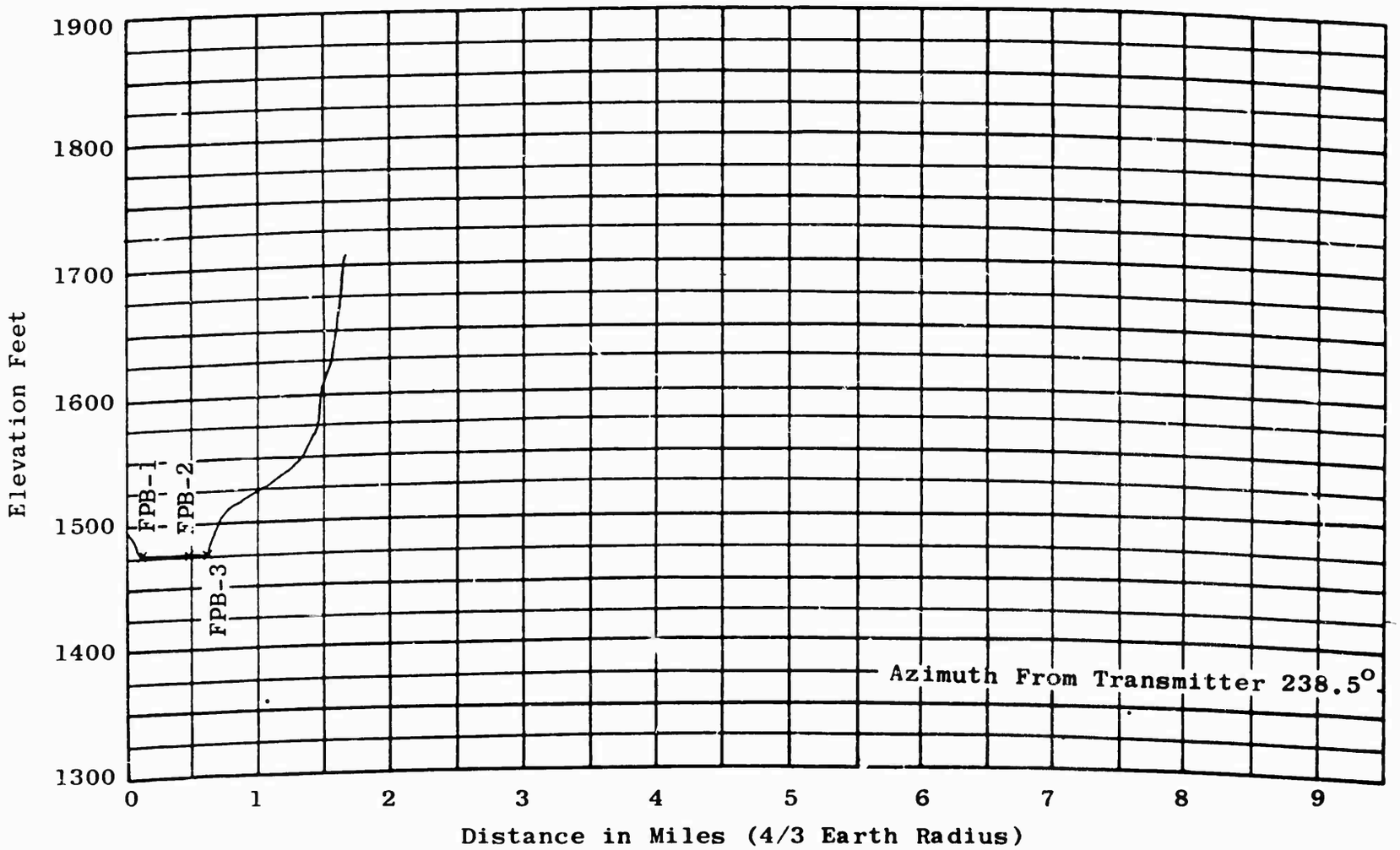

Figure 3.2 Terrain Profile Between Transmitter and Field Points FPB-1, FPB-2, and FPB-3

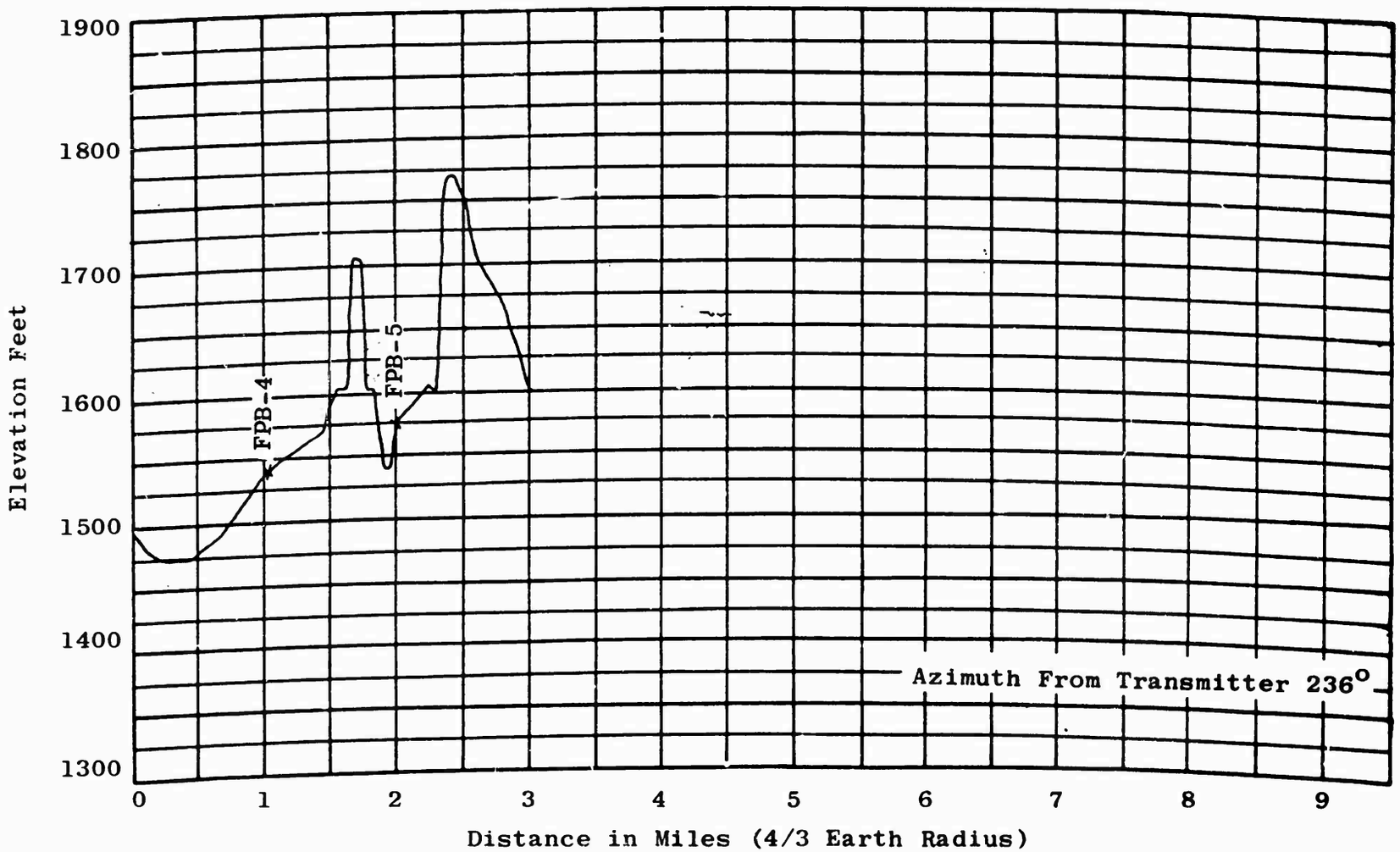

Figure 3.3 Terrain Profile Between Transmitter and Field Points FPB-4 and FPB-5

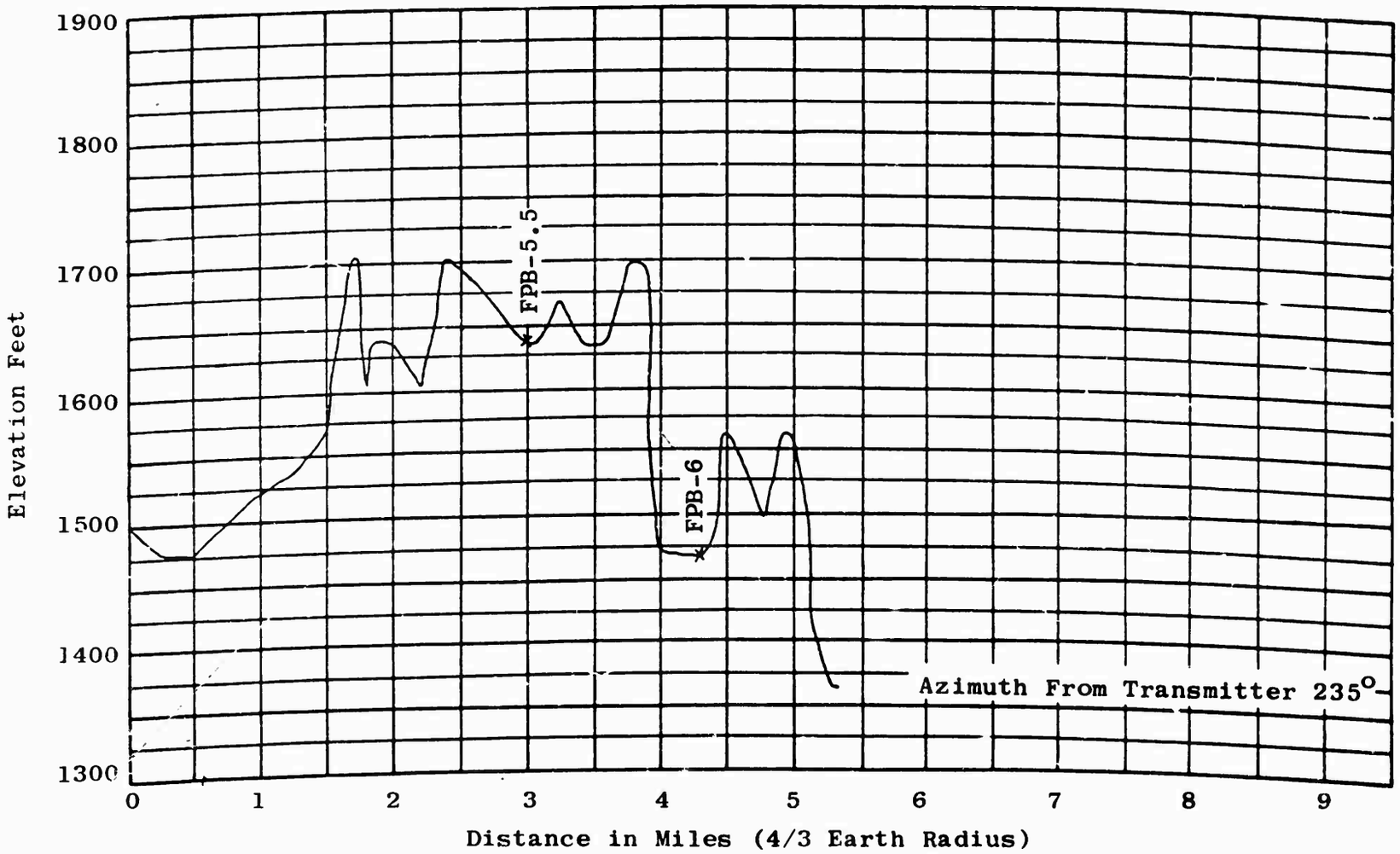

Figure 3.4 Terrain Profile Between Transmitter and Field Points FPB-5.5 and FPB-6

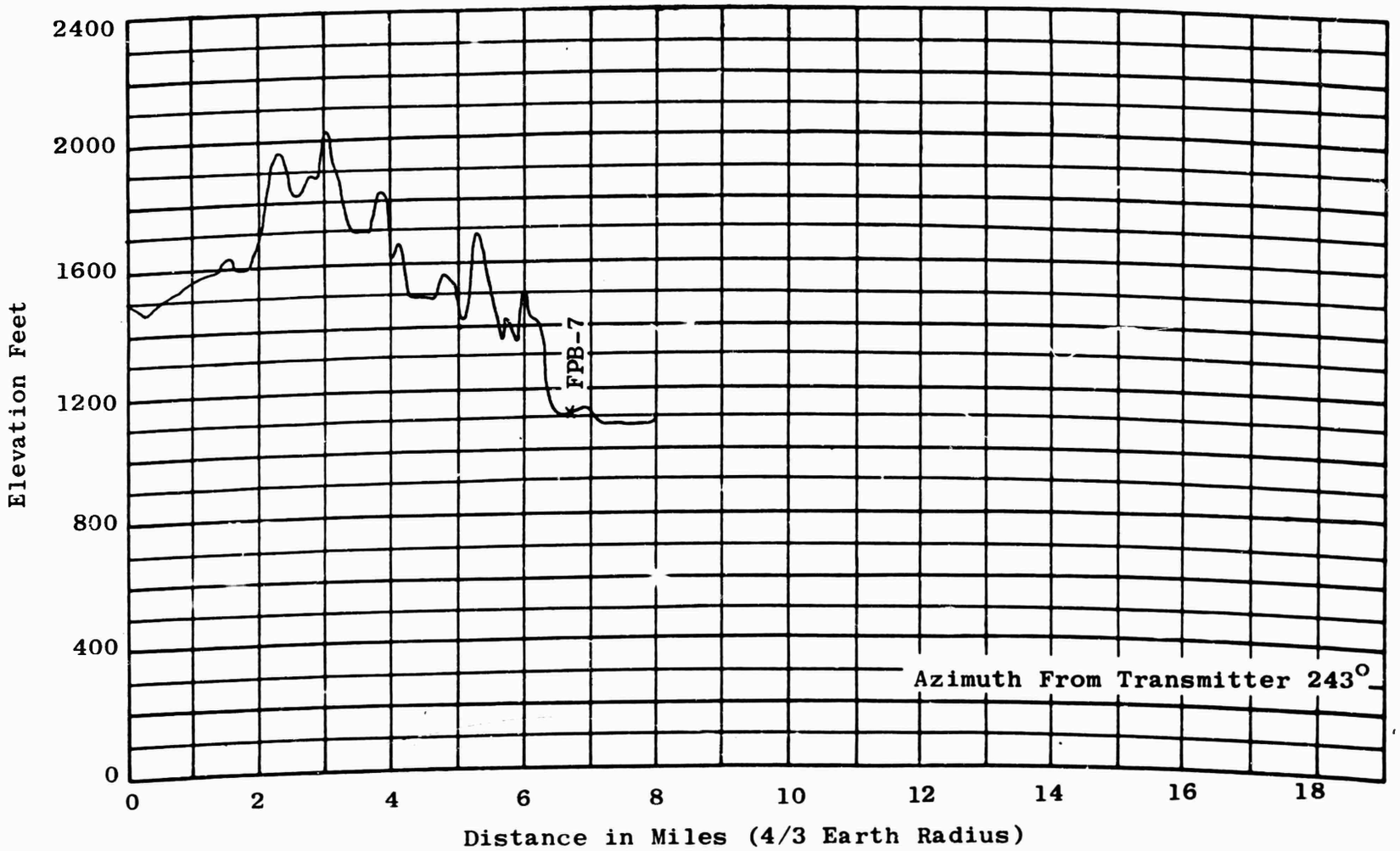

Figure 3.5 Terrain Profile Between Transmitter and Field Point FPB-7

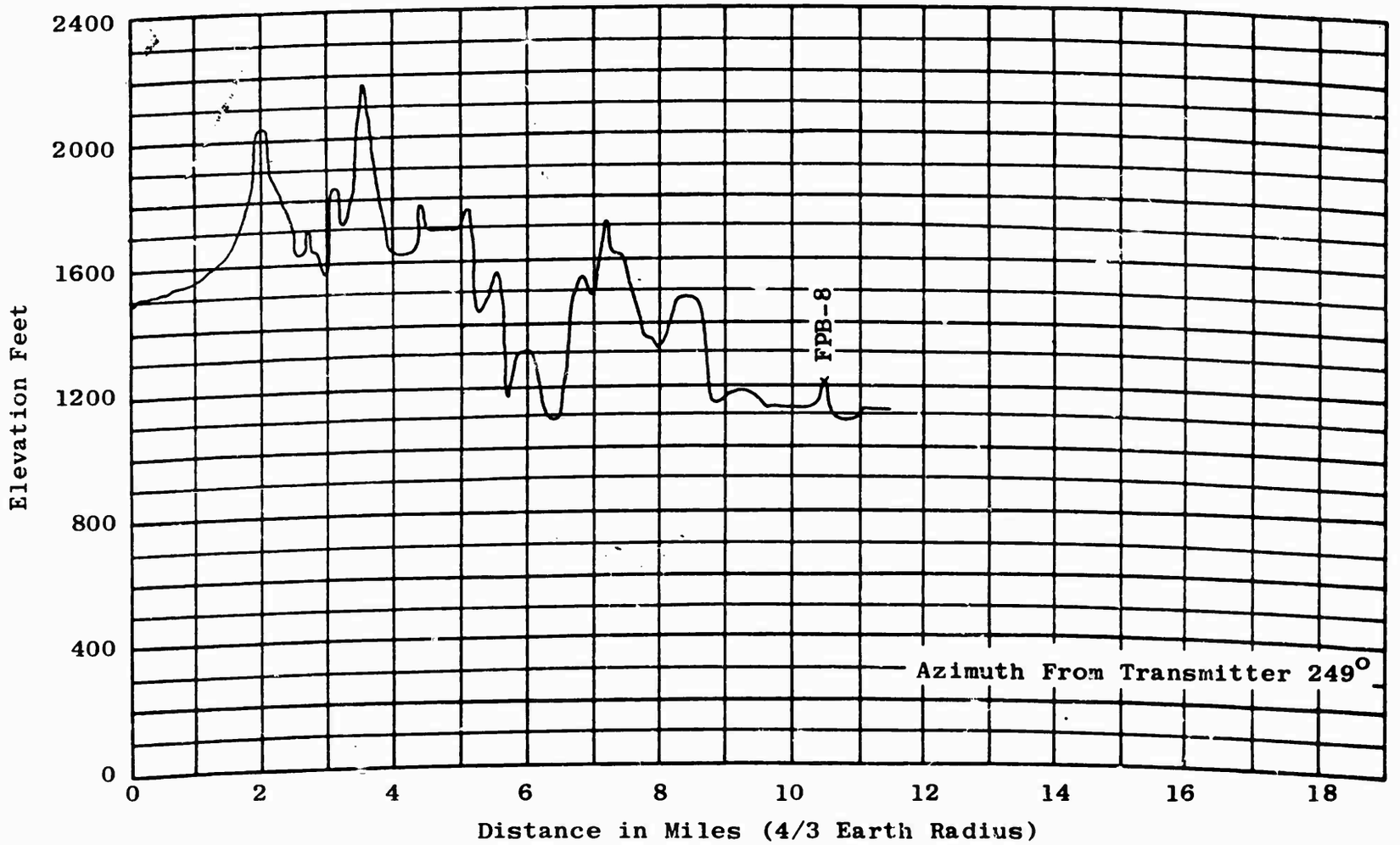

Figure 3.6 Terrain Profile Between Transmitter and Field Point FPB-8

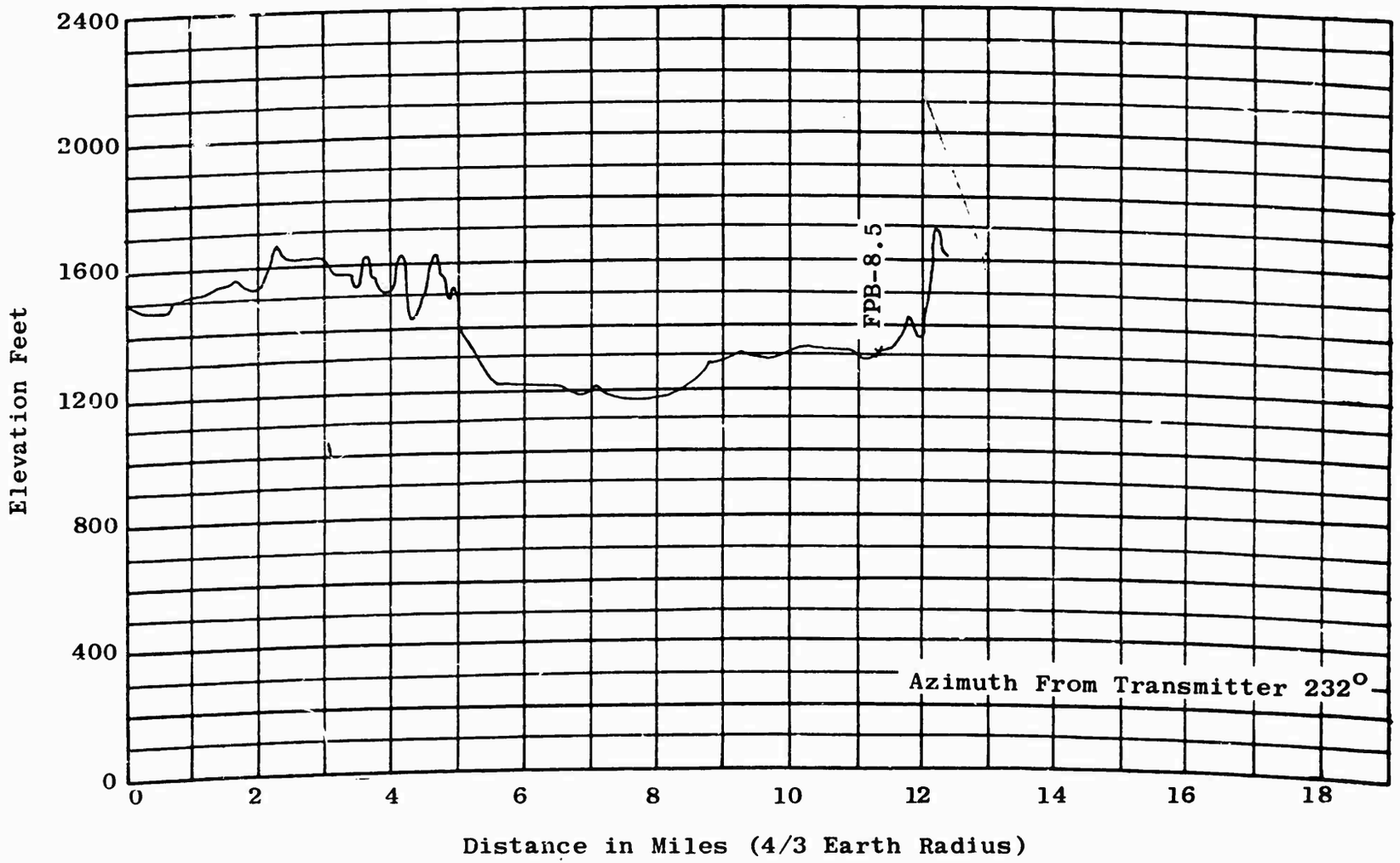

Figure 3.7 Terrain Profile Between Transmitter and Field Point FPB-8.5

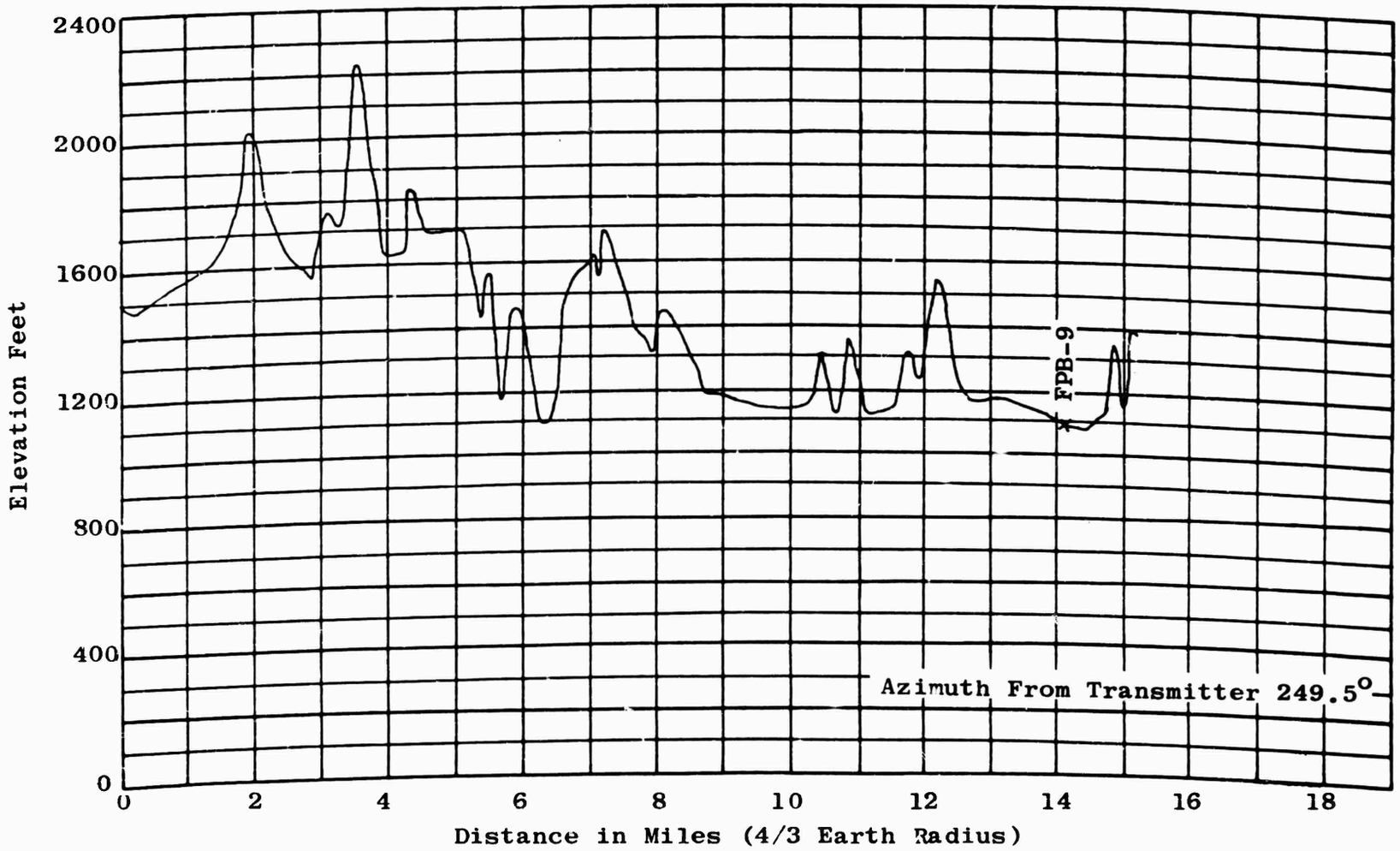

Figure 3.8 Terrain Profile Between Transmitter and Field Point FPB-9

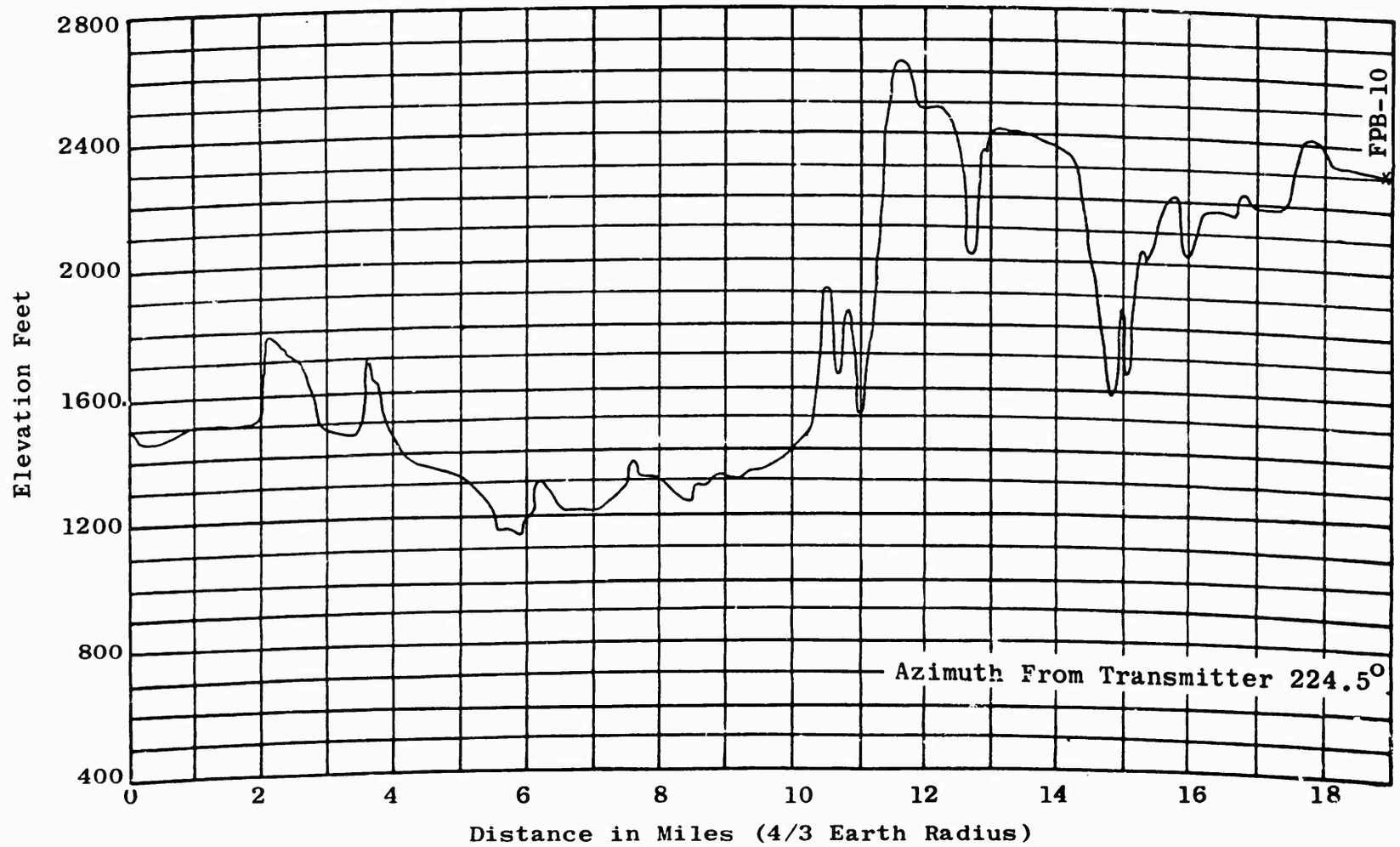

Figure 3.9 Terrain Profile Between Transmitter and Field Point FPB-10

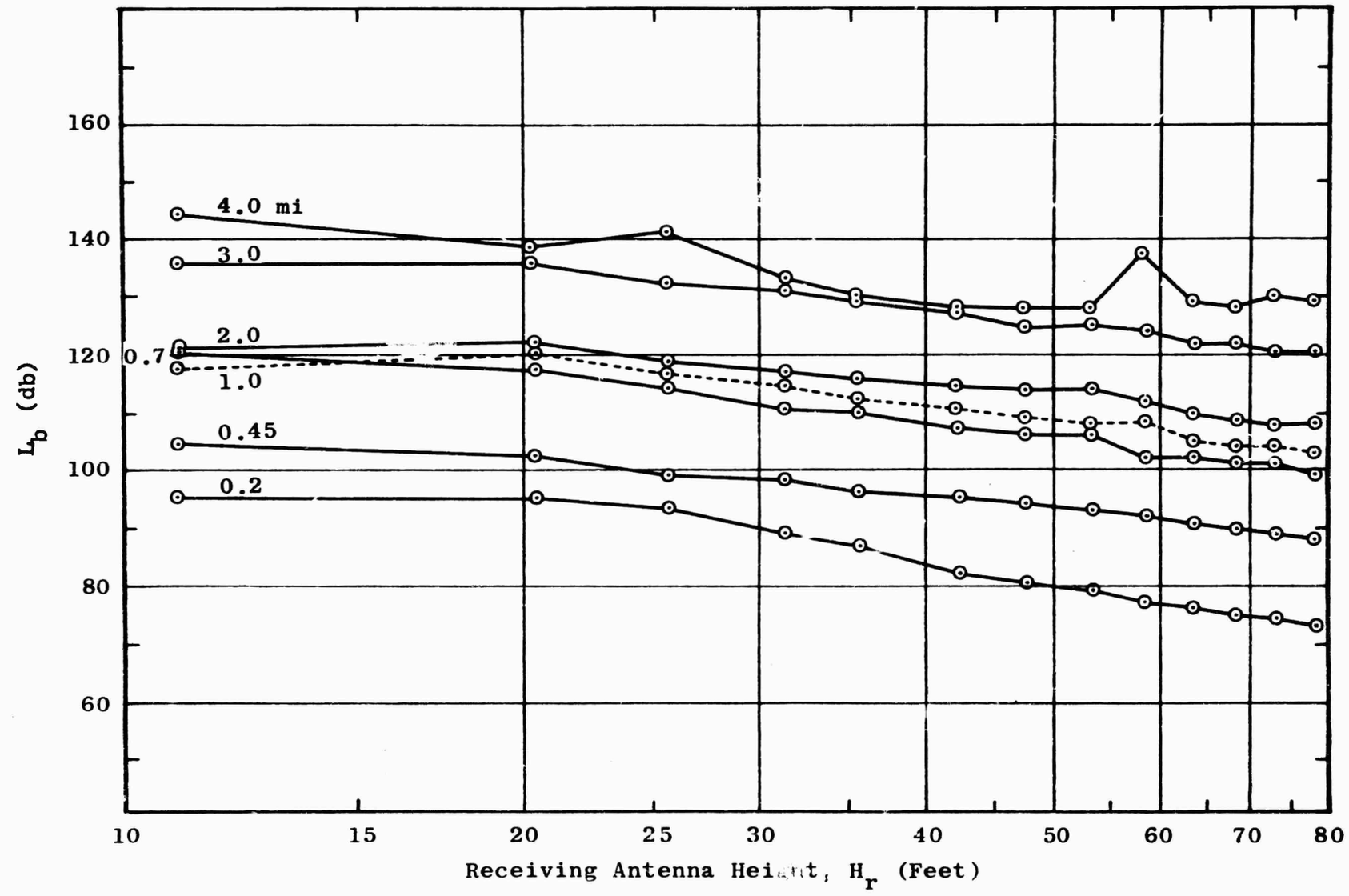

Figure 3.10 Variation of Basic Transmission Loss with Receiving Antenna Height
$L_b = F_A(25.5, 21, V, d, H_r)$

η_1 (dB)

17.0 kHz
14.0
7.0
10.5
4.0
3.5
3.0
1.0
0.7
0.45
0.35
(dB)

L_p (dB)

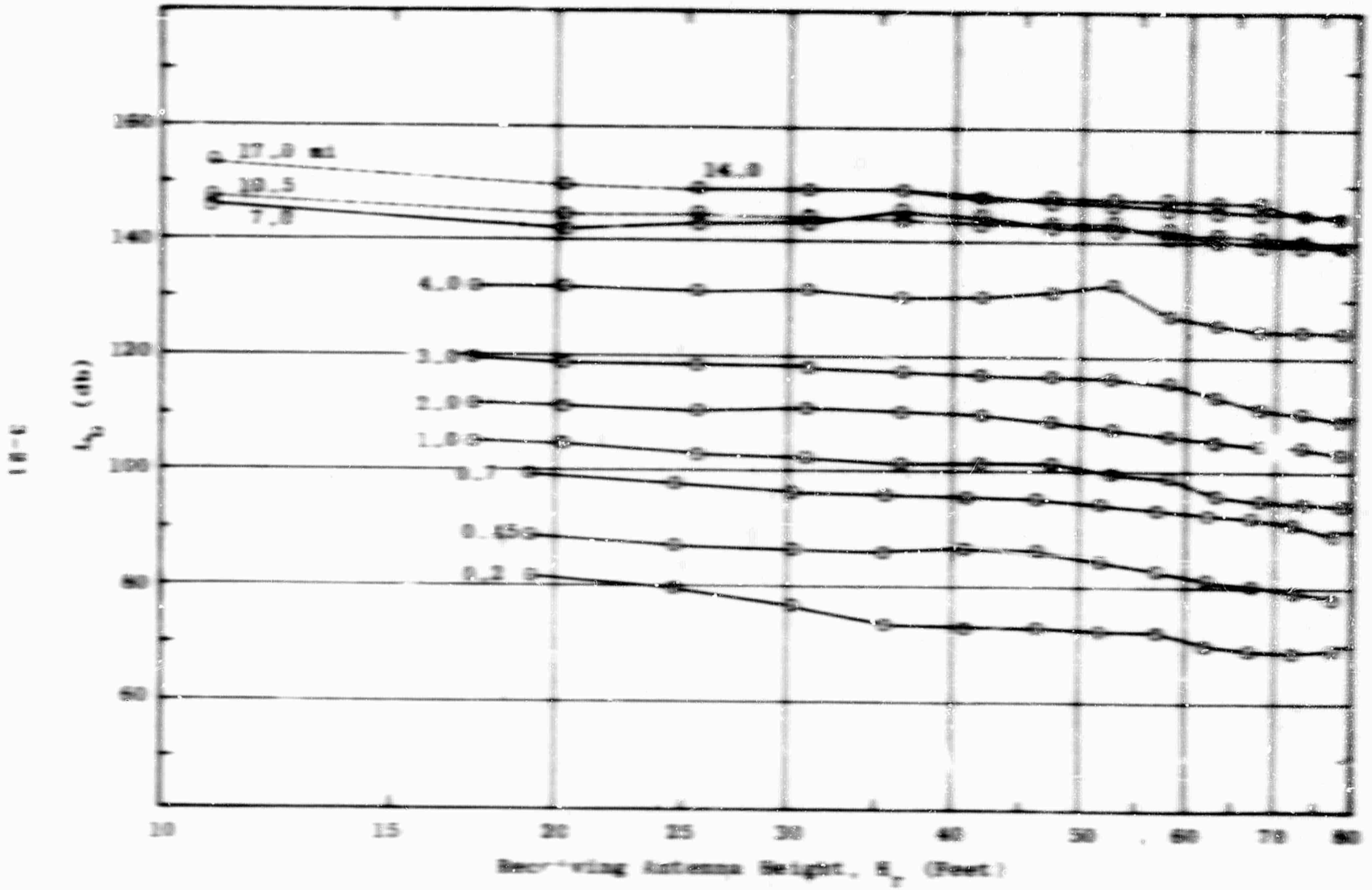

Figure 3.14 Variation of Basic Transmission Loss with Receiving Antenna Height
$L_b = F_A(50, 10, f, d, h_r)$

Figure 3.15 Reception of Radio Signals on Antennas

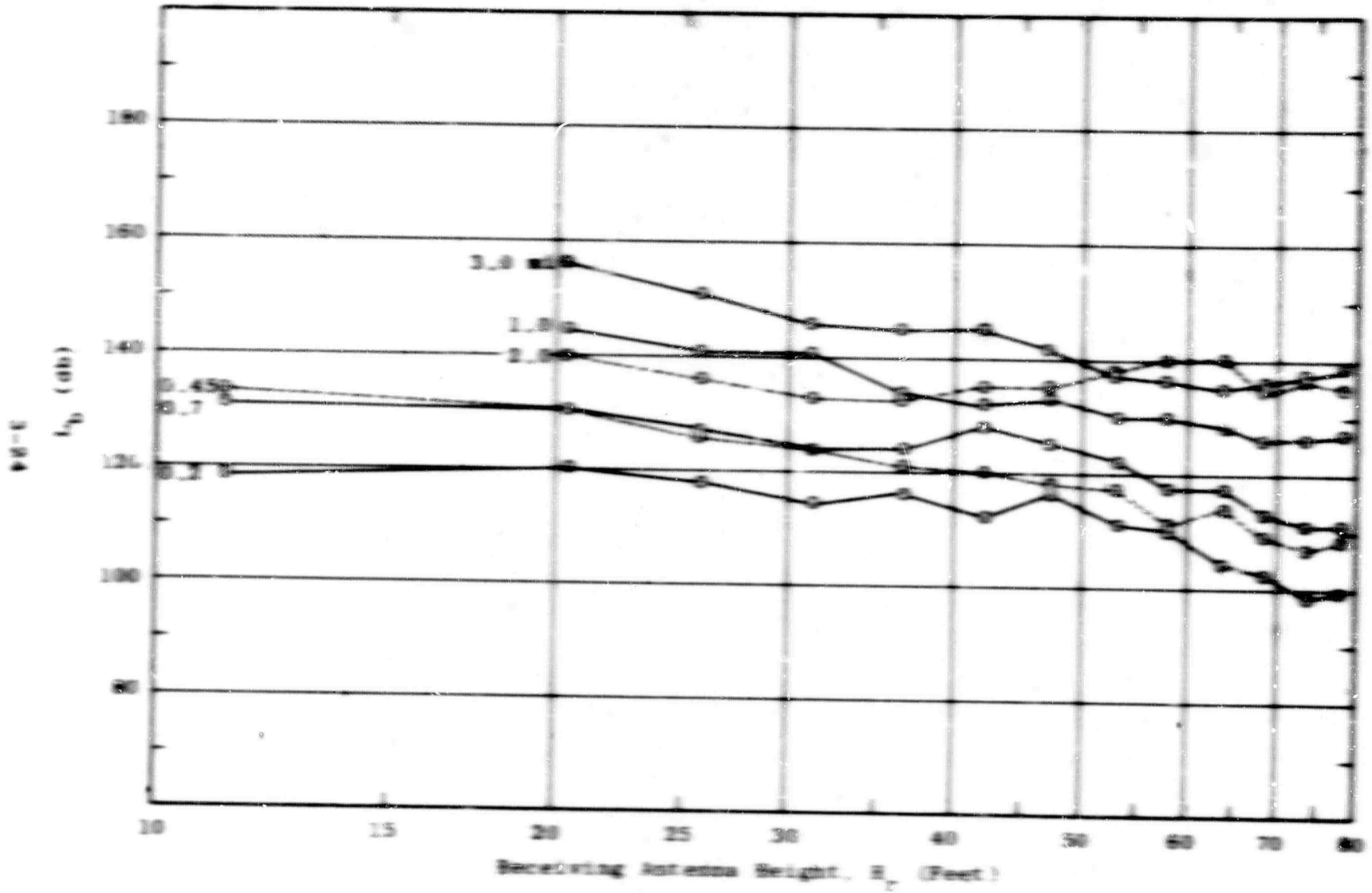

Figure 3.17 Variation of Basic Transmission Loss with Receiving Antenna Height
$L_b = F_4(250, 12, V, d, H_r)$

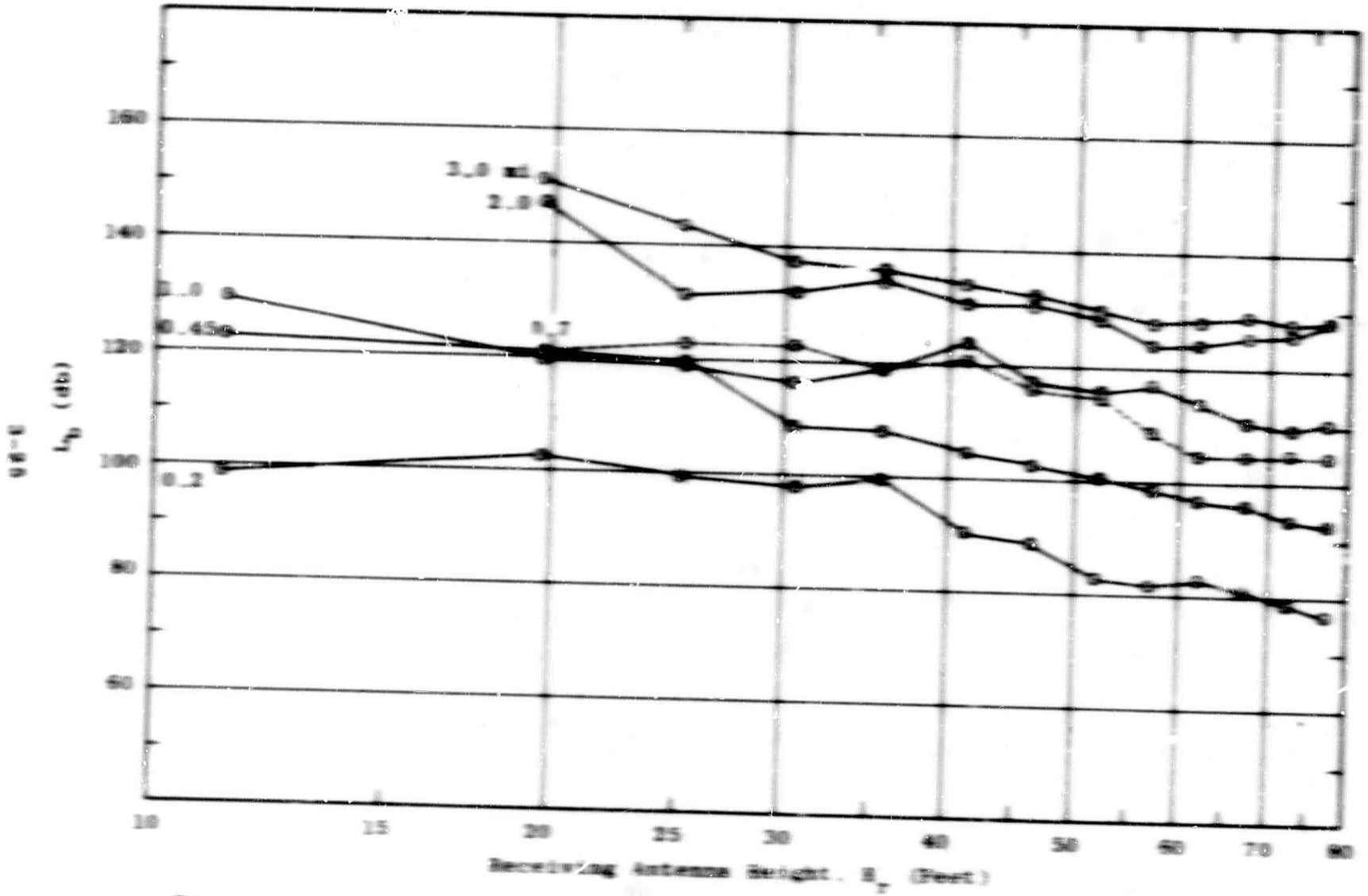

Figure 3.10 Variation of Basic Transmission Loss with Receiving Antenna Height
$L_b = F_A(250, 40, V, d, h_r)$

Figure 3.19 Variation of Basic Transmission Loss with Receiving Antenna Height (h_r) (f_c = 2.0, 3.0, 0.45, 0.7, 0.9 GHz)

Figure 3.11 Variation of Basic Transmission Loss with Receiver Antenna Height
$f_0 = f(60, 13, 4, h_1)$

Figure 3.22 Variation of Basic Transmission Loss with Receiving Antenna Height ($L_b = L_b(80, 80, V, 4, H_r)$)

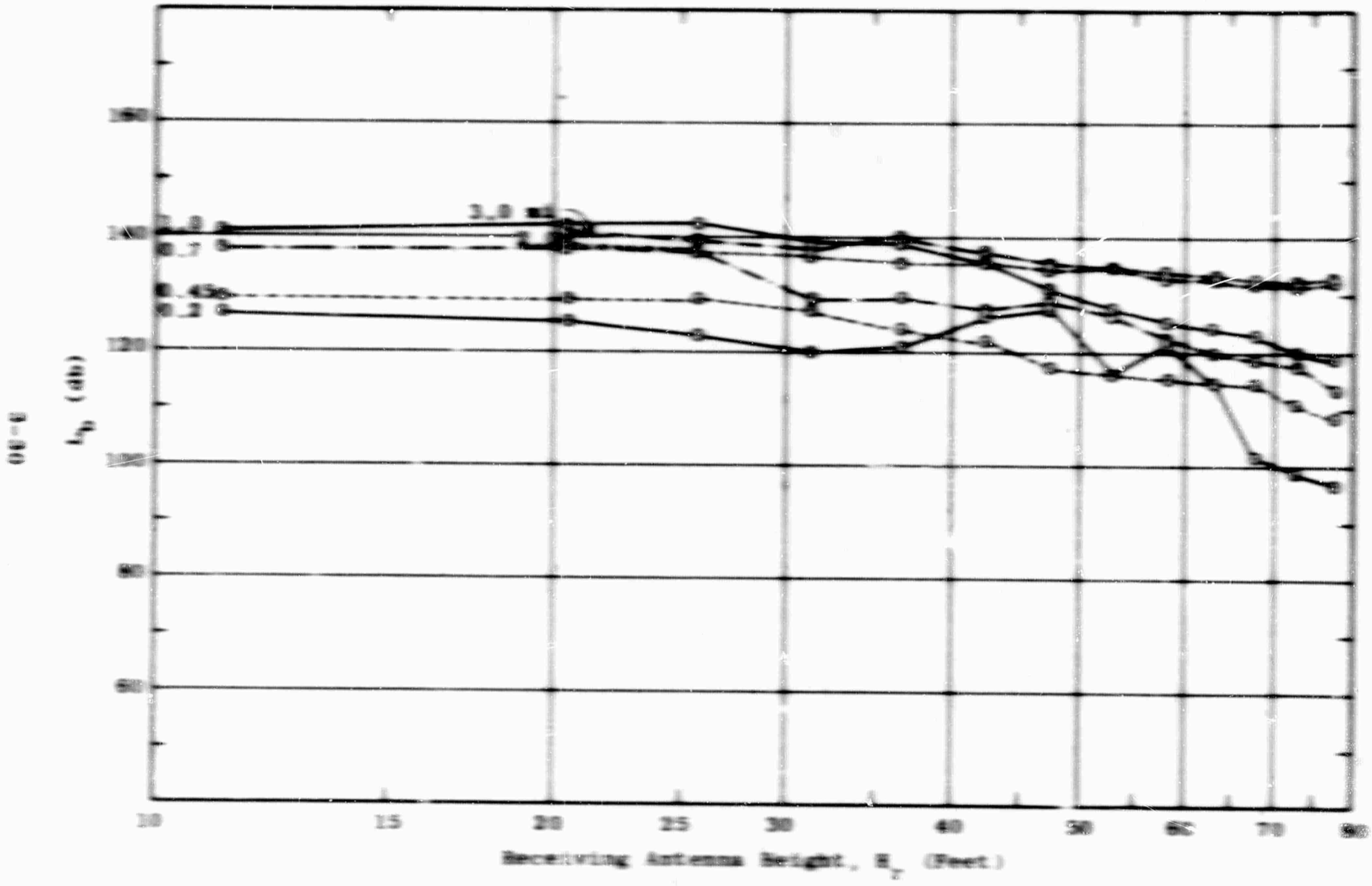

Figure 3.23 Variation of Basic Transmission Loss with Receiving Antenna Height
$L_b = F_4(400, 13, H, d, H_r)$

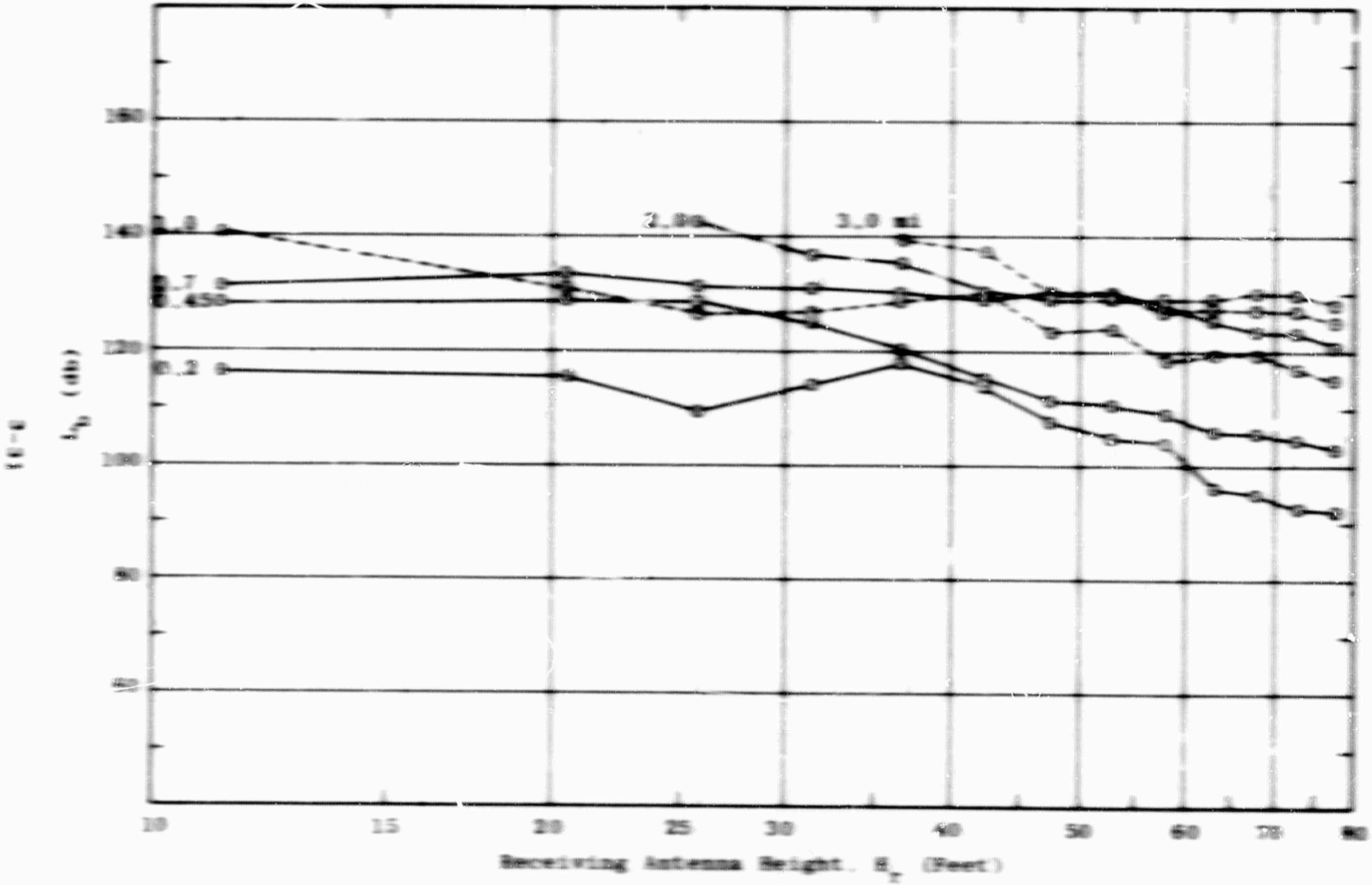

Figure 3.34 Variation of Basic Transmission Loss with Receiving Antenna Height
$L_b = F_A(400, 40, E, d, H_r)$

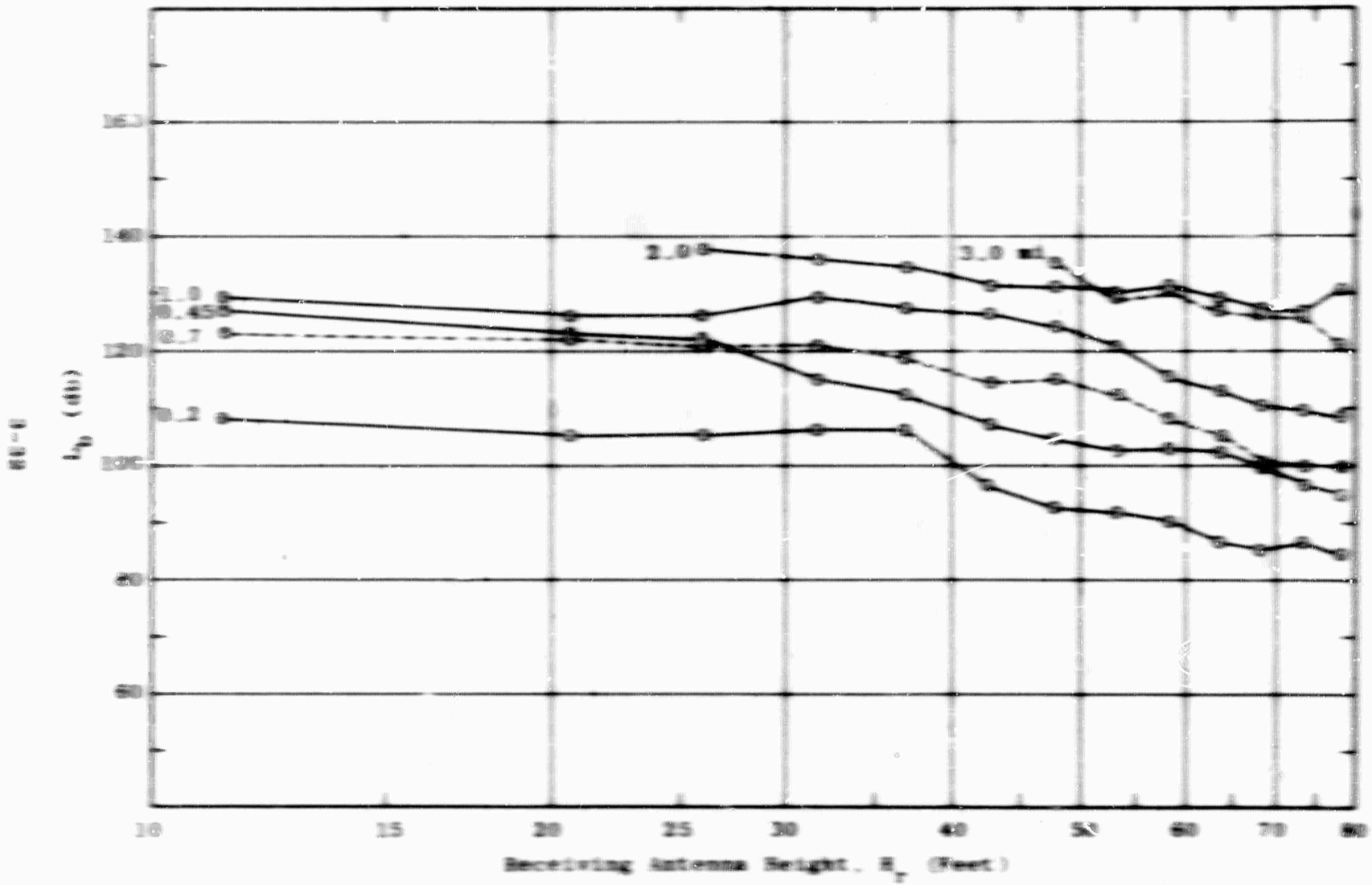

Figure 3.25 Variation of Basic Transmission Loss with Receiving Antenna Height
$L_b = F_A(400, 90, E, d, H_r)$

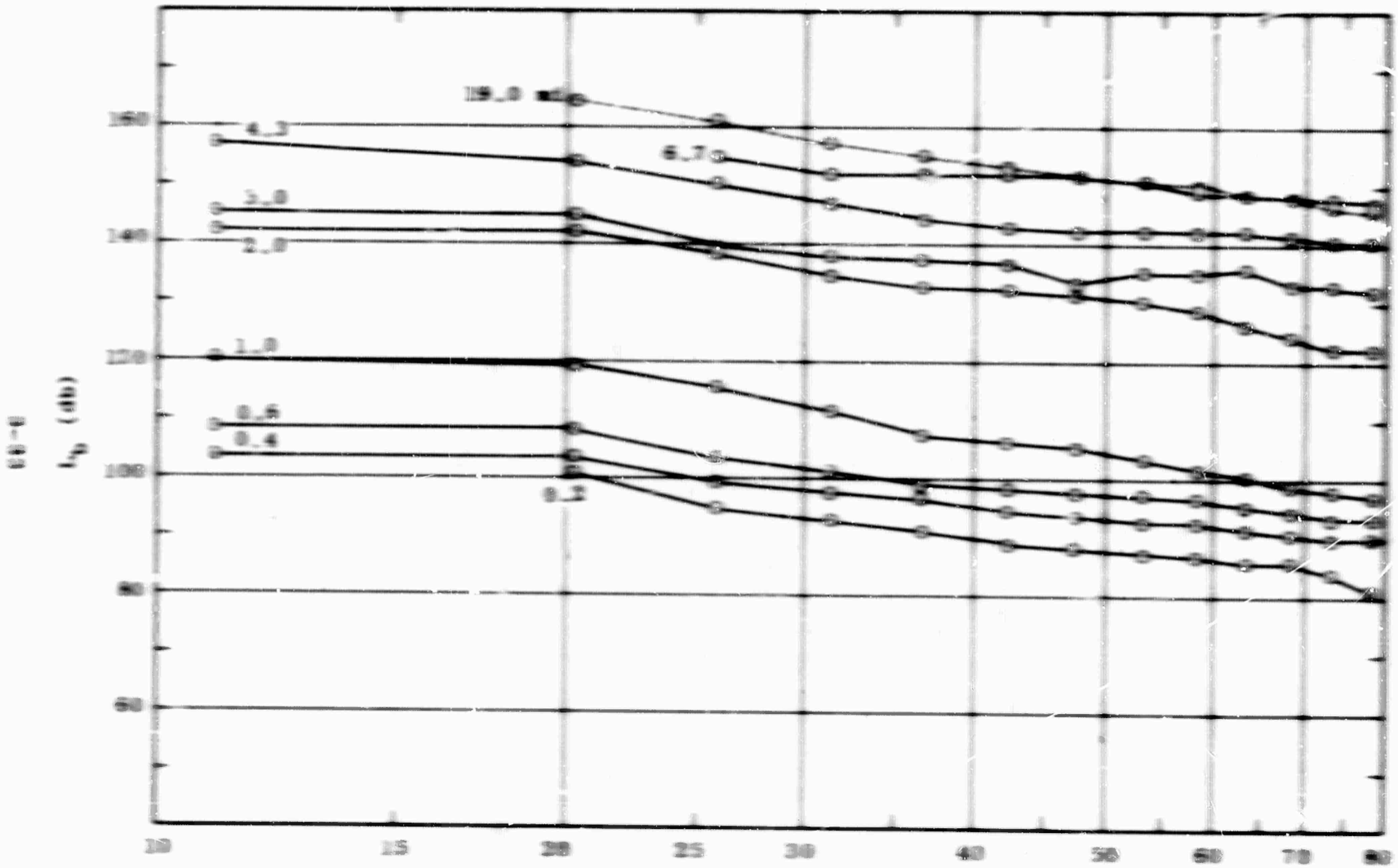

Figure 3.26 Variation of Basic Transmission Loss with Receiving Antenna Height
$L_b = F_3(25.5, 21, \nu, d, h_2)$

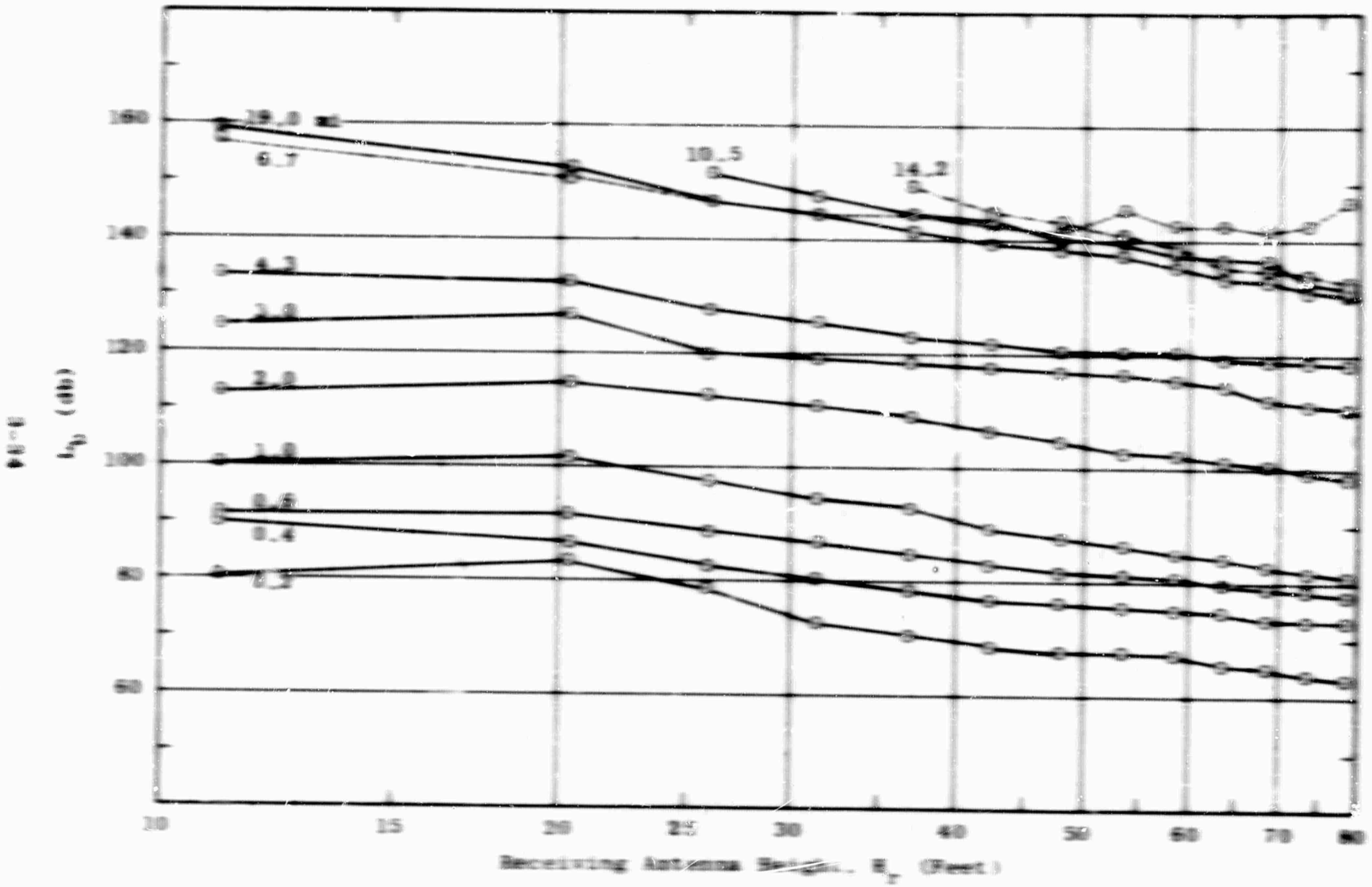

Figure 3.27 Variation of Basic Transmission Loss with Receiving Antenna Height
$L_b = F_3(25.5, 40, V, d, H_r)$

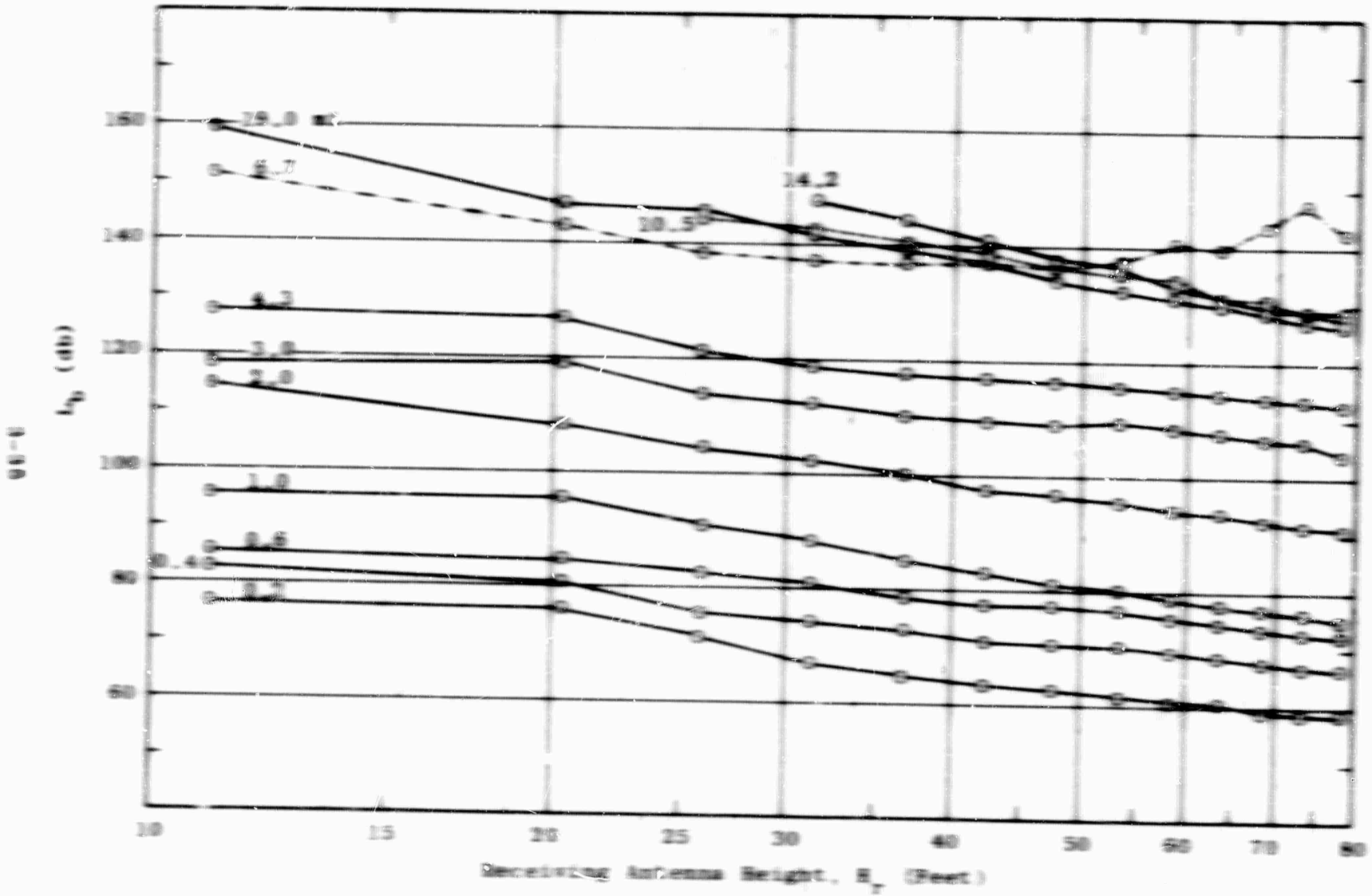

Figure 3.28 Variation of Basic Transmission Loss with Receiving Antenna Height
$L_b = F_3(25.5, 80, r, d, h_r)$

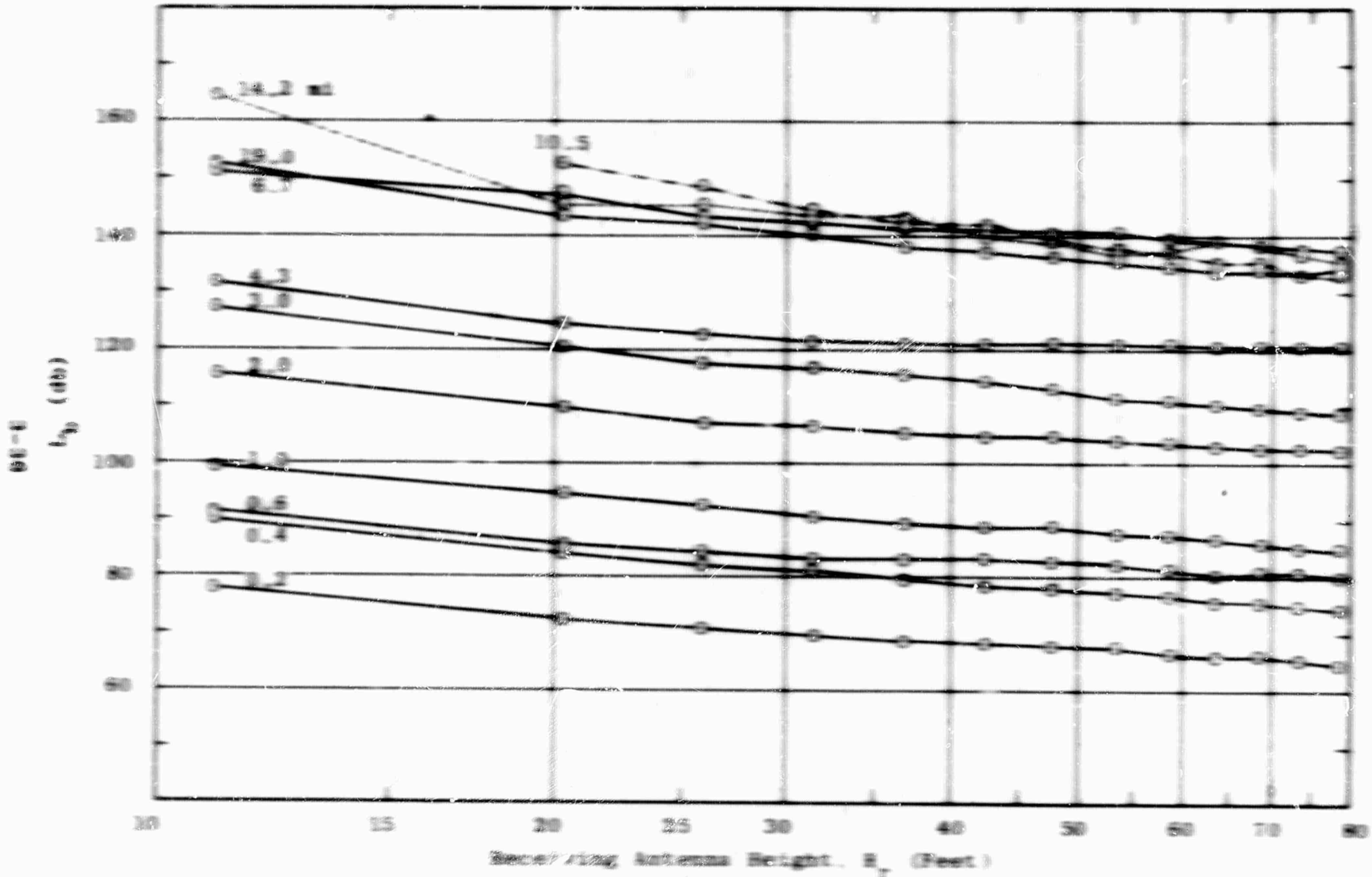

Figure 3.25 Variation of Basic Transmission Loss with Receiving Antenna Height
$L_b = F_3(35.5, 13, H, d, H_r)$

Figure 3.30 Variation of Basic Transmission Loss with Receiving Antenna Height
($L_b = F(25.5, 40, H_r, d, H_t)$)

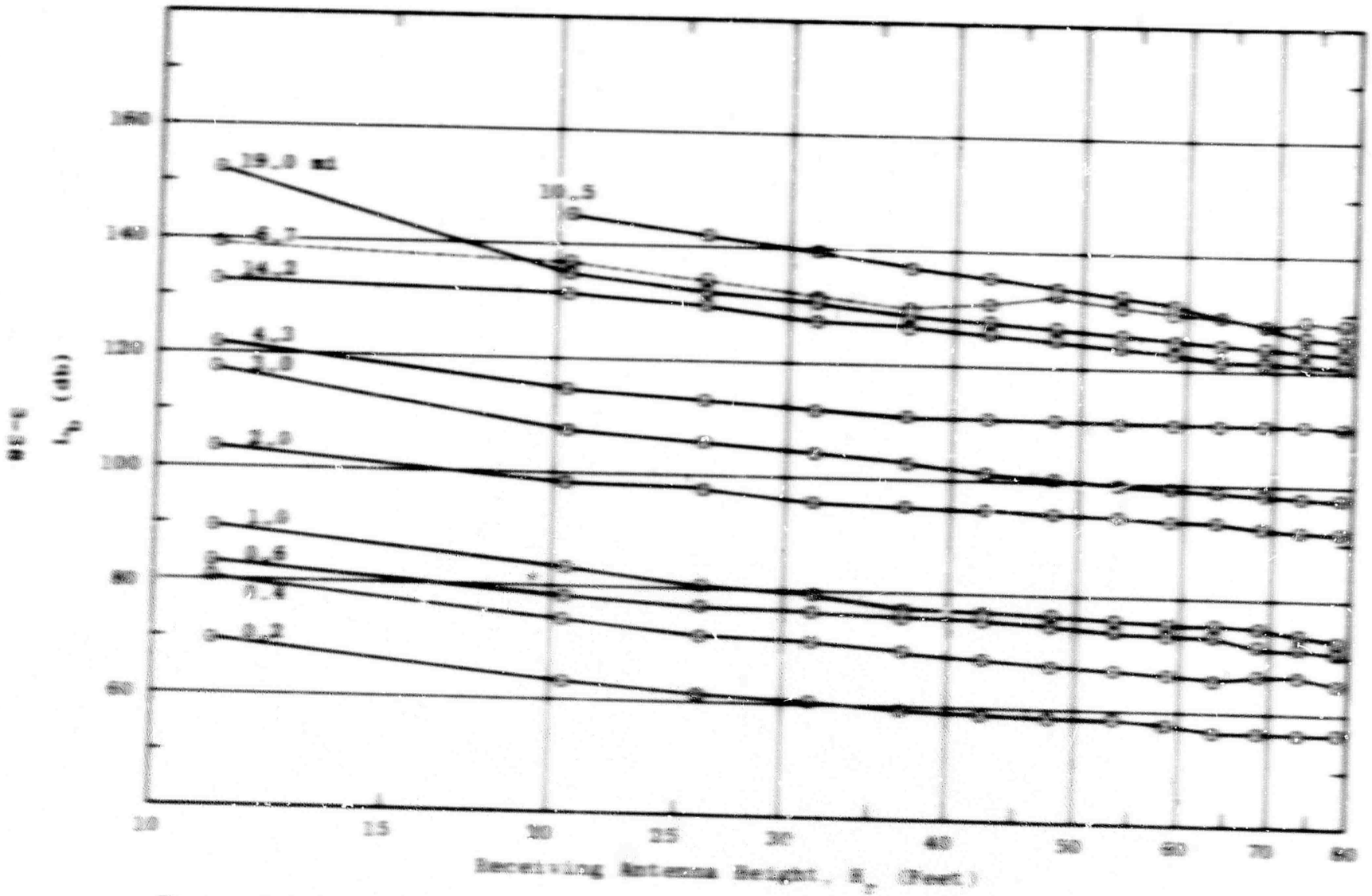

Figure 3.31 Variation of Basic Transmission Loss with Receiving Antenna Height
$L_b = F_3(25.5, 60, 8, 4, h_r)$

L_p (dB)

L_p (dB)

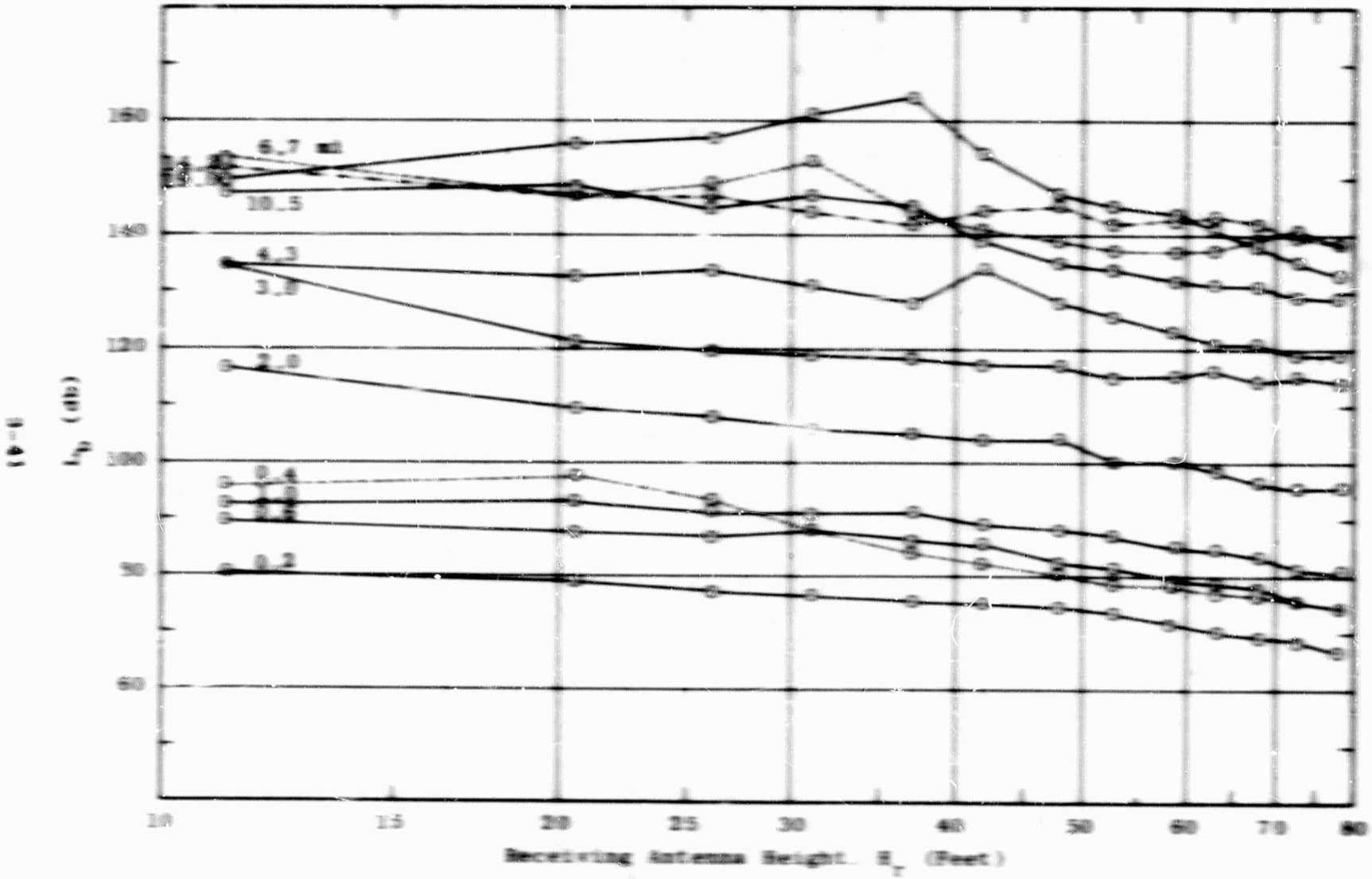

Figure 3.34 Variation of Basic Transmission Loss with Receiving Antenna Height

$L_b = F_3(50, 80, Y, d, H_r)$

η_T (dB)

L_n (dB)

3-43

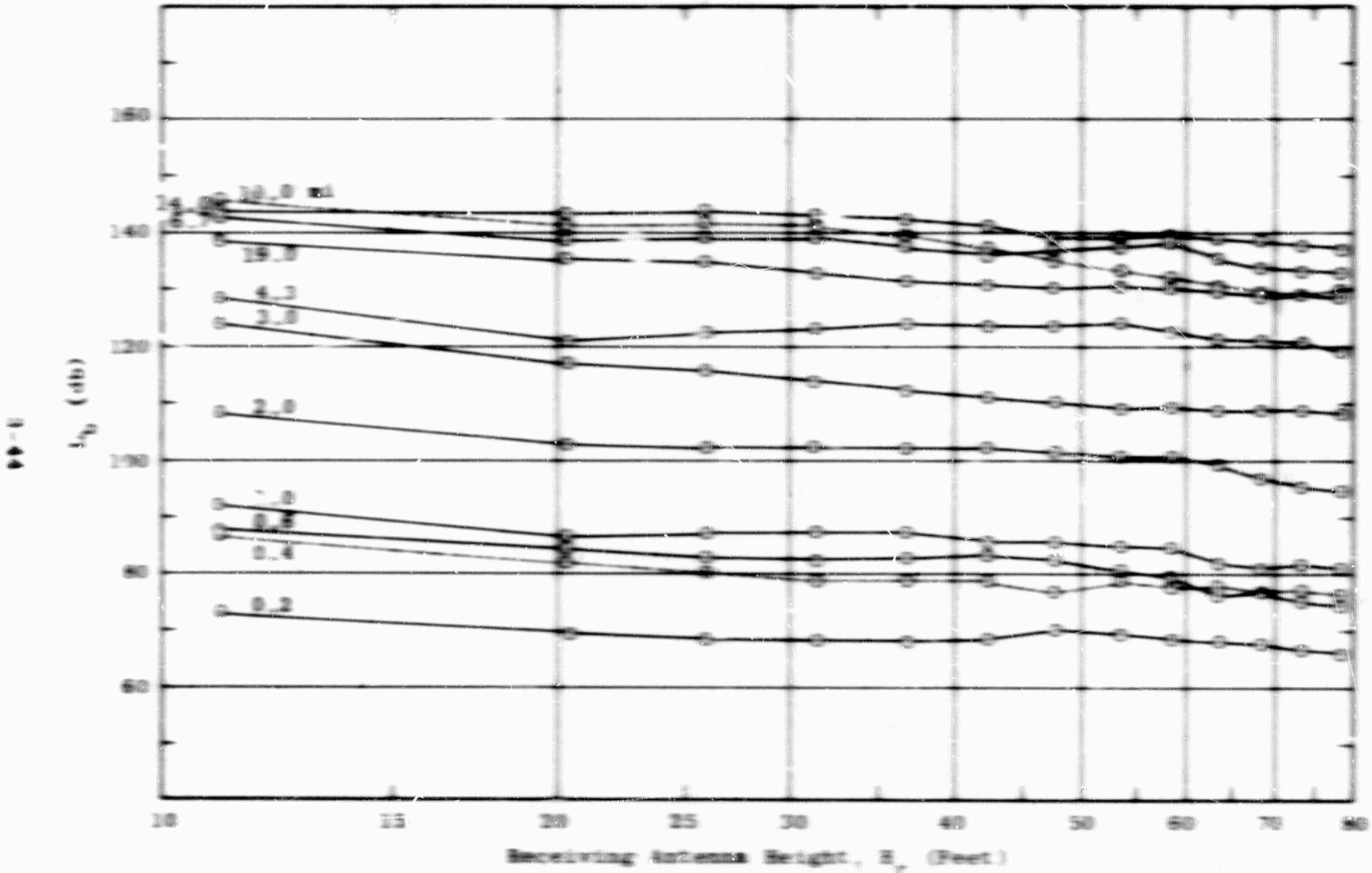

Figure 3.37 Variation of Basic Transmission Loss with Receiving Antenna Height
$L_b = F_3(50, 80, E, d, h_r)$

Figure 3.36 Variation of Basic Transmission Loss with Receiving Antenna Height (h_t = 4.3 m, D, V, d, β)

3-46

Figure 3-40 Variation of Basic Transmission Loss with Receiving Antenna Height (f_1 = 4.4 GHz, f_2 = 4.6 GHz)

Figure 3-43 Variation of Basic Propagation Loss with Receiving Antenna Height

Figure 3-17. Median Urban Noise Power Versus Receiver Antenna Height (f_c = 1.0, 0.5, 0.25, 0.1 MHz)

Figure 3.10 Variation of Basic Transonic Lift with Receiver Antenna Height

L_p (dB)

3-61

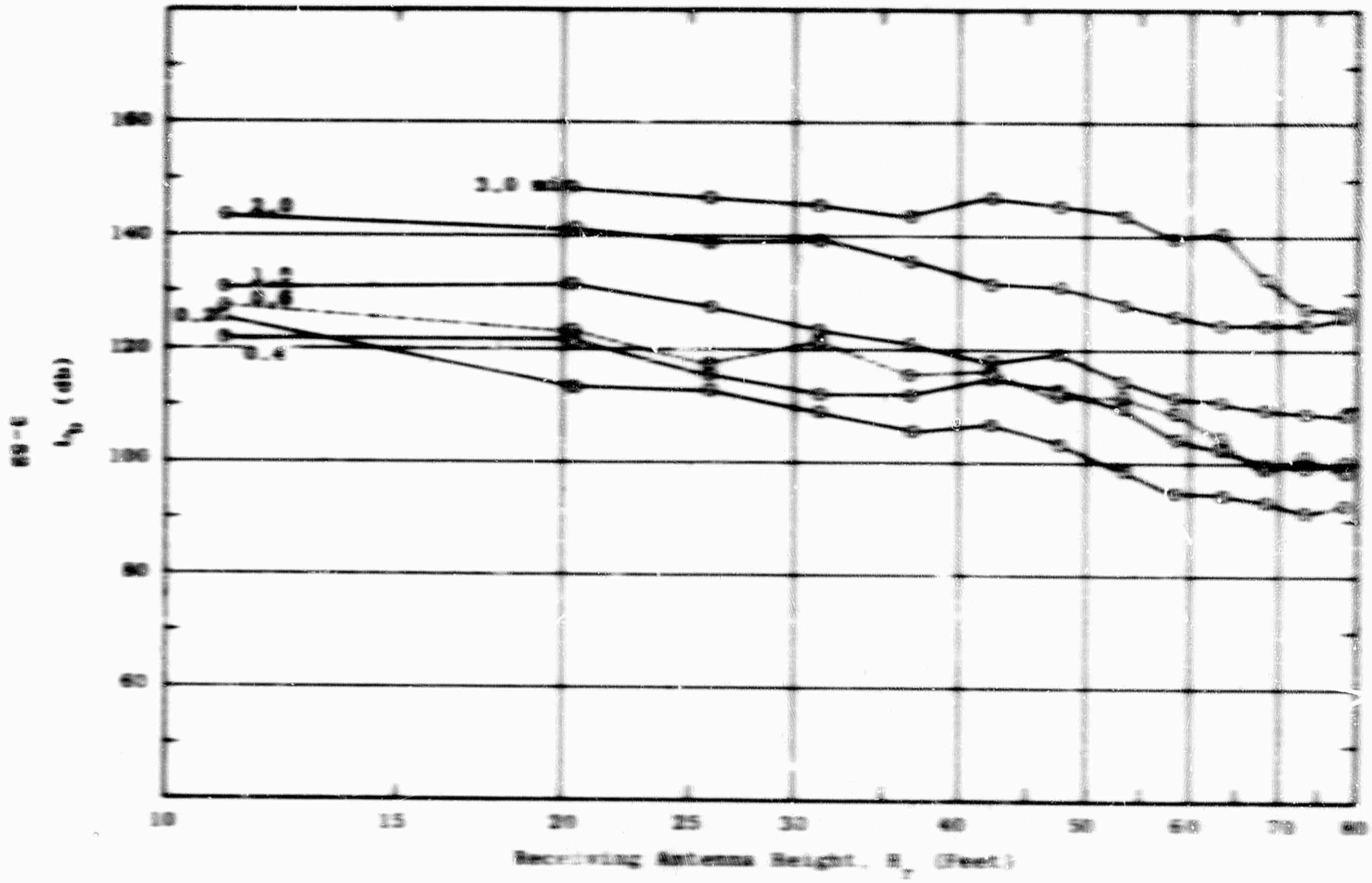

Figure 3.45 Variation of Basic Transmission Loss with Receiving Antenna Height
$L_b = F_3(250, 40, V, d, H_r)$

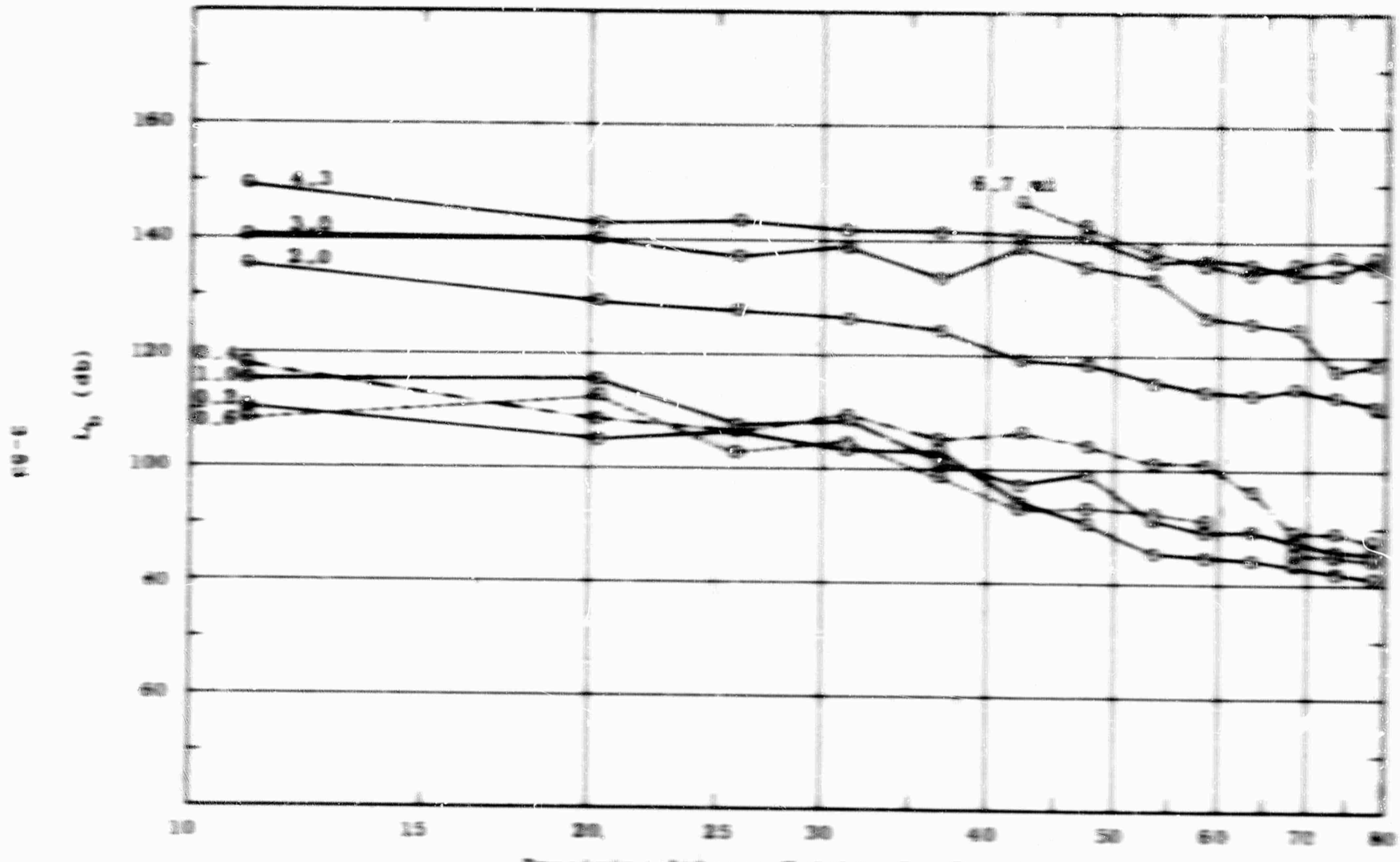

Figure 3.46 Variation of Basic Transmission Loss with Receiving Antenna Height
$L_b = F_3(250, 80, T, d, H_r)$

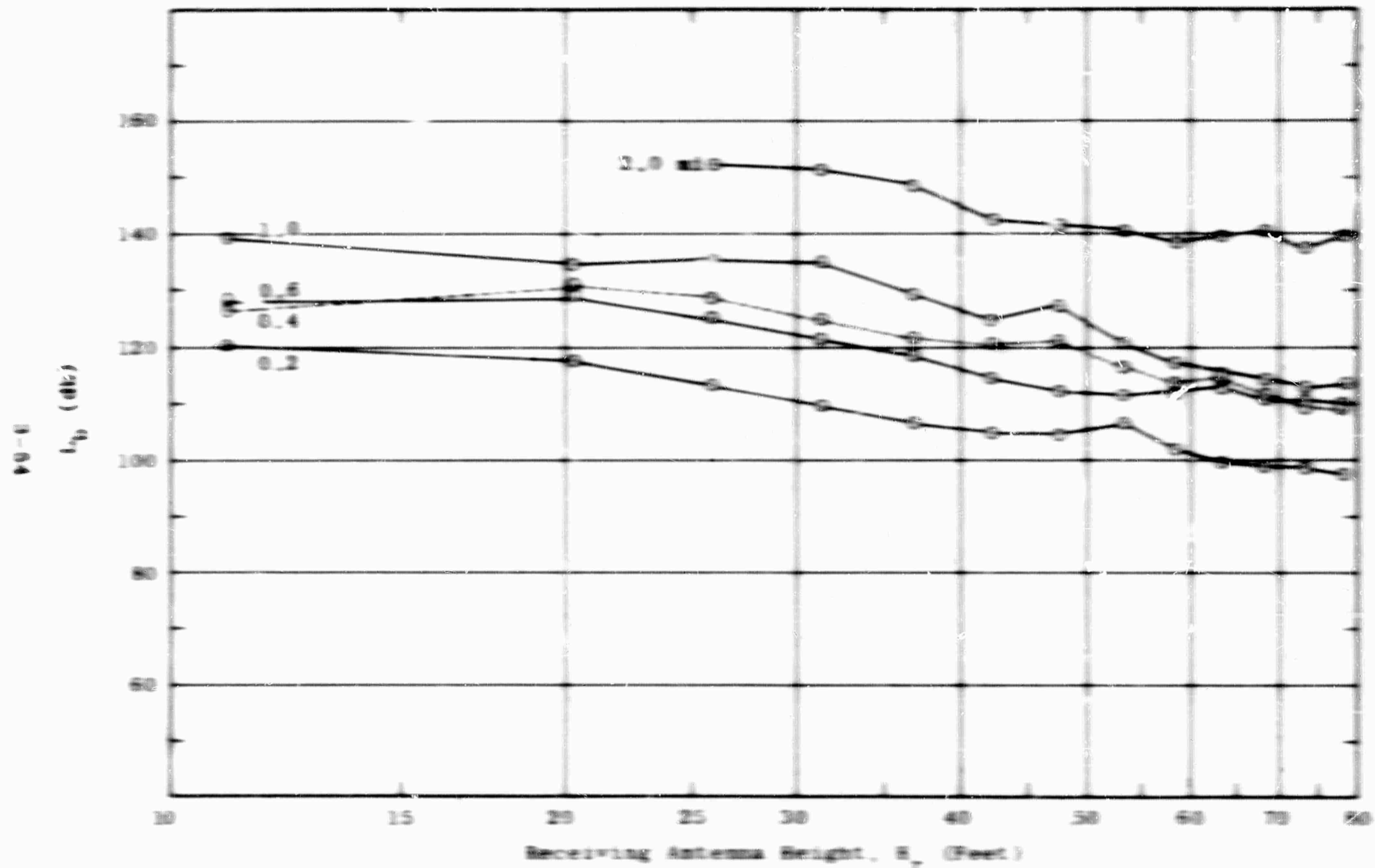

Figure 3.47 Variation of Basic Transmission Loss with Receiving Antenna Height
$L_b = F_3(250, 12, 8, d, h_r)$

Figure 3.4.9 Variation of Basic Transmission Loss with Receiving Antenna Height (h_r) for h_t = 15 ft, θ_t = 0°, ϕ_t = 0°, ϕ_r = 0°

L_p (dB)

Receiving Antenna Height, h_r (Feet)

Figure 1-49. Variation of Basic Propagation Loss with Receiving Antenna Height

Figure 3-58. Variation of Basic Transmission Loss with Receiving Antenna Height (h_r) for Various Transmitting Antenna Heights (h_t)

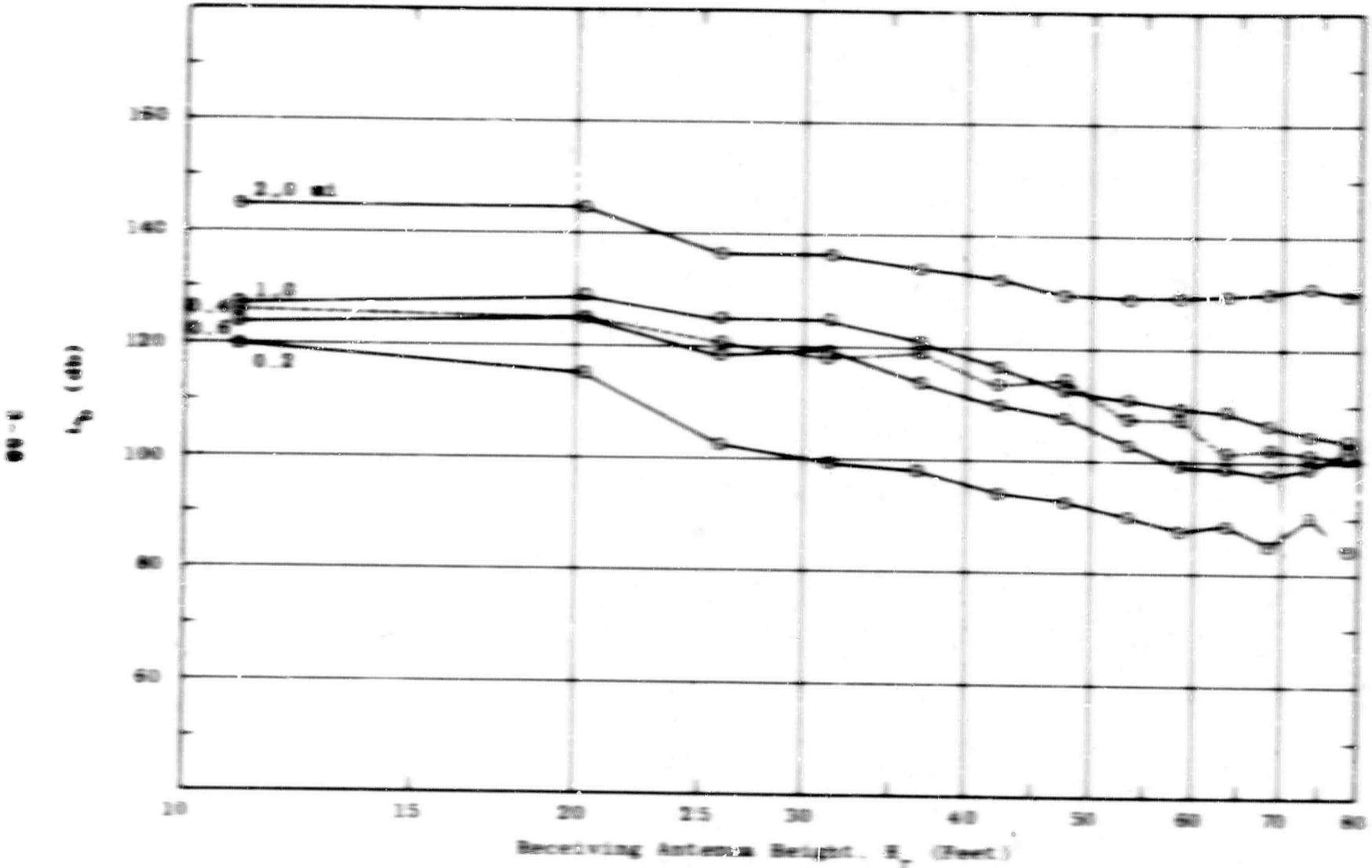

Figure 3.51 Variation of Basic Transmission Loss with Receiving Antenna Height
$L_b = F_3(400, 40, V, d, H_r)$

Figure 3.58 Variation of Basic Interference Lobe with Receiving Antenna Height
$h_r = h_r(\theta_0, \theta_1, \phi_1, \phi_2)$

L_p (dB)

Figure 3.56 Variation of Basic Propagation Loss with Receiving Antenna Height
$L_b = L_b(40, f, h_1, h_2)$

Receiving Antenna Height, h_1 (feet)

(dB) L_b

Figure 3.15 Variation of Basic Transmission Loss with Receiving Antenna Height

4. DATA ANALYSIS

4.1 Introduction

Now that sufficient quantities of tropical propagation data have been collected and reduced, an intensive program of data analysis has been started. Although far from complete, this program of data analysis has reached the point at which a number of interesting findings may be reported. In addition to reporting findings to date, this report emphasizes the methodologies which underlie the various analysis methods which are being applied.

A careful analysis of experimental results will serve many goals. Among these goals, three should be singled out as being of particular significance to this program. First, a thorough analysis of large quantities of measured data can often reveal inconsistencies which are almost inevitable in any large experiment.

The second key goal for tropical propagation analysis is to correctly characterize radio propagation as it really exists in the environment in which the measurements are made. Although the fulfillment of this goal is only one step toward the ultimate objectives of the program, there is much information of immediate importance to be gained from a correct knowledge of radio propagation in the particular type of environment in which measurements are being made in Thailand.

The third key goal for tropical propagation analysis is to develop a mathematical model which describes radio propagation as measured in the particular environment under study and identifies the key variables upon which

propagation losses depend. The model, with properly identified variables, will ultimately permit an extension of the results of the present series of experiments to a large number of other areas.

Thus, although the primary objective of data analysis is the development of a properly evaluated mathematical model, various stages of data analysis will also provide a constant check on data consistency and significance, and can also provide information of immediate interest prior to the completion of the ultimate mathematical model.

Along with the development of a mathematical model it is important to consider the physical model, that is, the physical concept of propagation through foliage.

Two basic types of propagation data are being taken. One type is field strength as a function of receiving antenna height as the variable and transmitting antenna height, distance, frequency, season and polarization as parameters. These measurements, which are taken at fixed field points, are referred to as "field point measurements" or simply FP measurements. The other basic type of propagation data is obtained from recordings of field strength as a function of distance in a vehicle which travels along carefully surveyed single trails. Here radial distance is the variable and transmitting antenna height, frequency, polarization and season serve as parameters. The results of these measurements are referred to as "vehicular data."

Two complete sets of data on each of two trail systems, designated Radial A and Radial B, are being collected. One set represents dry season conditions and the other represents wet season conditions. The field

point data presented in Section 3 of this report along with the data presented in Semiannual Report Number 4 and Semiannual Report Number 5 provide one essentially complete set of FP data for Radial A. Also, the new data presented in Section 3 of this report provides an essentially complete set of FP data for Radial B from 25.5 mc to 400 mc.

The data analysis presented in this report has been devoted to the complete set of Radial A FP data, and a significant sample of Radial A vehicular data. The data analysis begins with a study of the field point median data and the relationships of this data to several applicable theoretical models.

Next an analysis is made of the time and spatial variations of basic transmission loss in the vegetation. No long-term time variability measurements have been made. However, existing data concerning short-term time variability provides necessary information. Spatial variations which are studied include antenna height and distance. A study of the fine-grain variability of basic transmission loss is made as well as a study of the variation of the FP medians with antenna height. The vehicular data provides a great deal of important information concerning the statistical variations of basic transmission loss as a function of radial distance from the source.

Next, attention is directed toward a number of other factors which can affect propagation, such as climatology, vegetation and polarization. Finally, a brief discussion of the potential usefulness of the currently available data is given, with an example calculation.

The quantity of reduced data has recently reached the point at which intensive analysis may be made. Many interesting calculations present themselves as possibilities as a result of the first stages of data analysis described in this report. However, the emphasis at this point is on the methods of analysis rather than conclusions. It is far too easy to jump to premature conclusions before all the evidence is in. Such premature conclusions may overshadow the true meaning and significance of the data.

4.8 Analysis of Field Point Medians

At the outset it will be helpful to define the term "field point median." To define field point median, it is necessary to recall that measurements are made at each field point as a function of receiving antenna height. The total range of receiving antenna height is divided into a number of consecutive intervals, each of which is approximately 6 feet in length. The median value of recorded signal strength is chosen from each 6-foot interval. These medians go together to form what is referred to as the field point median data. In this section attention will be directed toward the analysis of one complete set of field point median data for Radial A.

4.8.1 Summary of Measured Data

The most convenient format for data presentation has been plots of median basic transmission loss as a function of receiving antenna height with distance, frequency, transmitting antenna height, polarization and season as parameters. Although convenient for basic data

presentation, this format is not the best for data analysis. Thus, by way of data summary, and to obtain a better analysis format, the two following families of curves are presented.

The first family extends from Figures 4.1A through 4.1B and gives basic transmission loss as a function of distance, based on the measured field point median data. Figures 4.1A through 4.1I pertain to vertical polarization and Figures 4.1J through 4.1R pertain to horizontal polarization. Frequency is the parameter for each curve. The distinguishing parameters are transmitting and receiving antenna heights. The data has been grouped so that a complete family of data with respect to frequency is given in each of the first three figures. At frequencies of 50 mc and above, standard transmitting antenna heights of 13 feet, 40 feet, and 80 feet were used. However, at frequencies lower than 50 mc with vertical polarization, transmitting antenna height is limited by basic antenna design considerations. This leads to minor difficulties in grouping data by transmitting antenna height. To the greatest extent possible, a consistent set of data has been chosen for each figure. In Figure 4.1A for example, the basic heights are 13 feet for transmitting and 30 feet for receiving. The actual transmitting antenna height at 19 mc for vertical polarization was 21 feet, which corresponds to an effective height of approximately 10 feet. This effective height of 10 feet is most directly comparable to a standard transmitting antenna height of 13 feet. There is noticeable inconsistency at 98.5 mc, shown in Figures 4.1A, 4.1B and 4.1C. The transmitting antenna for 98.5 mc, vertical polarization, is a 10-foot vertical whip. At 50 mc, the transmitting antenna is a vertical half-wave dipole

whose center is 13 feet above ground. The extent to which differences in effective antenna height explain the apparent inconsistency at 25.5 mc is currently under study. For frequencies lower than 12 mc, vertical polarization, the transmitting antennas become progressively longer. However, antenna height has no significant effect on basic path loss below 12 mc, as is shown in Section 4.3.2.1.

The actual antenna heights are marked on each curve if they differ from those given in the legend of the exhibit. For example, a notation 80'-20' beside a curve means that the data was taken with an 80-foot transmitting antenna and a 20-foot receiving antenna.

The 3-, 6- and 12-mc curves for horizontal polarization shown in Figures 4.1M, 4.1N and 4.1O appear to be inconsistent with the higher frequency curves. Possible reasons for this inconsistency are being carefully checked.

The second major family of data extends from Figure 4.2A through Figure 4.2R. This family is exactly the same as the previous family except in this latter case frequency appears as the variable. It becomes immediately obvious from an examination of Figures 4.2A, 4.2B and 4.2C that the basic transmission loss values for 25.5 mc, vertical polarization, appear to be too high. This possibility suggests itself since the loss at 25.5 mc does not appear to be consistent with the trend at 12 mc and 50 mc. The inconsistency noted at 25.5 mc in Figures 4.2A, 4.2B and 4.2C is identical to that noted previously in connection with Figures 4.1A, 4.1B and 4.1C. This possible inconsistency has a bearing on a later analysis so at this point it will be noted that a decrease in measured loss of approximately 10 db would make the data appear more

reasonable at the 13-foot transmitting antenna height. The detection of this apparent inconsistency provides an excellent example of the role that data analysis can play in ensuring the validity of experimental results.

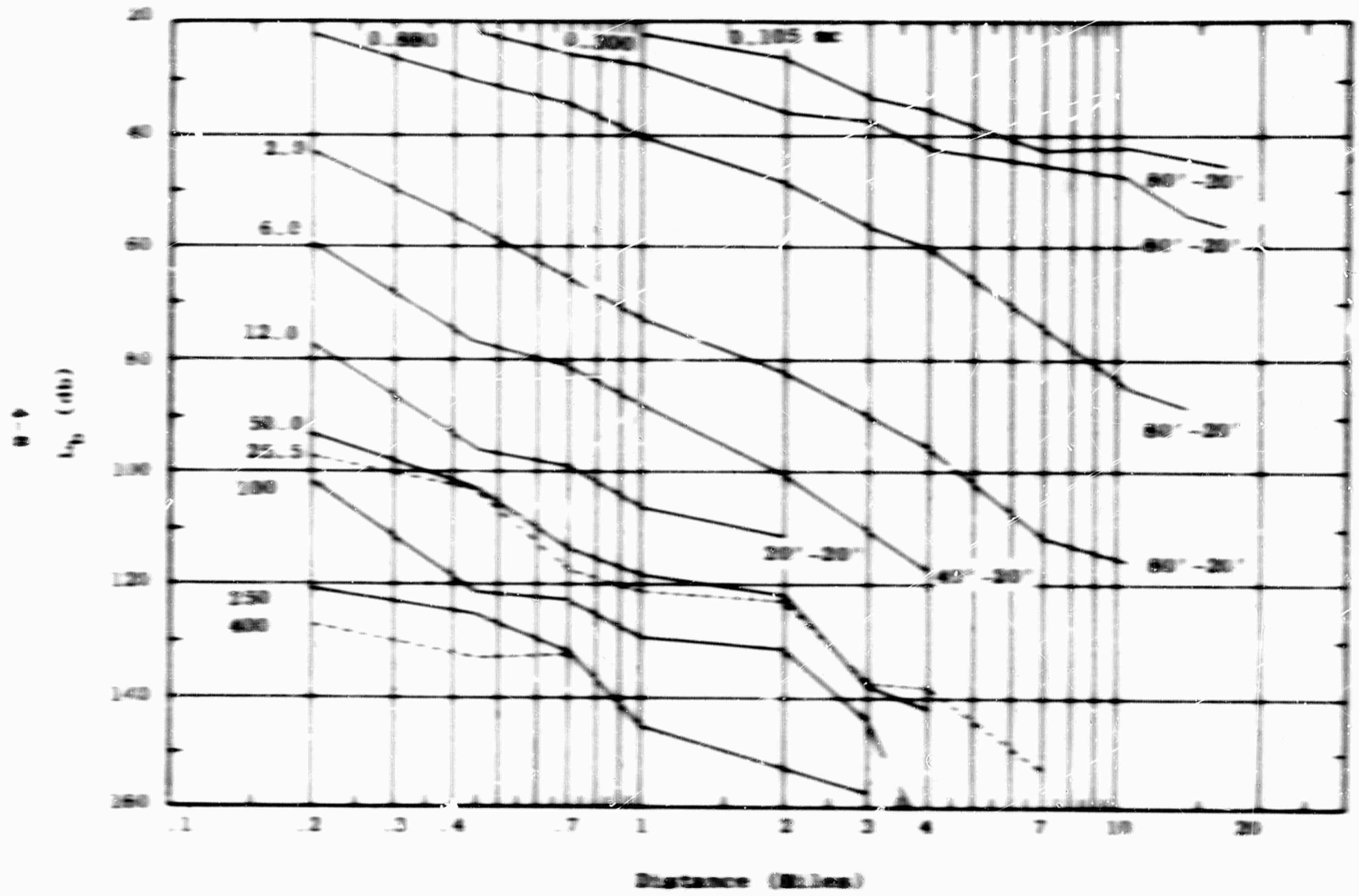

Figure 4.18 Measured Results, L_b vs Distance
$L_b = F_A(f, 12, V, \theta, 20)$

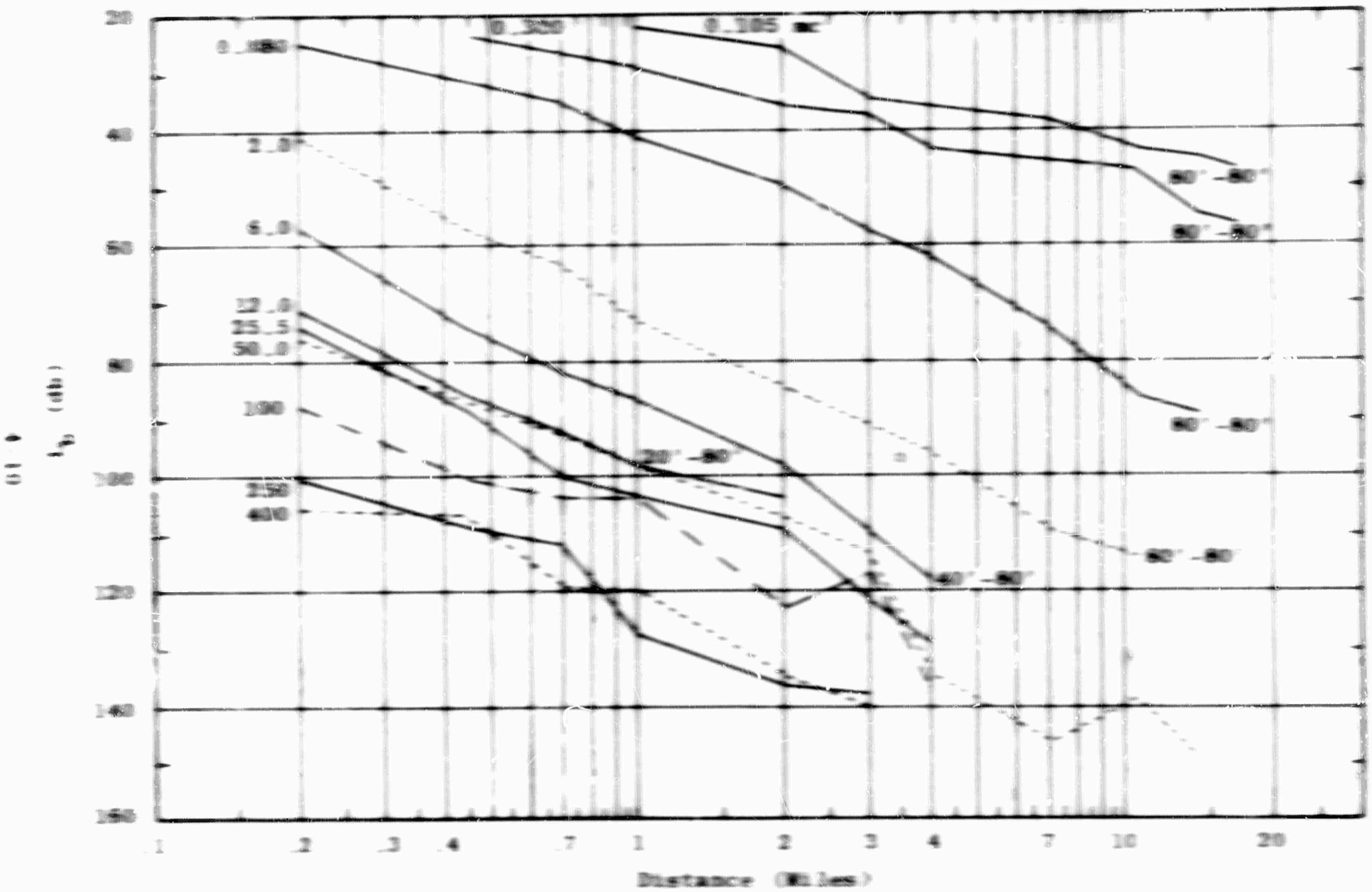

Figure 4.1C Measured Results, L_b Vs Distance
$L_b = F_A(f, 13, V, \geq 60)$

Figure 4-10 Measured Results, L_p vs Distance
$L_p = F(r, \theta, \phi, f, Z)$

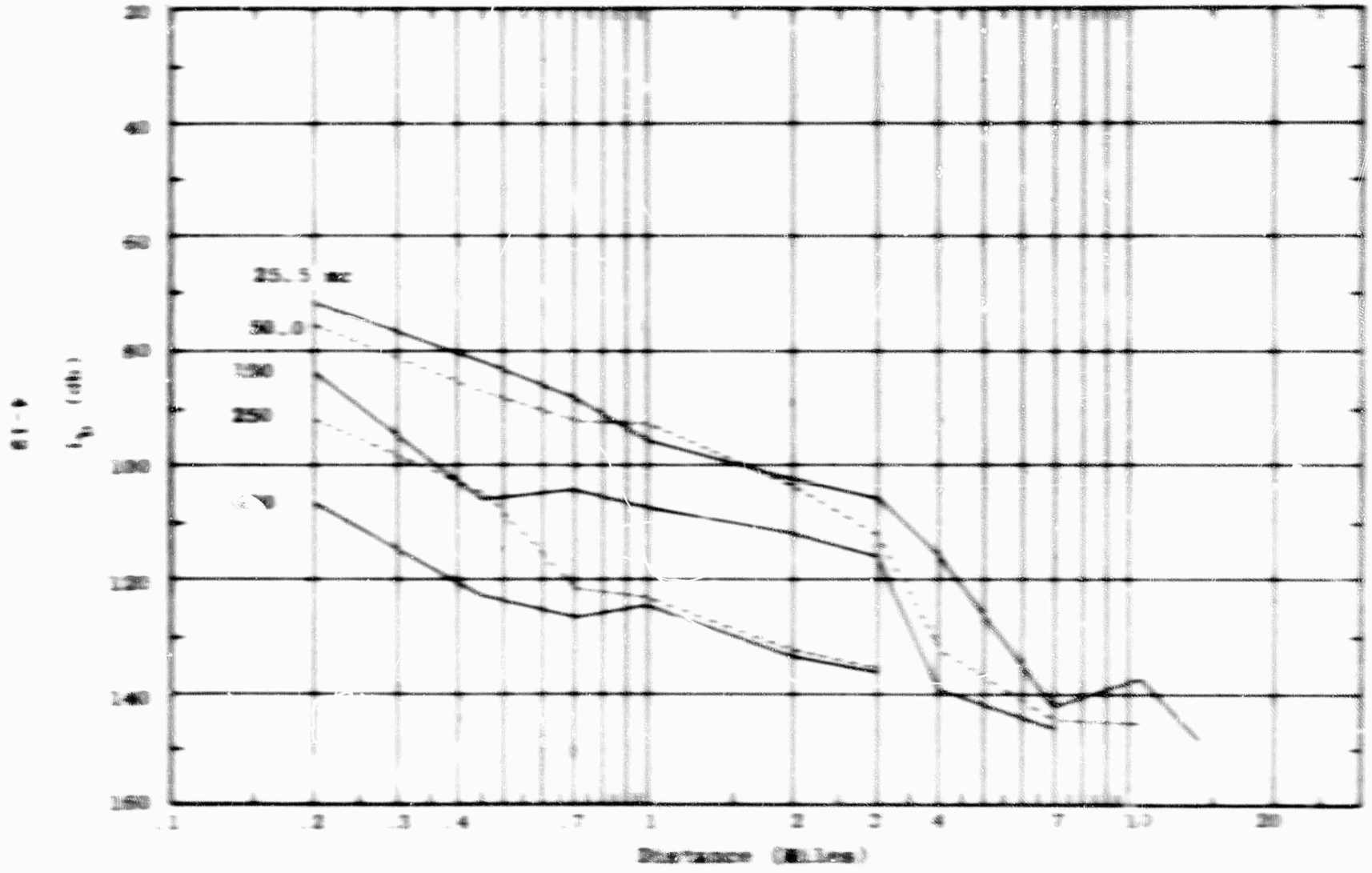

Figure 4.13 Measured Results, L_b vs Distance
$L_b = F_6(f, 40, 1, 2, 40)$

4-11

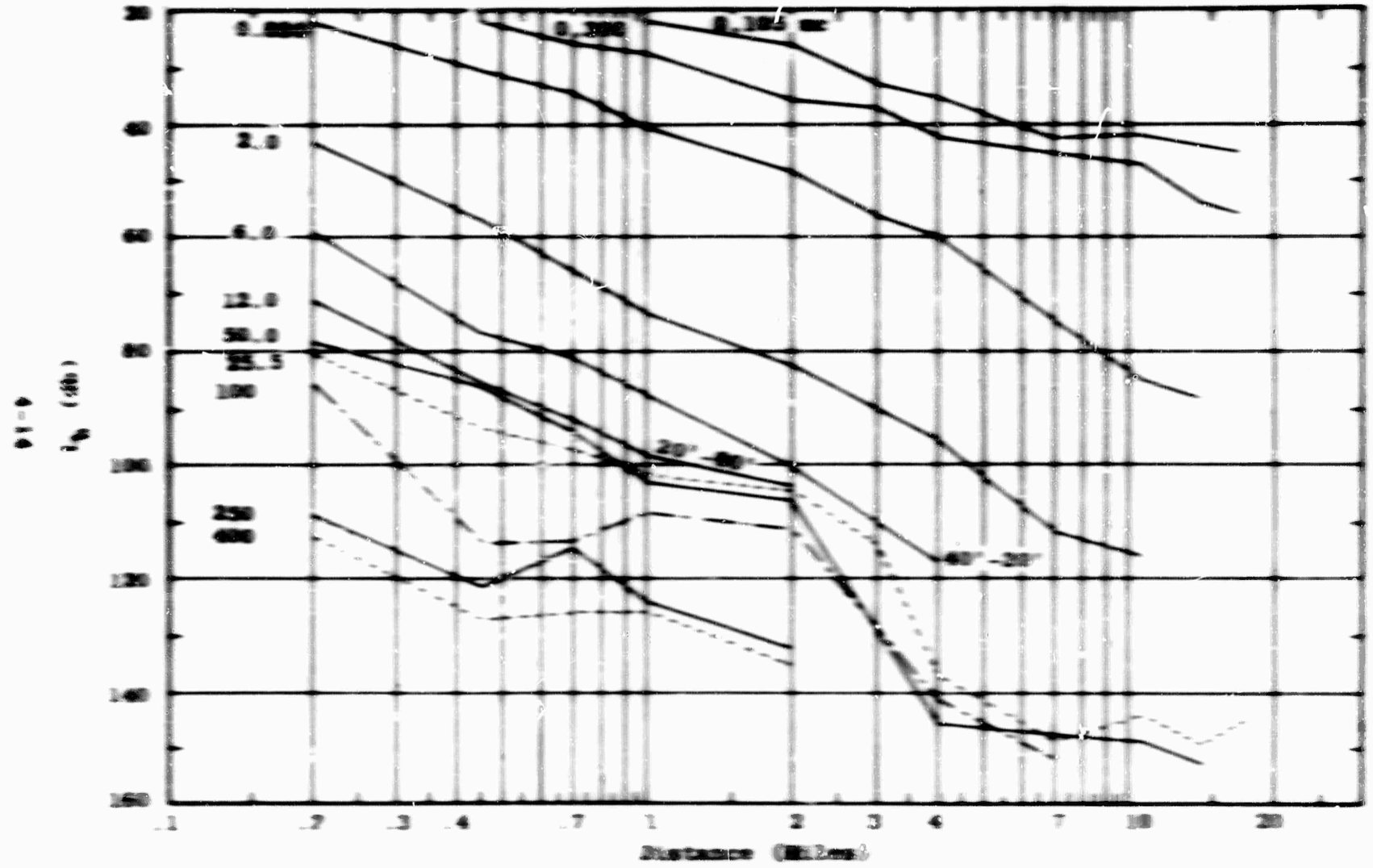

Figure 4.16 Measured Results, L_b Vs Distance
$L_b = F_4(d, \theta\theta, f, z, 2\theta)$

4-16

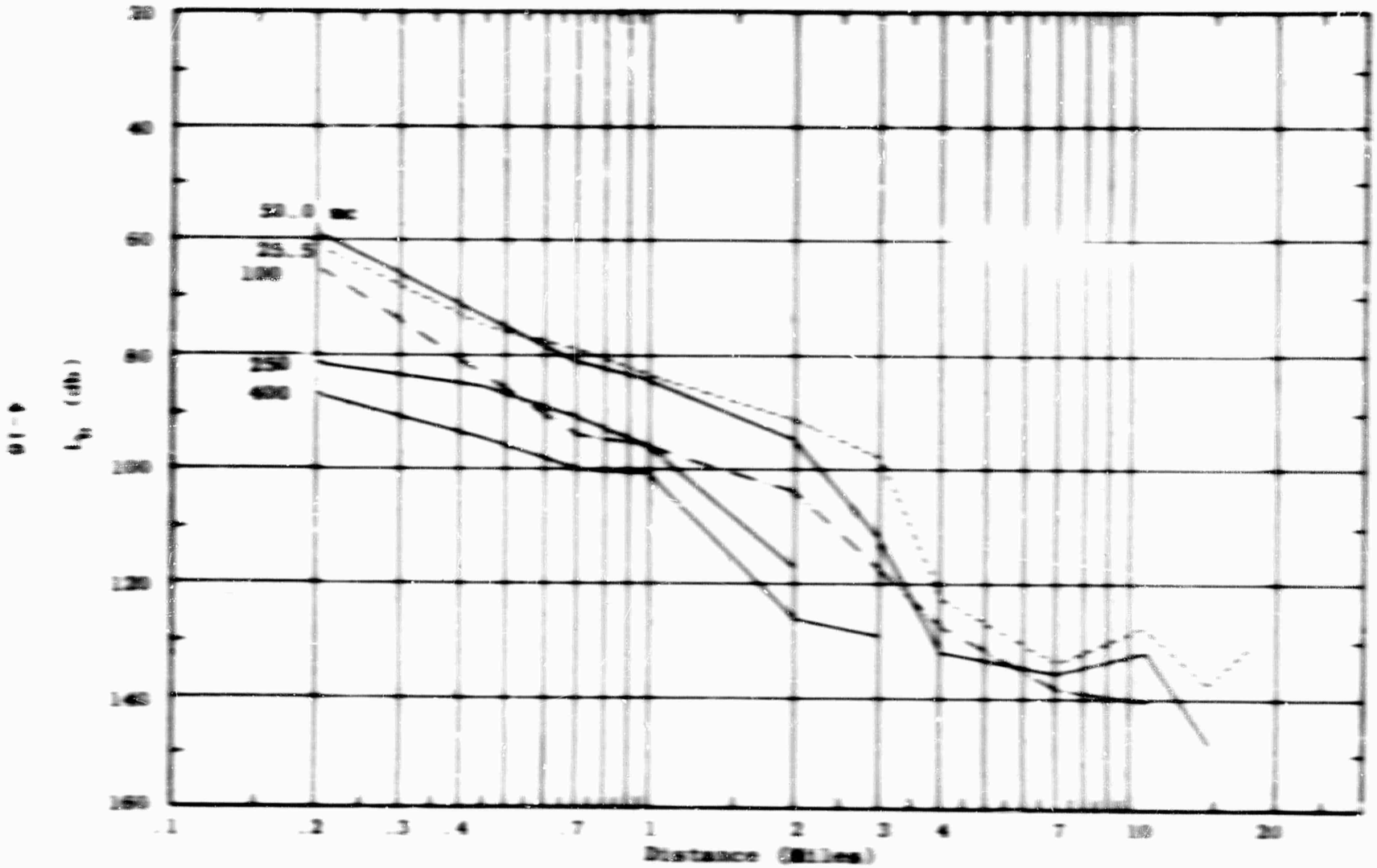

Figure 4.11 Measured Results, L_b Vs Distance
$L_b = F_A(f, 60, Y, Z, 60)$

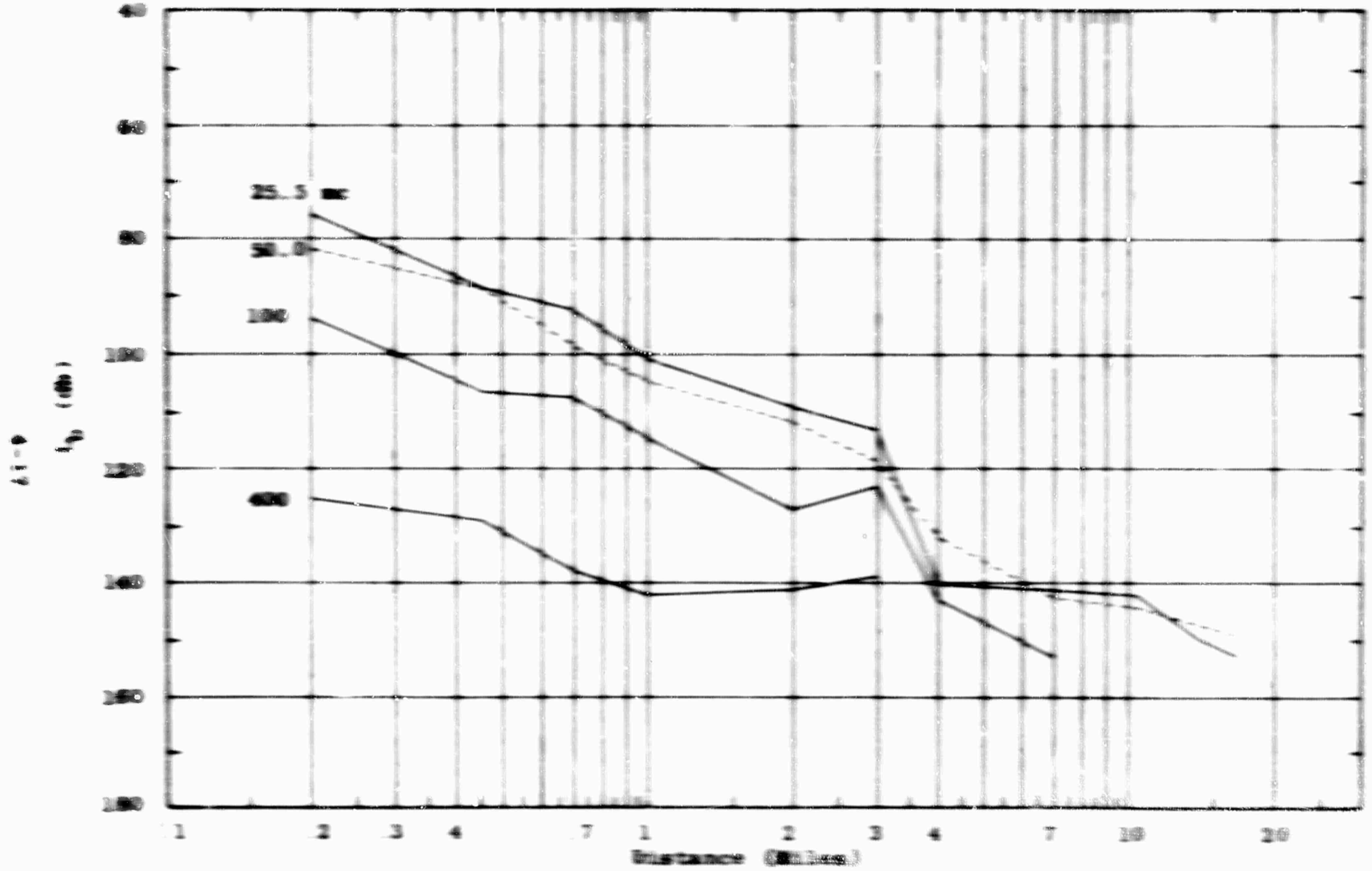
25.5 MC
50.0
100
400
1
2
3
4
7
1
2
3
4
7
10
20

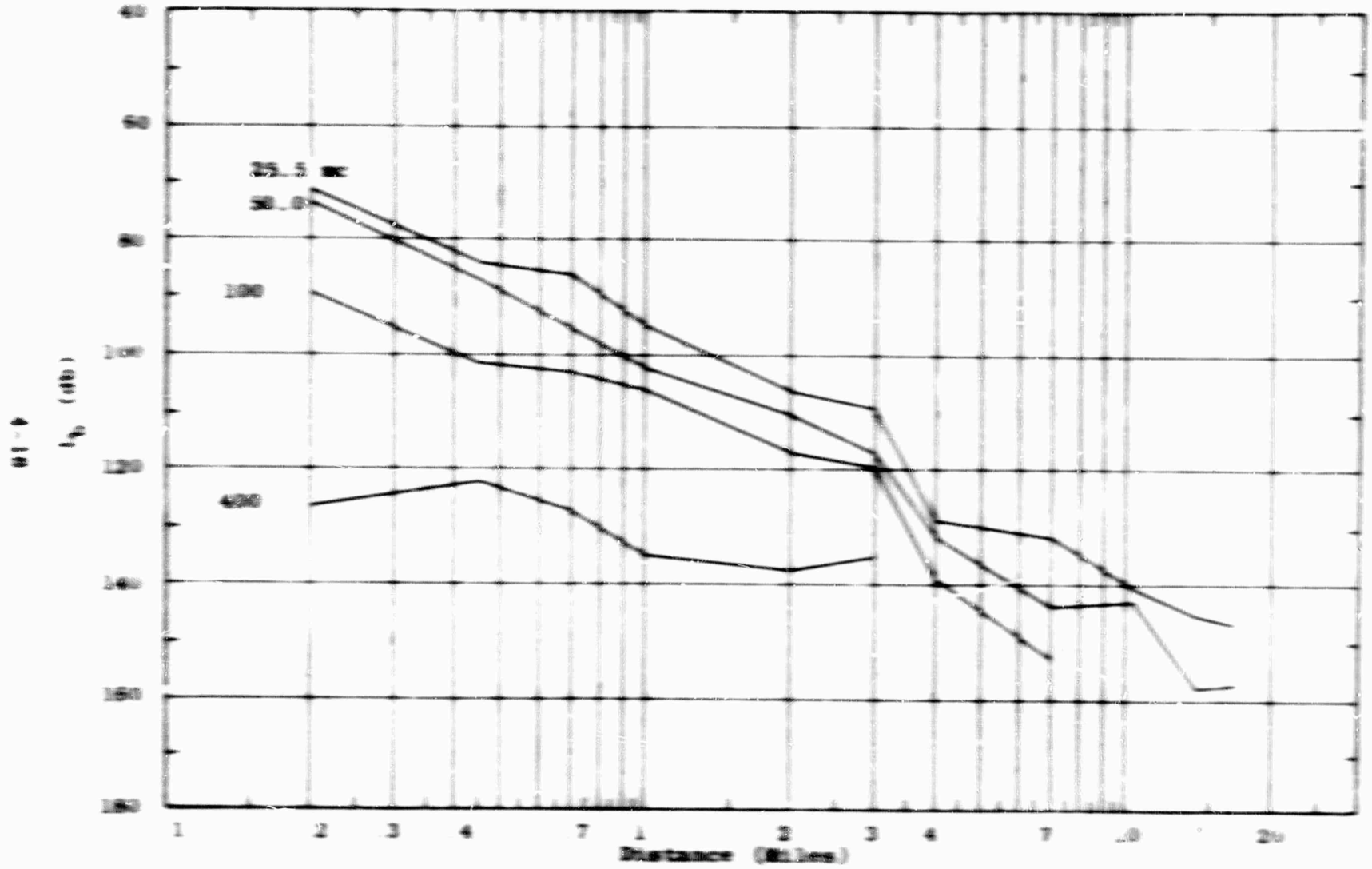

Figure 4.1E Measured Results, L_b Vs Distance
$L_b = F_A(f, 10, E, \zeta, 40)$

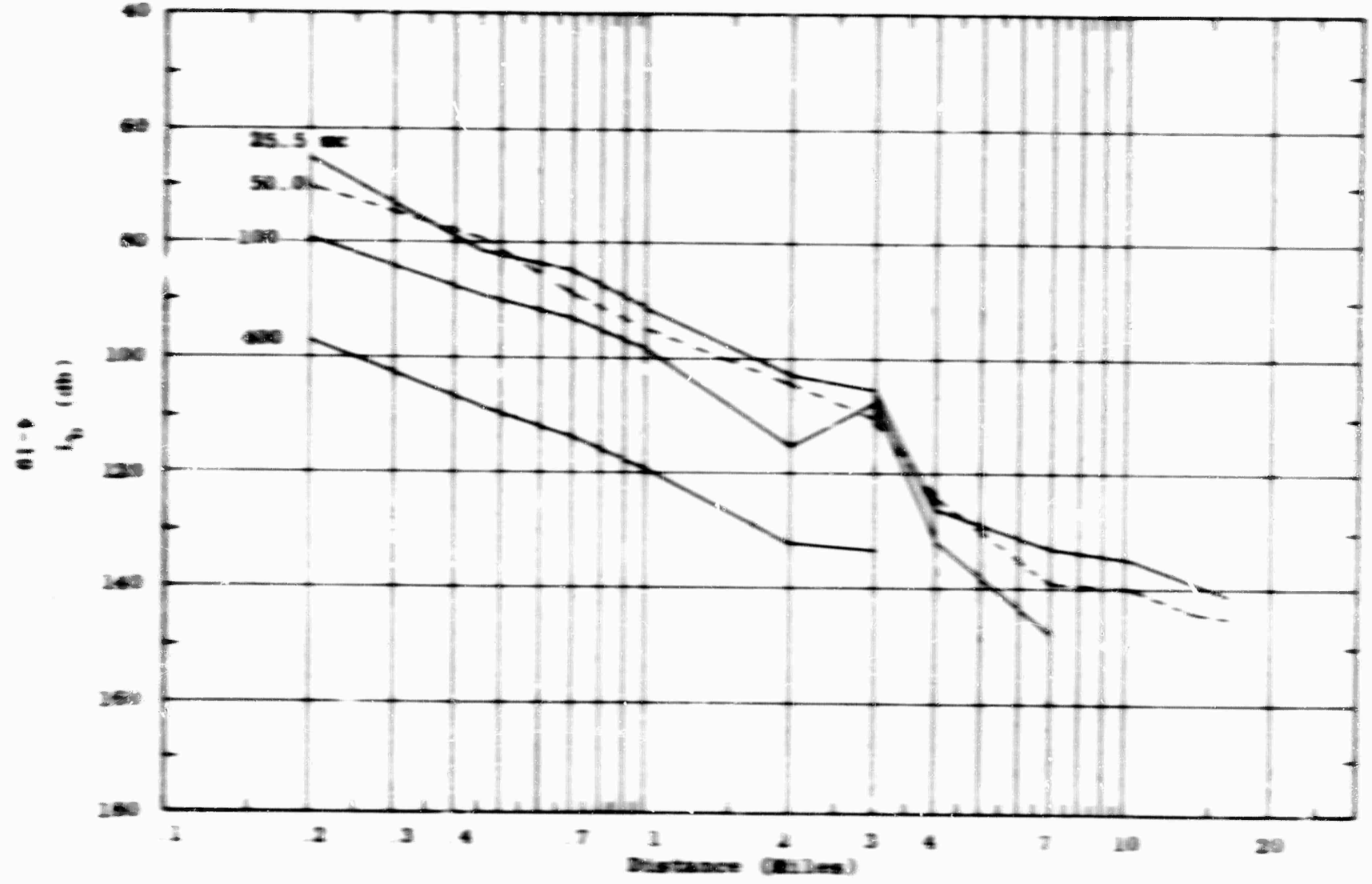

Figure 4.15 Measured Results, L_b Vs Distance
$L_b = F_4(f, 13, E, d, 50)$

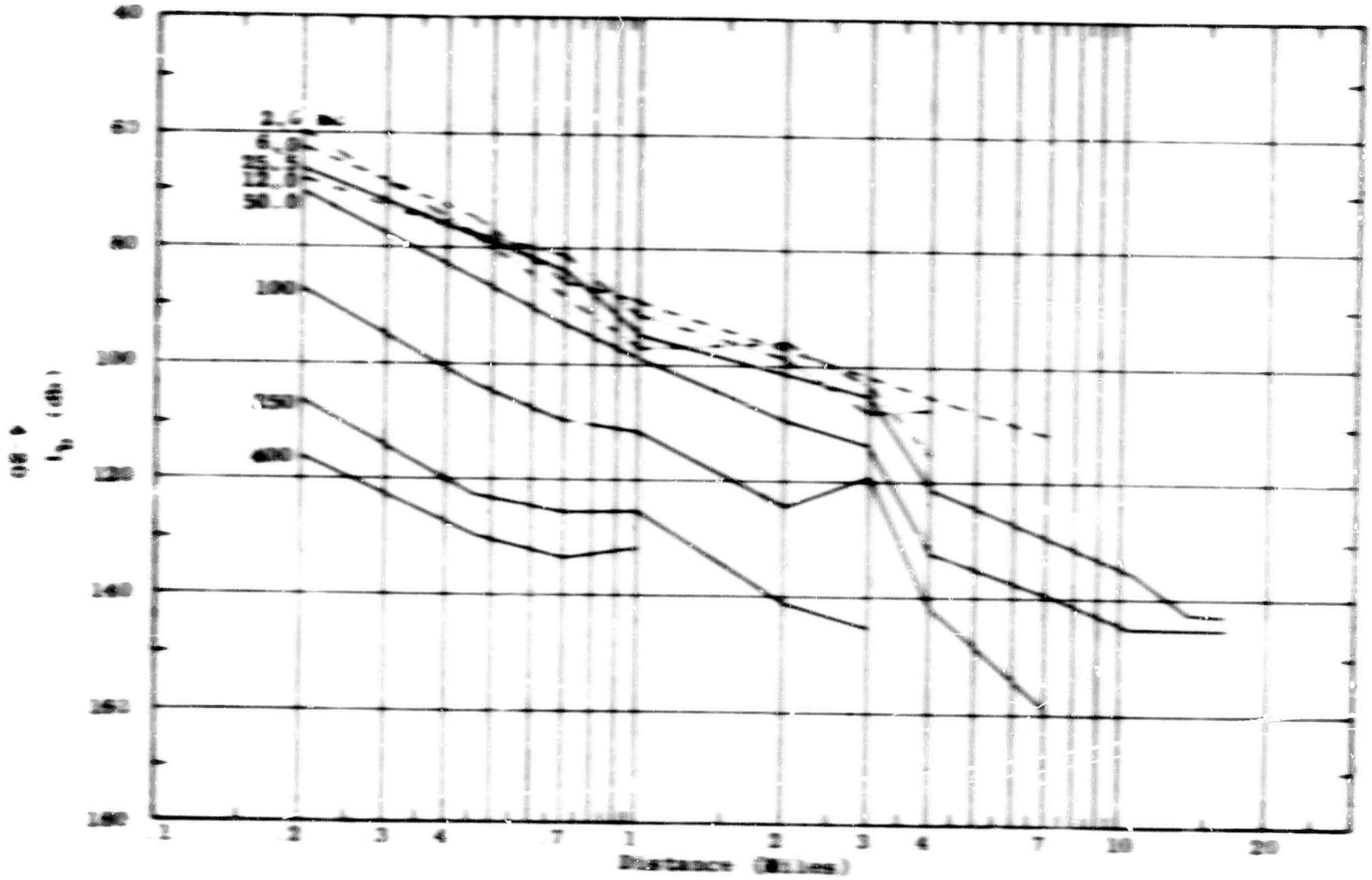

Figure 4.18 Measured Results, L_b Vs Distance
$L_b = F_3(f, 40, x, 2, 20)$

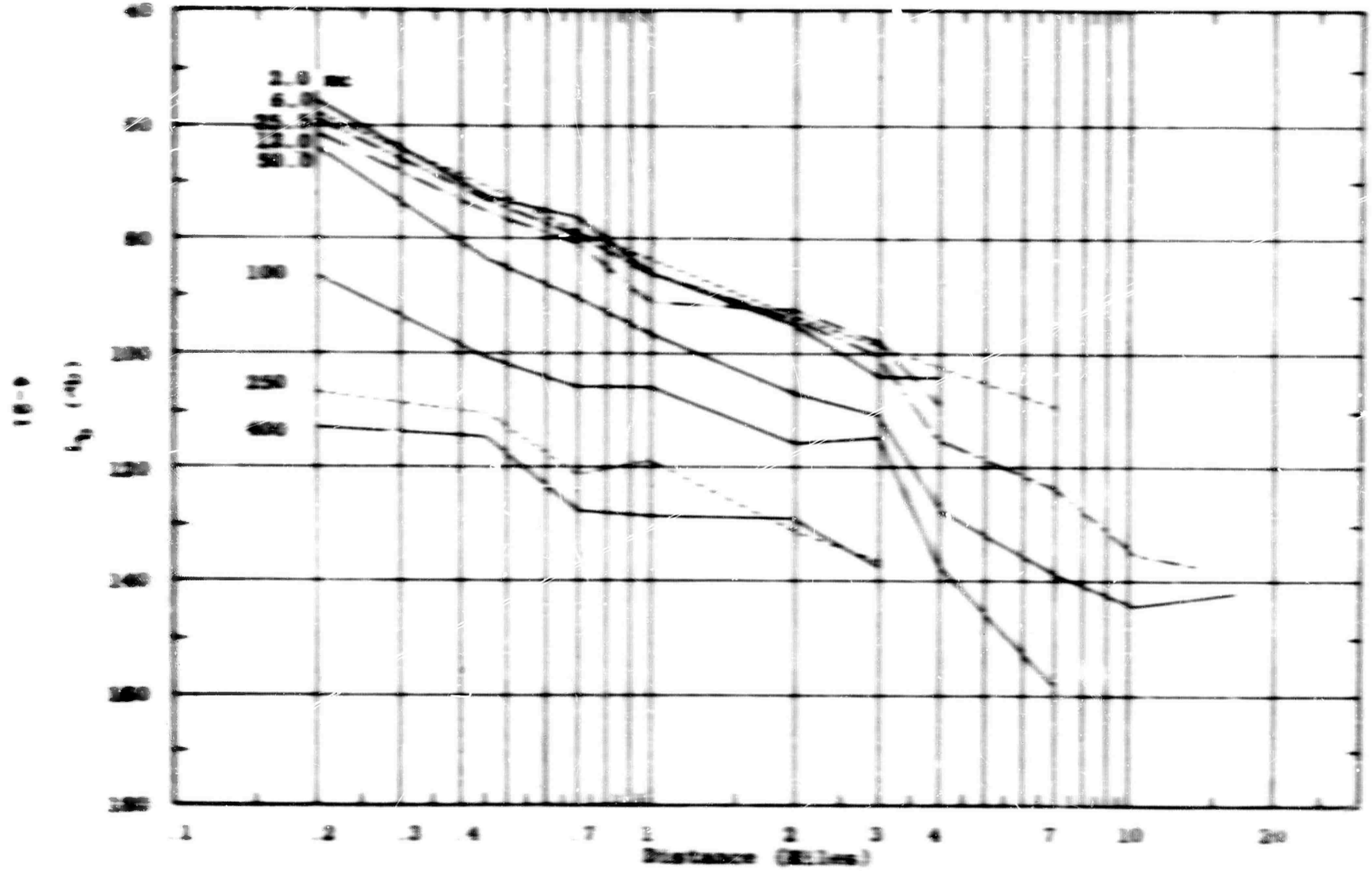

Figure 4.13 Measured Results, L_b Vs Distance
$L_b = F_6(t, 40, E, d, 40)$

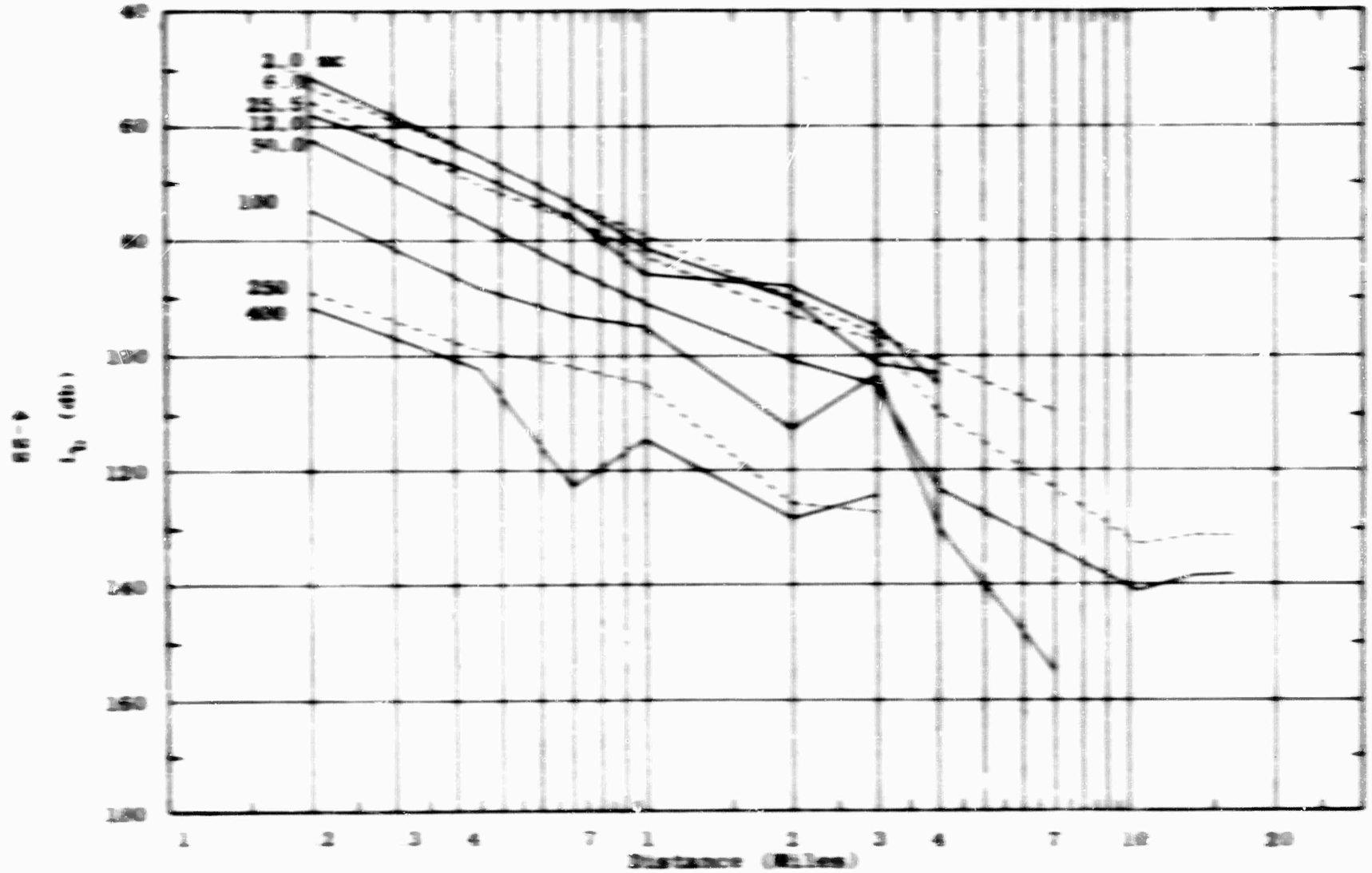

Figure 4.10 Measured Results, L_b vs Distance
$L_b = F_A(f, 40, E, d, 50)$

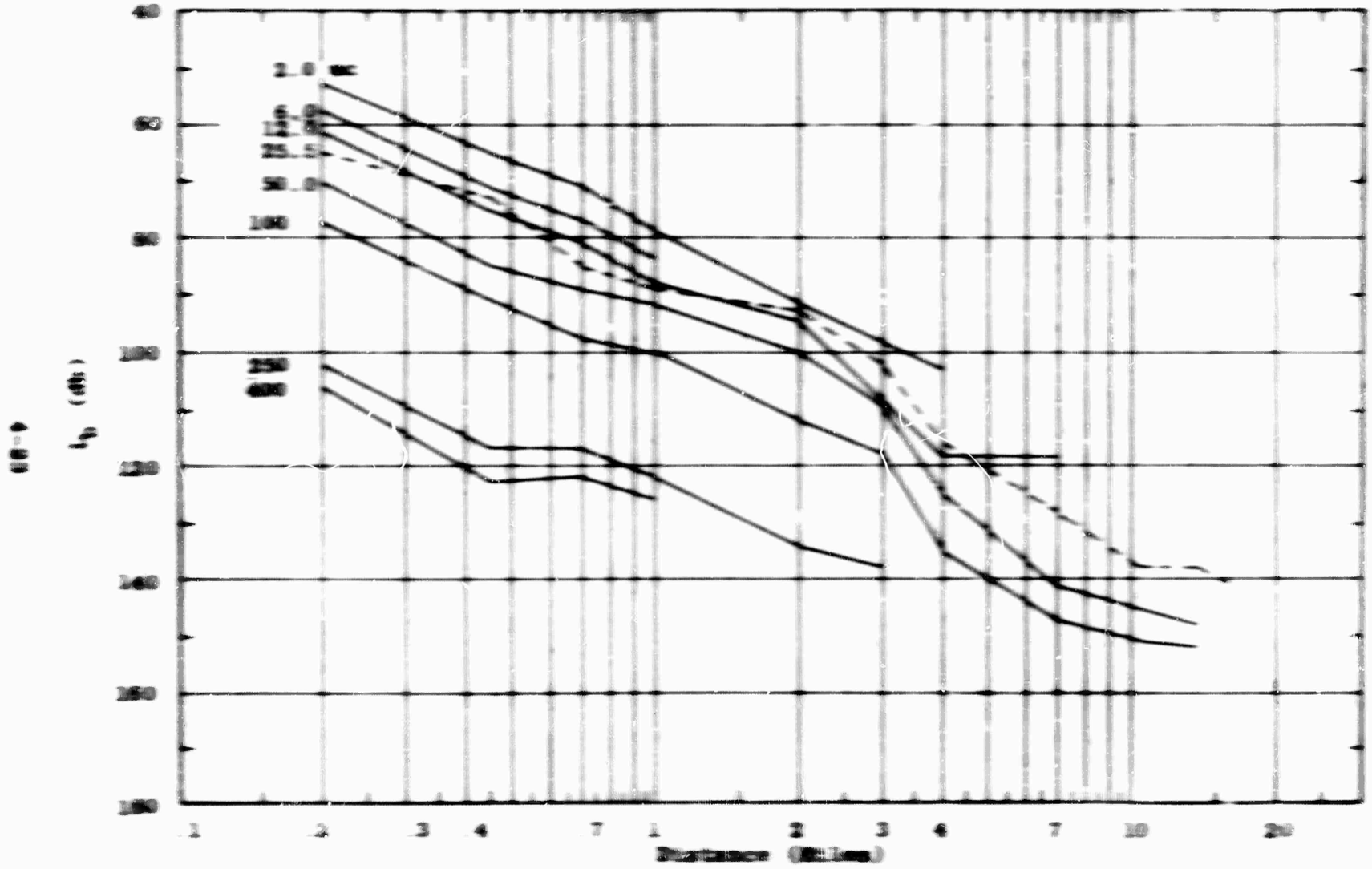

Figure 4.17 Measured Results, L_b Vs Distance
$L_b = F_4(f, H_b, E, d \geq 20)$

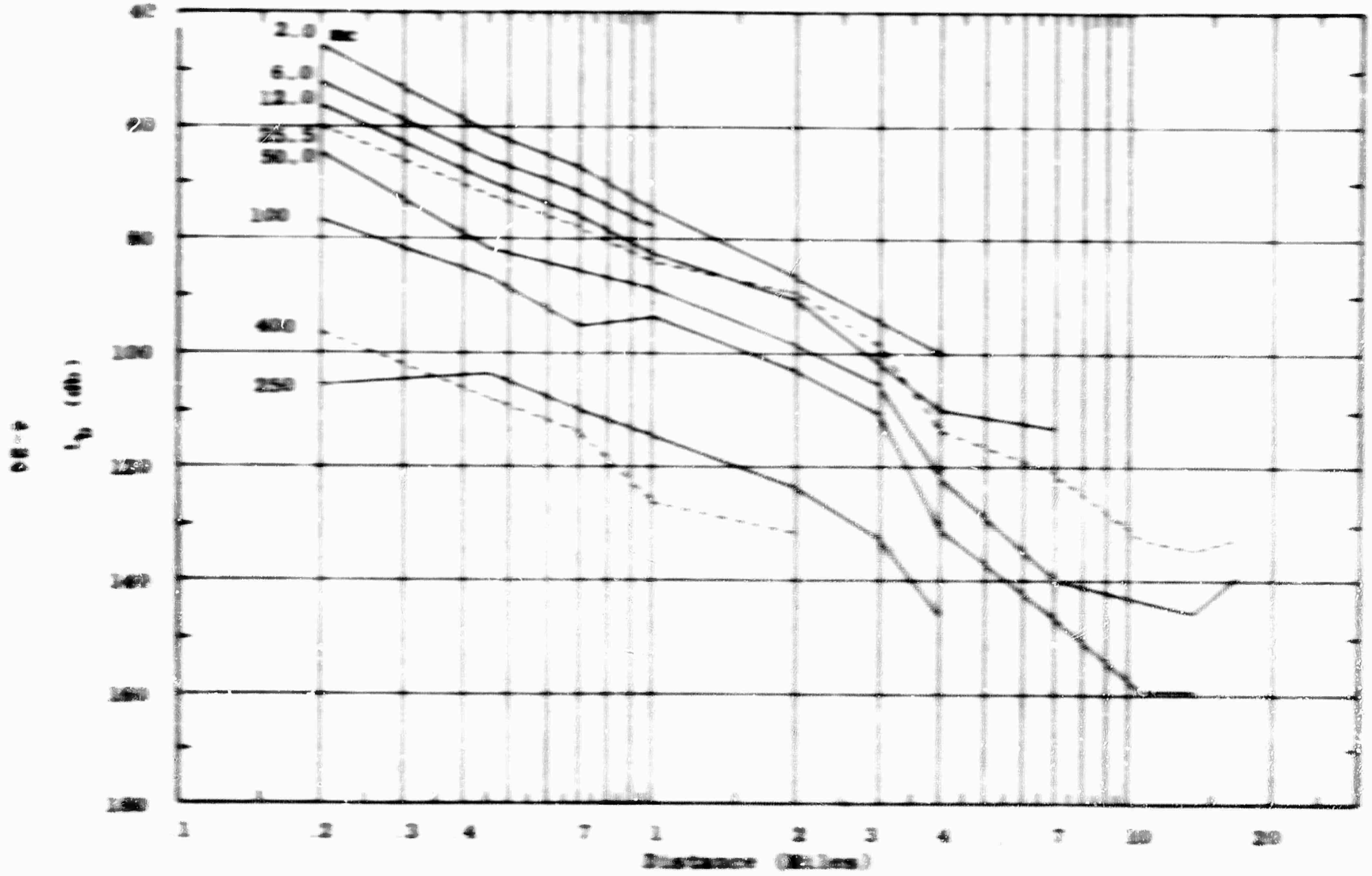
2.0
6.0
12.0
25.5
50.0
100
400
250
1
2
3
4
7
1
2
3
4
7
10
20

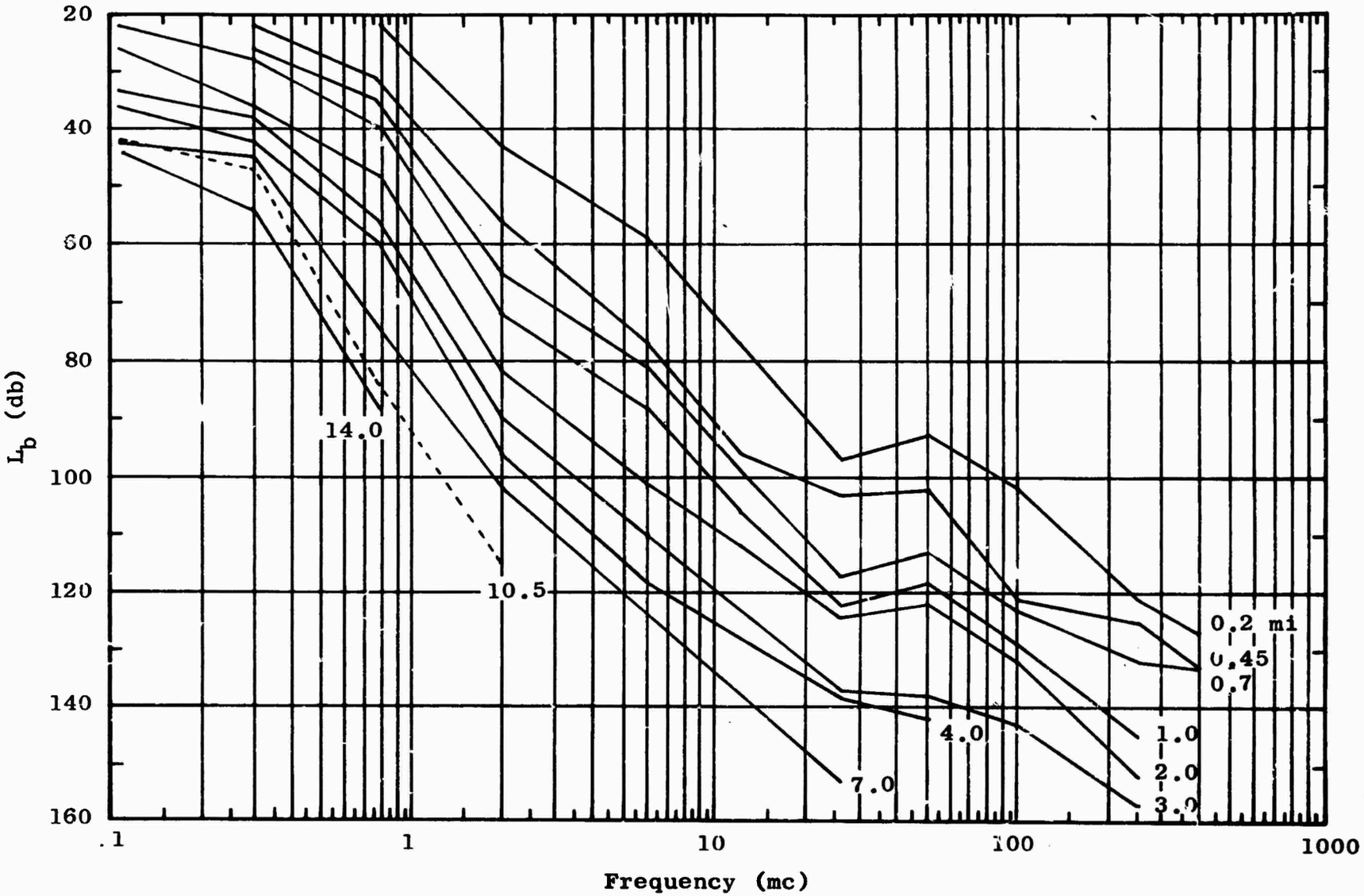

Figure 4.2A Measured Results, L_b Vs Frequency
$L_b = F_A(f, 13, V, d, 20)$

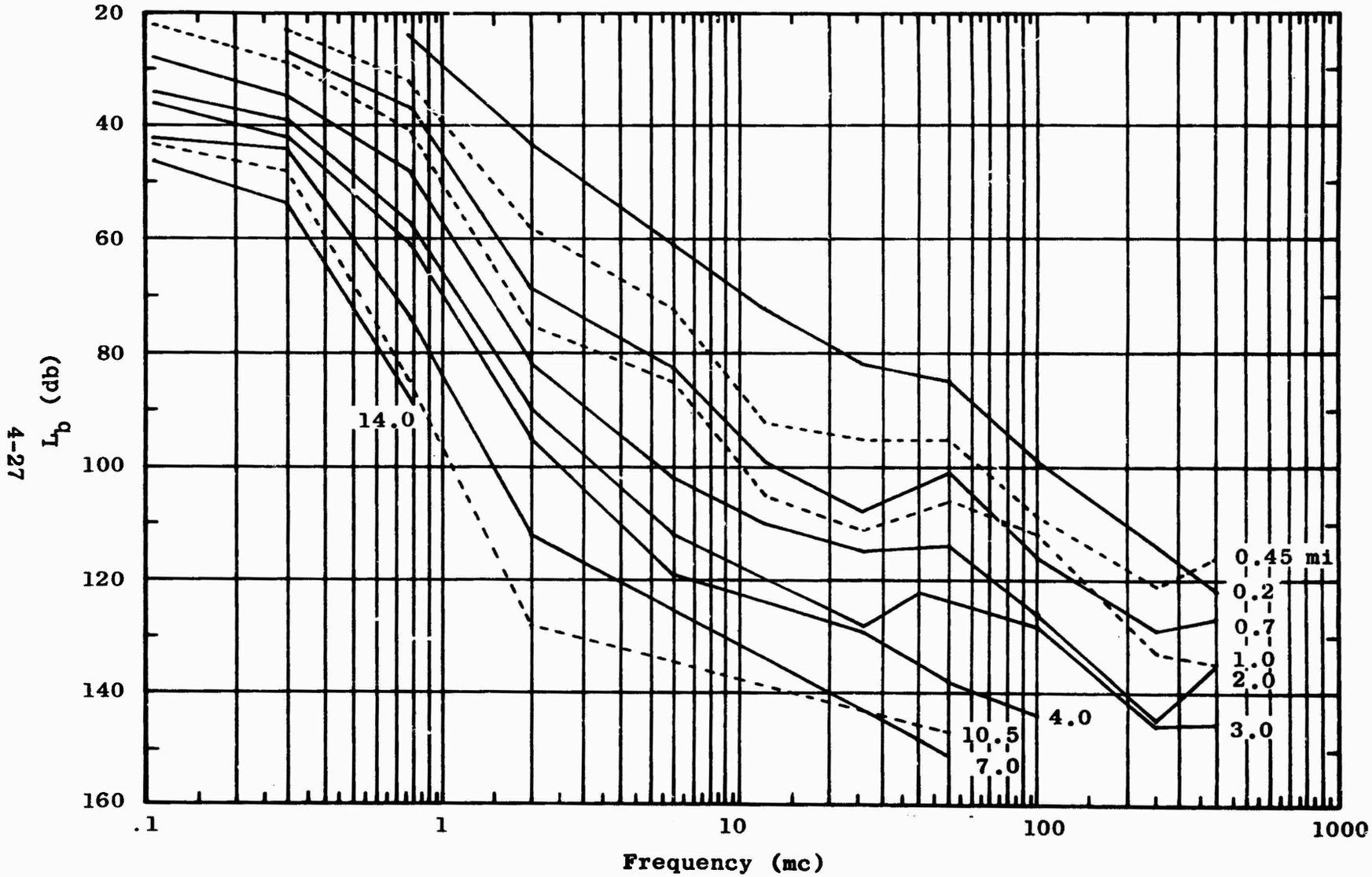

Figure 4.2B Measured Results, L_b Vs Frequency
$L_b = F_A(f, 13, V, d, 40)$

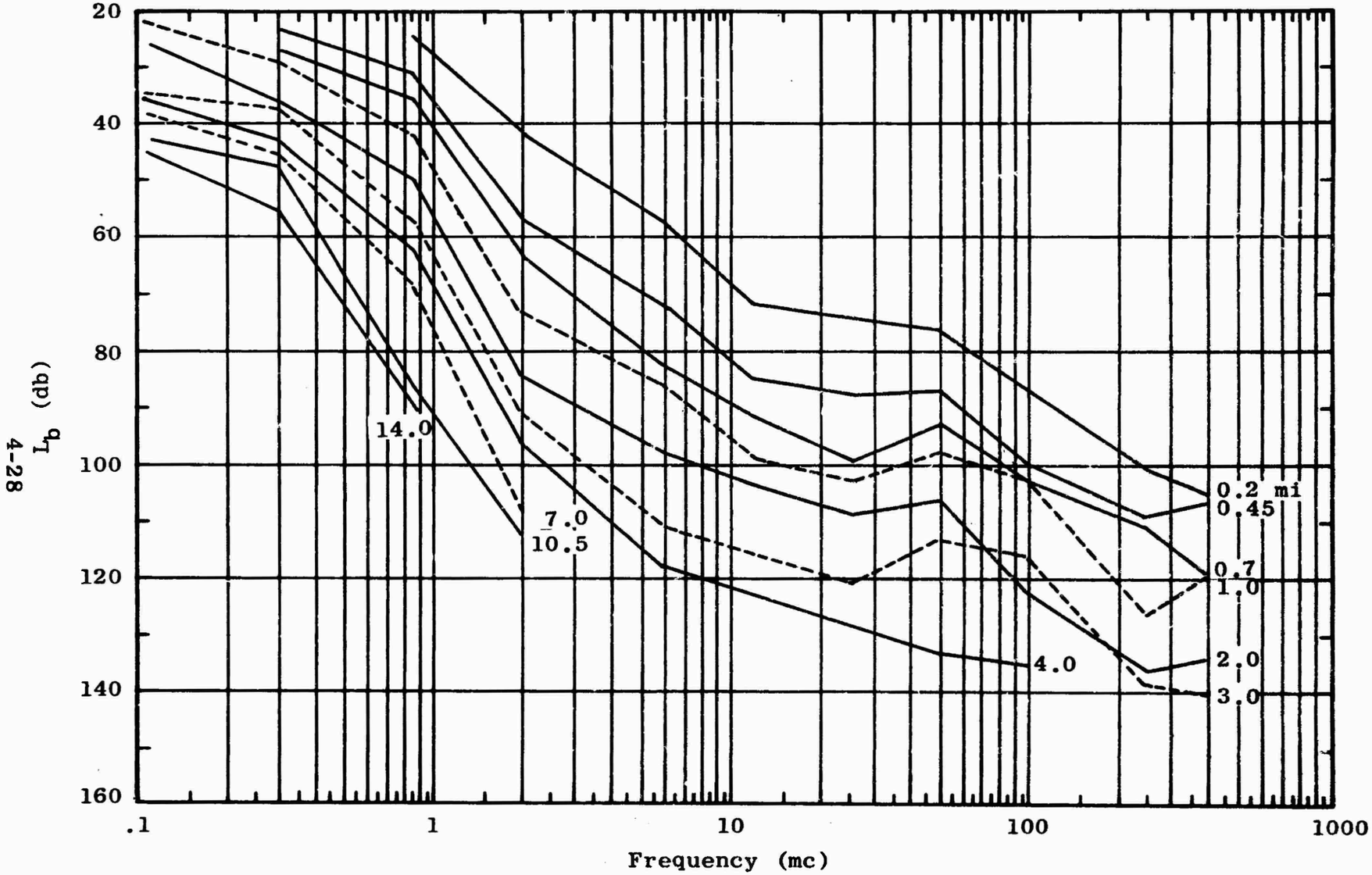

Figure 4.2C Measured Results, L_b Vs Frequency
$L_b = F_A(f, 13, V, d, 80)$

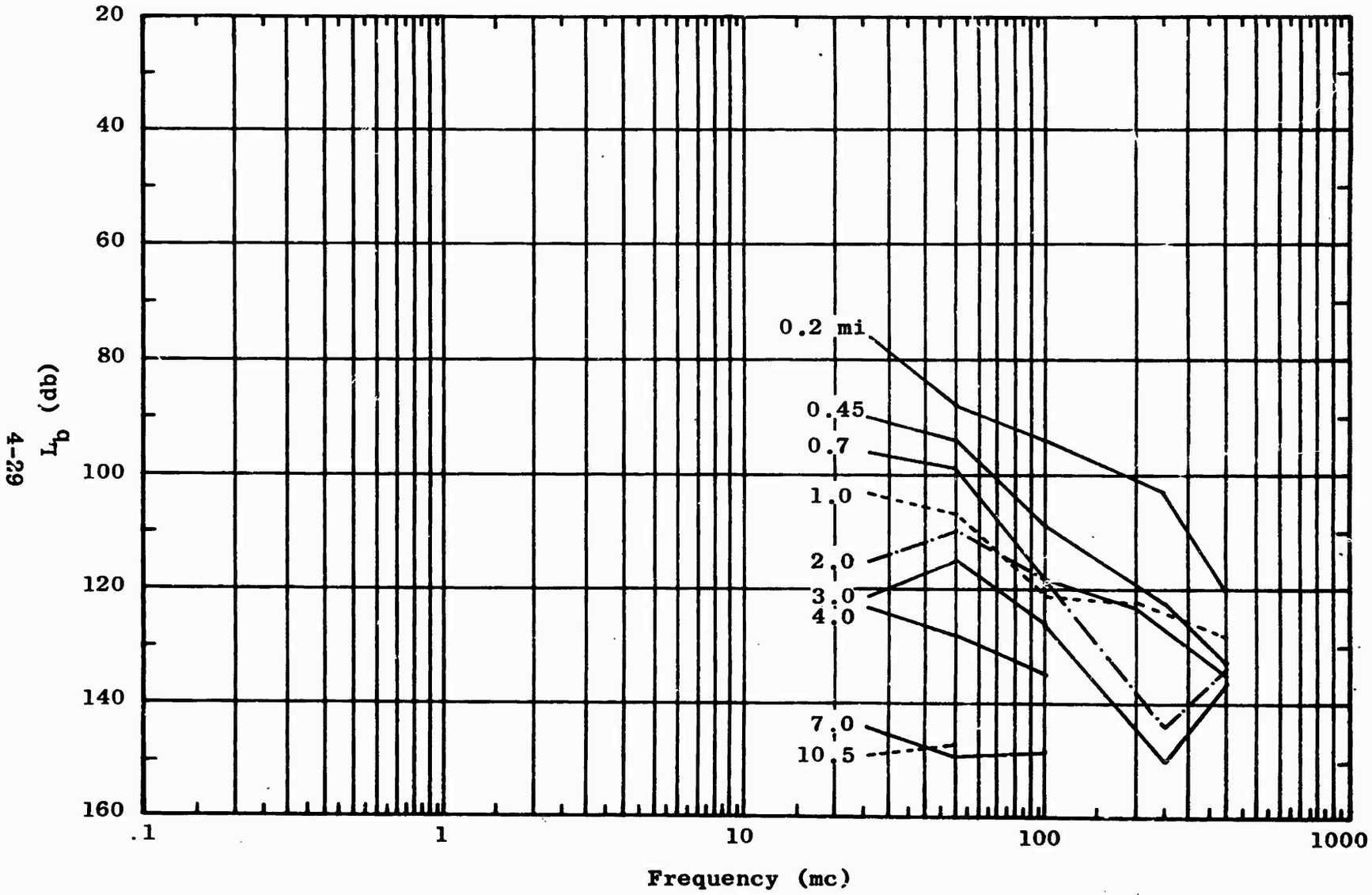

Figure 4.2D Measured Results, L_b Vs Frequency
$L_b = F_A(f, 40, V, d, 20)$

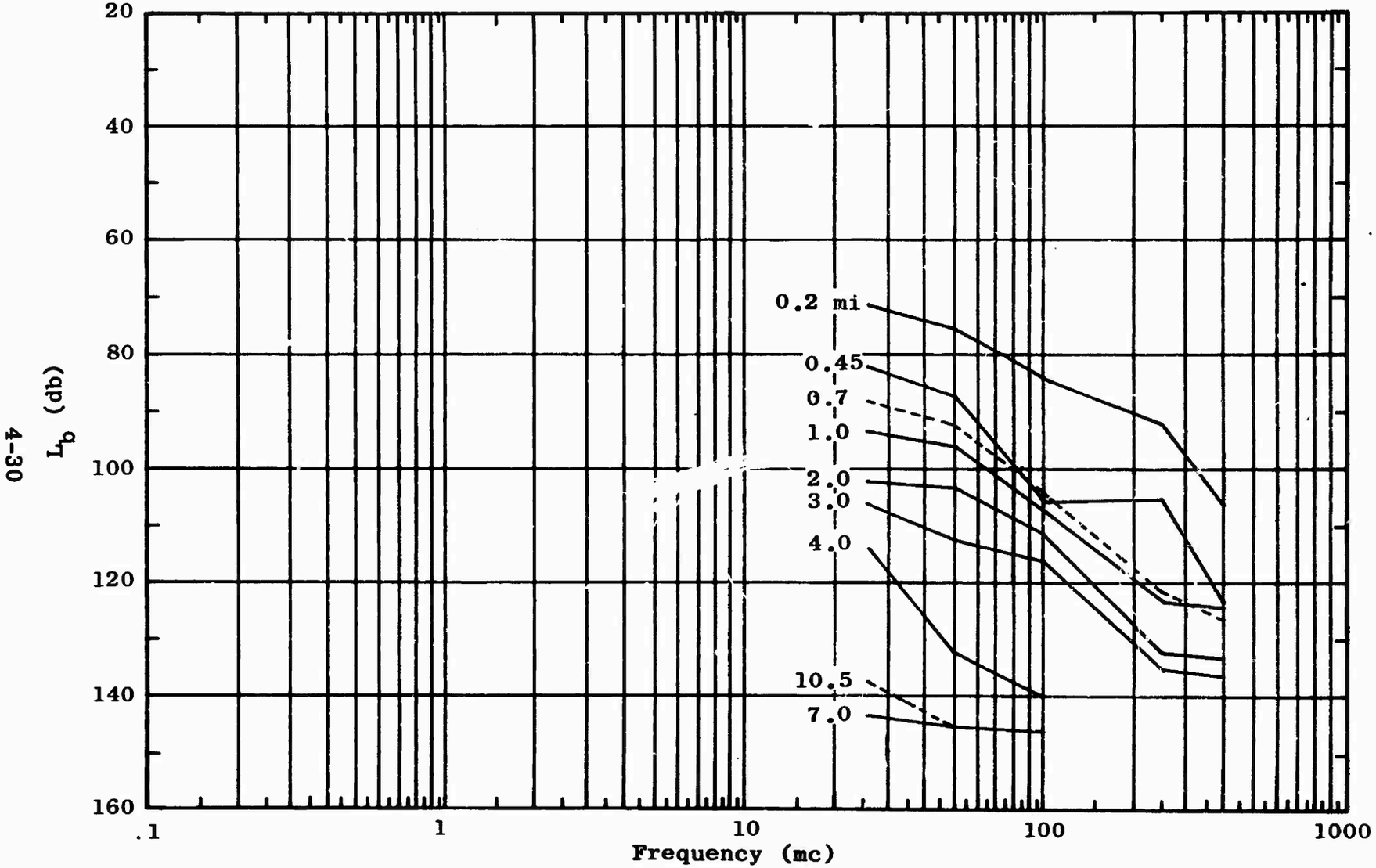

Figure 4.2E Measured Results, L_b Vs Frequency
$L_b = F_A(f, 40, V, d, 40)$

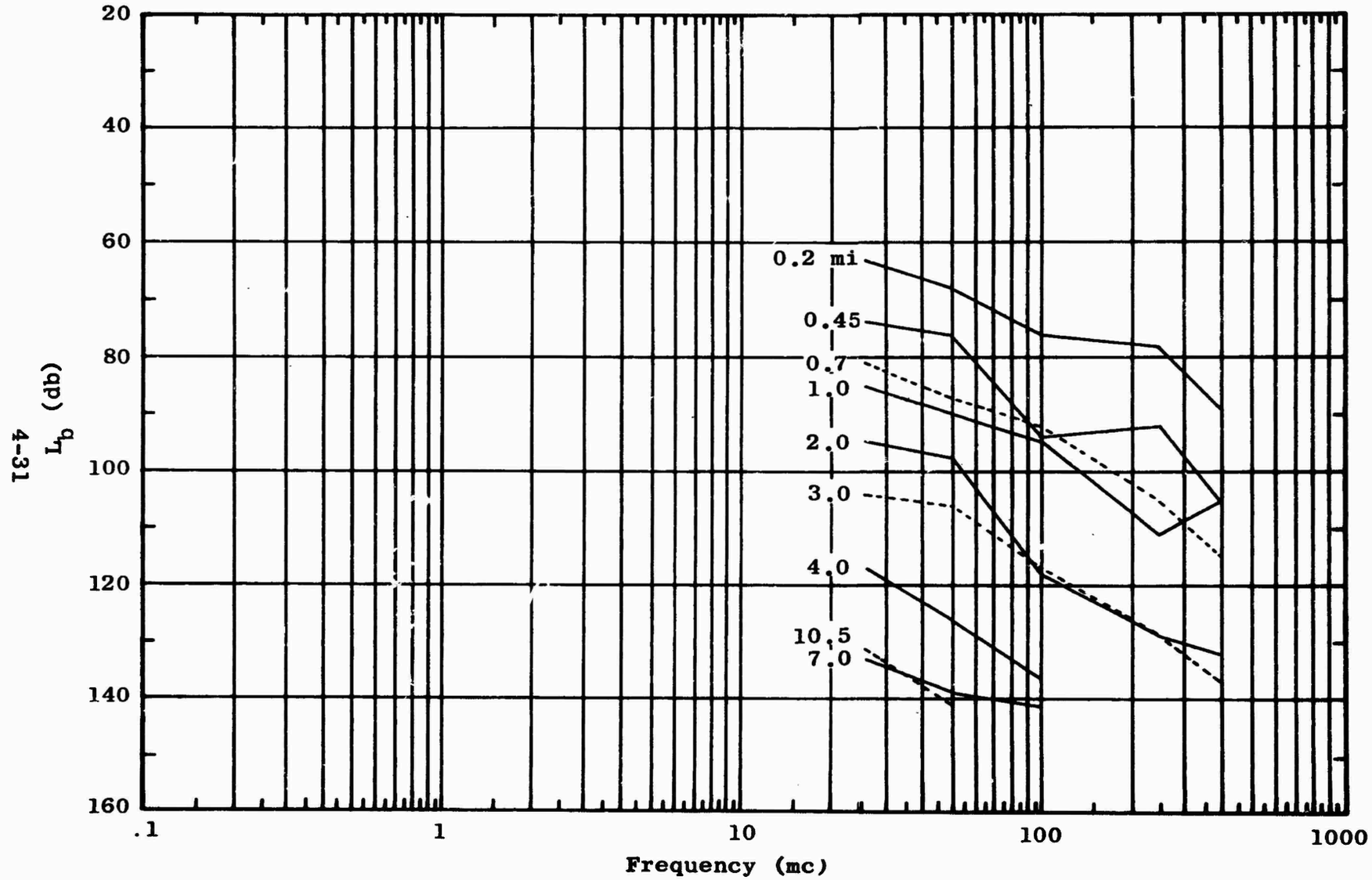

Figure 4.2F Measured Results, L_b Vs Frequency
$L_b = F_A(f, 40, V, d, 80)$

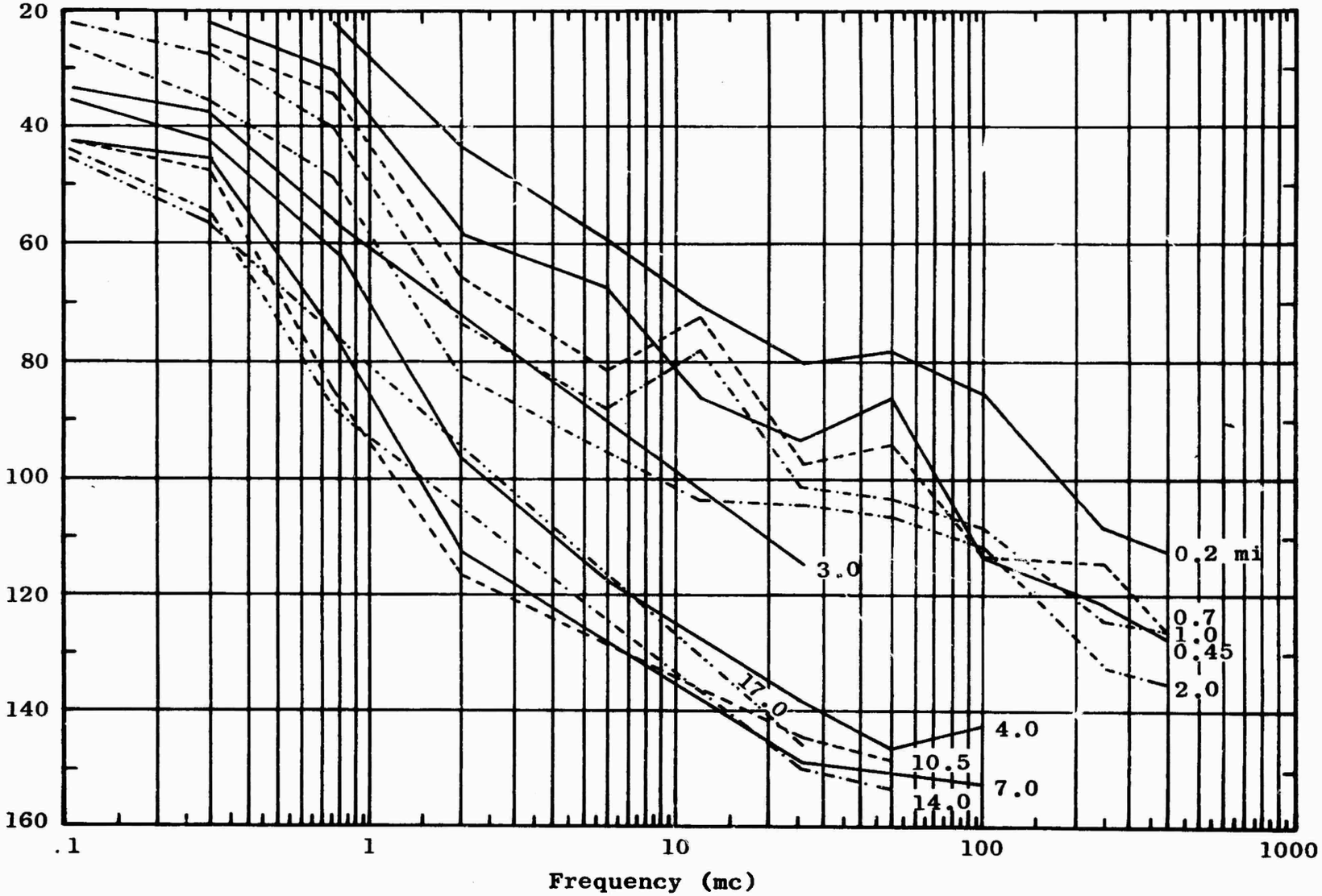

Figure 4.2G Measured Results, L_b Vs Frequency
$L_b = F_A(f, 80, V, d, 20)$

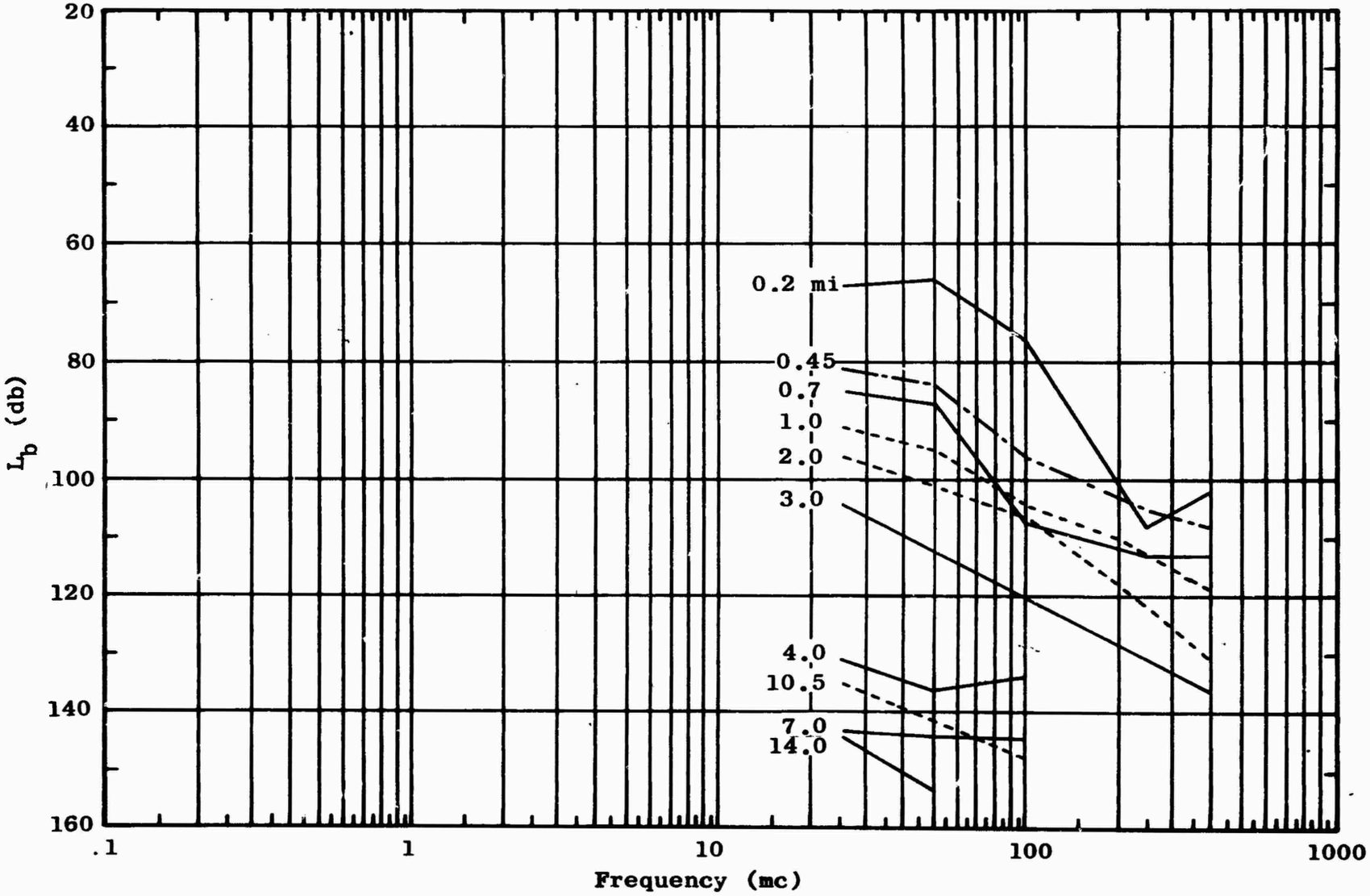

Figure 4.2H Measured Results, L_b Vs Frequency
$L_b = F_A(f, 80, V, d, 40)$

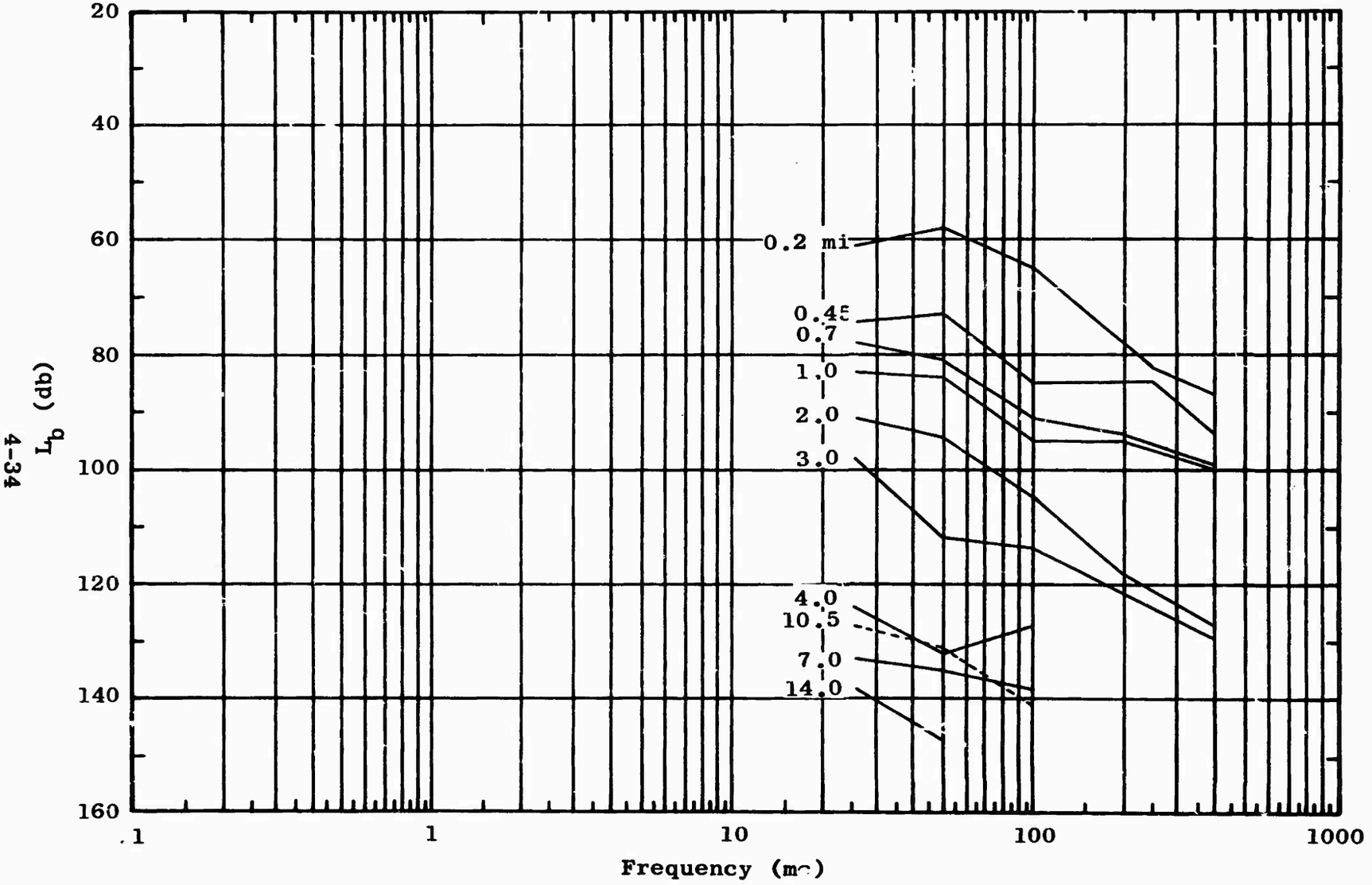

Figure 4.2I Measured Results, L_b Vs Frequency
$L_b = F_A(f, 80, V, d, 80)$

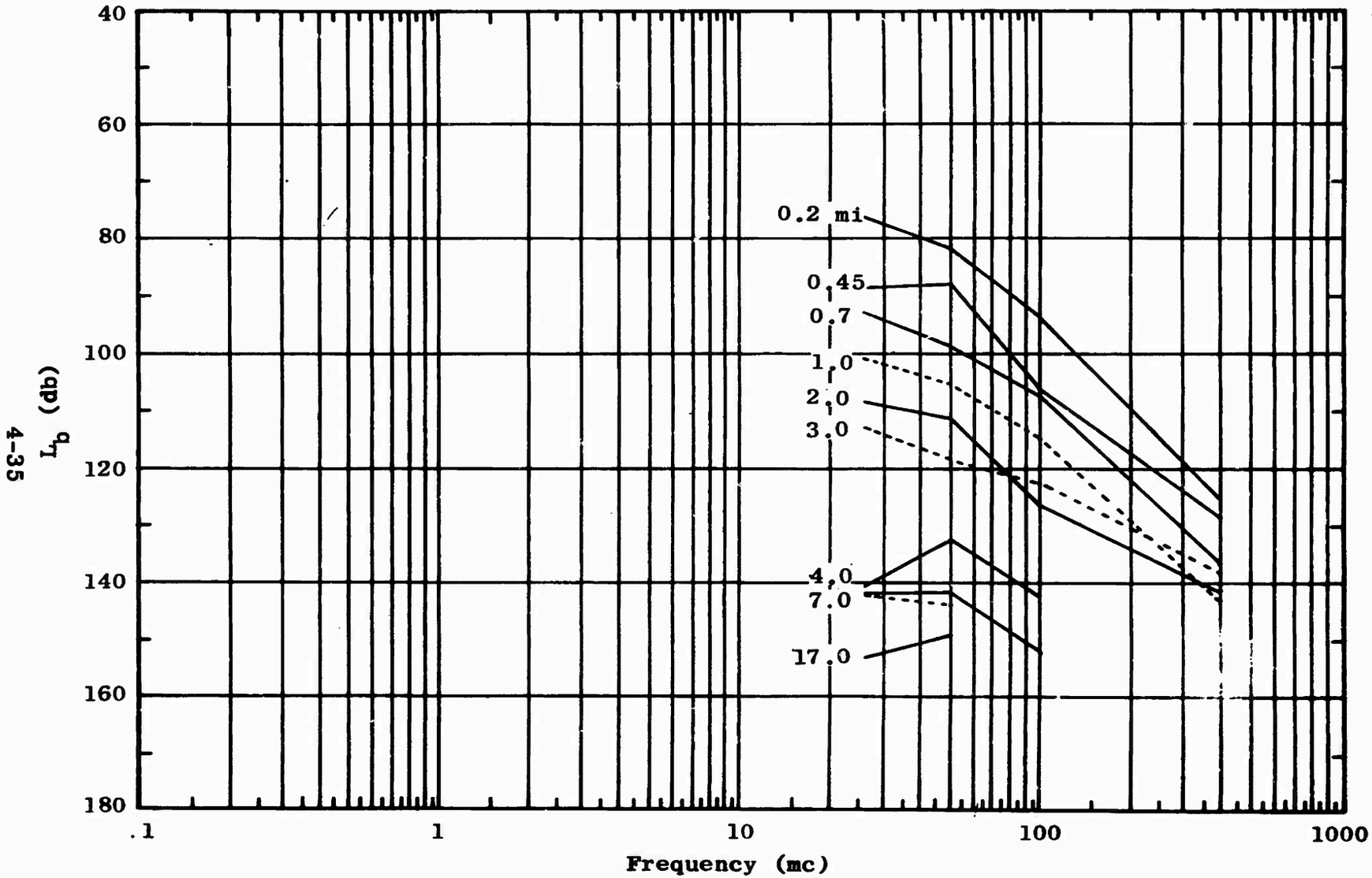

Figure 4.2J Measured Results, L_b Vs Frequency
$L_b = F_A(f, 13, H, d, 20)$

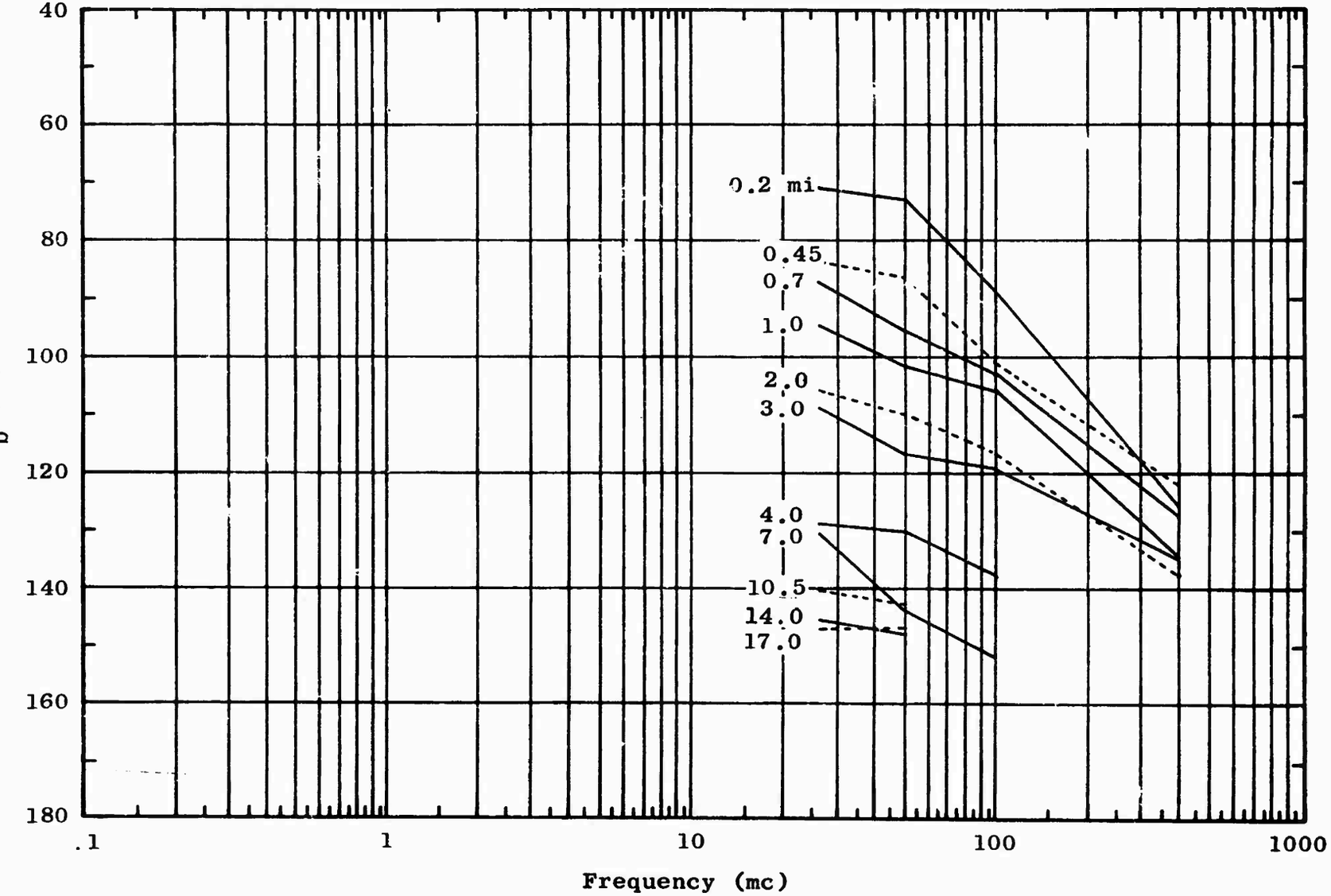

Figure 4.2K Measured Results, L_b Vs Frequency
$L_b = F_A(f, 13, H, d, 40)$

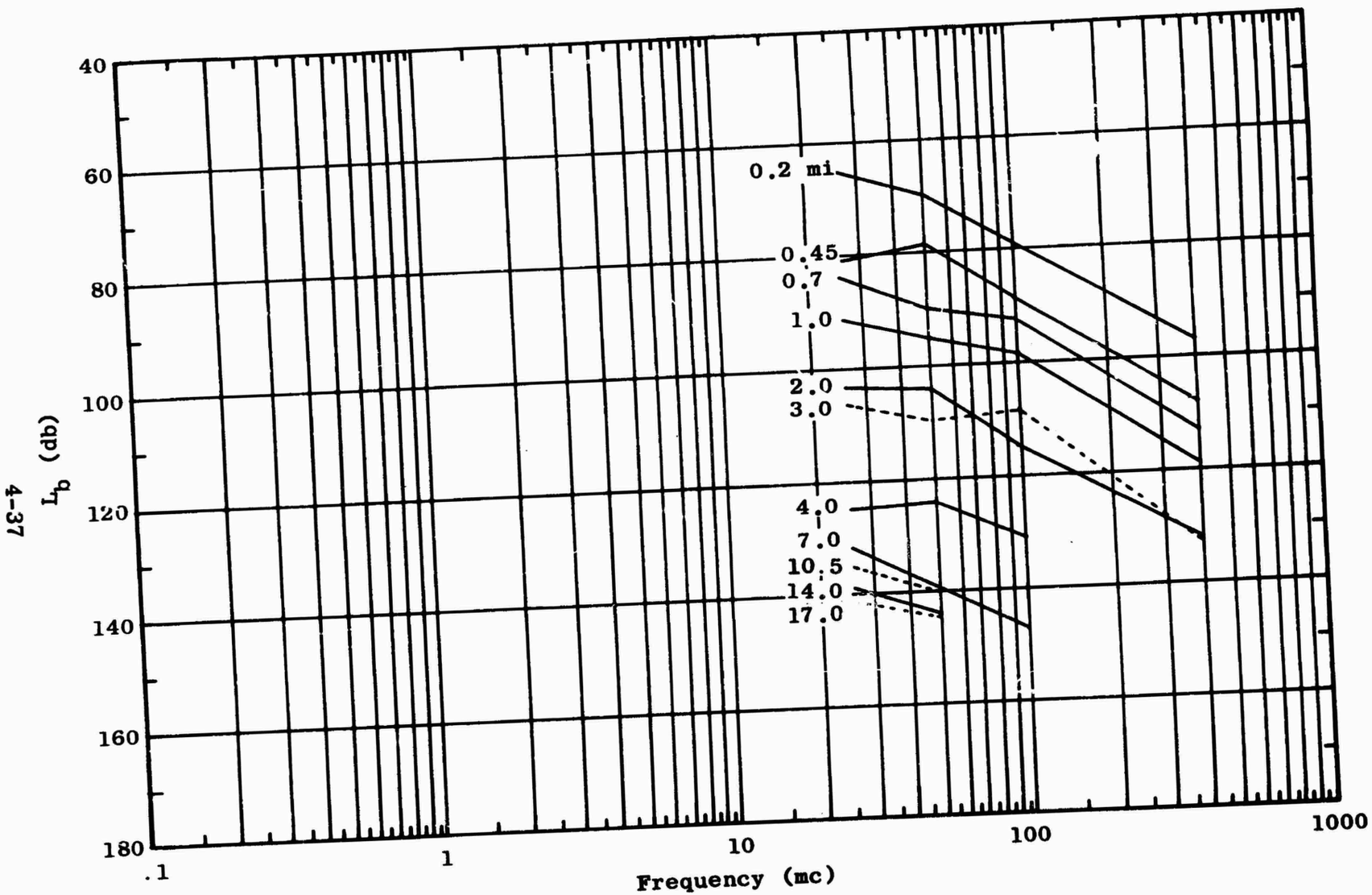

Figure 4.2L Measured Results, L_b Vs Frequency
$L_b = F_A(f, 13, H, d, 80)$

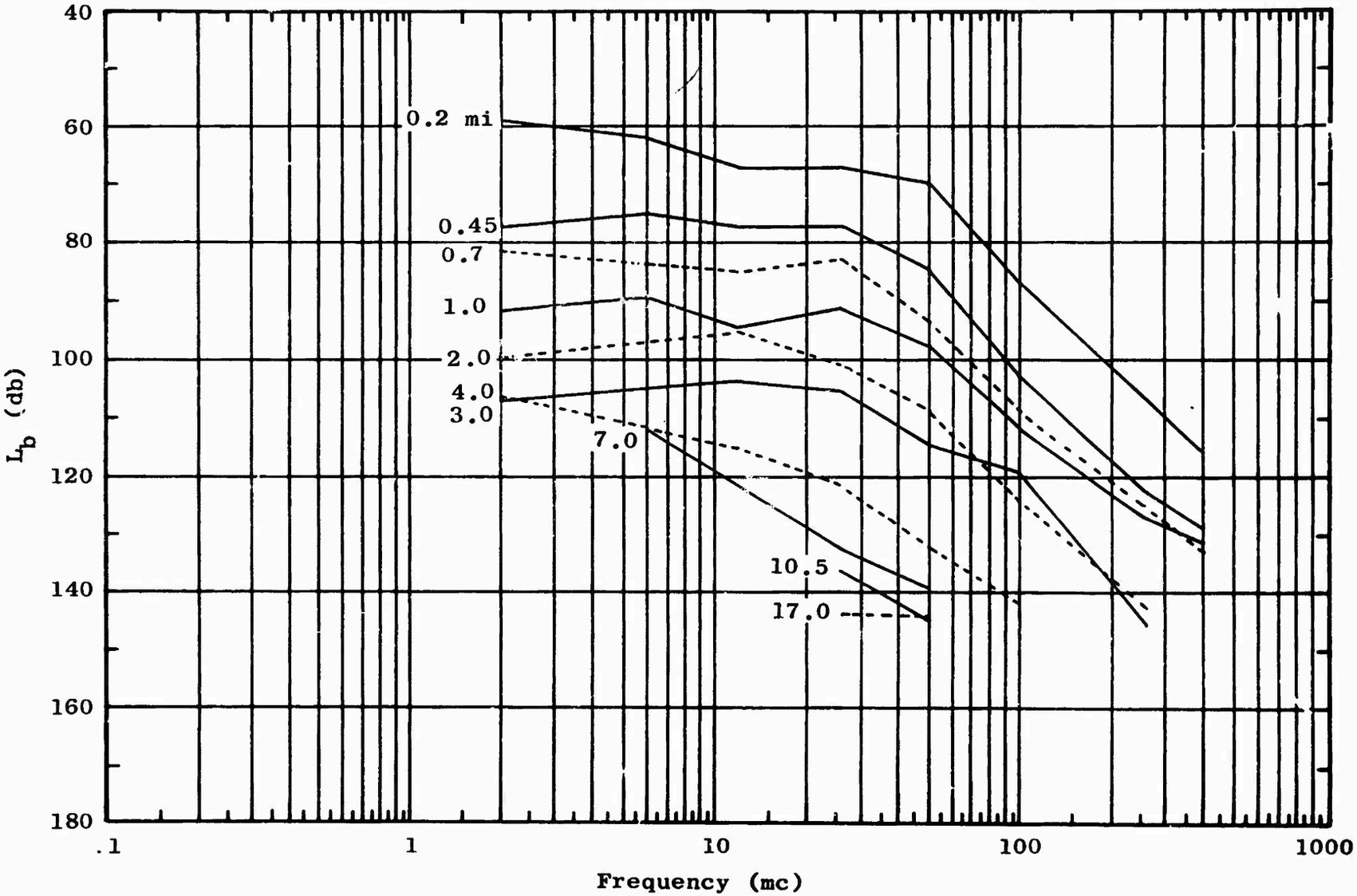

Figure 4.2M Measured Results, L_b Vs Frequency
$L_b = F_A(f, 40, H, d, 20)$

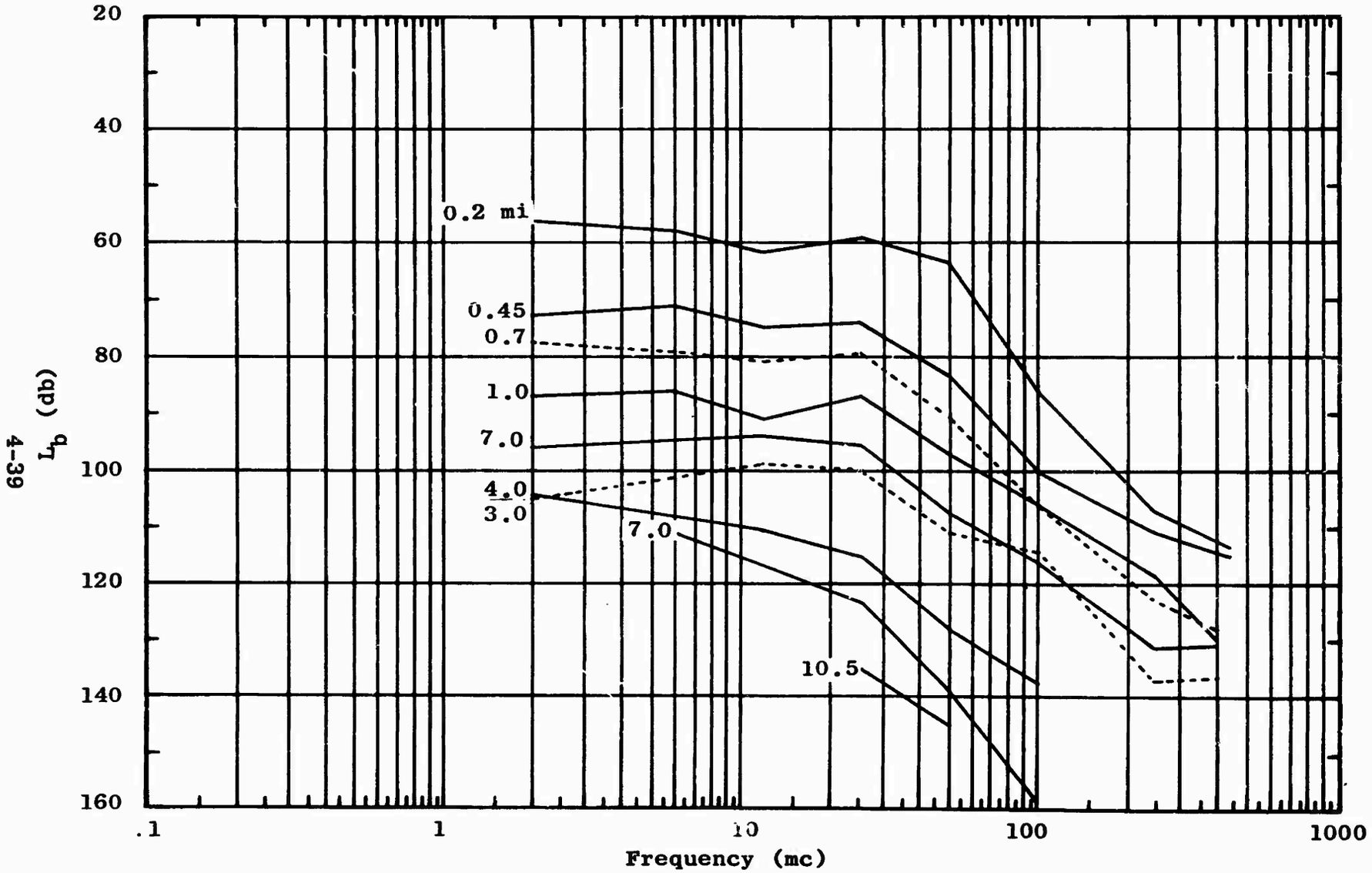

Figure 4.2N Measured Results, L_b Vs Frequency
$L_b = F_A(f, 40, H, d, 40)$

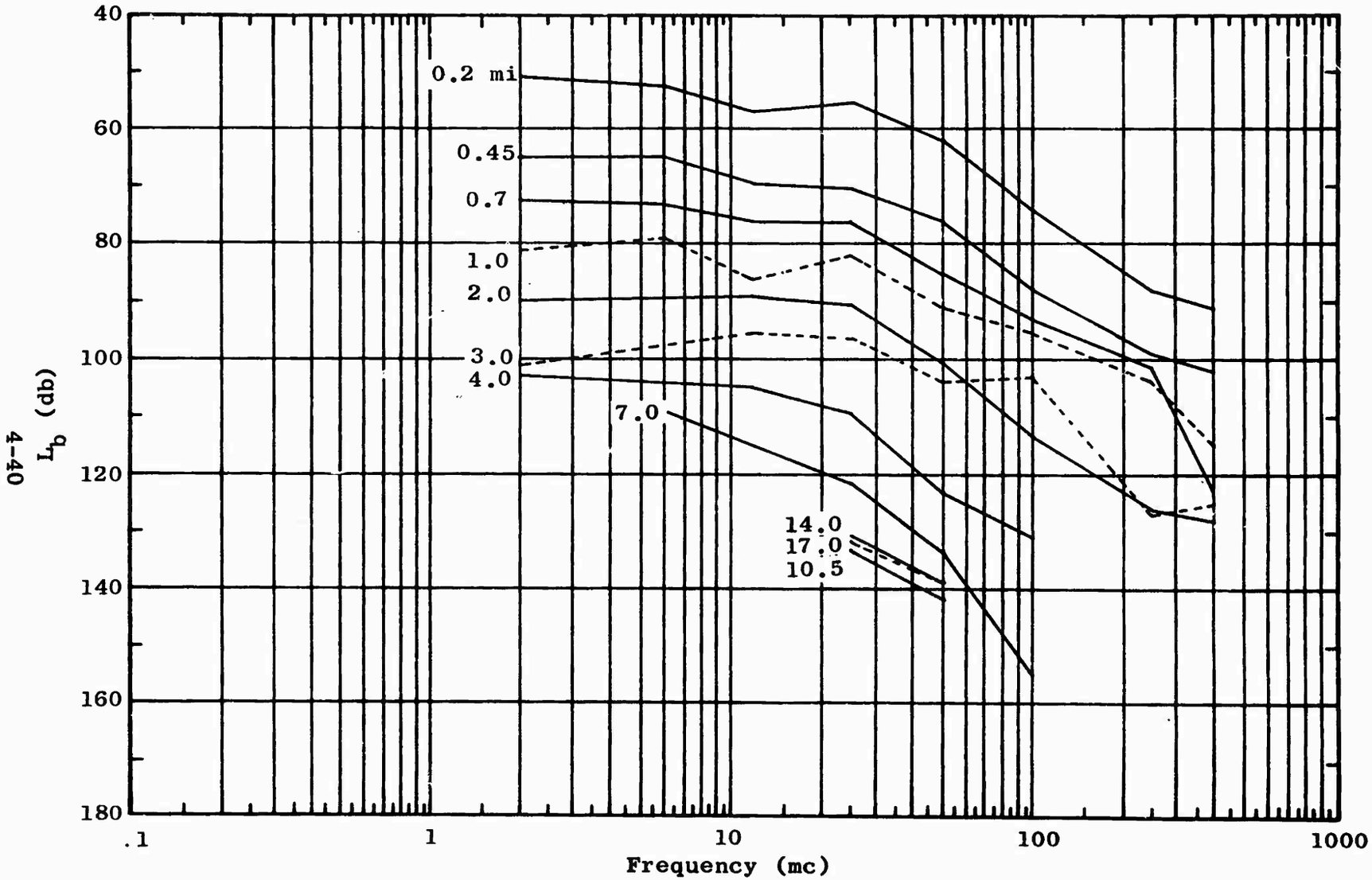

Figure 4.20 Measured Results, L_b Vs Frequency
$L_b = F_A(f, 40, H, d, 80)$

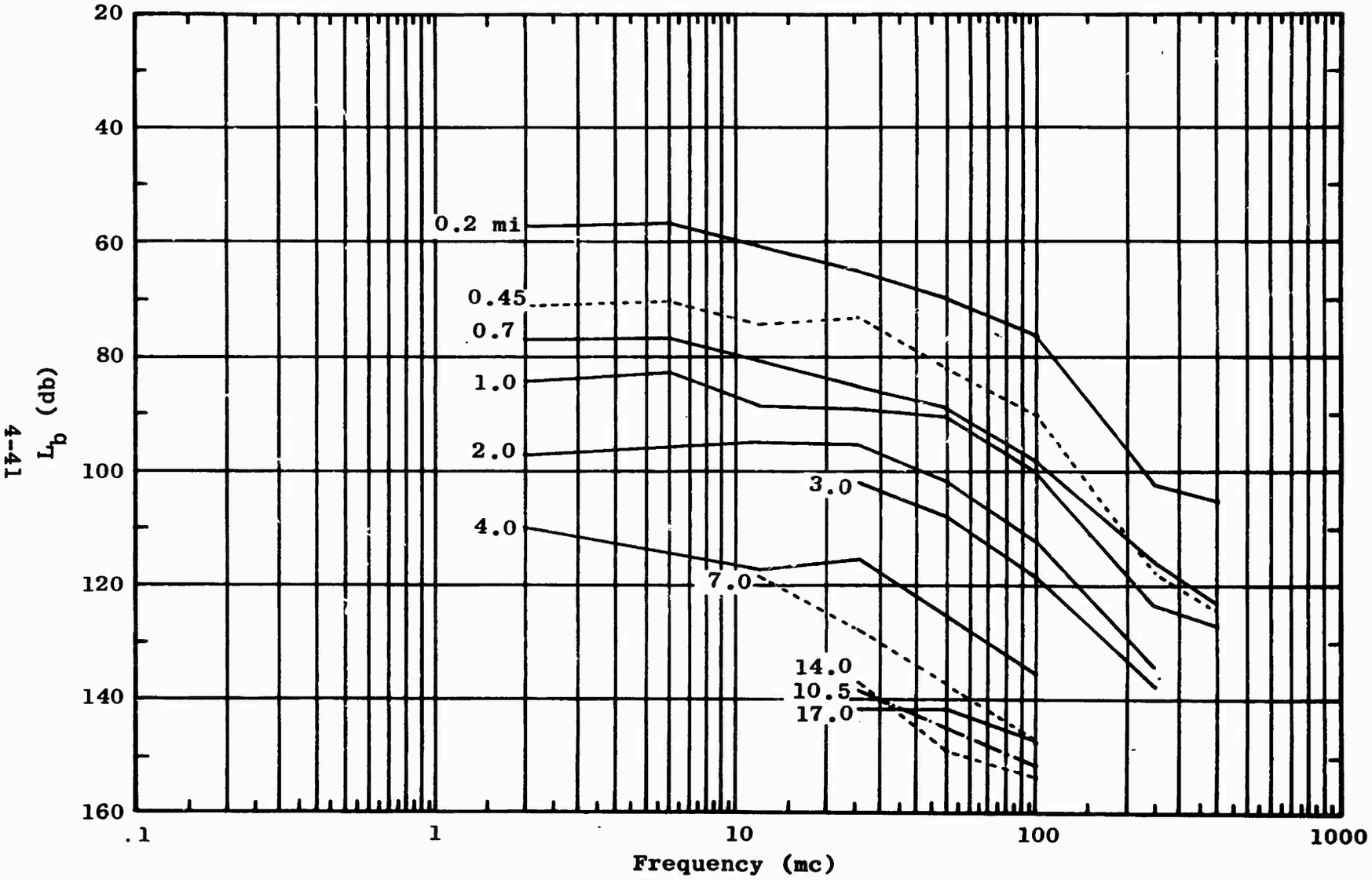

Figure 4.2P Measured Results, L_b Vs Frequency
$L_b = F_A(f, 80, H, d, 20)$

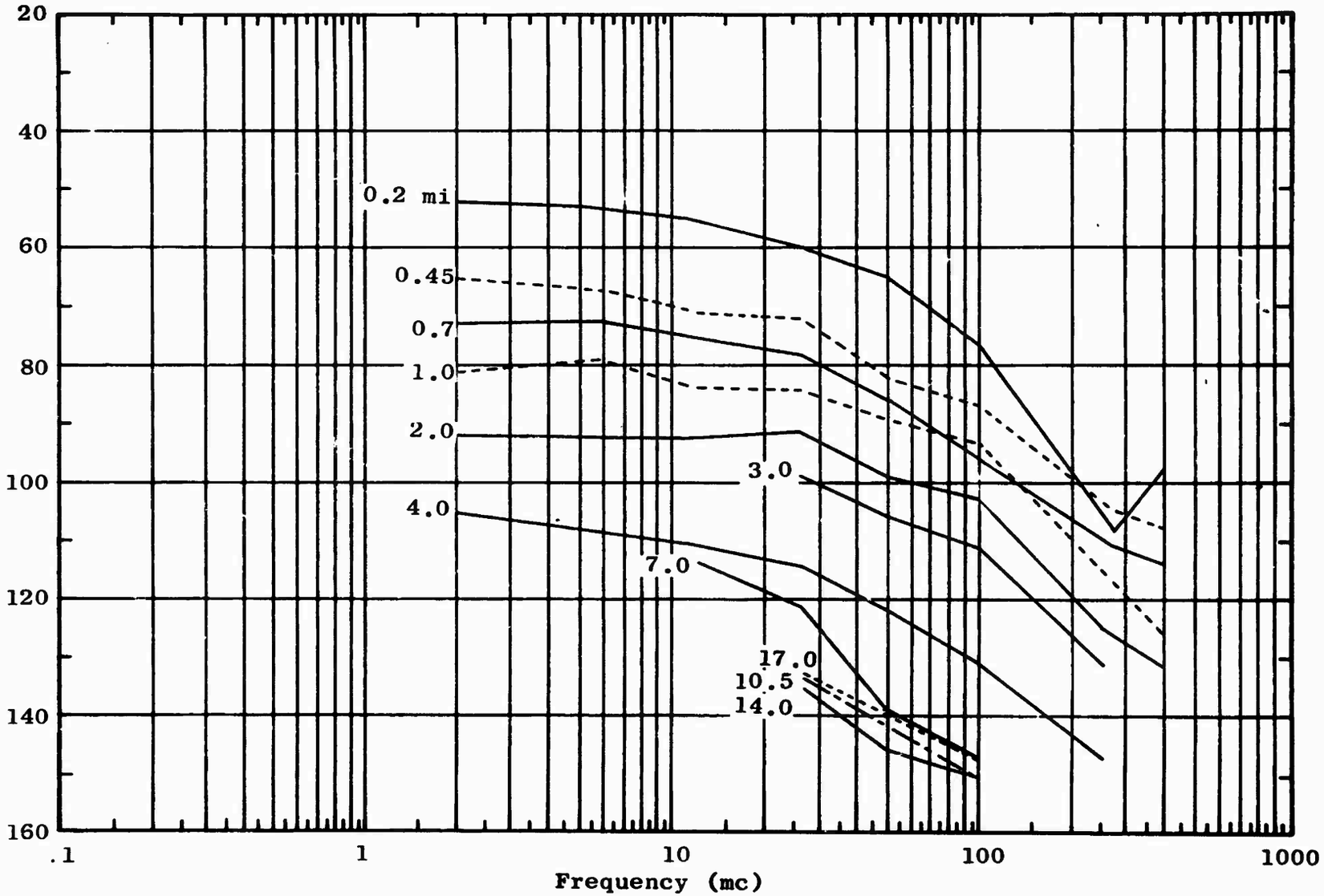

Figure 4.2Q Measured Results, L_b Vs Frequency
$L_b = F_A(f, 80, H, d, 40)$

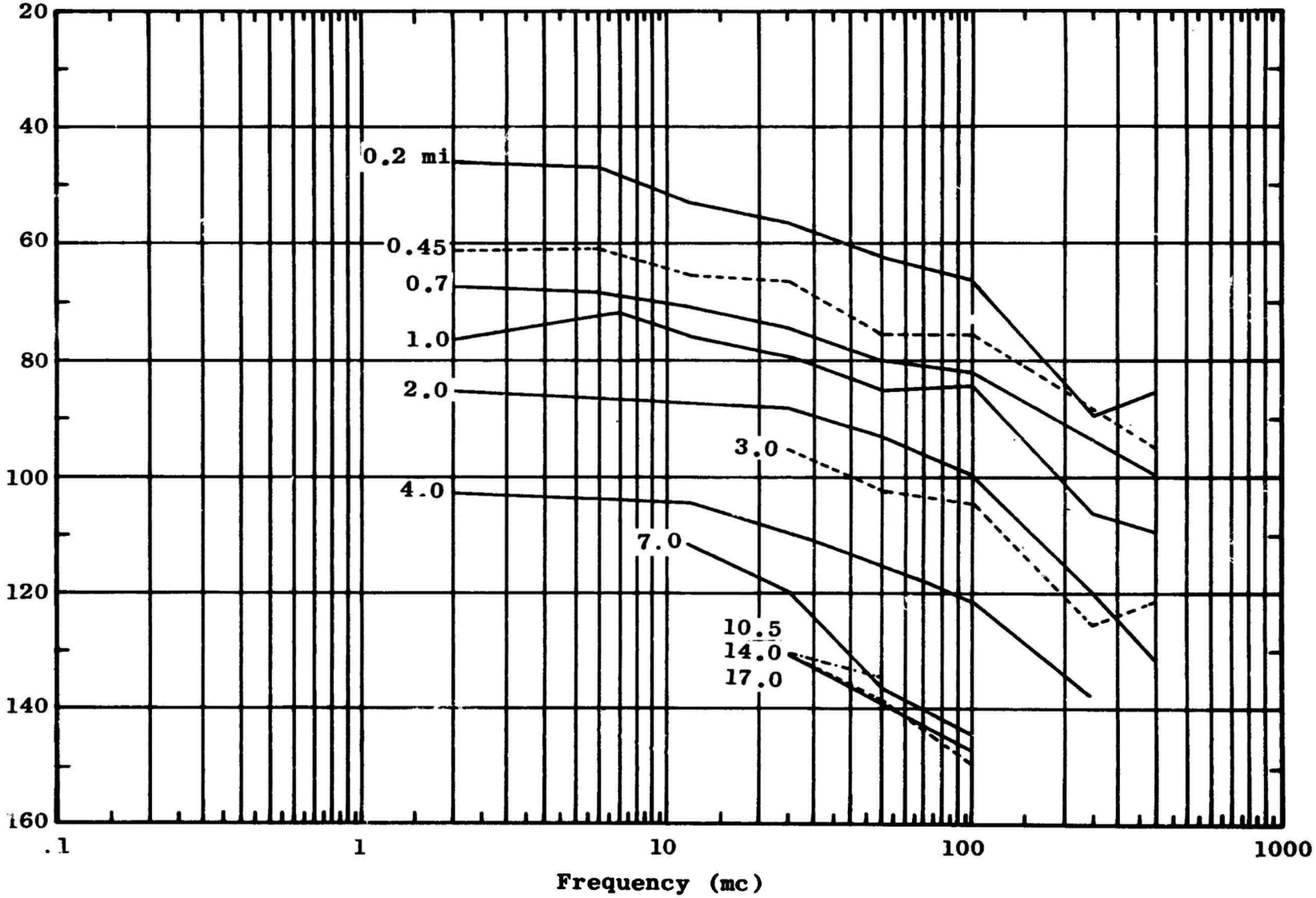

Figure 4.2R Measured Results, L_b Vs Frequency
$L_b = F_A(f, 80, H, d, 80)$

4.2.2 Theoretical Models

The first logical step in any attempt to develop a model which represents radio propagation in vegetated areas is to compare the measured results with values to be expected over similar paths which are not vegetated. Assuming it is possible to adequately describe propagation over unvegetated terrain, the differences are attributable to factors associated with the vegetation. Thus, one problem of considerable importance is a knowledge of propagation over treeless terrain. This problem has received considerable attention for many years. Although this problem has not been solved analytically, there are several possibilities for approximate solutions, a number of which will be given in the following sections.

4.2.2.1 NBS Model

An examination of the terrain profiles for Radial A which are given in Semiannual Report Number 4 indicates that the terrain is such that in the absence of vegetation, the transmitting and receiving antennas would always be intervisible at ranges of less than 1.5 miles. The terrain profiles further show that the two antennas would never be intervisible at ranges beyond 1.5 miles. In this section attention will be directed to the distance ranges beyond the radio horizon, i.e., ranges greater than 1.5 miles. In October 1955 Norton, Rice and Vogler published a paper designed to provide simple formulas suitable for estimating median transmission loss for paths extending beyond the

radio horizon.[1] These methods appear most recently in NBS Technical Note 101.[2]

Two general types of propagation paths are possible for Radial A at a separation distance of 1.5 miles or more. The first consists of those paths for which the transmitting and receiving antennas have the same radio horizon. The second consists of those paths for which the transmitting and receiving antennas have different radio horizons. In the first case the path is looked upon as a knife edge and in the second case the path is simply called a "rough-earth" path.

For knife-edge calculations the following loss formula is used.

$$L_{bk} = 36.57 + 20 \log d_{mi} + 20 \log f_{mc} + A(V) - G(\bar{H}_{te}) - G(\bar{H}_{re}) \quad (2)$$

For rough-earth calculations, the following formula is used.

$$L_{bd} = 10 \log d_{mi} + \frac{1}{2}C\left[K(k_{te}),b^{\circ}\right] + \frac{1}{2}C\left[K(k_{re}),b^{\circ}\right] + 16.67 \log f_{mc} - G\left[\bar{H}_t(k_{te})\right] - G\left[\bar{H}_r(k_{re})\right] + 10 \log C_o(k_t) + 10 \log C_c(k_r) + 488.69 f_{mc}^{\frac{1}{3}} \beta_o\left[K(k_t),b^{\circ}\right] C_o(k_t)\alpha_1 + \beta_o\left[K(k_r),b^{\circ}\right] C_o(k_r)\beta_1 \text{ db} \quad (3)$$

---

1. K. A. Norton, P. L. Rice, L. E. Vogler, "The Use of Angular Distance in Estimating Transmission Loss and Fading Range for Propagation Through a Turbulent Atmosphere Over Irregular Terrain," Proc. IRE, October 1955.

2. NBS Technical Note 101, "Transmission Loss Predictions for Tropospheric Communication Circuits," May 7, 1965.

The rather complicated terms in these two equations are presented and explained in Semiannual Report Number 2. These equations have been programmed on a digital computer and many comparisons have been made between measured and computed results. The results of the comparisons have neither conclusively supported nor invalidated the theoretical model, as will be demonstrated shortly. Much of the uncertainty arises from the factors $G(\bar{H}_{te})$ and $G(\bar{H}_{re})$, which appear in both the rough-earth and knife-edge equations. The function $G(\bar{H}_{te})$ represents in part the effects of reflection between the transmitting antennas and the terrain obstacle which forms the radio horizon for the transmitting antenna. This function is intimately dependent upon terrain details between the transmitter and its radio horizon. In addition, definite criteria as to when the function is to be used and when it is not to be used are not available. The function $G(\bar{H}_{re})$ includes the effects of reflection between the receiving antenna and the terrain obstacle which forms its radio horizon. There is the same uncertainty as to the applicability of $G(\bar{H}_{re})$ as with the applicability of $G(\bar{H}_{te})$.

In order to explore the effect of these $G(\bar{H})$ functions, data at 25.5 mc and 100 mc will be used as examples. Figure 4.3 compares measured results and NBS theoretical results. The points on the theoretical curve marked K correspond to points at which a knife edge was assumed to exist, i.e., where the transmitting and receiving antennas had common radio horizons. The points on the theoretical curve marked R correspond to points at which rough-earth conditions prevailed, i.e., points at which the two antennas had different radio horizons. Figure 4.3 shows that in many cases the theoretical loss is greater than measured loss. Figure 4.4 shows a similar comparison between measured data and the NBS model without the $G(\bar{H})$ functions. Figures 4.5

and 4.6 give a similar set of comparisons for 100 mc.

At each distance there are four loss figures which could be deduced from the theoretical model: (1) theory including both $G(\bar{H}_{te})$ and $G(\bar{H}_{re})$, (2) theory including $G(\bar{H}_{te})$ only, (3) theory including $G(\bar{H}_{re})$ only and (4) theory with neither of the $G(\bar{H})$ functions. Since there is a great deal of uncertainty as to just when the $G(\bar{H})$ functions are to be applied and when they are not, it is logical to ask if there is some combination of possible choices at each distance which fits the data well. First to be considered is the case of the closest possible fit to the measured data. Figure 4.7 shows the result of choosing the best possible fit from the four theoretical choices for path loss available at each distance. A theoretical point is marked T, if the theoretical calculation included $G(\bar{H}_{te})$ but not $G(\bar{H}_{re})$. A theoretical point is marked R if the reverse is true. If the point is marked, T,R, both functions were used, and if the point is not marked, neither function was used. Figure 4.7 applies to 25.5 mc. A similar comparison is shown in Figure 4.8 for 100 mc.

On the assumption that there is some effect from the vegetation, the same experiment was tried again with the goal of obtaining a best theoretical fit corresponding to a loss of approximately 10 db less than the measured data. The agreement was excellent for 25.5 mc, as is shown in Figure 4.9. The results at 100 mc are shown in Figure 4.10.

Results of the type shown in Figures 4.3 through 4.6 indicate that the theoretical formulas are not completely suitable as they now stand. However, results of the type shown in Figures 4.7 through 4.10 indicate that the methods might be applicable if proper criteria governing the use of the $G(\bar{H})$ functions could be established. This matter is receiving further study.

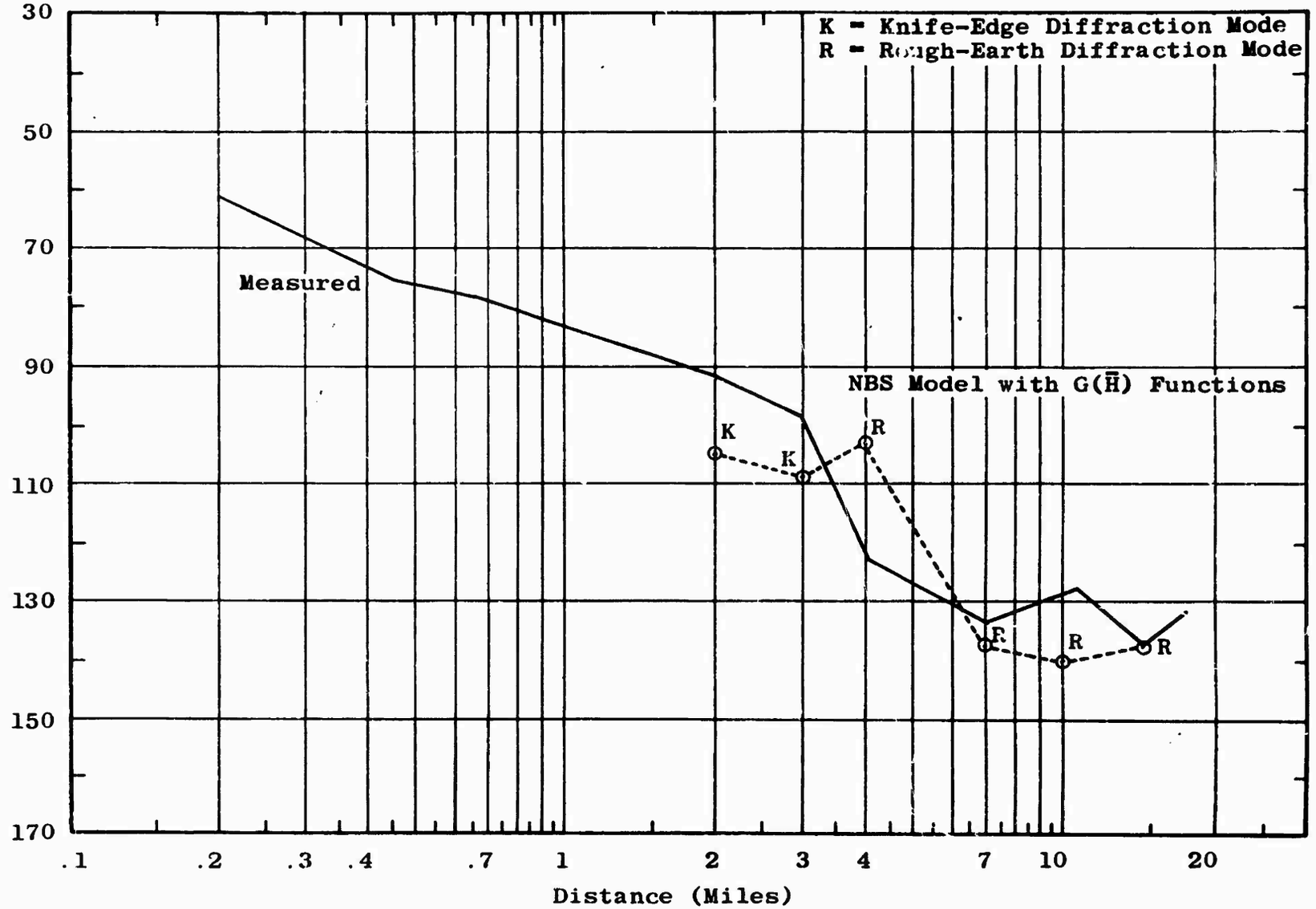

Figure 4.3 Comparison Between Measured Results and NBS Model Including $G(\bar{H})$ Functions
$L_b = F_A(25.5, 80, V, d, 80)$

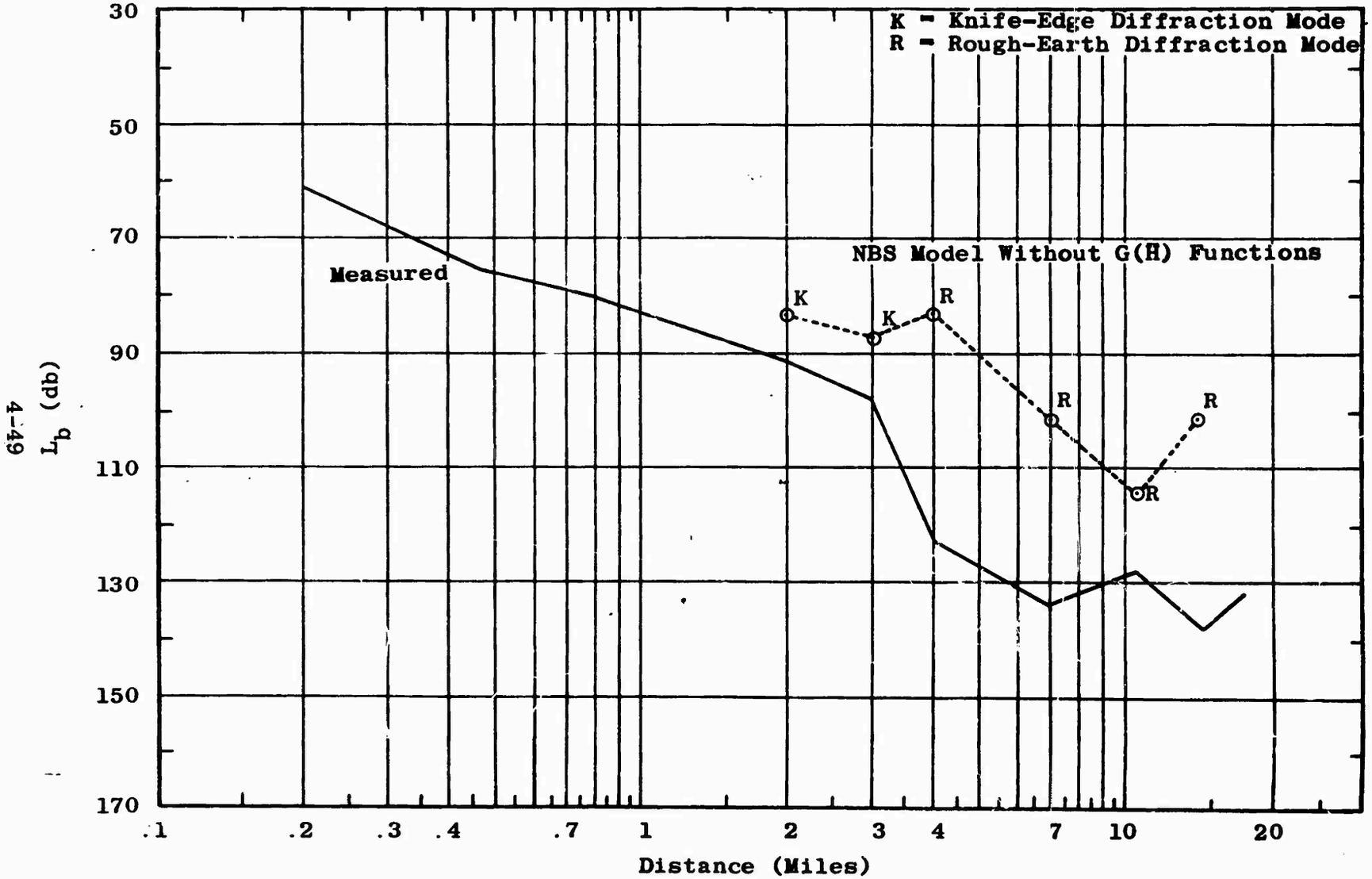

Figure 4.4 Comparison Between Measured Results and NBS Model Without G(H) Functions
$L_b = F_A(25.5, 80, V, d, 80)$

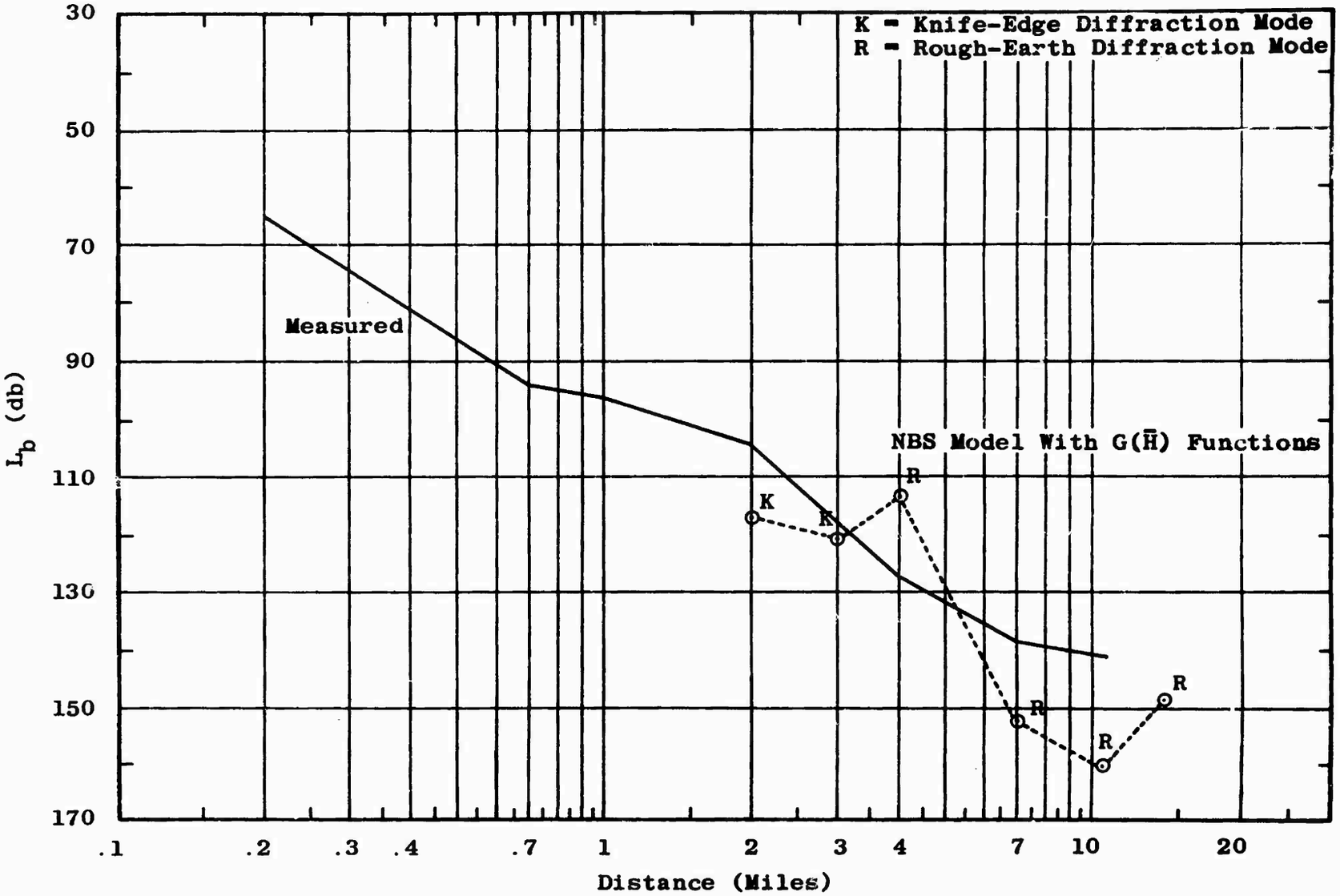

Figure 4.5 Comparison Between Measured Results and NBS Model Including $G(\bar{H})$ Functions
$L_b = F_A(100, 80, V, d, 80)$

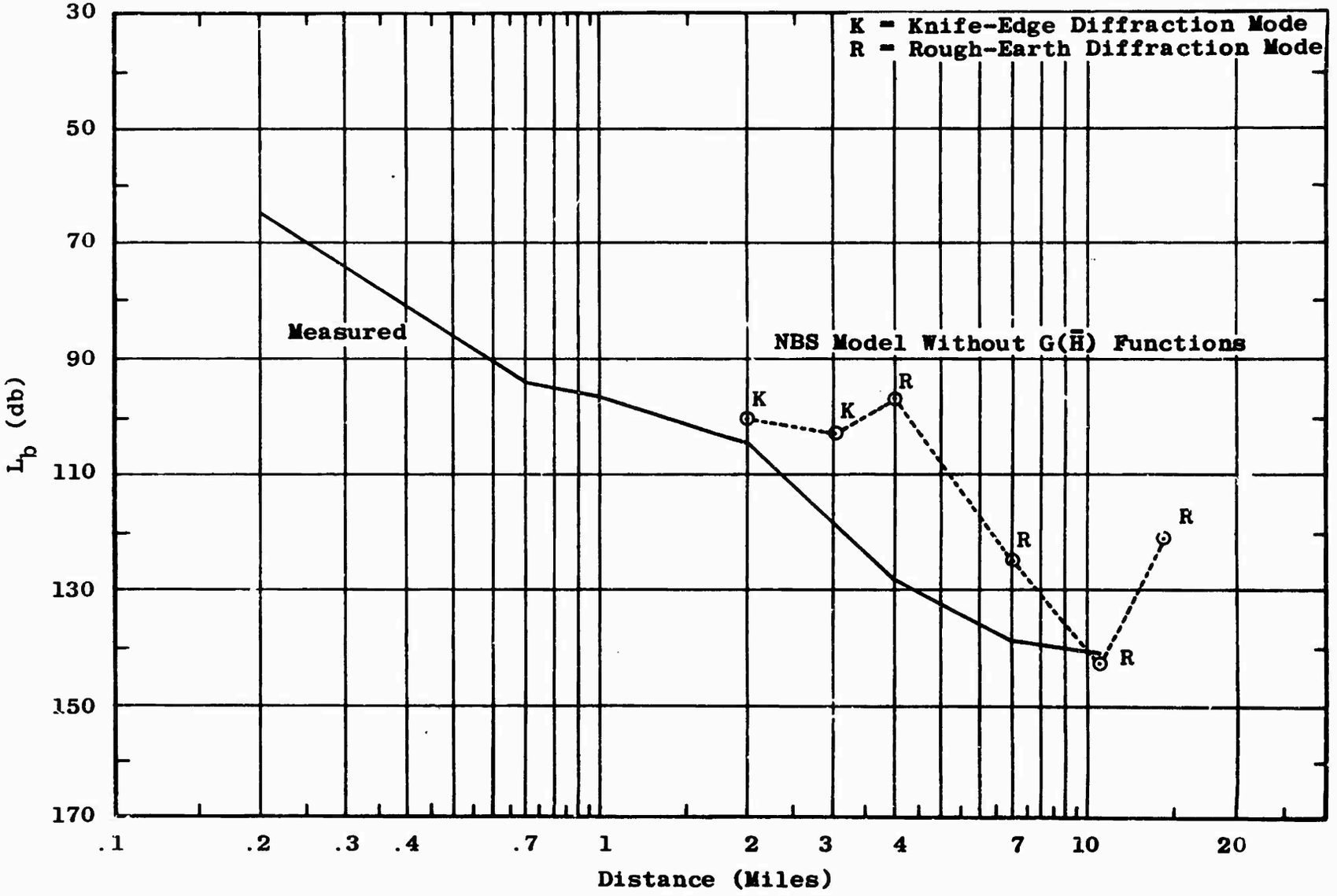

Figure 4.6 Comparison Between Measured Results and NBS Model Without G(H̄) Functions
$L_b = F_A(100, 80, V, d, 80)$

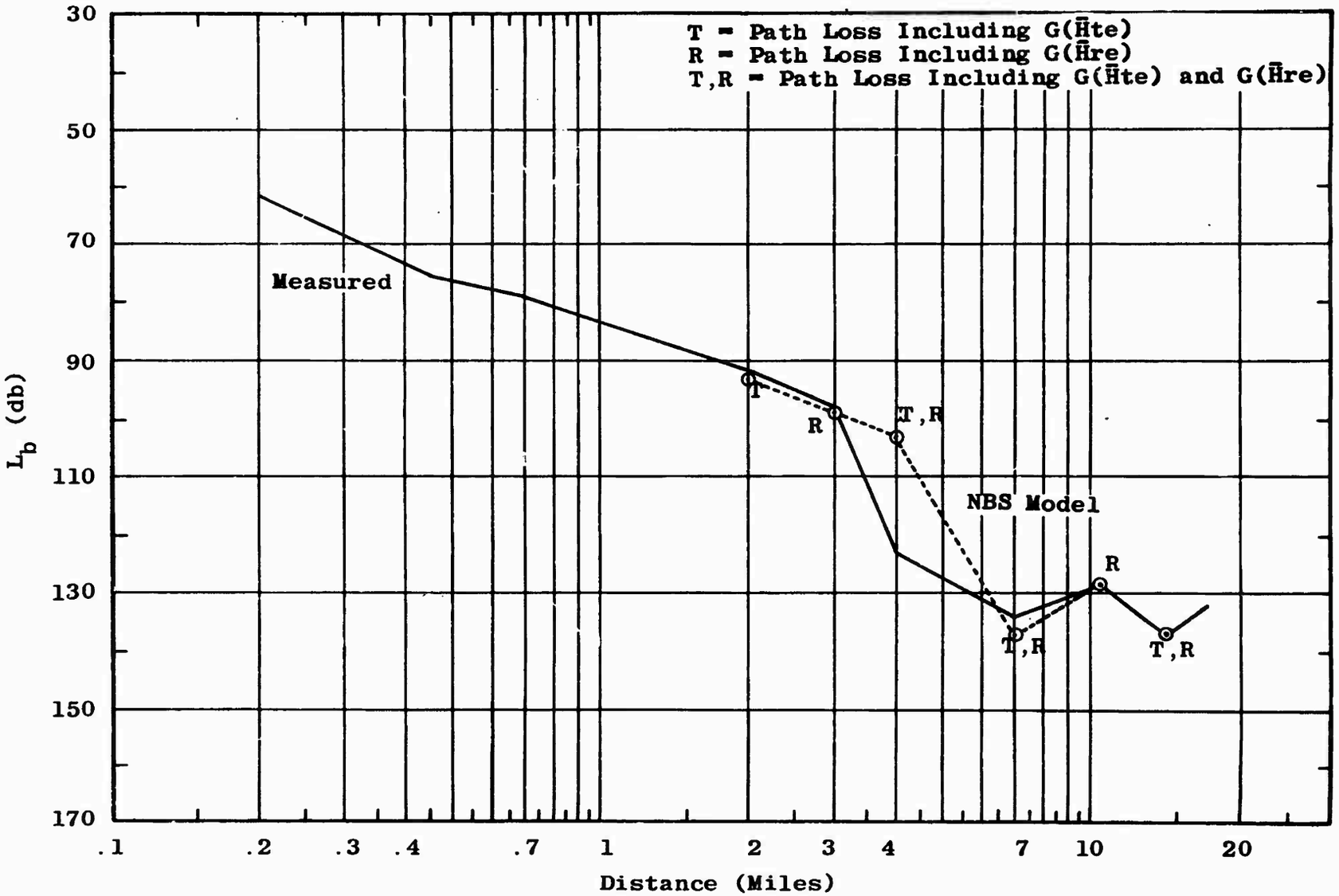

Figure 4.7 Best Fit to Measured Results
$L_b = F_A(25.5, 80, V, d, 80)$

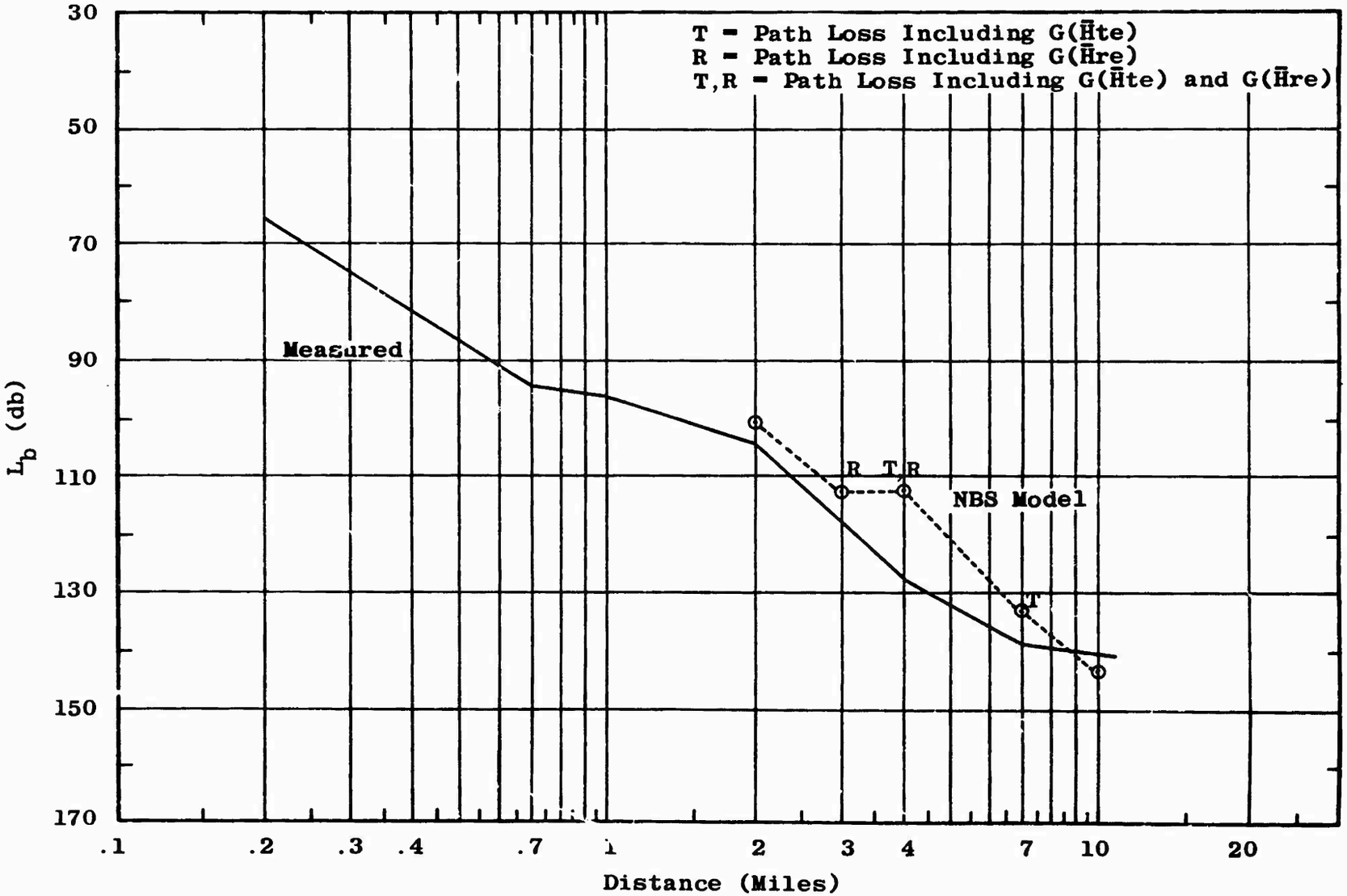

Figure 4.8 Best Fit to Measured Results
$L_b = F_A(100, 80, V, d, 80)$

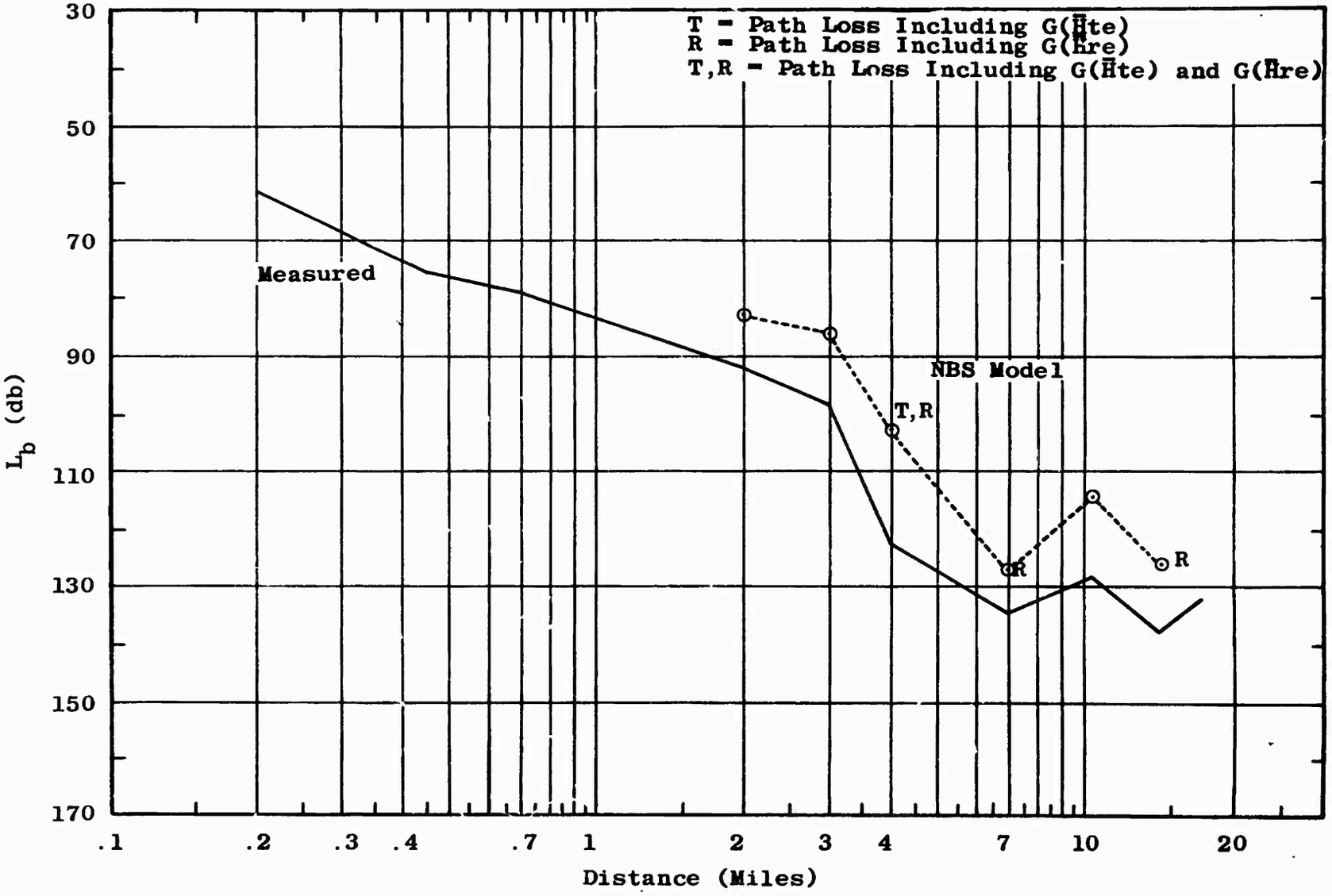

Figure 4.9 Best Fit 10 db Below Measured Results
$L_b = F_A(25.5, 80, V, d, 80)$

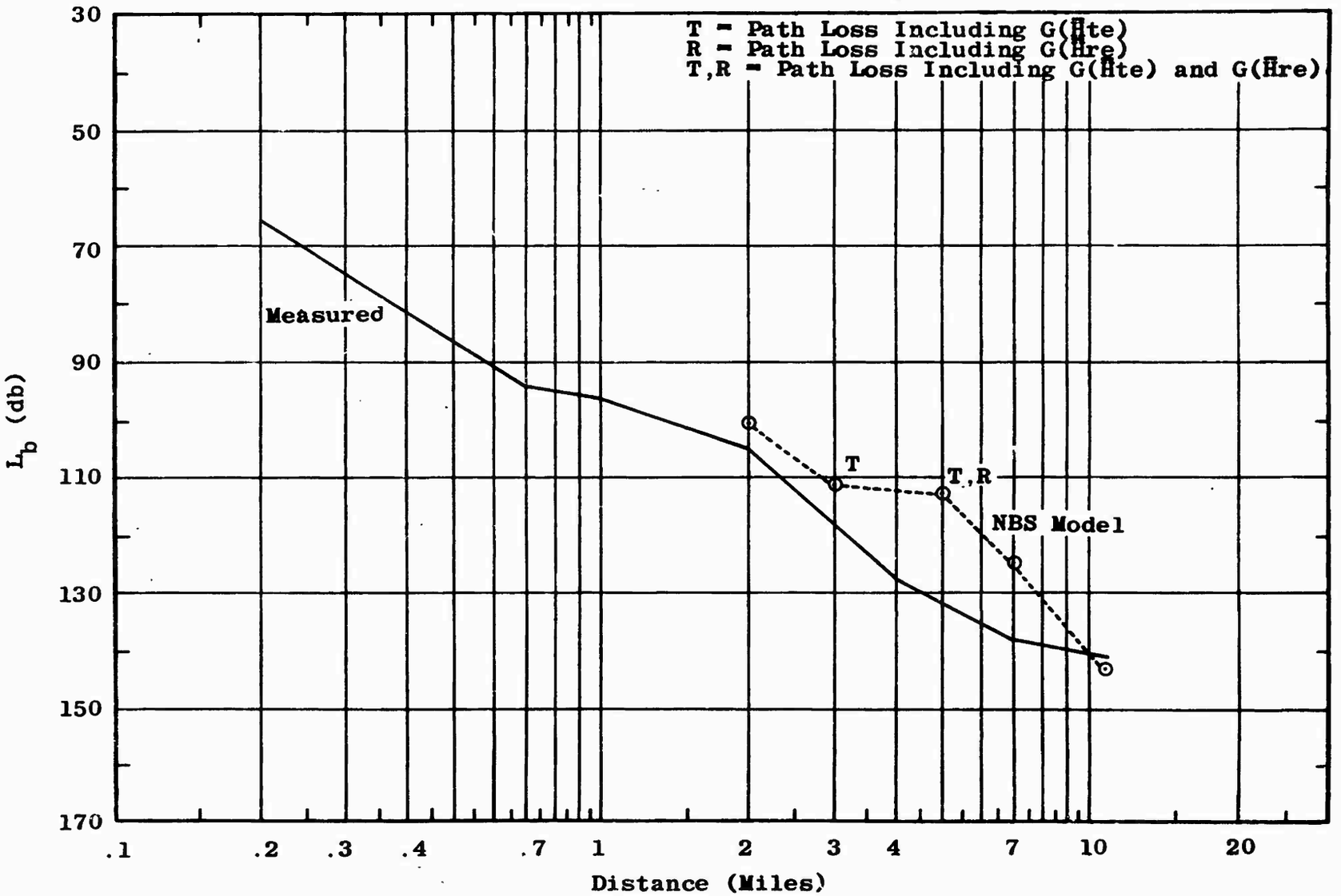

Figure 4.10 Best Fit 10 db Below Measured Results
$L_b = F_A(100, 80, V, d, 80)$

4.2.2.2 Computer-Induced Statistical Terrain Model

The NBS model is being explored with the hope that it will predict terrain effects with reasonable accuracy when terrain details are known. In this way a realistic assessment of the effect of vegetation may be made.

The NBS methods are relatively complex and require a detailed knowledge of terrain. It is not anticipated that the method would ever be practical for operational predictions. However, the model, if valid, could be used to artificially sample a range of possible terrain profiles and generate a statistic which realistically represents the propagation over rough terrain.

One attempt has been made to generate a statistic with the NBS model. Ten straight-line radials were drawn from the transmitting site through the area occupied by Radial A. The 10 radials cover Trail A as shown in Figure 4.11. Propagation loss was calculated by means of a computer as a function of distance along each of the 10 radials. A sample of the results is shown in Figure 4.12. The results shown in Figure 4.12 include both $G(\bar{H})$ functions. The primary information of interest is the median value and range of loss values at each distance. As Figure 4.12 shows, the range of possible loss values as predicted by the NBS model is quite large. The data which has been obtained in this way is referred to as the "computer-induced statistic."

Figure 4.13 compares measured data at 25.5 mc and the median of the computer-induced statistic, including and excluding the $G(\bar{H})$ functions. Figure 4.14 provides the same comparison at 100 mc.

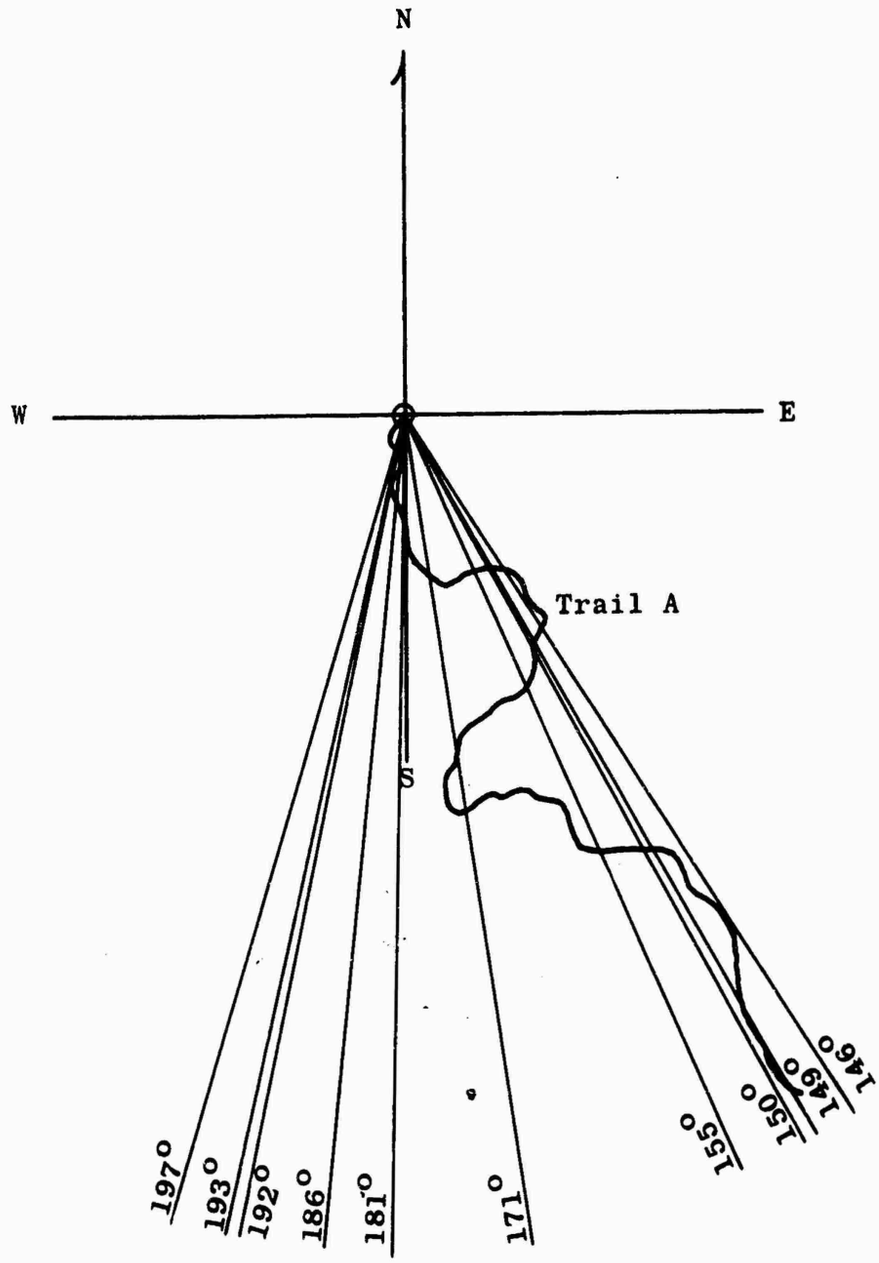

Figure 4.11 Radials Used to Obtain Computer-Induced Statistic

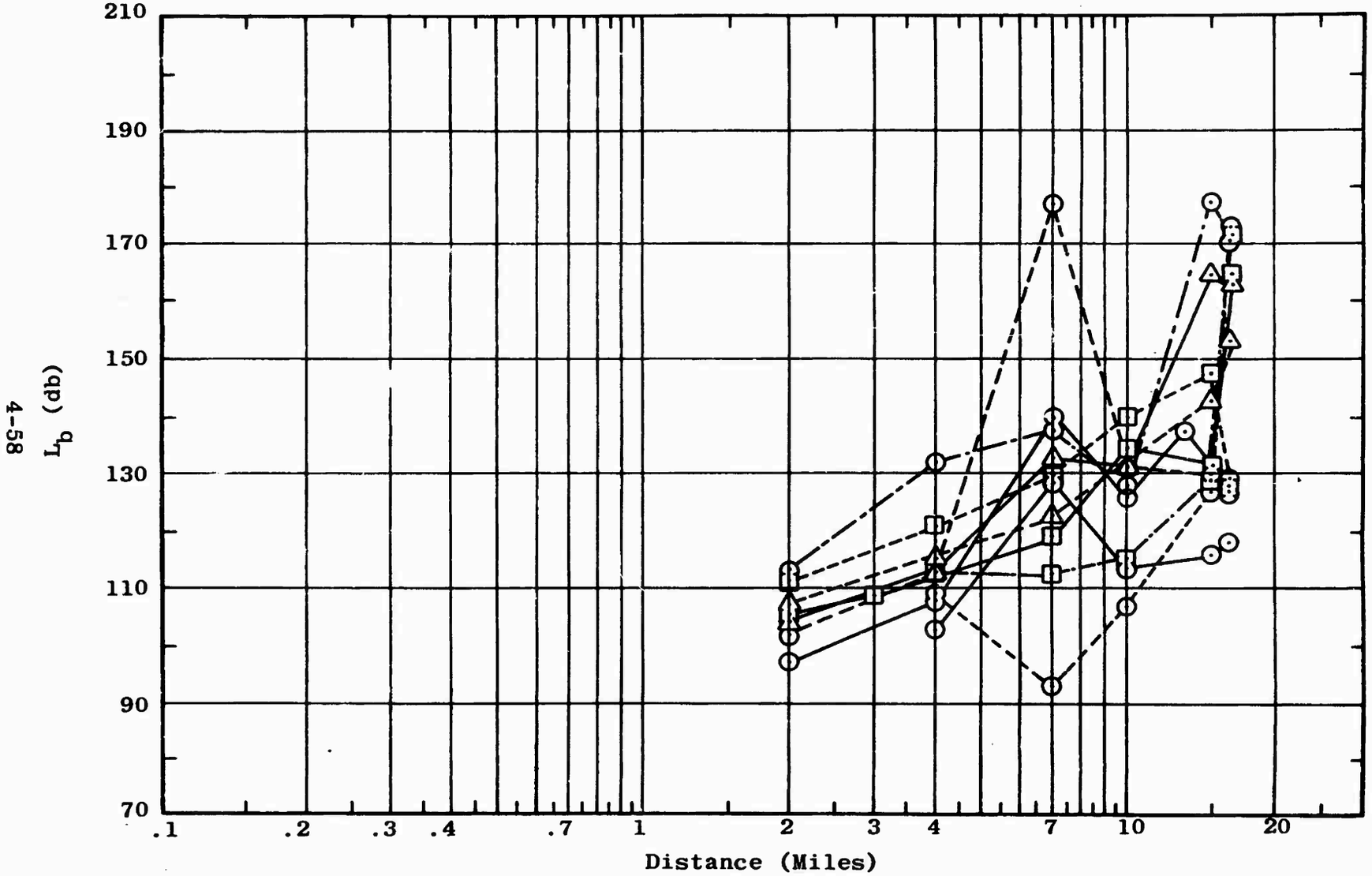

Figure 4.12 Composite of L_b Along Ten Radials
$L_b = F_A(25.5, 80, V, d, 80)$

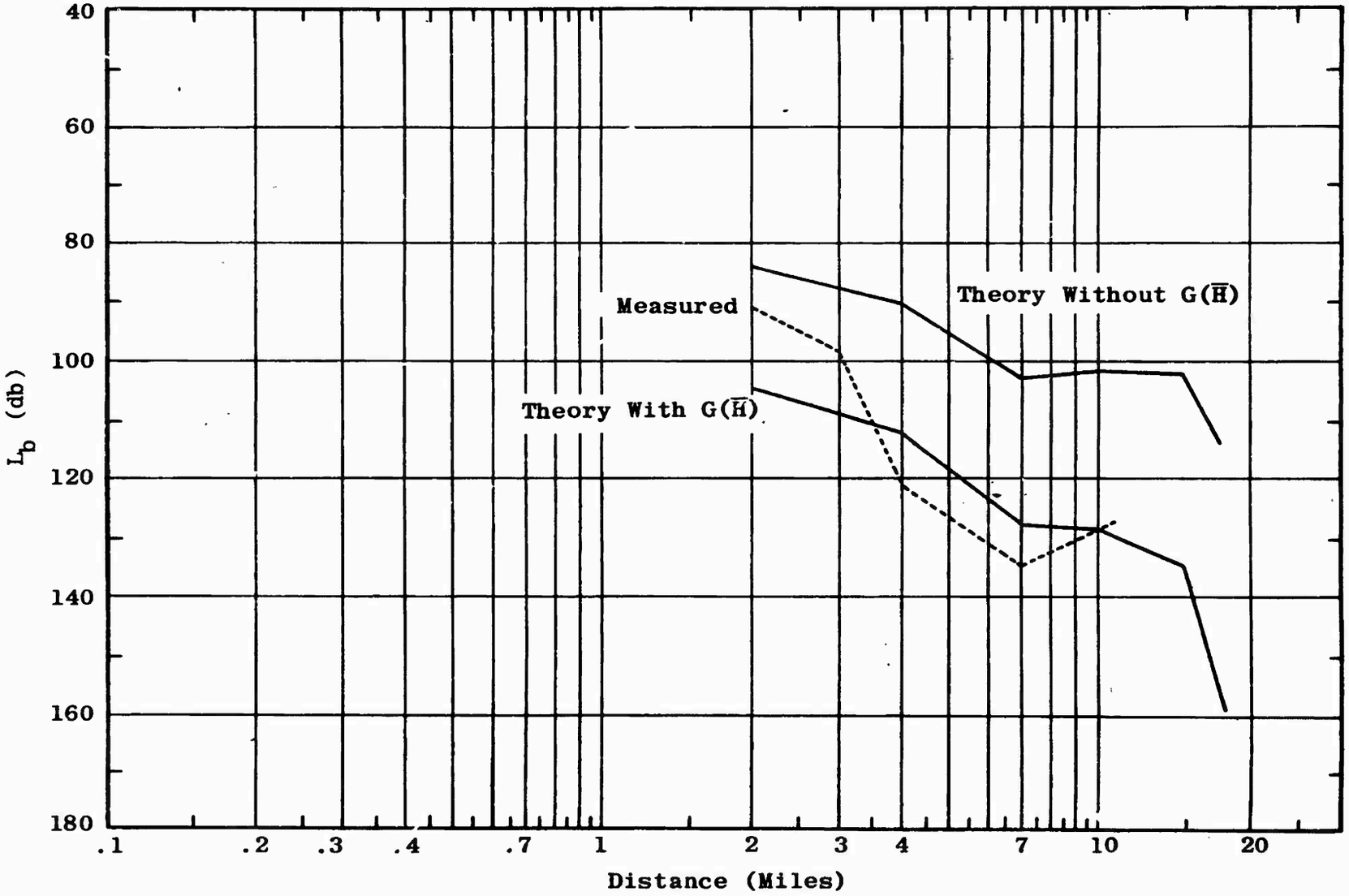

Figure 4.13 Comparison Between Measured Results and Computer-Induced Terrain Statistic $L_b = F_A(25.5, 80, V, d, 80)$

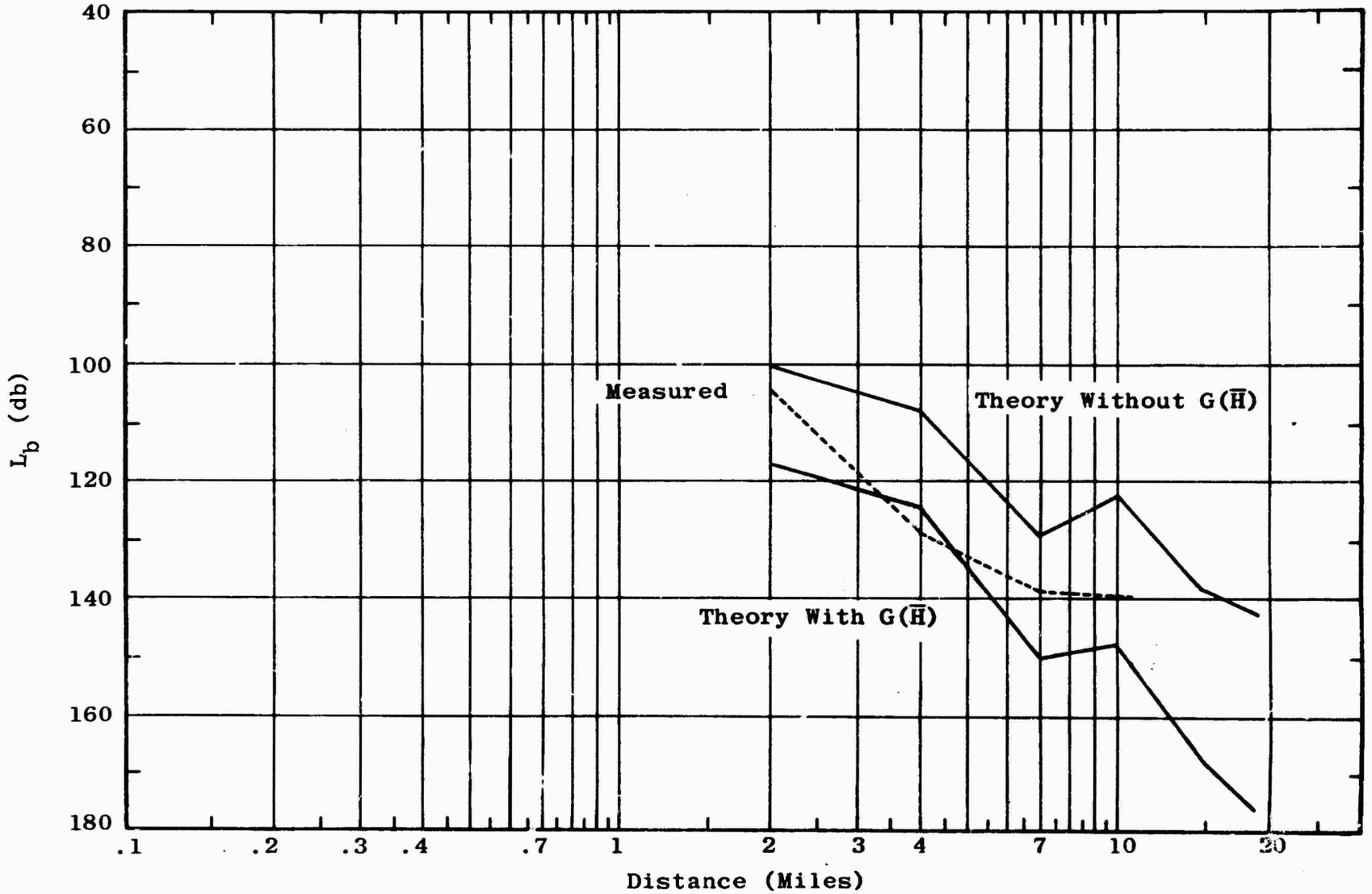

Figure 4.14 Comparison Between Measured Results and Computer-Induced Terrain Statistic $L_b = F_A(100, 80, V, d, 80)$

4.2.2.3 Smooth-Earth Model

The smooth-earth propagation equations presented by Norton[3] in 1941 have been compared with measured data. In the medium high-frequency range and below, the smooth-earth model has been found to closely represent the propagation loss for short distances when the path is void of foliage. Figure 4.15 gives the smooth-earth model for a ground conductivity, σ, of 0.03 mhos per meter and a relative permittivity, ε, of 15. Figures 4.16A through 4.16K compare the smooth-earth model to measured data. For the three low frequencies, two smooth-earth curves are shown. One curve represents a "good" ground while the other is typical of very poor ground. The purpose of plotting the range of loss for extreme values of ground constants was to investigate the possibility of attributing the measured loss, in excess of free-space loss, totally to ground losses. This investigation was not made in the HF range since an apparent foliage effect is present.

In Figure 4.15 the effect of interference between a direct ray and a ground-reflected ray can just begin to be seen. A similar effect is common to the 100-mc measured data although the effect is much more pronounced in the measured data. The smooth-earth model also shows a falling off in the distance range from 0.2 to 0.5 miles at 250 and 400 mc. A similar falling off is found in almost all of the measured 250- and 400-mc data.

---

3. K. A. Norton, "The Calculation of Ground-Wave Field Intensity over a Finitely Conducting Spherical Earth," Proc. IRE, pp. 623-639, December 1941.

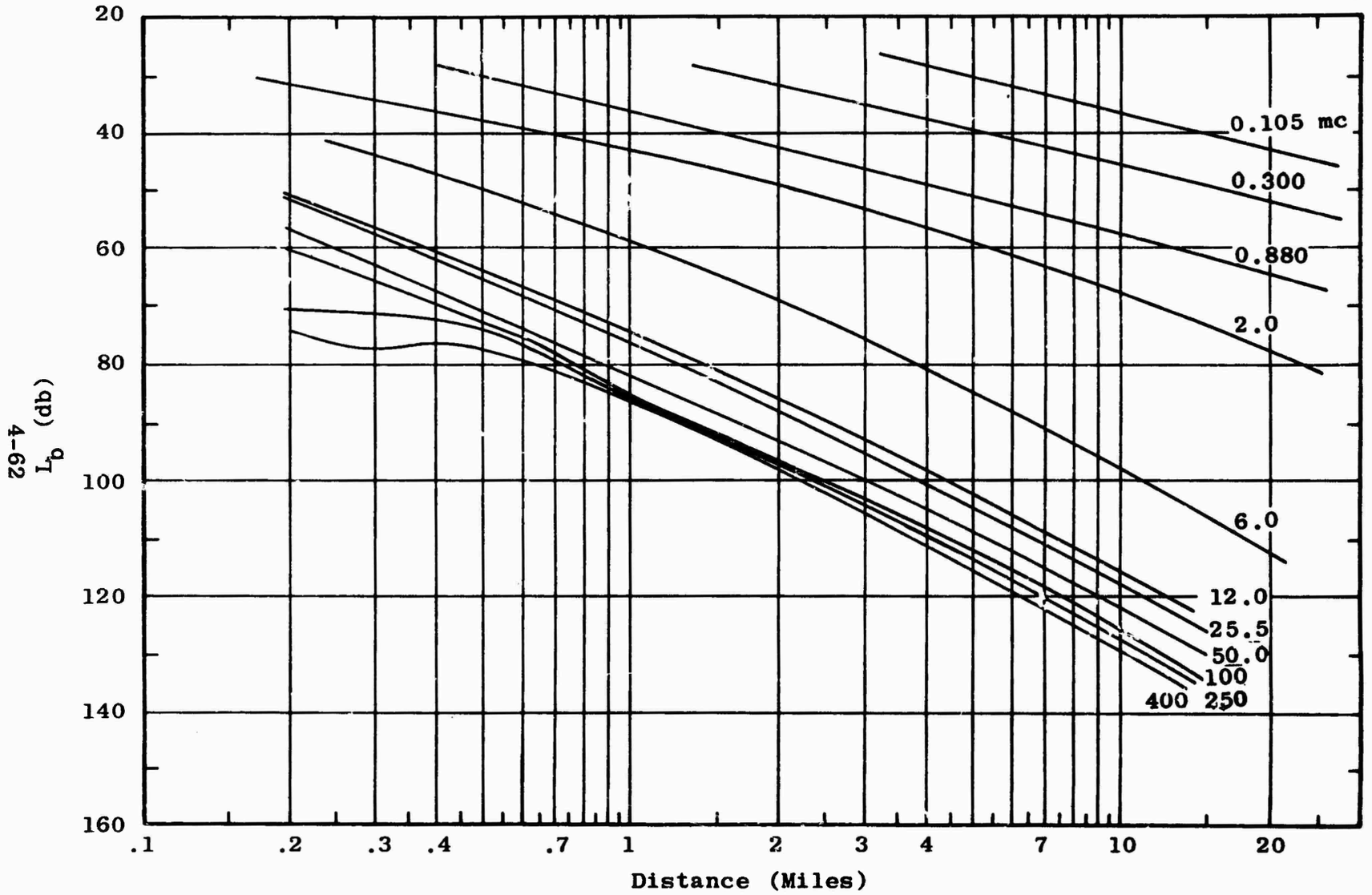

Figure 4.15 Smooth-Earth Model
$L_b = F_A(f, 80, V, d, 20)$

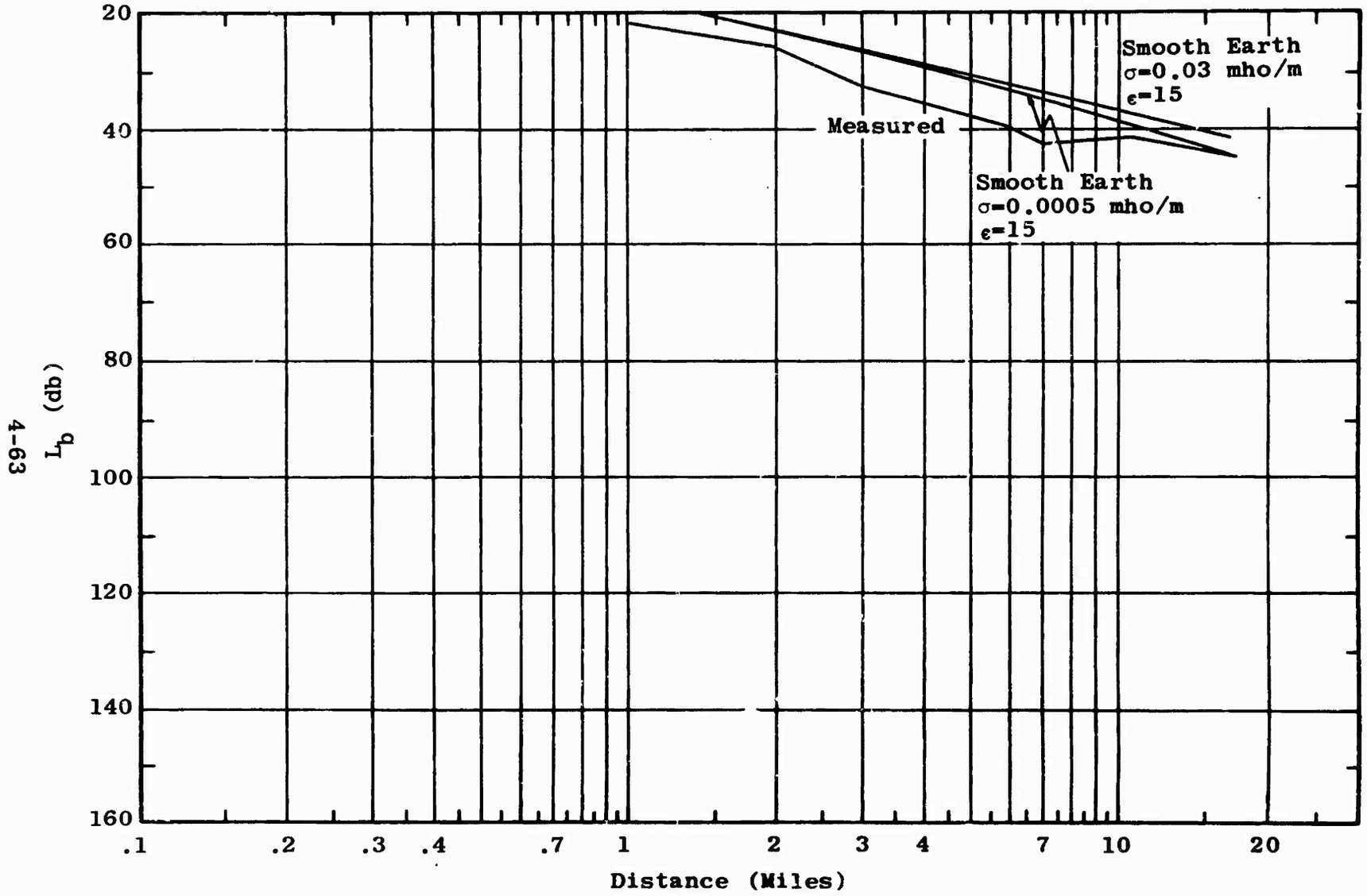

Figure 4.16A Comparison Between Measured Results and Smooth-Earth Model
$L_b = F_A(0.105, 80, V, d, 20)$

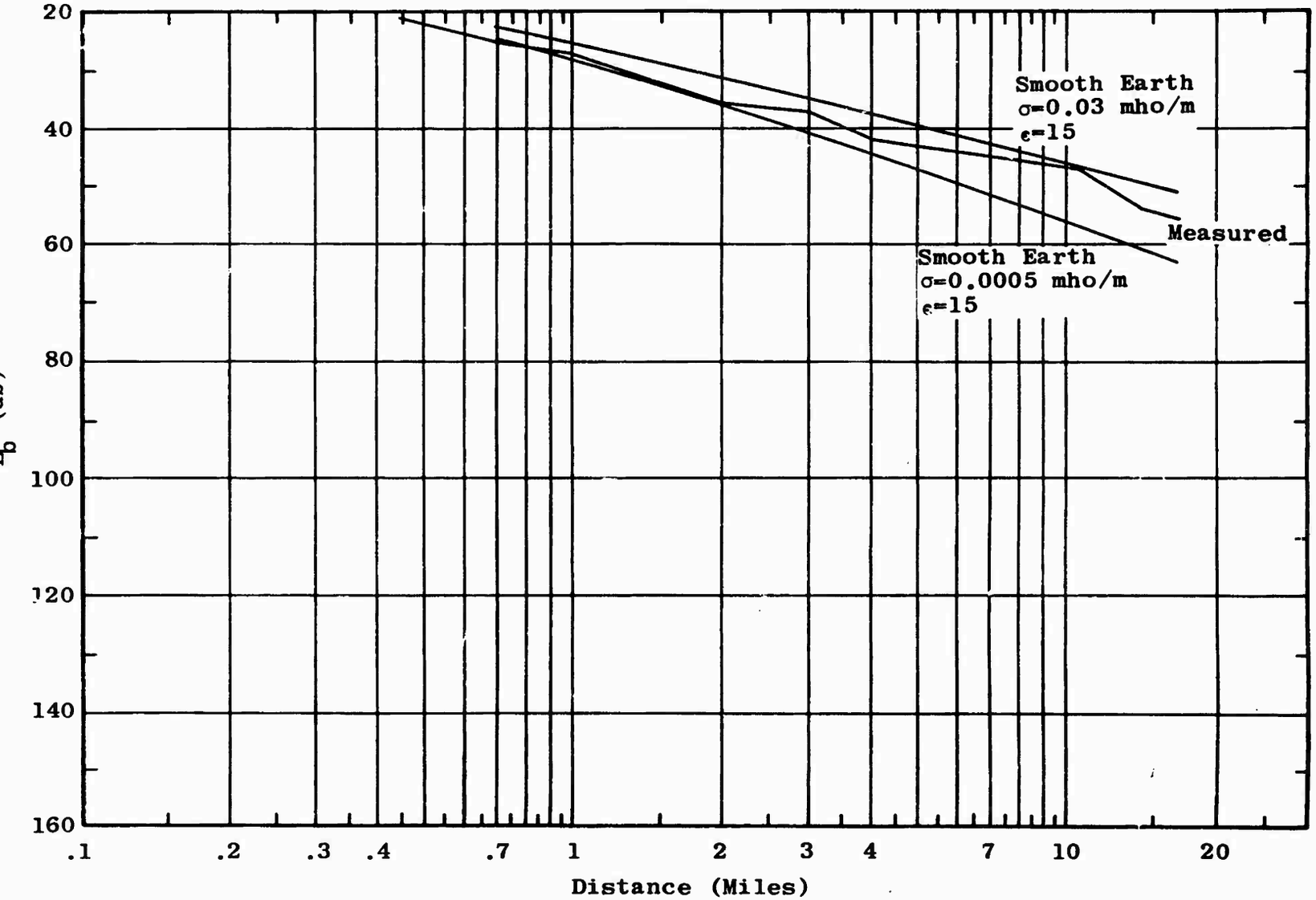

Figure 4.16B Comparison Between Measured Results and Smooth-Earth Model
$L_b = F_A(0.300, 80, V, d, 20)$

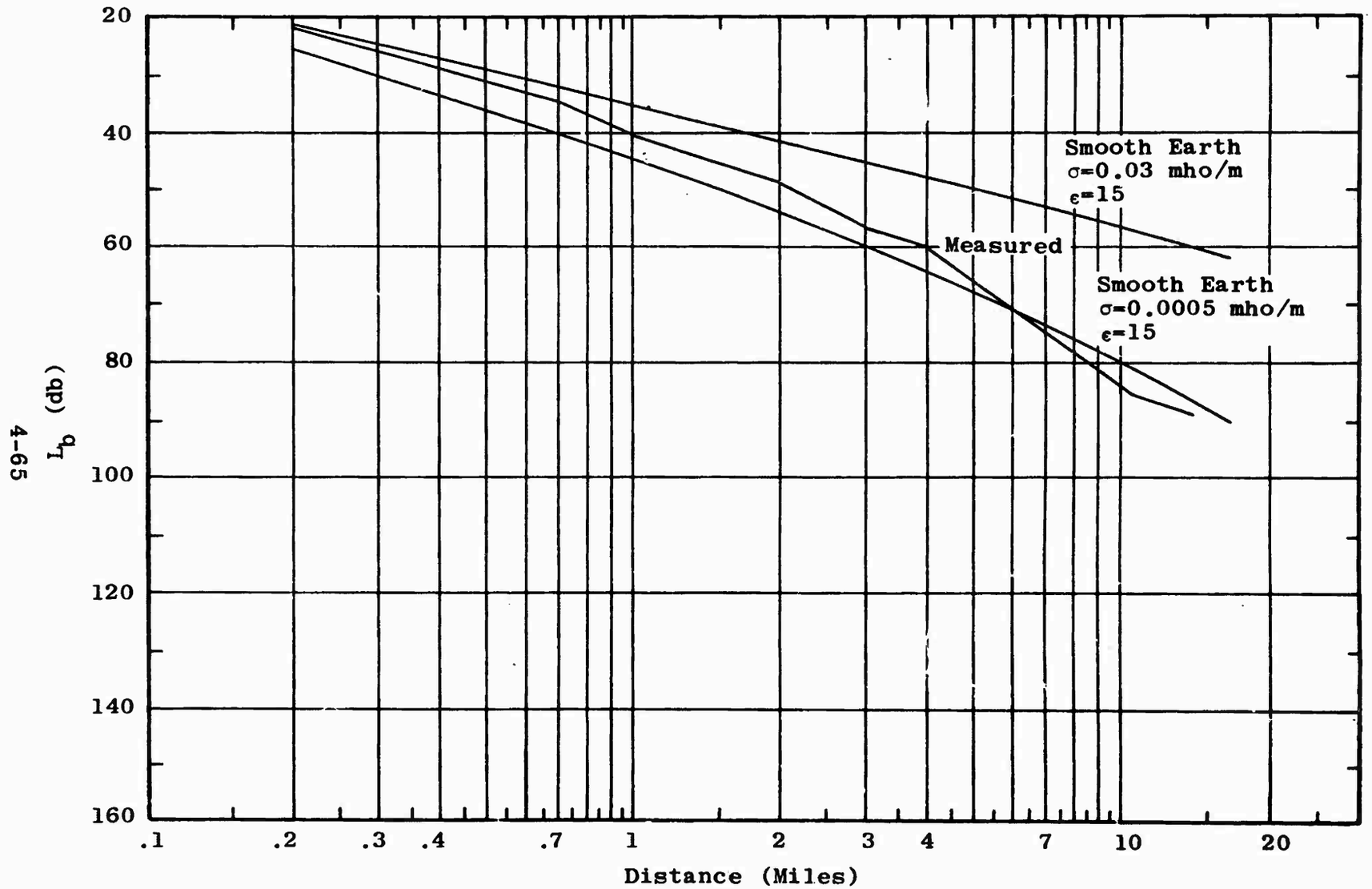

Figure 4.16C Comparison Between Measured Results and Smooth-Earth Model
$L_b = F_A(0.880, 80, V, d, 20)$

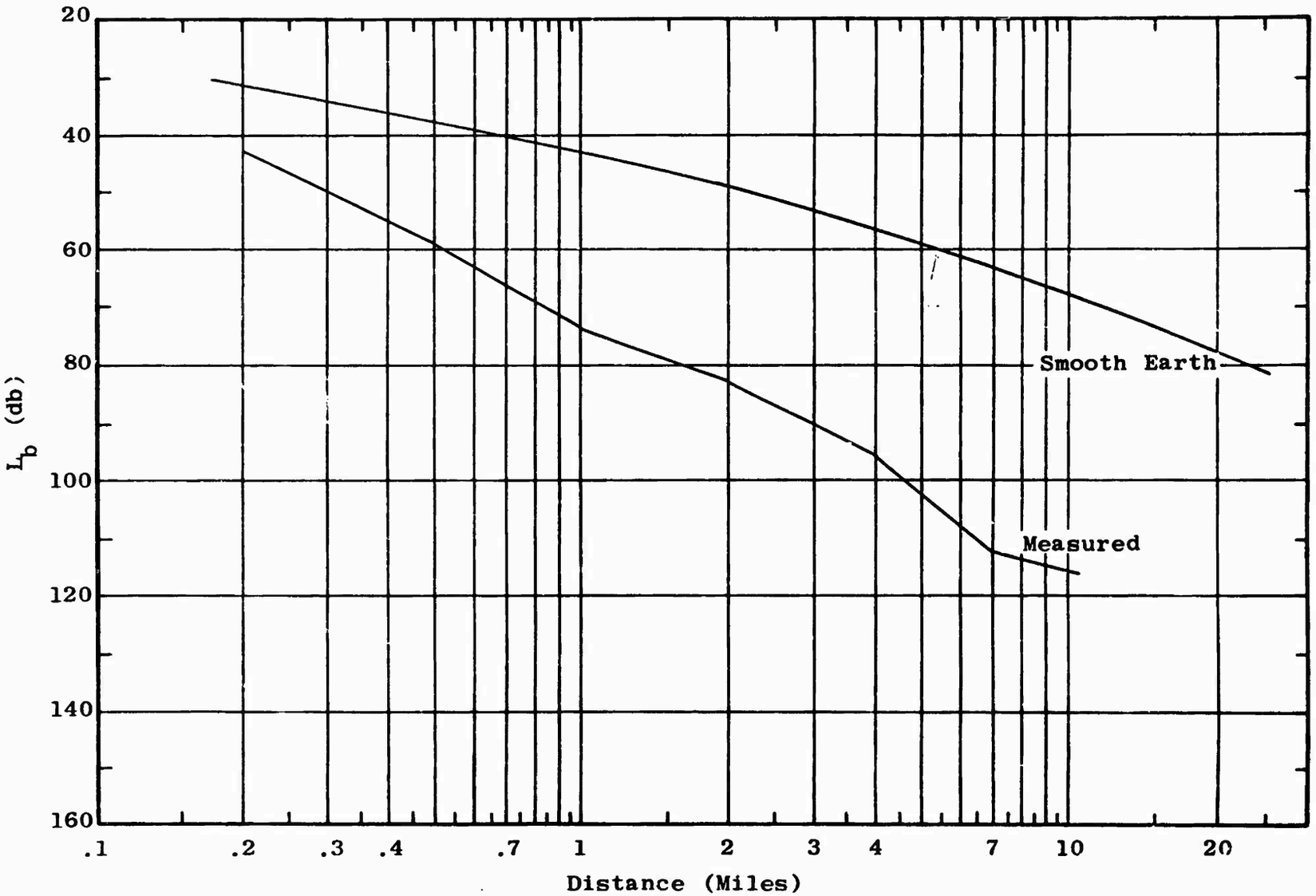

Figure 4.16D Comparison Between Measured Results and Smooth-Earth Model
$L_b = F_A(2.0, 80, v, d, 20)$

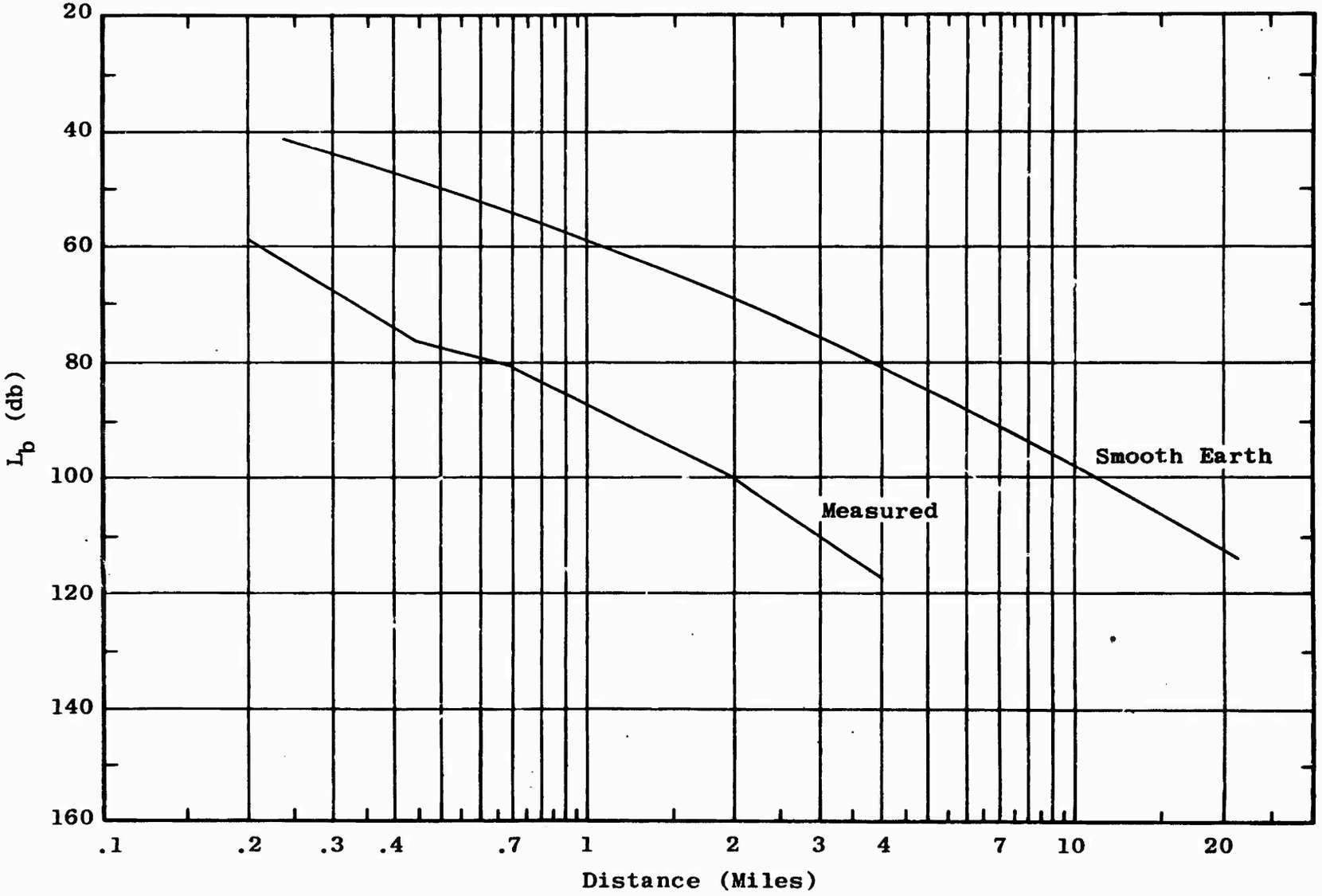

Figure 4.16E Comparison Between Measured Results and Smooth-Earth Model
$L_b = F_A(6.0, 40, V, d, 20)$

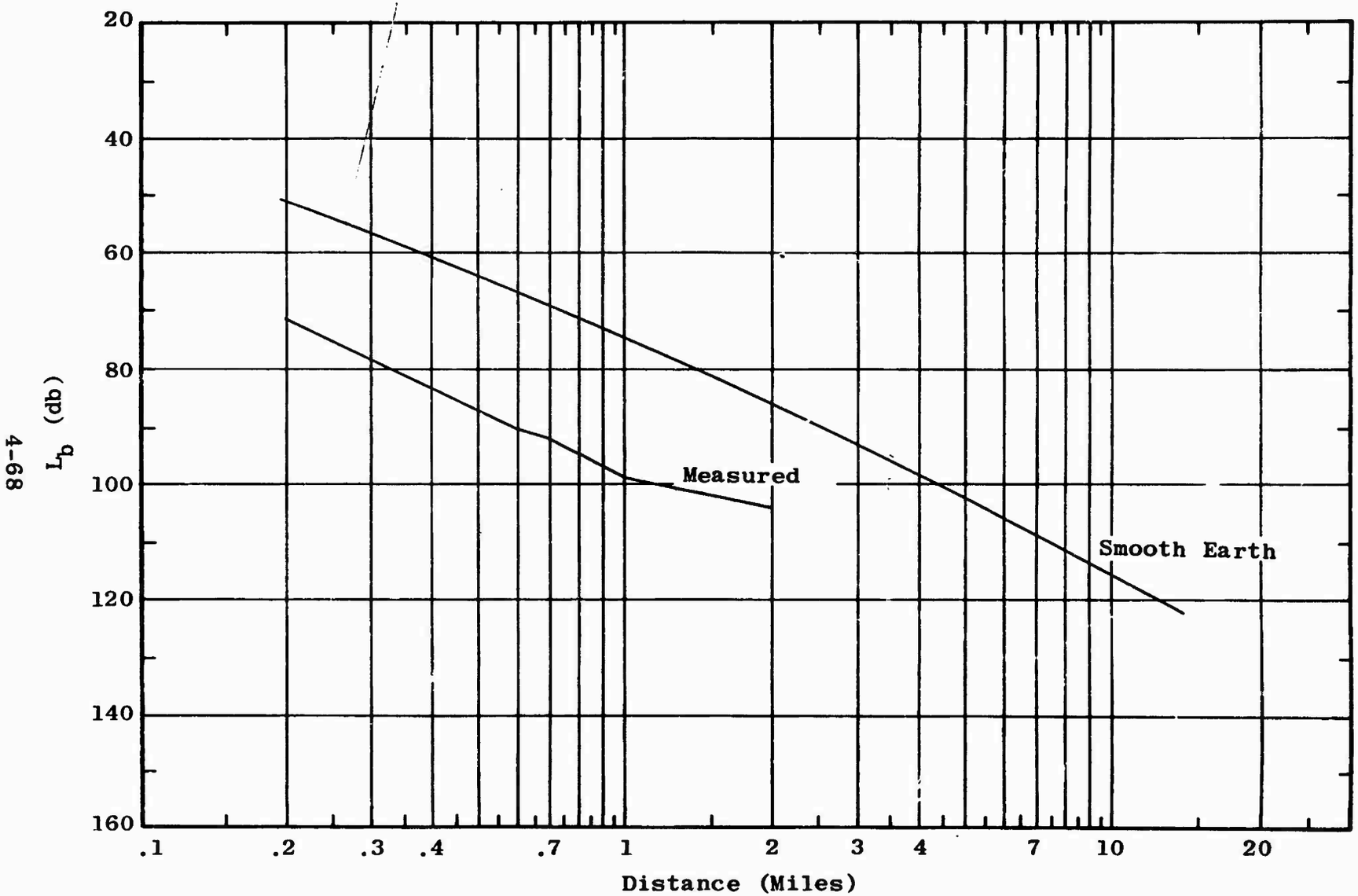

Figure 4.16F Comparison Between Measured Results and Smooth-Earth Model
$L_b = F_A(12.0, 80, V, d, 20)$

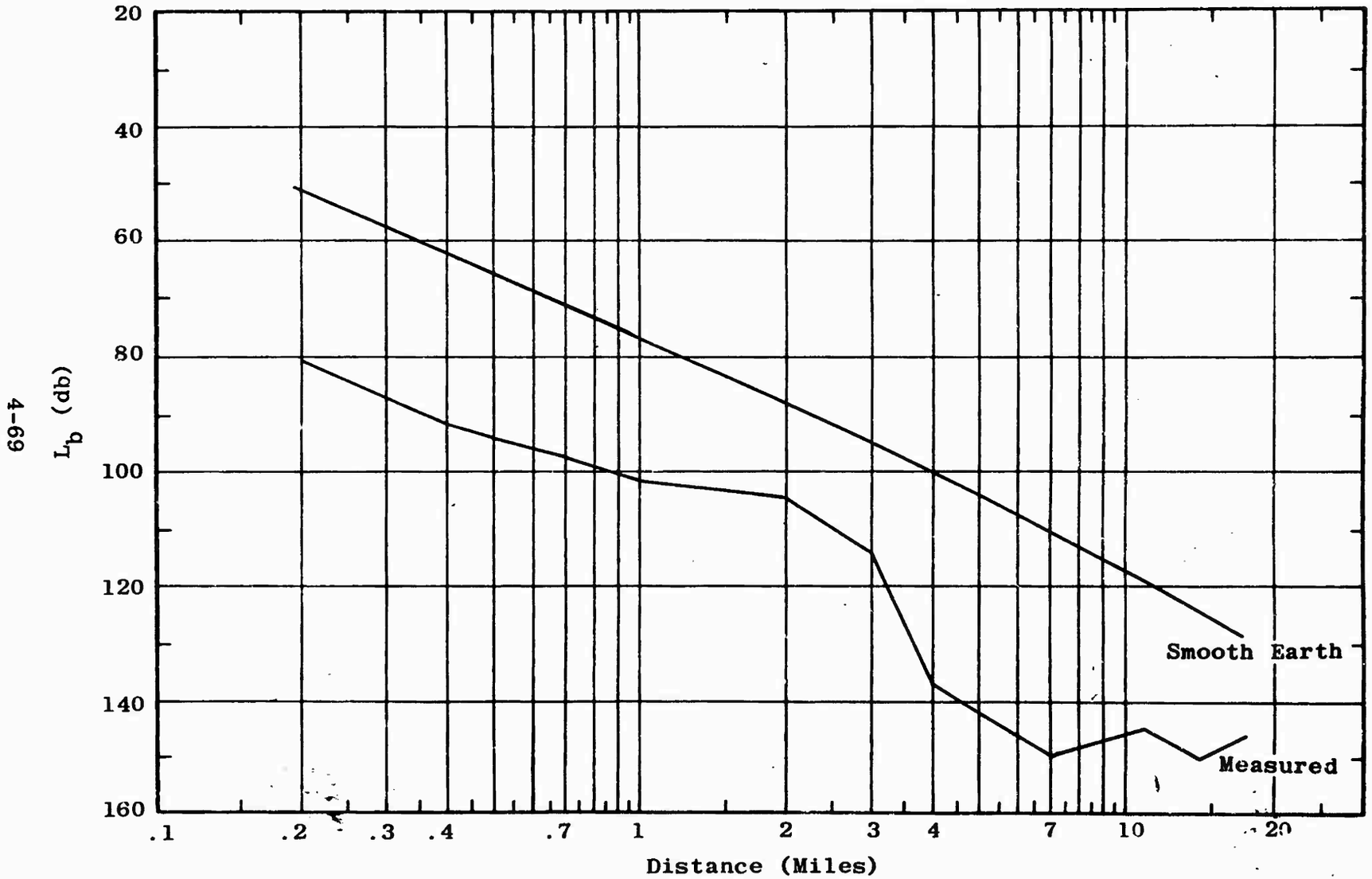

Figure 4.16G Comparison Between Measured Results and Smooth-Earth Model

$L_b = F_A(25.5, 80, V, d, 20)$

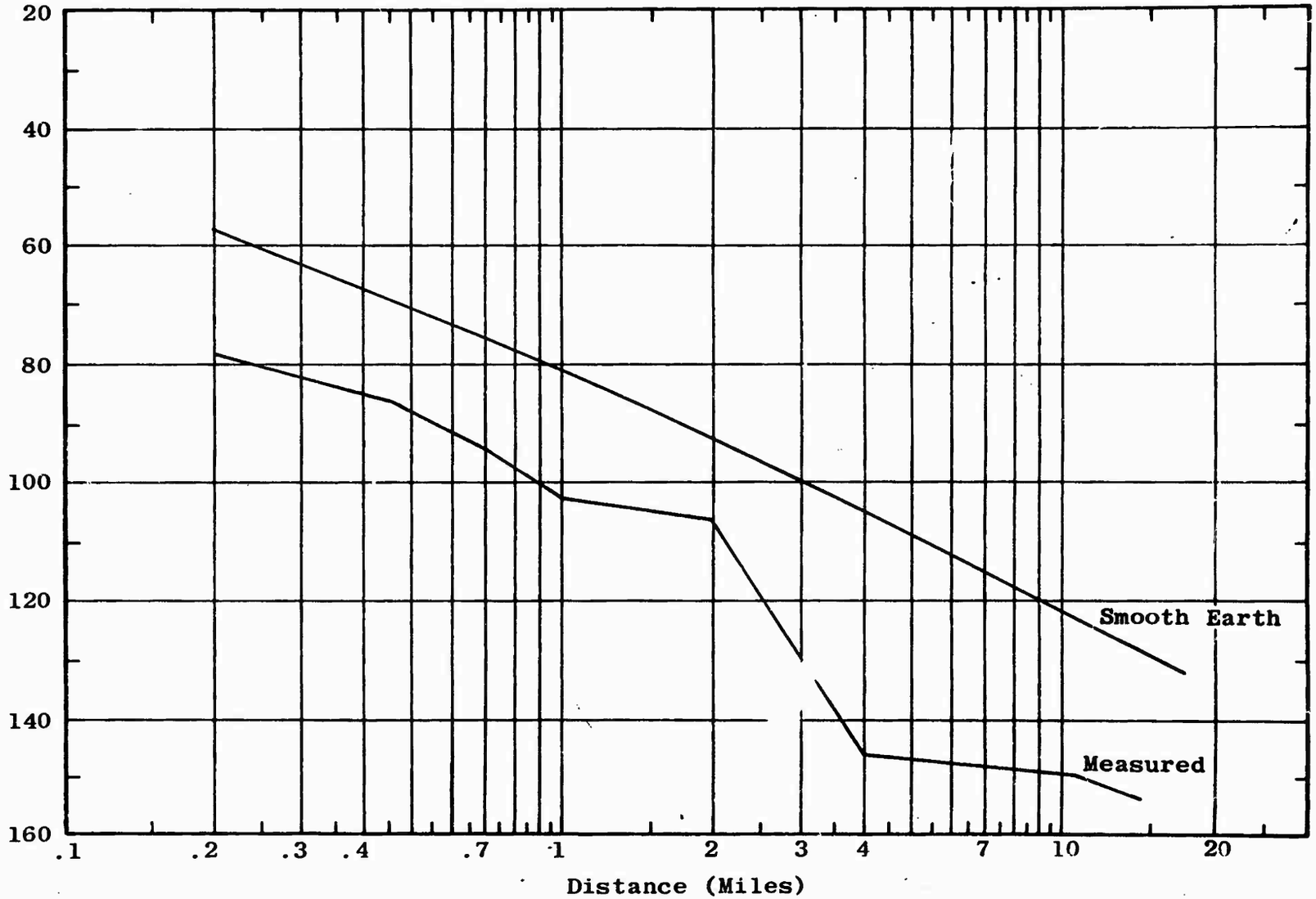

Figure 4.16H Comparison Between Measured Results and Smooth-Earth Model
$L_b = F_A(50.0, 80, V, d, 20)$

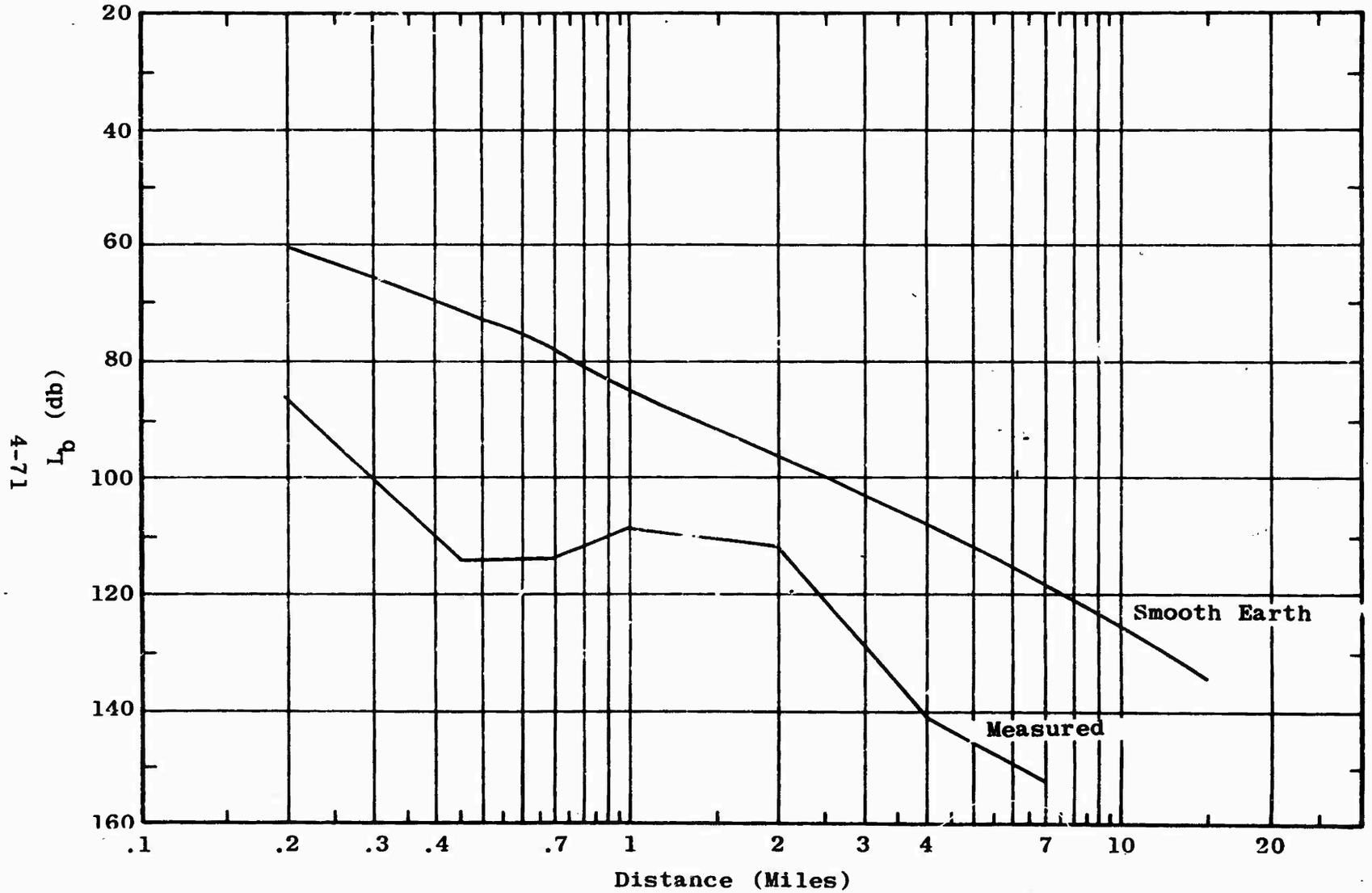

Figure 4.16I Comparison Between Measured Results and Smooth-Earth Model
$L_b = F_A(100, 80, V, d, 20)$

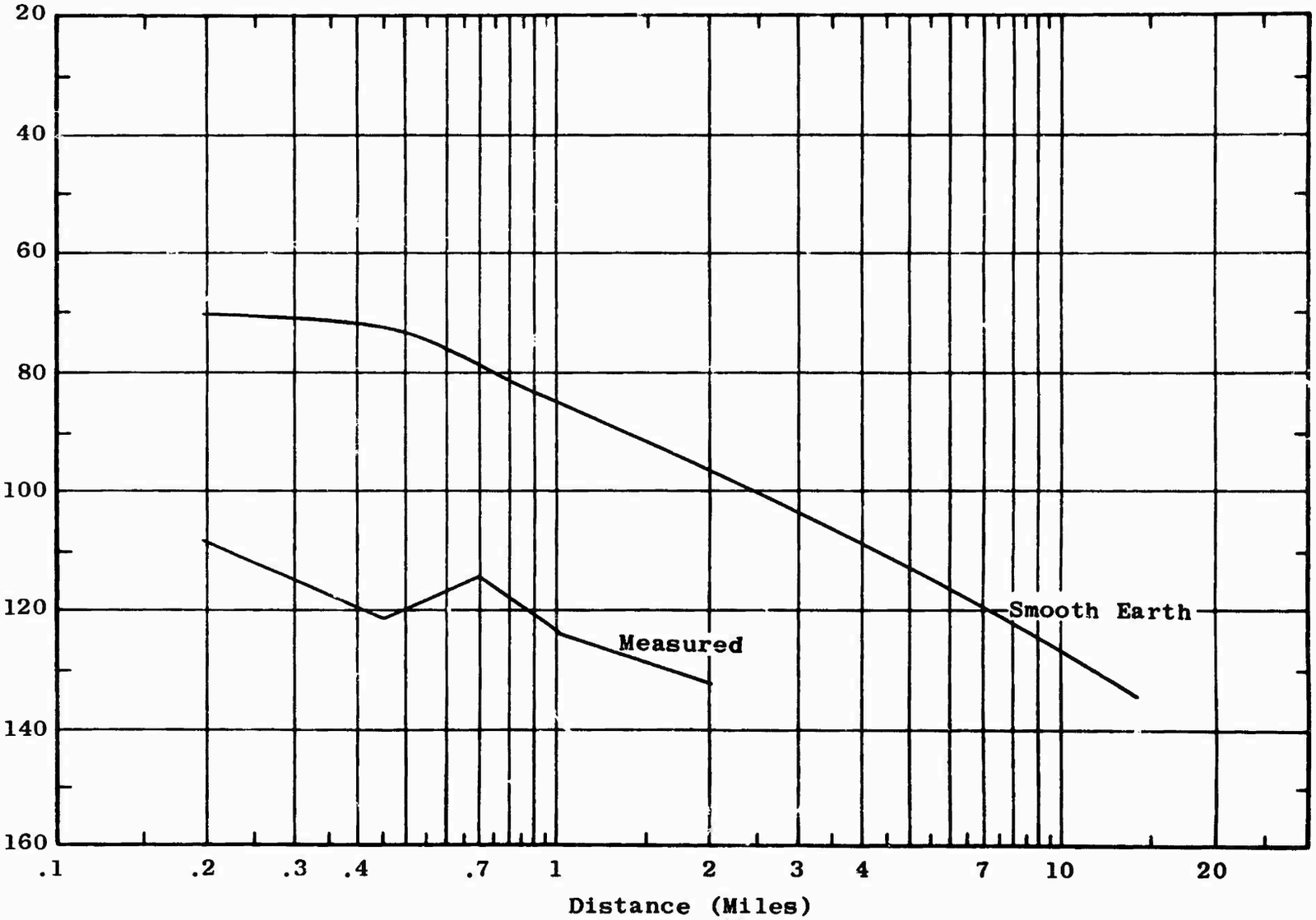

Figure 4.16J Comparison Between Measured Results and Smooth-Earth Model
$L_b = F_A(250, 80, V, d, 20)$

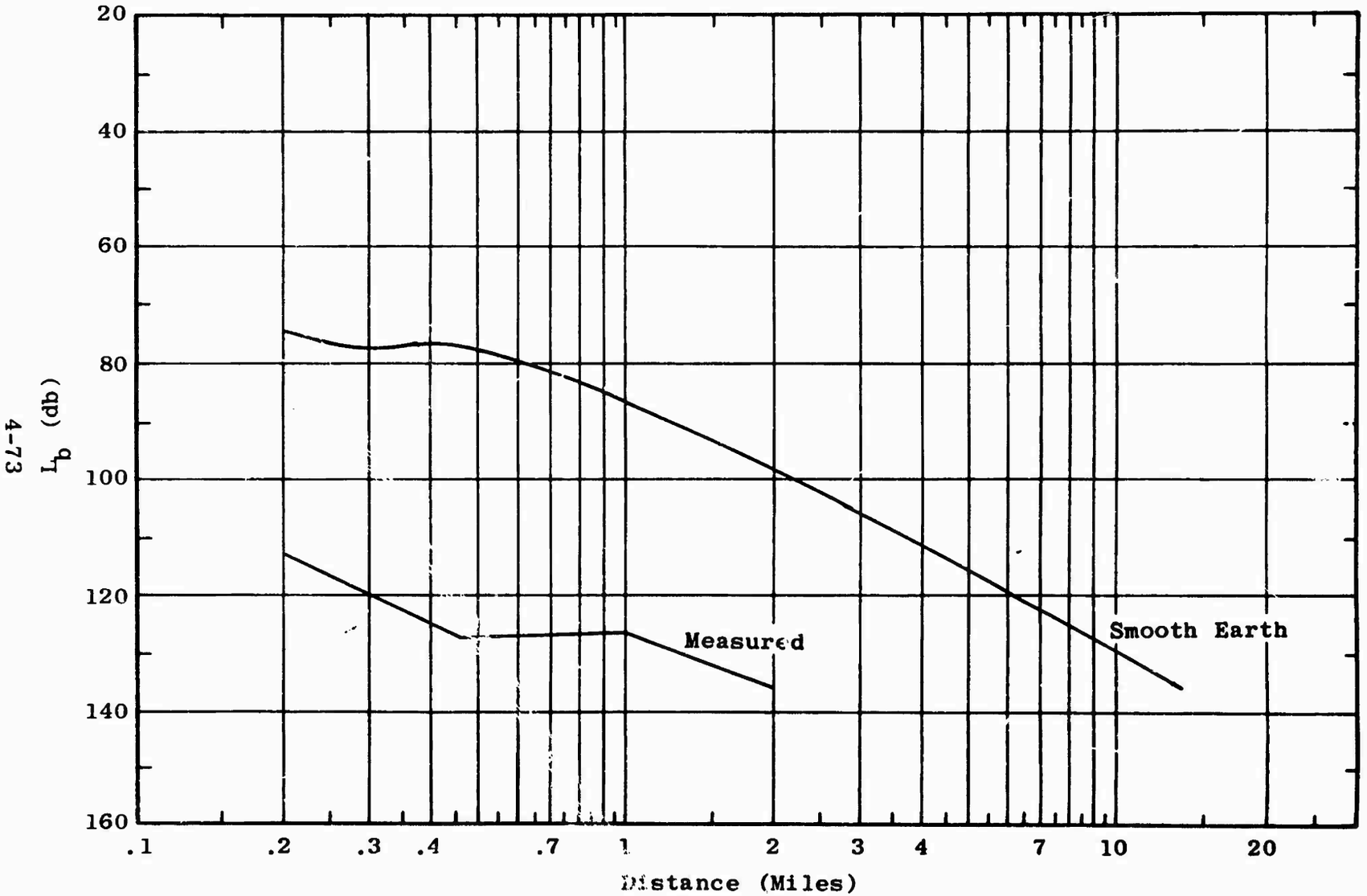

Figure 4.16K Comparison Between Measured Results and Smooth-Earth Model
$L_b = F_A(400, 80, V, d, 20)$

4.2.2.4 Egli's Rough-Earth Model

The National Bureau of Standards is currently working on a statistical model for rough terrain. This model is based upon the analysis of a large number of propagation measurements which have been made within the United States. It is very likely that the NBS statistical model and the data which went into the model will be an invaluable aid in identifying terrain effects in the tropical vegetation data. Unfortunately, this program has not been completed and data is not yet available.

A terrain model based on a more limited set of terrain data has been suggested by Egli.[4] The Egli model is discussed in detail in Semiannual Report Number 1. This model is based upon the plane earth propagation equations plus a statistical terrain factor. Consider Egli's equation,

$$E_{50} = \frac{40\ h_1\ h_2 \sqrt{P_t}}{95\ d^2} \quad \mu v/m \qquad (4)$$

where

E_{50} = median field over all locations d miles away

P_t = power transmitted in watts

h_1, h_2 = transmitting and receiving antenna heights in feet

d = separation distance in miles.

---

4. J. J. Egli, "Radio Propagation Above 40 mc Over Irregular Terrain," Proc. IRE, October 1957.

The basic transmission loss equation can be expressed as

$$L_b = 36.57 + 20 \log f_{mc} + 20 \log E_o - 20 \log E \quad (5)$$

where

$$E_o = 4.359 \times 10^3 \sqrt{P_t} \ \mu v/m \text{ for a half-wave dipole.}$$

Taking E in the above equation to be Egli's E_{50} and introducing a vegetation or "foliage" factor, F.F., the following equation results.

$$L_b = 116.57 + 20 \log f_{mc} + 40 \log d_{mi} - 20 \log (h_1 \ h_2) + F.F. \quad (6)$$

where the two antenna heights are measured in feet.

The foliage factor, F.F., which appears in the above equation was derived from available measured data. The foliage factor for horizontal and vertical polarization is shcwn plotted on Figure 4.17. It is interesting to note that the foliage factor for both horizontal and vertical polarization follows a straight line except at 25 mc. Since Egli's model was derived for frequencies of 40 mc and above, there is some question of its applicability at 25 mc. However, a possible discrepancy of some 10 db in measured data at 25 mc for vertical polarization was noted in Section 4.2.1. It is interesting to note that a resolution of this discrepancy at 25 mc would tend to make the foliage factor at 25 mc follow the straight line predicted at the other frequencies.

The foliage factor as deduced by comparing Egli's statistical terrain model with measured data has an increasing effect with frequency. The effect for horizontal polarization is less than the effect for vertical polarization at the lower

frequencies but tends toward the same value at higher frequencies. The foliage factor does not appear to be dependent upon distance, which may be surprising in view of results presented in previous reports. This matter, too, needs further study to resolve.

Egli's model predicts a normal distribution about each median value whose standard deviation is a function of distance. The statistical terrain parameters suggested by Egli are summarized below.

Frequency (mc)	Standard Deviation (db)	10% to 90% Range (db)
25	4.6(estimated)	12(estimated)
50	6.1	16
100	7.7	20
250	9.2	24
400	10.7	28

In order to compare the model based on Egli's terrain factors with measured data, the following procedure was used. Basic transmission loss curves based on measured data were prepared at each polarization and frequency for the following pairs of transmitter-receiver antenna heights: 80-80, 80-40, 80-20, 40-80, 40-40, 40-20, 13-80, 13-40, and 13-20 feet. Equation 6 was used to predict a corresponding set of propagation curves. Each predicted curve was subtracted from the corresponding measured curve and the difference was plotted as shown in Figure 4.18. A figure similar to Figure 4.18 was prepared for each frequency and polarization. The conglomeration of curves shown in Figure 4.18 was discarded and only the upper and lower envelopes were retained. Figures 4.19A through 4.19J show these envelopes for the various frequencies and polarizations considered. Superimposed

on these envelopes of measured data are hree straight lines. The middle straight line represents the median prediction and the two outer straight lines represent the 10 per cent and 90 per cent limits of Egli's terrain factor. These figures show that the over-all comparison is quite good. In general, the effect of terrain can be seen to decrease the loss from that expected at 1 to 2 miles and increase the loss from that expected at about 7 miles. This is due to the gross features of the particular set of profiles which pertain to Radial A and would probably average out over a large number of different terrain profiles.

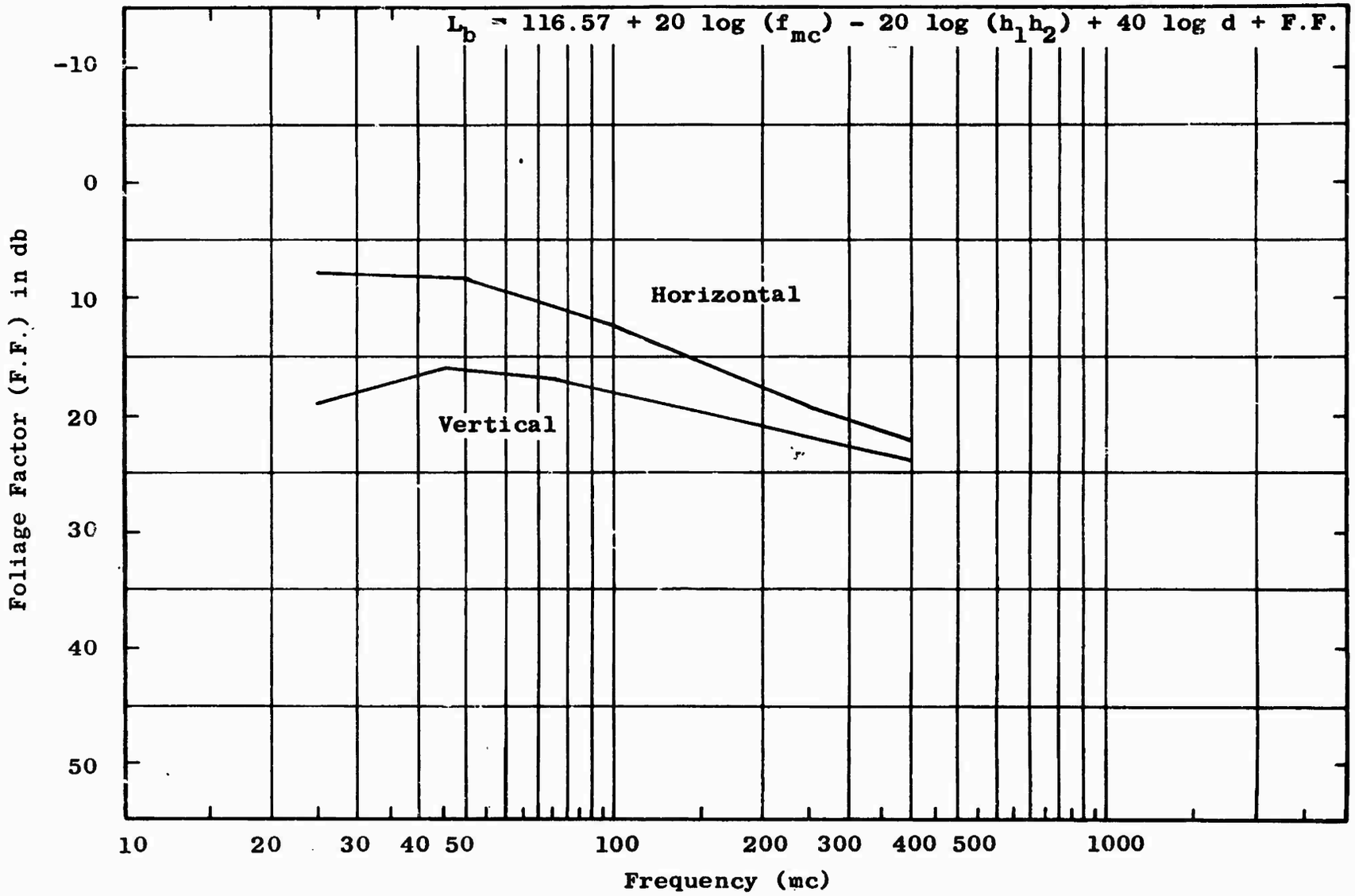

Figure 4.17 Foliage Factor (F.F.)

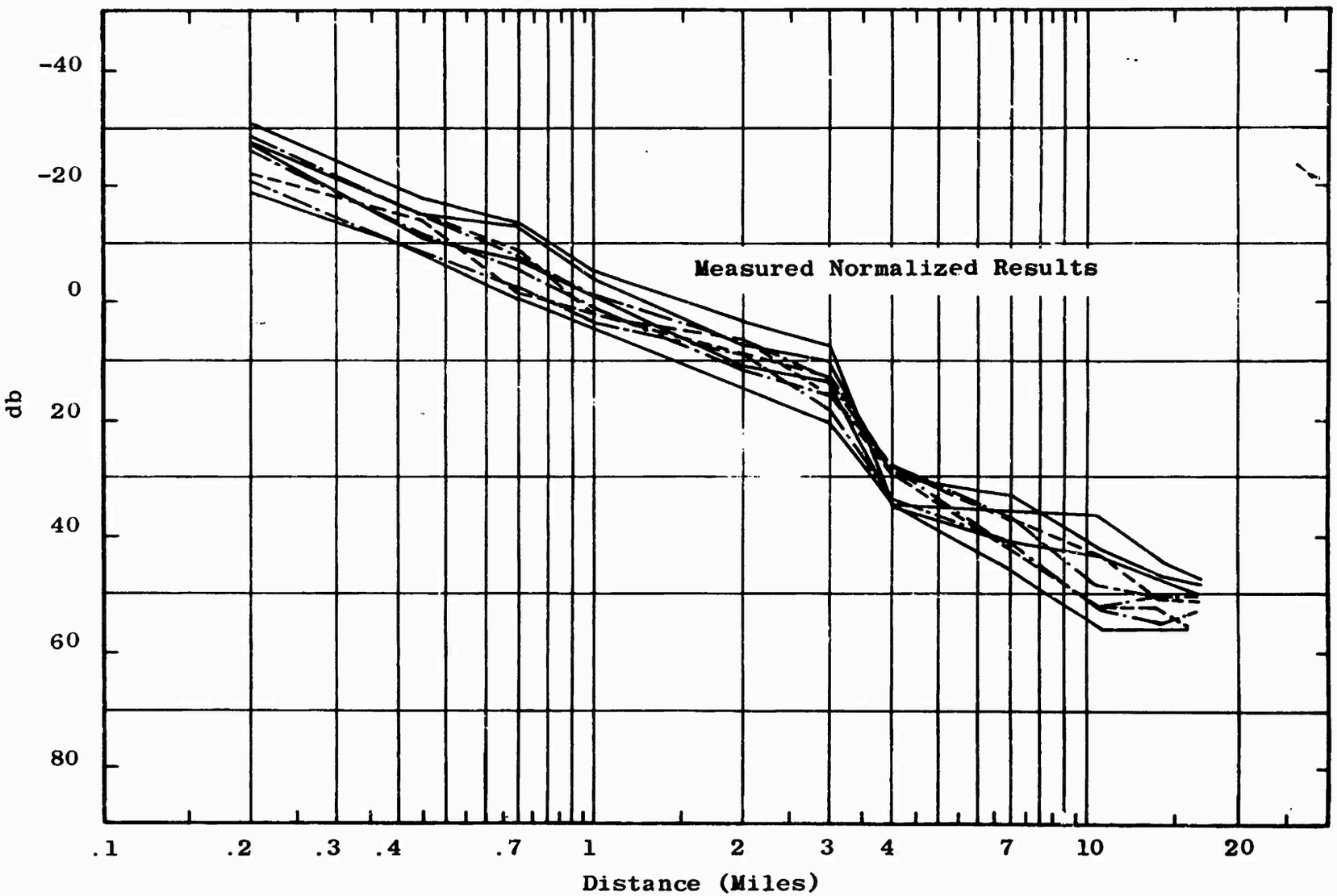

Figure 4.18 Sample Composite of Measured Results Normalized to Egli Model

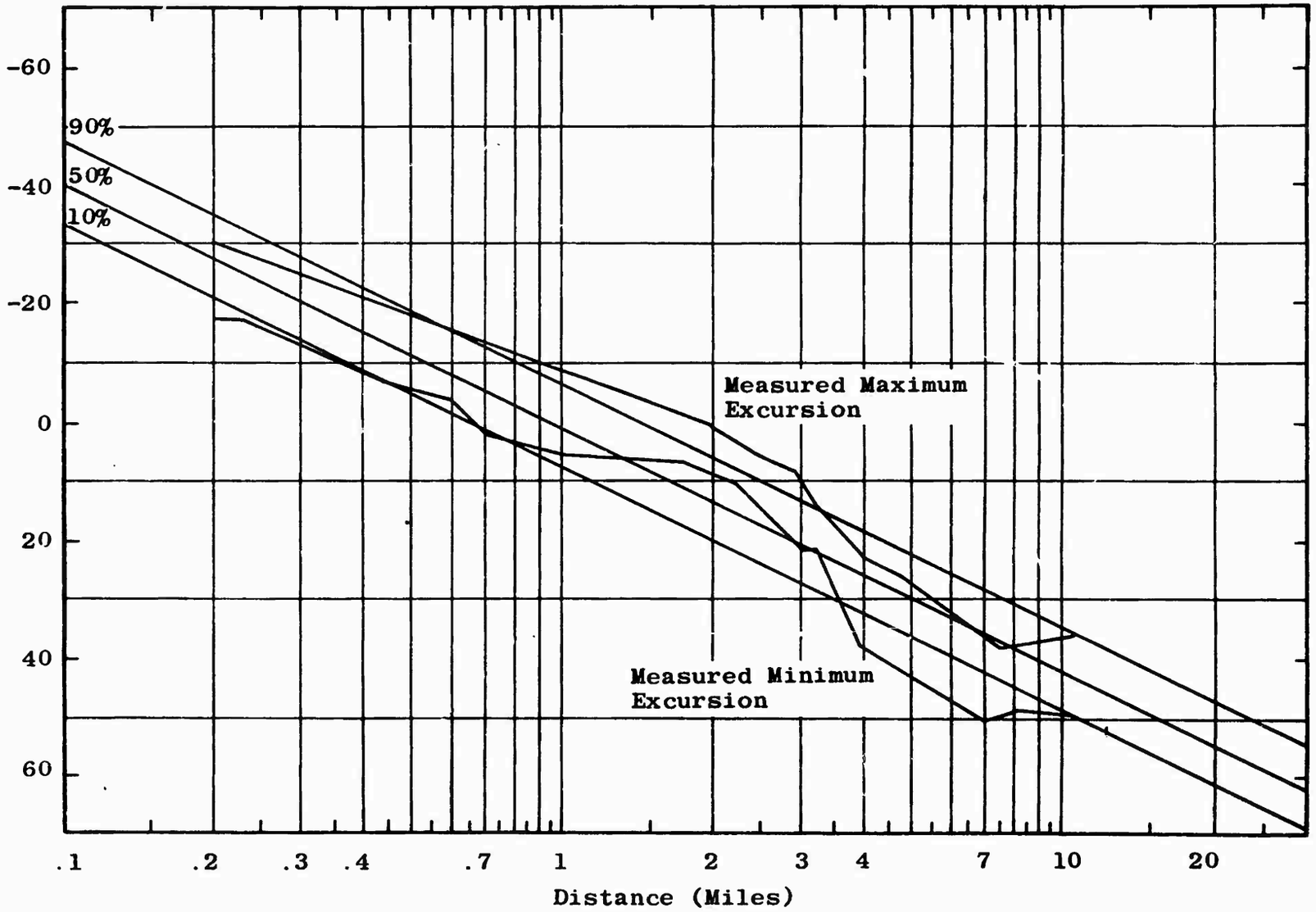

Figure 4.19A Comparison Between Measured Results and Egli Model
$L_b = F_A(25.5, 13\text{-}80, V, d, \quad \text{-}80)$

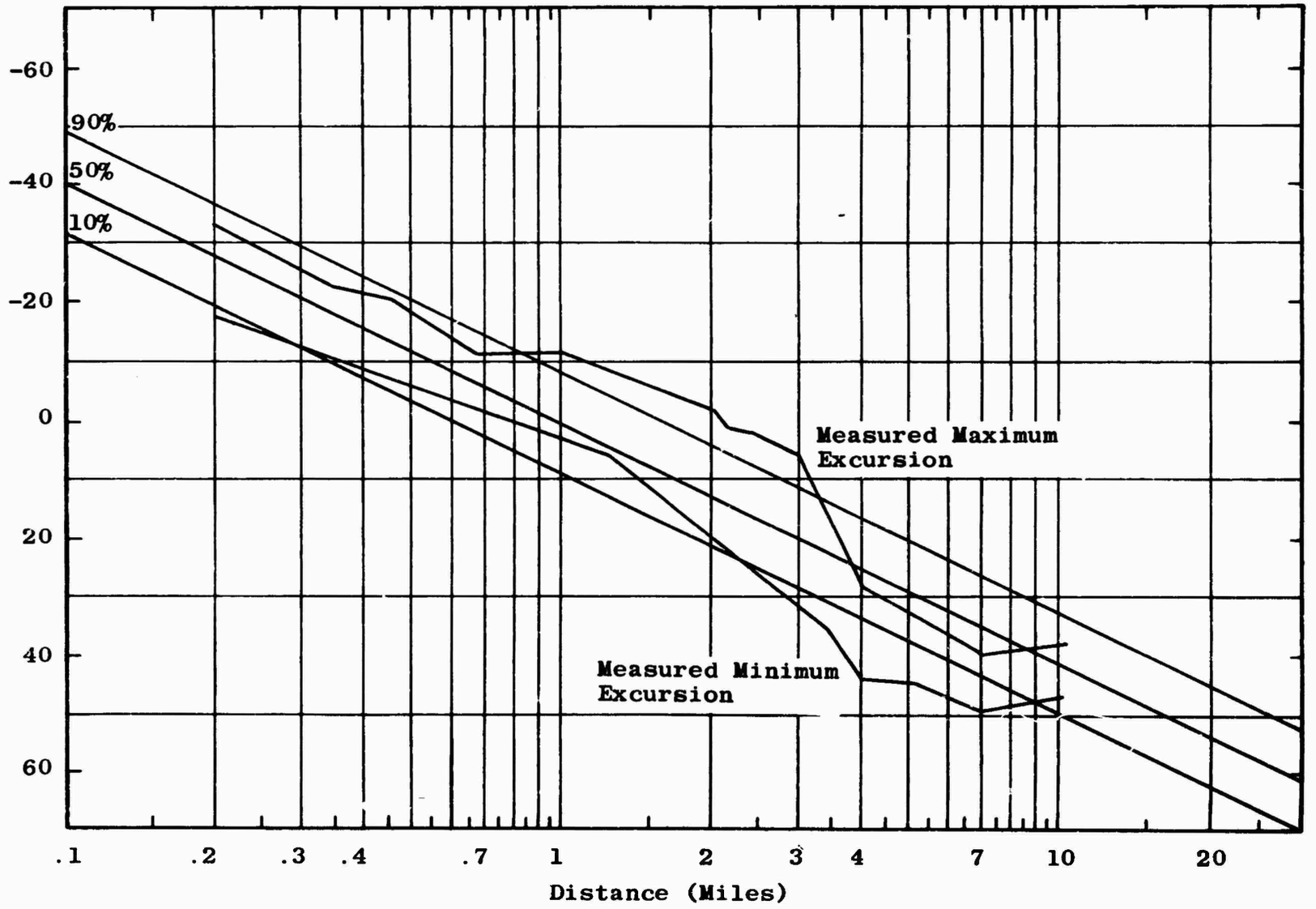

Figure 4.19B Comparison Between Measured Results and Egli Model
$L_b = F_A(50, 13\text{-}80, V, d, 20\text{-}80)$

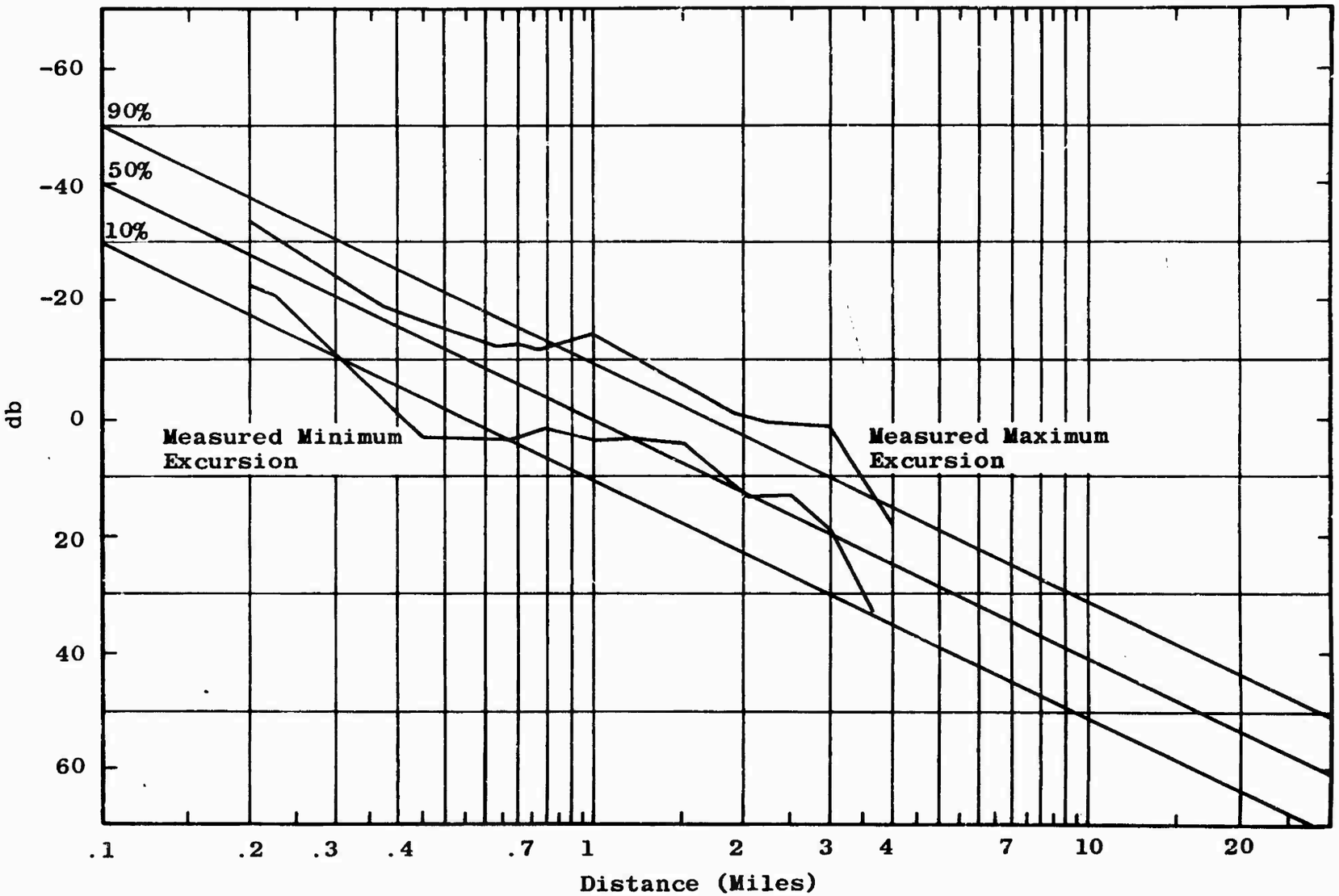

Figure 4.19C Comparison Between Measured Results and Egli Model
$L_b = F_A(100, 13\text{-}80, V, d, 13\text{-}80)$

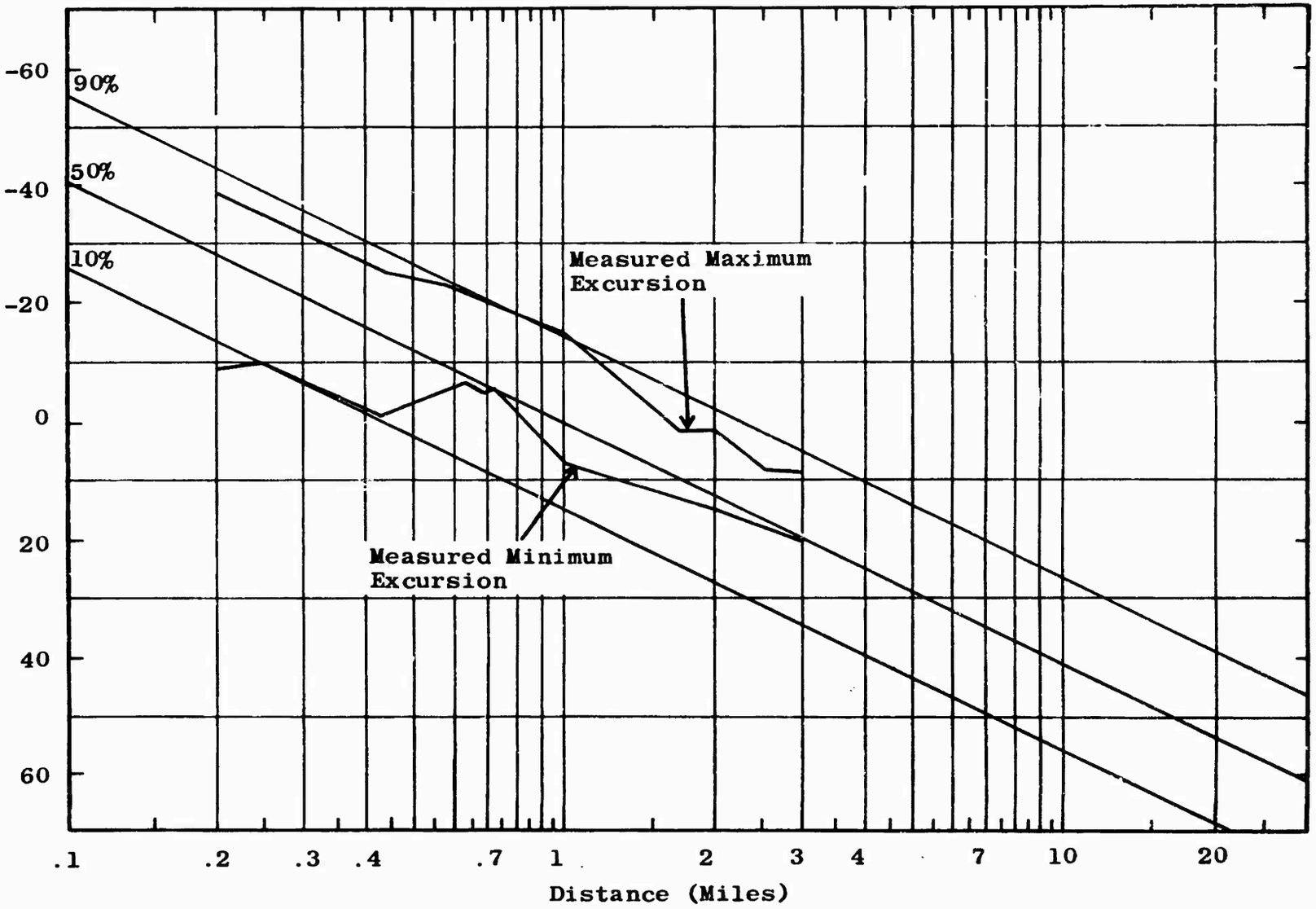

Figure 4.19D Comparison Between Measured Results and Egli Model
$L_b = F_A(250, 13\text{-}80, V, d, 20\text{-}80)$

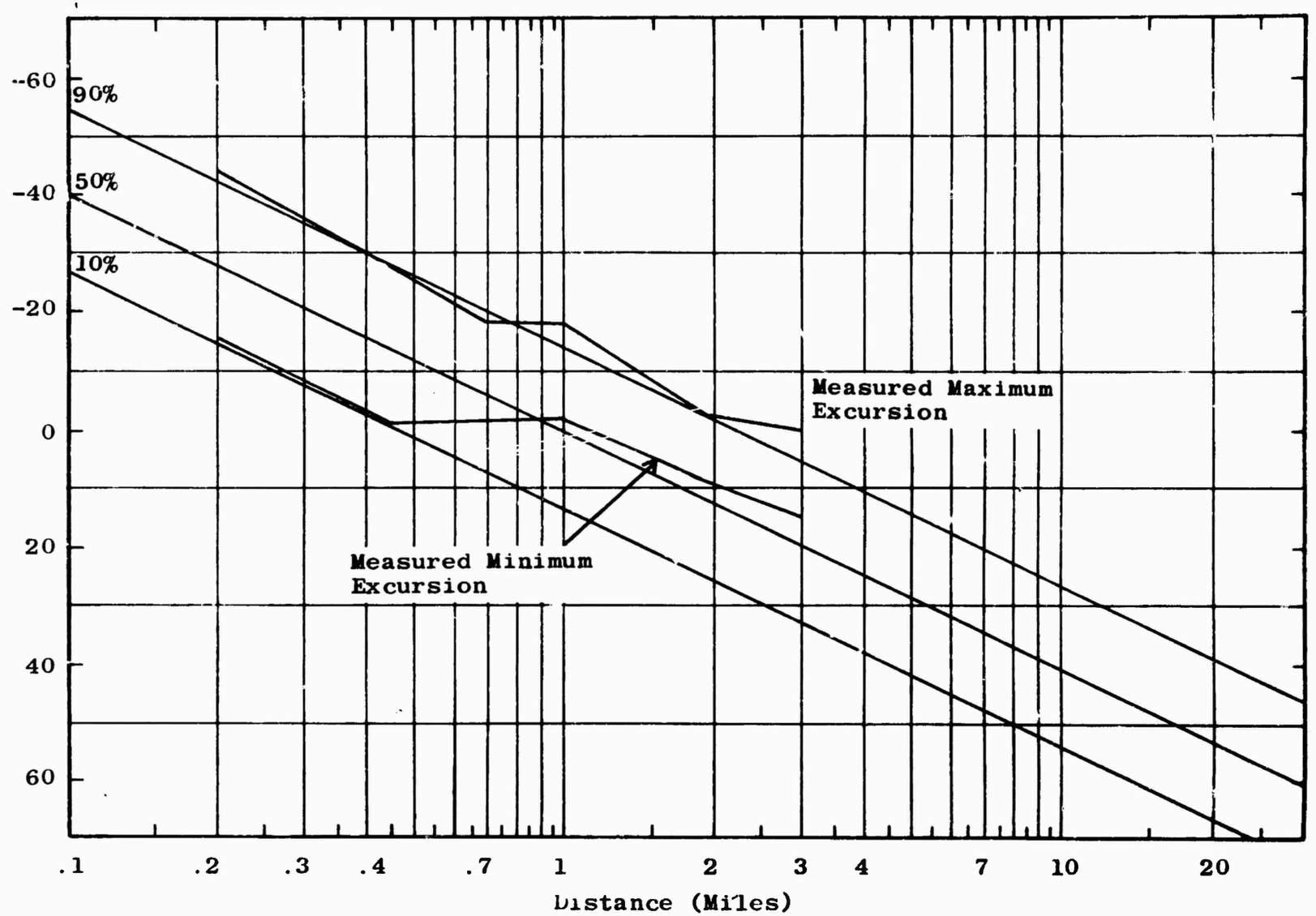

Figure 4.19E Comparison Between Measured Results and Egli Model
$L_b = F_A(400, 13\text{-}80, V, d, 13\text{-}80)$

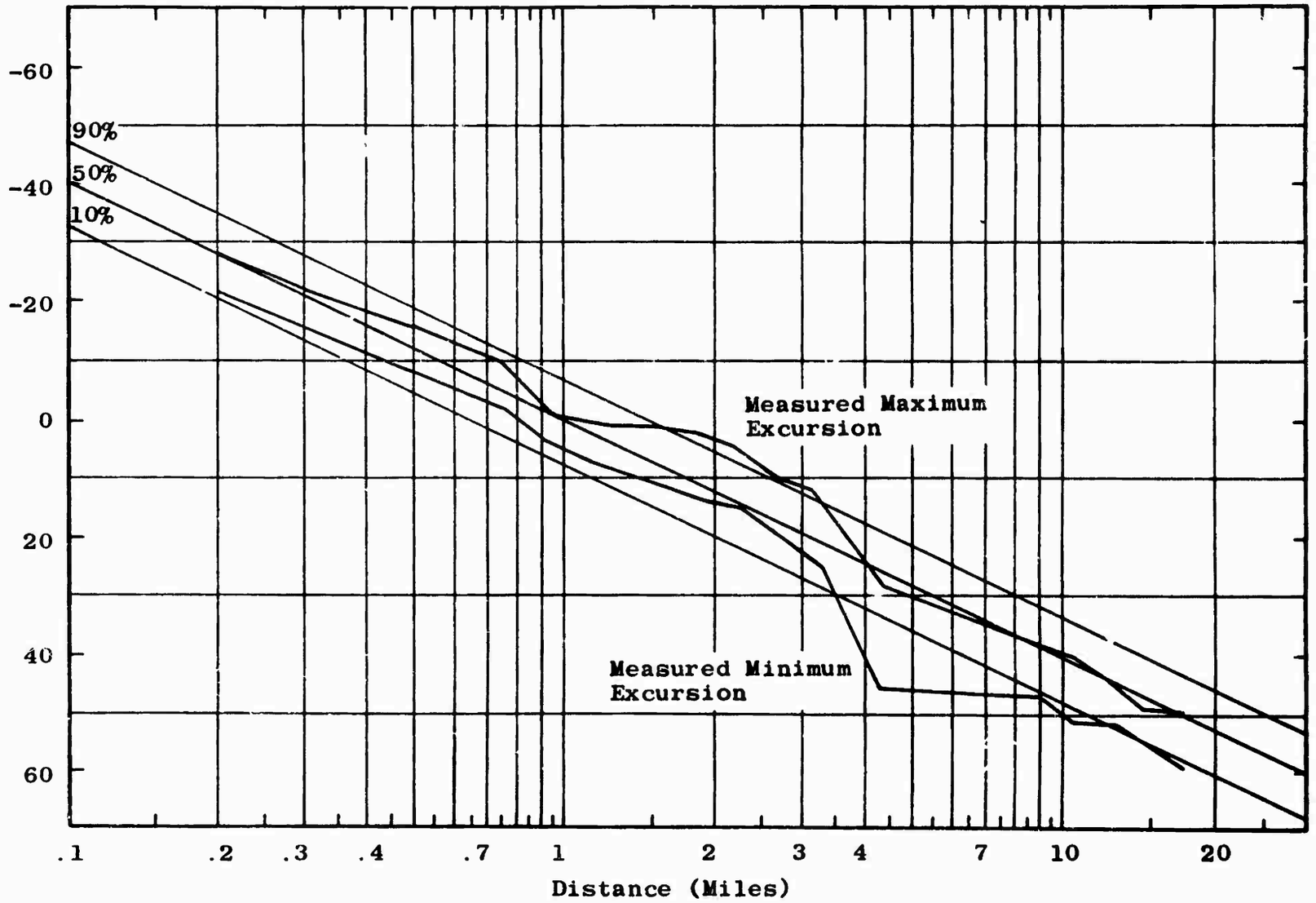

Figure 4.19F Comparison Between Measured Results and Egli Model
$L_b = F_A(25.5, 13\text{-}80, H, d, 20\text{-}80)$

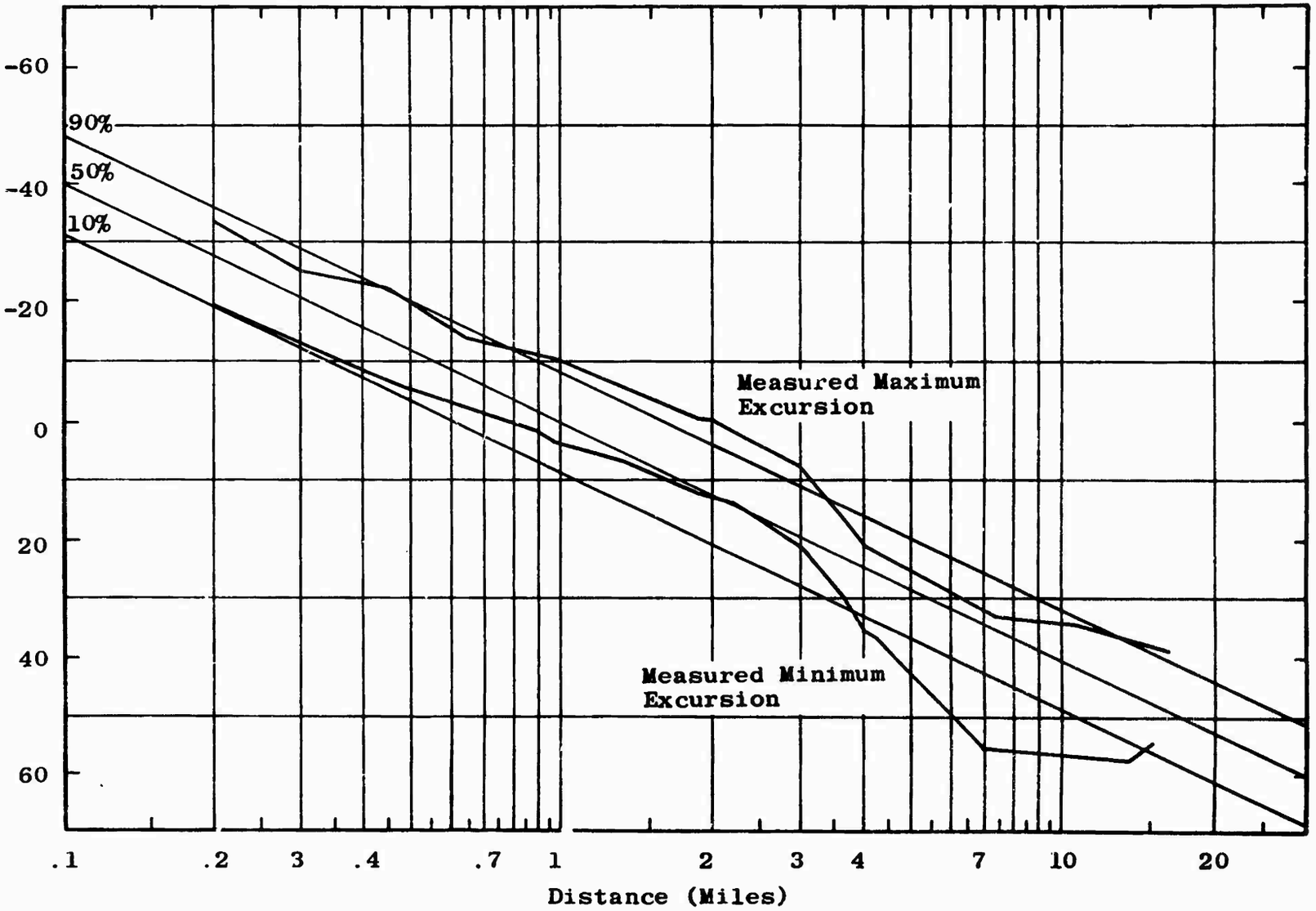

Figure 4.19G Comparison Between Measured Results and Egli Model
$L_b = F_A(50, 13\text{-}80, H, d, 20\text{-}80)$

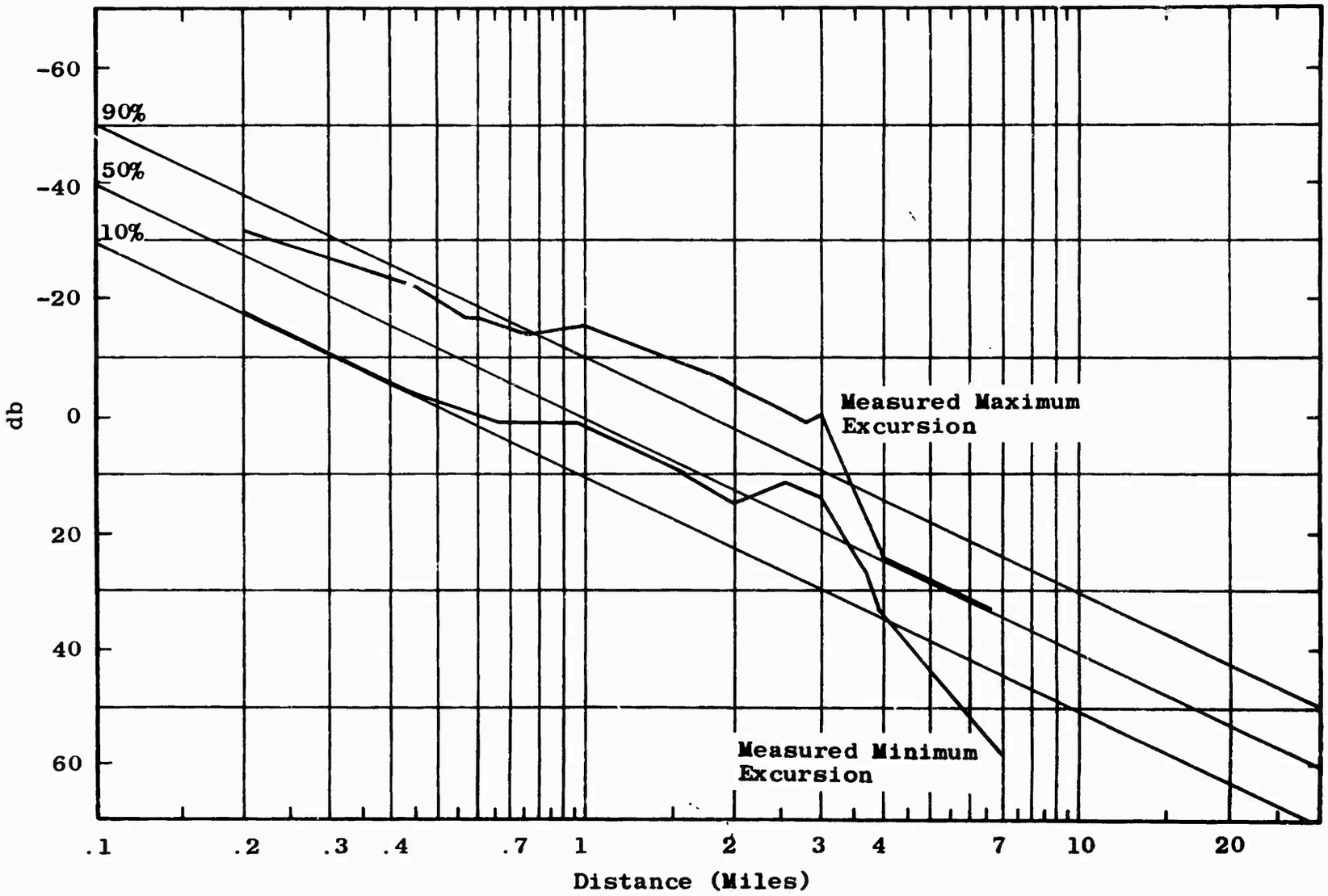

Figure 4.19H Comparison Between Measured Results and Egli Model
$I_b = F_A(100, 13\text{-}80, H, d, 20\text{-}80)$

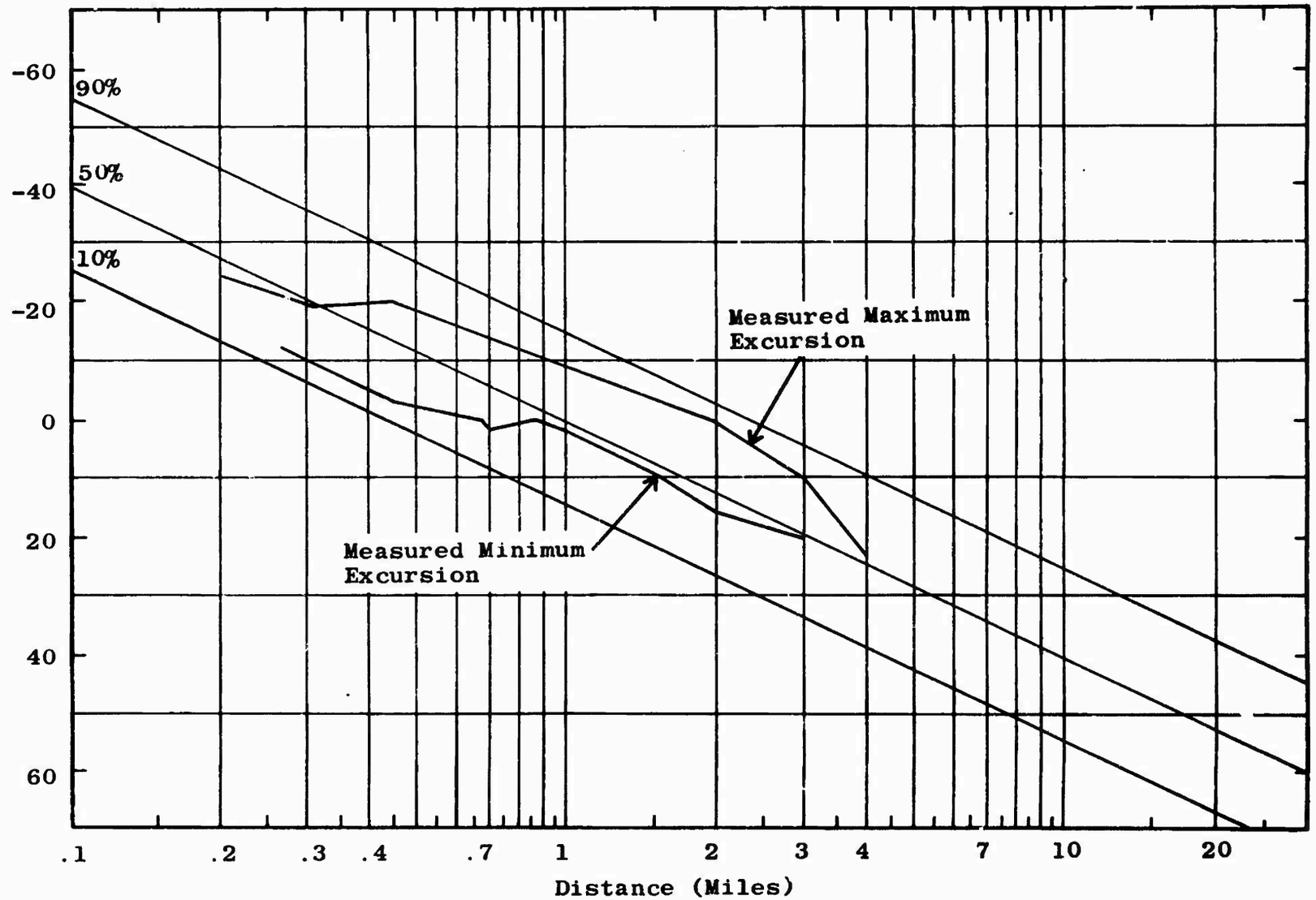

Figure 4.19I Comparison Between Measured Results and Egli Model
$L_b = F_A(250, 13\text{-}80, H, d, 20\text{-}80)$

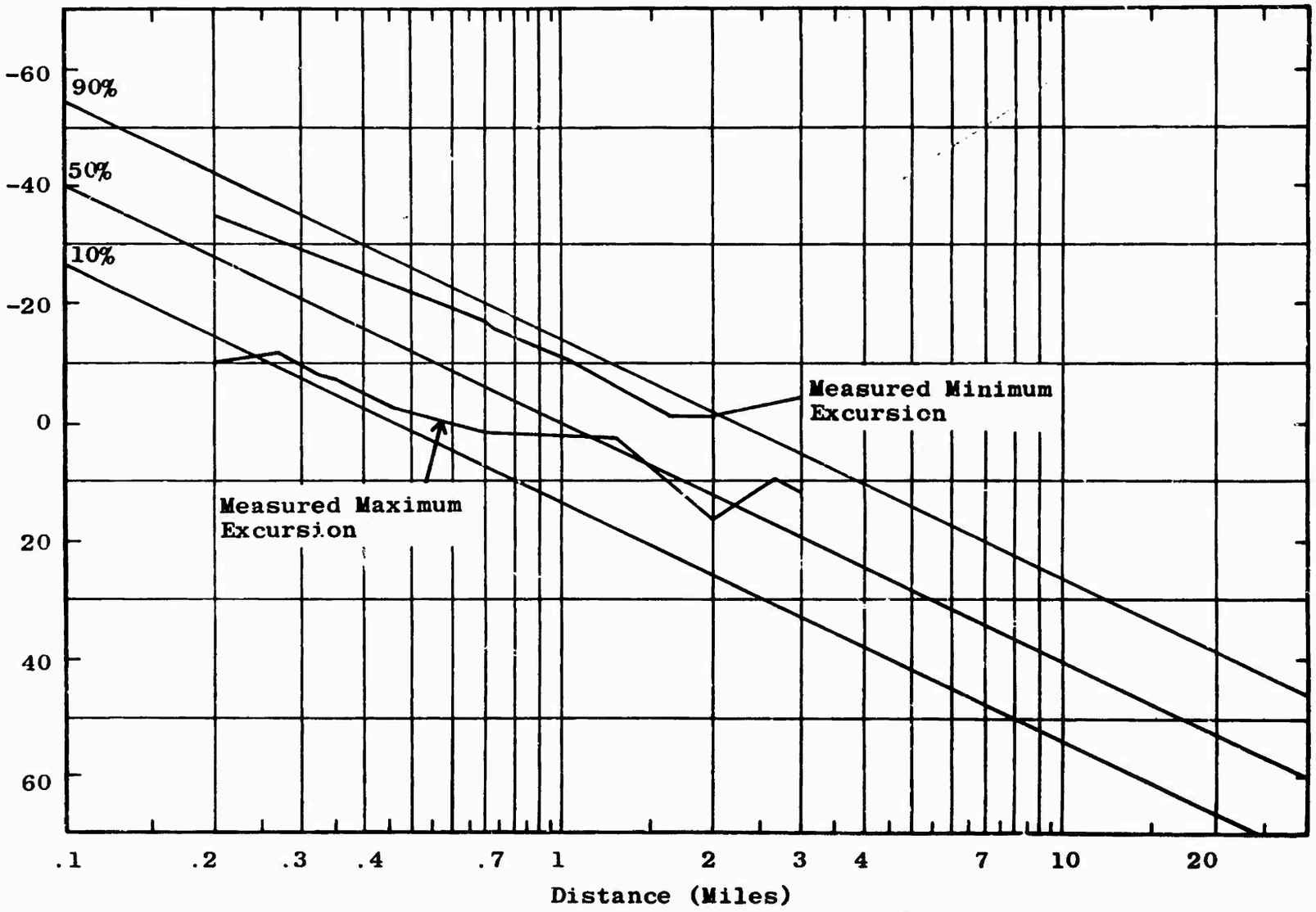

Figure 4.19J Comparison Between Measured Results and Egli Model
$L_b = F_A(400, 13\text{-}80, H, d, 20\text{-}80)$

4.3 Time and Spatial Variations of L_b

4.3.1 Time Variability

Since this program is primarily interested in the study of propagation losses as a function of spatial variables, no comprehensive study has been made of time variables of path loss. However, recordings of signal strength vs time are made for short periods of time as a routine procedure of the field point measurement program. This data is useful in improving the accuracy of the field strength measurements.

Tables IIa through IIr summarize the time variability noted at various frequencies and polarizations along Radial A. The table is subdivided by frequency and polarization. The first column within each subdivision of these tables gives the numerical identifier of the field point at which the measurement was made. The second column gives the radial distance between the transmitter site and the field point. The third and fourth columns give the transmitting and receiving antenna height. The fifth column gives the maximum variation which was observed in the received field over the time period given in the sixth column. In all cases, the signal which was received was the same standard test signal used for all field point measurements.

This data provides a valuable insight into the short-term time variability within the foliated environment.

The range of variation indicated by the data is relatively small. Thus, short-term time variability is in general not a primary factor at the ranges and under the propagation conditions covered by these measurements.

Table IIa. Short-Term Time Variability

$L_b = F_A(0.105, H_t, V, d, H_r)$

Field Point	Distance (Miles)	H_t (Feet)	H_r (Feet)	Maximum Variation (db)	Time Period (Minutes)
1	0.2	80	8	0	0.56
3	0.7	80	8	0.5	0.60
5	2.0	80	8	0	0.65
5.5	3.0	80	8	0.2	0.50
6	4.0	80	8	0.1	0.62
7	7.0	80	8	0.2	0.55
8	10.5	80	8	0.2	0.25
9	14.0	80	8	0.4	0.39
10	17.0	80	8	0.1	0.53

Table IIb. Short-Term Time Variability

$L_b = F_A(0.300, H_t, V, d, H_r)$

Field Point	Distance (Miles)	H_t (Feet)	H_r (Feet)	Maximum Variation (db)	Time Period (Minutes)
1	0.2	80	8	0.3	0.66
2	0.45	80	8	0.4	0.75
3	0.7	80	8	0	0.50
5.5	3.0	80	8	0	0.49
7	7.0	80	8	0.5	0.50
8	10.5	80	8	0.2	0.28
9	14.0	80	8	0.1	0.53
10	17.0	80	8	0	0.36

Table IIc. Short-Term Time Variability

$L_b = F_A(0.880, H_t, V, d, H_r)$

Field Point	Distance (Miles)	H_t (Feet)	H_r (Feet)	Maximum Variation (db)	Time Period (Minutes)
1	0.2	80	8	0.2	0.58
2	0.45	80	8	0.5	0.44
3	0.7	80	8	0.9	0.70
5.5	3.0	80	8	0	0.62
6	4.0	80	8	0.2	0.46
7	7.0	80	8	0.6	0.30
8	10.5	80	8	0.7	0.80
9	14.0	80	8	0.4	0.44

Table IId. Short-Term Time Variability

$L_b = F_A(2, H_t, V, d, H_r)$

Field Point	Distance (Miles)	H_t (Feet)	H_r (Feet)	Maximum Variation (db)	Time Period (Minutes)
4	1.0	80	4	0	0.40
4	1.0	80	8	0.2	0.38
8	10.5	80	8	2.2	0.94
9	14.0	80	8	1.2	0.92
10	17.0	80	8	1.3	1.14

Table IIe. Short-Term Time Variability

$L_b = F_A(6, H_t, V, d, H_r)$

Field Point	Distance (Miles)	H_t (Feet)	H_r (Feet)	Maximum Variation (db)	Time Period (Minutes)
4	1.0	40	8	0	0.42
5	2.0	40	4	0	0.20
5	2.0	40	8	0.2	0.28

Table IIf. Short-Term Time Variability

$L_b = F_A(25.5, H_t, V, d, H_r$

Field Point	Distance (Miles)	H_t (Feet)	H_r (Feet)	Maximum Variation (db)	Time Period (Minutes)
1	0.2	80	11	0.5	1.20
2	0.45	80	11	1.2	1.06
3	0.7	80	11	0.3	0.80
4	1.0	80	11	0.9	0.78
5	2.0	80	11	0.6	0.86
5.5	3.0	80	11	0.55	0.66
6	4.0	80	11	0.7	0.76
10	17.0	80	11	2.0	0.34
1	0.2	13	8	0.85	0.66
2	0.45	13	18	0.3	0.58
2	0.45	13	82	2.1	0.84
3	0.7	13	8	0.1	0.30
3	0.7	13	82	0.2	1.22
4	1.0	13	8	0.1	0.94
4	1.0	13	82	0	0.64
5	2.0	13	8	1.3	1.48
5	2.0	13	82	2.9	1.06
5.5	3.0	13	8	1.4	0.84
5.5	3.0	13	82	0.8	0.76
6	4.0	13	82	1.5	1.50

Table IIg. Short-Term Time Variability

$L_b = F_A(50, H_t, V, d, H_r)$

Field Point	Distance (Miles)	H_t (Feet)	H_r (Feet)	Maximum Variation (db)	Time Period (Minutes)
8	10.5	80	7	0	0.40
8	10.5	80	11	0	0.31
1	0.2	40	11	1.2	0.52
1	0.2	40	81	0	1.00
4	1.0	40	17	0	0.84
4	1.0	40	81	0	0.52
5	2.0	40	17	0	0.62
5	2.0	40	81	0	1.04
5.5	3.0	40	11	0.5	0.48
5.5	3.0	40	81	0.8	0.68
6	4.0	40	11	0.2	0.60
7	7.0	40	81	0.4	0.70
8	10.5	40	17	1.6	0.30
8	10.5	40	81	0	0.70
9	14.0	40	17	1.8	0.79
9	14.0	40	81	0.2	0.74
1	0.2	13	17	1.3	0.98
1	0.2	13	81	0.7	0.68
2	0.45	13	17	0	0.60
2	0.45	13	81	0	0.54
3	0.7	13	17	0	0.78
3	0.7	13	81	0	0.92
4	1.0	13	17	0.9	2.57
4	1.0	13	81	1.0	0.91
5	2.0	13	17	0.8	1.30
5	2.0	13	81	0	0.60
8	10.5	13	11	0.1	0.19
8	10.5	13	82	0.5	1.22
9	14.0	13	82	0	0.36

Table IIh. Short-Term Time Variability

$L_b = F_A(100, H_t, V, d, H_r)$

Field Point	Distance (Miles)	H_t (Feet)	H_r (Feet)	Maximum Variation (db)	Time Period (Minutes)
1	0.2	40	11	3.0	0.86
2	0.45	40	11	0.7	0.58
3	0.7	40	11	1.5	0.41
5.5	3.0	40	11	0	0.20
6	4.0	40	11	1.2	0.47
7	7.0	40	11	5.0	0.46
1	0.2	13	11	6.0	1.27
5.5	3.0	13	11	1.5	1.42
5.5	3.0	13	82	1.7	3.16
6	4.0	13	66	2.5	0.85
6	4.0	13	82	2.3	2.18

Table IIi. Short-Term Time Variability

$L_b = F_A(250, H_t, V, d, H_r)$

Field Point	Distance (Miles)	H_t (Feet)	H_r (Feet)	Maximum Variation (db)	Time Period (Minutes)
1	0.2	40	17	1.0	0.34
1	0.2	40	82	0.5	0.44
2	0.47	40	11	2.0	1.30
3	0.7	40	17	0.4	0.22
4	1.0	40	11	0.6	0.76
5	2.0	40	82	2.1	0.50
5.5	3.0	40	81	0.8	0.84
6	4.0	40	81	0.2	0.44
1	0.2	13	18	1.5	0.56
1	0.2	13	82	0.8	0.34
3	0.7	13	11	0	0.[illegible]0
4	1.0	13	18	0.1	0.67
5	2.0	13	82	1.0	0.44
5.5	3.0	13	82	0.7	0.88

Table IIj. Short-Term Time Variability

$L_b = F_A(400, H_t, V, d, H_r)$

Field Point	Distance (Miles)	H_t (Feet)	H_r (Feet)	Maximum Variation (db)	Time Period (Minutes)
1	0.2	80	11	1.5	0.66
2	0.45	80	11	0	0.39
3	0.7	80	11	2.6	0.57
3	0.7	40	11	1.4	0.65
1	0.2	13	11	0	0.52
1	0.2	13	82	1.1	0.77
2	0.45	13	11	0	0.40
3	0.7	13	11	0	1.84
3	0.7	13	82	1.7	1.76
4	1.0	13	11	0.4	1.13
4	1.0	13	81	1.1	0.78
5.5	3.0	13	11	0.7	1.16

Table IIk. Short-Term Time Variability

$L_b = F_A(2, H_t, H, d, H_r)$

Field Point	Distance (Miles)	H_t (Feet)	H_r (Feet)	Maximum Variation (db)	Time Period (Minutes)
1	0.2	40	8	1.8	1.08
2	0.45	40	8	1.6	0.70
3	0.7	40	8	1.3	0.50
5.5	3.0	40	8	0.1	0.51

Table III. Short-Term Time Variability

$L_b = F_A(6, H_t, H, d, H_r)$

Field Point	Distance (Miles)	H_t (Feet)	H_r (Feet)	Maximum Variation (db)	Time Period (Minutes)
4	1.0	80	4	0	0.46
4	1.0	80	8	0.1	0.40
1	0.2	40	8	0	0.44
2	0.45	40	8	0.6	3.01
5.5	3.0	40	8	1.0	0.50
7	7.0	40	8	0.3	0.22

Table IIm. Short-Term Time Variability

$L_b = F_A(12, H_t, H, d, H_r)$

Field Point	Distance (Miles)	H_t (Feet)	H_r (Feet)	Maximum Variation (db)	Time Period (Minutes)
1	0.2	80	8	0	0.40
5.5	3.0	40	8	0.1	0.46

Table IIn. Short-Term Time Variability

$L_b = F_A(25.5, H_t, H, d, H_r)$

Field Point	Distance (Miles)	H_t (Feet)	H_r (Feet)	Maximum Variation (db)	Time Period (Minutes)
1	0.2	80	8	0	0.82
1	0.2	80	18	0.2	1.40
2	0.45	80	8	0	0.68
2	0.45	80	82	0.2	0.66
5	2.0	80	11	0	0.48
5	2.0	80	82	0.5	0.82
5.5	3.0	80	11	0.2	0.20
5.5	3.0	80	78	0.8	0.88
6	4.0	80	11	0.4	0.72
6	4.0	80	78	0.9	0.68
7	7.0	80	18	1.2	0.52
7	7.0	80	78	0.6	0.36
8	10.5	80	18	4.0	0.86
8	10.5	80	78	3.0	1.32
9	14.0	80	17	0.4	0.44
9	14.0	80	78	0	0.68
10	17.0	80	78	1.1	0.48
1	0.2	40	17	1.3	0.53
1	0.2	40	81	1.3	0.50
2	0.45	40	18	0	0.60
2	0.45	40	82	0	0.43
3	0.7	40	17	0.4	1.36
3	0.7	40	81	0.3	1.56
4	1.0	40	17	0	0.32
4	1.0	40	81	0.2	0.48
5	2.0	40	17	0.2	0.46
5	2.0	40	81	1.0	0.48

Table IIn(Continued). Short-Term Time Variability

$L_b = F_A(25.5, H_t, H, d, H_r)$

Field Point	Distance (Miles)	H_t (Feet)	H_r (Feet)	Maximum Variation (db)	Time Period (Minutes)
5.5	3.0	40	81	0.4	0.34
6	4.0	40	14	0.7	0.34
6	4.0	40	81	0.9	0.34
7	7.0	40	17	0	0.71
7	7.0	40	78	0	0.56
8	10.5	40	17	0.4	0.75
8	10.5	40	81	0.2	0.63
9	14.0	40	17	0	0.32
9	14.0	40	81	0.1	0.54
2	0.45	13	18	0	0.60
2	0.45	13	82	0	0.61
3	0.70	13	18	2.2	3.48
4	1.0	13	18	0.3	0.74
4	1.0	13	82	0.6	0.99
5	2.0	13	18	0.7	1.38
5	2.0	13	82	0.1	2.36
5.5	3.0	13	18	0.1	0.40
7	7.0	13	82	0.2	1.50
8	10.5	13	11	0.1	0.71
8	10.5	13	82	0.1	1.23

Table IIo. Short-Term Time Variability

$L_b = F_A(50, H_t, H, d, H_r)$

Field Point	Distance (Miles)	H_t (Feet)	H_r (Feet)	Maximum Variation (db)	Time Period (Minutes)
1	0.2	80	11	0.4	0.70
2	0.45	80	11	1.0	0.86
3	0.7	80	11	0.5	0.96
4	1.0	80	11	0.4	0.69
5	2.0	80	11	0.6	0.96
5.5	3.0	80	11	0.5	1.40
5.5	3.0	80	82	0.2	0.60
6	4.0	80	11	1.4	0.90
2	0.45	40	11	0.4	0.40
2	0.45	40	81	0	1.16
3	0.7	40	11	0.3	0.55
3	0.7	40	81	0	0.32
4	1.0	40	11	0	0.68
4	1.0	40	81	0	0.80
5	2.0	40	11	0	0.70
5.5	3.0	40	11	0	0.97
8	10.5	40	17	0.5	0.38
8	10.5	40	81	0.4	0.57
9	14.0	40	81	0.6	0.57
10	17.0	40	17	0.4	0.63
10	17.0	40	81	0.2	0.73
3	0.7	13	17	0	0.68
3	0.7	13	81	1.1	0.52
4	1.0	13	17	0.2	0.84
4	1.0	13	81	0.4	1.48
5	2.0	13	18	0.5	0.61
5	2.0	13	81	0.3	1.05
5.5	3.0	13	18	0.1	0.40
5.5	3.0	13	81	0.4	0.92
6	4.0	13	18	0.5	0.62

Table IIo (Continued). Short-Term Time Variability

$L_b = F_A(50, H_t, H, d, H_r)$

Field Point	Distance (Miles)	H_t (Feet)	H_r (Feet)	Maximum Variation (db)	Time Period (Minutes)
6	4.0	13	81	0.7	0.84
7	7.0	13	82	0.2	0.95
8	10.5	13	82	0.4	1.75

Table IIp. Short-Term Time Variability

$L_b = F_A(100, H_t, H, d, H_r)$

Field Point	Distance (Miles)	H_t (Feet)	H_r (Feet)	Maximum Variation (db)	Time Period (Minutes)
3	0.7	80	17	0.9	0.59
3	0.7	80	81	1.8	1.92
4	1.0	80	17	1.5	0.80
4	1.0	80	81	0.9	0.85
5	2.0	80	11	0.9	0.70
5.5	3.0	80	17	0.5	0.65
5.5	3.0	80	81	0.2	0.92
6	4.0	80	18	0.9	0.59
6	4.0	80	82	0.9	1.46
7	7.0	80	17	0	0.68
7	7.0	80	78	0	0.69
8	10.5	80	78	0.6	0.78
9	14.0	80	78	0.9	0.51
3	0.7	40	17	0.9	1.11
3	0.7	40	81	0.7	0.90
4	1.0	40	17	0	0.51
4	1.0	40	81	0.2	0.56
5	2.0	40	17	0.4	0.92
5	2.0	40	81	0.4	0.66

Table IIp (Continued). Short-Term Time Variability

$L_b = F_A(100, H_t, H, d, H_r)$

Field Point	Distance (Miles)	H_t (Feet)	H_r (Feet)	Maximum Variation (db)	Time Period (Minutes)
5.5	3.0	40	17	0	0.44
5.5	3.0	40	81	0	0.22
6	4.0	40	18	0	0.46
6	4.0	40	81	0	0.50
7	7.0	40	17	0	0.58
7	7.0	40	81	0	0.40
1	0.2	13	17	0.5	1.14
1	0.2	13	81	0.6	1.20
2	0.45	13	11	0	0.88
3	0.7	13	11	0	0.94
4	1.0	13	17	0	0.80
4	1.0	13	81	0.4	1.06
5	2.0	13	18	0.4	0.65
5	2.0	13	81	0.6	0.60
5.5	3.0	13	17	0	0.80
5.5	3.0	13	81	0	0.52
7	7.0	13	81	0	2.08

Table IIq. Short-Term Time Variability

$L_b = F_A(250, H_t, H, d, H_r)$

Field Point	Distance (Miles)	H_t (Feet)	H_r (Feet)	Maximum Variation (db)	Time Period (Minutes)
1	0.2	80	18	0.7	0.62
1	0.2	80	82	1.3	0.56
2	0.45	80	11	0.9	0.90
2	0.45	80	82	0.4	0.73
3	0.7	80	11	2.0	0.80
3	0.7	80	82	0	0.66
4	1.0	80	78	0	0.40
5.5	3.0	80	11	0.4	0.60
6	4.0	80	17	0	0.55
6	4.0	80	81	0	0.62
1	0.2	40	11	2.0	0.80
1	0.2	40	78	1.4	1.24
2	0.45	40	11	0	1.00
2	0.45	40	78	1.4	1.06
5.5	3.0	40	17	0.6	0.70
5.5	3.0	40	78	0.6	0.52
6	4.0	40	78	0	0.95

Table IIr. Short-Term Time Variability

$L_b = F_A(400, H_t, H, d, H_r)$

Field Point	Distance (Miles)	H_t (Feet)	H_r (Feet)	Maximum Variation (db)	Time Period (Minutes)
1	0.2	80	11	0.6	1.22
2	0.45	80	11	2.2	0.50
3	0.7	80	81	1.0	1.14
4	1.0	80	11	0.7	0.84
4	1.0	80	82	0.8	1.80
5.5	3.0	80	11	0	0.73
1	0.2	40	11	0.6	0.80
2	0.45	40	11	1.0	0.62
3	0.7	40	11	0	0.82
3	0.7	40	82	0.6	0.98
4	1.0	40	11	0.6	0.46
4	1.0	40	81	0.7	0.32
5	2.0	40	11	0.2	1.57
5.5	3.0	40	11	0	0.30
1	0.2	13	11	0	0.30
2	0.45	13	11	0.1	0.94
3	0.7	13	11	0	0.44
4	1.0	13	11	0	0.60
4	1.0	13	81.6	2.1	1.49
5.5	3.0	13	11	1.3	0.51

4.3.2 Variation with Antenna Height

4.3.2.1 Fine-Grain Variability

Figures 4.20A through 4.20P are examples of the fine-grain variability of received field strength as a function of receiving antenna height. Two types of curves are plotted in the above figures. The dashed curves represent field point median data of the type shown in Figures 3.10 through 3.55. The solid curves are plotted directly from the strip chart recordings of field strength made at the time of measurement. The field strength data is taken from the recordings, converted to basic transmission loss, and plotted directly as the solid curves in Figures 4.20A through 4.20P. Thus, the variations appearing in the solid curves in the above figures are the same as the variations in field strength which appear on the strip chart recordings.

Fine-grain variability is defined as the difference between the median value of basic transmission loss (dashed curve) and the actual value of basic transmission loss (solid curve) at a particular receiving antenna height. As Figure 4.20A shows, for a frequency of 880 kc, vertical polarization, there is almost no fine-grain variability. In fact, there is essentially no change of any kind in propagation loss with height. Figure 4.20B demonstrates that for vertical polarization at 12 mc there is a definite decrease in propagation loss with increasing antenna height, but there is no significant fine-grain variability. At 100 mc, as Figure 4.20C shows, there is a noticeable fine-grain variability for a transmitting antenna height of 13 feet. However, the variability is slightly less for a transmitting antenna height of 80 feet, as shown in Figure 4.20D.

Figures 4.20E and 4.20F provide examples of a fine-grain variability that is more apparent at the higher transmitting antenna height than at the lower. This phenomenon may

be significant and is receiving further study.

Figures 4.20G through 4.20P show a noticeable fine-grain variability for both horizontal and vertical polarization at 250 and 400 mc. Table III provides a summary of the maximum fine-grain variation for a cross section of Radial A data. The maximum fine-grain variation is defined as the maximum difference in db between a dotted curve and a solid curve of the type shown in Figures 4.20A through 4.20P.

Table III shows that the fine-grain variability tends to increase with increasing frequency for close distances, but tends to remain constant with frequency at the farther distances. The information presented in Figures 4.20A through 4.20P and in Table III is submitted to provide a sample of the basic characteristics of fine-grain variability with antenna height. An intensive analysis of fine-grain variability with antenna height and its correlation with fine-grain variability as a function of distance is in process.

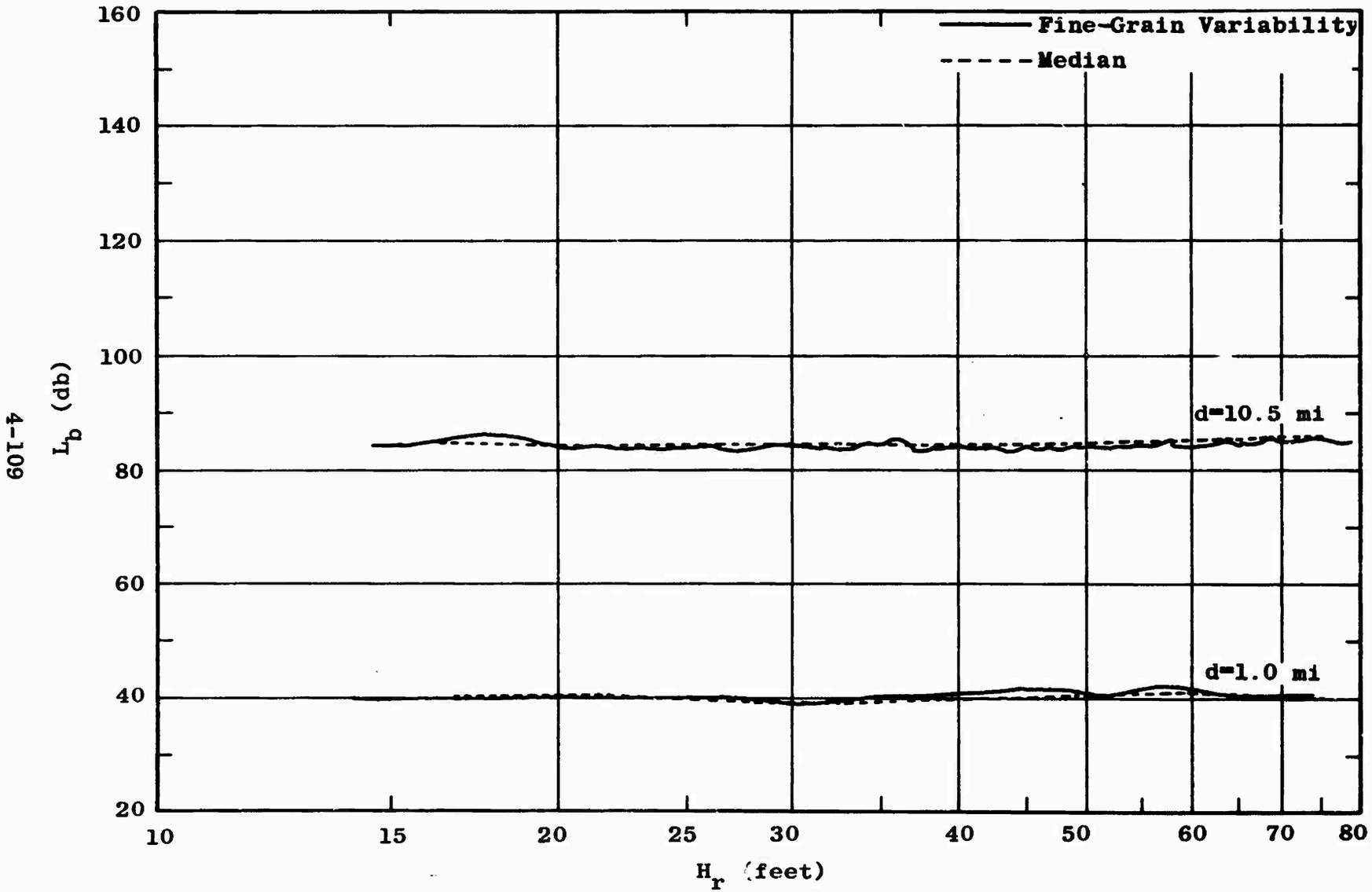

Figure 4.20A Fine-Grain Variability as a Function of Receiving Antenna Height
$L_b = F_A(0.880, 80, V, d, H_r)$

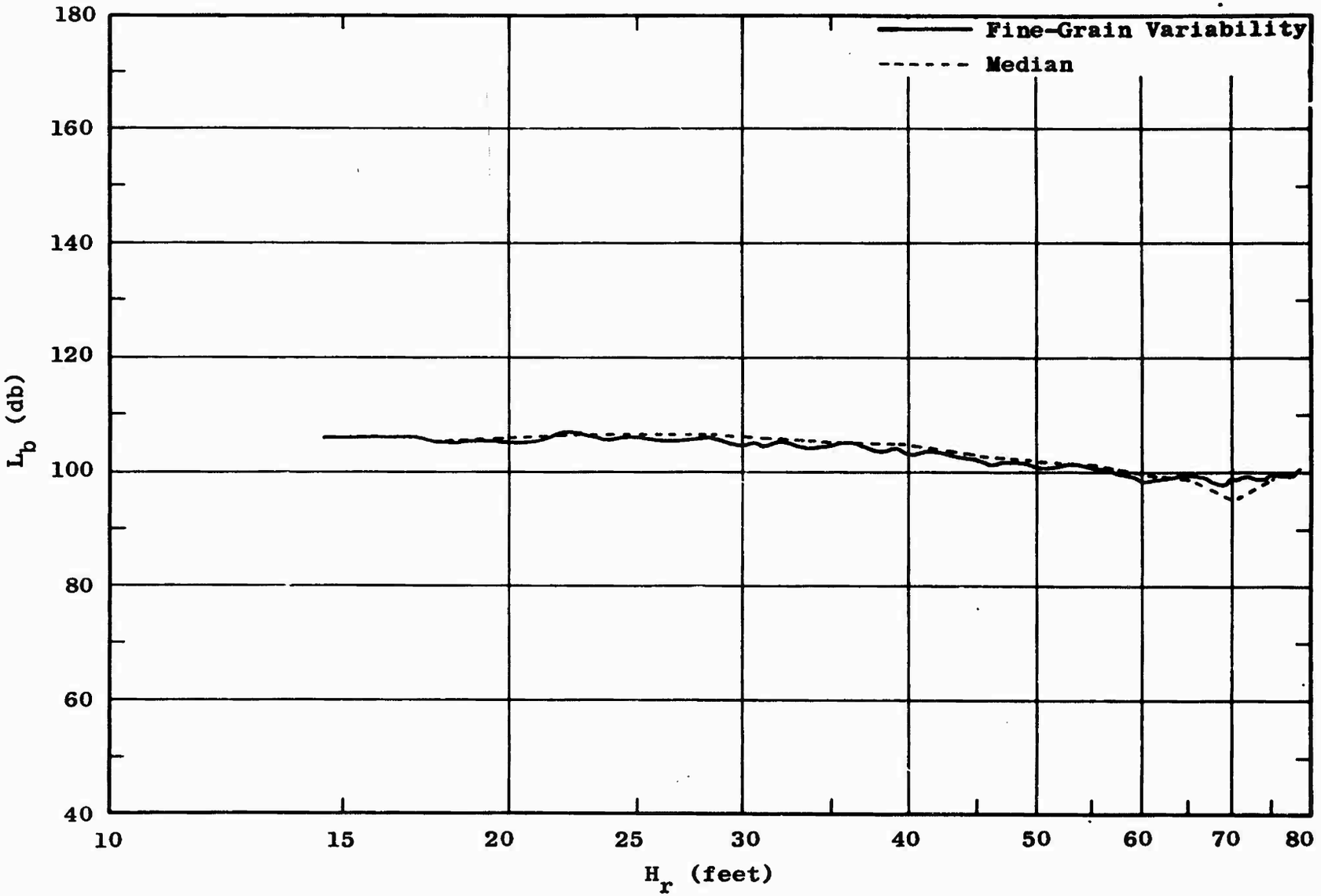

Figure 4.20B Fine-Grain Variability as a Function of Receiving Antenna Height
$L_b = F_A(12, 21, V, 1.0, H_r)$

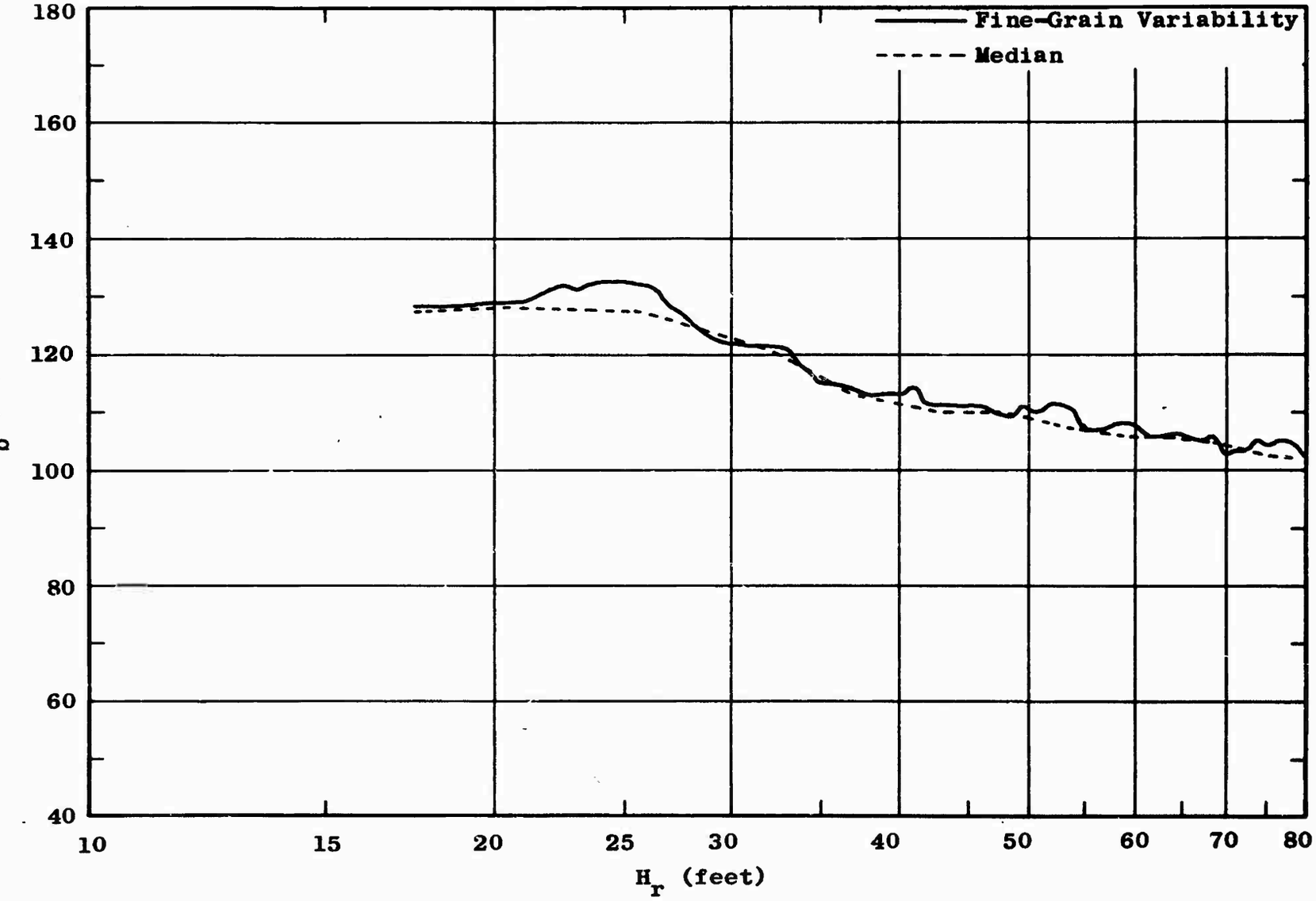

Figure 4.20C Fine-Grain Variability as a Function of Receiving Antenna Height
$L_b = F_A(100, 13, V, 1.0, H_r)$

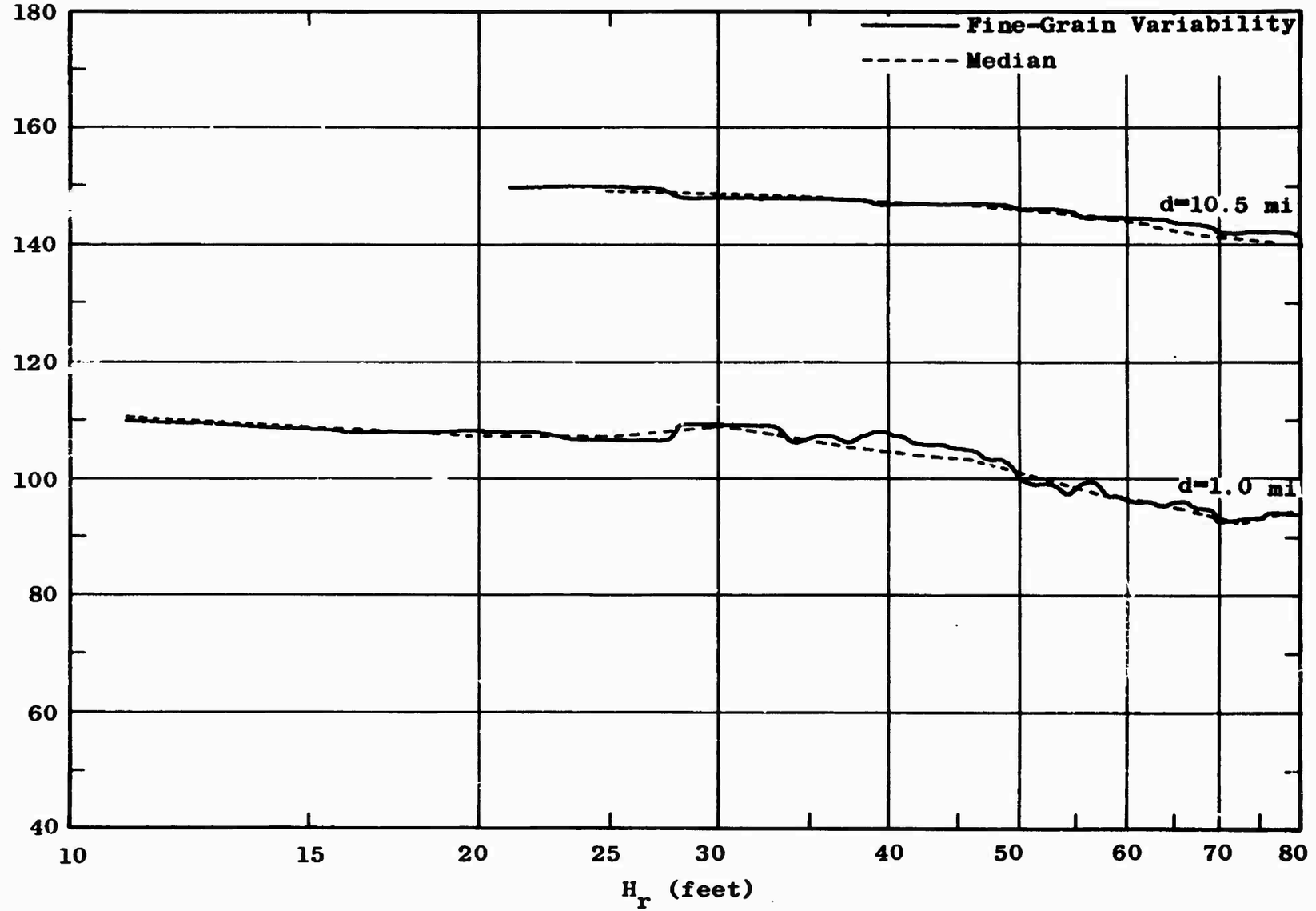

Figure 4.20D Fine-Grain Variability as a Function of Receiving Antenna Height
$L_b = F_A(100, 80, V, d, H_r)$

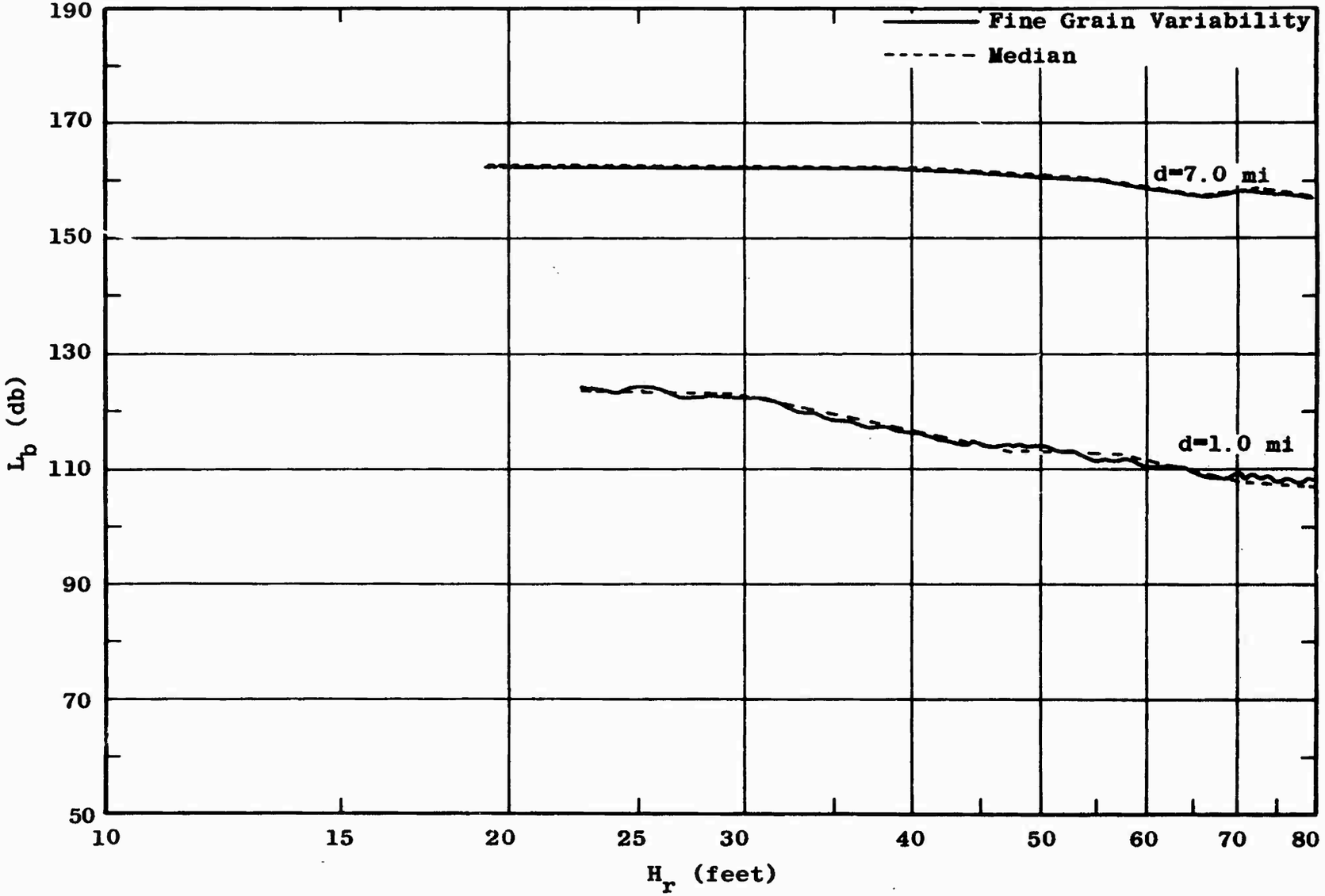

Figure 4.20E Fine-Grain Variability as a Function of Receiving Antenna Height
$L_A = F_b(100, 13, H, d, H_r)$

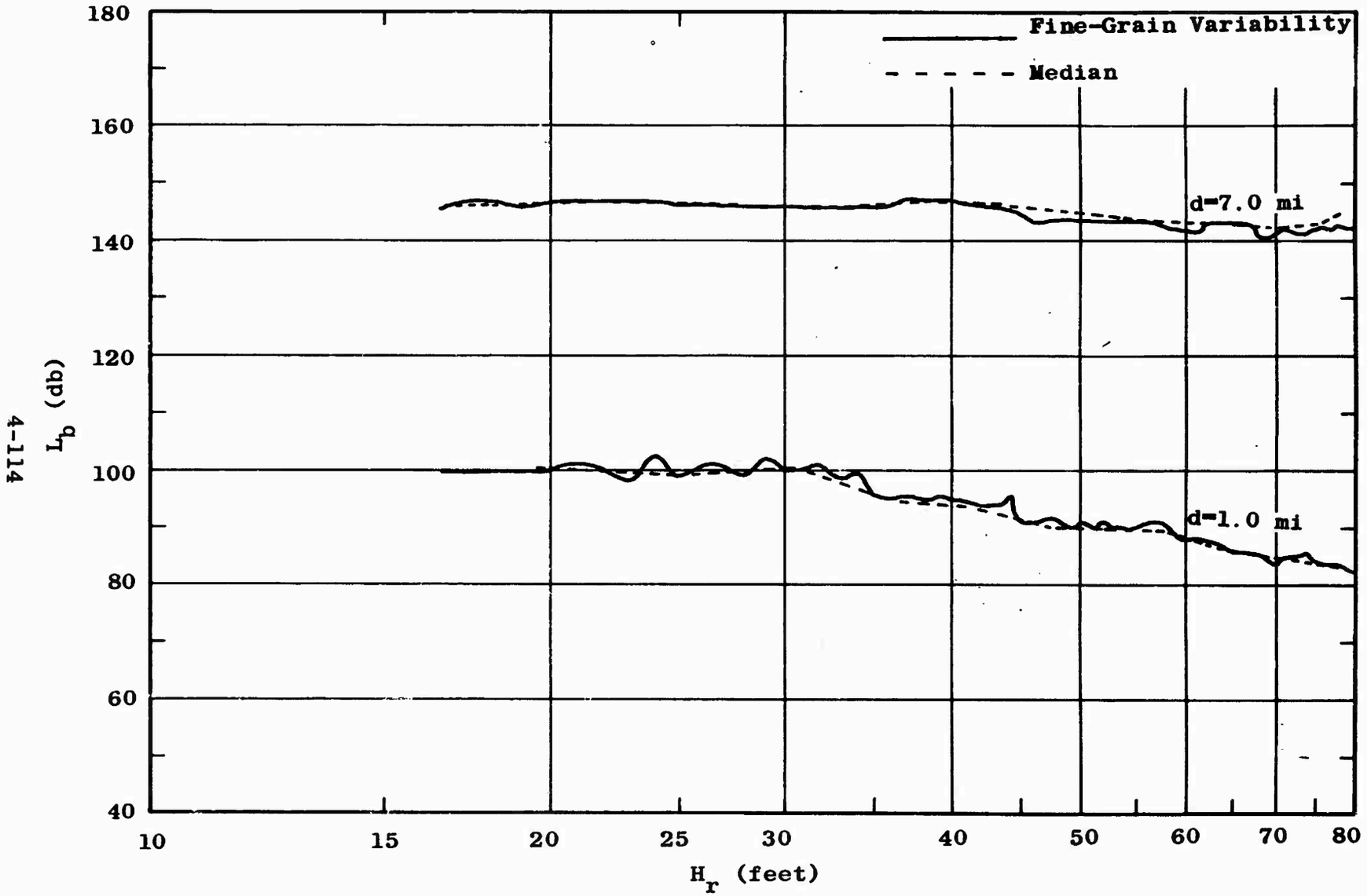

Figure 4.20F Fine-Grain Variability as a Function of Receiving Antenna Height
$L_b = F_A(100, 80, H, d, H_r)$

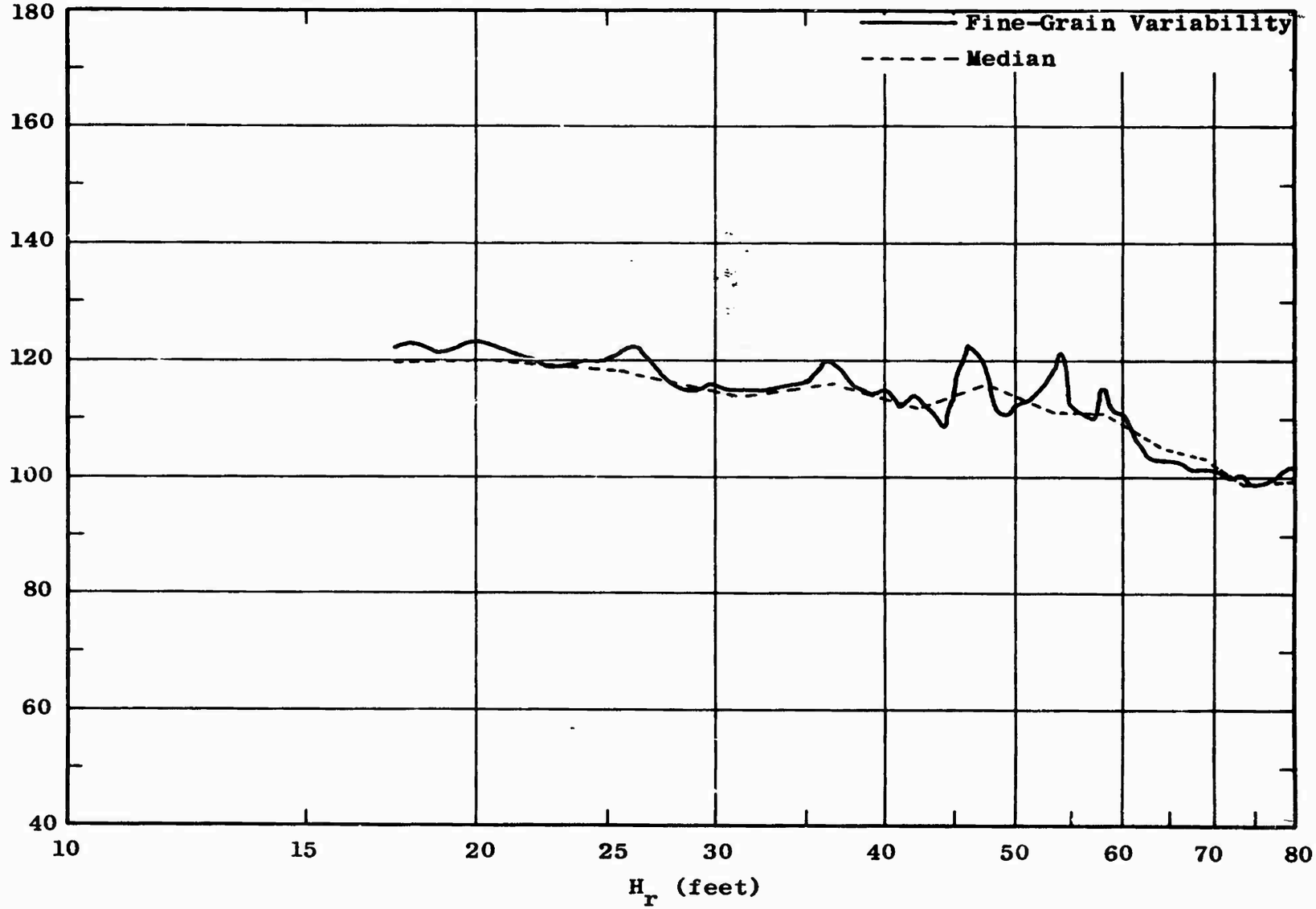

Figure 4.20G Fine-Grain Variability as a Function of Receiving Antenna Height
$L_b = F_A(250, 13, V, 0.2, H_r)$

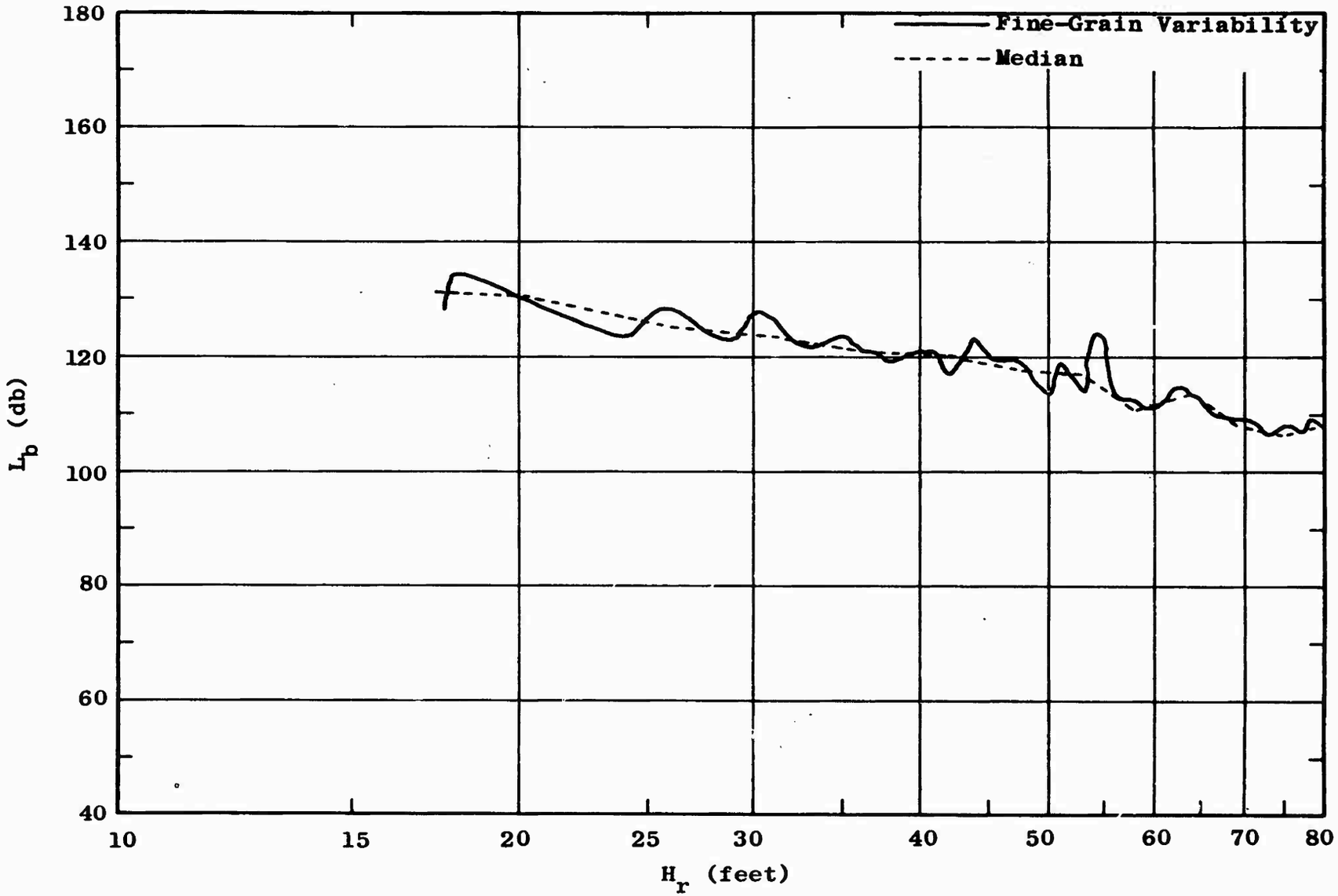

Figure 4.20H Fine-Grain Variability as a Function of Receiving Antenna Height
$L_b = F_A(250, 13, V, 0.45, H_r)$

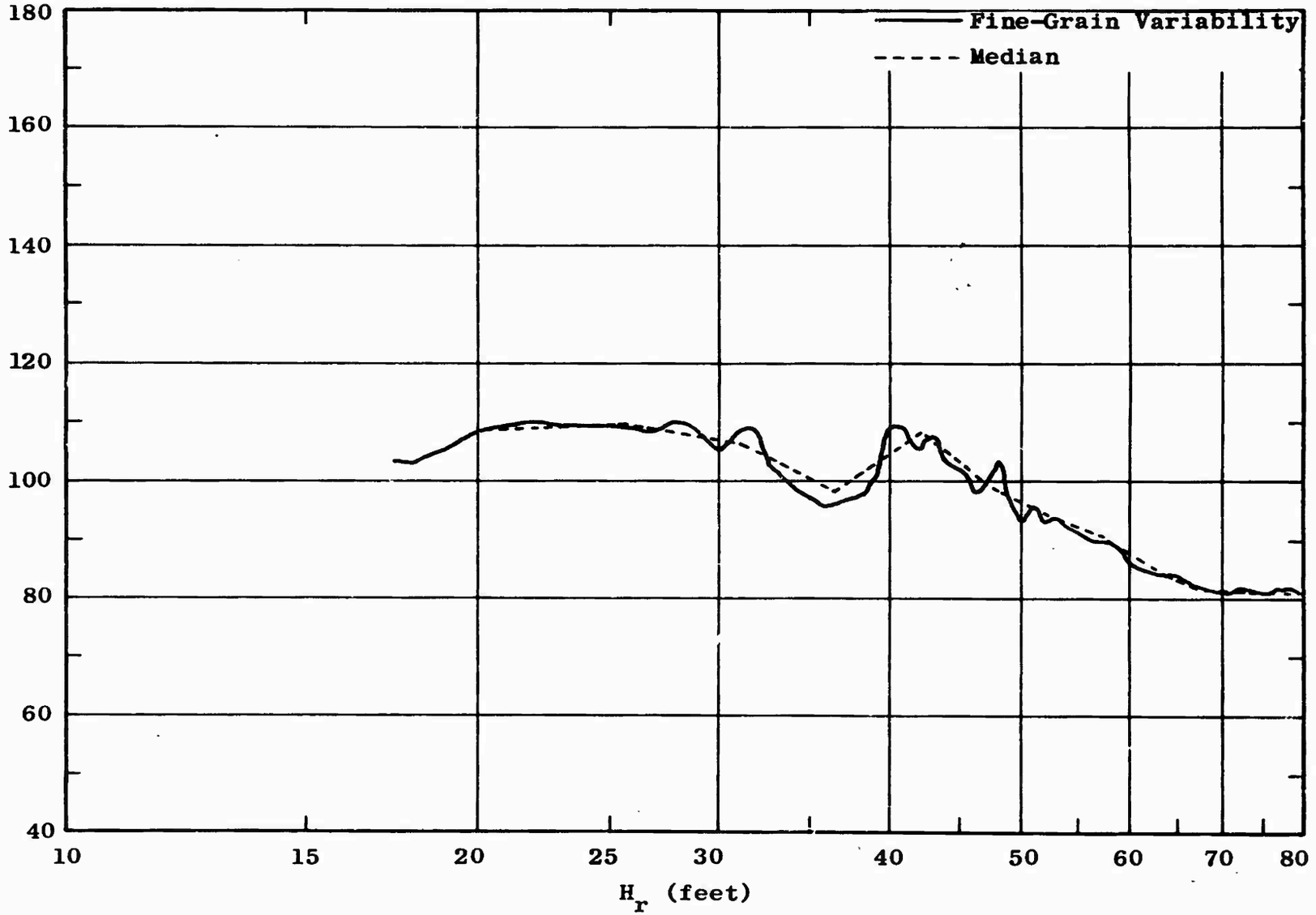

Figure 4.20I Fine-Grain Variability as a Function of Receiving Antenna Height
$L_b = F_A(250, 80\ V, 0.2, H_r)$

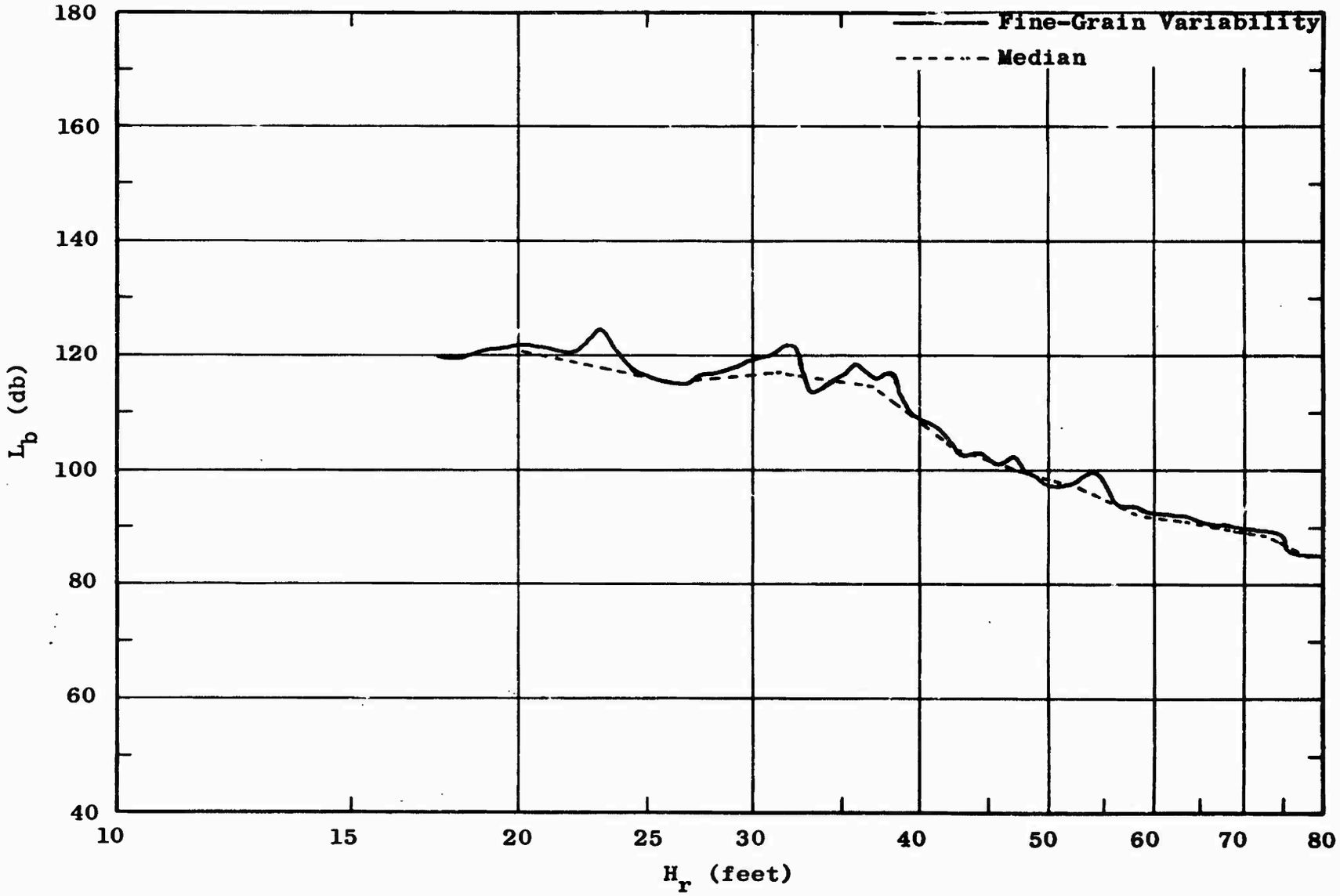

Figure 4.20J Fine-Grain Variability as a Function of Receiving Antenna Height
$L_b = F_A(250, 80, V, 0.45, H_r)$

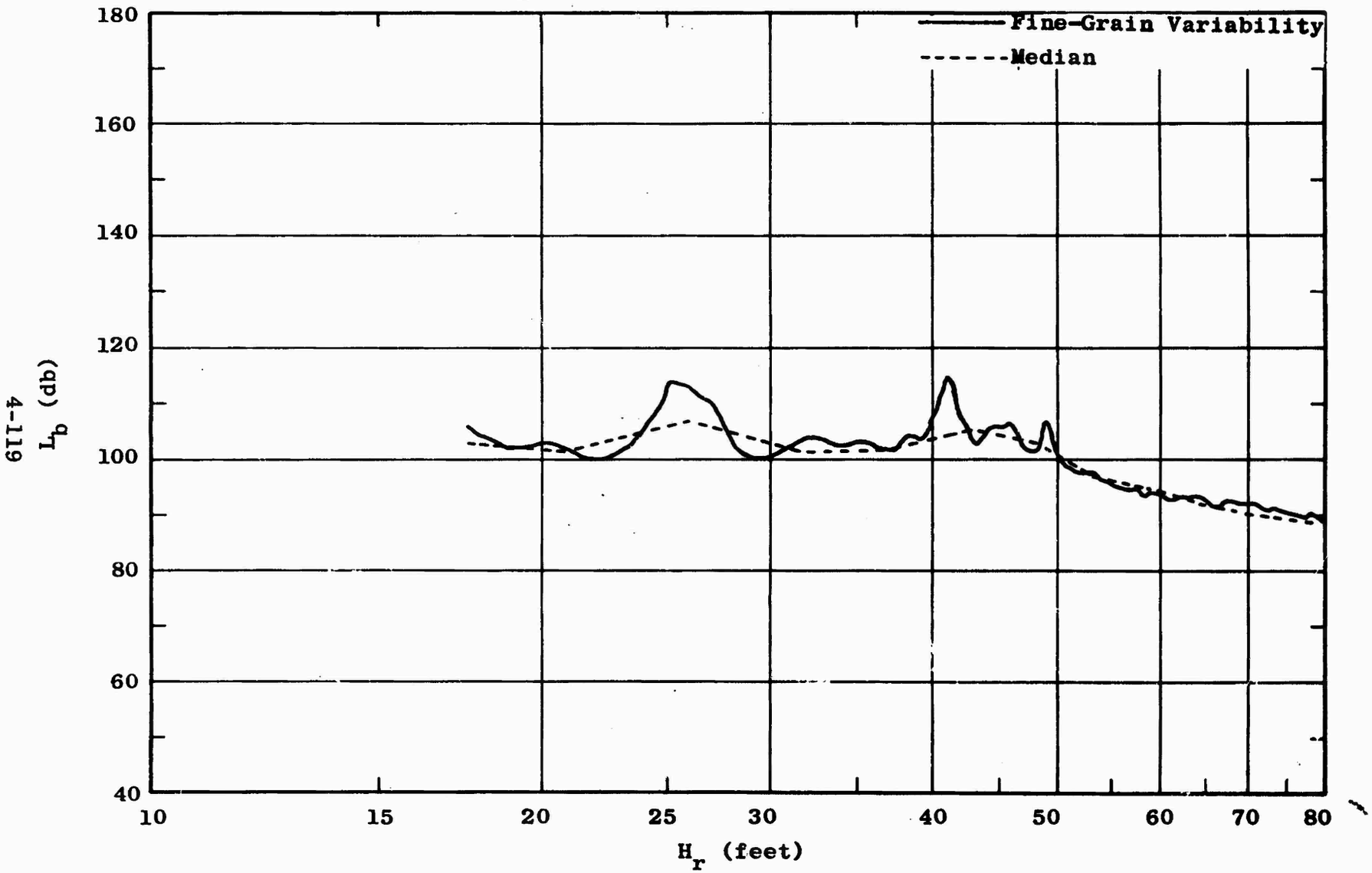

Figure 4.20K Fine-Grain Variability as a Function of Receiving Antenna Height
$L_b = F_A(250, 80, H, 0.2, H_r)$

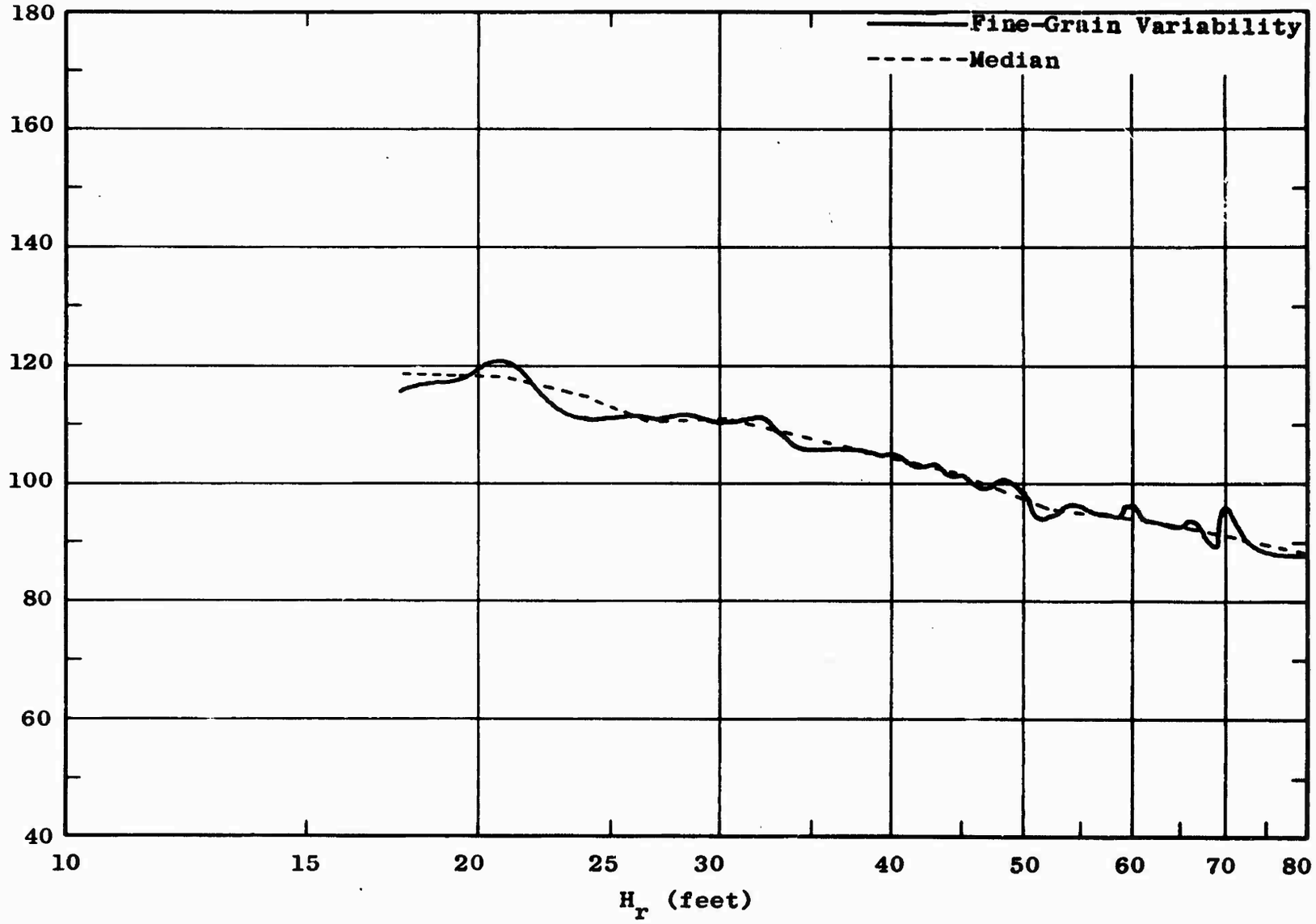

Figure 4.20L Fine-Grain Variability as a Function of Receiving Antenna Height
$L_b = F_A(250, 80, H, 0.45, H_r)$

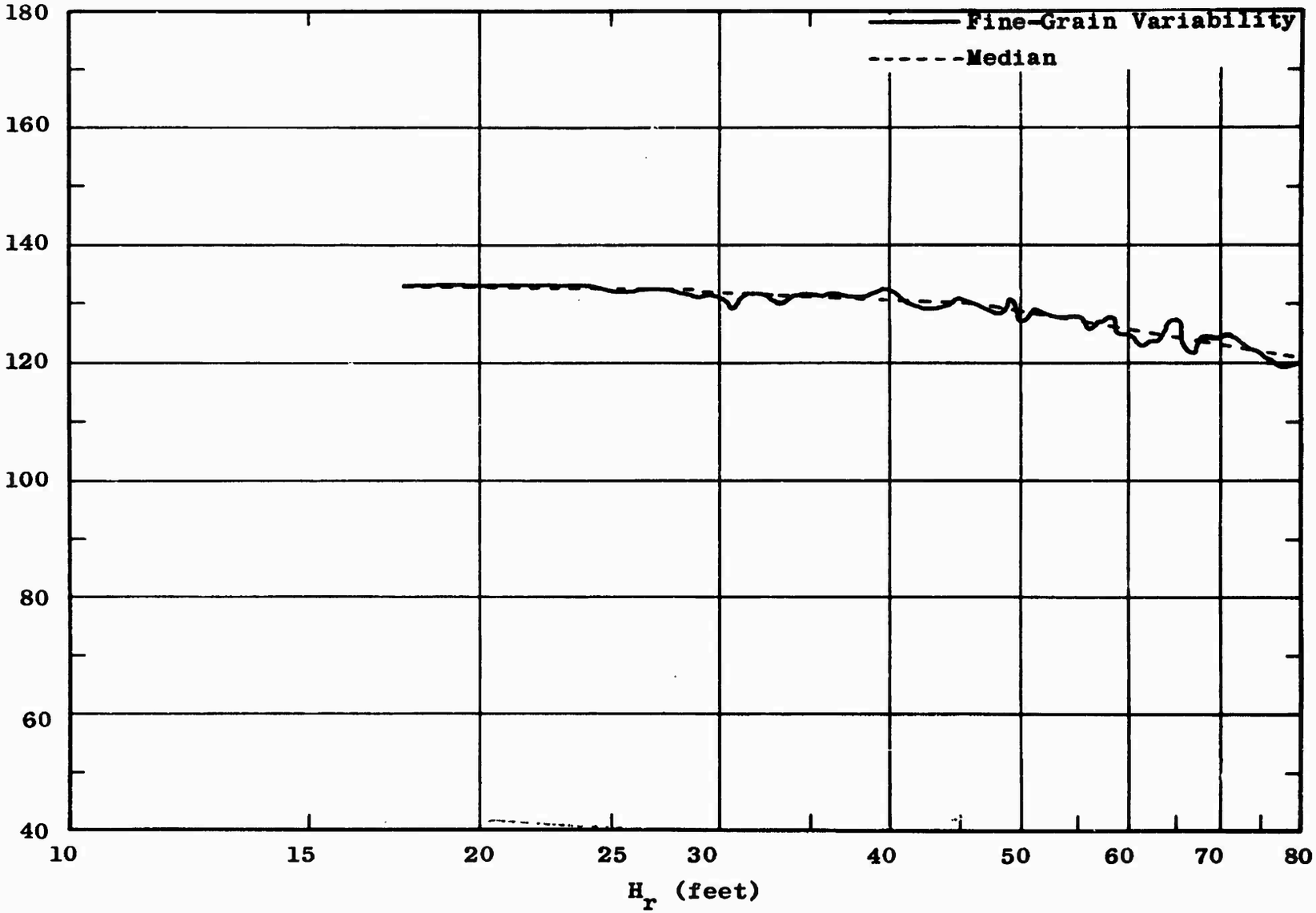

Figure 4.20M Fine-Grain Variability as a Function of Receiving Antenna Height
$L_b = F_A(400, 13, V, 1.0, H_r)$

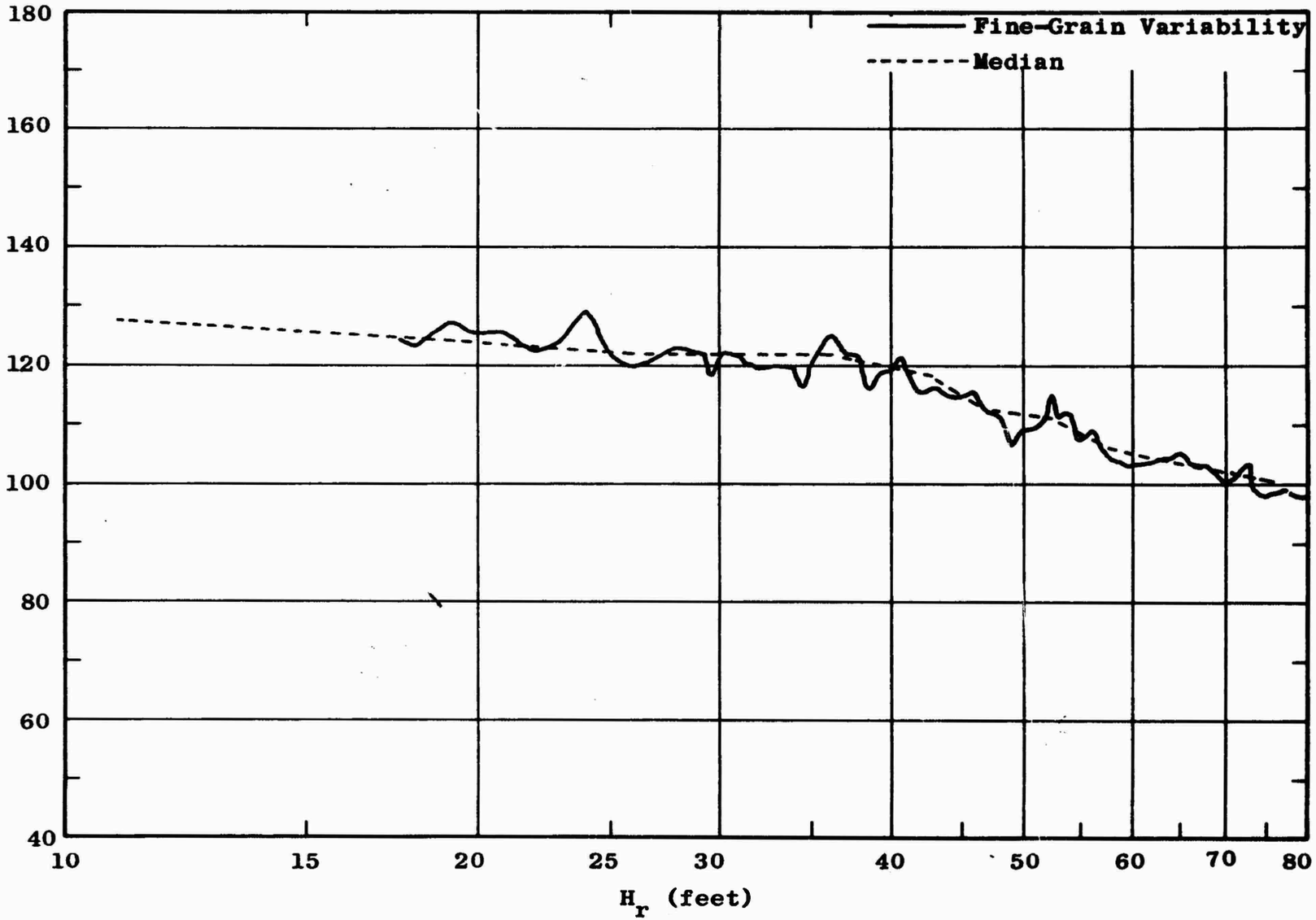

Figure 4.20M Fine-Grain Variability as a Function of Receiving Antenna Height
$L_b = F_A(400, 80, V, 1.0, H_r)$

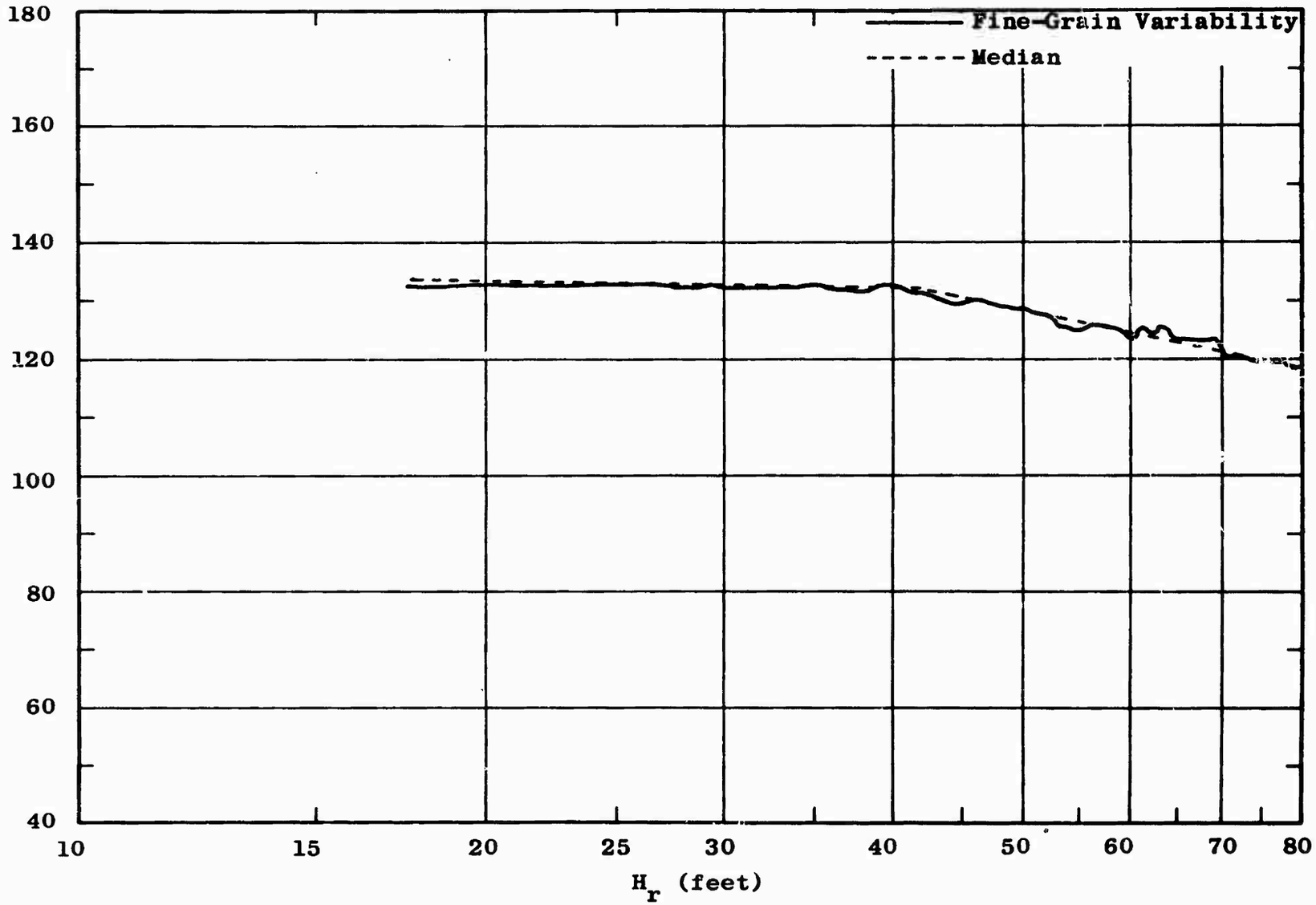

Figure 4.200 Fine-Grain Variability as a Function of Receiving Antenna Height
$L_b = F_A(400, 13, H, 1.0, H_r)$

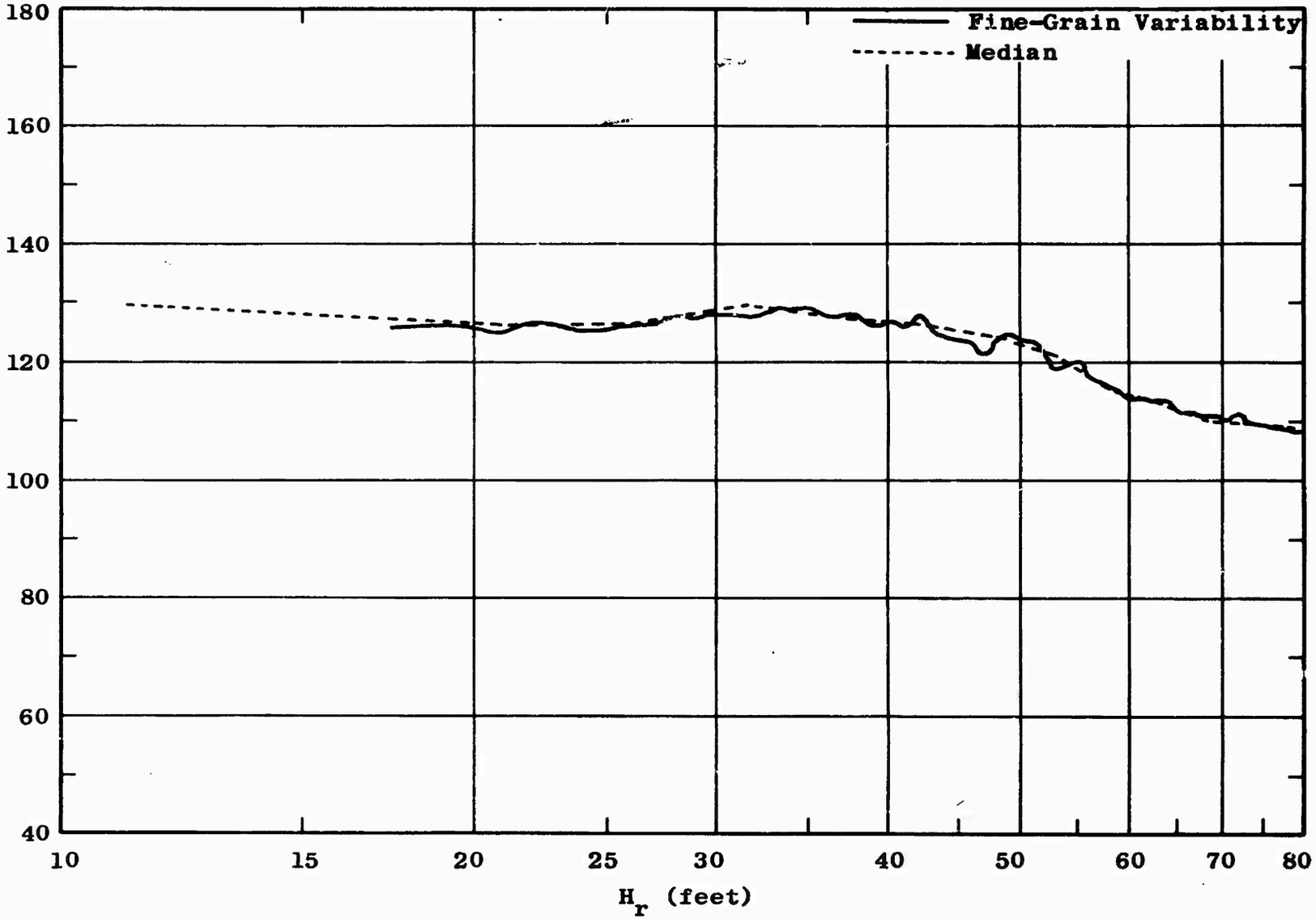

Figure 4.20P Fine-Grain Variability as a Function of Receiving Antenna Height
$L_b = F_A(400, 80, H, 1.0, H_r)$

Table III

FINE-GRAIN VARIABILITY

Frequency (mc)	H_t (Ft)	Pol.	Distance (Miles)	Max. Variation From Median (db)
0.880	80	V	1	1.0
0.880	80	V	10.5	1.5
12	21	V	1	1.5
12	21	V	2.0	2.0
12	40	H	1	1.2
12	40	H	4.0	1.0
100	80	V	1	2.0
100	80	V	10.5	1.0
100	80	H	1	2.0
100	80	H	7	1.0
100	13	V	1	4.0
100	13	V	4.0	3.0
100	13	H	1	2.0
100	13	H	7	1.0
400	80	V	1	6.0
400	80	V	2	4.0
400	80	H	1	3.0
400	80	H	3	2.0
400	13	V	1	4.0
400	13	V	3	1.0
400	13	H	1	2.0
400	13	H	3	1.0

4.3.2.2 Variability of Field Point Medians with Antenna Height

4.3.2.2.1 Comparison of L_b vs Distance for Various Receiving Antenna Heights

Figures 4.21A through 4.21HH provide a comparison of the basic transmission loss vs distance curves for three receiving antenna heights. In general, the three receiving antenna heights used for comparison were 20, 40, and 80 feet.

Figure 4.21A shows that there is no significant height effect for vertical polarization until a frequency of approximately 12 mc is reached. At 12 mc, the difference in basic transmission loss with a 20-foot receiving antenna and with an 80-foot receiving antenna is approximately 8 db.

Figures 4.21B through 4.21F show the effect of receiving antenna height for frequencies of 25.5 mc and above, vertical polarization, and a transmitting antenna height of 80 feet.

Figures 4.21G through 4.21K give a similar comparison for a transmitting antenna height of 40 feet. Figures 4.21L through 4.21P provide the same comparison for the 13-foot transmitting antenna height.

Figures 4.21Q through 4.21HH give a similar set of comparisons for horizontal polarization. Figure 4.21Q shows that there is a significant height effect for frequencies as low as 2 mc on horizontal polarization, whereas, there appears to be no significant height effect at either 2 or 6 mc for vertical polarization.

Comparing Figures 4.21E and 4.21B, for example, shows that the magnitude of the height effect for horizontal polarization is significantly less than that of the height

effect for vertical polarization.

Figures 4.21A through 4.21HH tend to indicate that the height effect is independent of distance except for possible terrain effects at the higher frequencies.

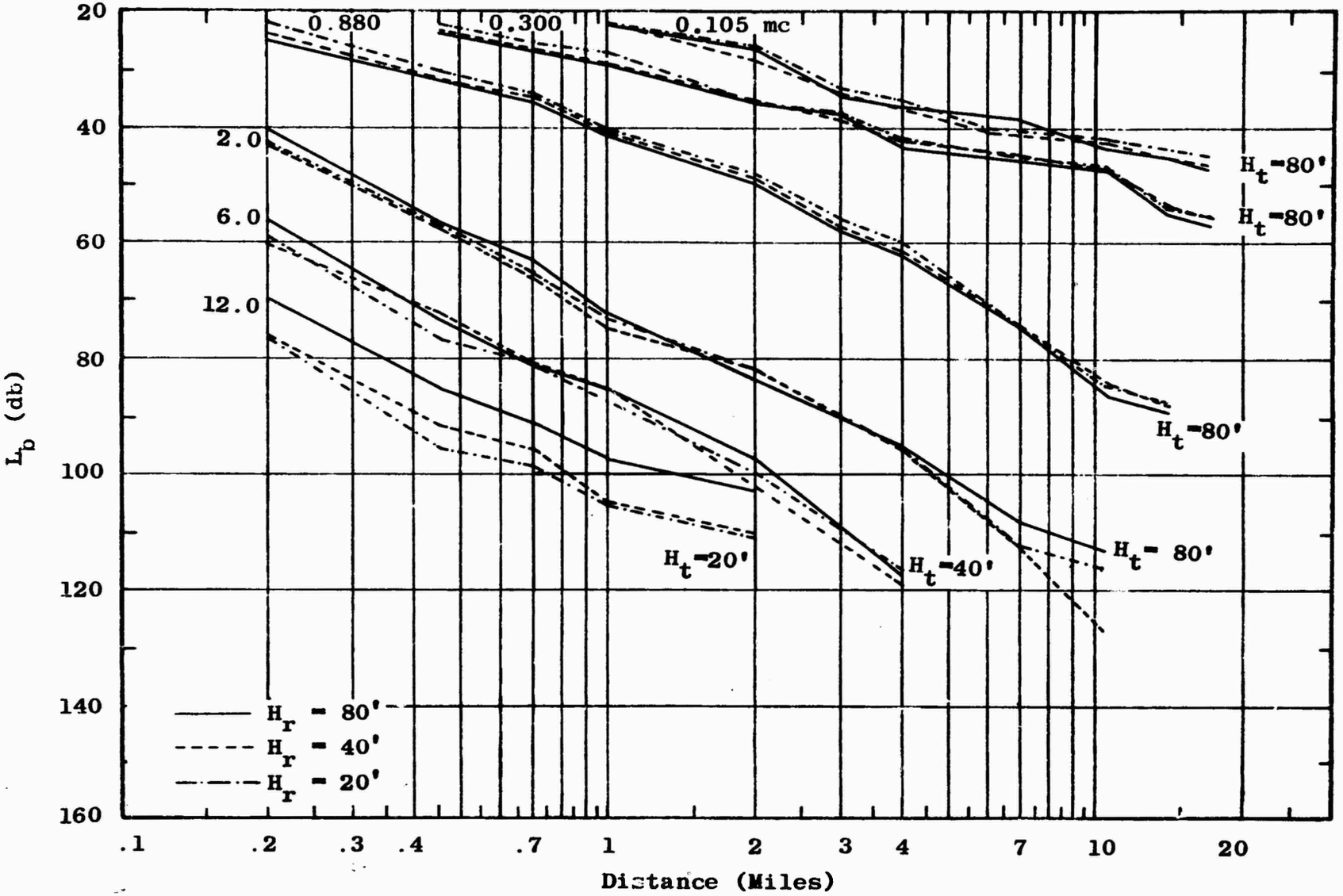

Figure 4.21A Comparison of L_b vs Distance for Various Receiving Antenna Heights
$L_b = F_A(f, H_t, V, d, H_r)$

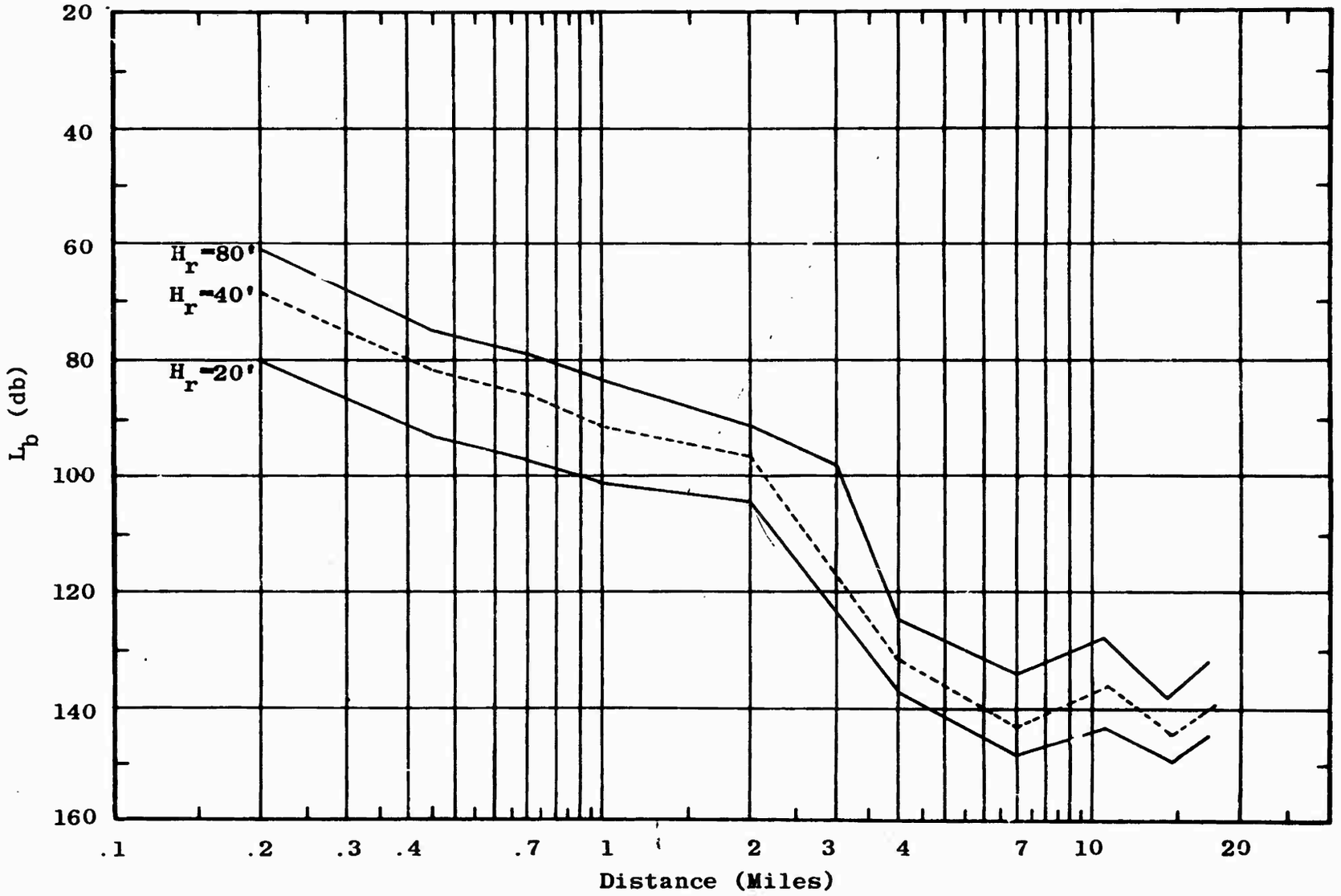

Figure 4.21B Comparison of L_b vs Distance for Various Receiving Antenna Heights
$L_b = F_A(f, H_t, V, d, H_r)$

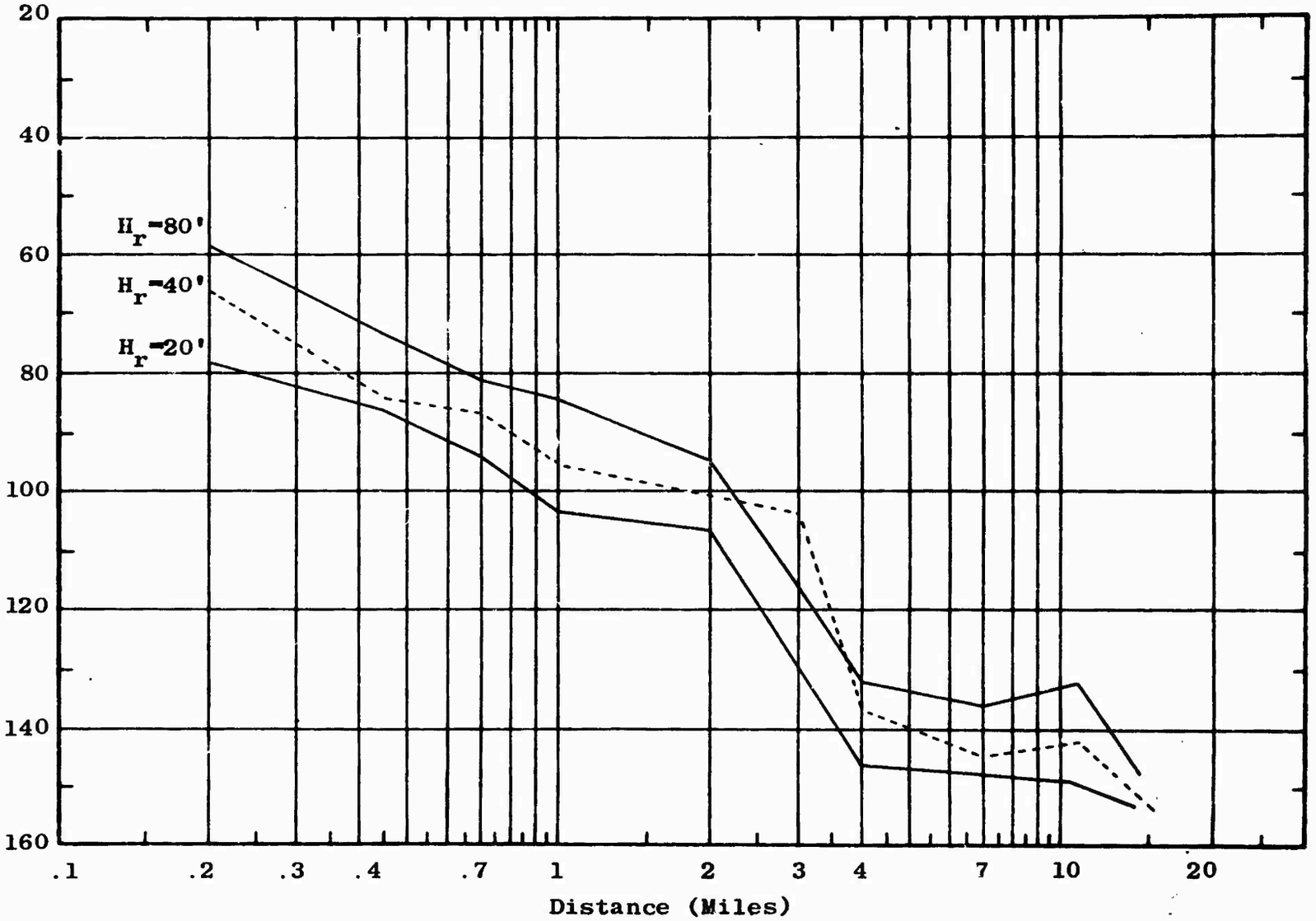

Figure 4.21C Comparison of L_b vs Distance for Various Receiving Antenna Heights
$L_b = F_A(50, 80, V, d, H_r)$

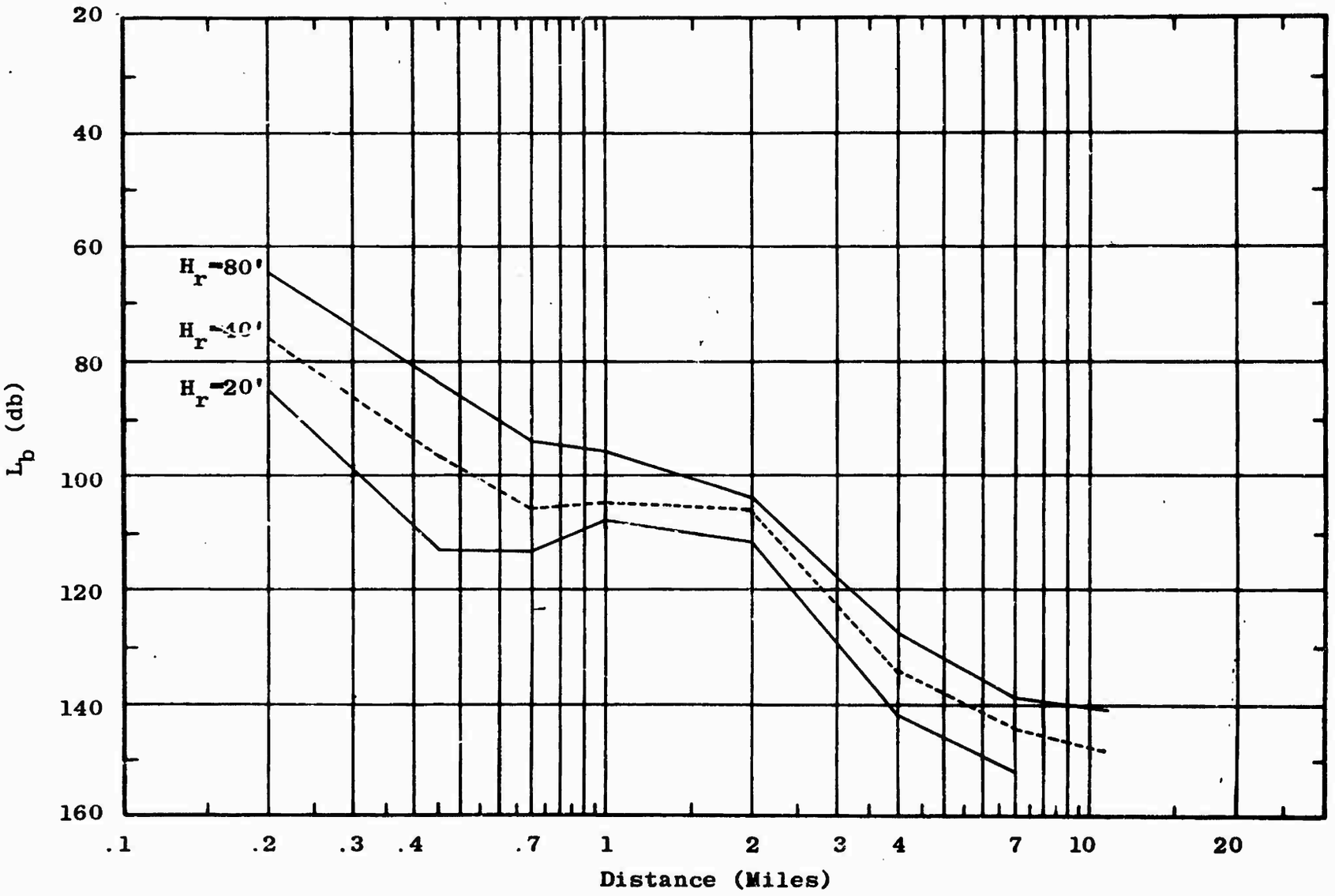

Figure 4.21D Comparison of L_b vs Distance for Various Receiving Antenna Heights
$L_b = F_A(100, 80, V, d, H_r)$

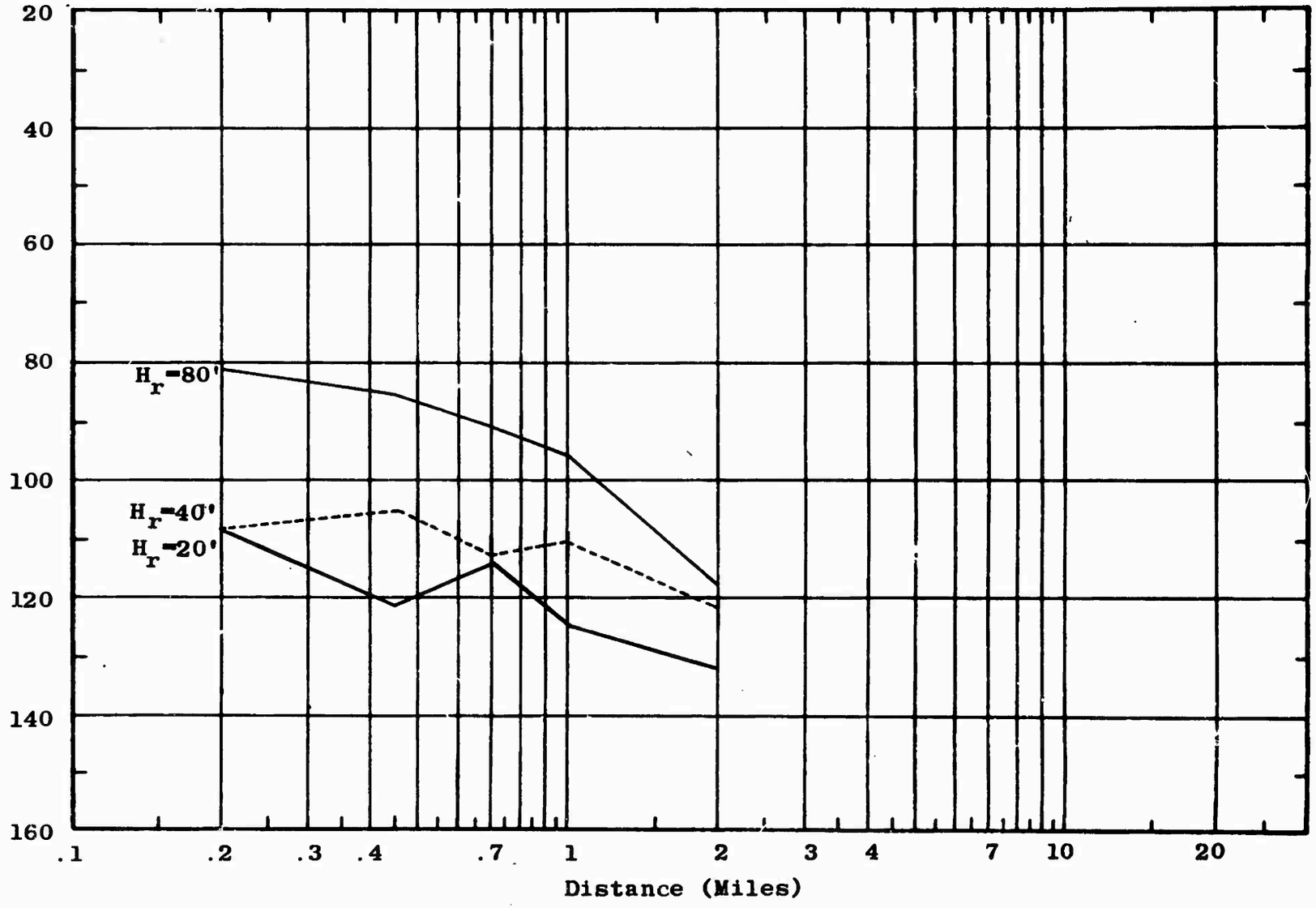

Figure 4.21E Comparison of L_b vs Distance for Various Receiving Antenna Heights
$L_b = F_A(250, 80, V, d, H_r)$

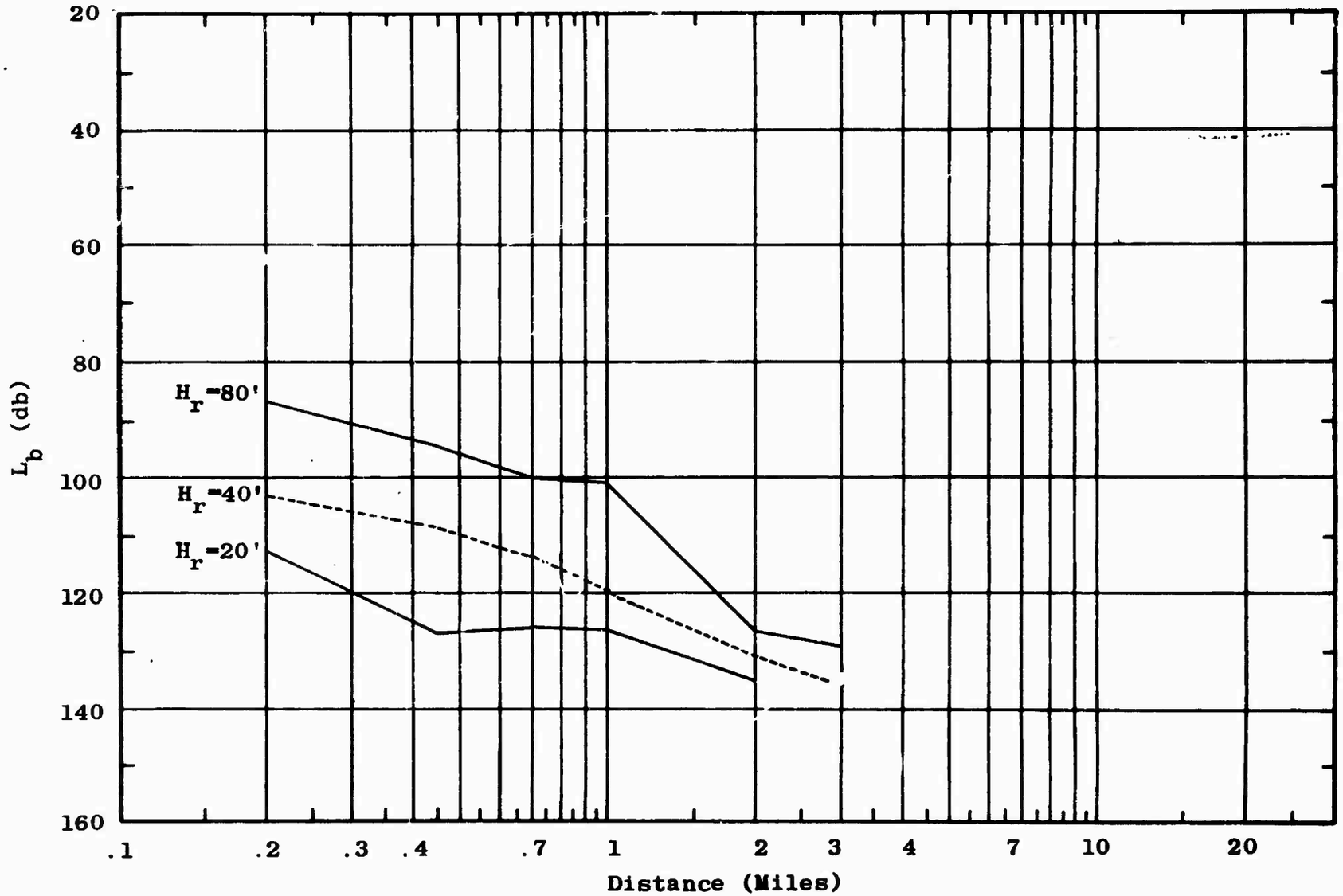

Figure 4.21F Comparison of L_b vs Distance for Various Receiving Antenna Heights
$L_b = F_A(400, 80, V, d, H_r)$

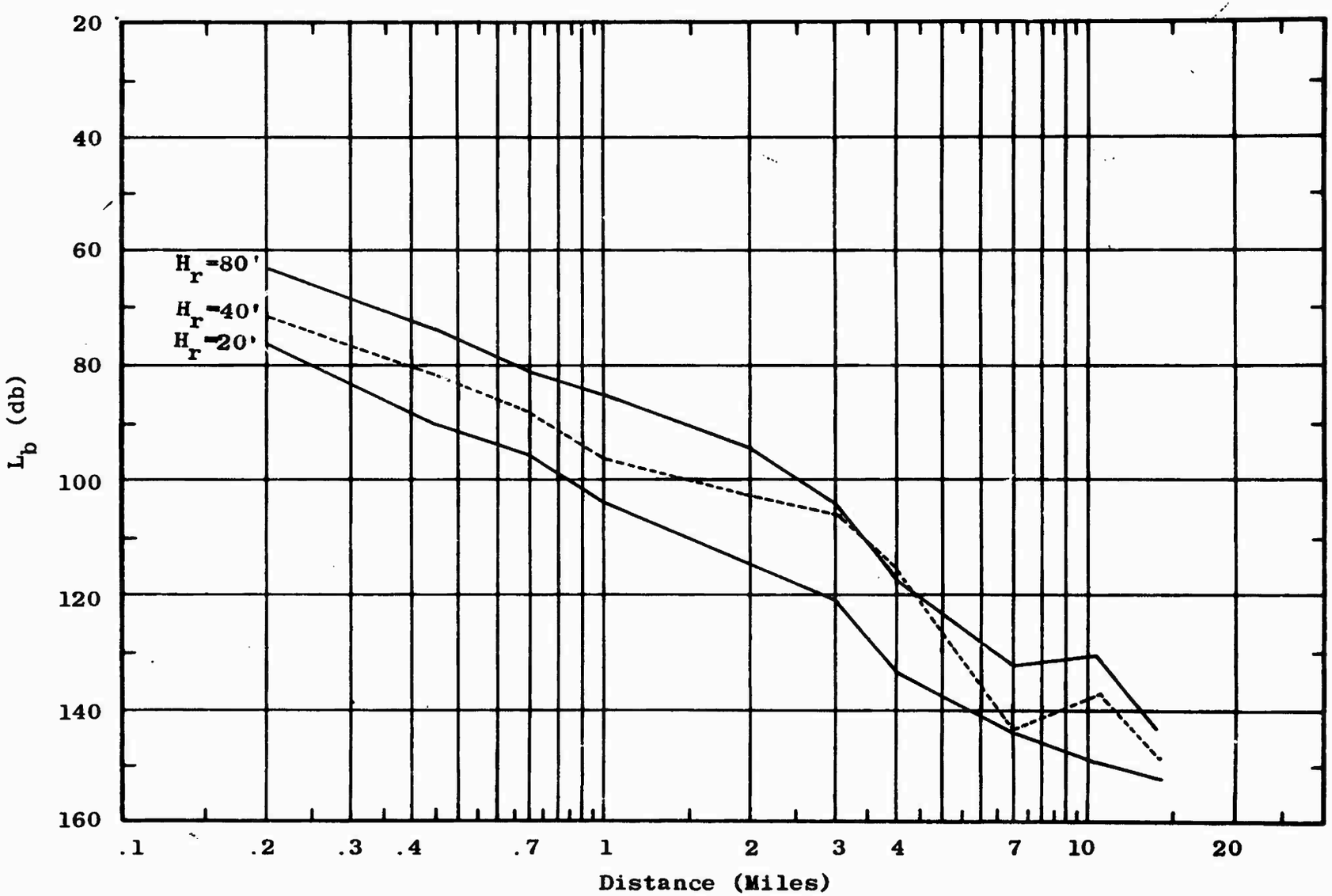

Figure 4.21G Comparison of L_b vs Distance for Various Receiving Antenna Heights
$L_b = F_A(25.5, 40, V, d, H_r)$

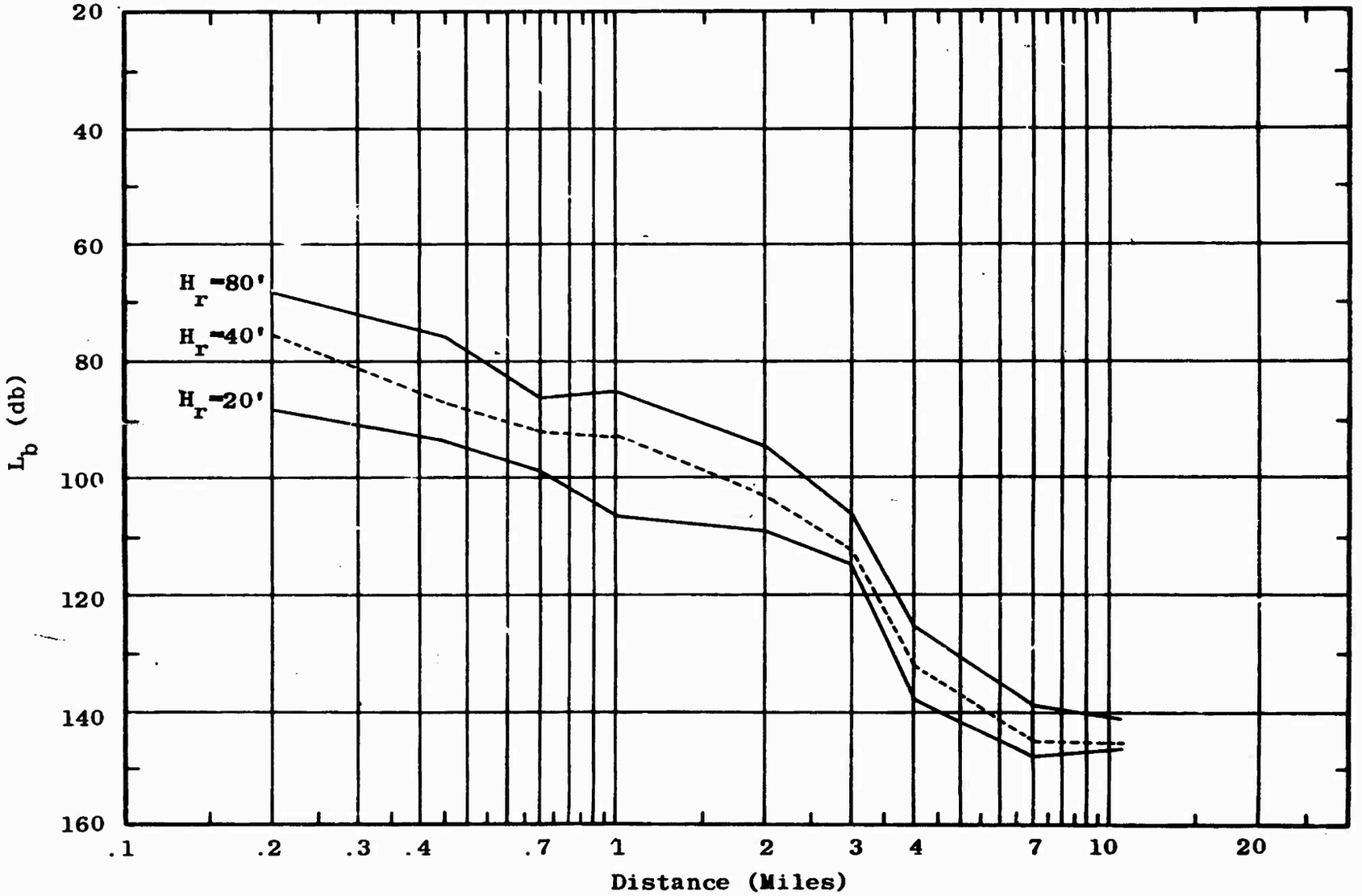

Figure 4.21H Comparison of L_b vs Distance for Various Receiving Antenna Heights
$L_b = F_A(50.0, 40, V, d, H_r)$

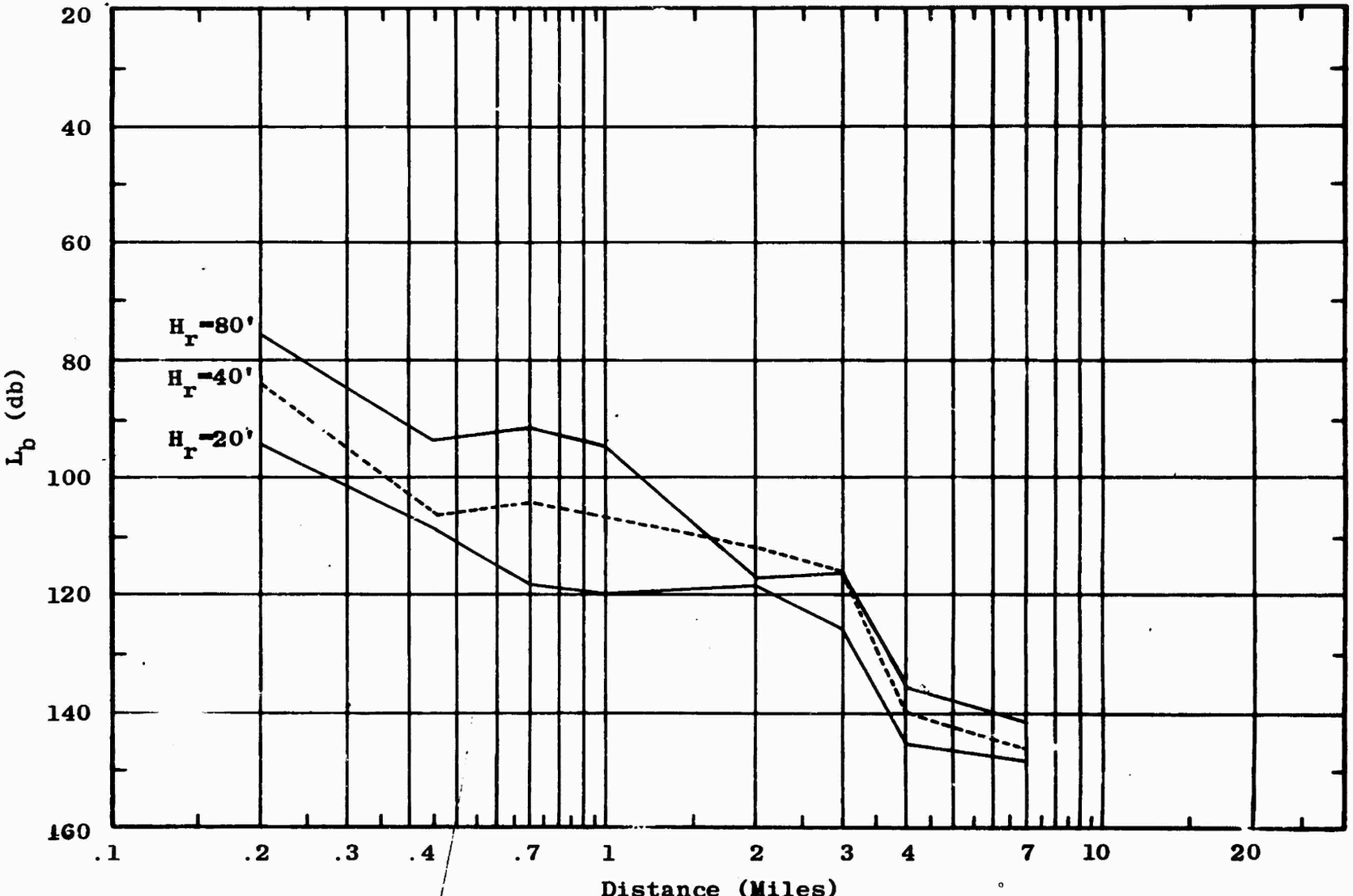

Figure 4.21I Comparison of L_b vs Distance for Various Receiving Antenna Heights
$L_b = F_A(100, 40, V, d, H_r)$

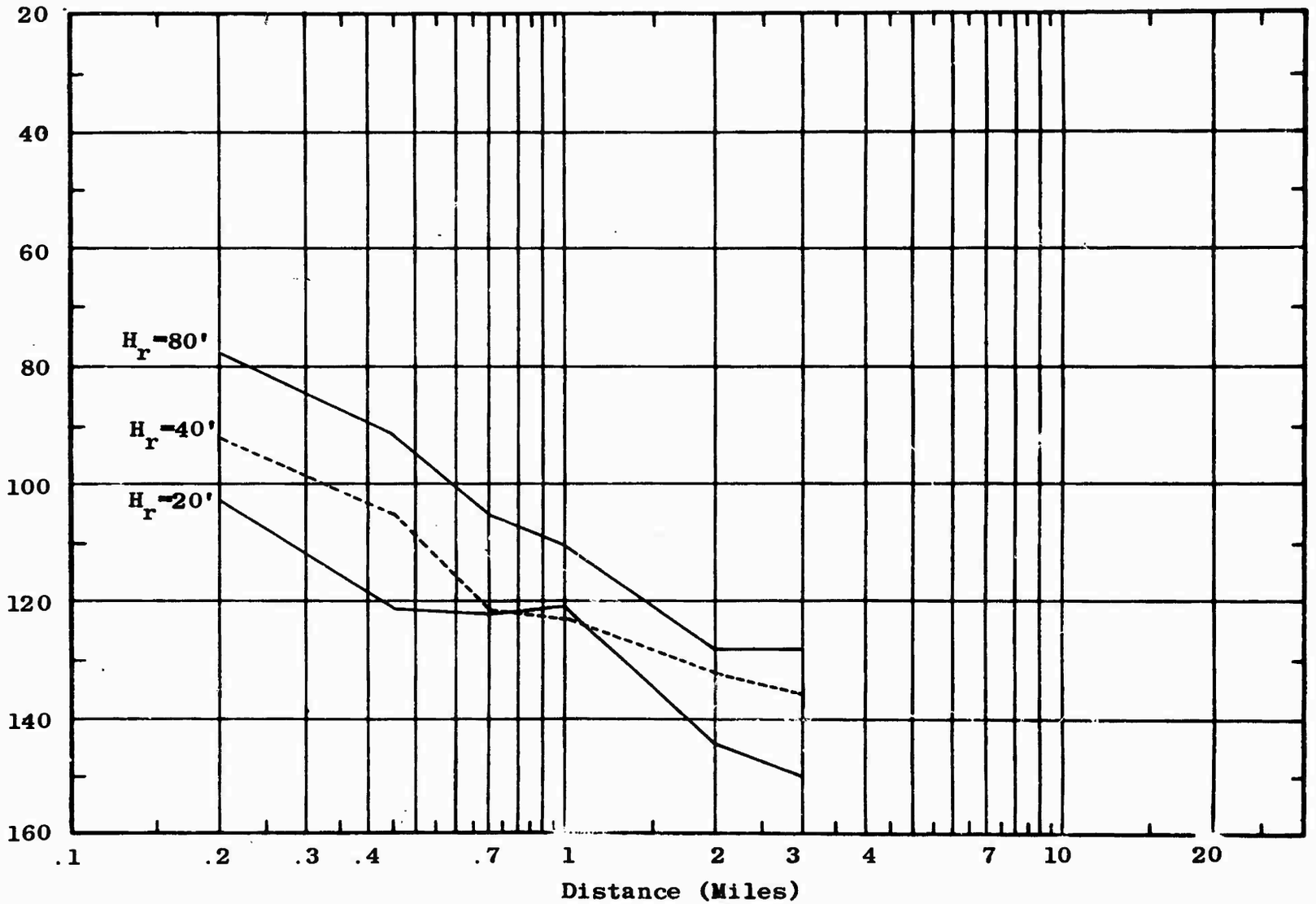

Figure 4.21J Comparison of L_b vs Distance for Various Receiving Antenna Heights
$L_b = F_A(250, 40, V, d, H_r)$

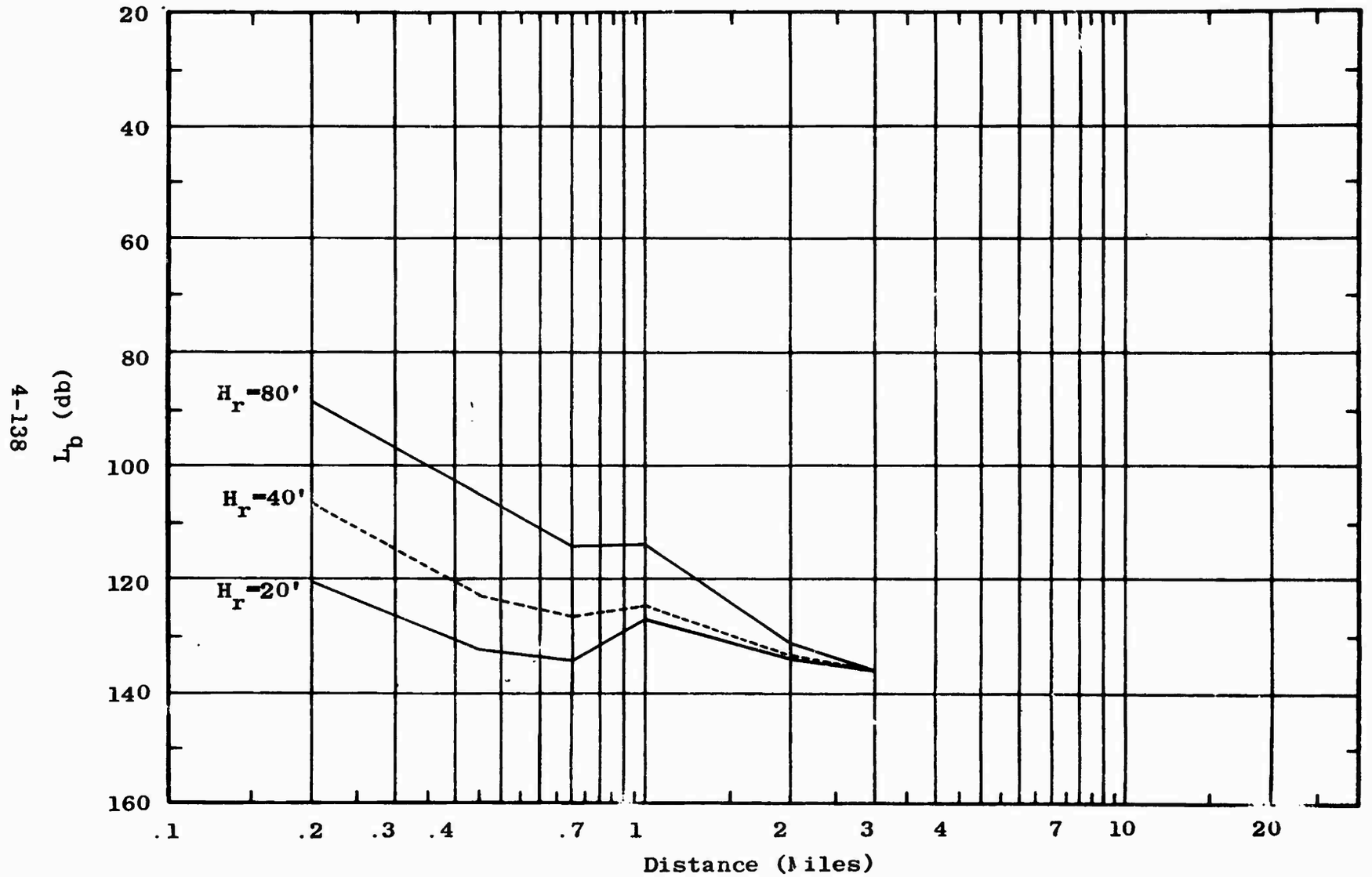

Figure 4.21K Comparison of L_b vs Distance for Various Receiving Antenna Heights
$L_b = F_A(400, 40, V, d, H_r)$

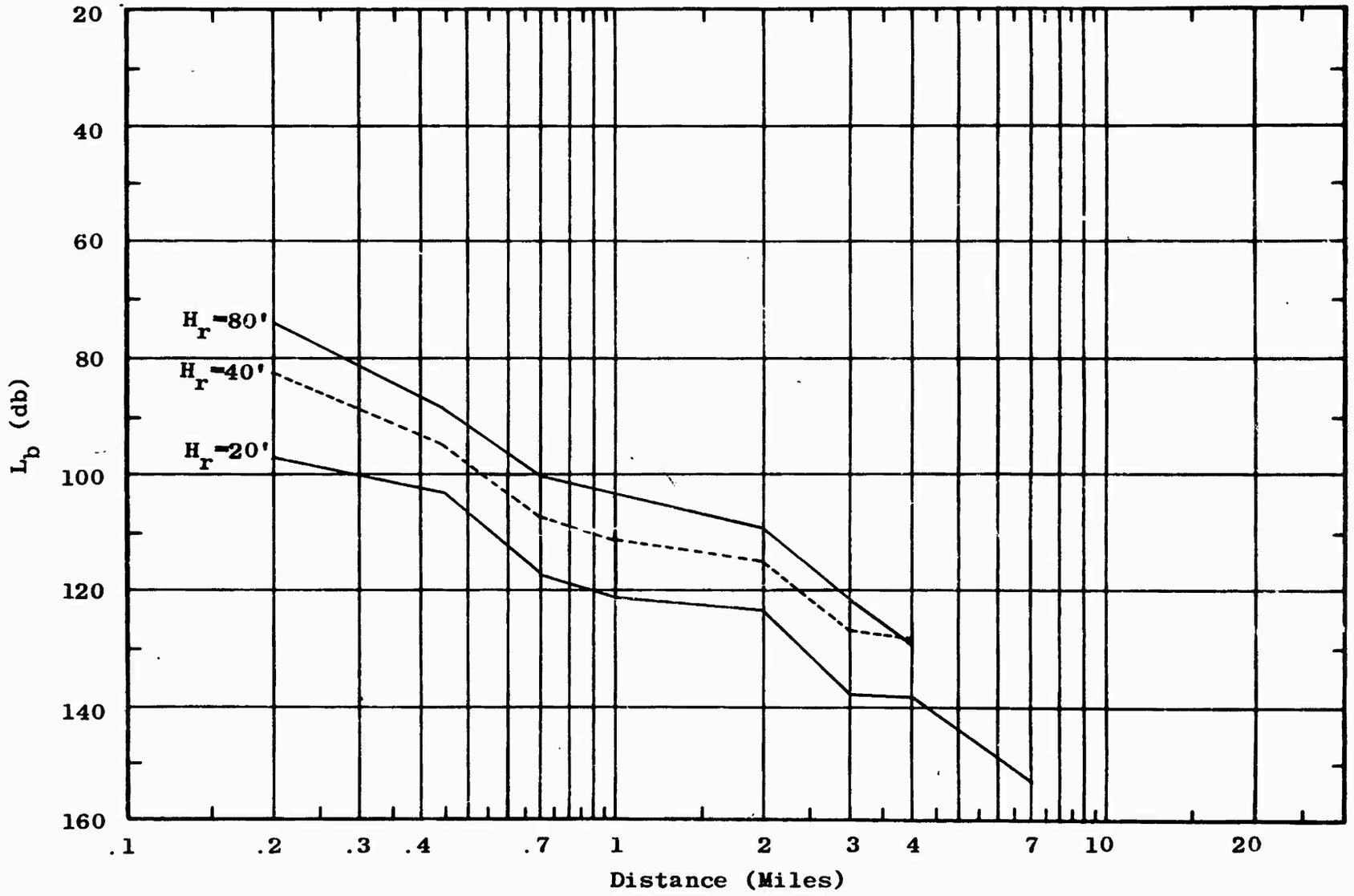

Figure 4.21L Comparison of L_b vs Distance for Various Receiving Antenna Heights
$L_b = F_A(25.5, 13, V, d, H_r)$

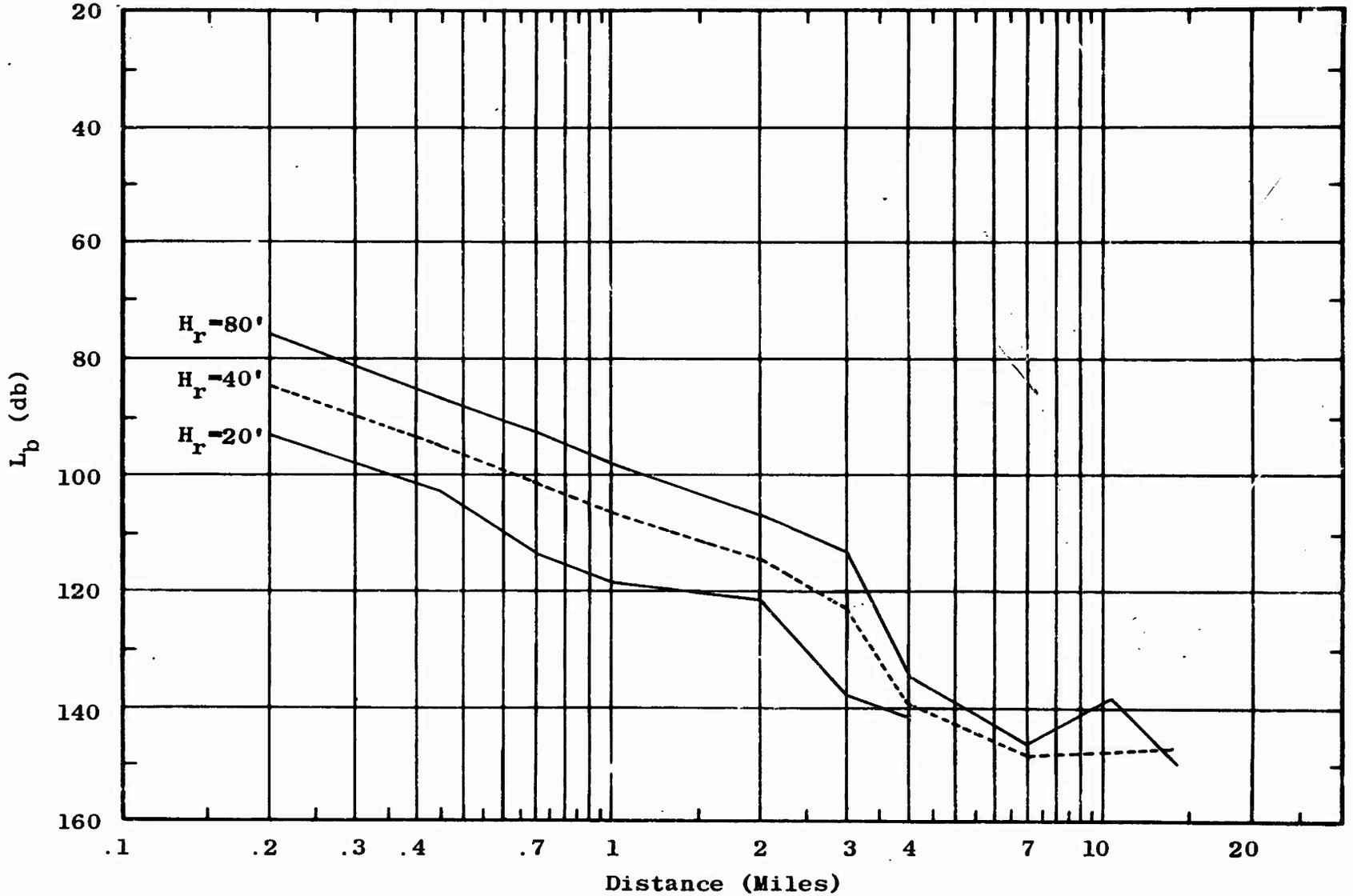

Figure 4.21M Comparison of L_b vs Distance for Various Receiving Antenna Heights
$L_b = F_A(50, 13, V, d, H_r)$

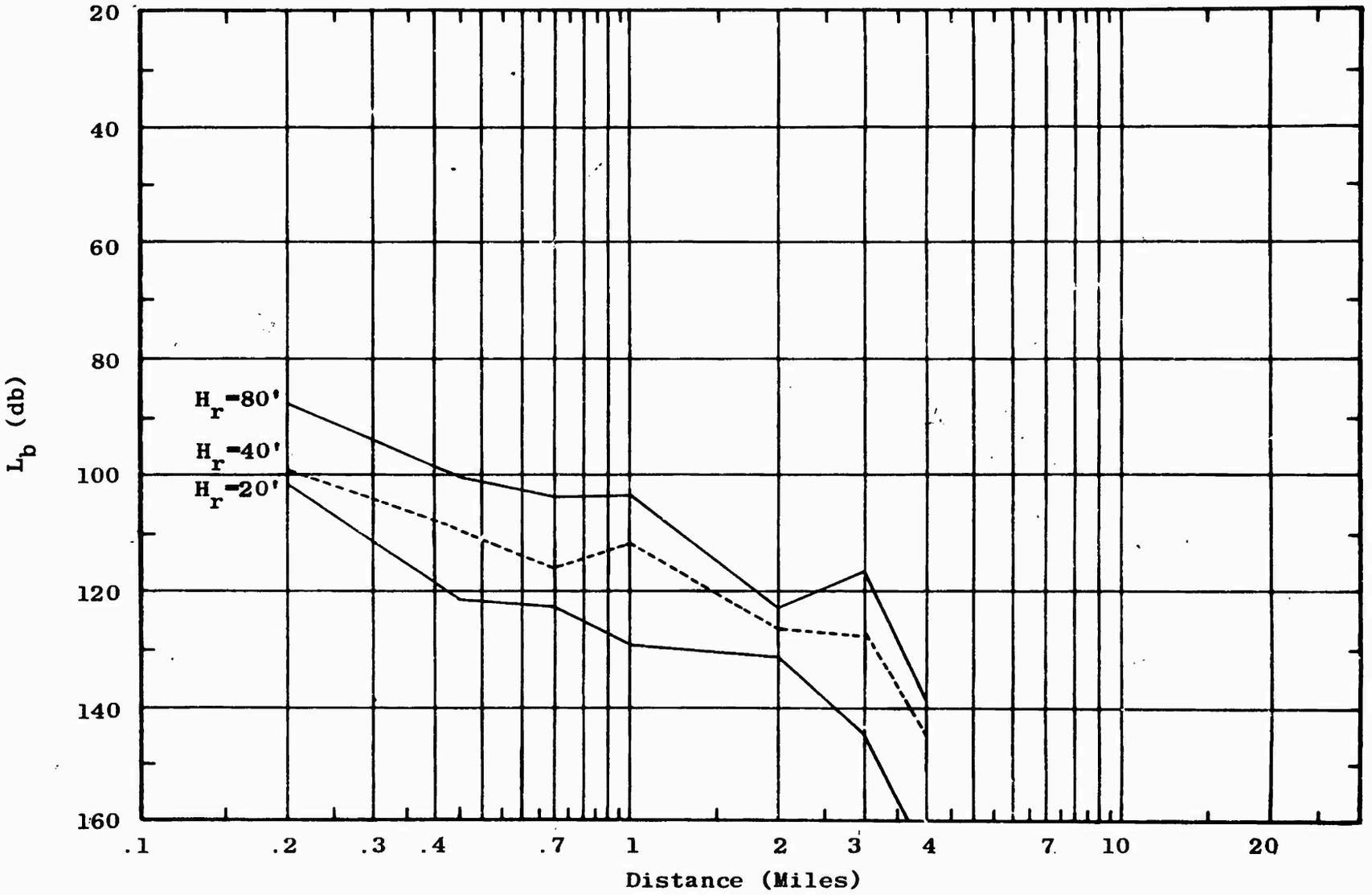

Figure 4.21N Comparison of L_b vs Distance for Various Receiving Antenna Heights
$L_b = F_A(100, 13, V, d, H_r)$

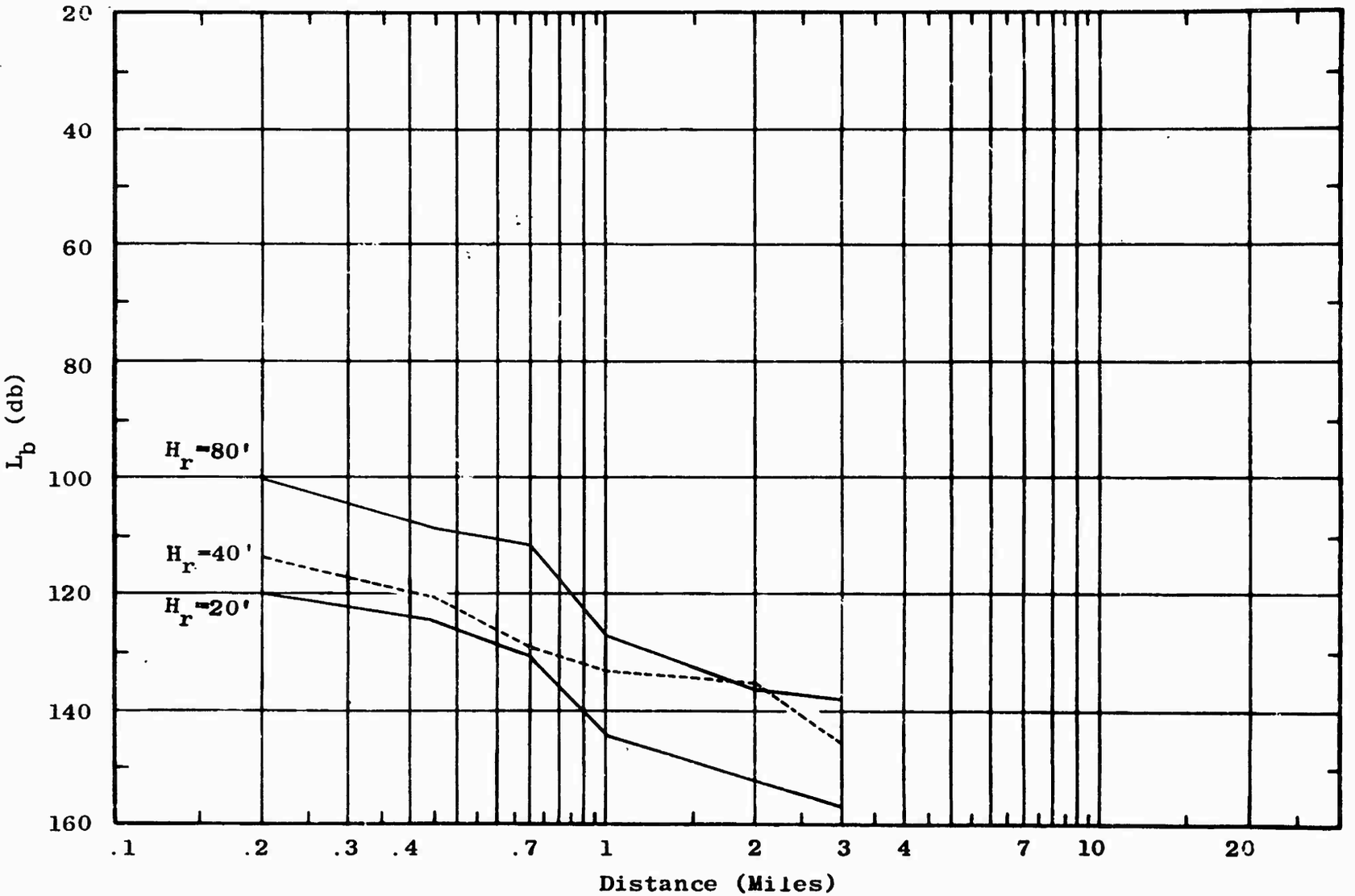

Figure 4.210 Comparison of L_b vs Distance for Various Receiving Antenna Heights
$L_b = F_A(250, 13, V, d, H_r)$

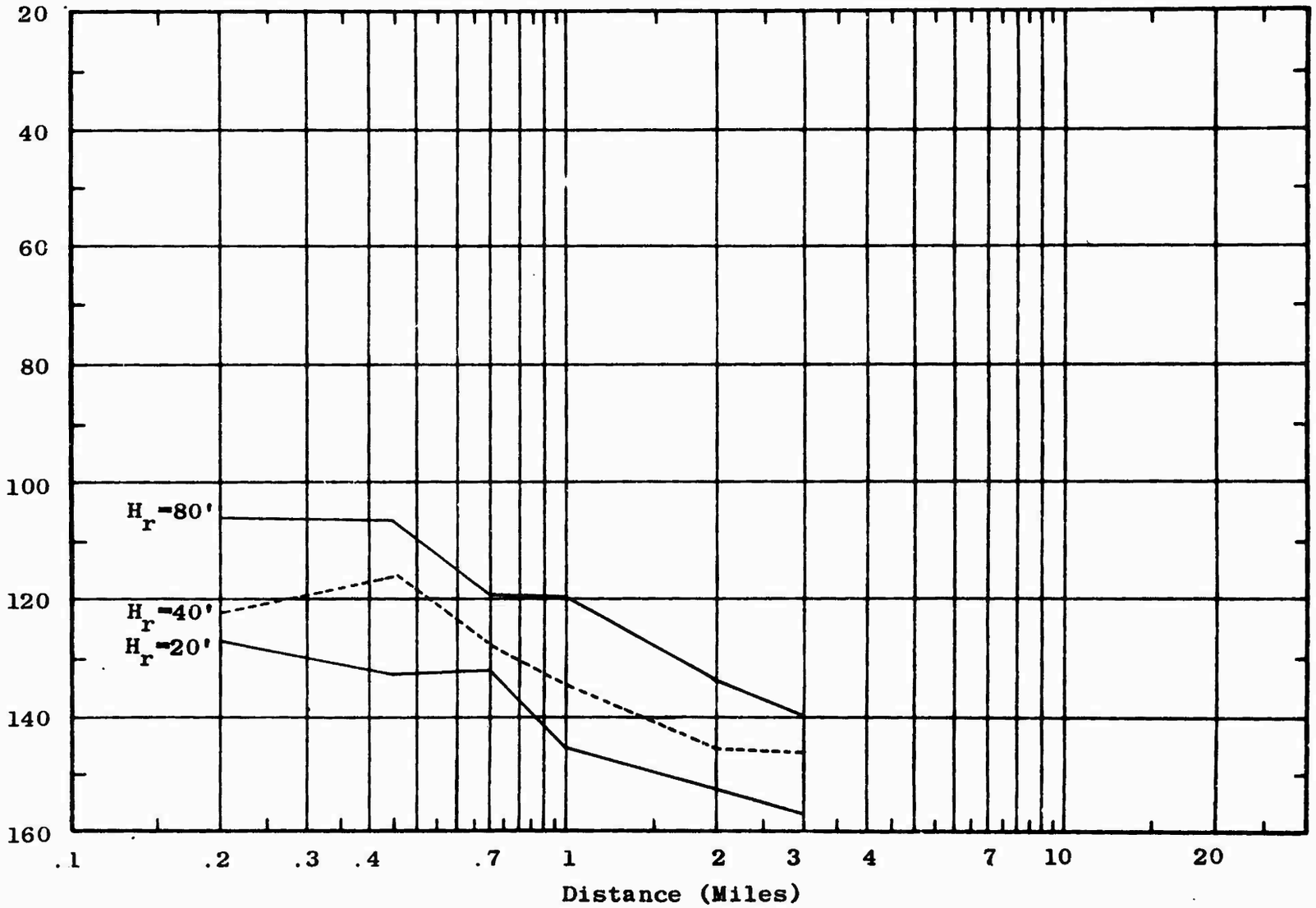

Figure 4.21P Comparison of L_b vs Distance for Various Receiving Antenna Heights
$L_b = F_A(400, 13, V, d, H_r)$

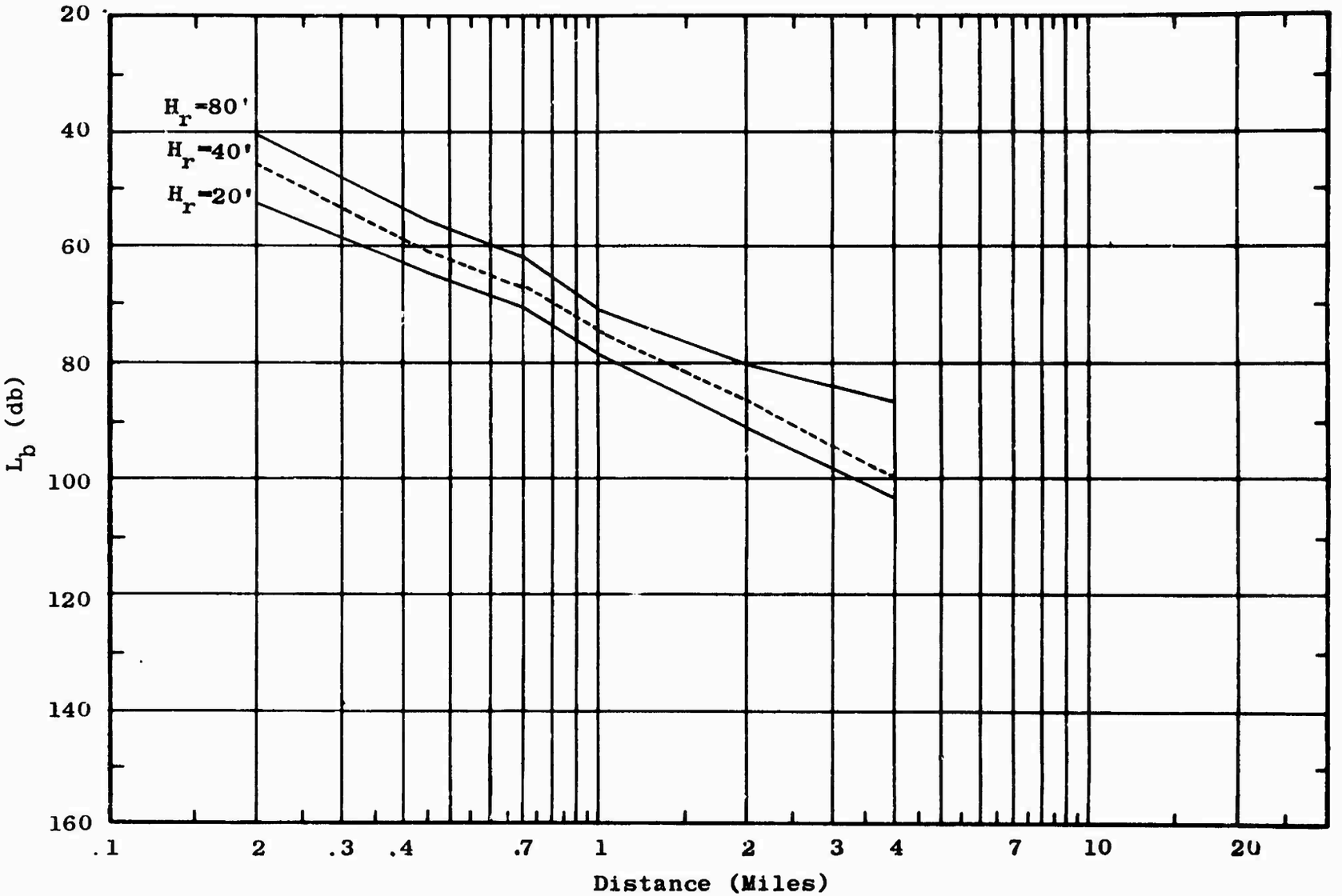

Figure 4.21Q Comparison of L_b vs Distance for Various Receiving Antenna Heights
$L_b = F_A(2.0, 80, H, d, H_r)$

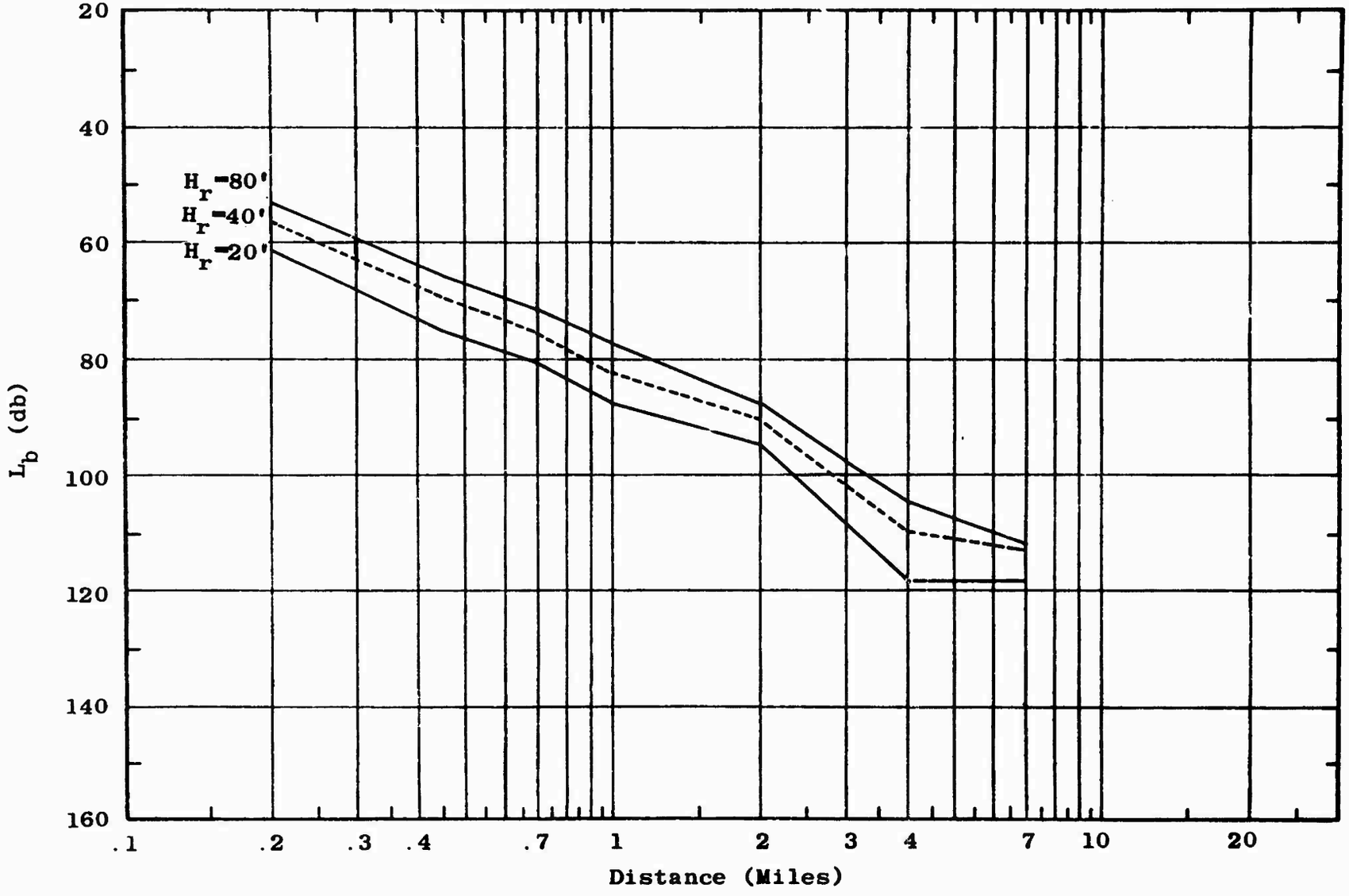

Figure 4.21R Comparison of L_b vs Distance for Various Receiving Antenna Heights
$L_b = F_A(12.0, 80, H, d, H_r)$

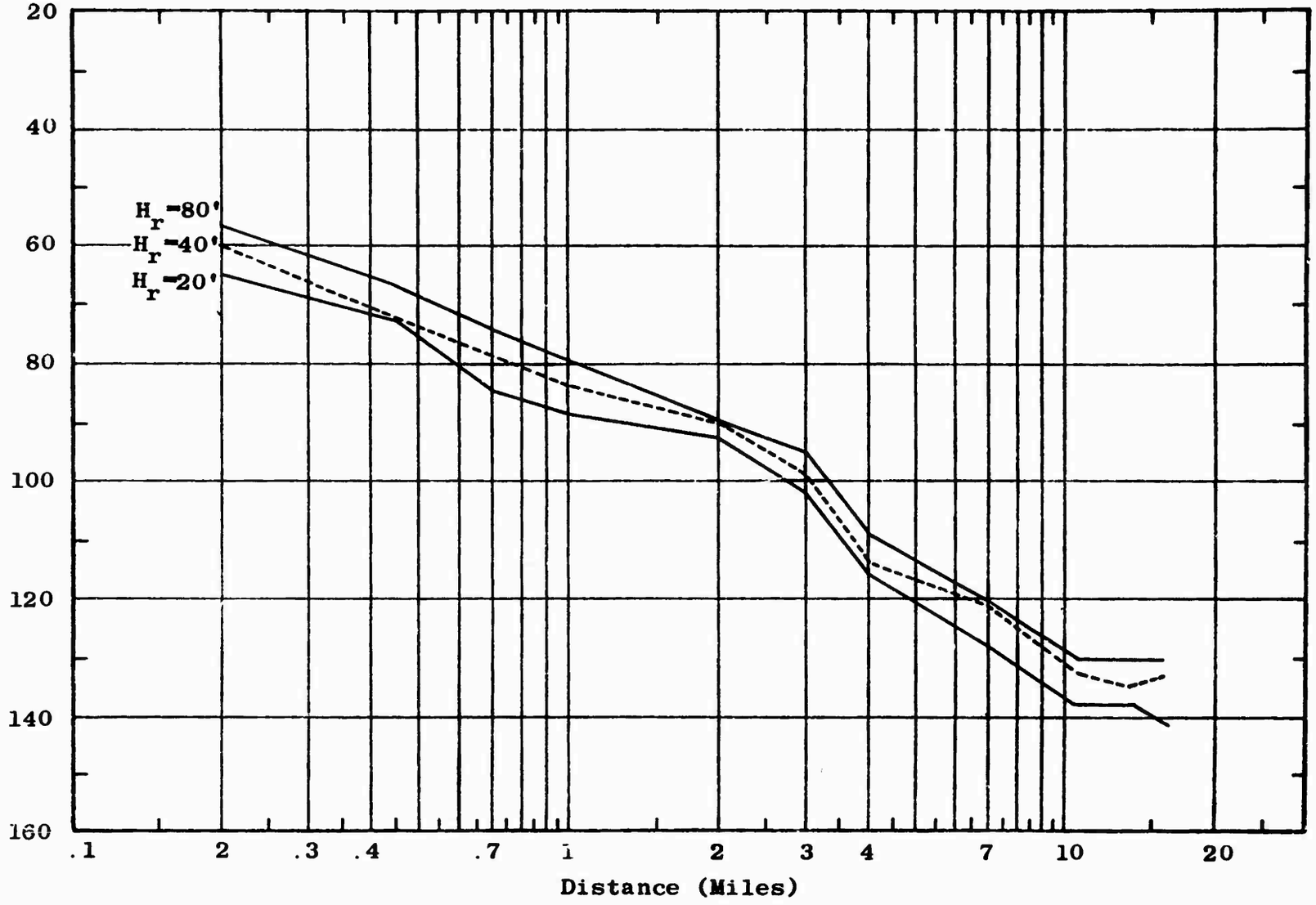

Figure 4.21S Comparison of L_b vs Distance for Various Receiving Antenna Heights
$L_b = F_A(25.5, 80, H, d, H_r)$

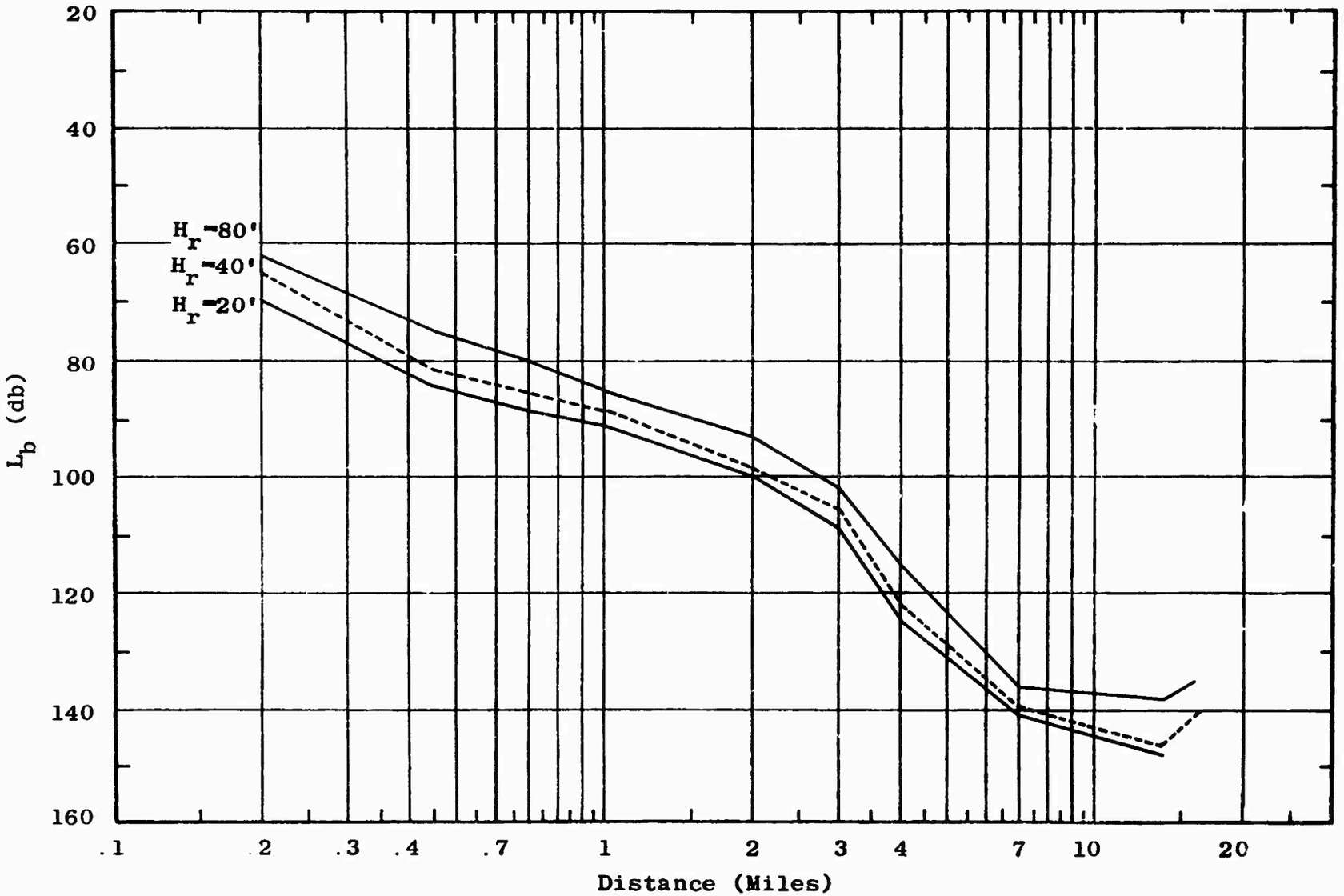

Figure 4.21T Comparison of L_b vs Distance for Various Receiving Antenna Heights
$L_b = F_A(50, 80, H, d, H_r)$

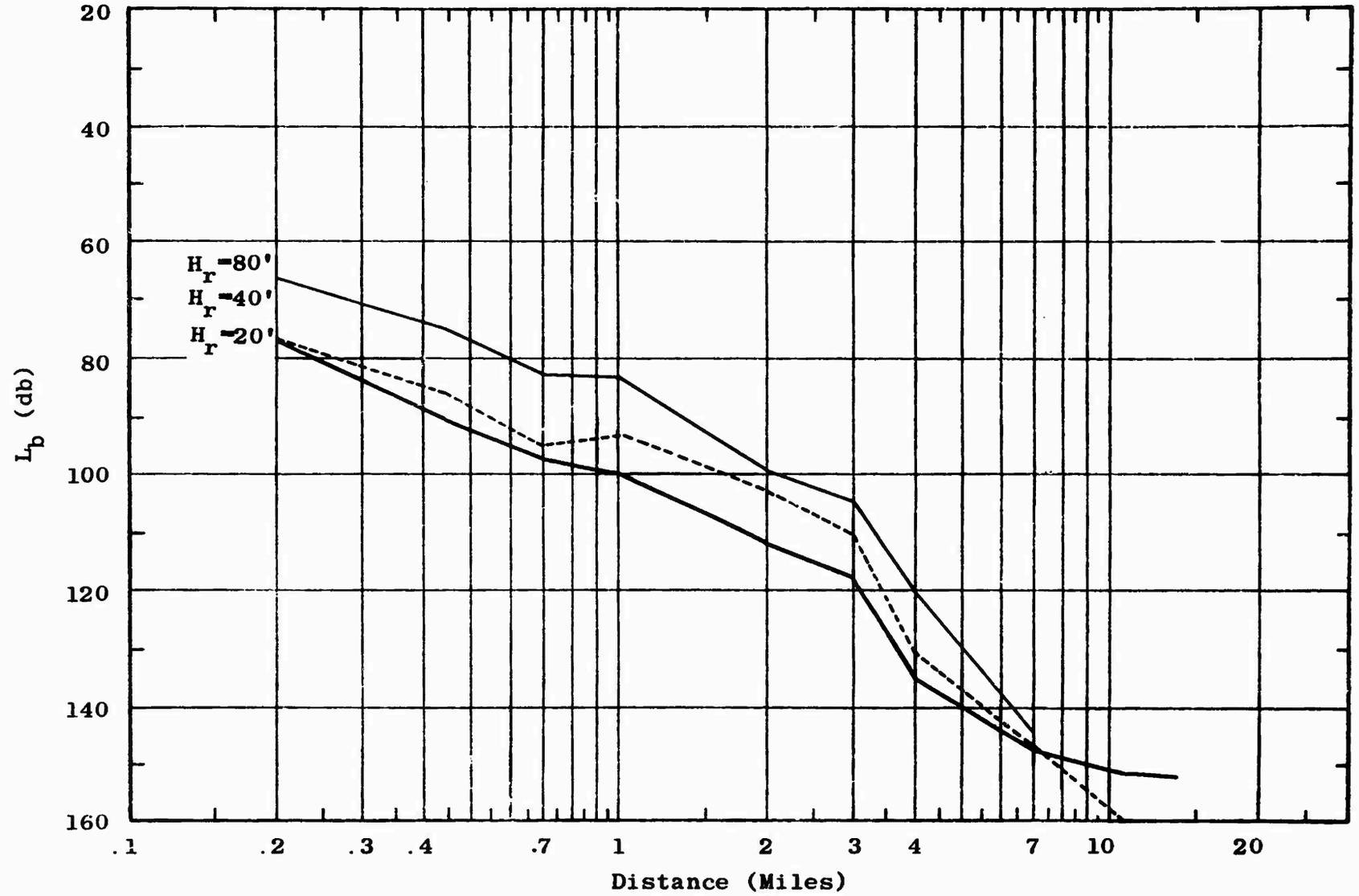

Figure 4.21U Comparison of L_b vs Distance for Various Receiving Antenna Heights
$L_b = F_A(100, 80, H, d, H_r)$

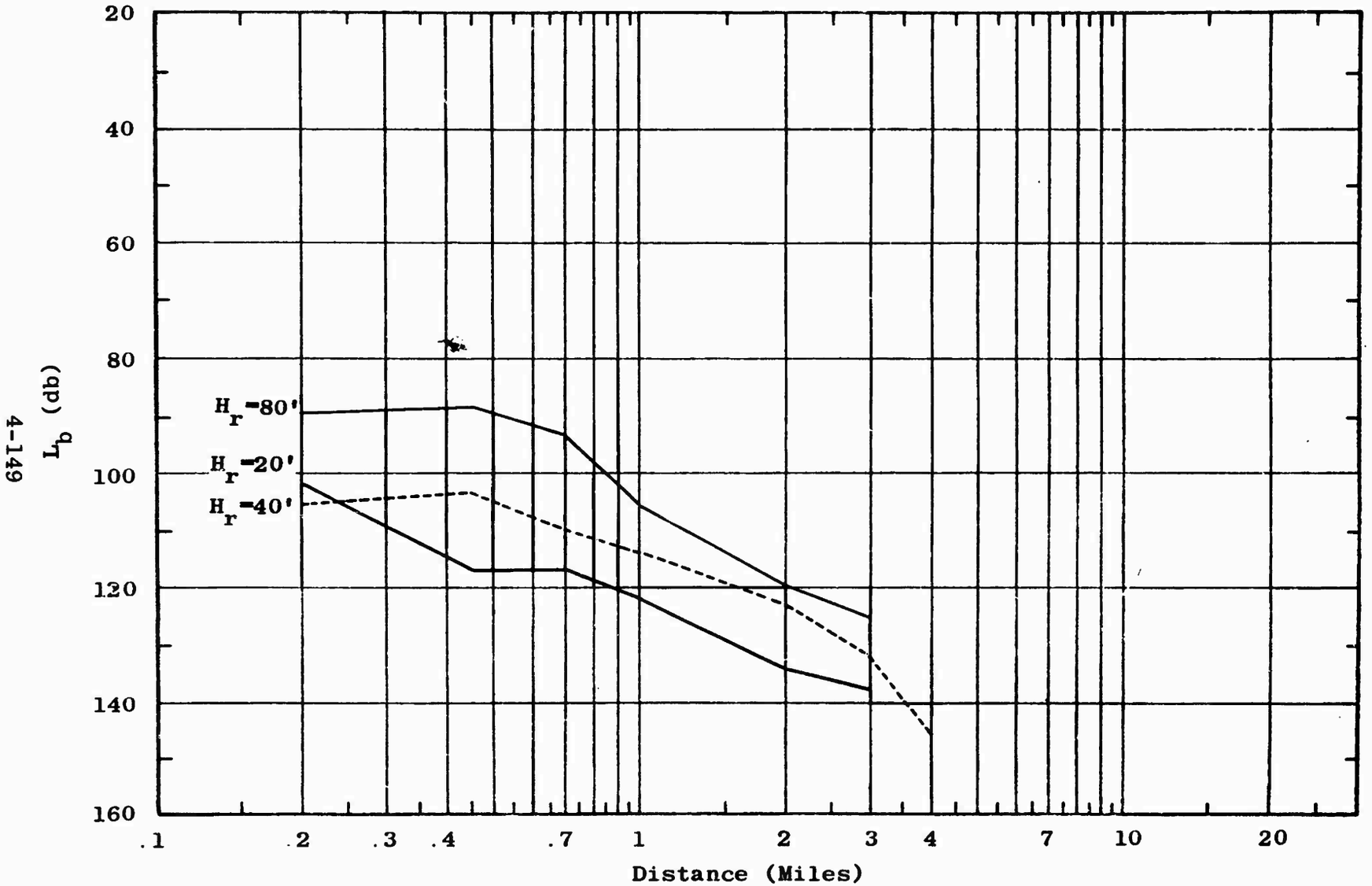

Figure 4.21V Comparison of L_b vs Distance for Various Receiving Antenna Heights
$L_b = F_A(250, 80, H, d, H_r)$

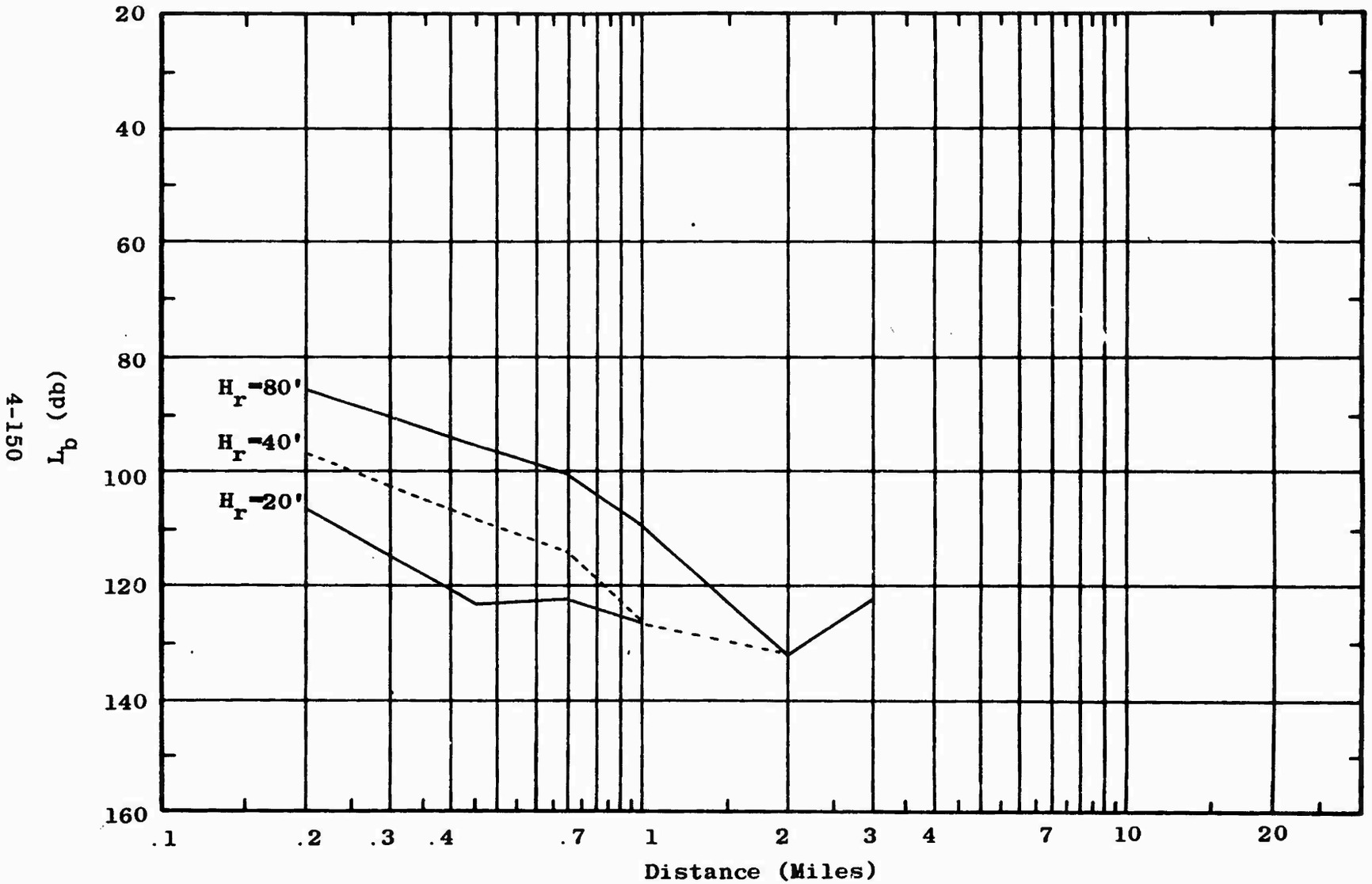

Figure 4.21W Comparison of L_b vs Distance for Various Receiving Antenna Heights
$L_b = F_A(400, 80, H, d, H_r)$

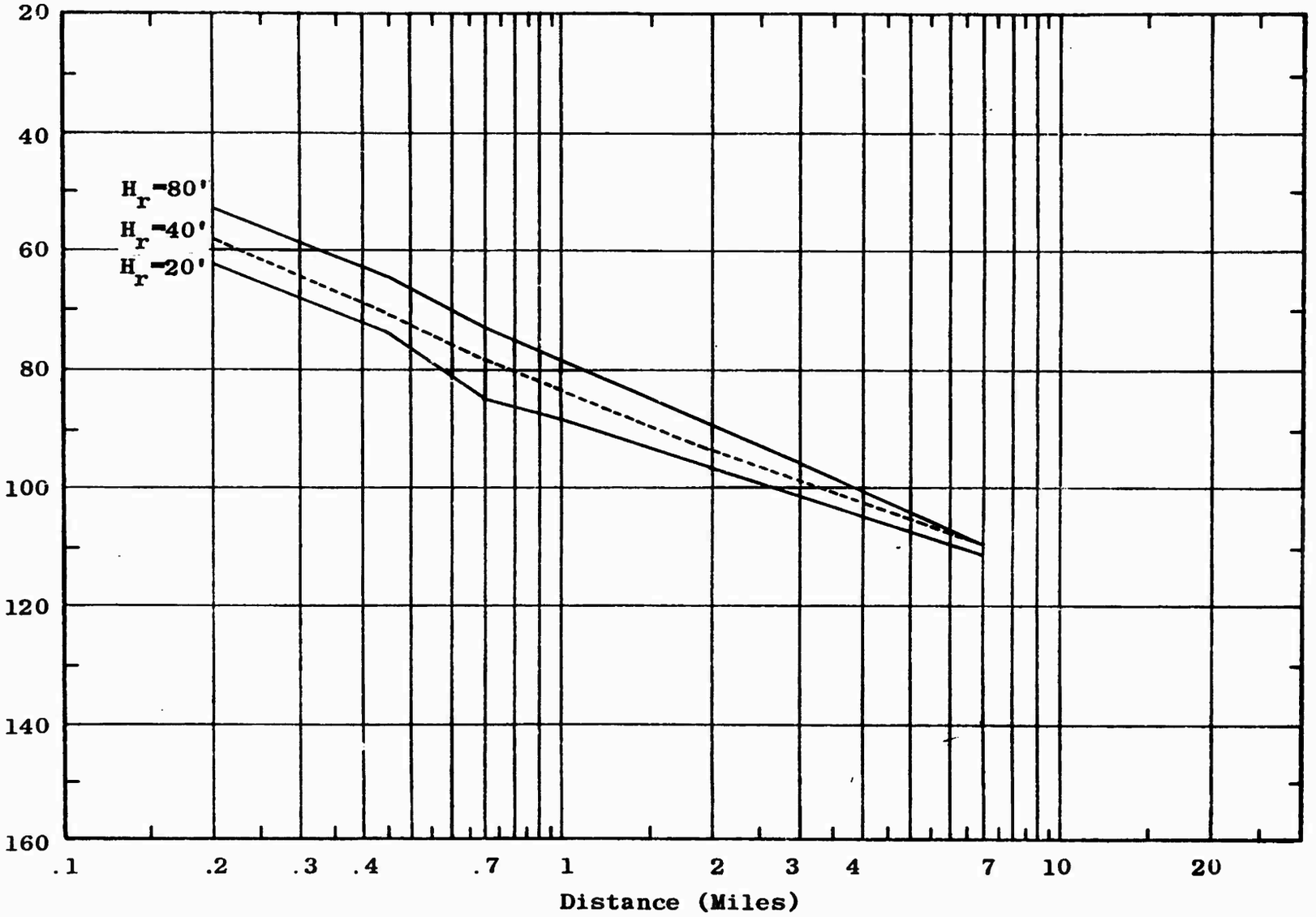

Figure 4.21X Comparison of L_b vs Distance for Various Receiving Antenna Heights
$L_b = F_A(6.0, 40, H, d, H_r)$

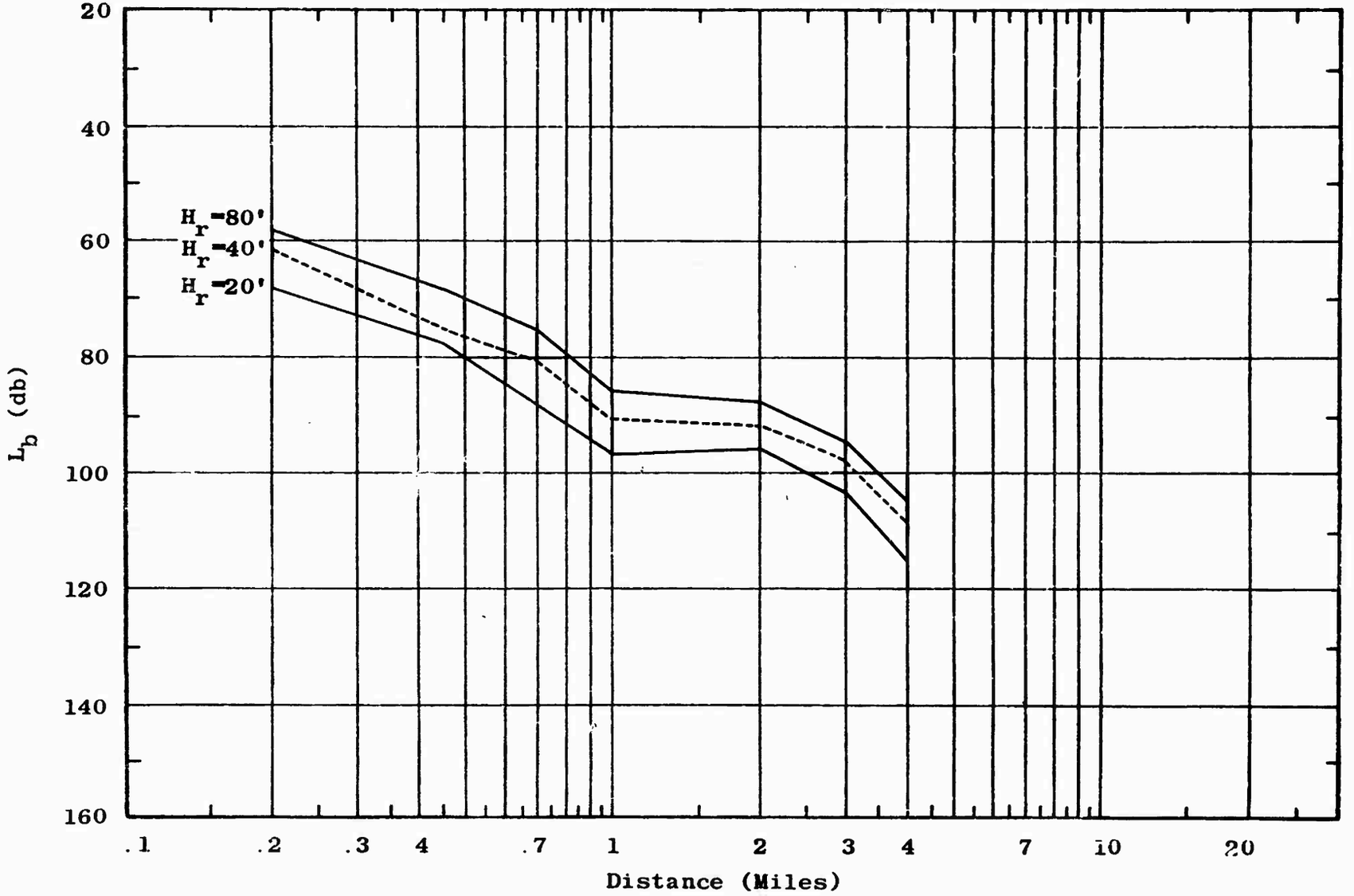

Figure 4.21Y Comparison of L_b vs Distance for Various Receiving Antenna Heights
$L_b = F_A(12.0, 40, H, d, H_r)$

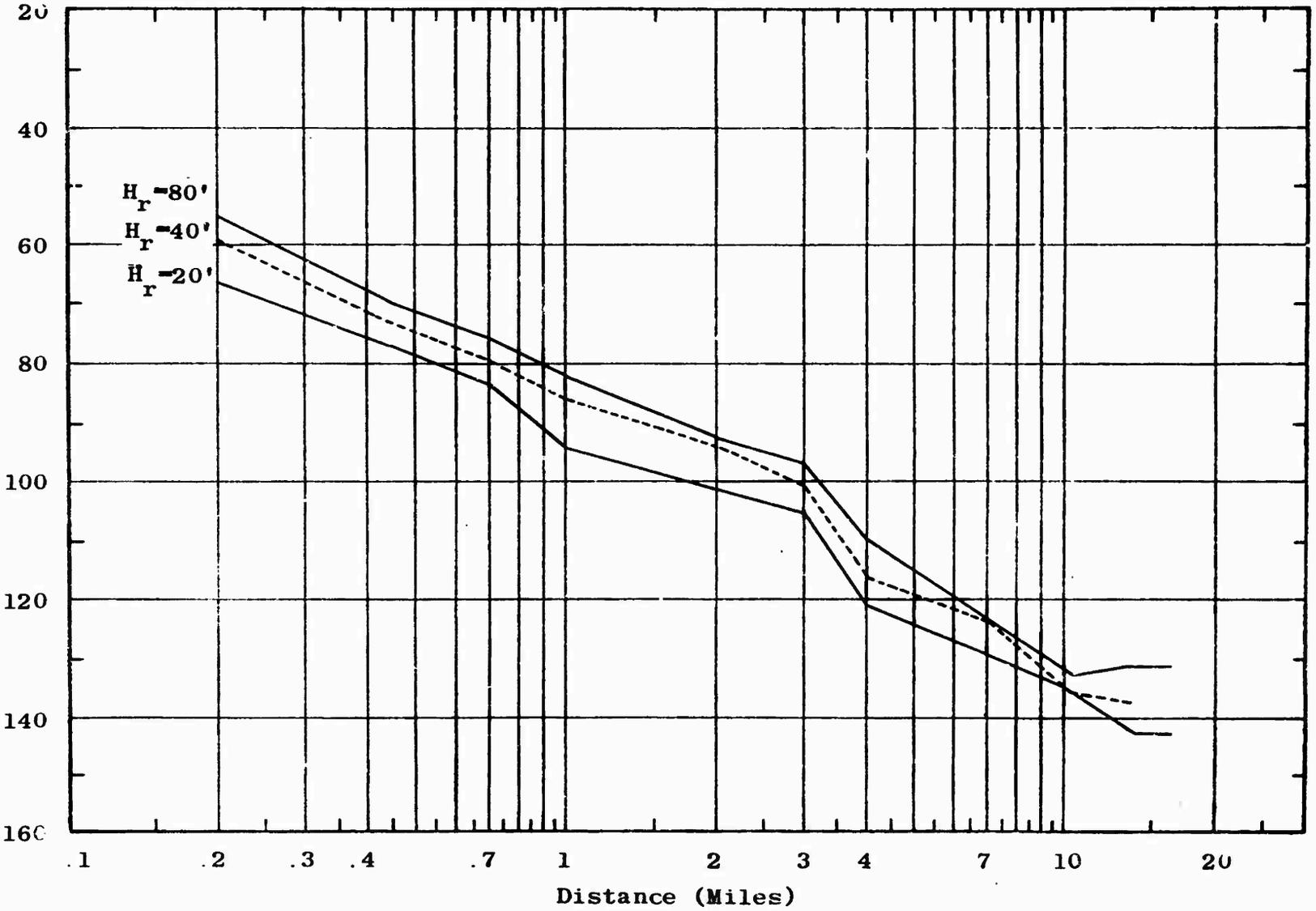

Figure 4.21Z Comparison of L_b vs Distance for Various Receiving Antenna Heights
$L_b = F_A(25.5, 40, H, d, H_r)$

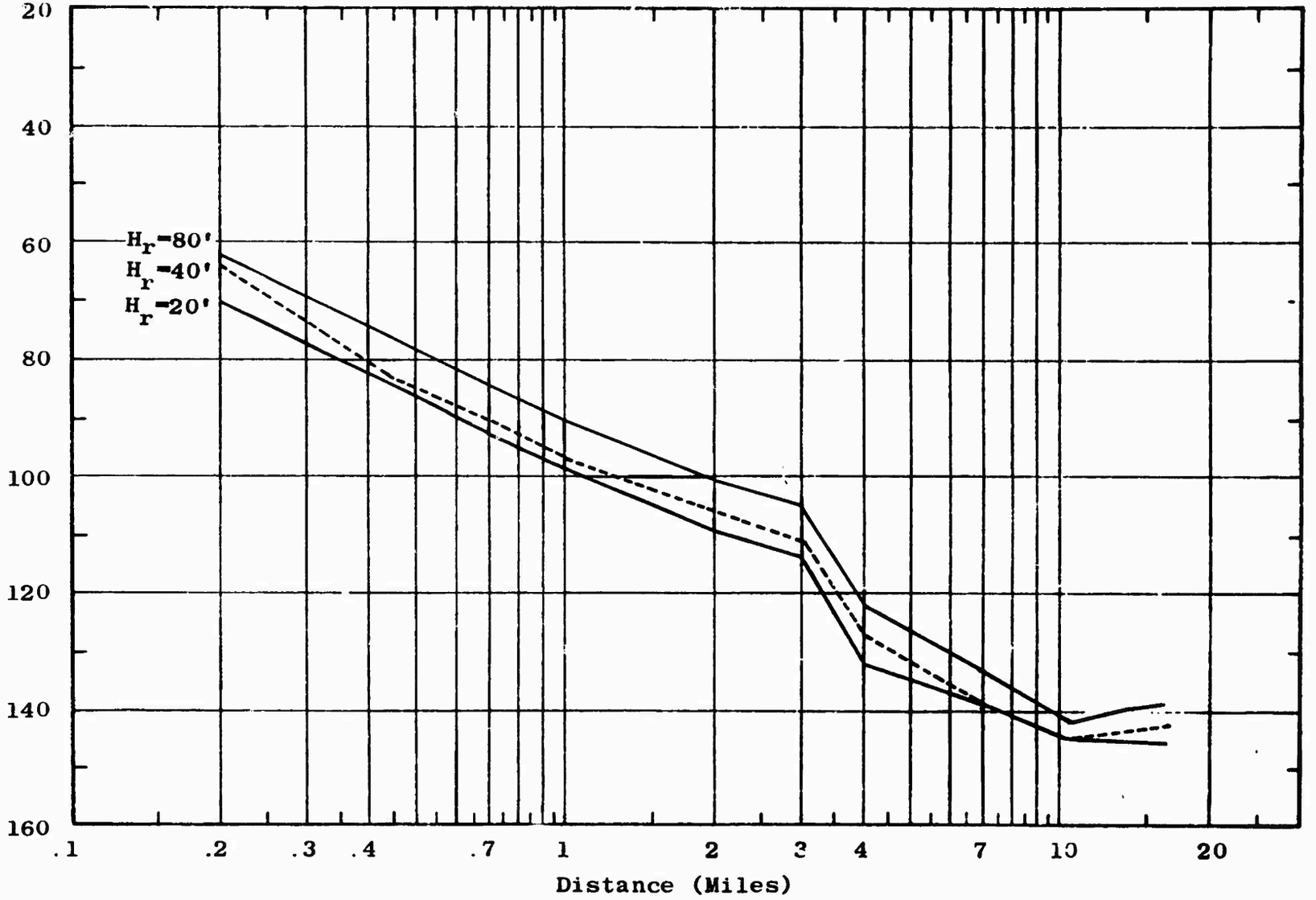

Figure 4.21AA Comparison of L_b vs Distance for Various Receiving Antenna Heights
$L_b = F_A(50, 40, H, d. H_r)$

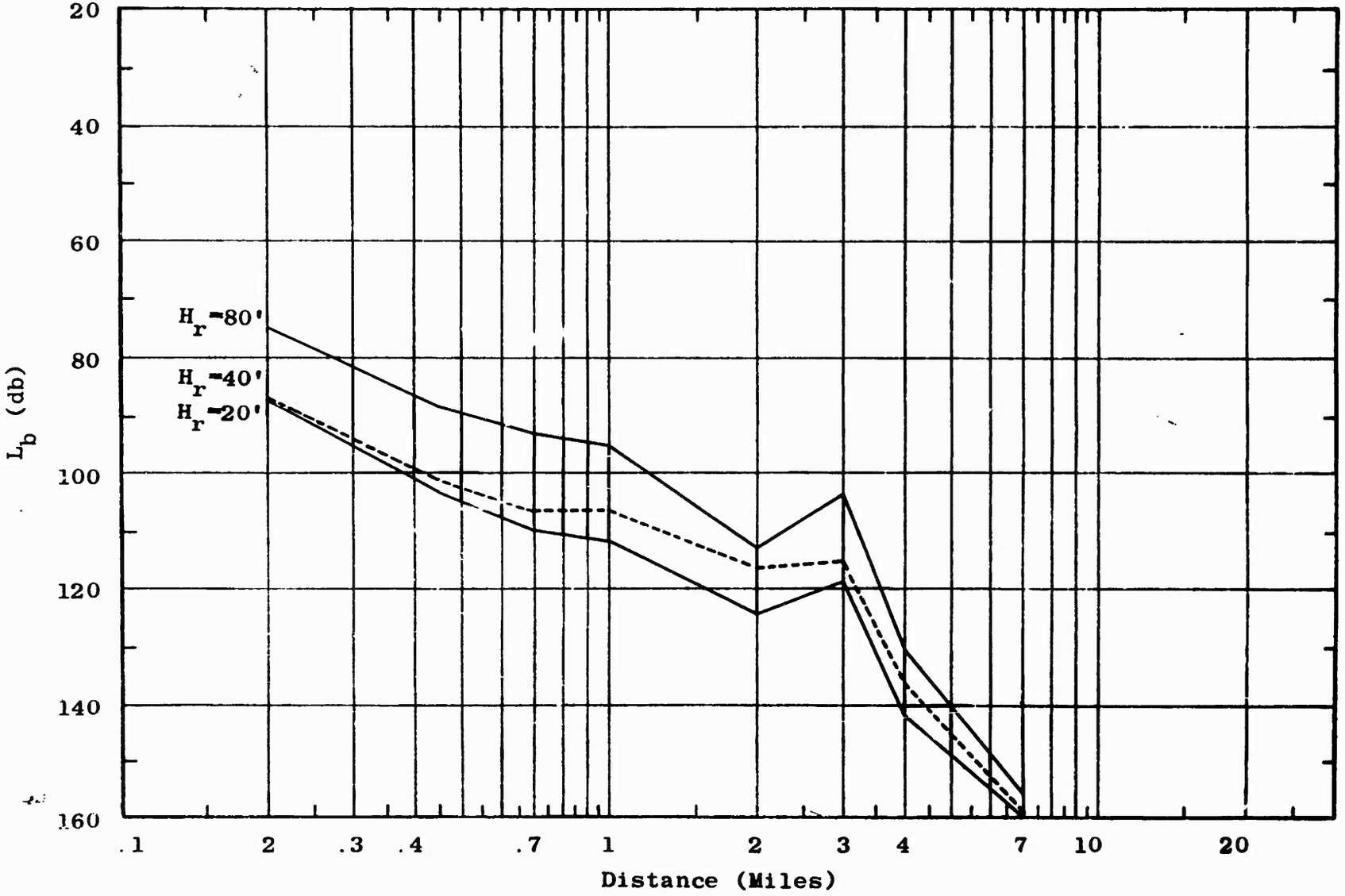

Figure 4.21BB Comparison of L_b vs Distance for Various Receiving Antenna Heights
$L_b = F_A(100, 40, H, d, H_r)$

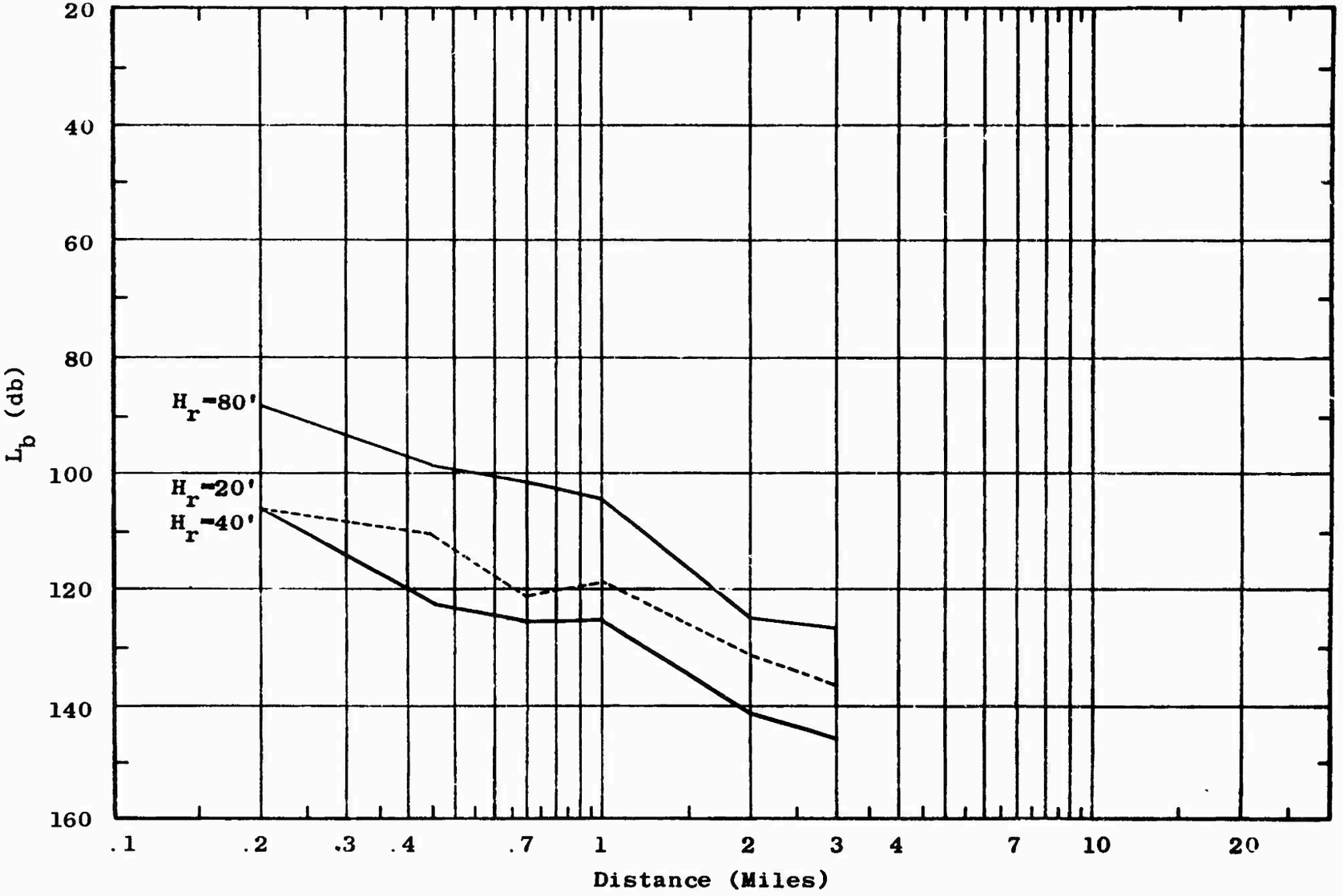

Figure 4.21CC Comparison of L_b vs Distance for Various Receiving Antenna Heights
$L_b = F_A(250, 40, H, d, H_r)$

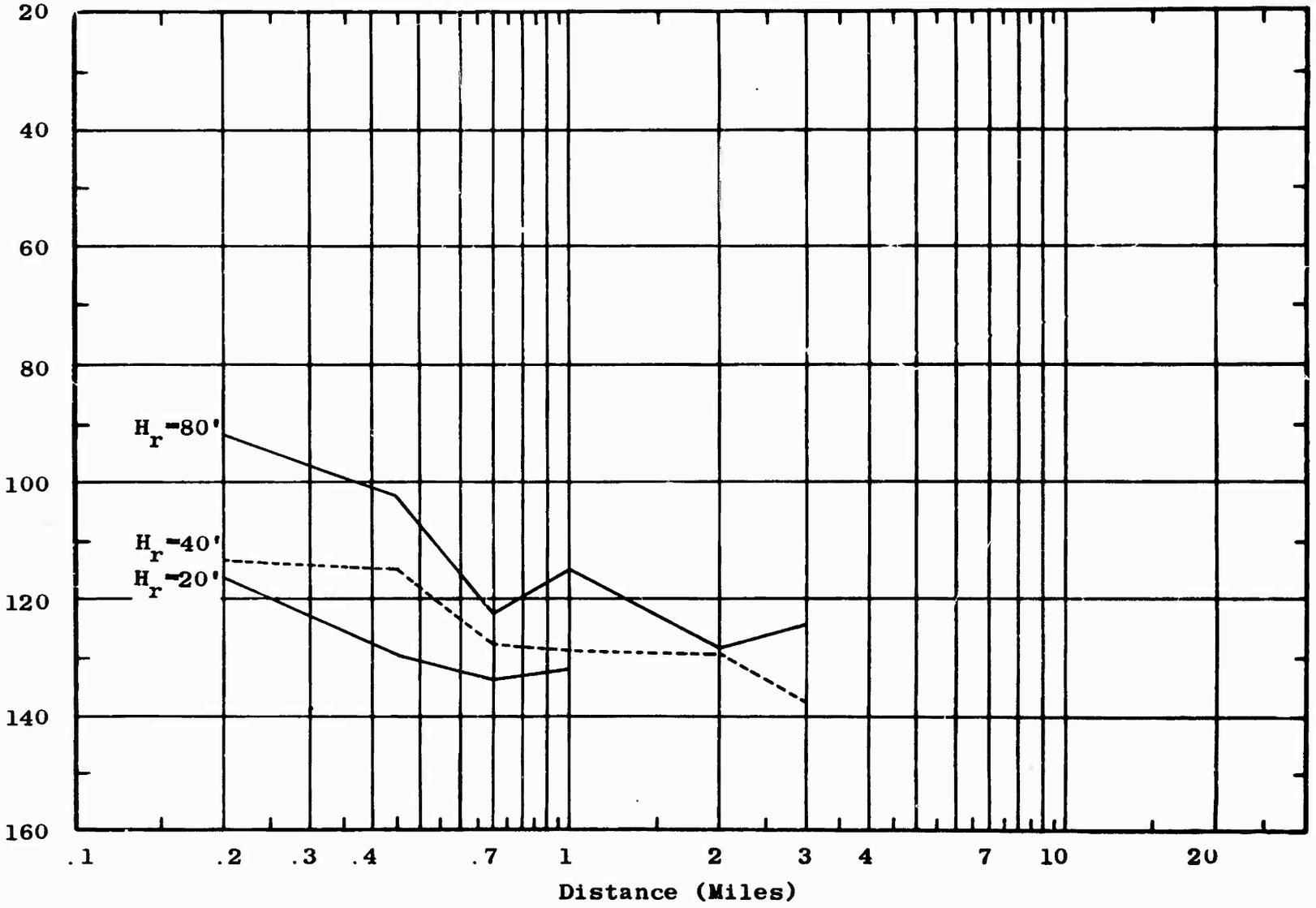

Figure 4.21DD Comparison of L_b vs Distance for Various Receiving Antenna Heights
$L_b = F_A(400, 40, H, d, H_r)$

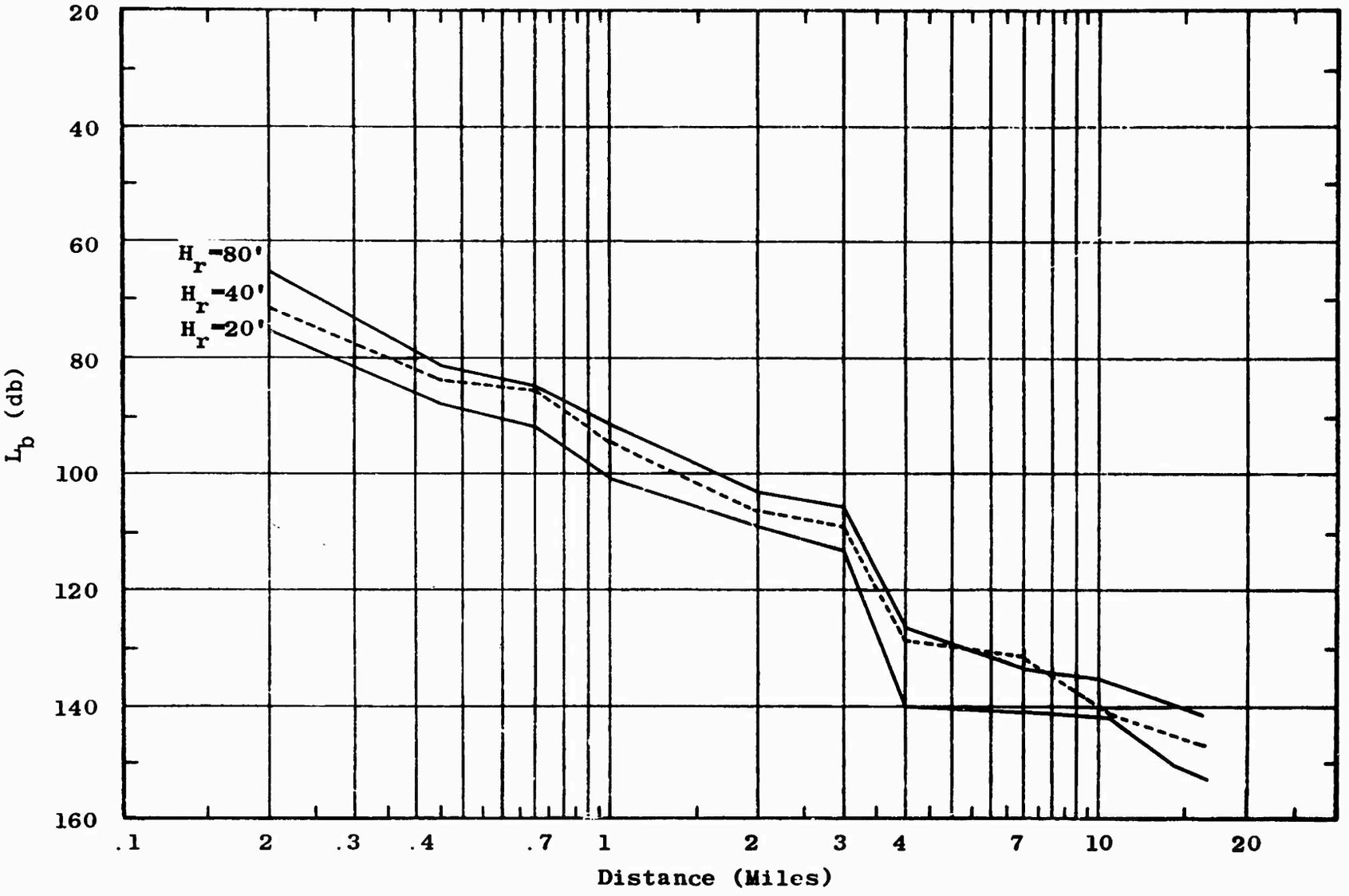

Figure 4.21EE Comparison of L_b vs Distance for Various Receiving Antenna Heights
$L_b = F_A(25.5, 13, H, d, H_r)$

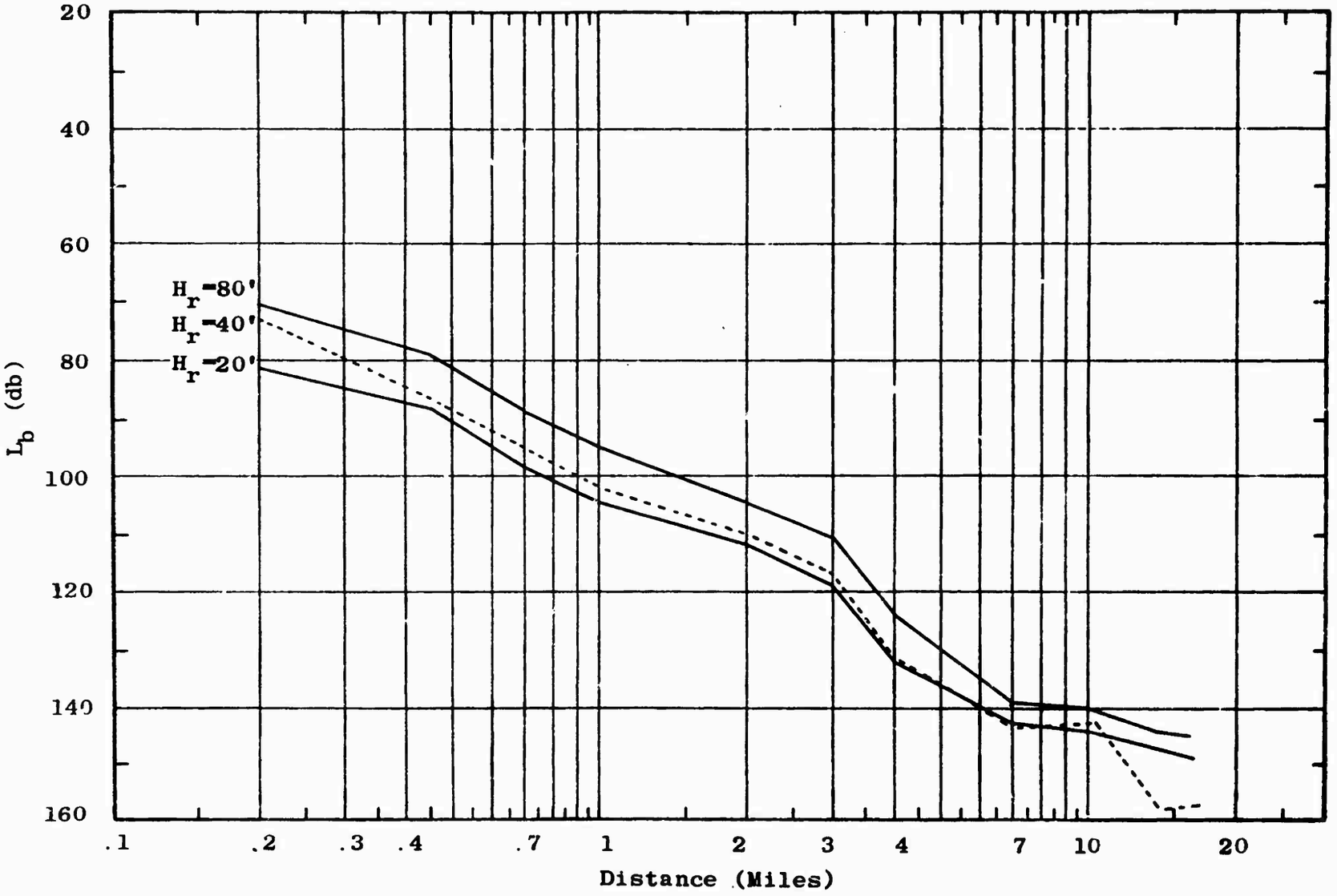

Figure 4.21FF Comparison of L_b vs Distance for Various Receiving Antenna Heights
$L_b = F_A(50, 13, H, d, H_r)$

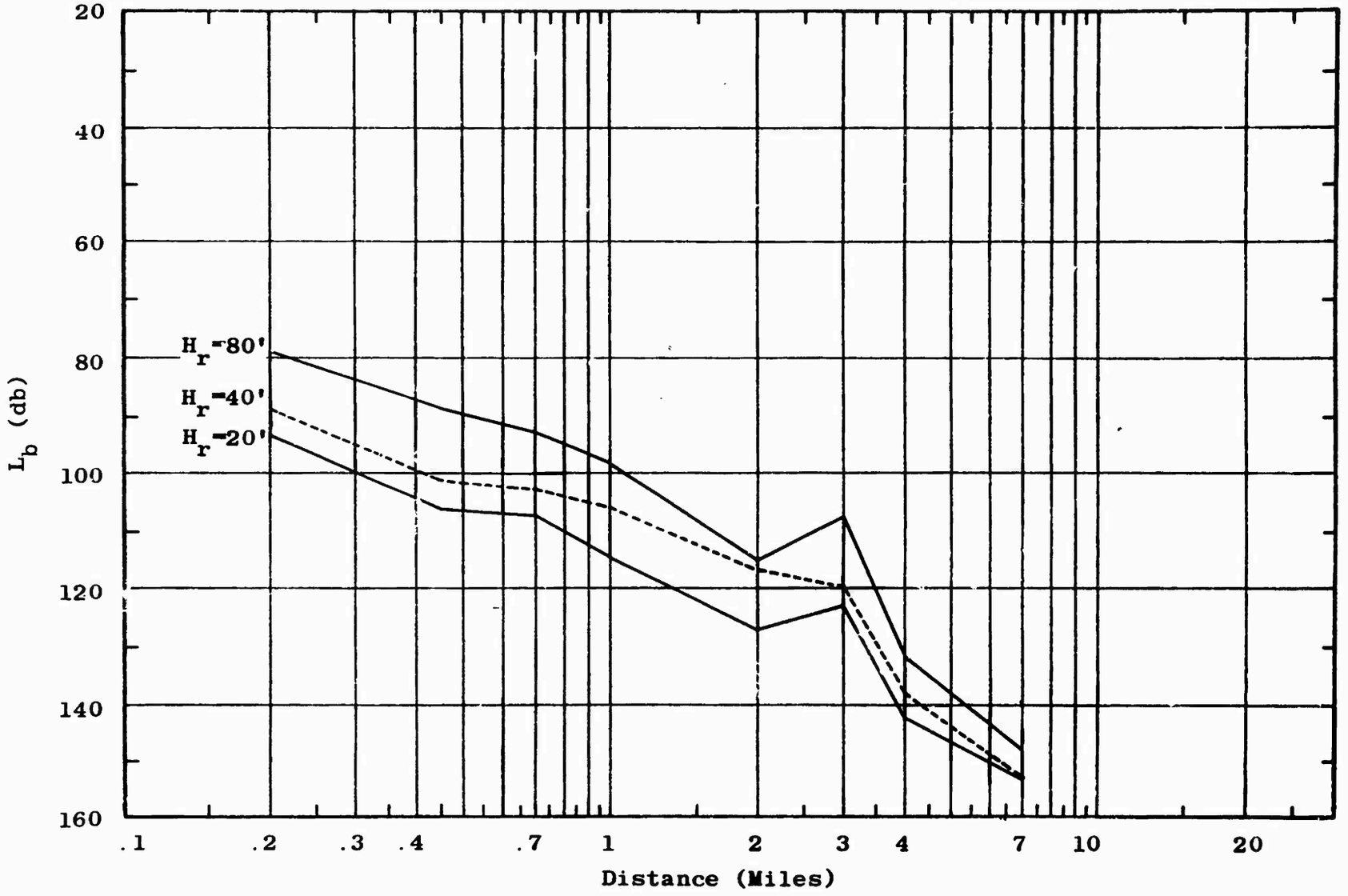

Figure 4.21GG Comparison of L_b vs Distance for Various Receiving Antenna Heights
$L_b = F_A(100, 13, H, d, H_r)$

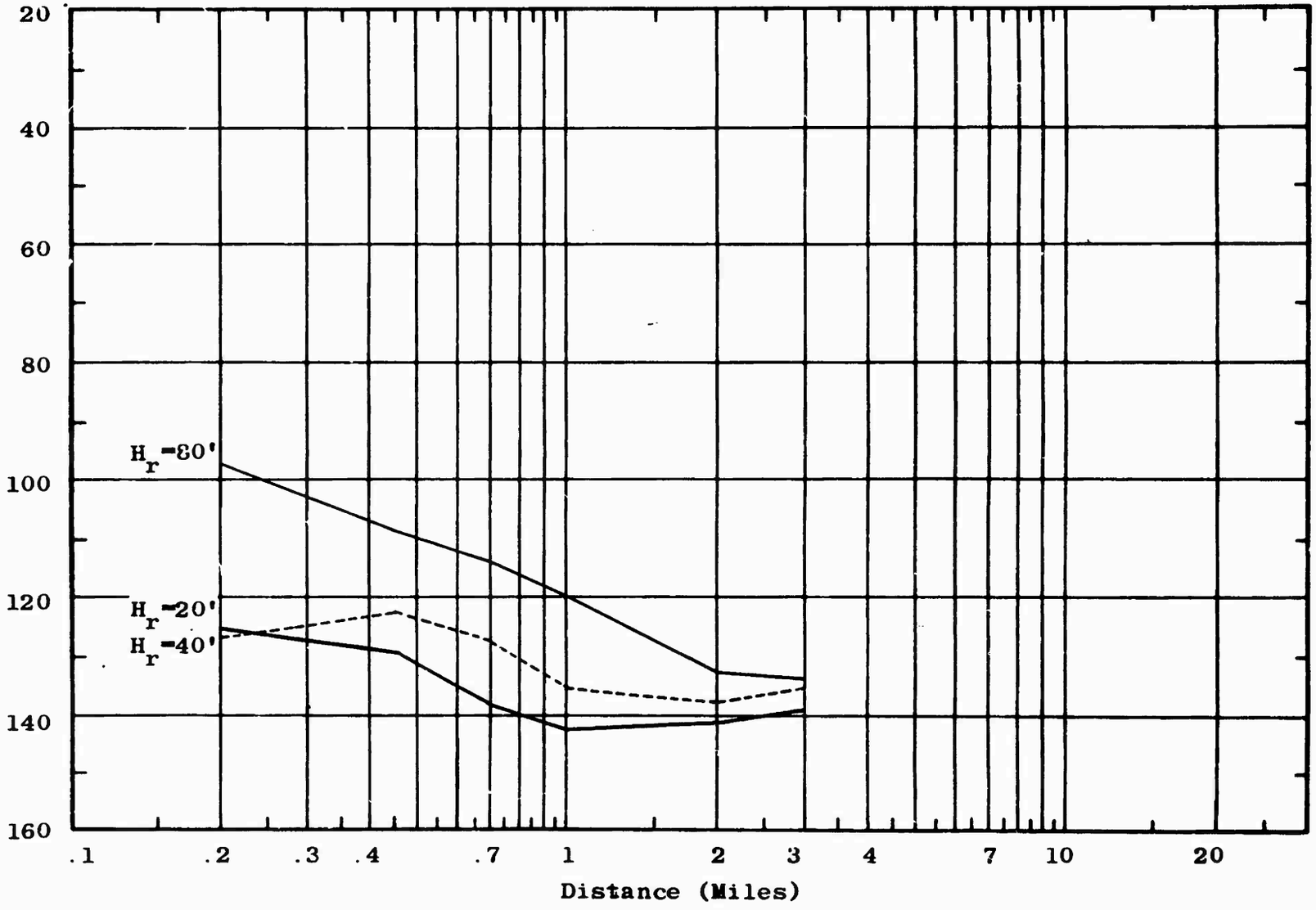

Figure 4.21HH Comparison of L_b vs Distance for Various Receiving Antenna Heights
$L_b = F_A(400, 13, H, d, H_r)$

4.3.2.2.2 Comparison of Height Variation with Smooth-Earth Model

Height functions for beyond-the-horizon transmission under smooth-earth conditions have been calculated by the methods described in Appendix A. The differences between the height variations noted in the median measured field point data and these theoretical smooth-earth height function curves should correspond to the combined effects of foliage and terrain on height variability of propagation loss.

In order to examine the height variability of measured field point data, the curves for basic transmission loss vs receiving antenna height have been replotted as shown in Figure 4.22. Each family of the type shown in Figure 4.22 is for a fixed frequency, polarization and transmitting antenna height. Each curve on Figure 4.22 corresponds to a different radial distance. These distances range from 0.2 to 17 miles.

The basic transmission loss curves shown in Figure 4.22 have been shifted vertically so that all curves within a family are at the same value for a receiving antenna height of 20 feet. This normalization of basic transmission loss at 20 feet allows a study of the height variation alone.

Results of the type shown in Figure 4.22 have been summarized by vertical bars of the type shown in Figure 4.23A. The top of the vertical bar represents the maximum vertical excursion of the family at a particular receiving antenna height; the bottom of the vertical bar represents the minimum vertical excursion. The mark falling somewhere between the top and bottom of the vertical bar marks the median. Thus all the basic transmission loss curves in a particular family would pass through a vertical bar. Half the curves would pass through that portion of the bar between the maximum value and the median while the other half of the curves

in a particular family would pass through that portion of the vertical bar between the median and the minimum value.

An examination of many families of curves of the type shown in Figure 4.22 indicates that there is no apparent trend in the height effect with distance. This bears out a similar conclusion which can be drawn as a result of studying Figures 4.21A through 4.21HH. However, there is an apparent difference in the height variability for distances closer than 2 miles as opposed to all distances beyond 2 miles. Two miles marks the dividing line between paths which would be line-of-sight in the absence of foliage and paths which would not be line-of-sight in the absence of foliage.

Figures 4.23A through 4.23LL provide a comparison of the theoretical smooth-earth height variability and the height variability observed in measured data for distances of 2 miles or more.

The vertical bars summarize the measured data in the manner described. The dotted curve on these figures represents the smooth-earth height function, normalized to the measured data at a receiving antenna height of 20 feet. As Figures 4.23A through 4.23Q show, the theoretical smooth-earth height function matches measured data reasonably well in almost every case for horizontal polarization.

Figures 4.23R through 4.23LL show a reasonable correspondence for vertical polarization.

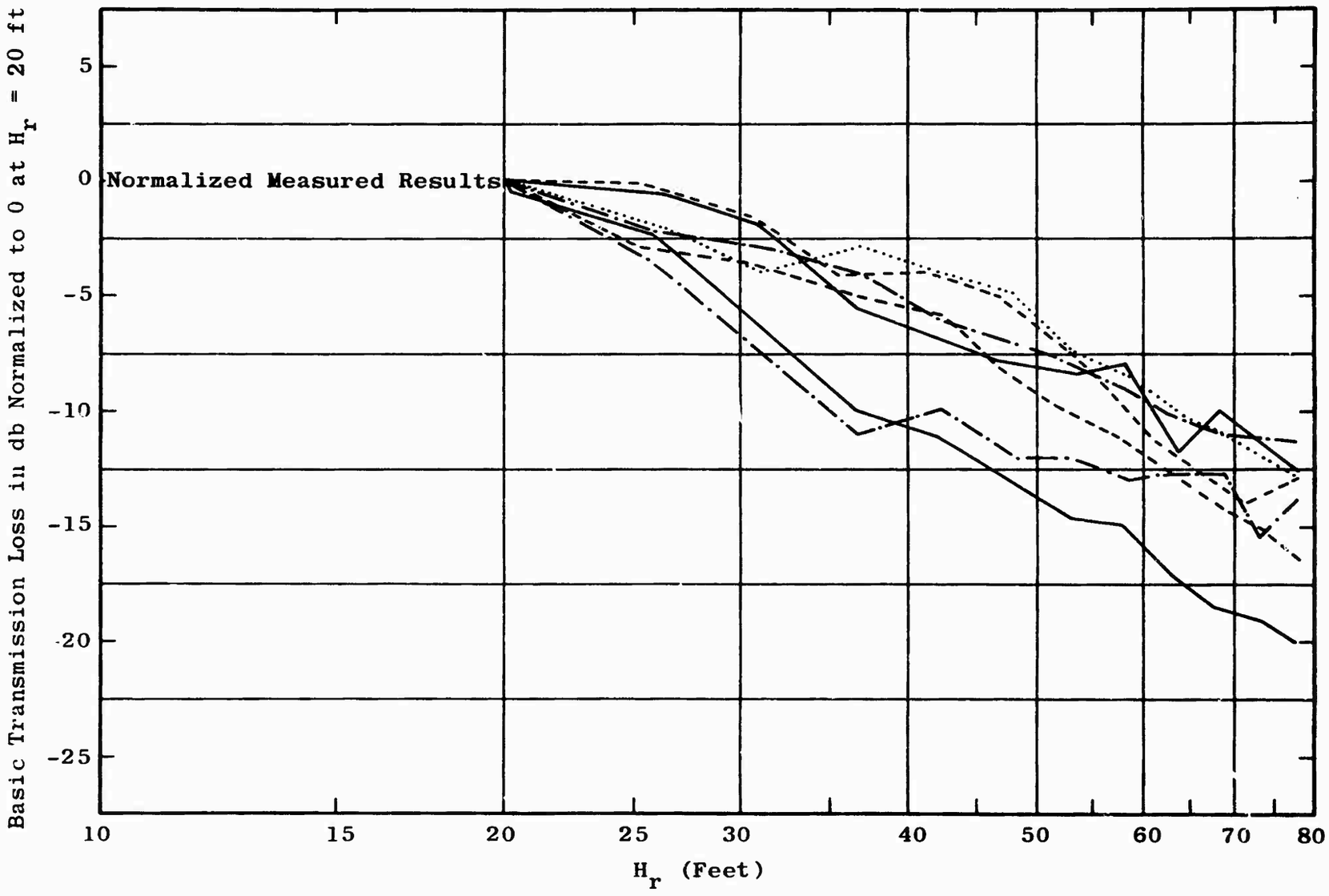

Figure 4.22 Sample Composite of Measured Antenna Height Functions
$L_b = F_A(50, 80, V, d, H_r)$

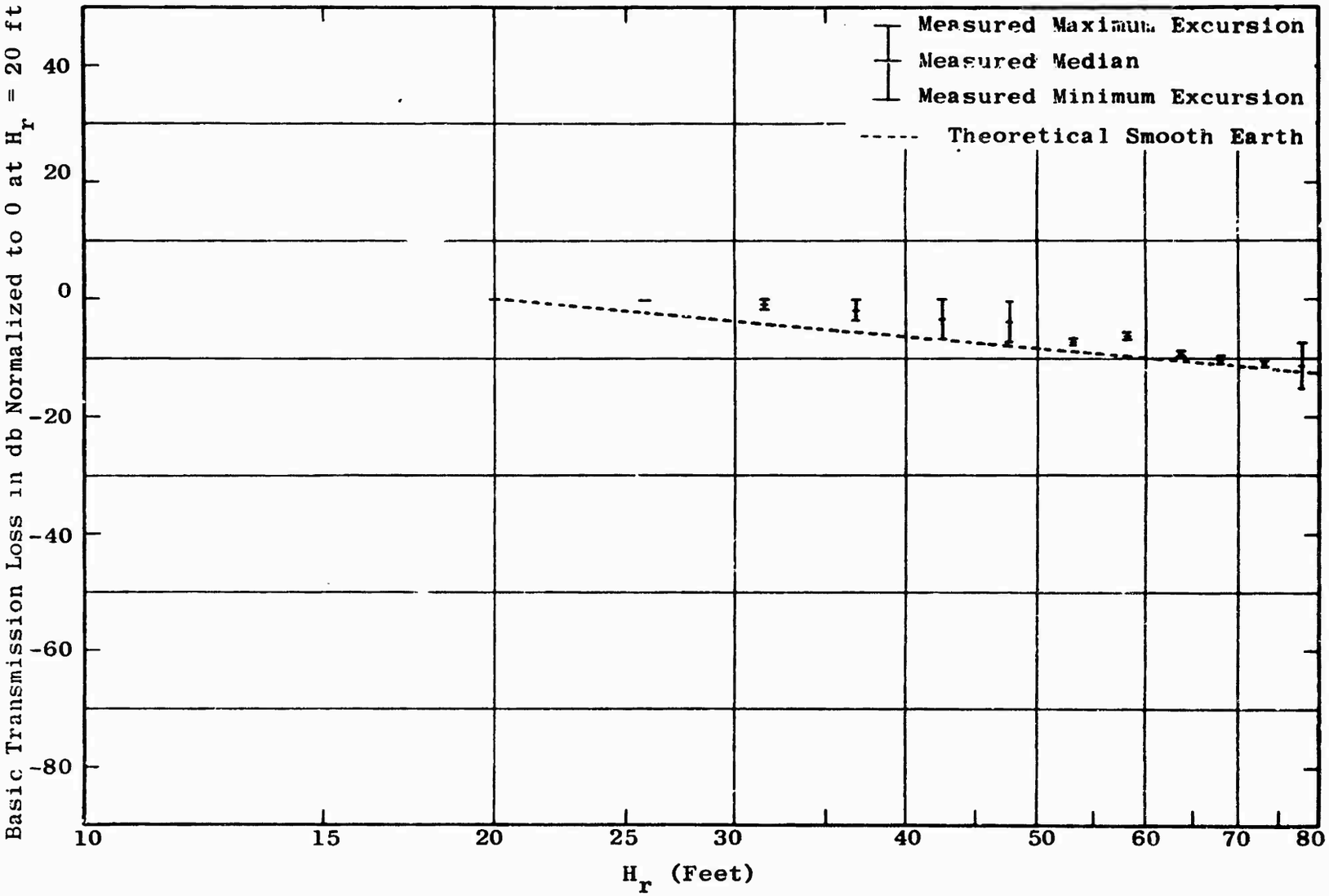

Figure 4.23A Comparison Between Measured and Theoretical Smooth-Earth Functions
$L_b = F_A(400, 80, H, \geq 2, H_r)$

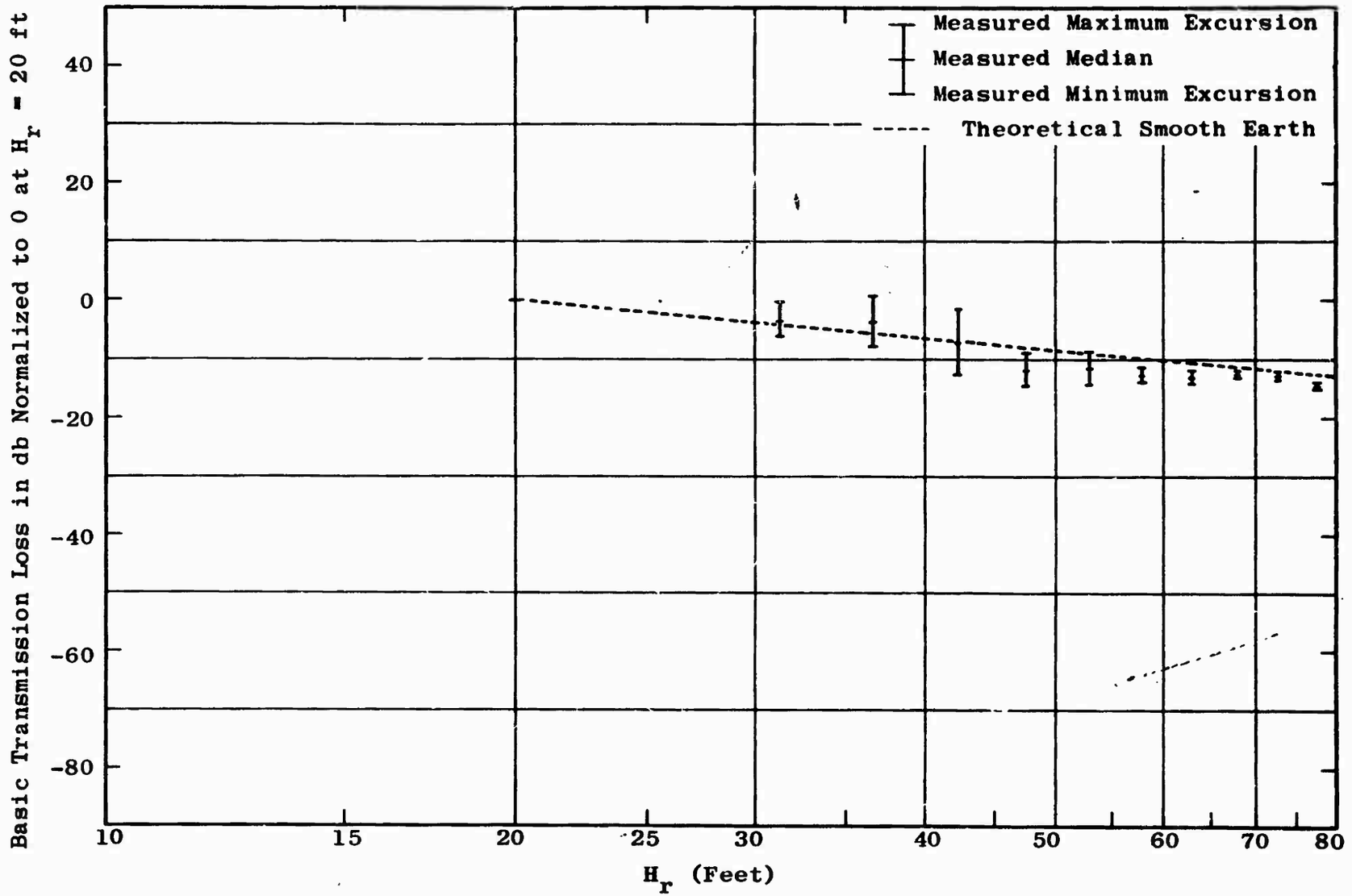

Figure 4.23B Comparison Between Measured and Theoretical Smooth-Earth Functions
$L_b = F_A(400, 40, H, \geq 2, H_r)$

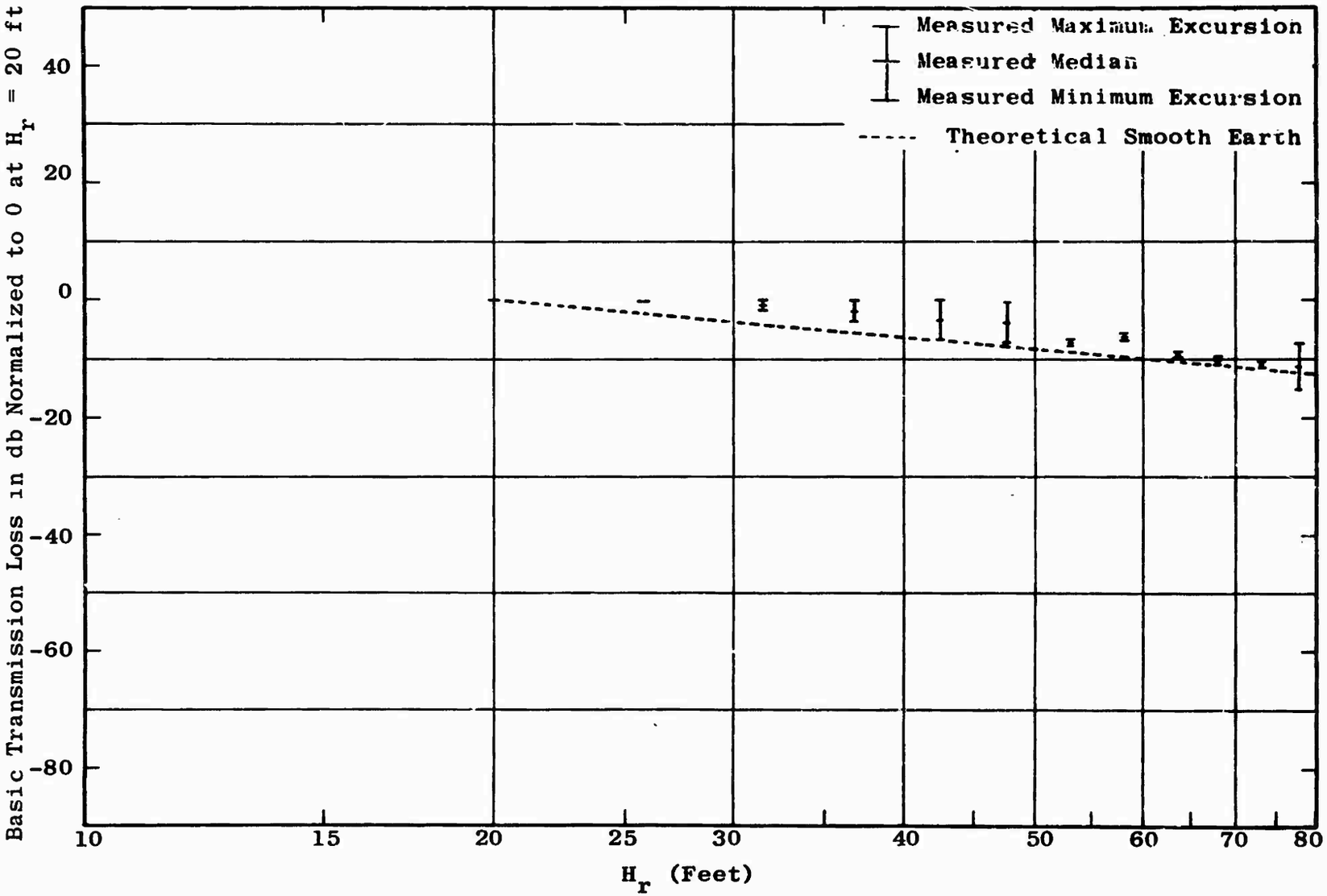

Figure 4.23A Comparison Between Measured and Theoretical Smooth-Earth Functions
$L_b = F_A(400, 80, H, \geq 2, H_r)$

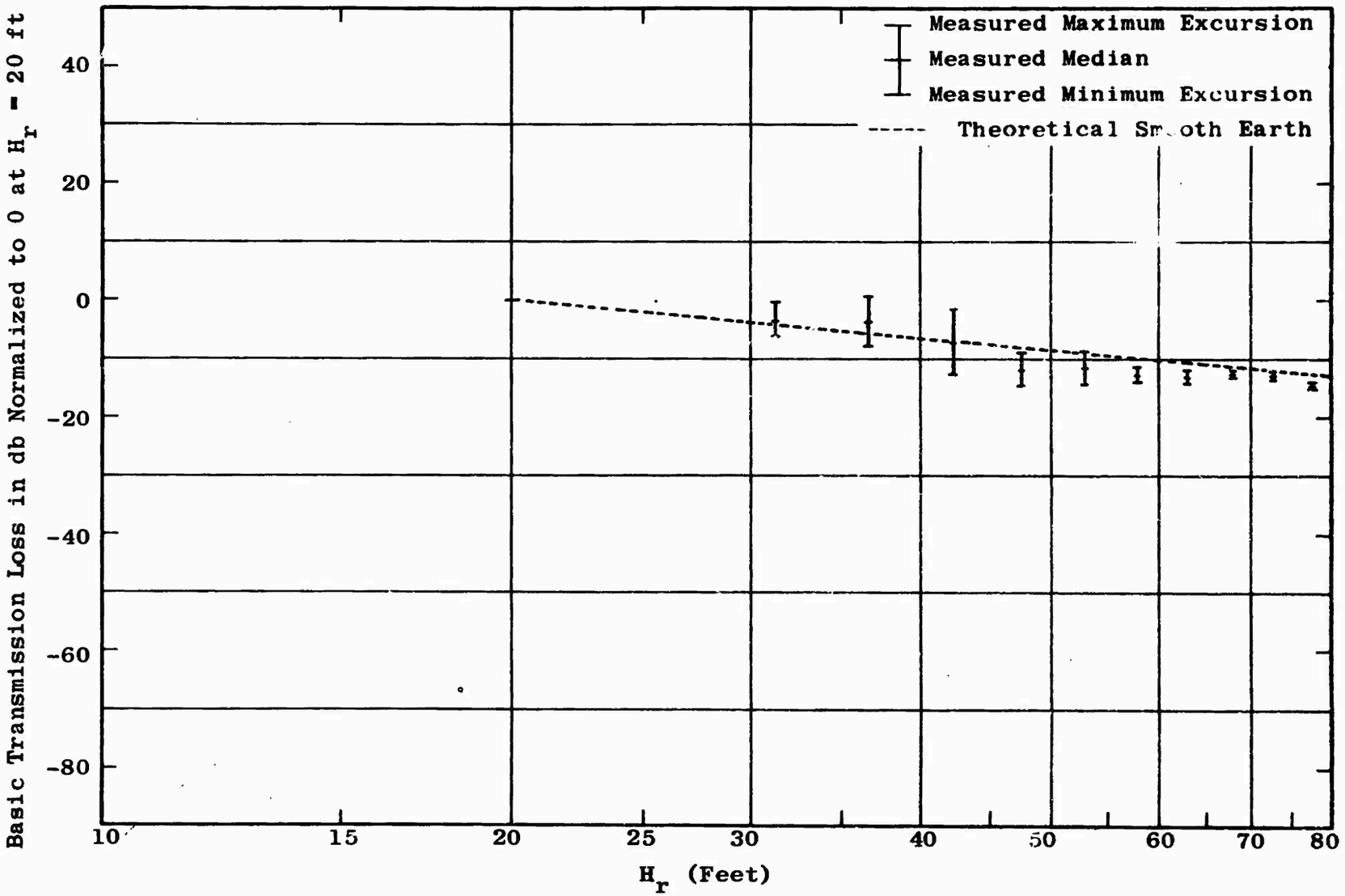

Figure 4.23B Comparison Between Measured and Theoretical Smooth-Earth Functions
$L_b = F_A(400, 40, H, \geq 2, H_r)$

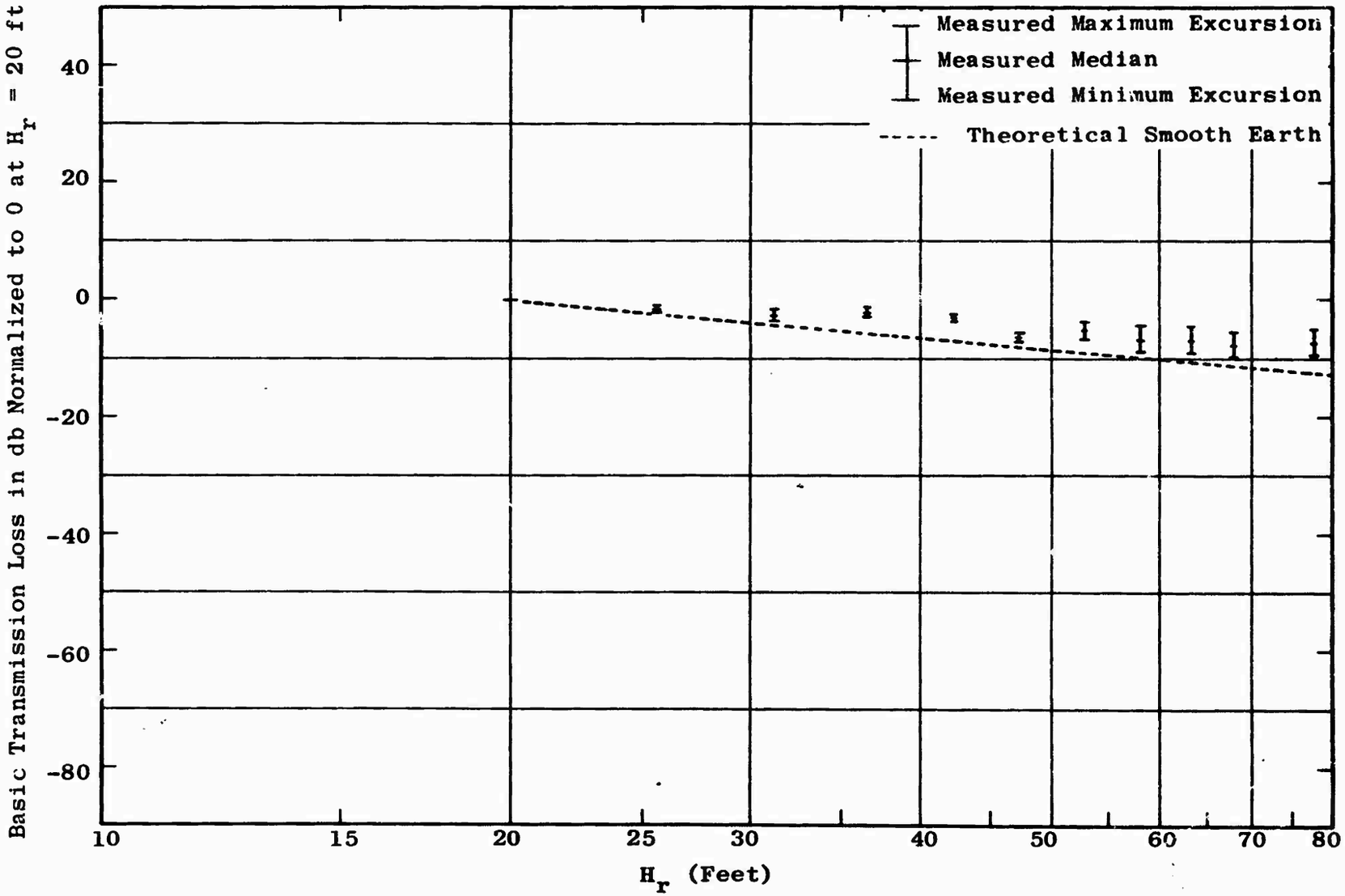

Figure 4.23C Comparison Between Measured and Theoretical Smooth-Earth Functions
$L_b = F_A(400, 13, H, \geq 2, H_r)$

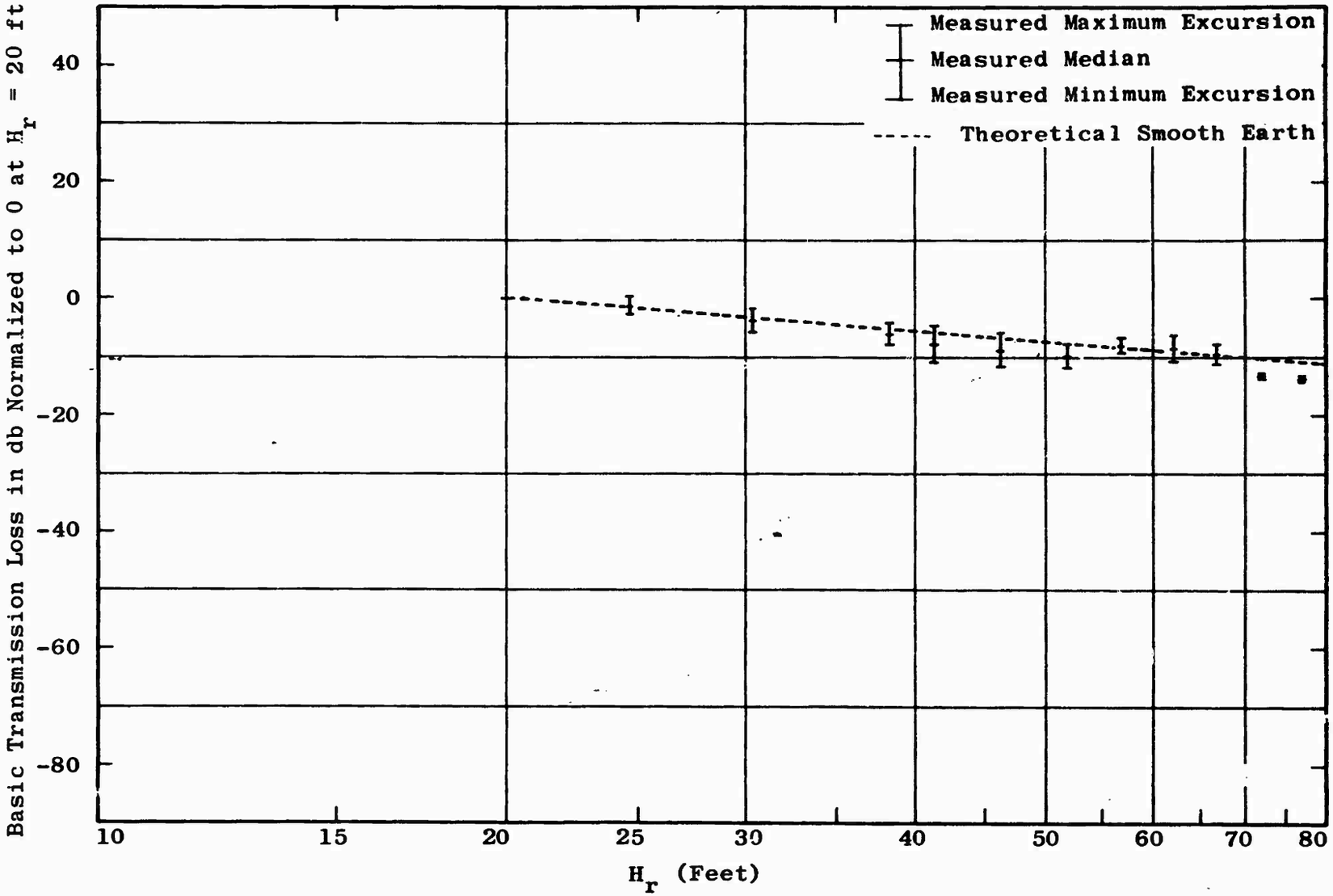

Figure 4.23D Comparison Between Measured and Theoretical Smooth-Earth Functions
$L_b = F_A(250, 80, H, \geq 2, H_r)$

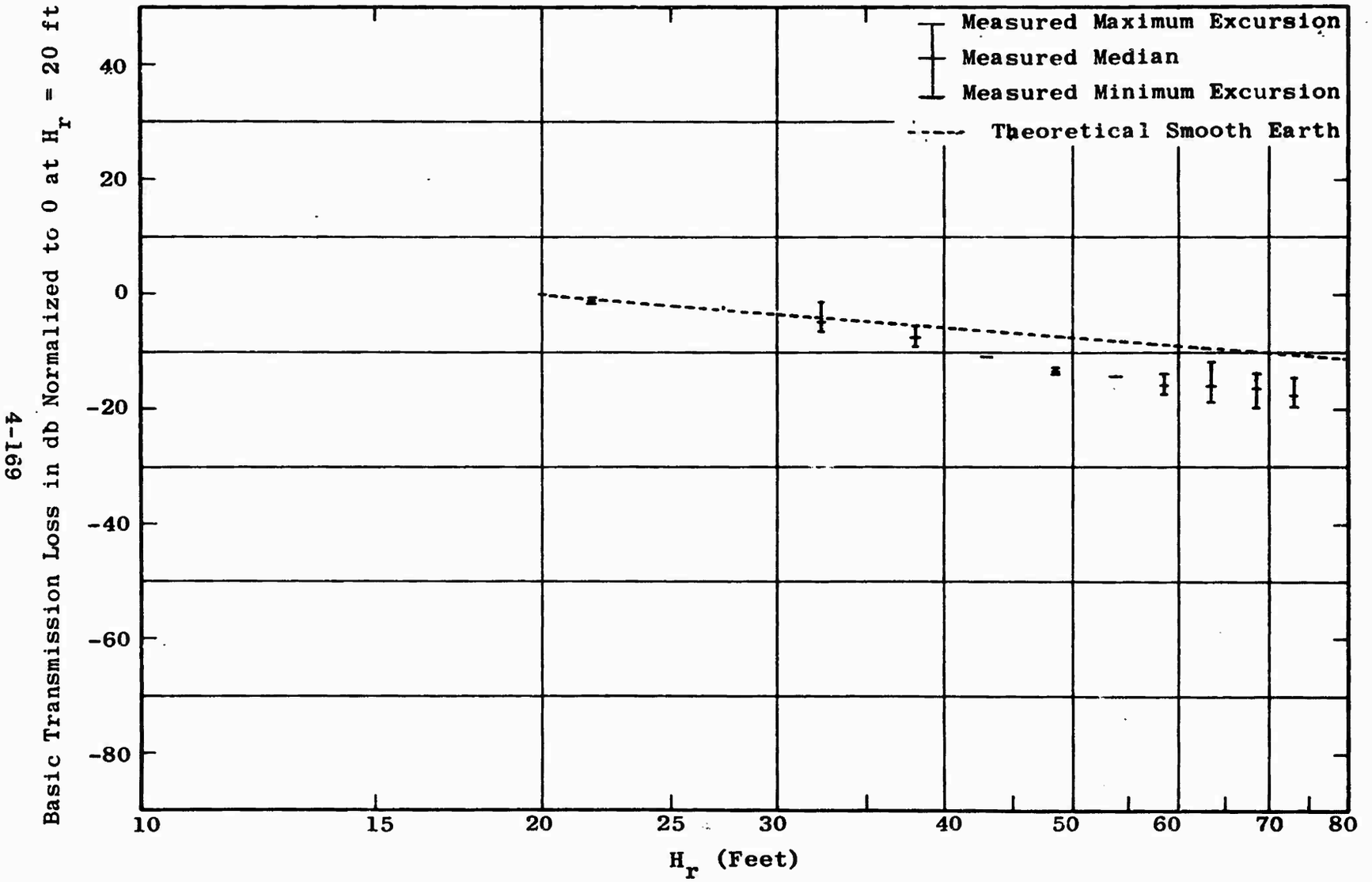

Figure 4.23E Comparison Between Measured and Theoretical Smooth-Earth Functions
$L_b = F_A(250, 40, H, \geq 2, H_r)$

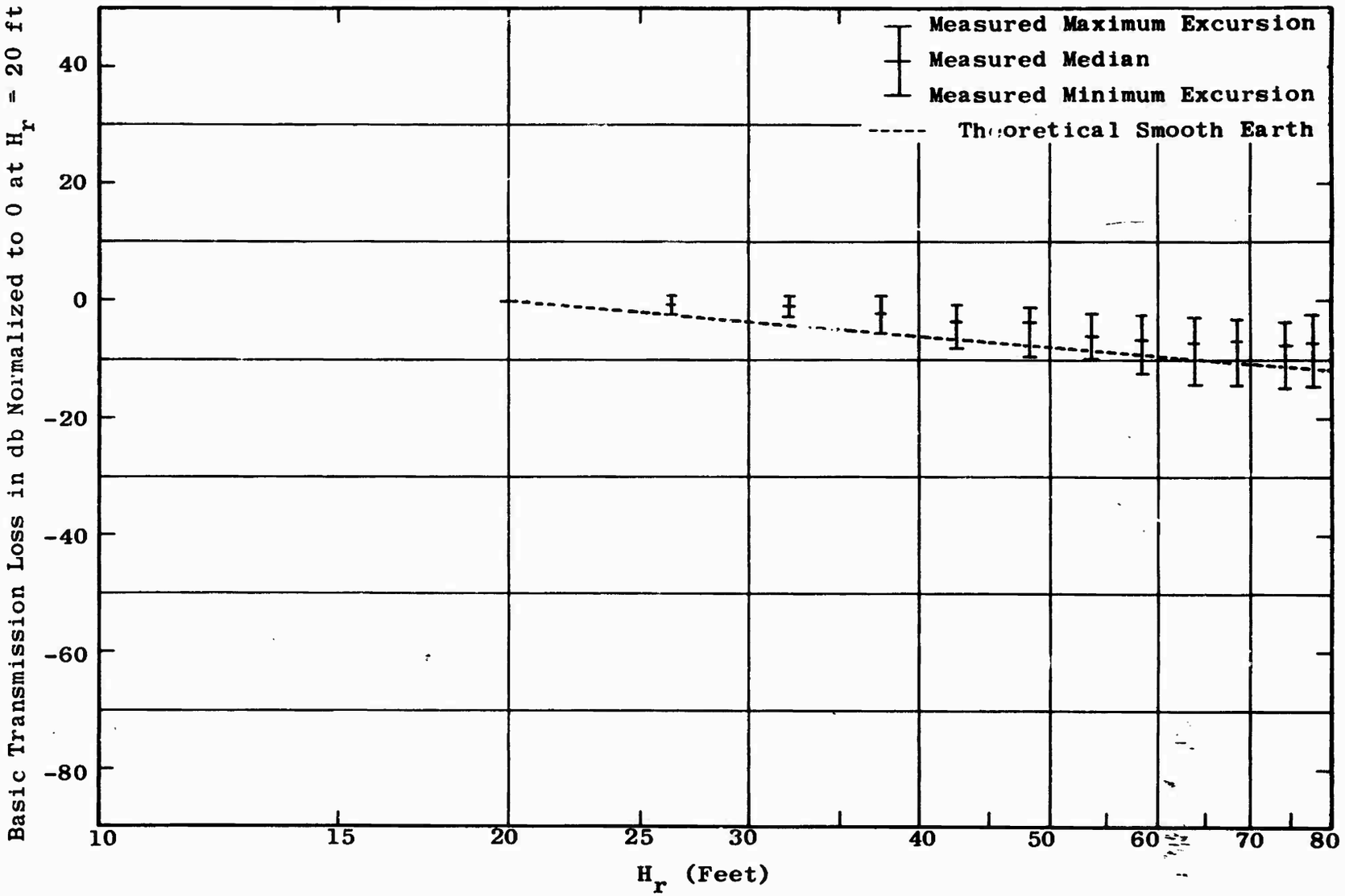

Figure 4.23F Comparison Between Measured and Theoretical Smooth-Earth Functions
$L_b = F_A(100, 80, H, \geq 2, H_r)$

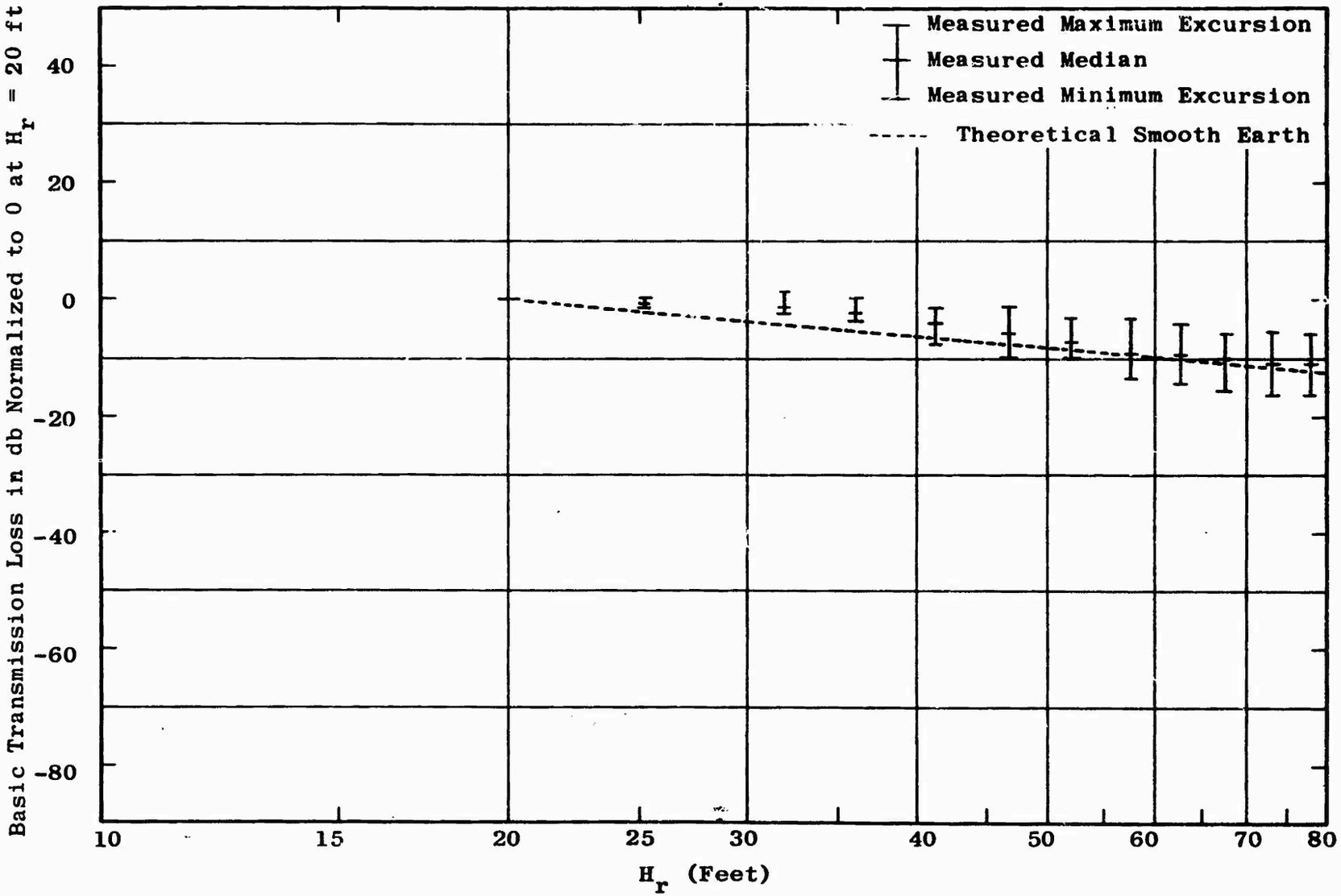

Figure 4.23G Comparison Between Measured and Theoretical Smooth-Earth Functions
$L_b = F_A(100, 40, H, \geq 2, H_r)$

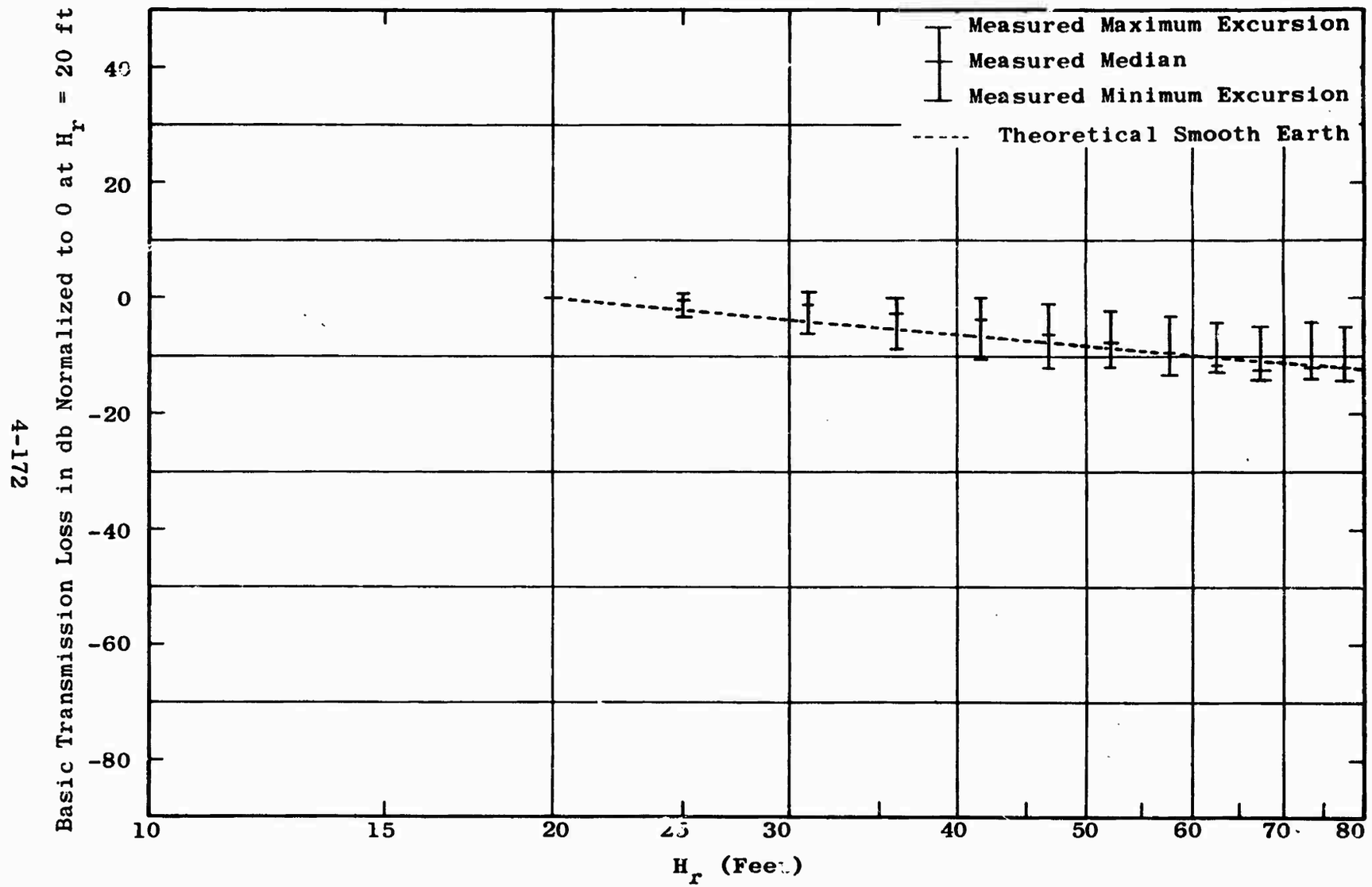

Figure 4.23H Comparison Between Measured and Theoretical Smooth-Earth Functions
$L_b = F_A(100, 13, H, \geq 2, H_r)$

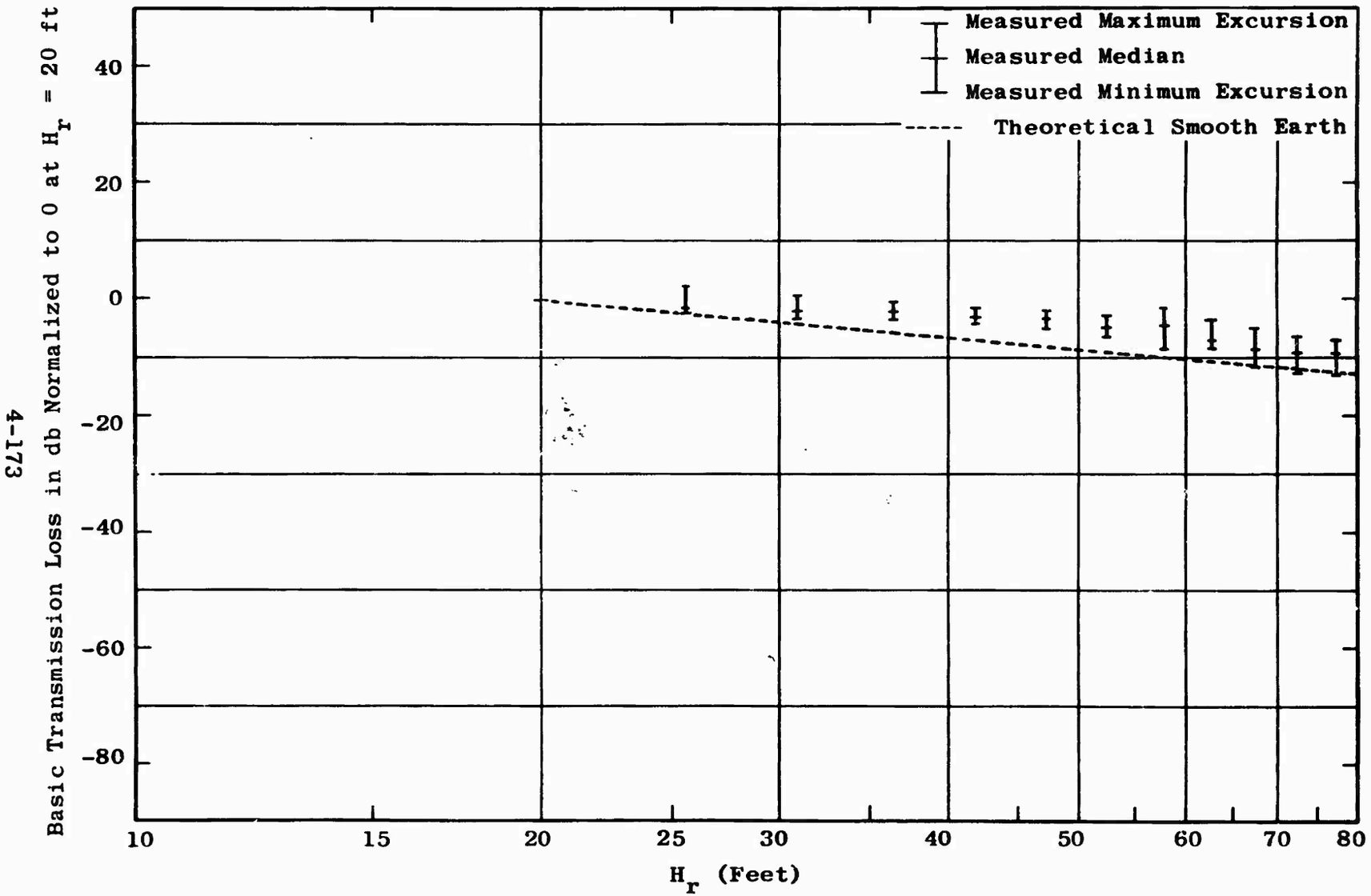

Figure 4.23I Comparison Between Measured and Theoretical Smooth-Earth Functions
$L_b = F_A(50, 80, H, \geq 2, H_r)$

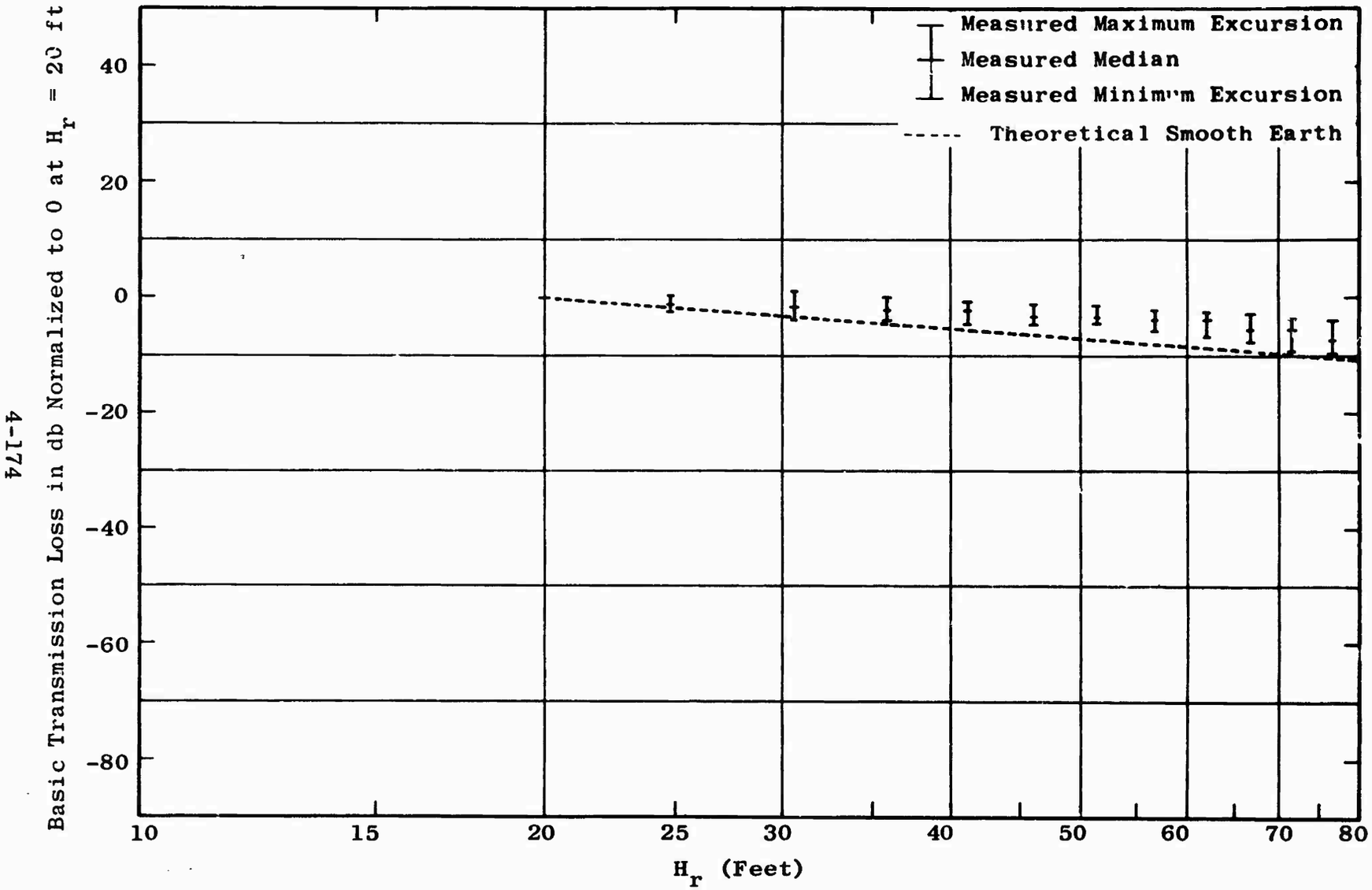

Figure 4.23J Comparison Between Measured and Theoretical Smooth-Earth Functions
$L_b = F_A(50, 40, H, \geq 2, H_r)$

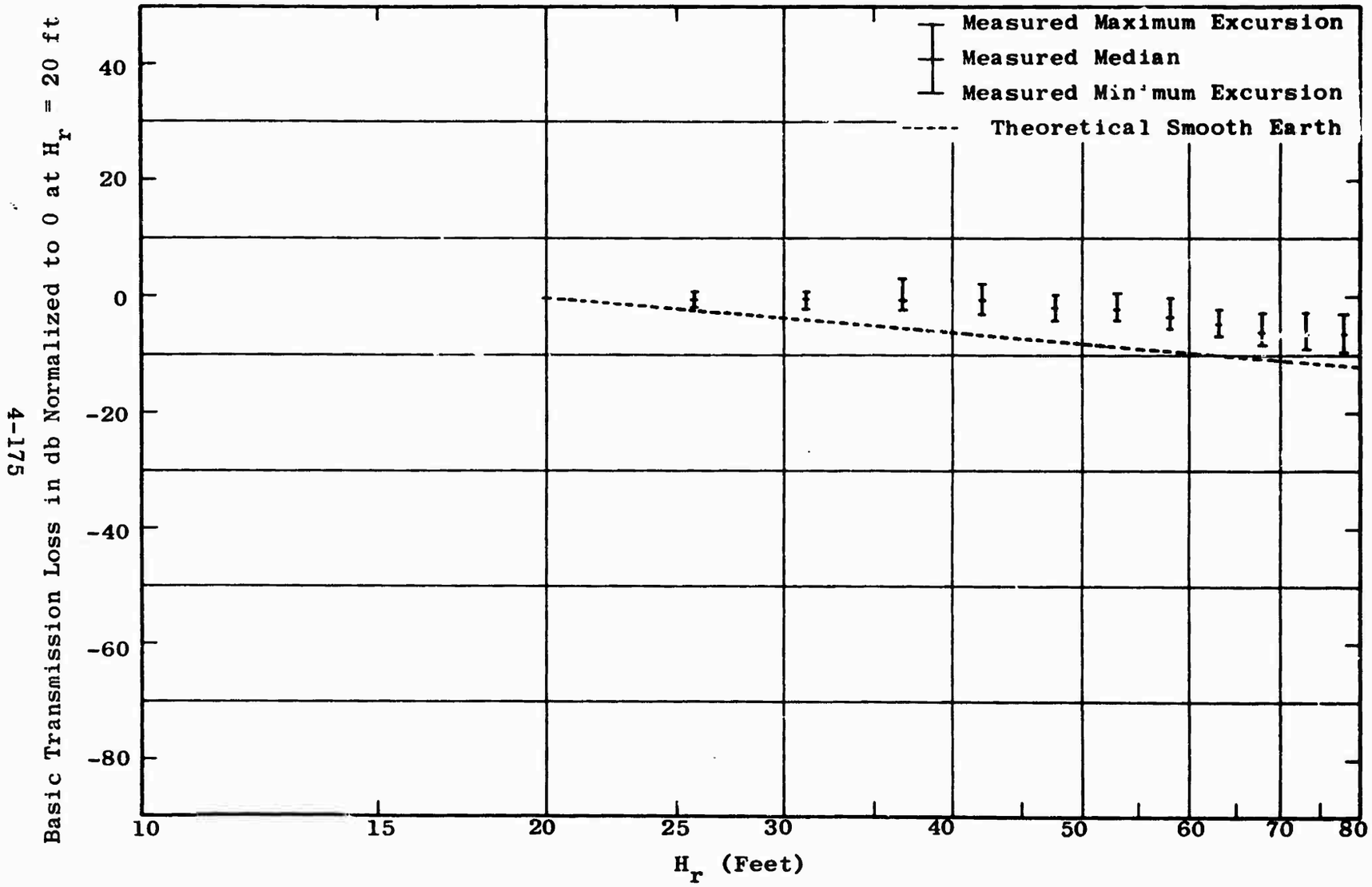

Figure 4.23K Comparison Between Measured and Theoretical Smooth-Earth Functions
$L_b = F_A(50, 13, H, \geq 2, H_r)$

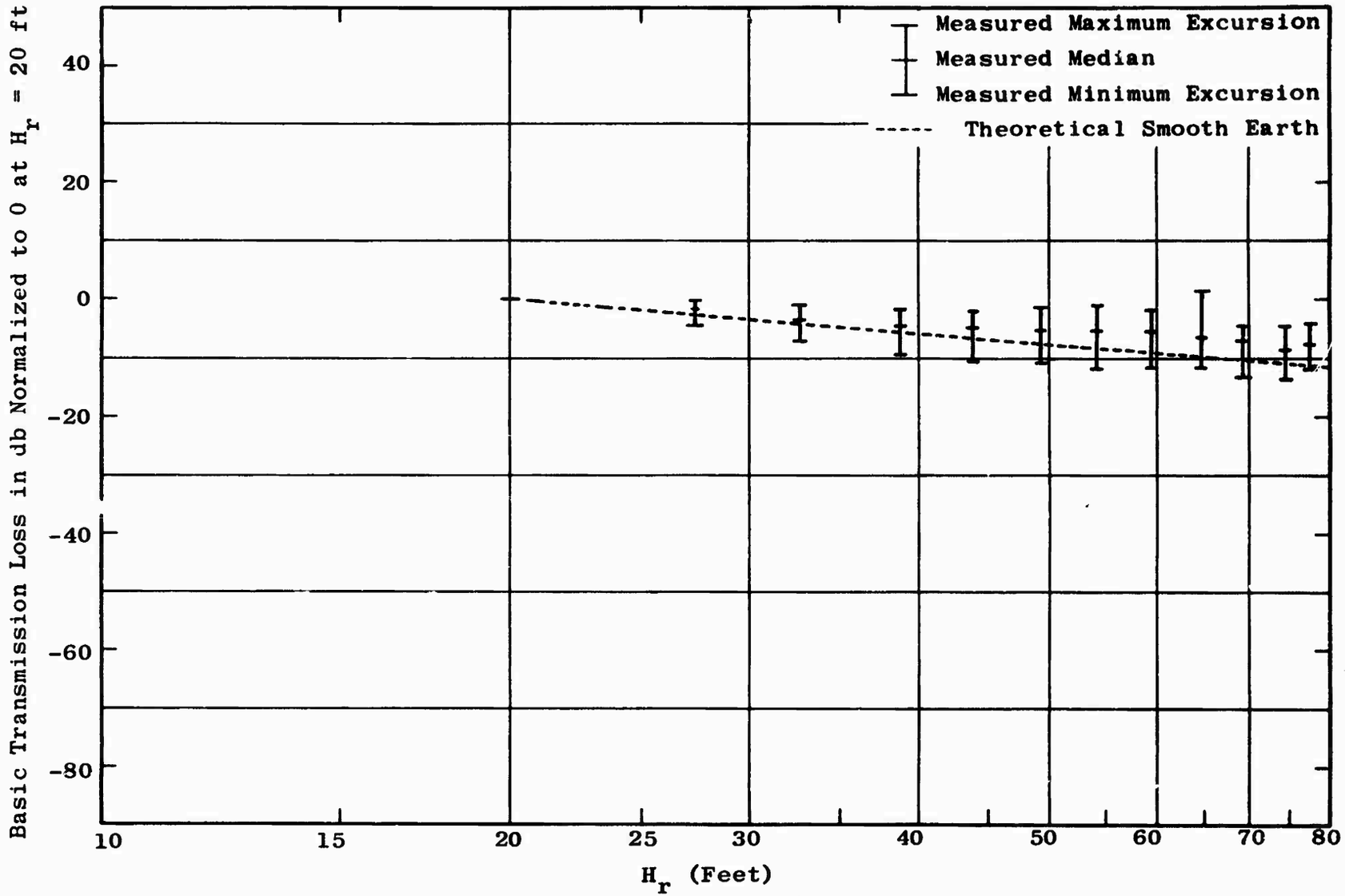

Figure 4.23L Comparison Between Measured and Theoretical Smooth-Earth Functions
$L_b = F_A(25.5, 80, H, \geq 2, H_r)$

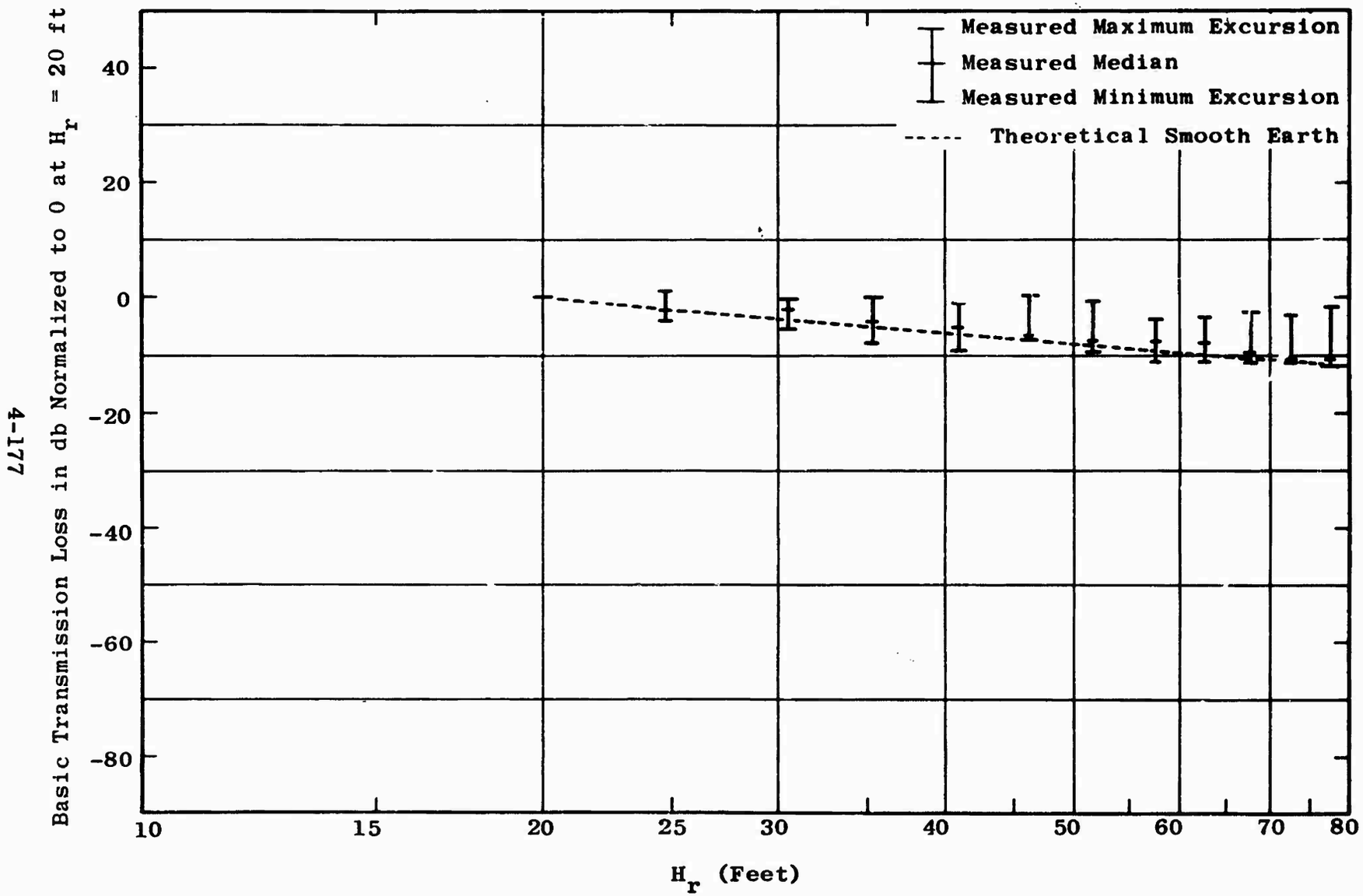

Figure 4.23M Comparison Between Measured and Theoretical Smooth-Earth Functions
$L_b = F_A(25.5, 40, H, \geq 2, H_r)$

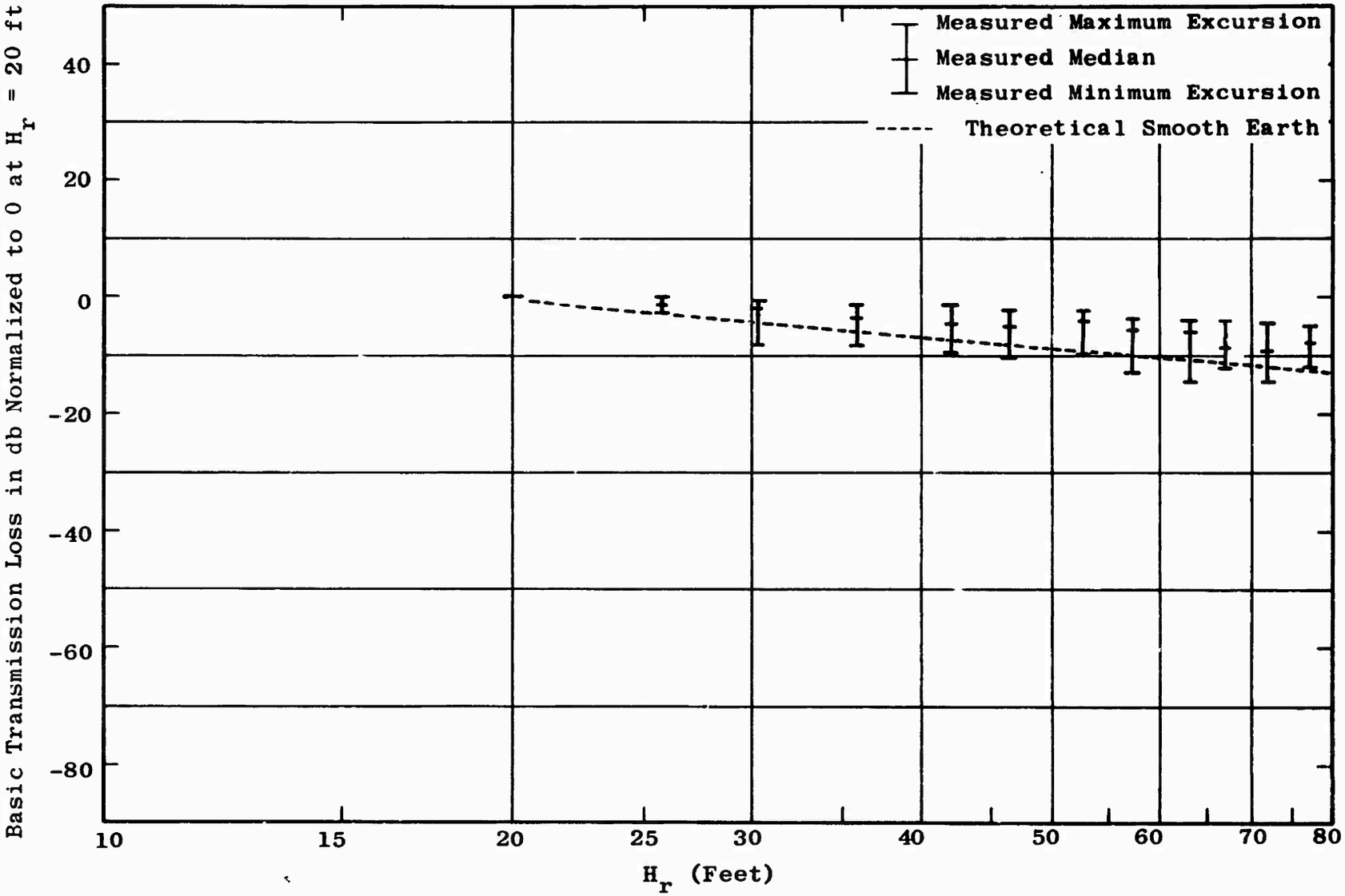

Figure 4.23N Comparison Between Measured and Theoretical Smooth-Earth Functions
$L_b = F_A(25.5, 13, H, \geq 2, H_r)$

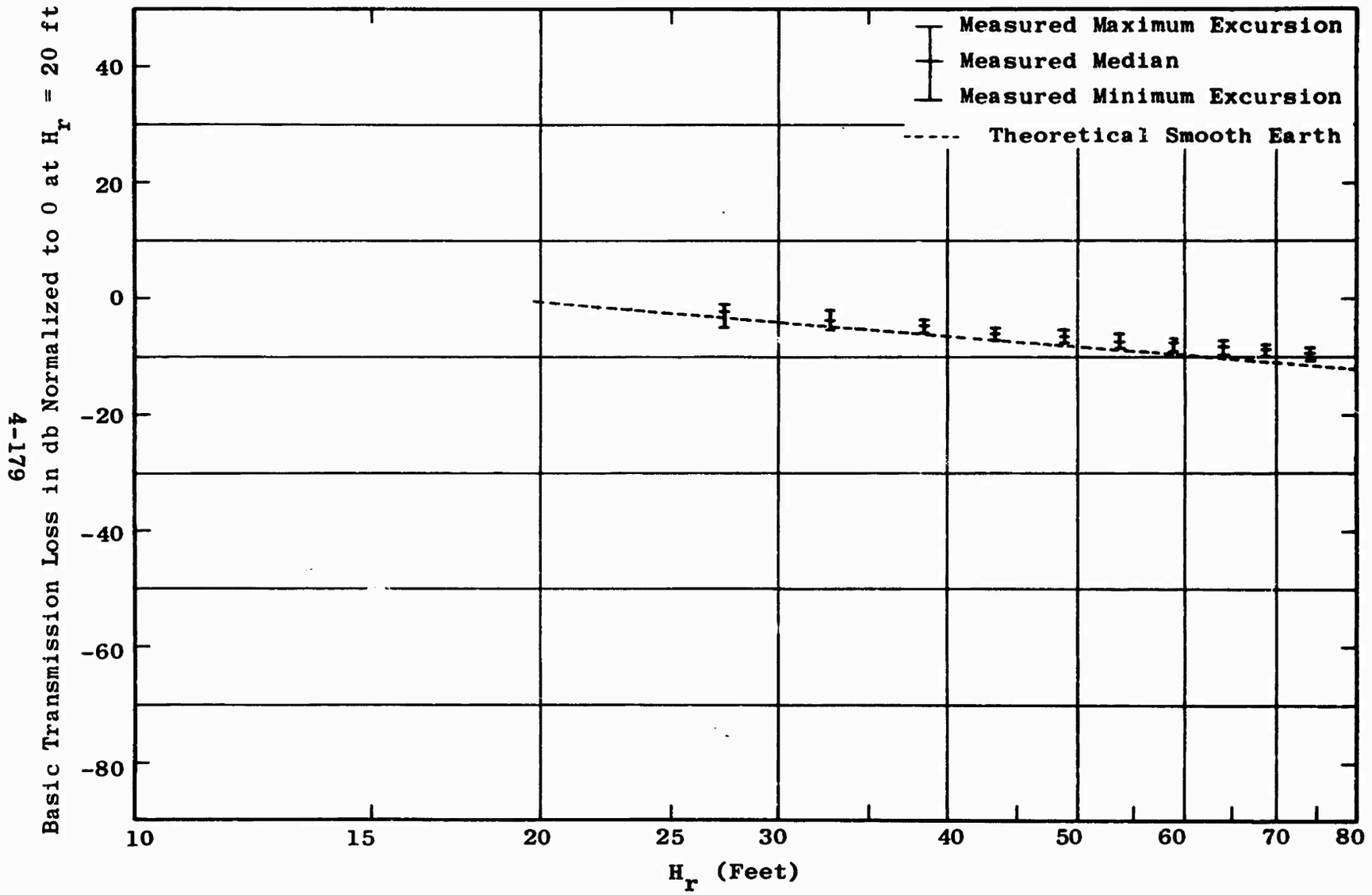

Figure 4.230 Comparison Between Measured and Theoretical Smooth-Earth Functions

$L_b = F_A(12.0, 40, H, \geq 2, H_r)$

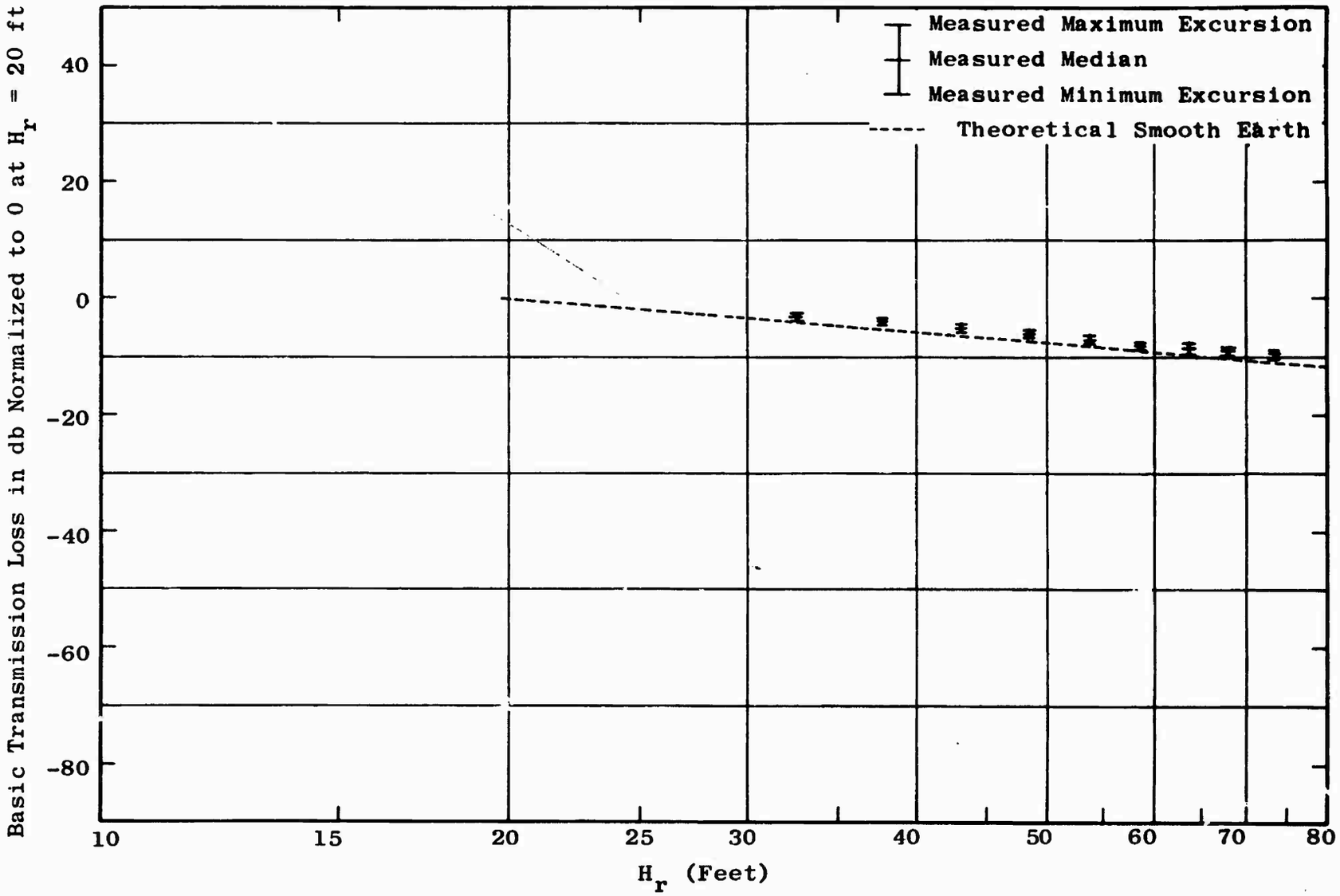

Figure 4.23P Comparison Between Measured and Theoretical Smooth-Earth Functions
$L_b = F_A(6.0, 40, H, \geq 2, H_r)$

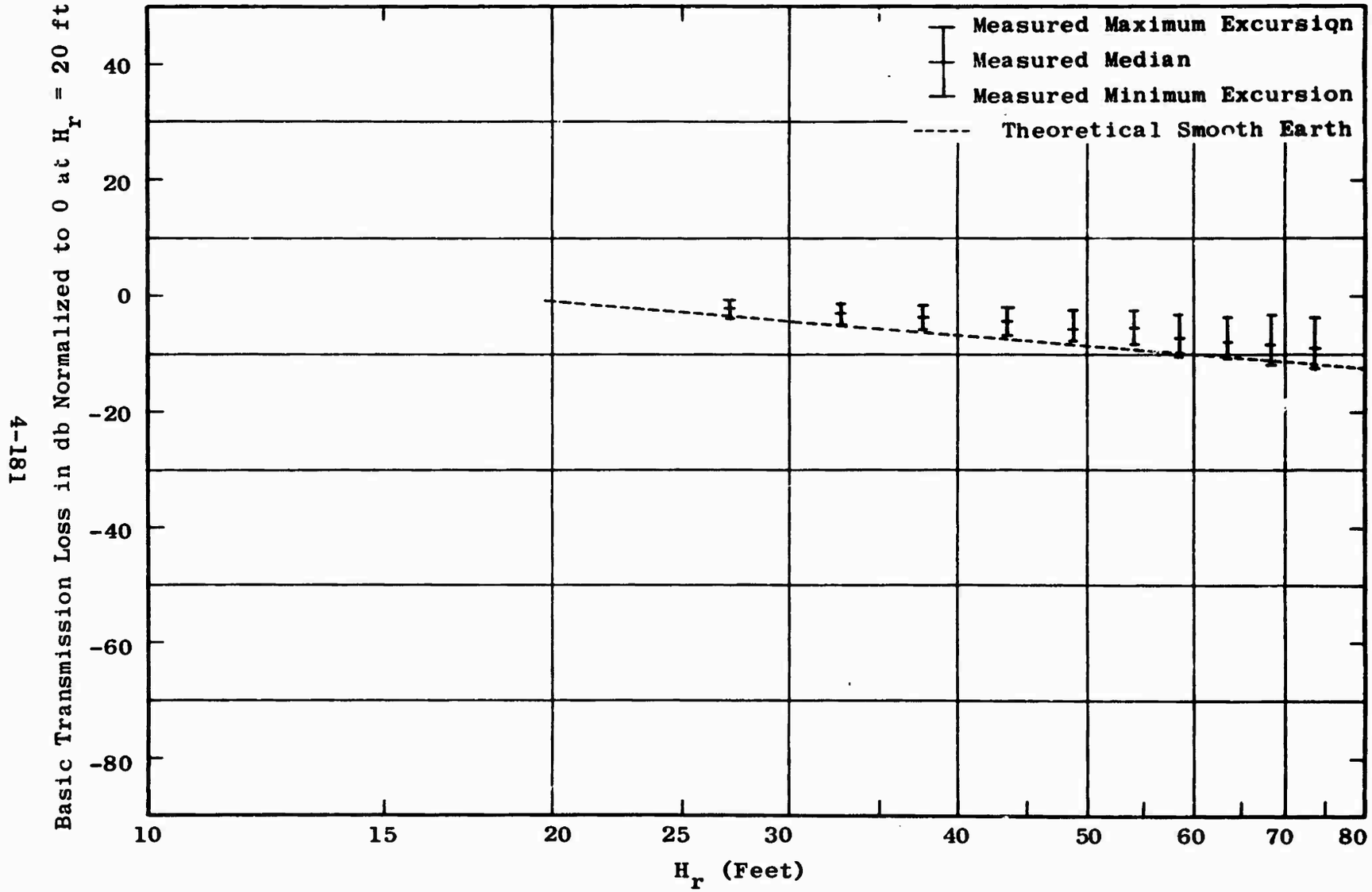

Figure 4.23Q Comparison Between Measured and Theoretical Smooth-Earth Functions
$L_b = F_A(2.0, 40, H, \geq 2, H_r)$

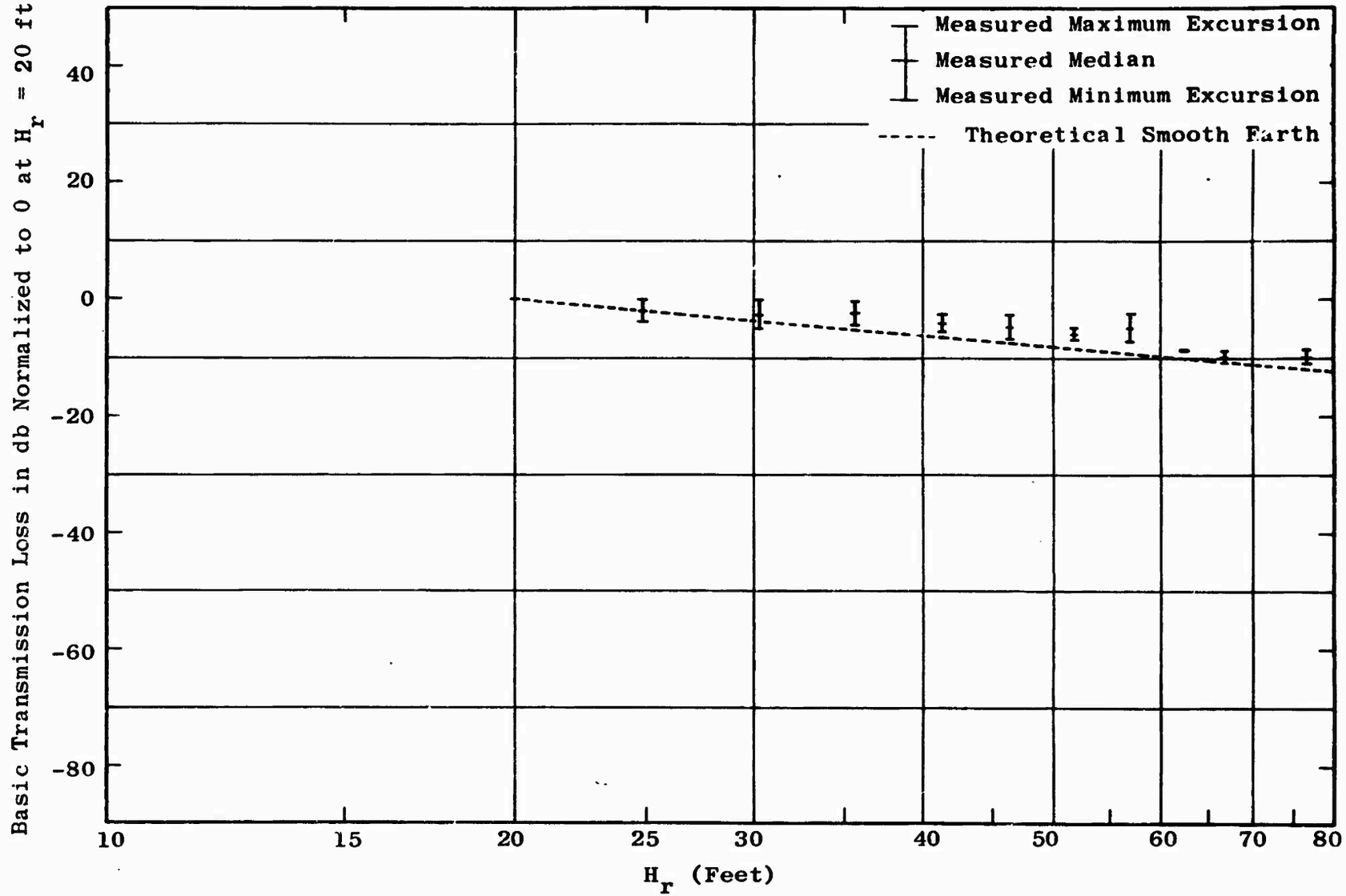

Figure 4.23R Comparison Between Measured and Theoretical Smooth-Earth Functions
$L_b = F_A(400, 80, V, \geq 2, H_r)$

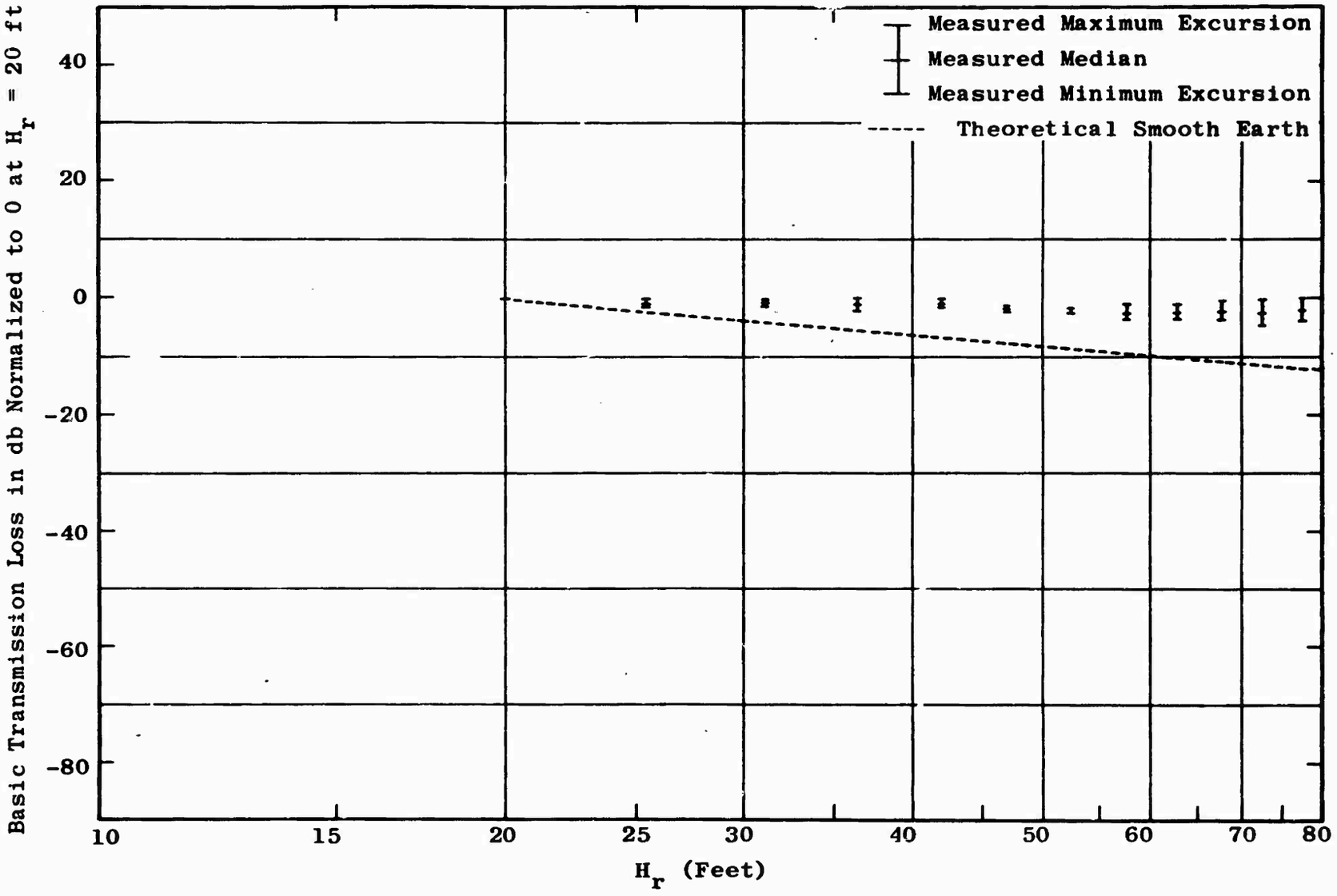

Figure 4.23S Comparison Between Measured and Theoretical Smooth-Earth Functions
$L_b = F_A(400, 40, V, \geq 2, H_r)$

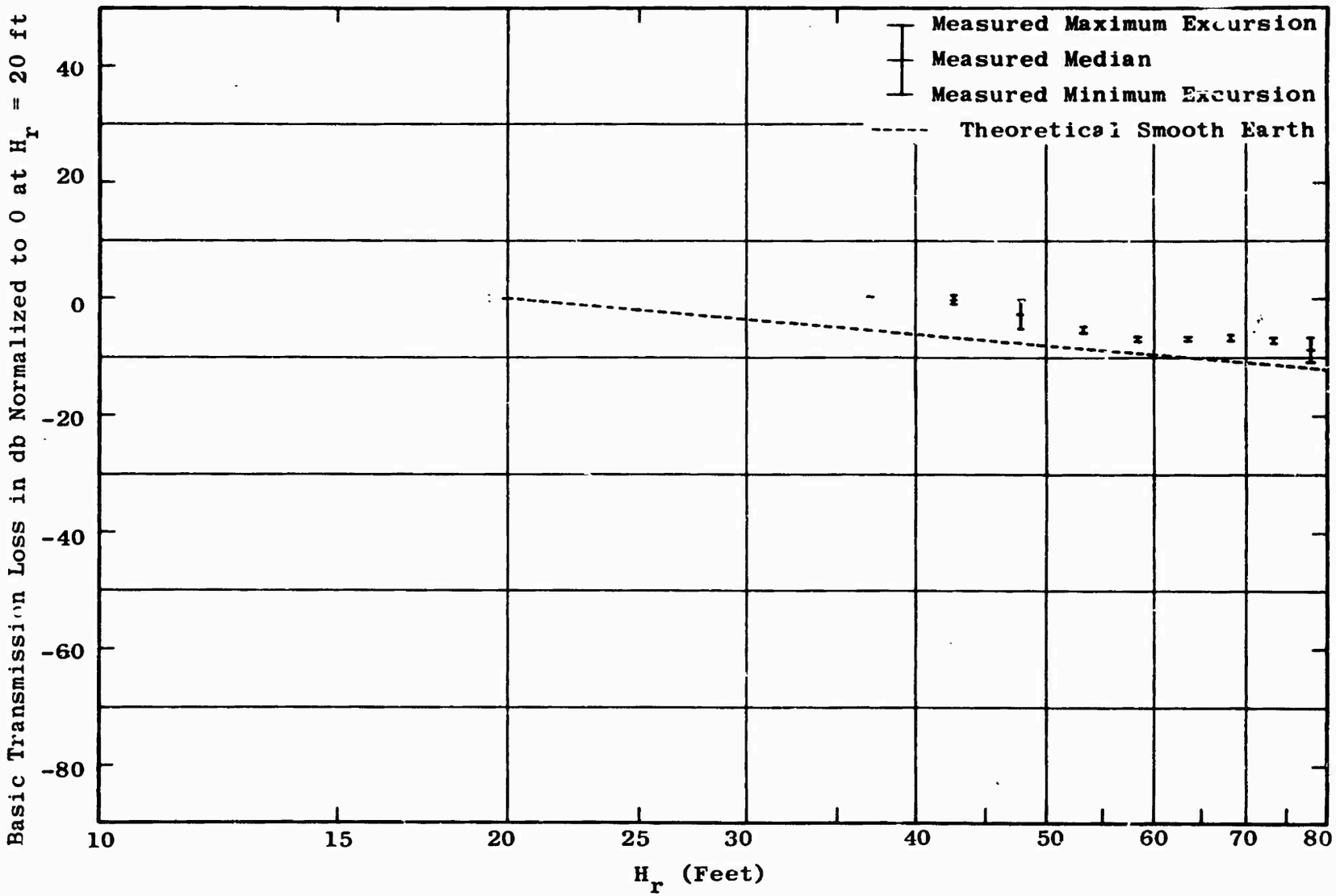

Figure 4.23T Comparison Between Measured and Theoretical Smooth-Earth Functions
$L_b = F_A(400, 13, V_1 \geq 2, H_r)$

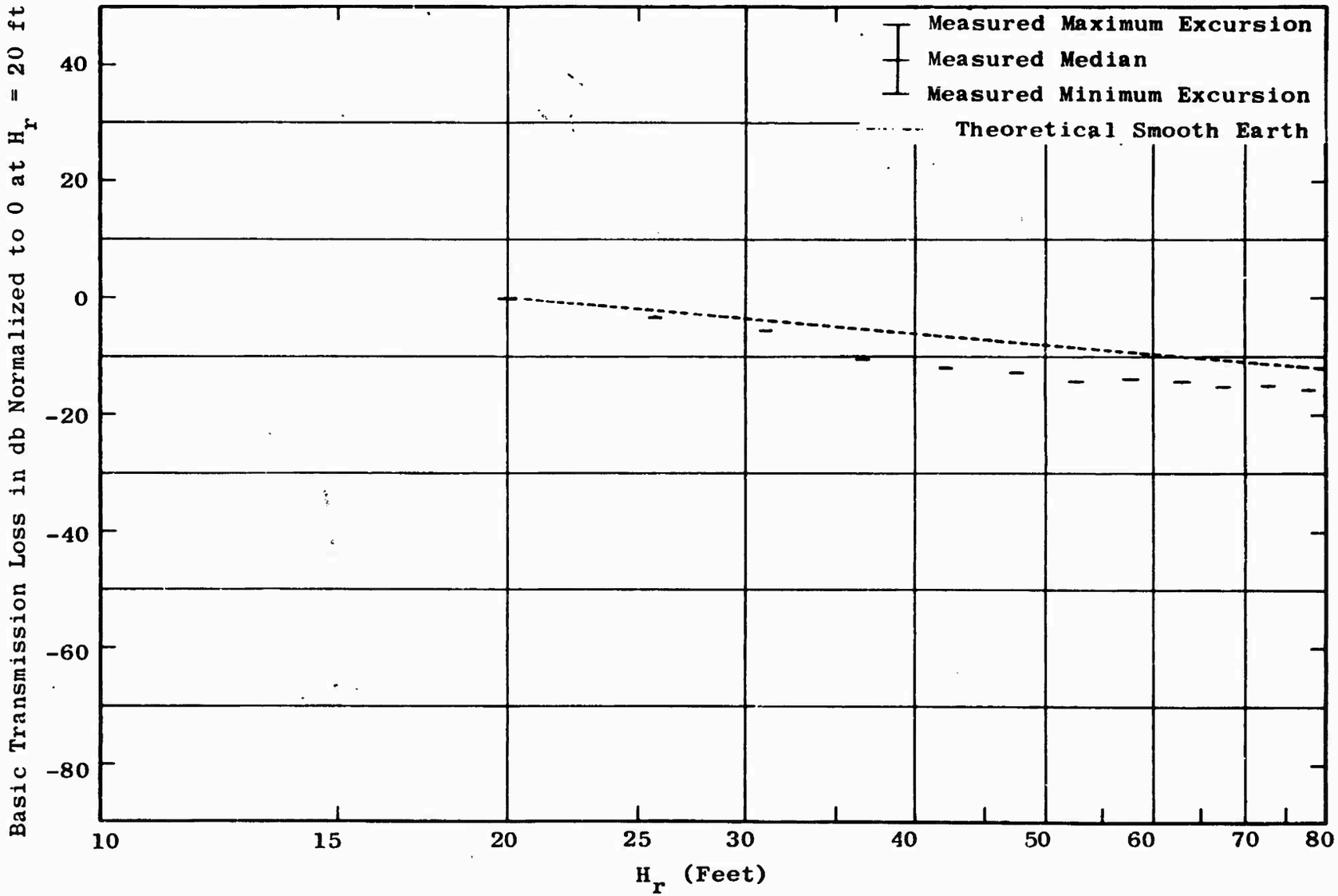

Figure 4.23U Comparison Between Measured and Theoretical Smooth-Earth Functions
$L_b = F_A(250, 80, V, \geq 2, H_r)$

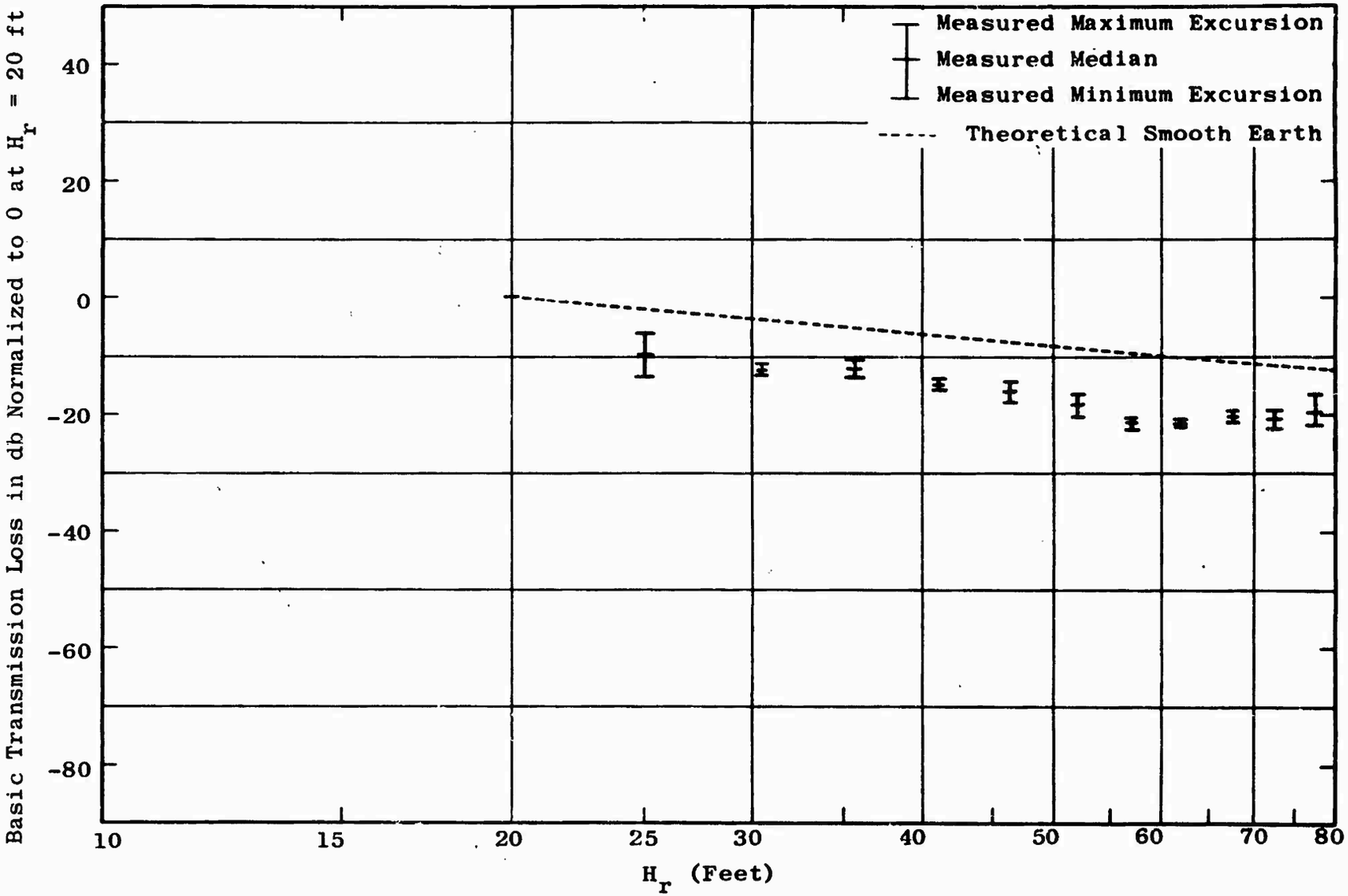

Figure 4.23V Comparison Between Measured and Theoretical Smooth-Earth Functions
$L_b = F_A(250, 40, V, \geq 2, H_r)$

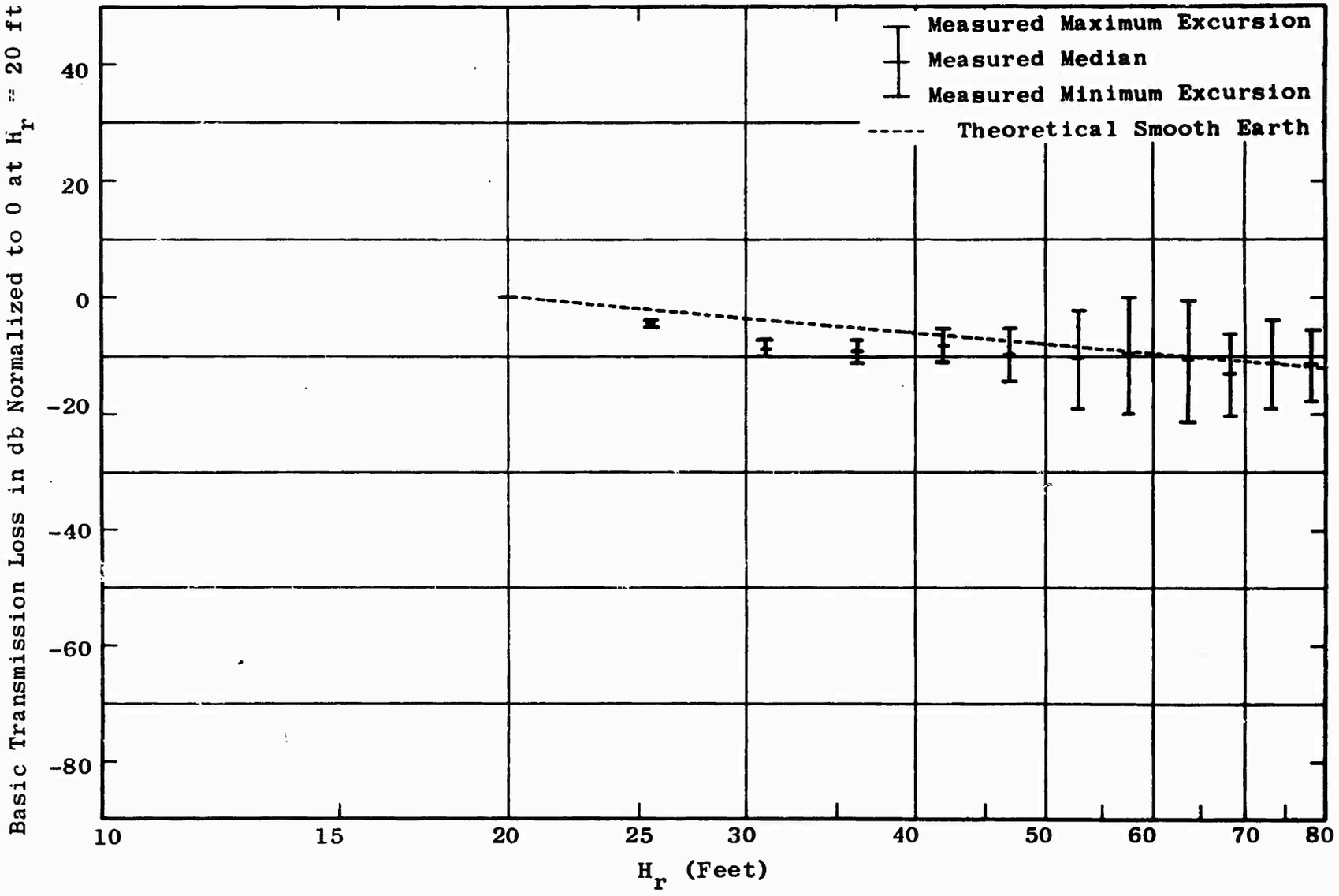

Figure 4.23W Comparison Between Measured and Theoretical Smooth-Earth Functions
$L_b = F_A(250, 13, V, \geq 2, H_r)$

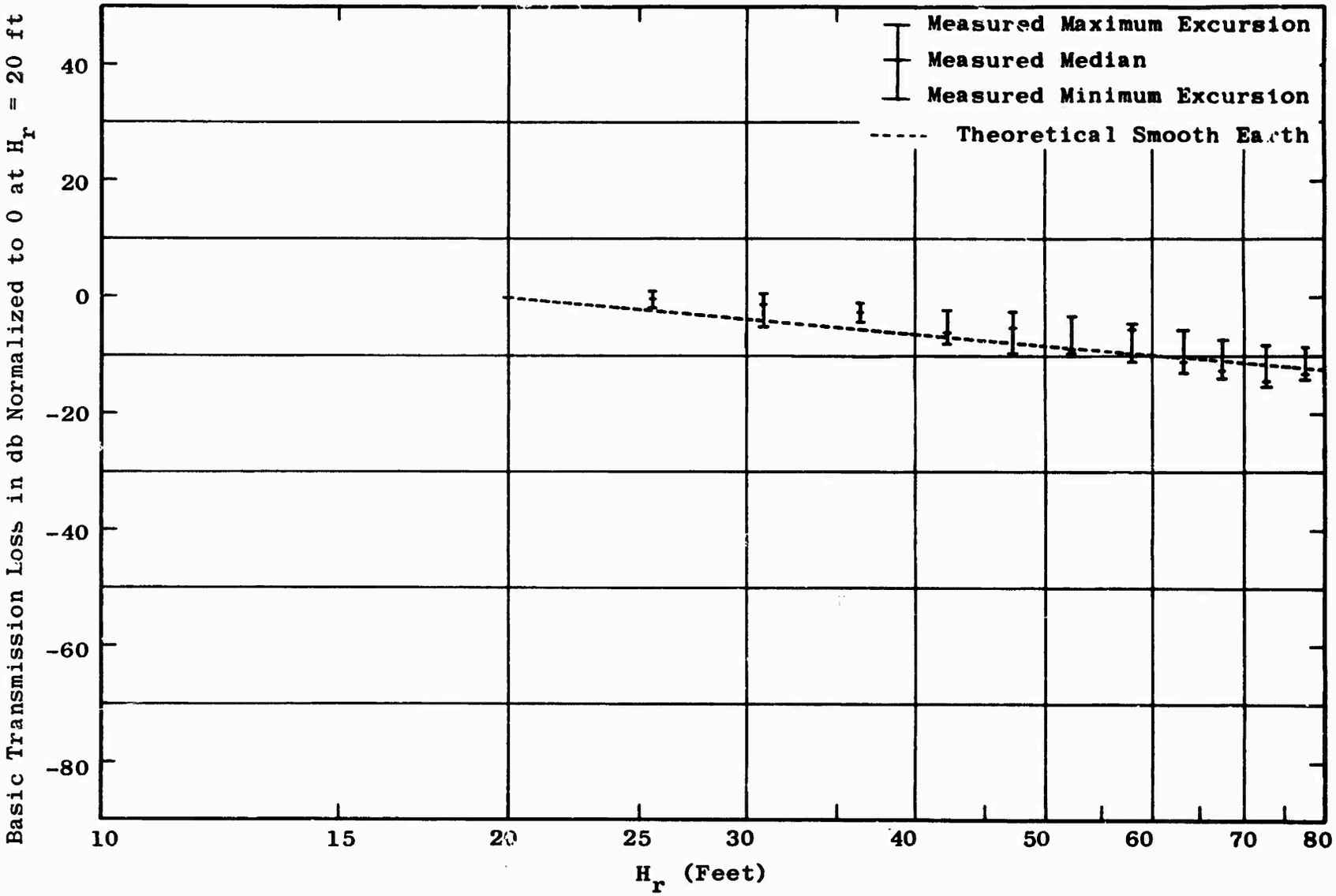

Figure 4.23X Comparison Between Measured and Theoretical Smooth-Earth Functions
$L_b = F_A(100, 80, V, \geq 2, H_r)$

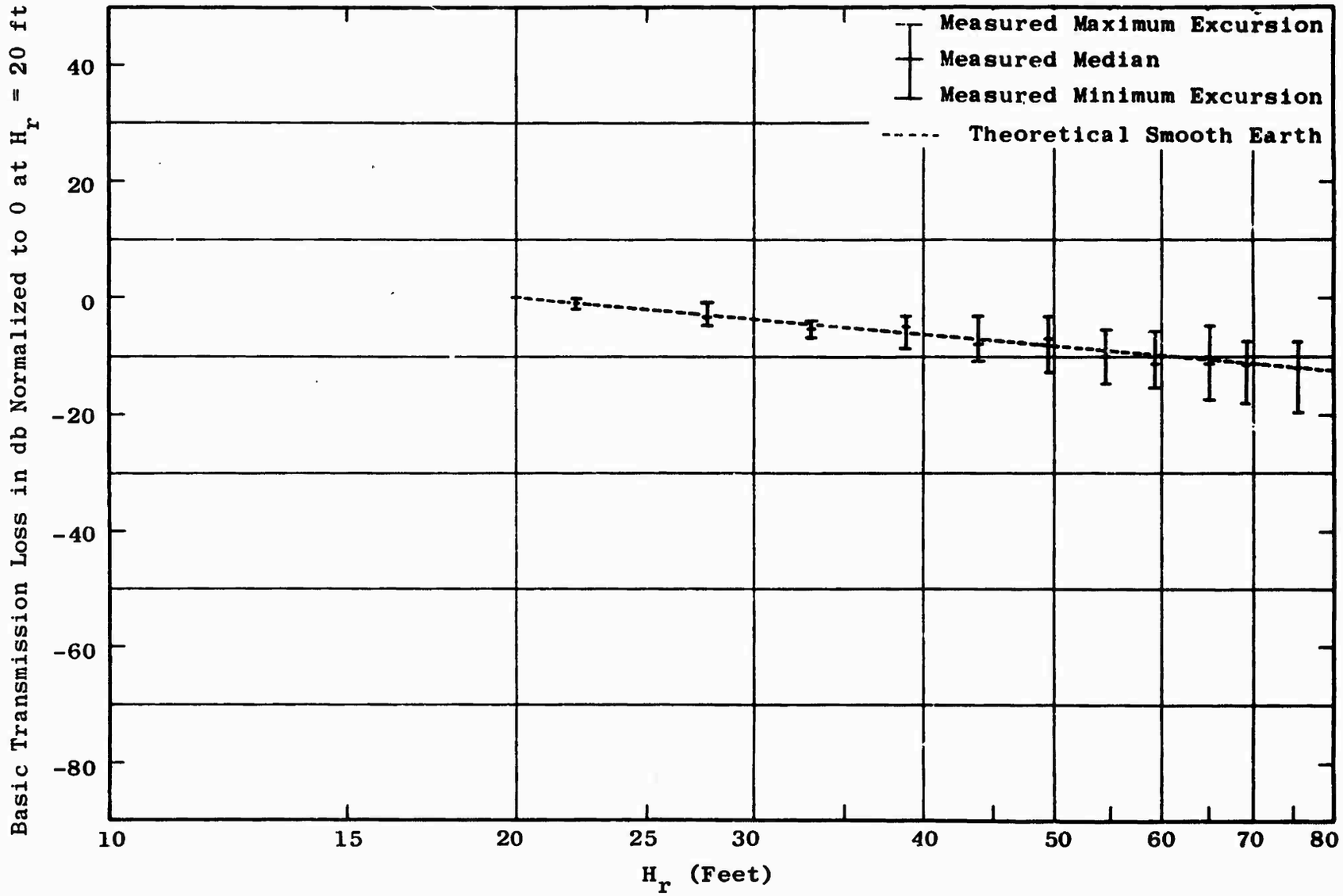

Figure 4.23Y Comparison Between Measured and Theoretical Smooth-Earth Functions
$L_b = F_A(100, 40, V, \geq 2, H_r)$

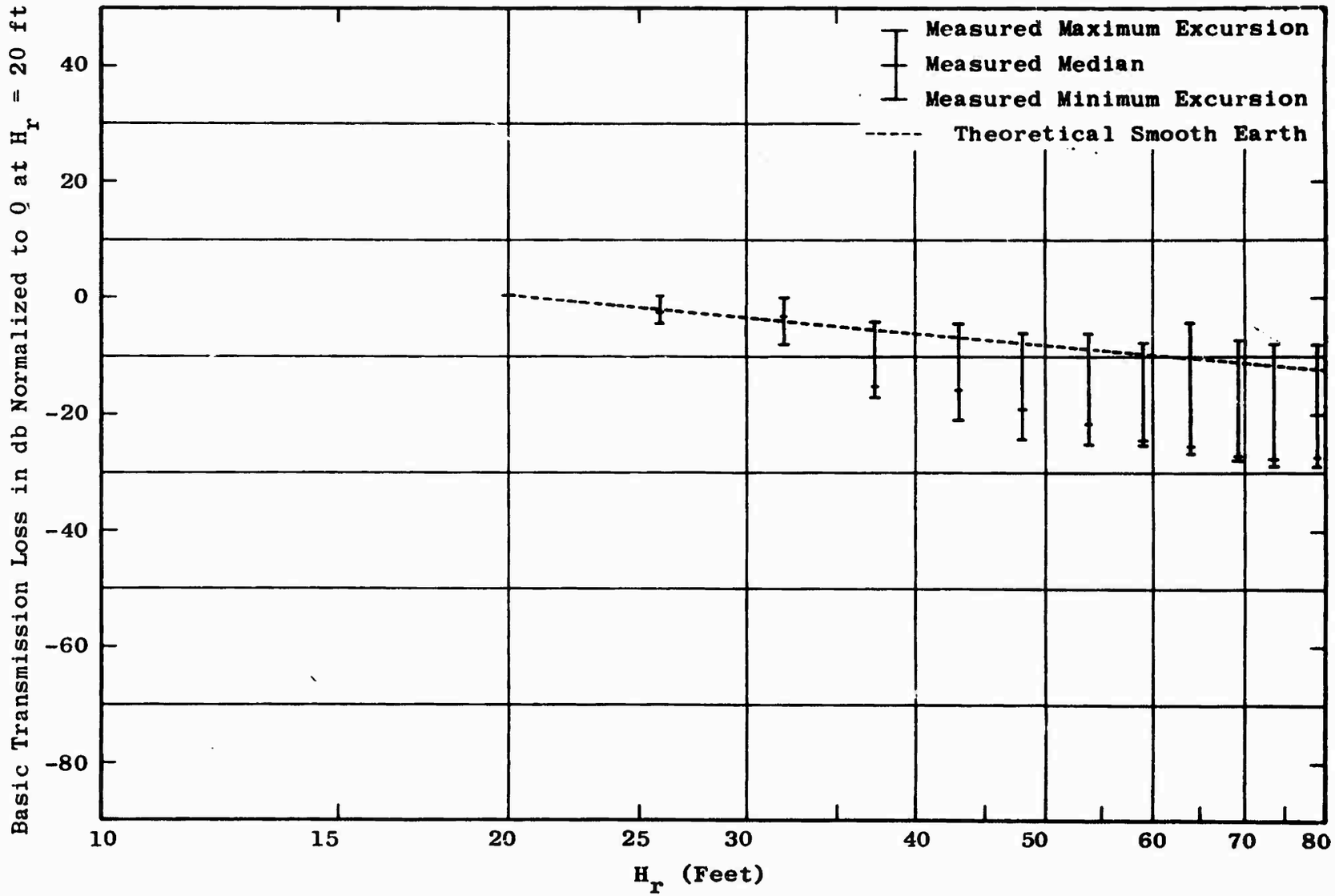

Figure 4.23Z Comparison Between Measured and Theoretical Smooth-Earth Functions
$L_b = F_A(100, 13, V, \geq 2, H_r)$

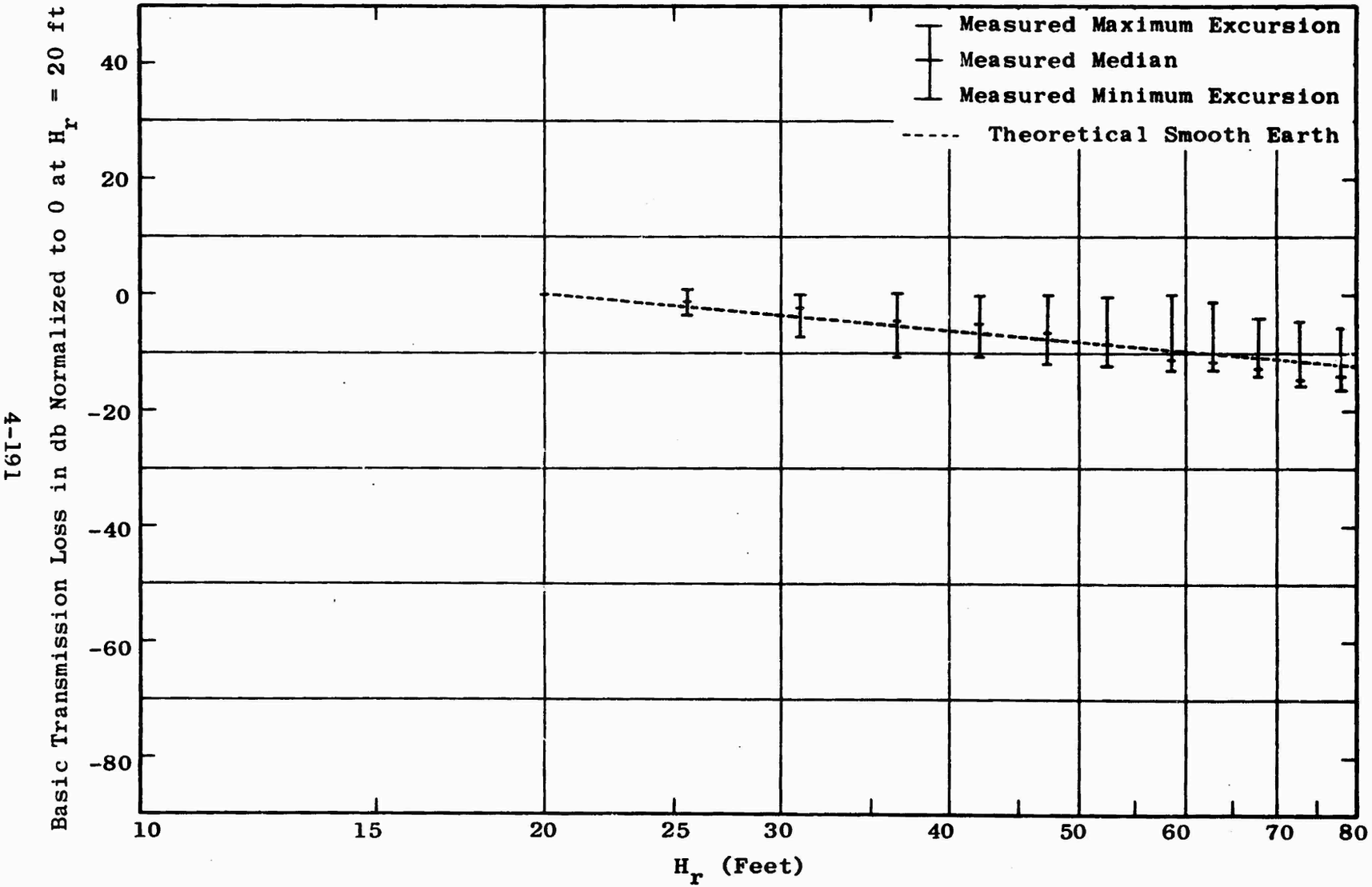

Figure 4.23AA Comparison Between Measured and Theoretical Smooth-Earth Functions
$L_b = F_A(50, 80, V, \geq 2, H_r)$

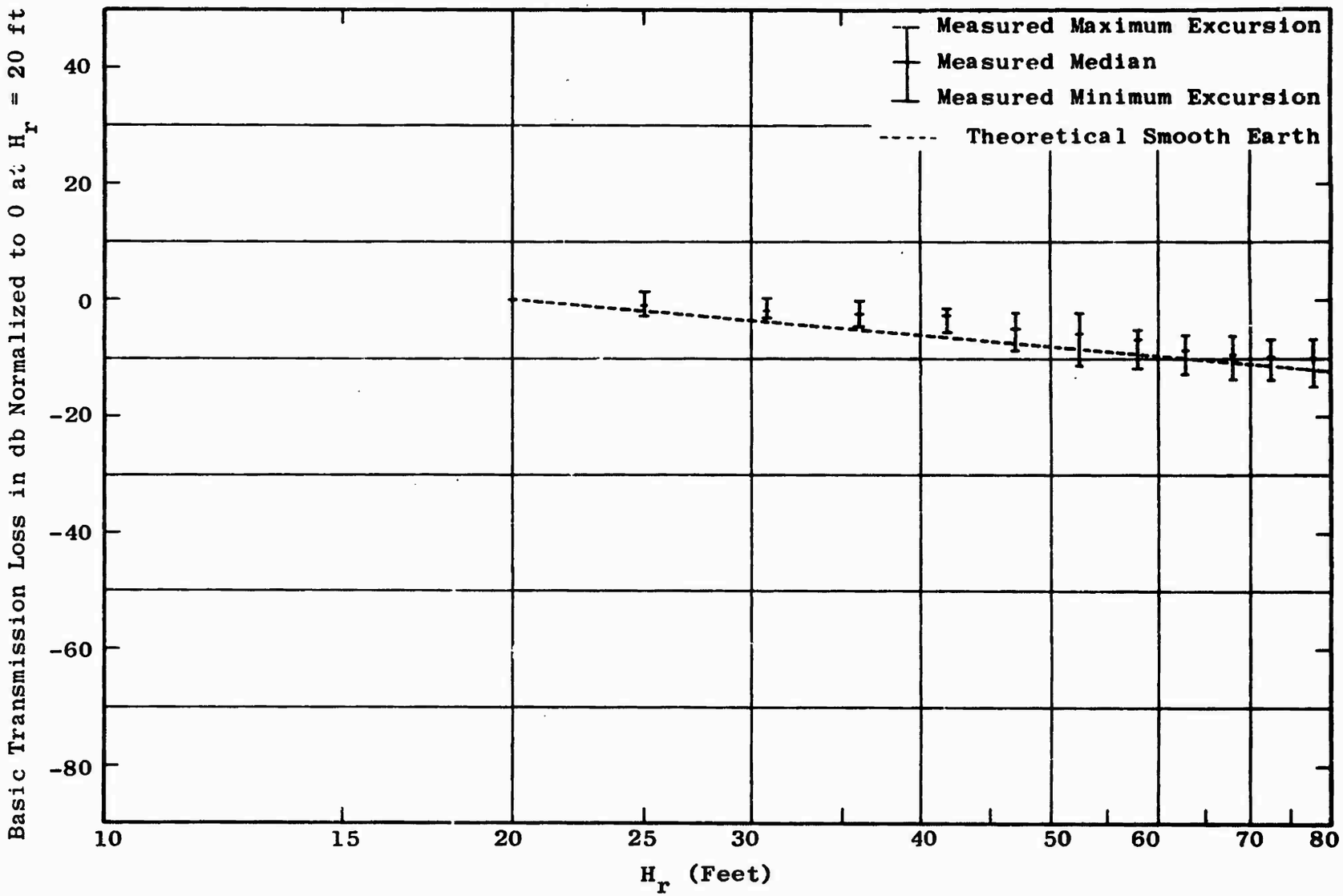

Figure 4.23BB Comparison Between Measured and Theoretical Smooth-Earth Functions
$L_b = F_A(50, 40, V, \geq 2, H_r)$

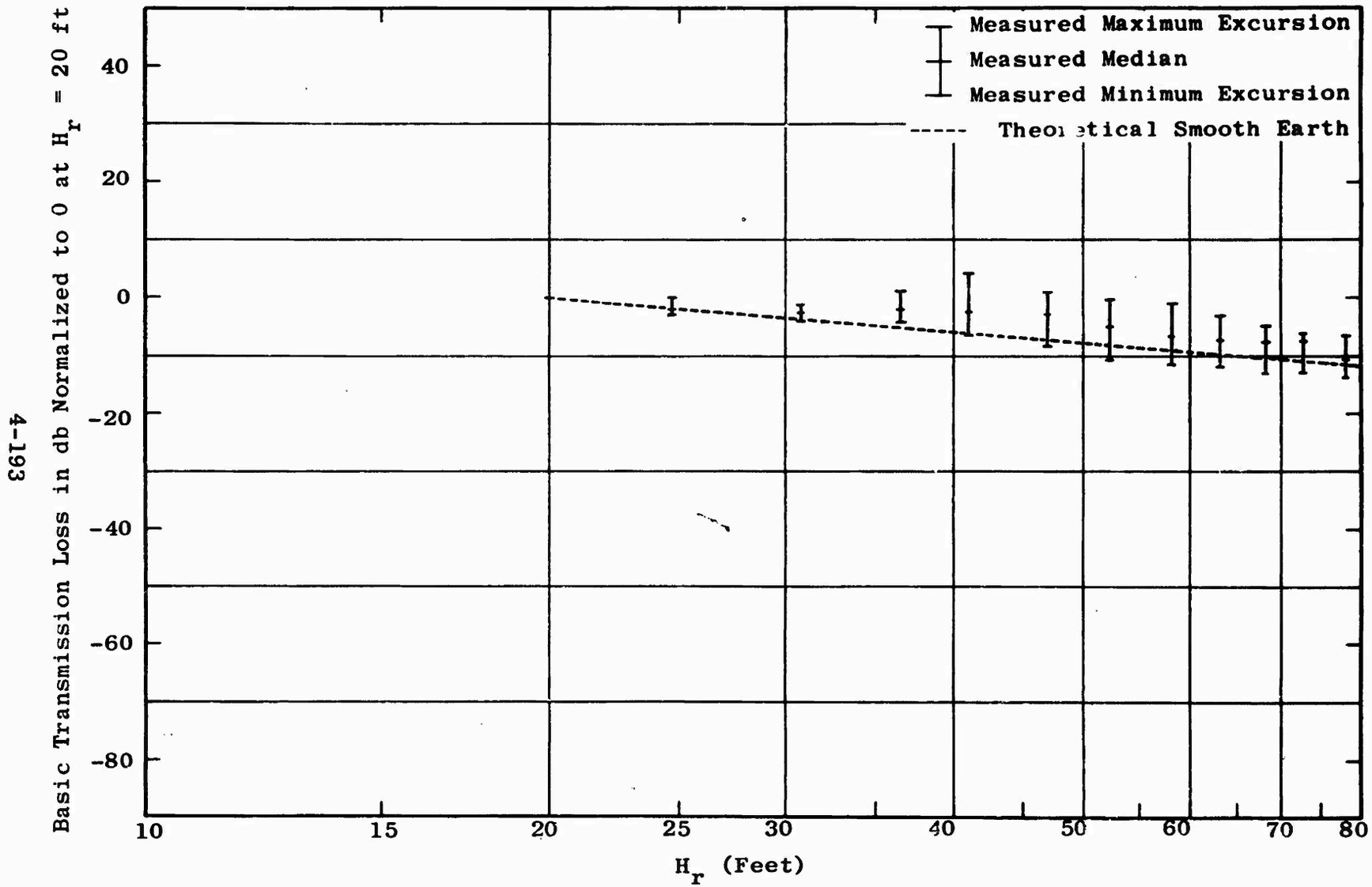

Figure 4.23CC Comparison Between Measured and Theoretical Smooth-Earth Functions
$L_b = F_A(50, 13, V, \geq 2, H_r)$

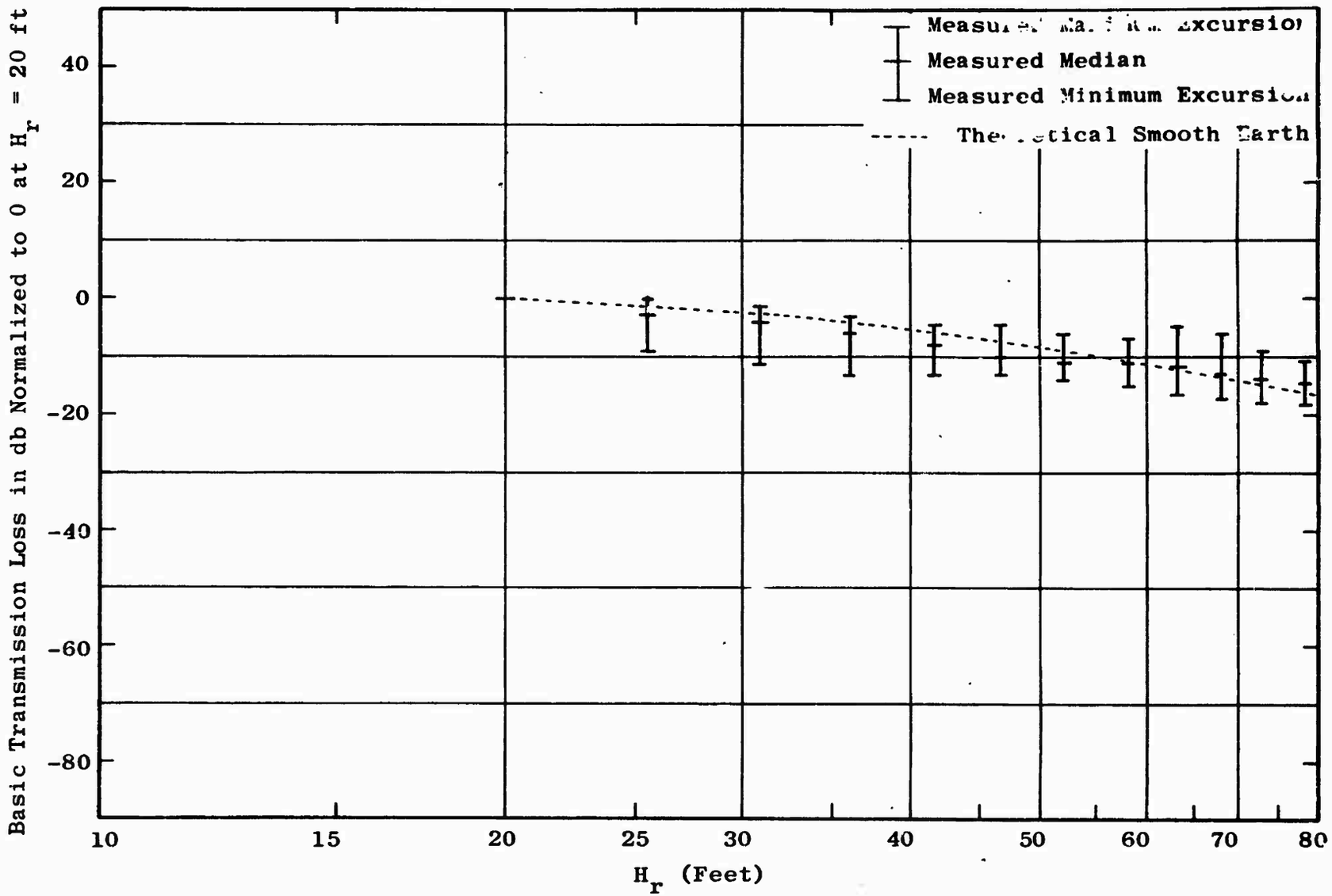

Figure 4.23DD Comparison Between Measured and Theoretical Smooth-Earth Functions
$L_b = F_A(25.5, 80, V, \geq 2, H_r)$

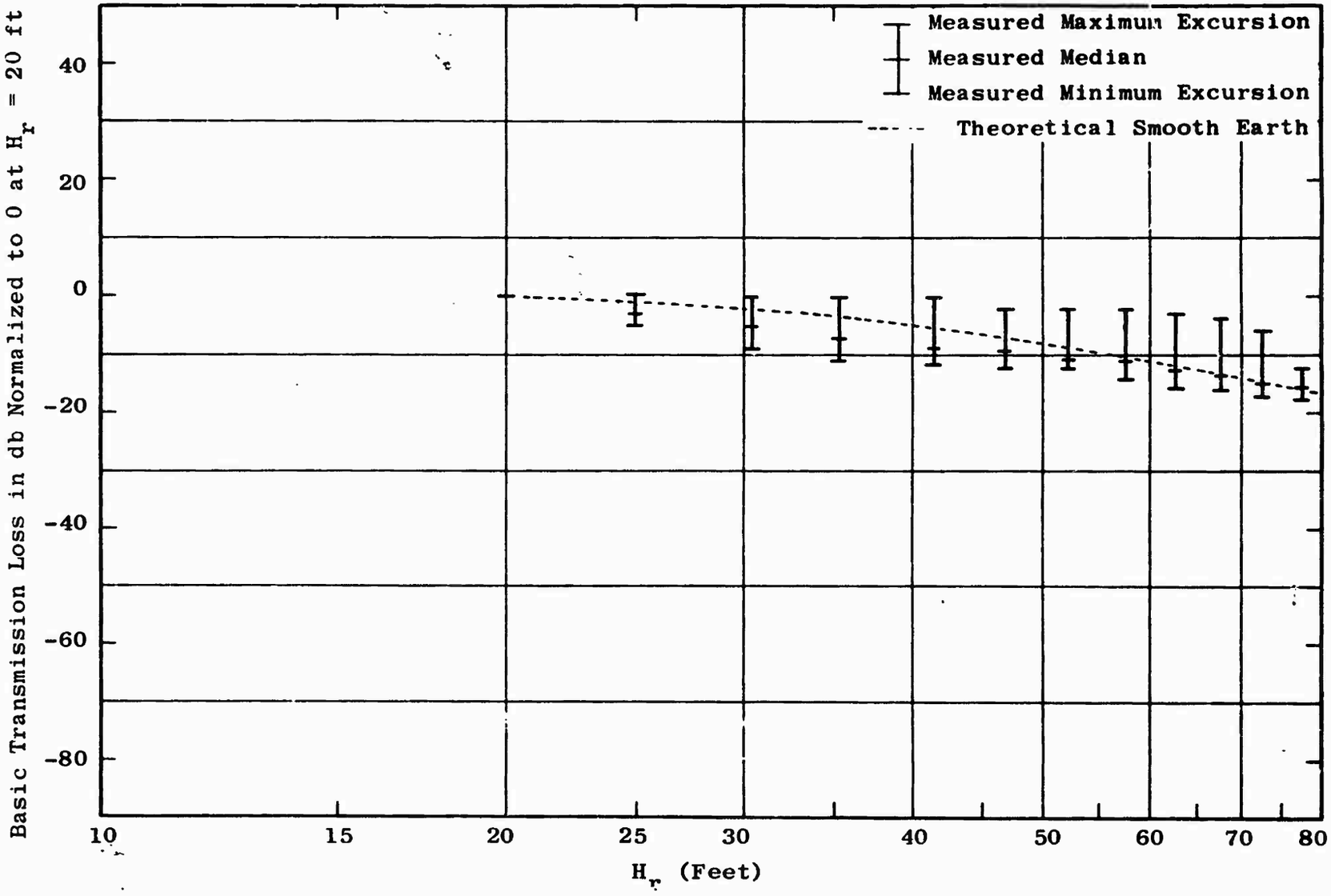

Figure 4.23EE Comparison Between Measured and Theoretical Smooth-Earth Functions
$L_b = F_A(25.5, 40, V, \geq 2, H_r)$

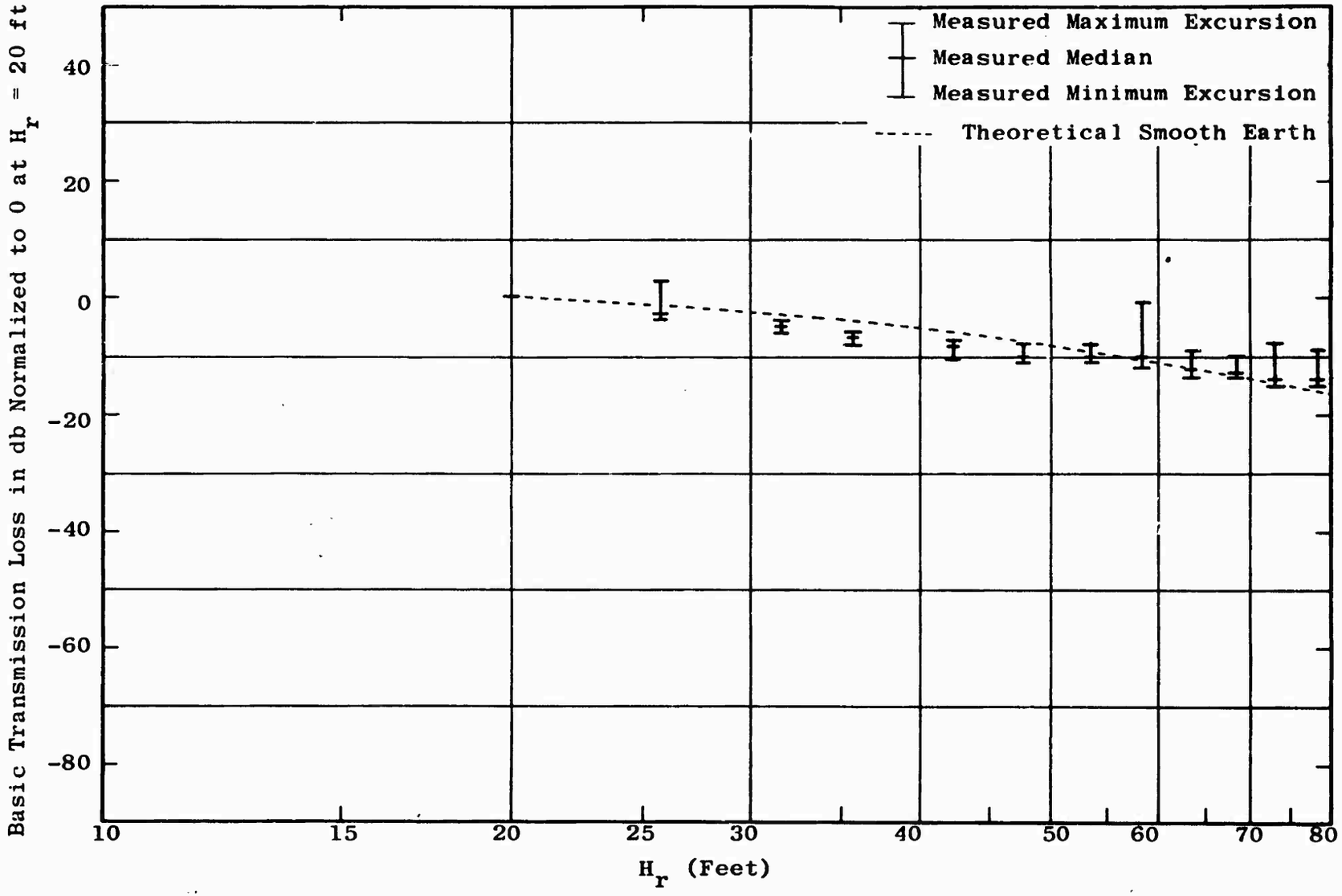

Figure 4.23FF Comparison Between Measured and Theoretical Smooth-Earth Functions
$L_b = F_A(25.5,\ 13,\ V,\ 2,\ H_r)$

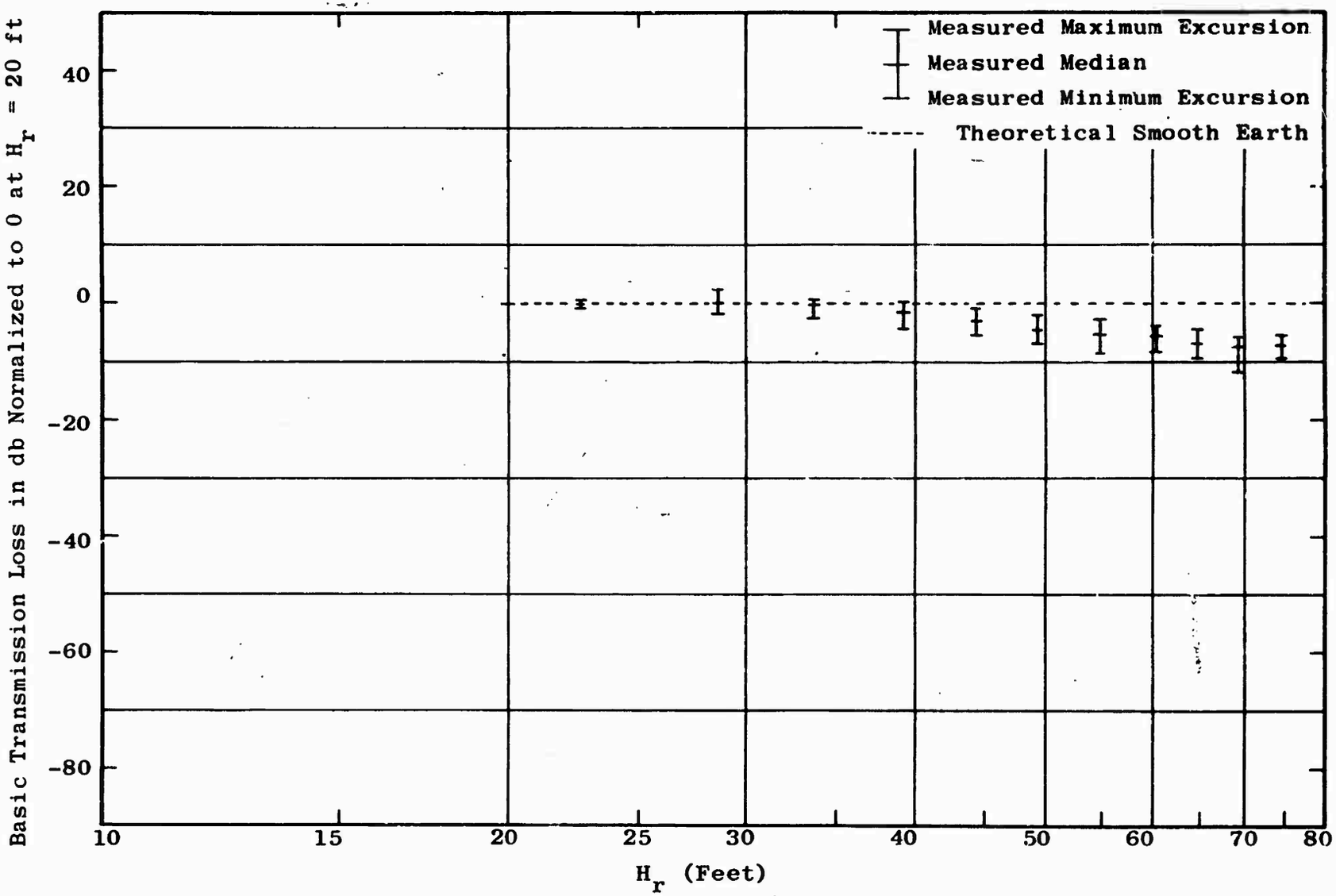

Figure 4.23GG Comparison Between Measured and Theoretical Smooth-Earth Functions
$L_b = F_A(12.0, 21, V, \geq 2, H_r)$

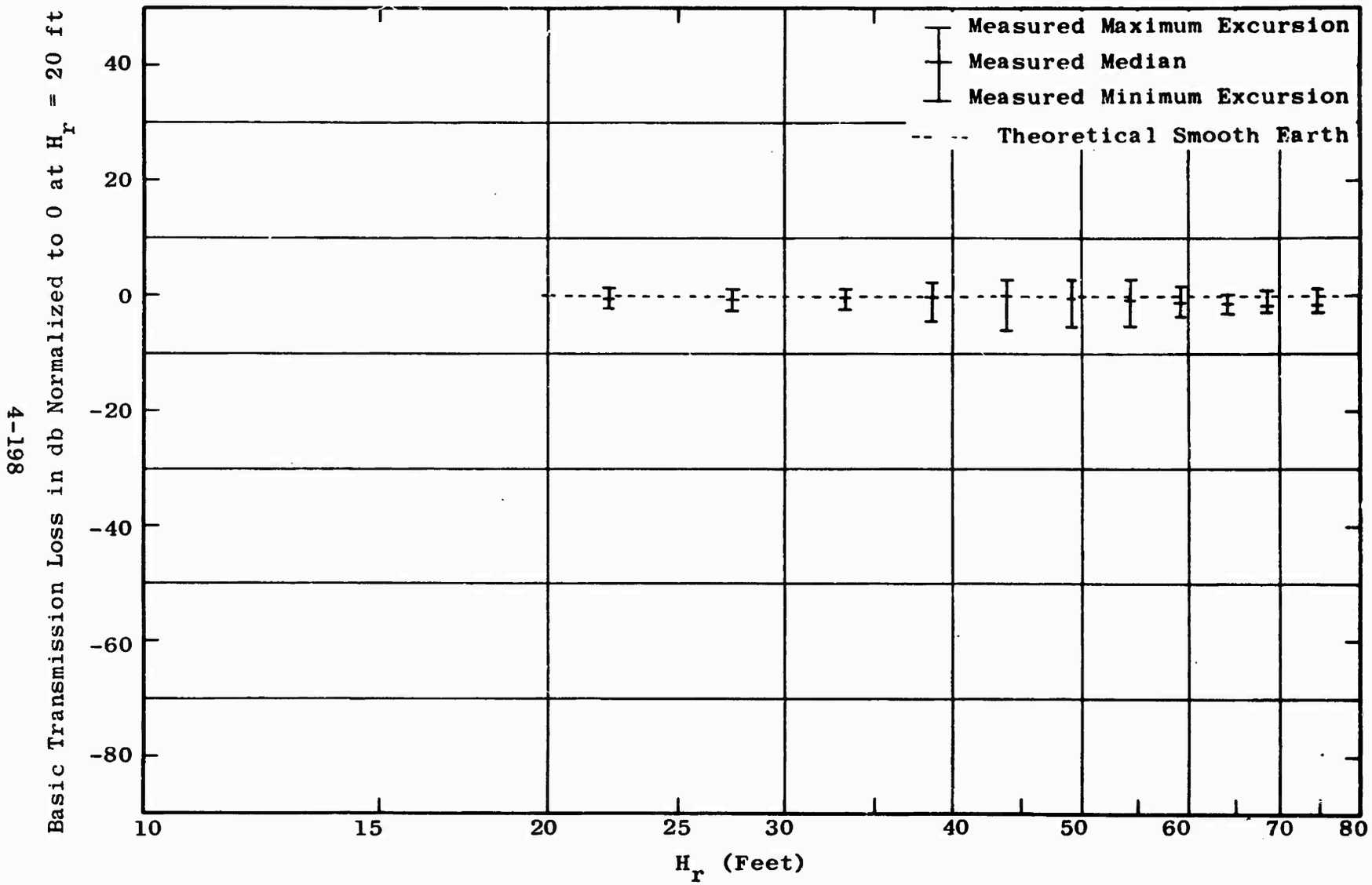

Figure 4.23HH Comparison Between Measured and Theoretical Smooth-Earth Functions
$L_b = F_A(6.0, 40, V, \geq 2, H_r)$

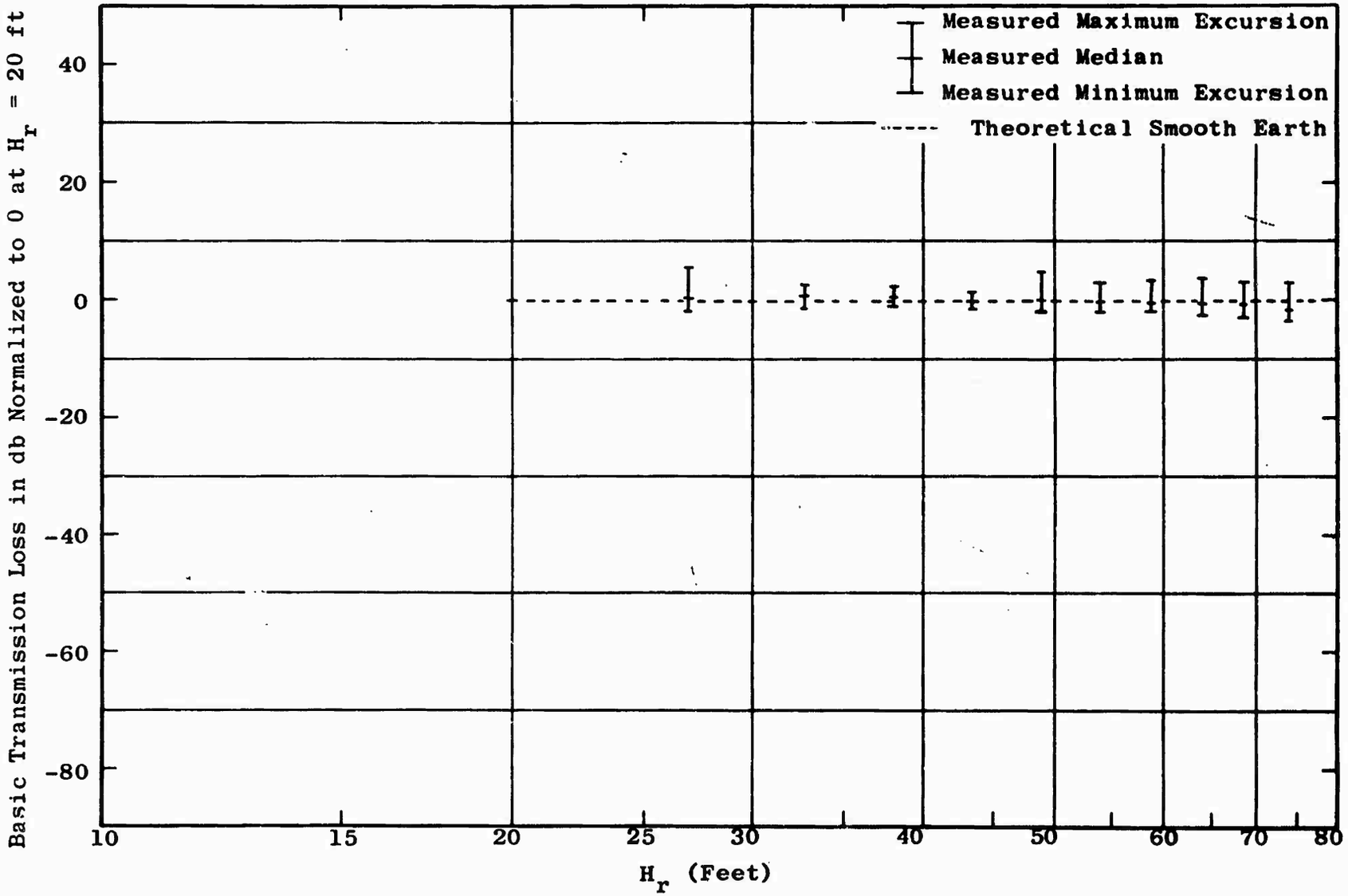

Figure 4.23II Comparison Between Measured and Theoretical Smooth-Earth Functions
$L_b = F_A(2.0, 80, V, \geq 2, H_r)$

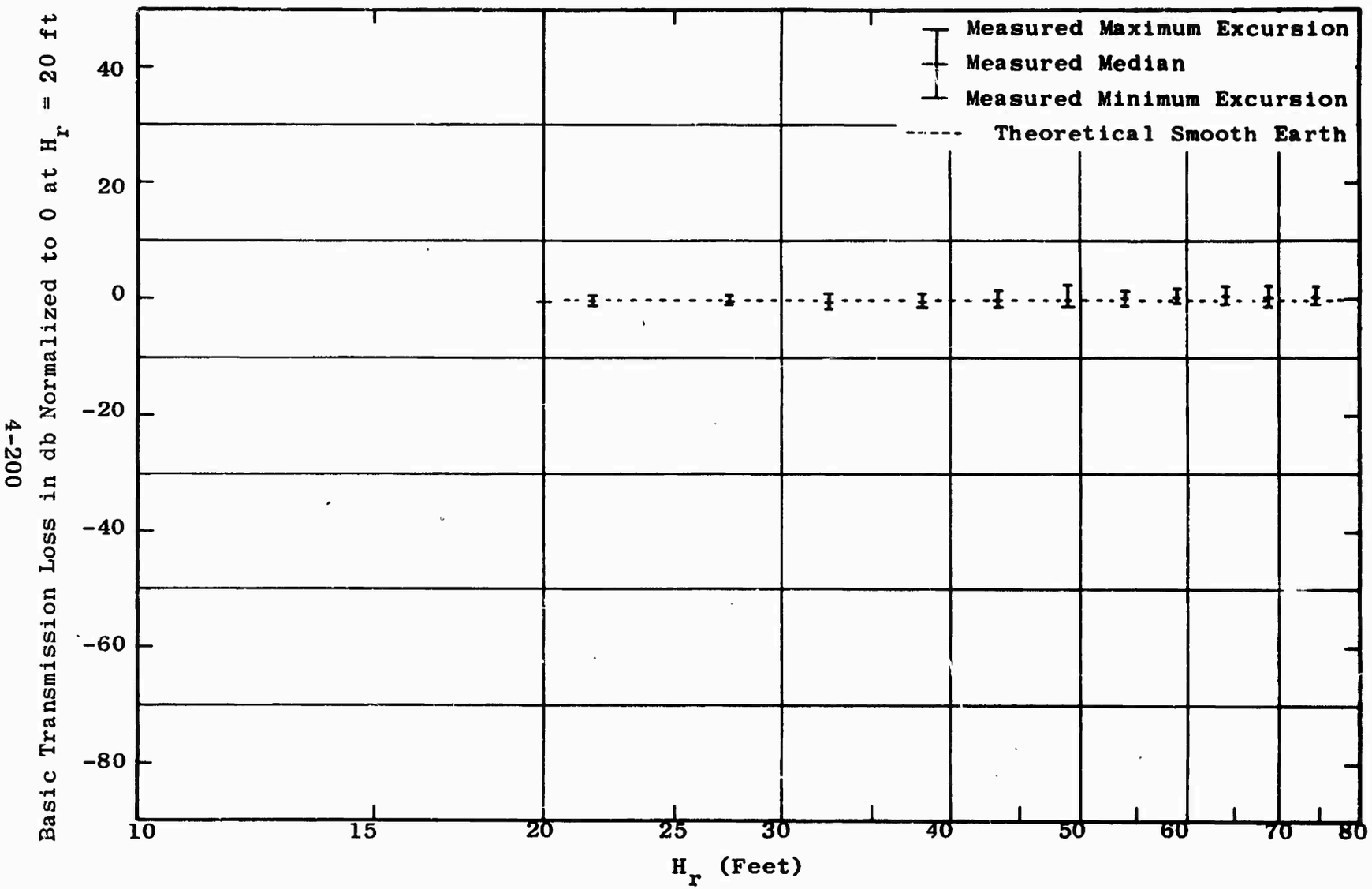

Figure 4.23JJ Comparison Between Measured and Theoretical Smooth-Earth Functions
$L_b = F_A(0.880, 80, V, \geq 2, H_r)$

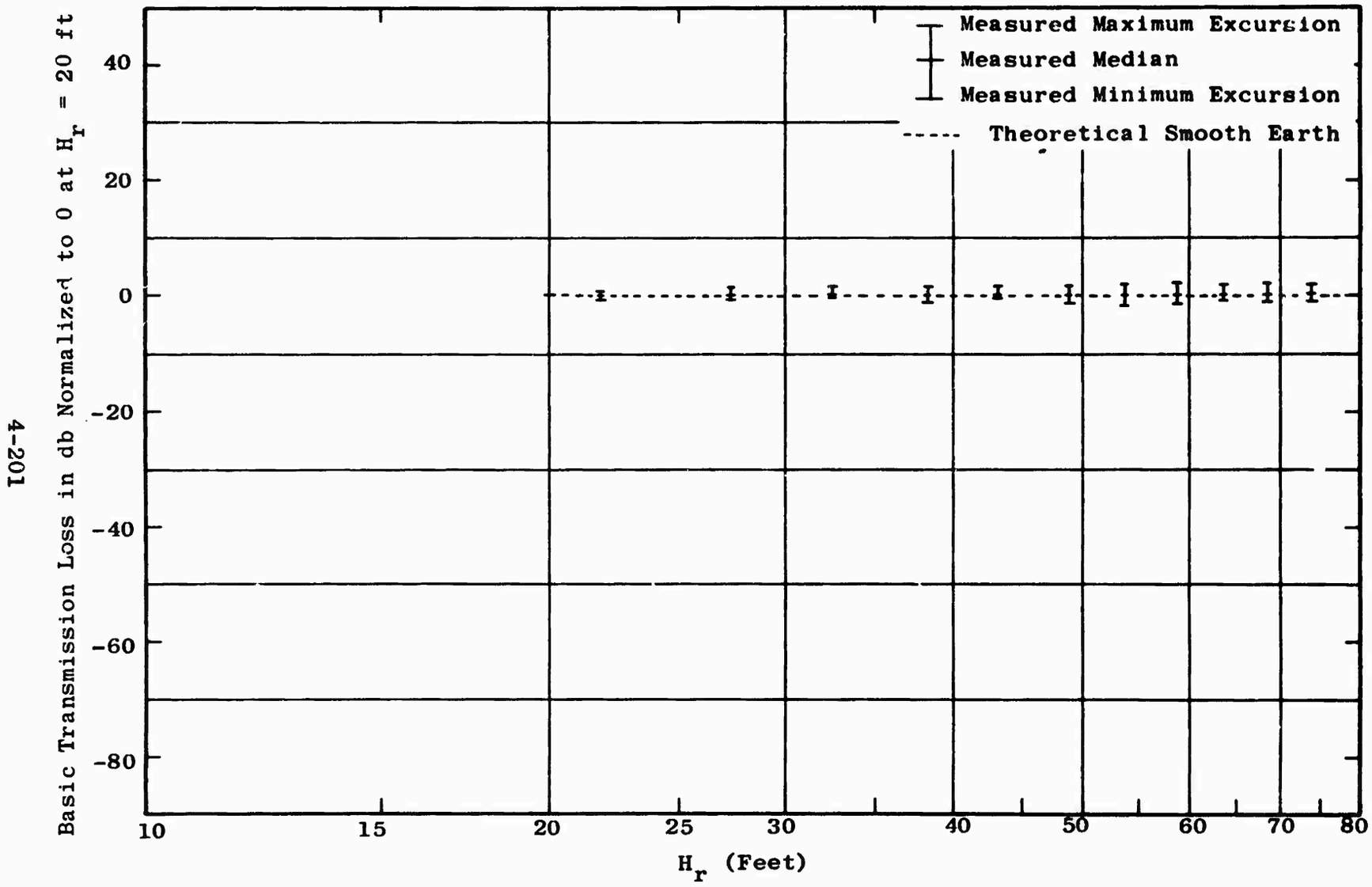

Figure 4.23KK Comparison Between Measured and Theoretical Smooth-Earth Functions
$L_b = F_A(0.300, 80, V, \geq 2, H_r)$

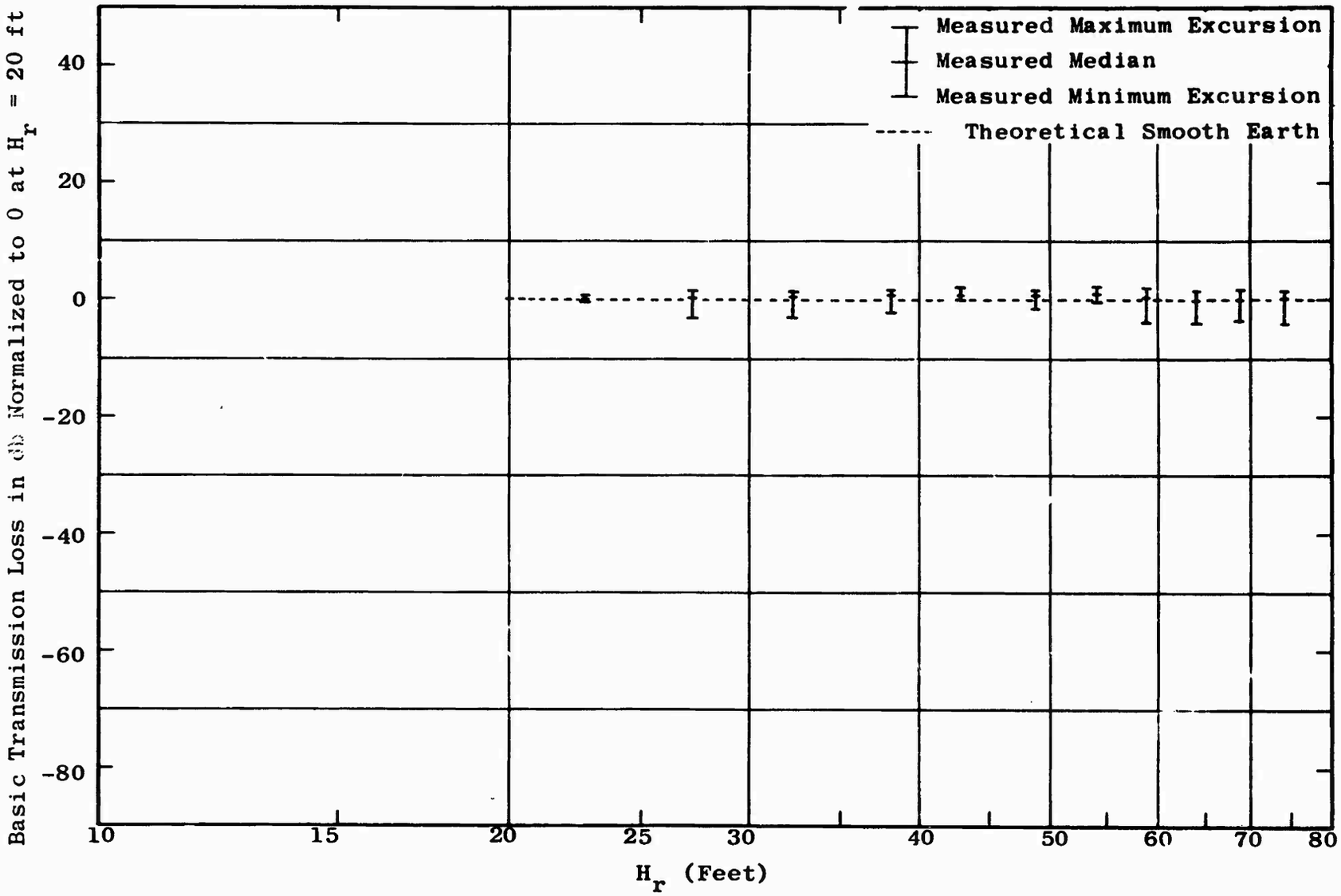

Figure 4.23LL Comparison Between Measured and Theoretical Smooth-Earth Functions
$L_b = F_A(0.105, 80, V, \geq 2, H_r)$

4.3.2.2.3 Comparison of Height Variation with NBS Model

A comparison similar to that made between the measured height variability and the smooth-earth height functions was made between measured height variability and the NBS terrain model described in Section 4.2.2.1.

The NBS method used for this comparison included both $G(\bar{H})$ functions. The results of the comparison appear in Figures 4.24A through 4.24J. The vertical bars represent the measured data in exactly the same way as in Figures 4.23A through 4.23LL. The NBS method was used to compute loss for all distances between 2 and 17 miles and the resulting curves were normalized at a receiving antenna height of 20 feet in the same way as the measured data. The upper solid curve on Figures 4.24A through 4.24J represents the theoretical maximum over all distances between 2 and 17 miles for the frequency, polarization and transmitting antenna height mentioned on each figure. The middle solid curve represents the median of all theoretically calculated curves and the lower solid curve represents the theoretical minimum.

Figures 4.24A through 4.24E show relatively good correlation for horizontal polarization. Figures 4.24F through 4.24J show equally good correlation for vertical polarization.

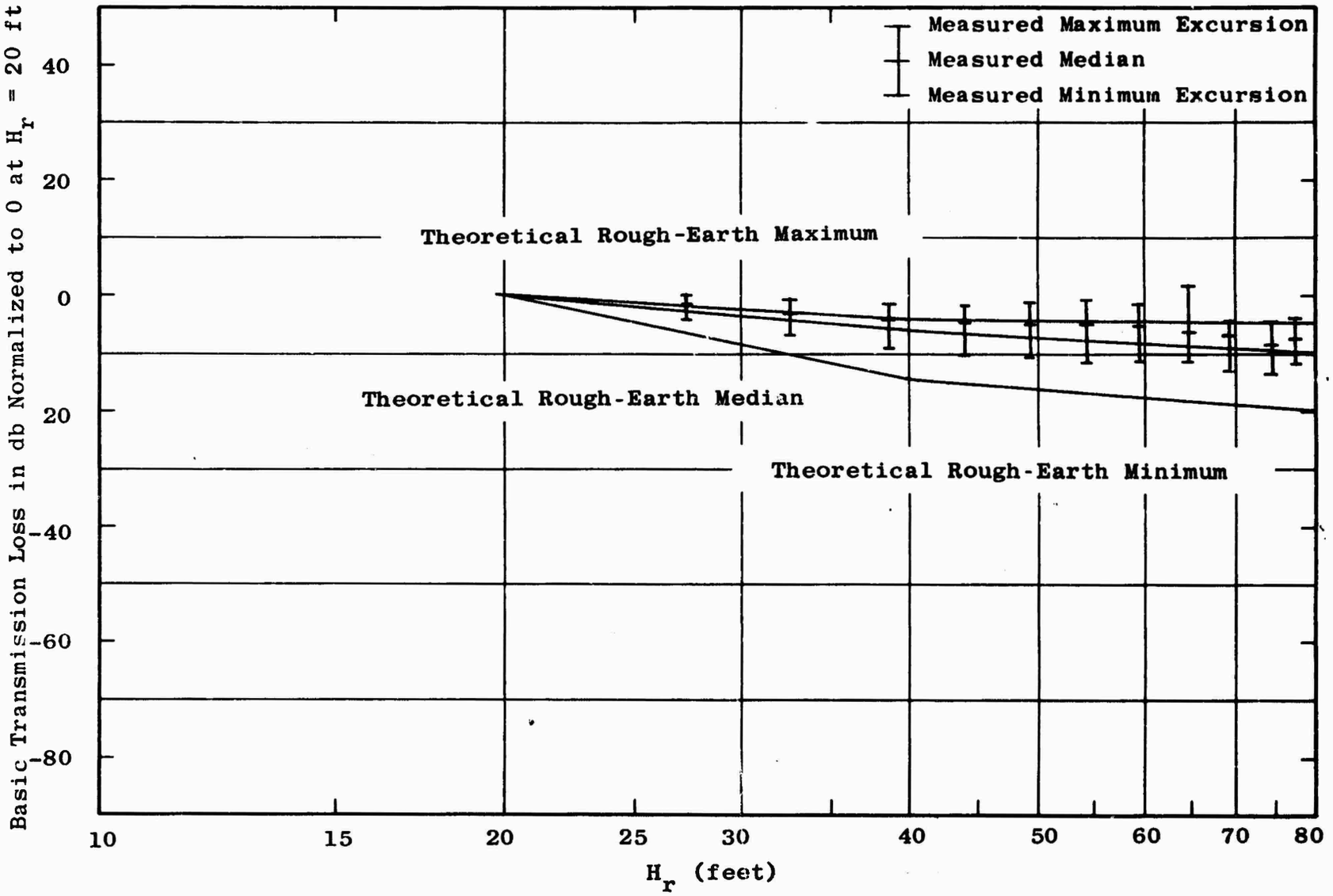

Figure 4.24A Comparison Between Measured and Theoretical Rough-Earth Height Functions
$L_b = F_A(25.5, 80, H, d, H_r)$

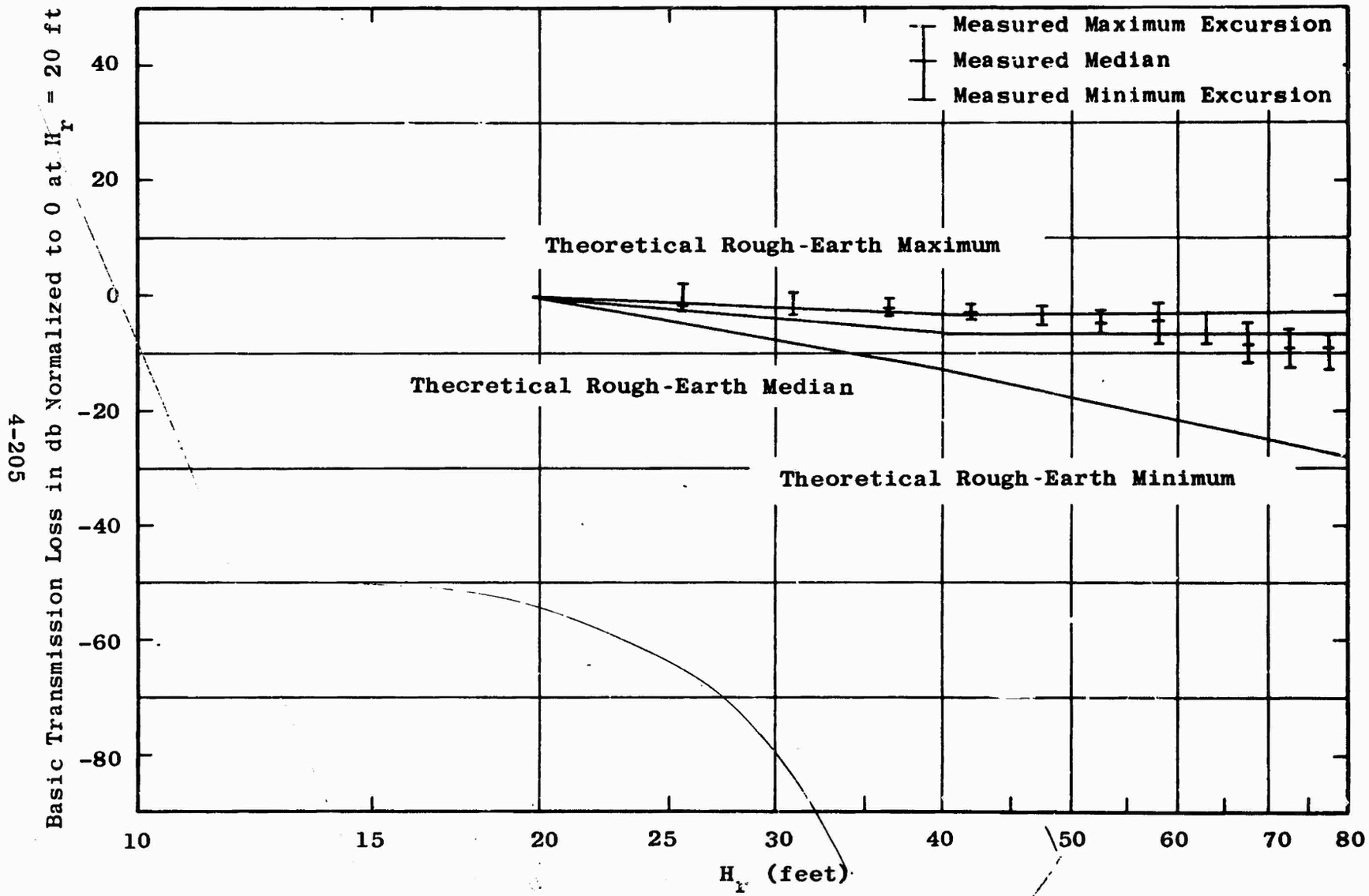

Figure 4.24B Comparison Between Measured and Theoretical Rough-Earth Height Functions
$L_b = F_A(50, 80, H, d, H_r)$

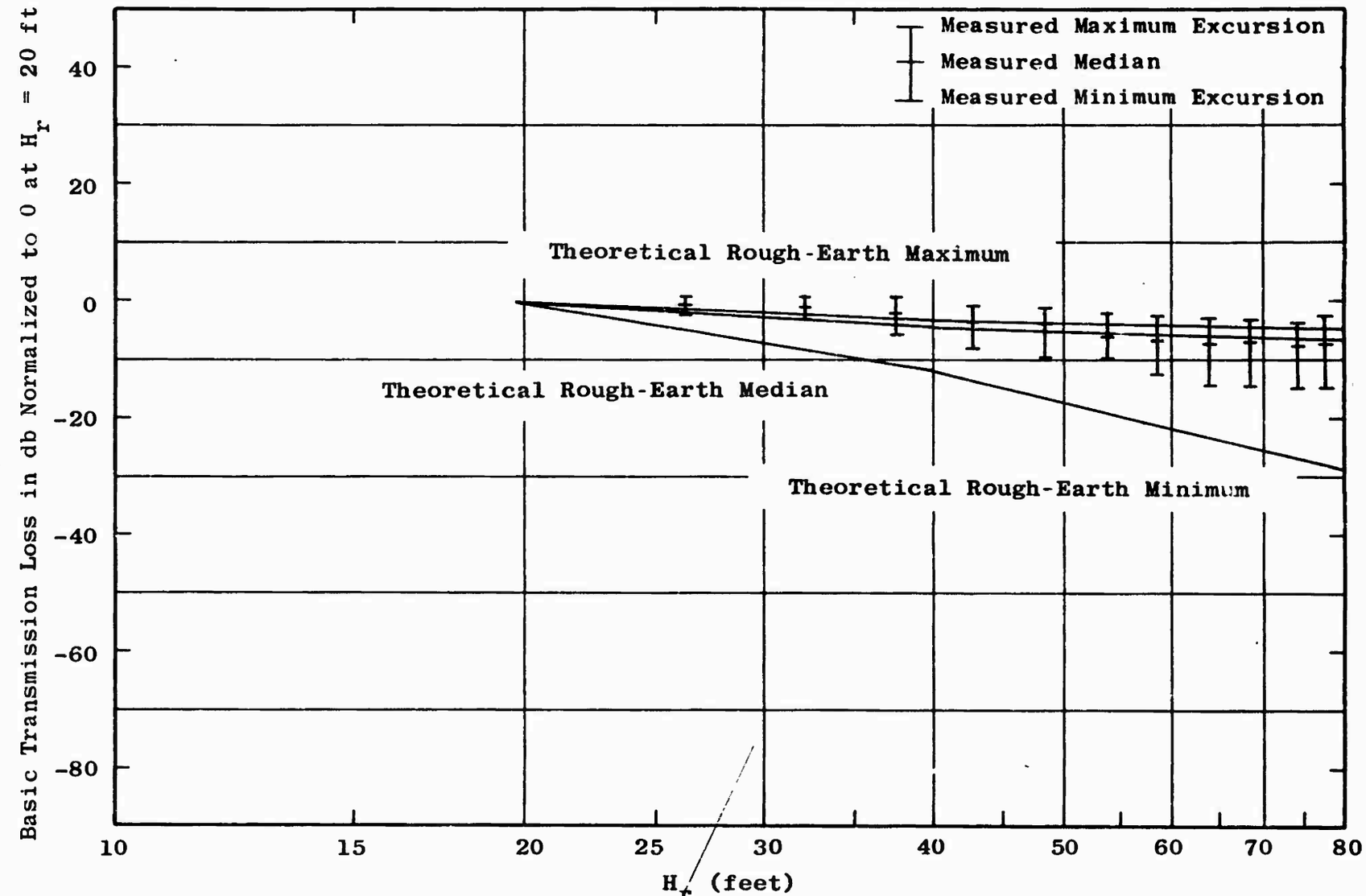

Figure 4.24C Comparison Between Measured and Theoretical Rough-Earth Height Functions
$L_b = F_A(100, 80, H, d, H_r)$

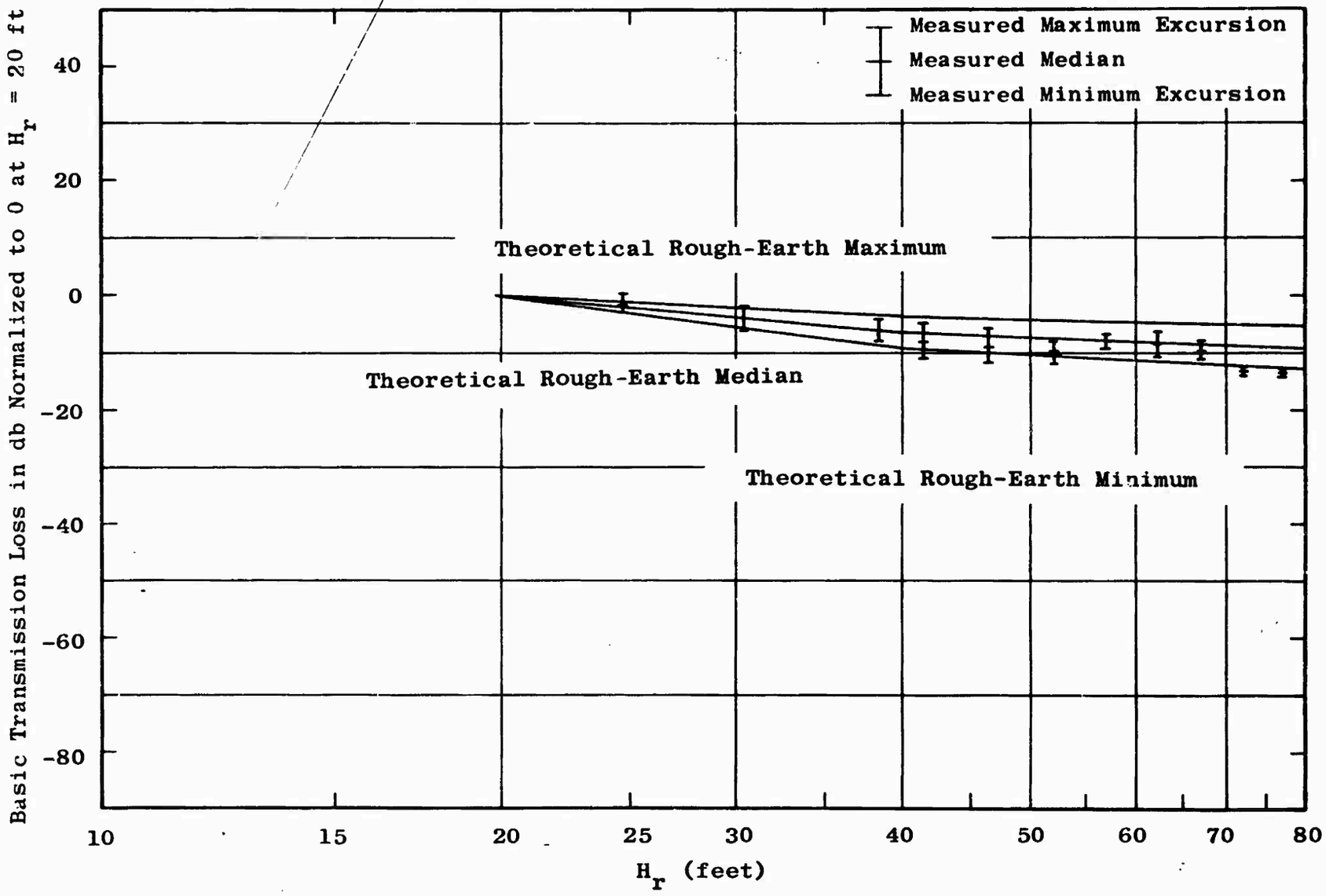

Figure 4.24D Comparison Between Measured and Theoretical Rough-Earth Height Functions
$L_b = F_A(250, 80, H, d, H_r)$

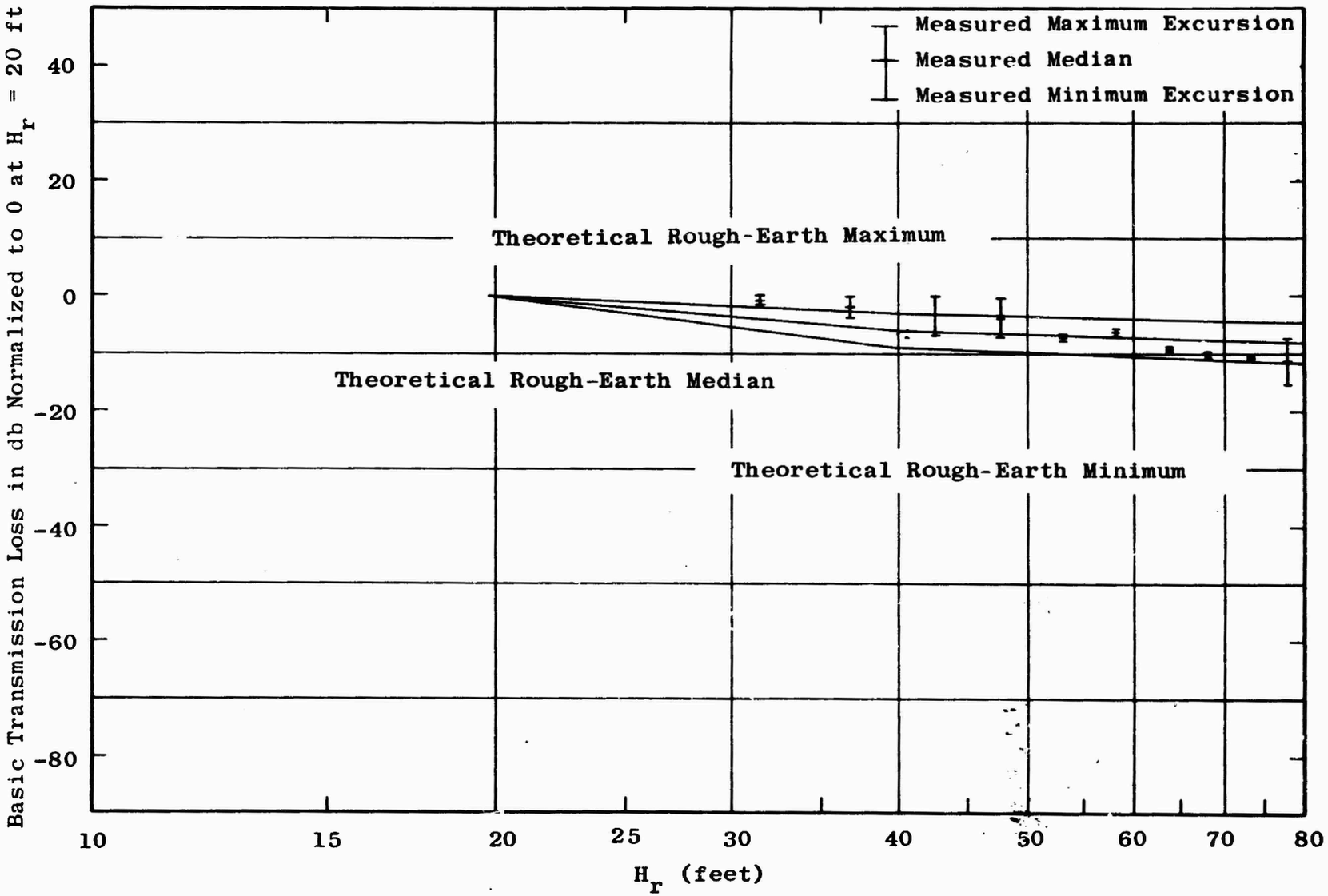

Figure 4.24E Comparison Between Measured and Theoretical Rough-Earth Height Functions
$L_b = F_A(400, 80, H, d, H_r)$

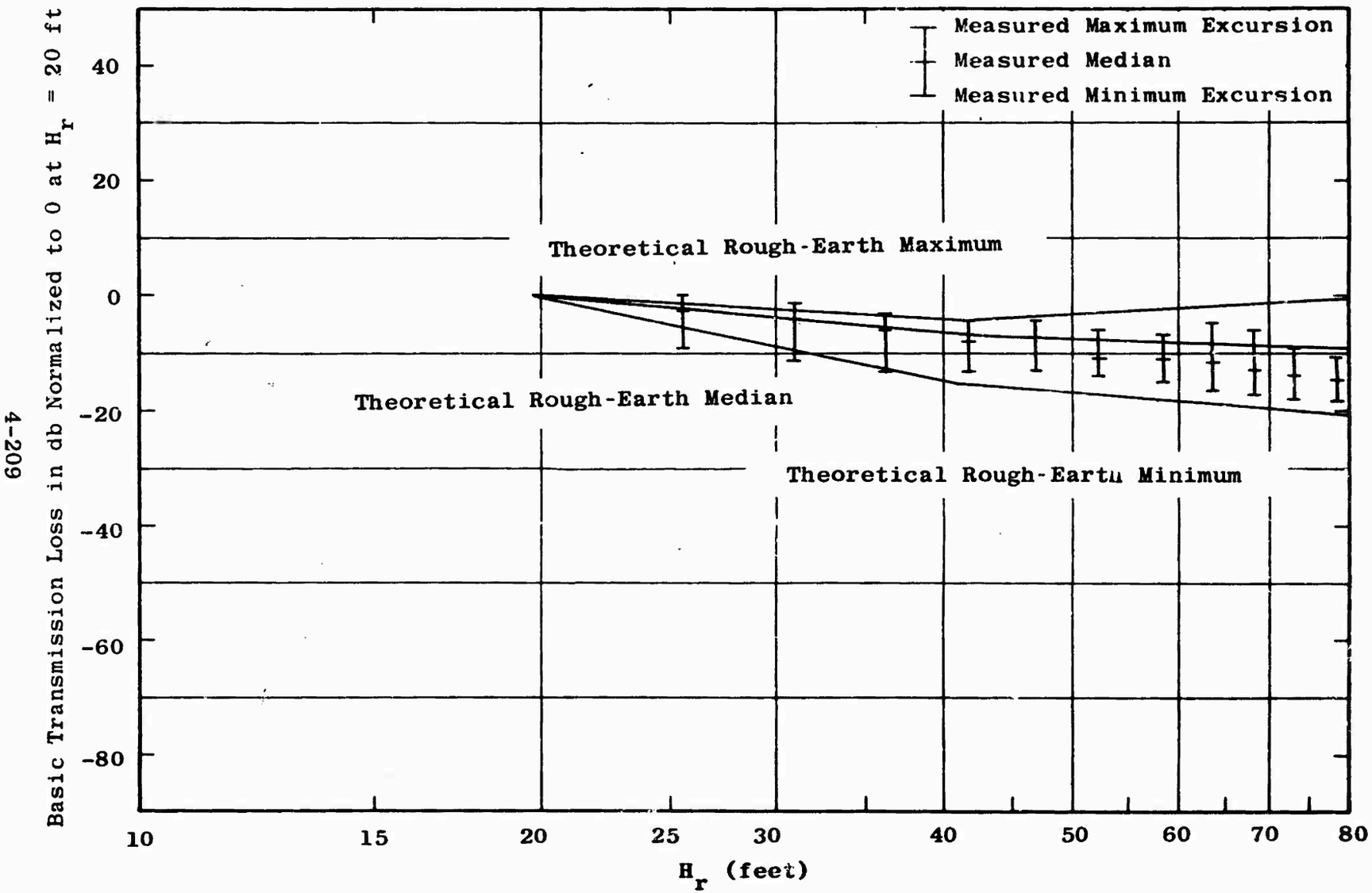

Figure 4.24F Comparison Between Measured and Theoretical Rough-Earth Height Functions
$L_b = F_A(25.5, 80, V, d, H_r)$

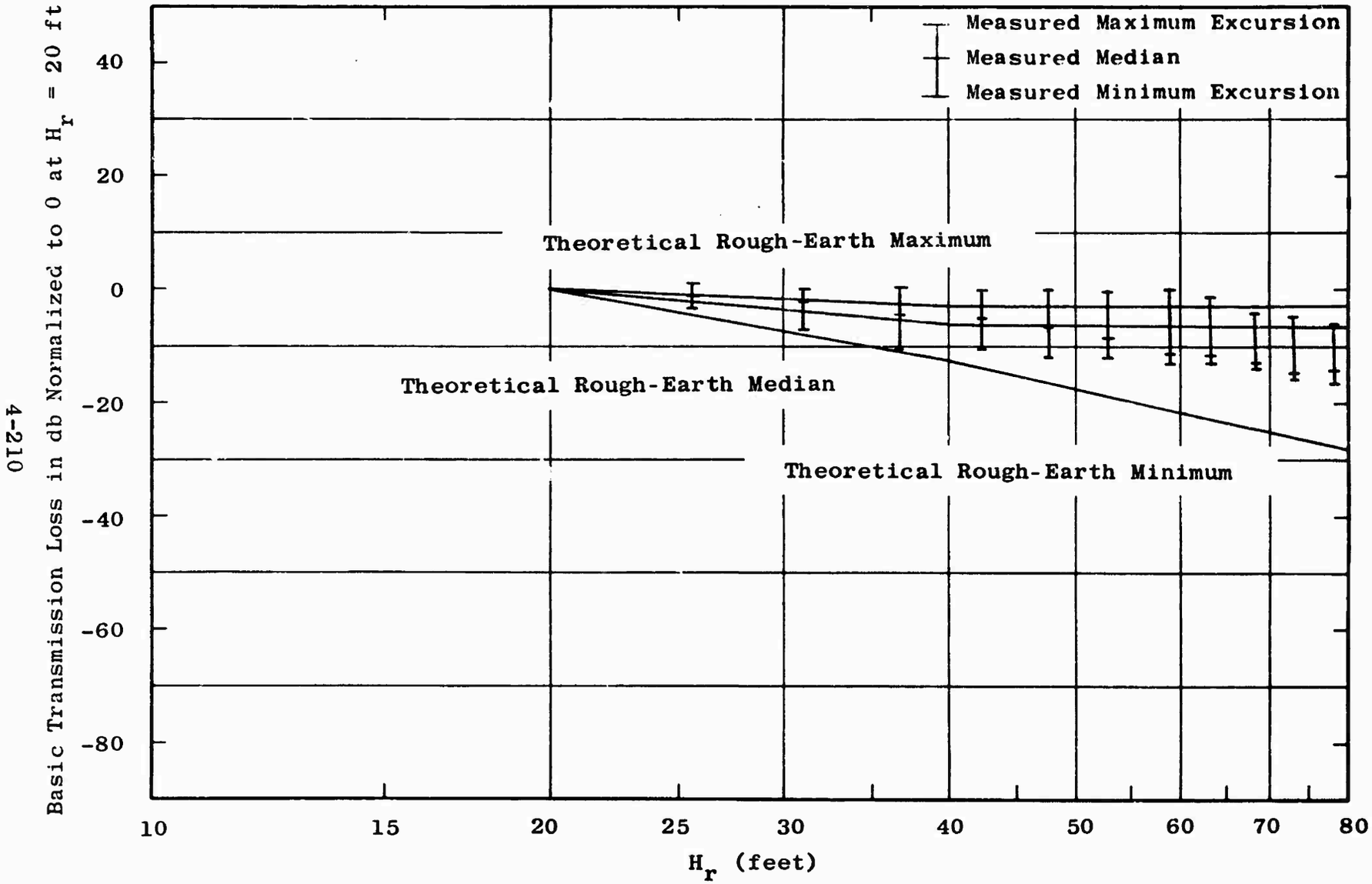

Figure 4.24G Comparison Between Measured and Theoretical Rough-Earth Height Functions
$L_b = F_A(50, 80, V, d, H_r)$

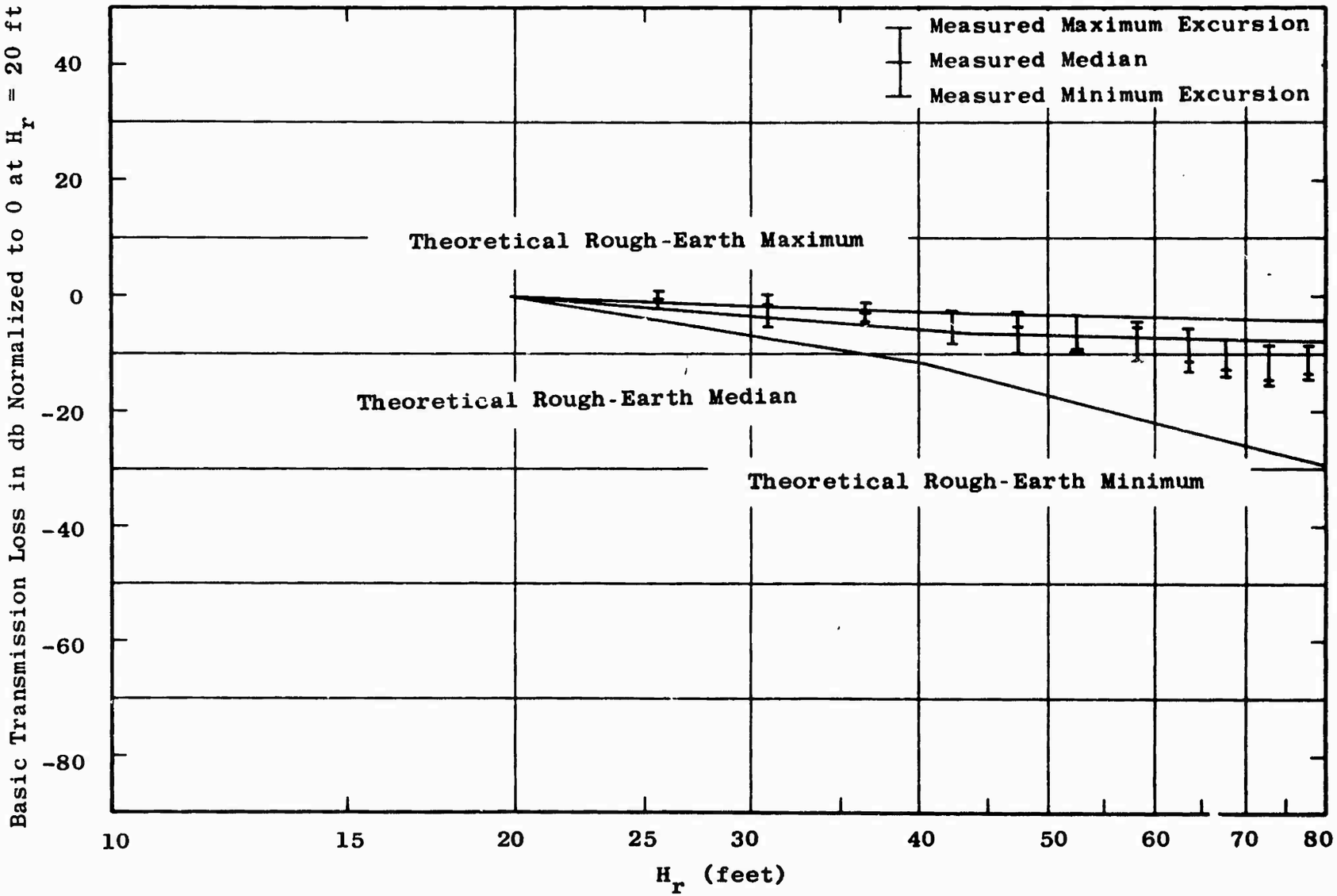

Figure 4.24H Comparison Between Measured and Theoretical Rough-Earth Height Functions
$L_b = F_A(100, 80, V, d, H_r)$

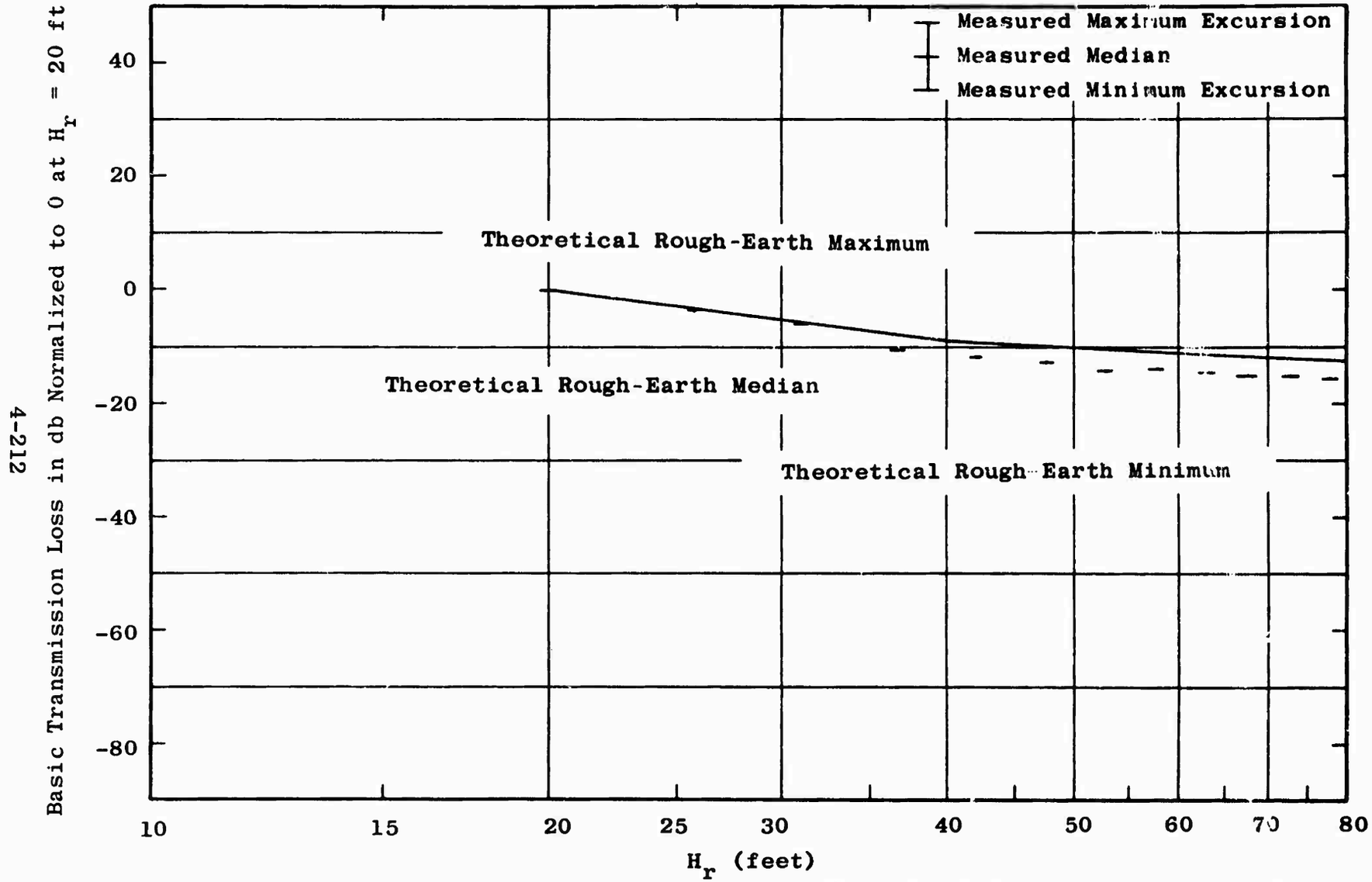

Figure 4.24I Comparison Between Measured and Theoretical Rough-Earth Height Functions
$L_b = F_A(250, 80, V, d, H_r)$

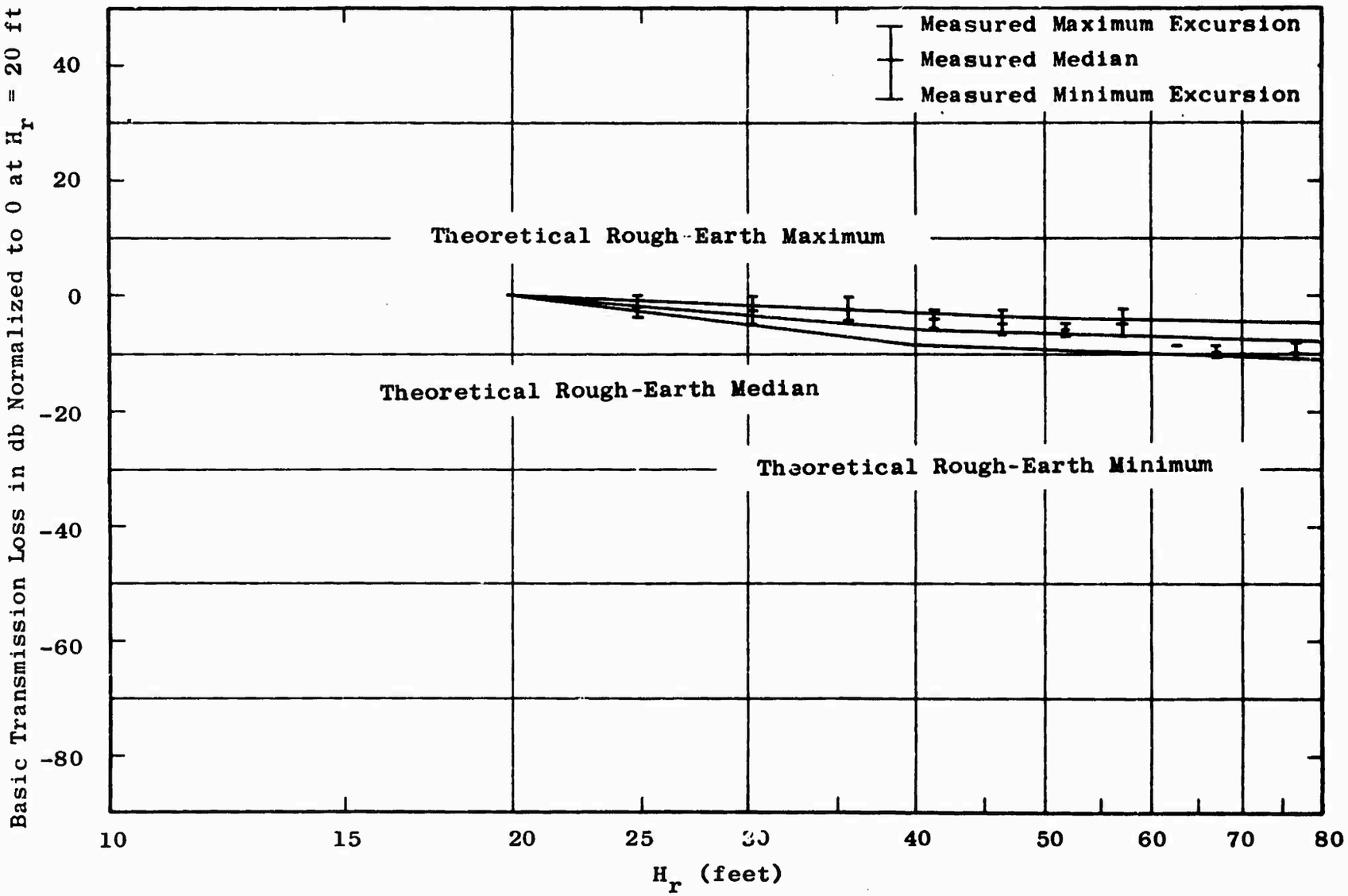

Figure 4.24J Comparison Between Measured and Theoretical Rough-Earth Height Functions
$L_b = F_A(400, 80, V, d, H_r)$

4.3.2.2.4 Comparison of Height Variations for d < 2 Miles and d ≥ 2 Miles

Since there is a distinct difference in path geometry for distances less than 2 miles and distances greater than 2 miles, it is of interest to compare measured height functions in these two categories. Figures 4.25A through 4.25CC provide this comparison. The vertical bars represent the range of measured data for distances of less than 2 miles while the solid curves represent the range and median value for measured data at distances of 2 miles or more.

Figures 4.25A through 4.25N show that, in general, the height function is the same in both regions for horizontal polarization. However, Figures 4.25O through 4.25CC show that for vertical polarization the propagation loss generally tends to decrease less rapidly with height for distances greater than 2 miles than for distances of less than 2 miles.

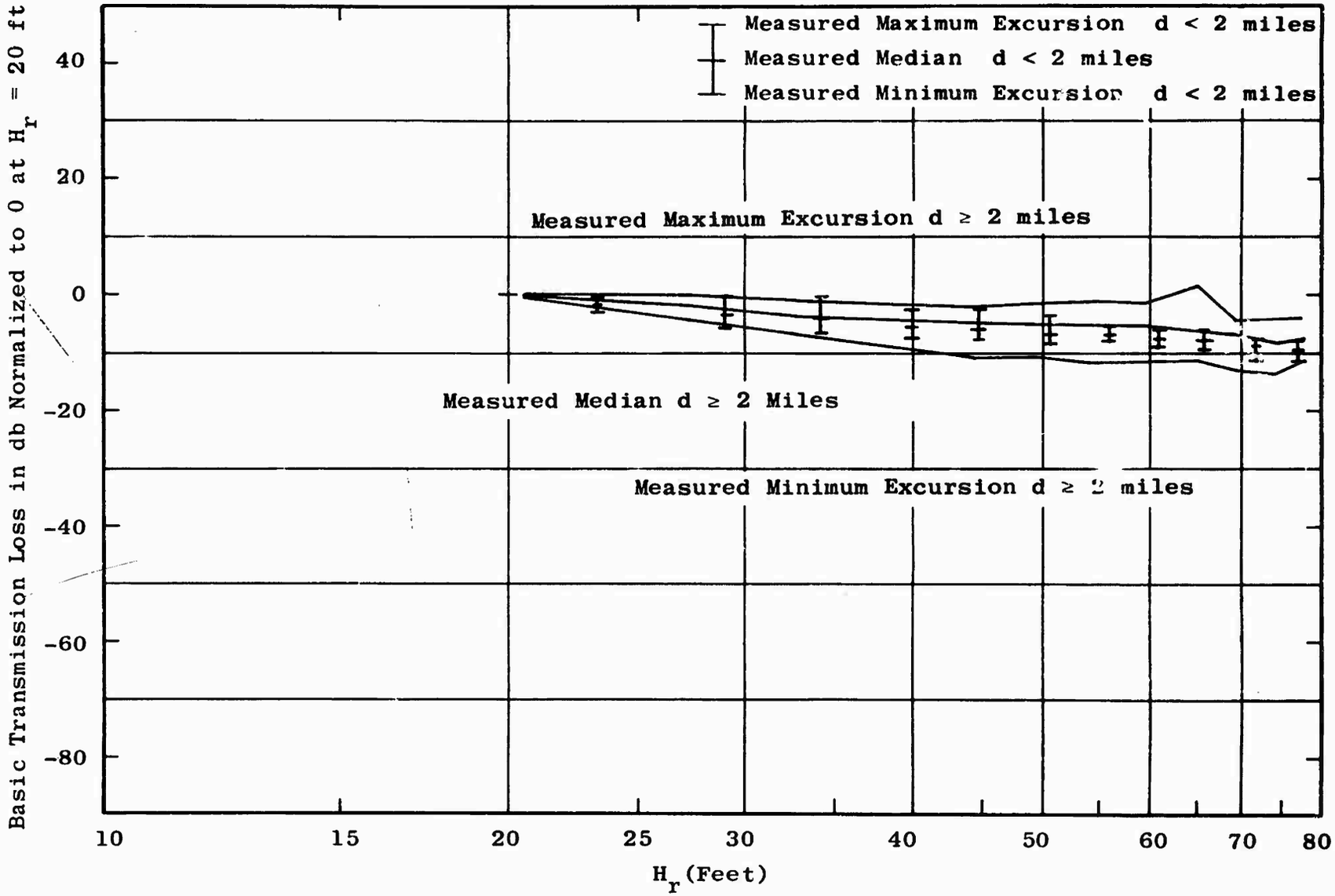

Figure 4.25A Comparison Between Measured Height Functions for d < 2 Miles and d ≥ 2 Miles
$L_b = F_A(25.5, 80, H, d, H_r)$

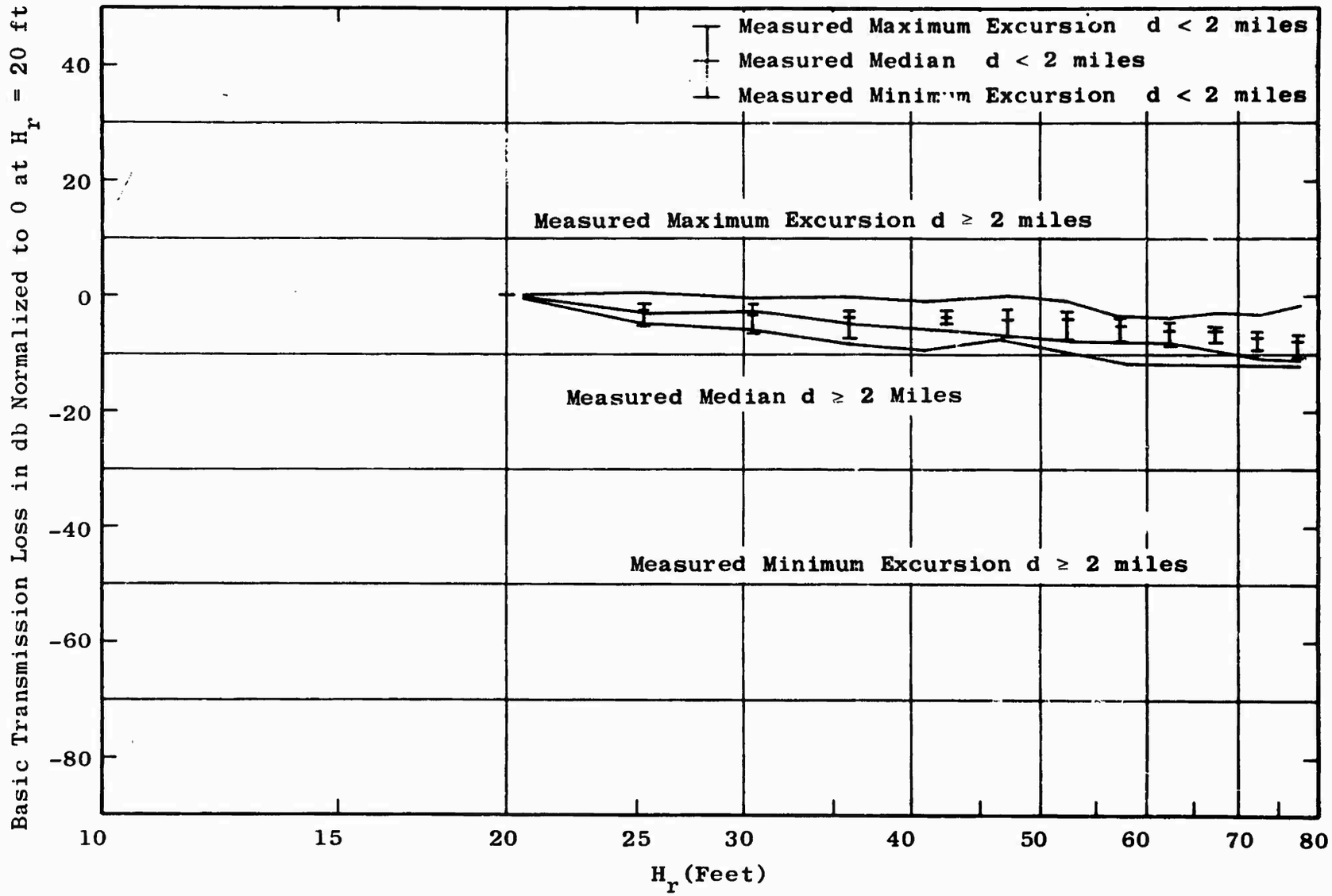

Figure 4.25B Comparison Between Measured Height Functions for d < 2 Miles and d ≥ 2 Miles
$L_b = F_A(25.5, 40, H, d, H_r)$

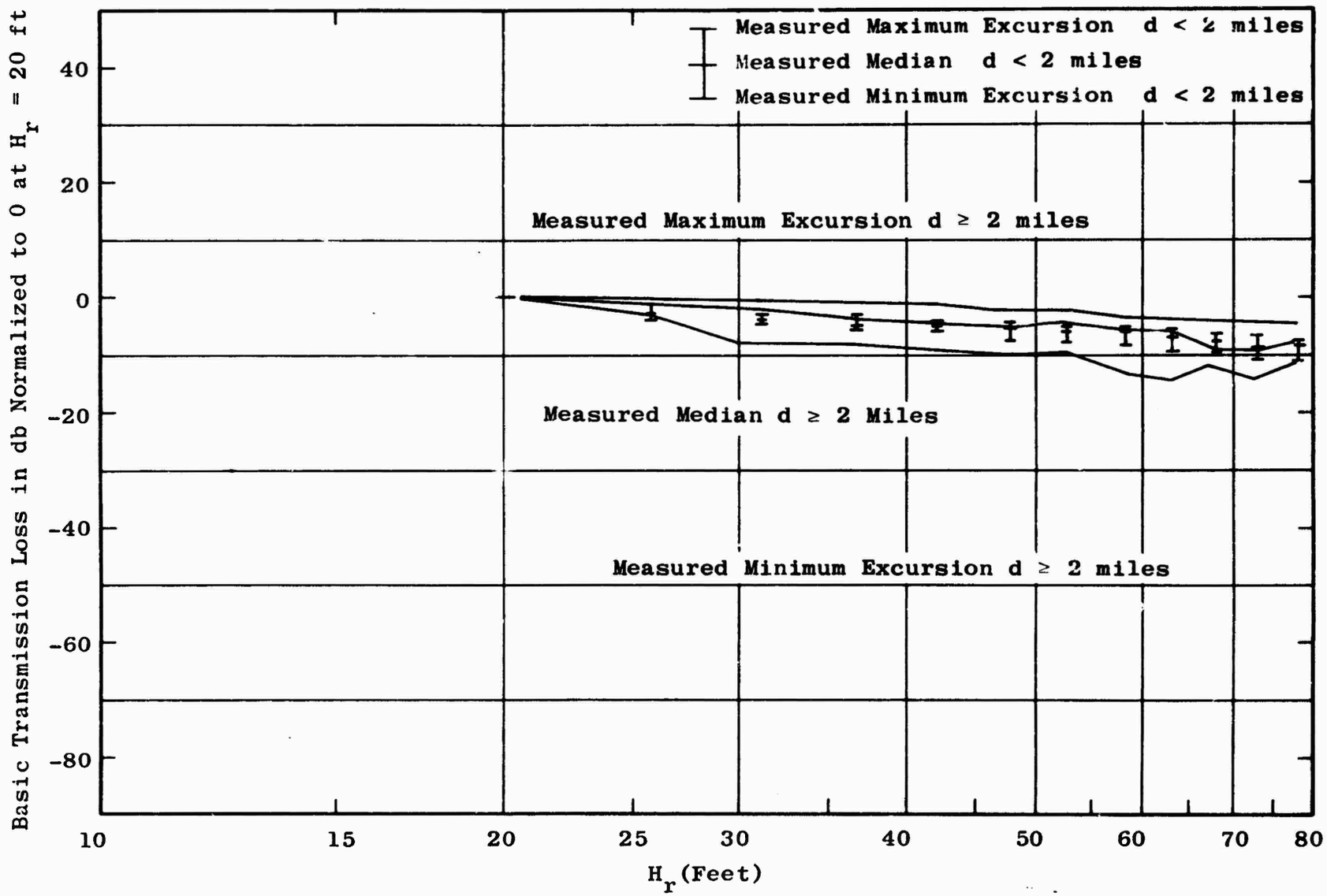

Figure 4.25C Comparison Between Measured Height Functions for d < 2 Miles and d ≥ 2 Miles
$L_b = F_A(25.5, 13, H, d, h_r)$

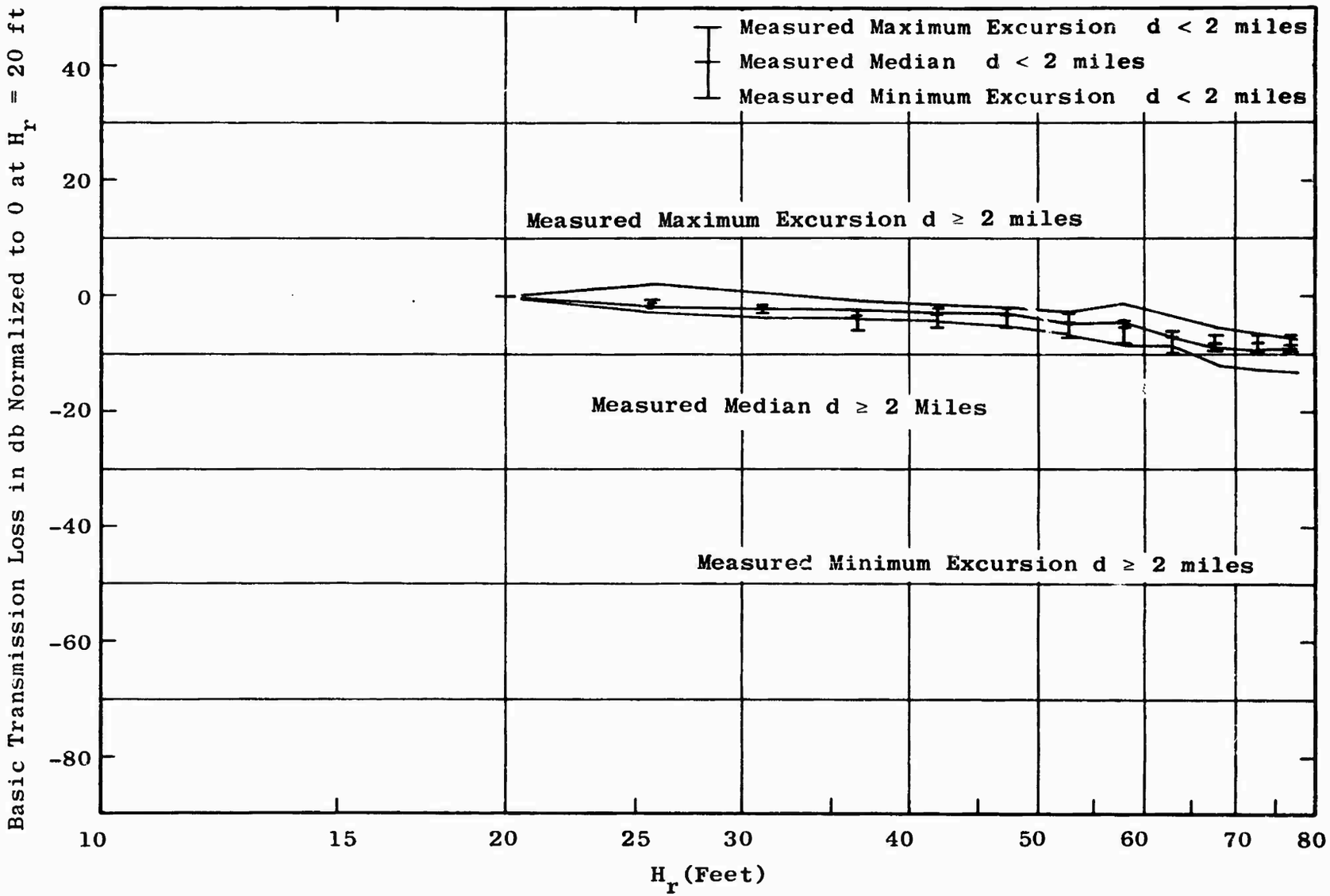

Figure 4.25D Comparison Between Measured Height Functions for d < 2 Miles and d ≥ 2 Miles
$L_b = F_A(50.0, 80, H, d, H_r)$

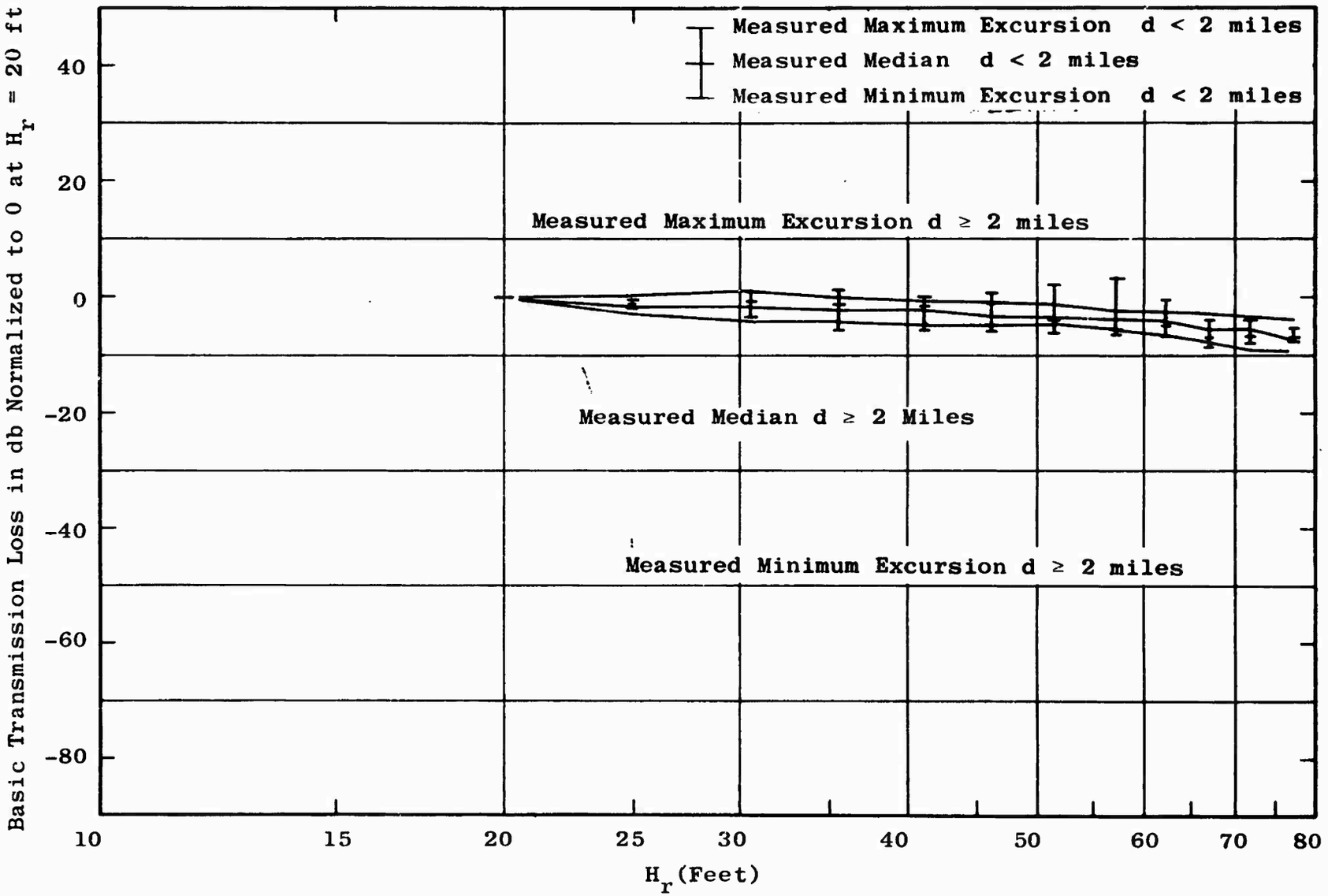

Figure 4.25E Comparison Between Measured Height Functions for d < 2 Miles and d ≥ 2 Miles
$L_b = F_A(50.0, 40, H, d, H_r)$

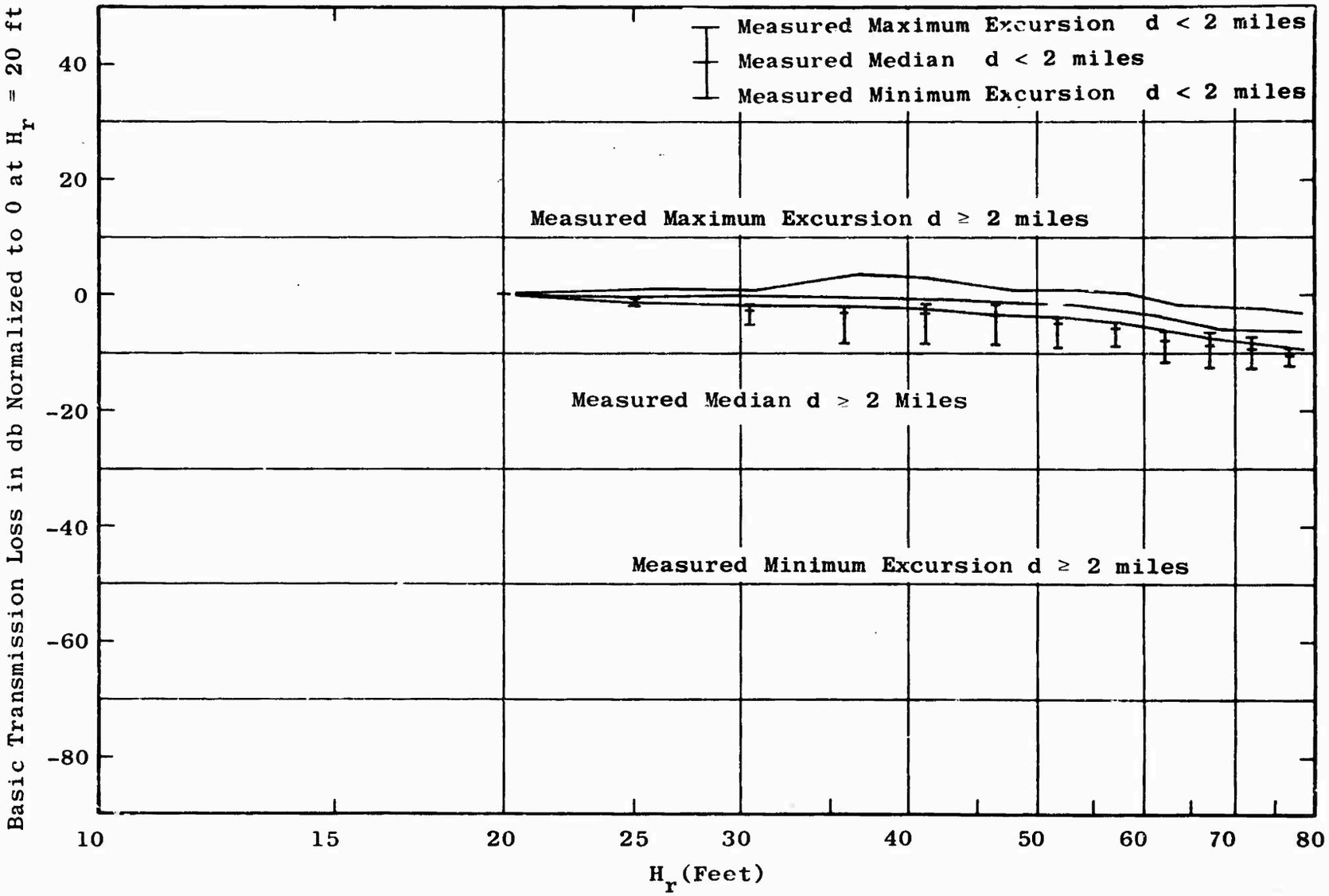

Figure 4.25F Comparison Between Measured Height Functions for d < 2 Miles and d ≥ 2 Miles
$L_b = F_A(50.0, 13, H, d, H_r)$

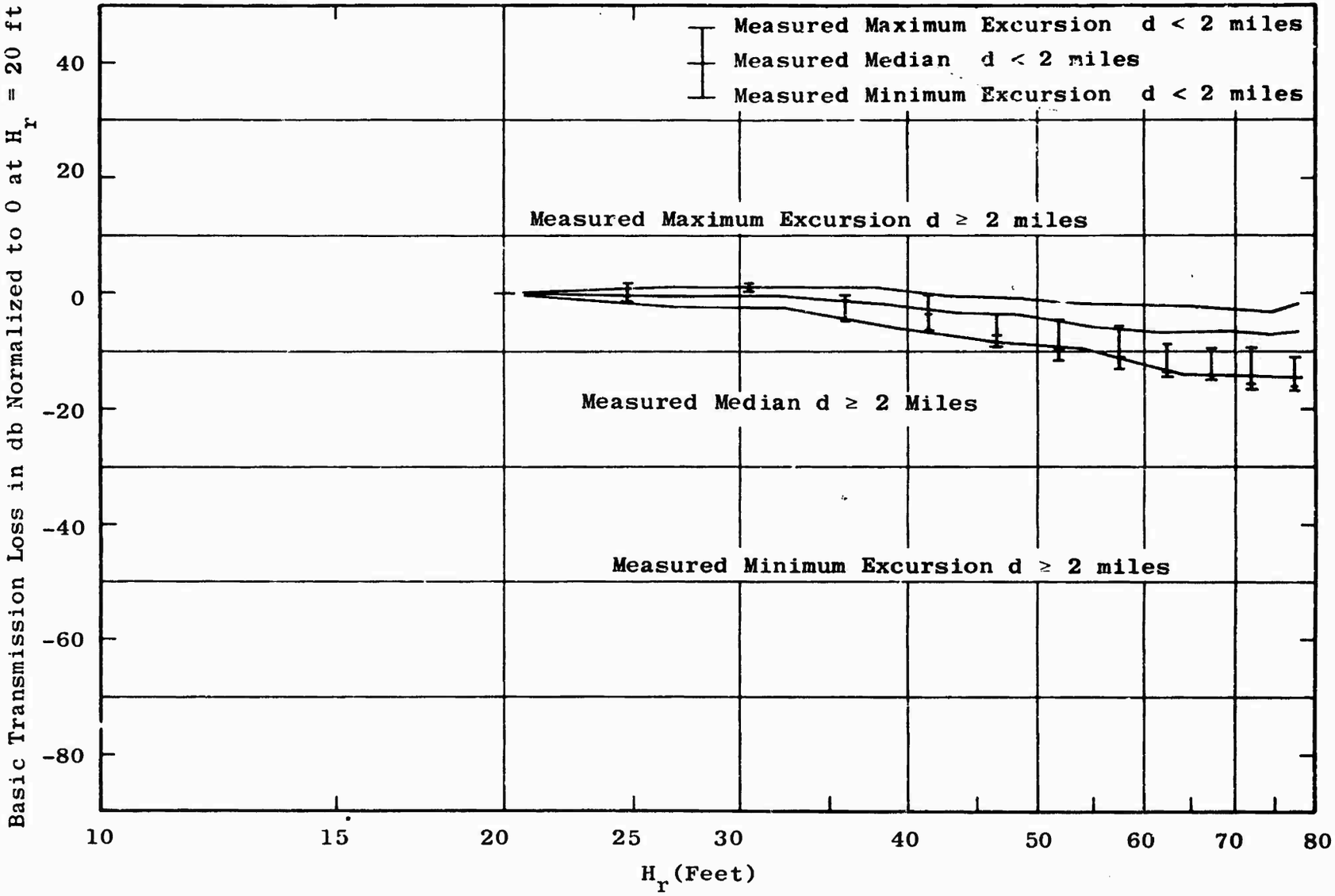

Figure 4.25G Comparison Between Measured Height Functions for d < 2 Miles and d ≥ 2 Miles
$L_b = F_A(100, 80, H, d, H_r)$

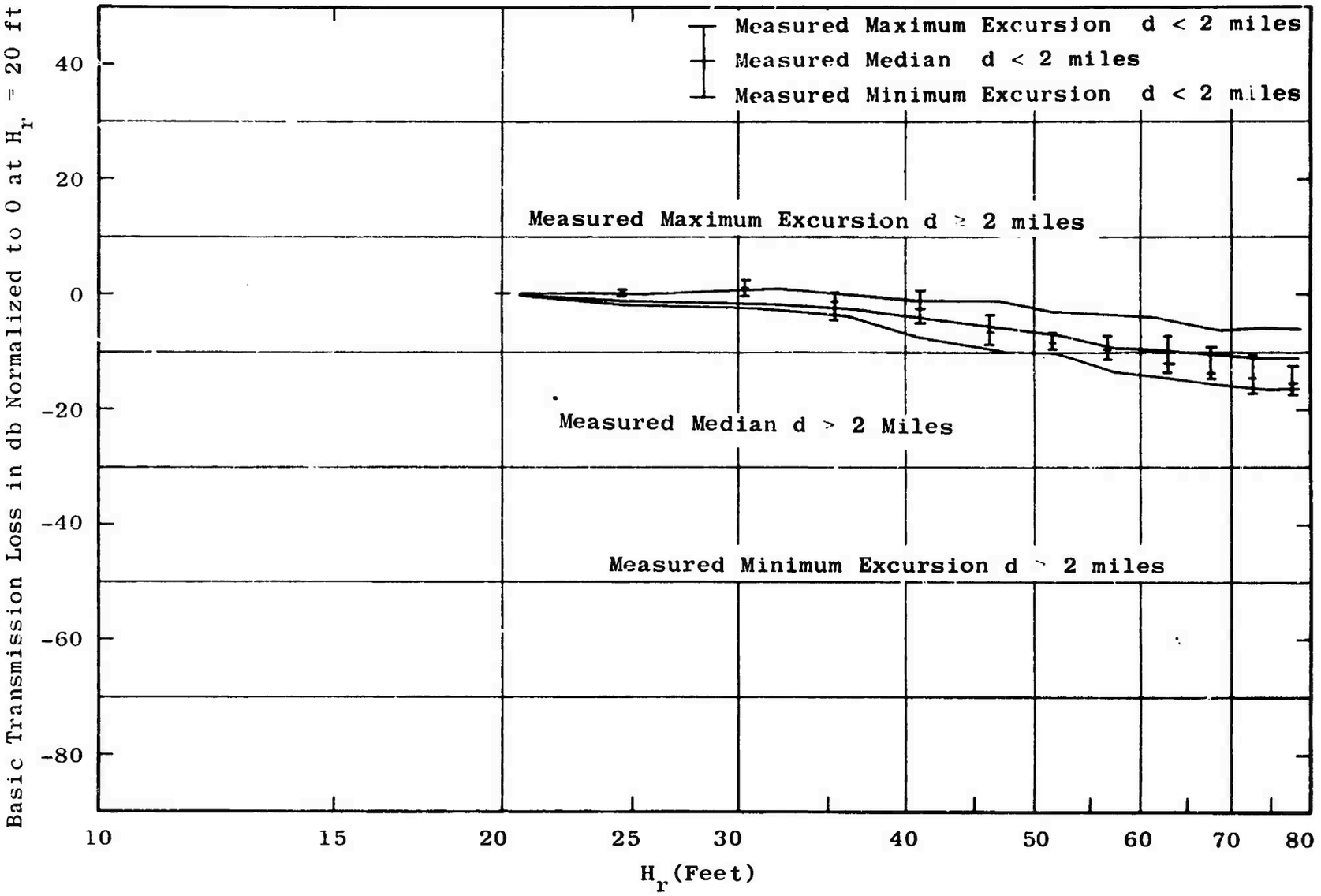

Figure 4.25H Comparison Between Measured Height Functions for d < 2 Miles and d > 2 Miles
$L_b = F_A(100, 40, H, d, H_r)$

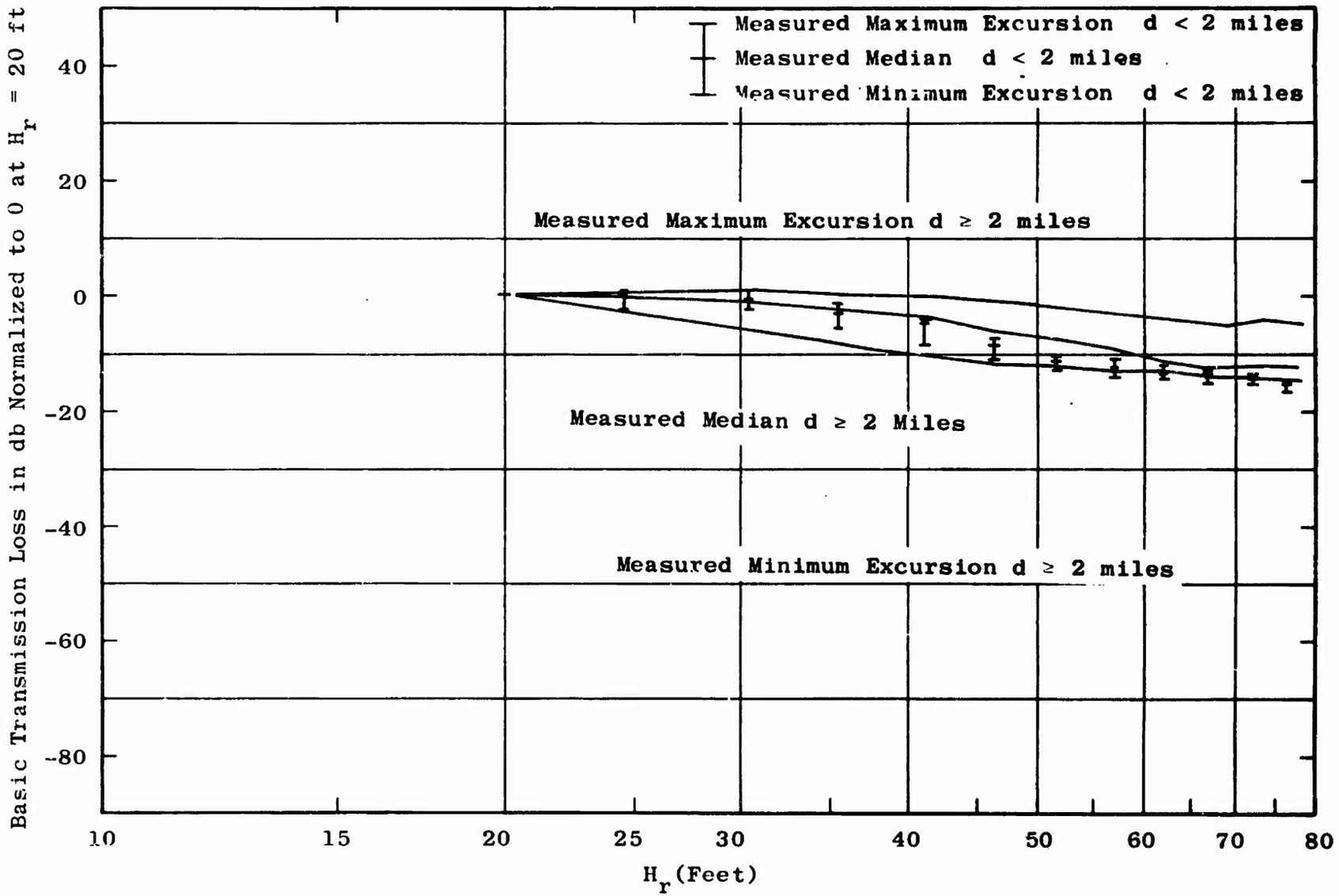

Figure 4.25I Comparison Between Measured Height Functions for d < 2 Miles and d ≥ 2 Miles
$L_b = F_A(100\ \ 13, H, d, H_r)$

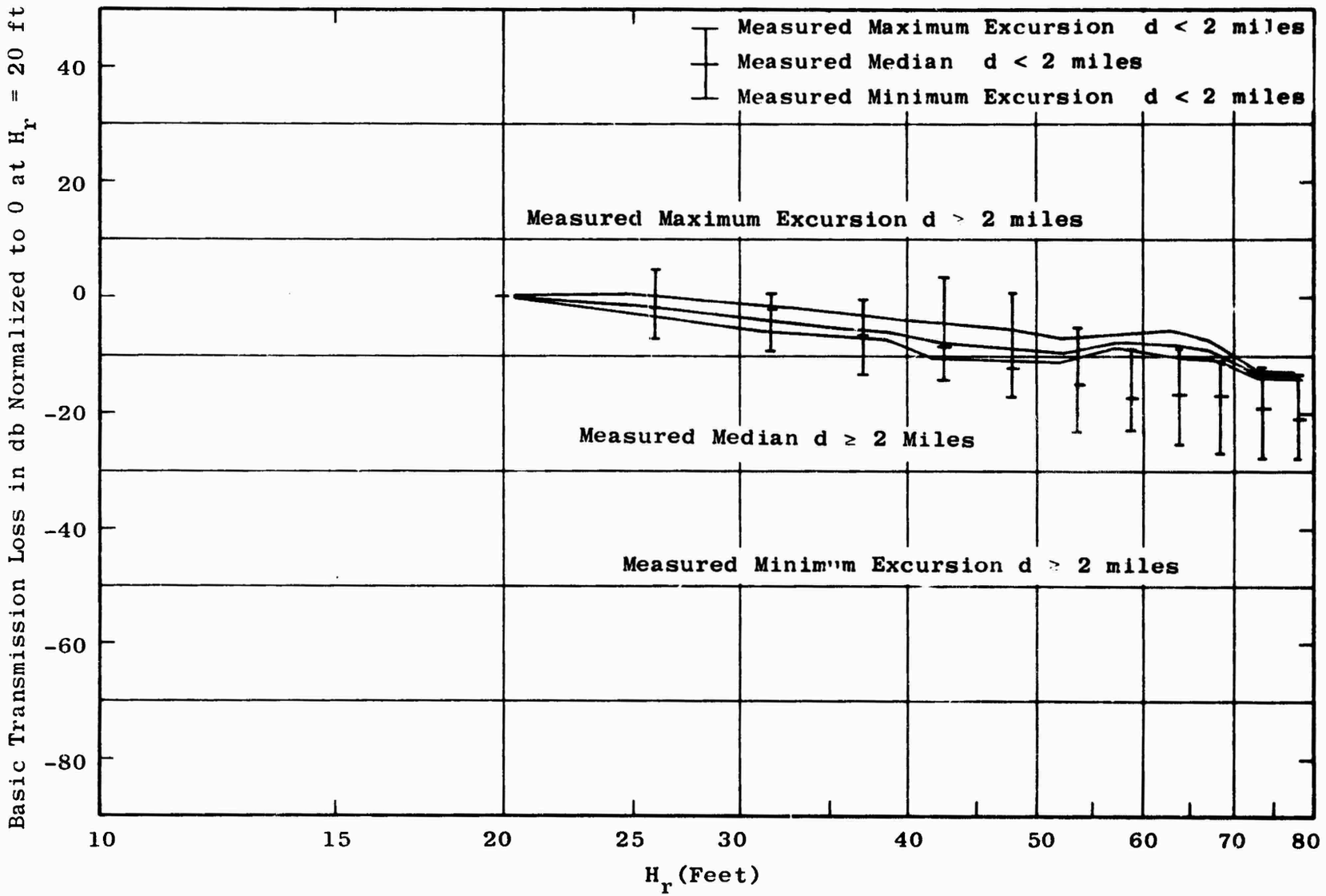

Figure 4.25J Comparison Between Measured Height Functions for d < 2 Miles and d > 2 Miles
$L_b = F_A(250, 80, H, d, H_r)$

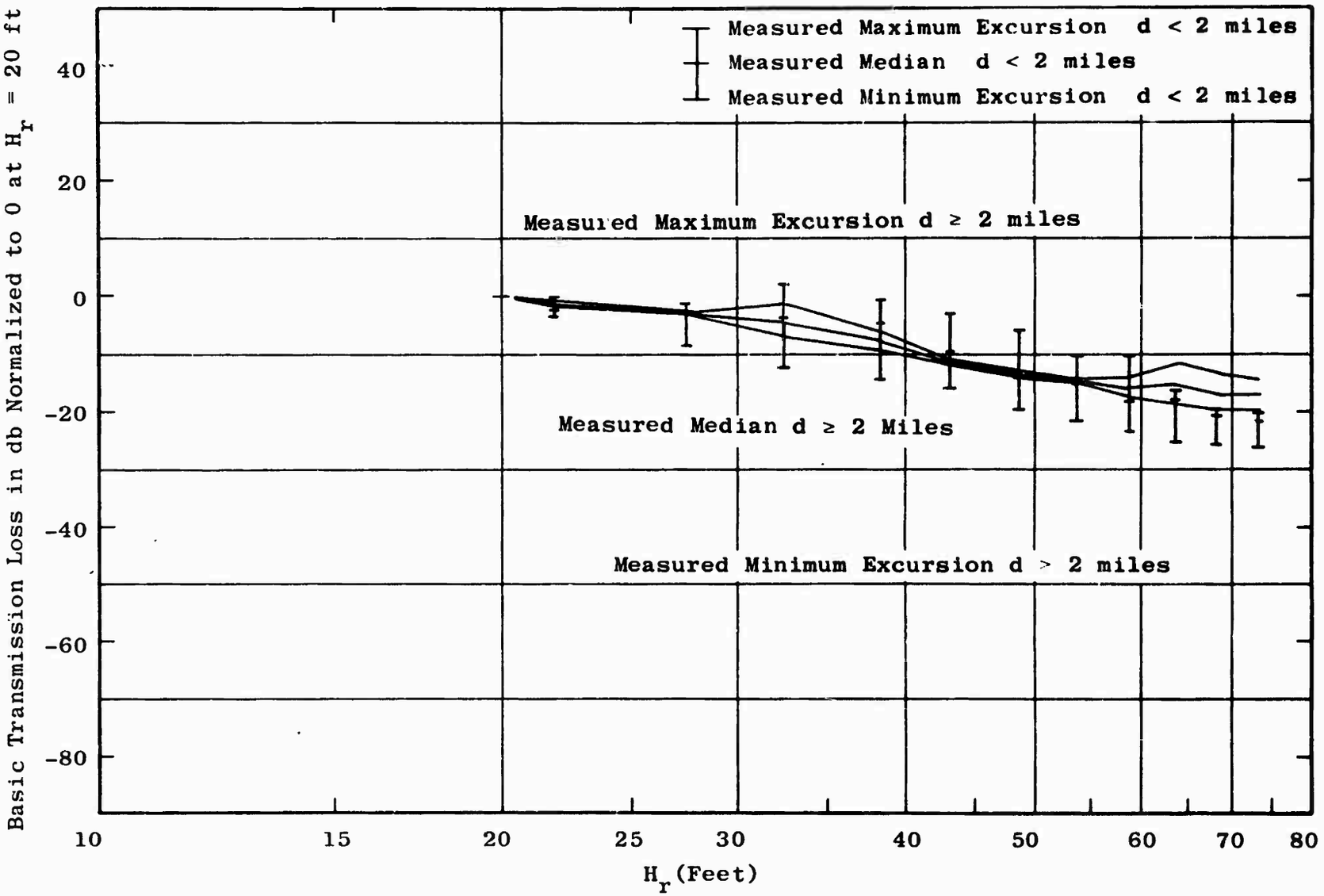

Figure 4.25K Comparison Between Measured Height Functions for d < 2 Miles and d ≥ 2 Miles
$L_b = F_A(250, 40, H, d, H_r)$

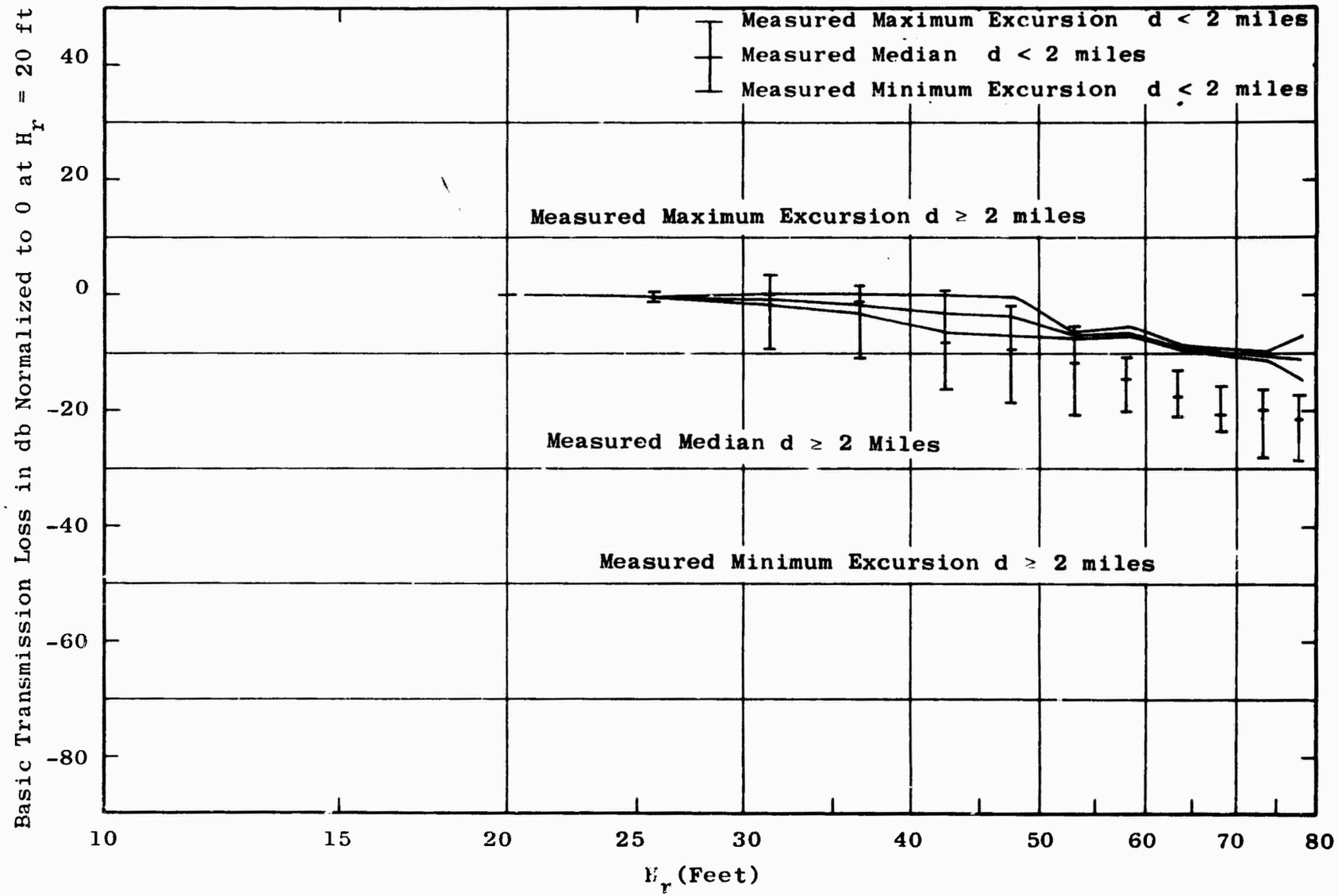

Figure 4.25L Comparison Between Measured Height Functions for d < 2 Miles and d ≥ 2 Miles
$L_b = F_A(400, 80, H, d, H_r)$

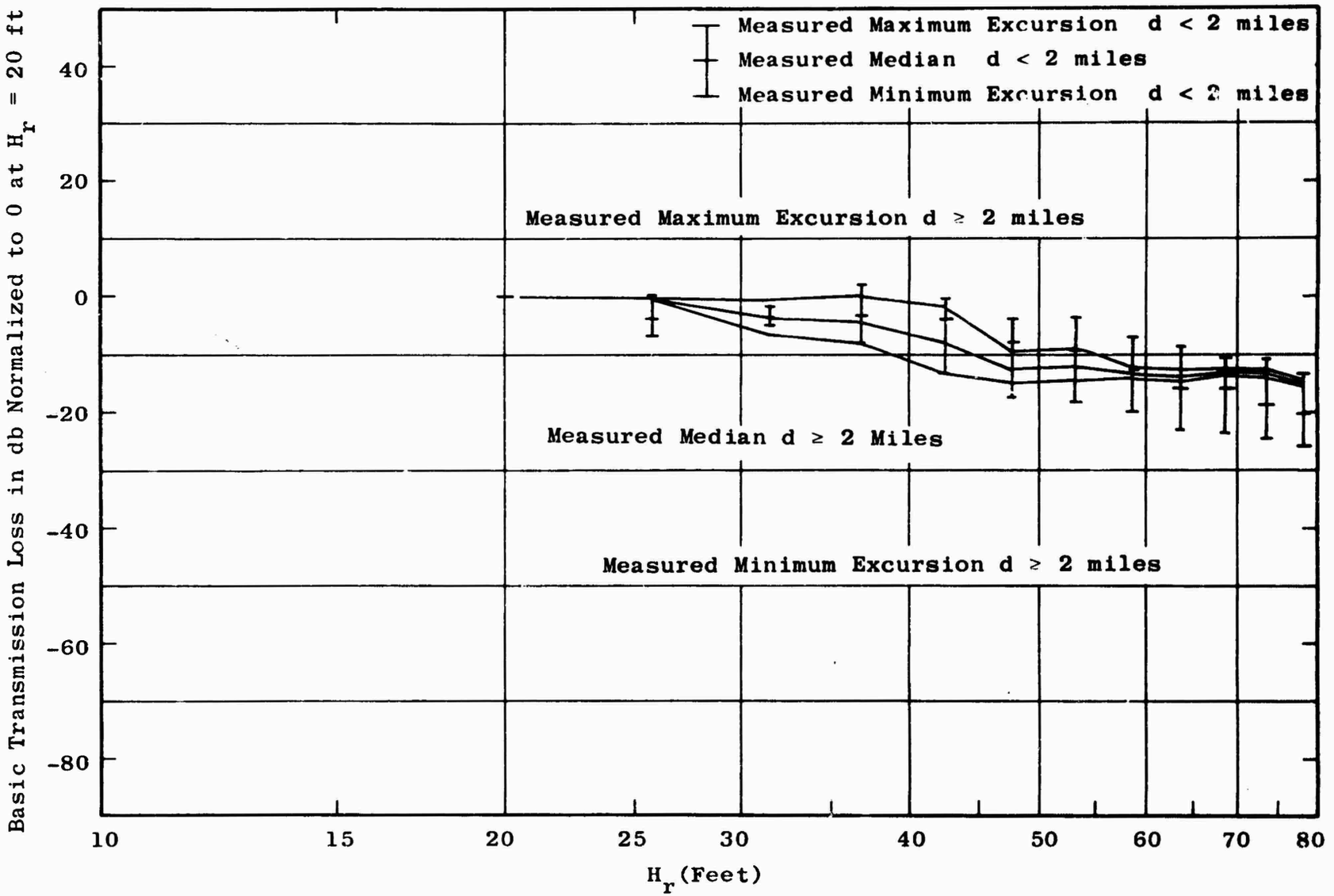

Figure 4.25M Comparison Between Measured Height Functions for d < 2 Miles and d ≥ 2 Miles
$L_b = F_A(400, 40, H, d, H_r)$

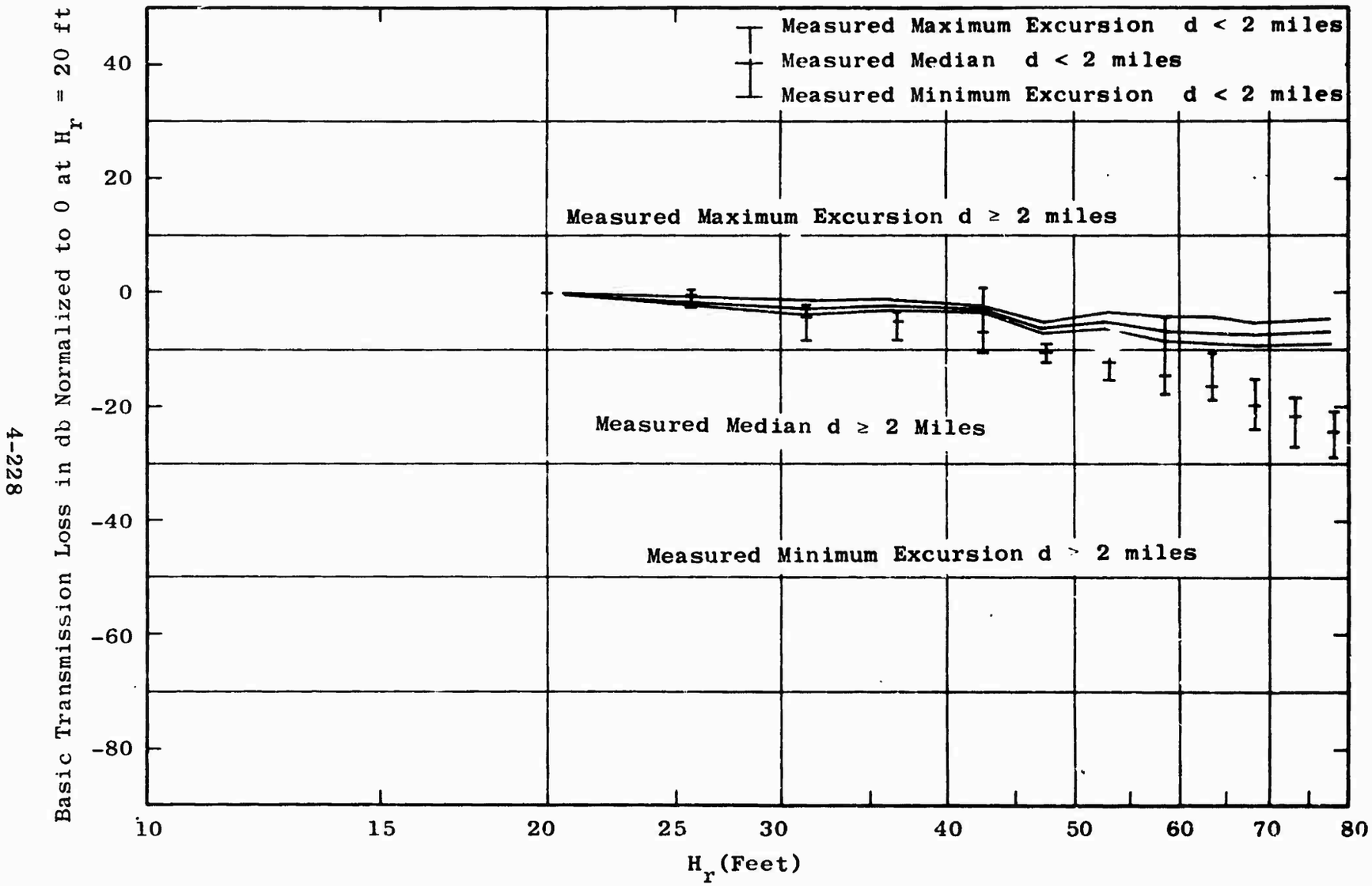

Figure 4.25N Comparison Between Measured Height Functions for d < 2 Miles and d ≥ 2 Miles
$L_b = F_A(400, 13, H, d, H_r)$

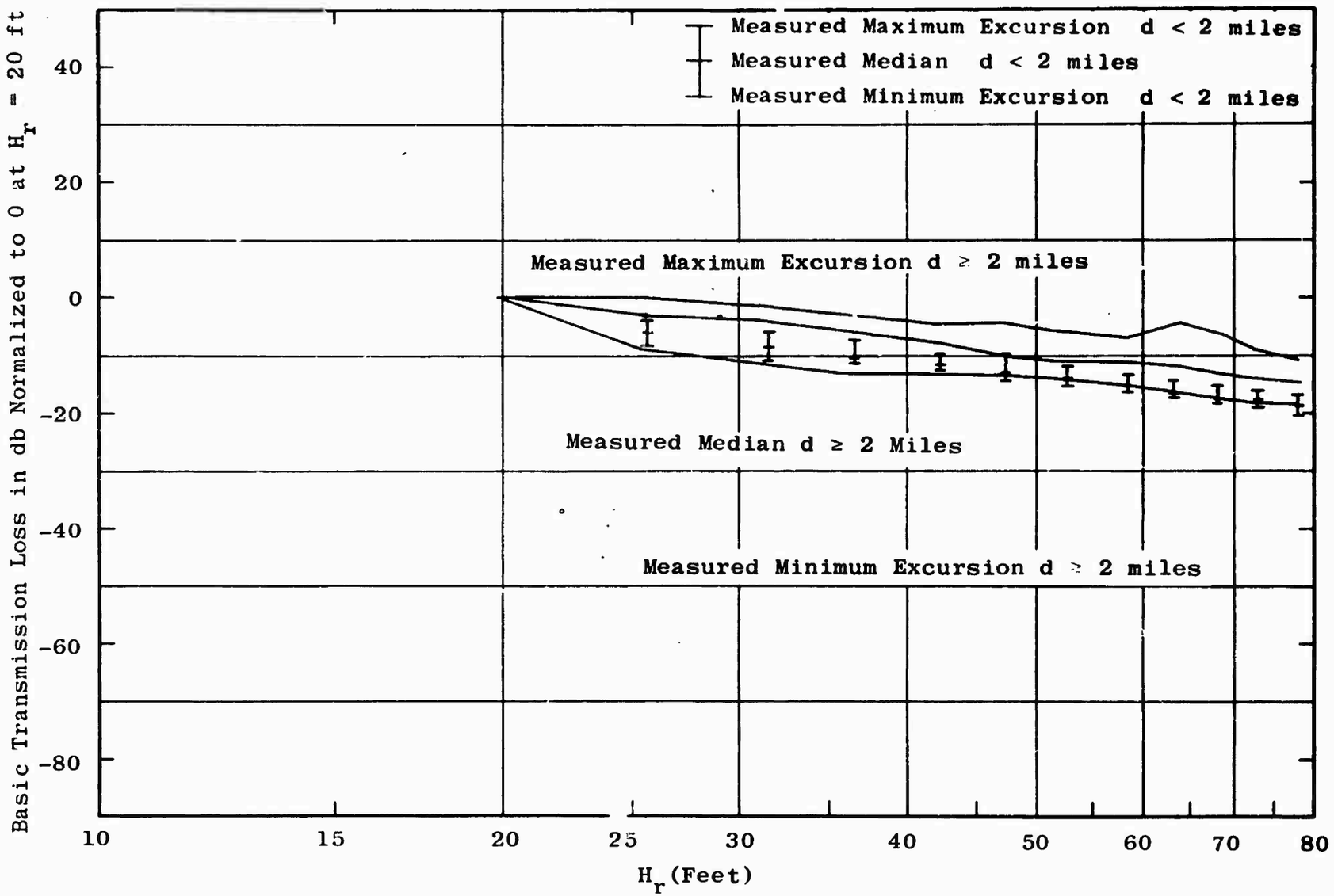

Figure 4.250 Comparison Between Measured Height Functions for d < 2 Miles and d ≥ 2 Miles
$L_b = F_A(25.5, 80, V, d, H_r)$

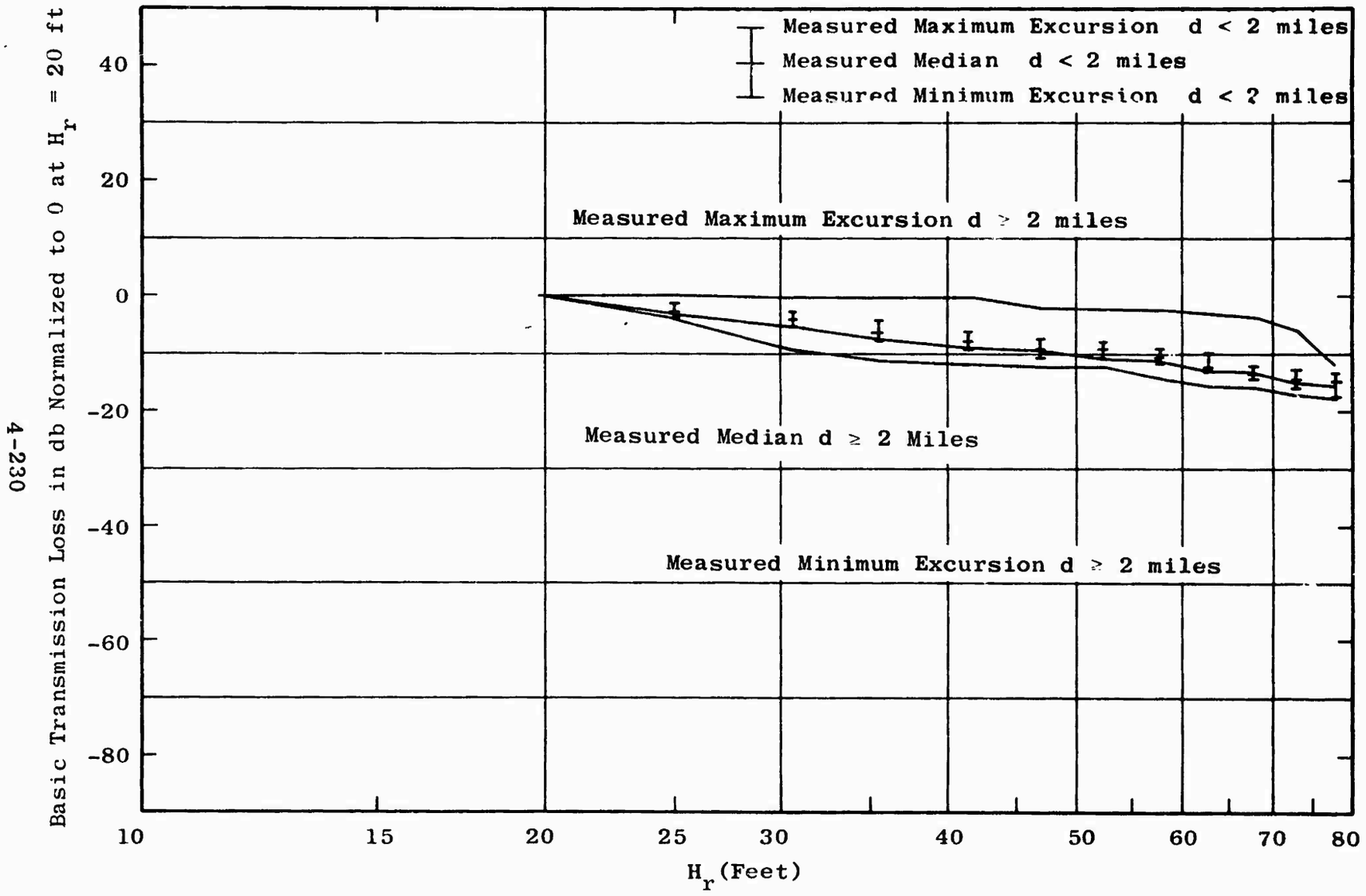

Figure 4.25P Comparison Between Measured Height Functions for d < 2 Miles and d ≥ 2 Miles
$L_b = F_A(25.5, 40, V, d, H_r)$

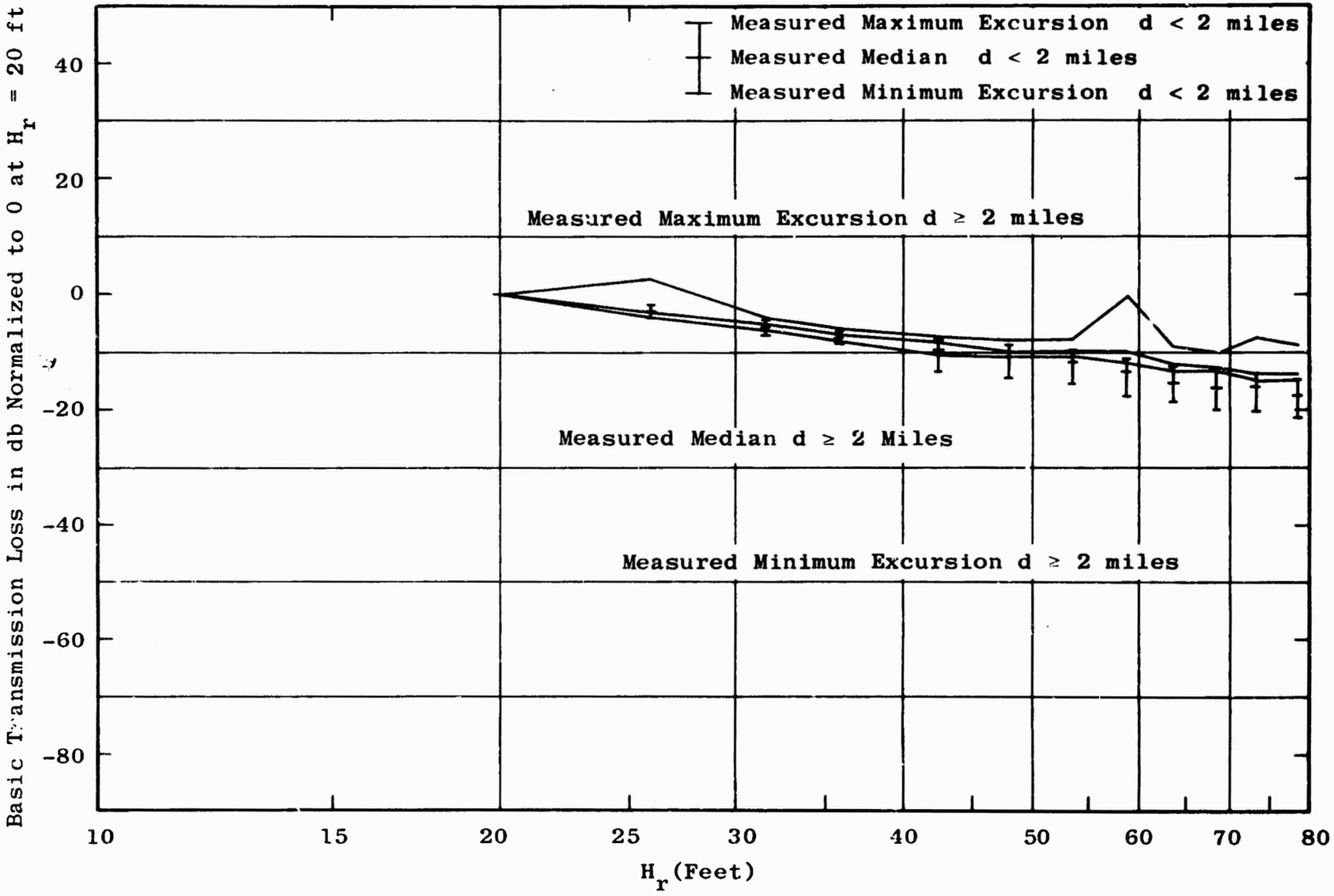

Figure 4.25Q Comparison Between Measured Height Functions for d < 2 Miles and d ≥ 2 Miles
$L_b = F_A(25.5, 13, V, d, H_r)$

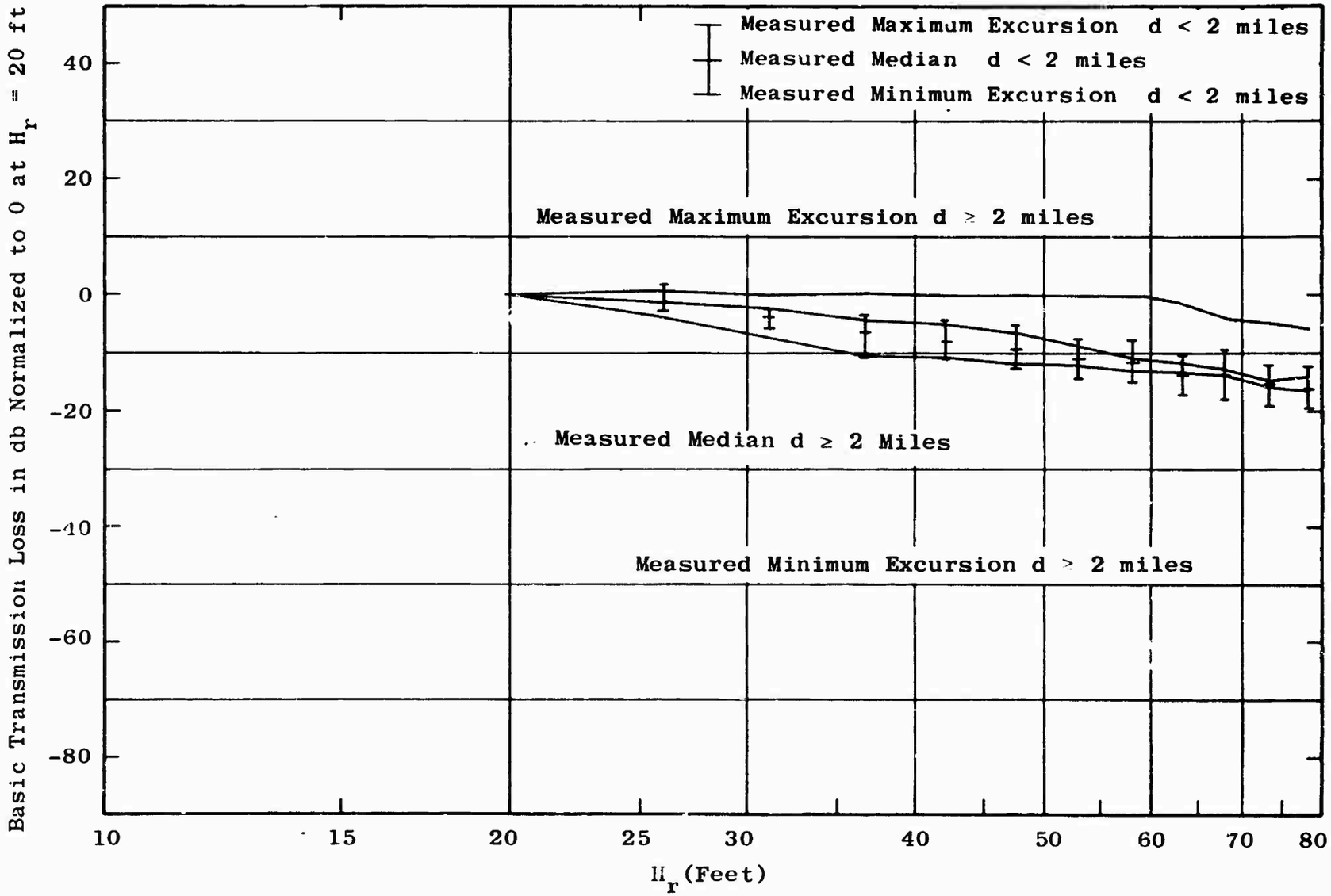

Figure 4.25R Comparison Between Measured Height Functions for d < 2 Miles and d ≥ 2 Miles
$L_b = F_A(50, 80, V, d, H_r)$

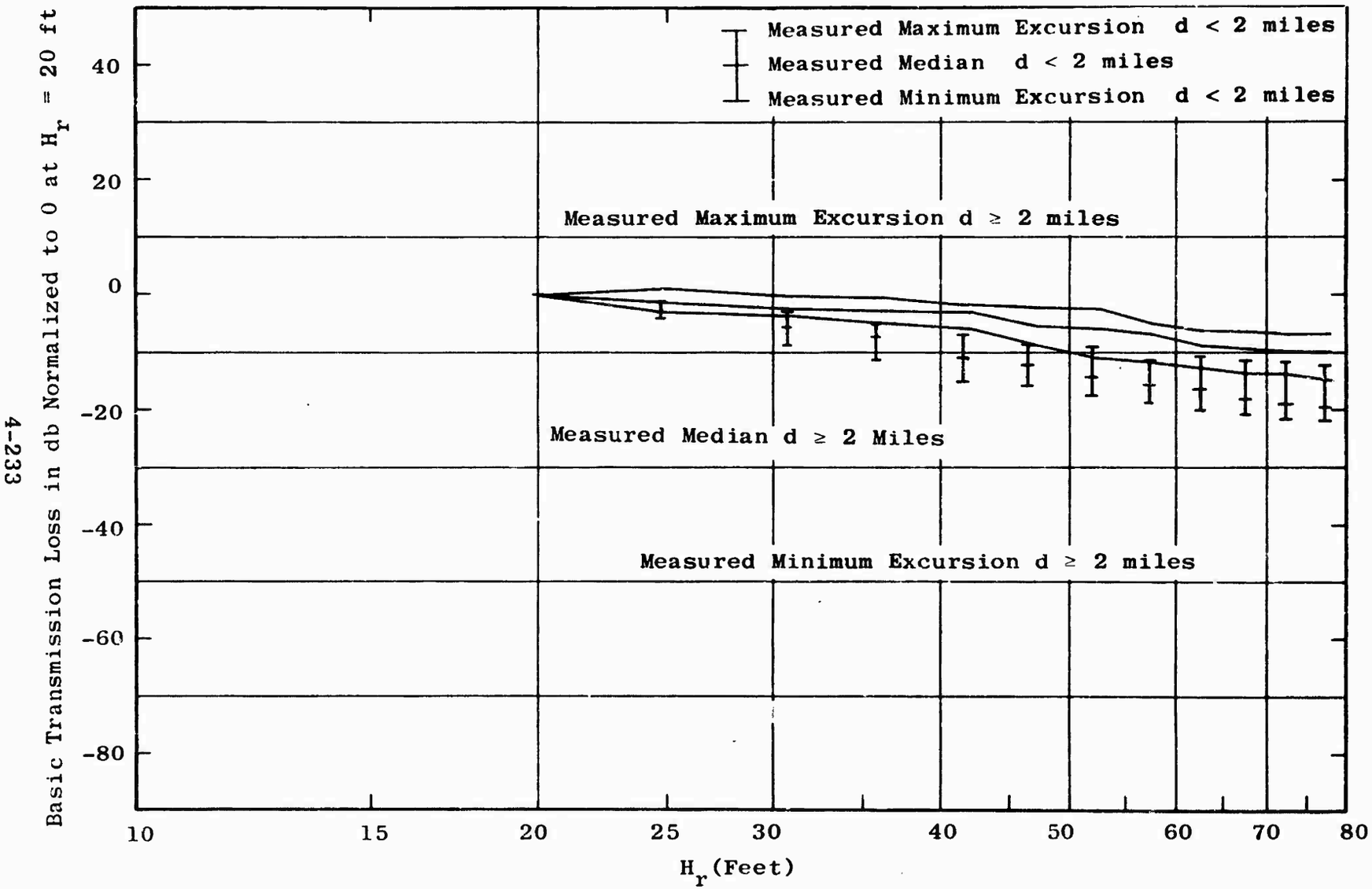

Figure 4.25S Comparison Between Measured Height Functions for d < 2 Miles and d ≥ 2 Miles
$L_b = F_A(50, 40, V, d, H_r)$

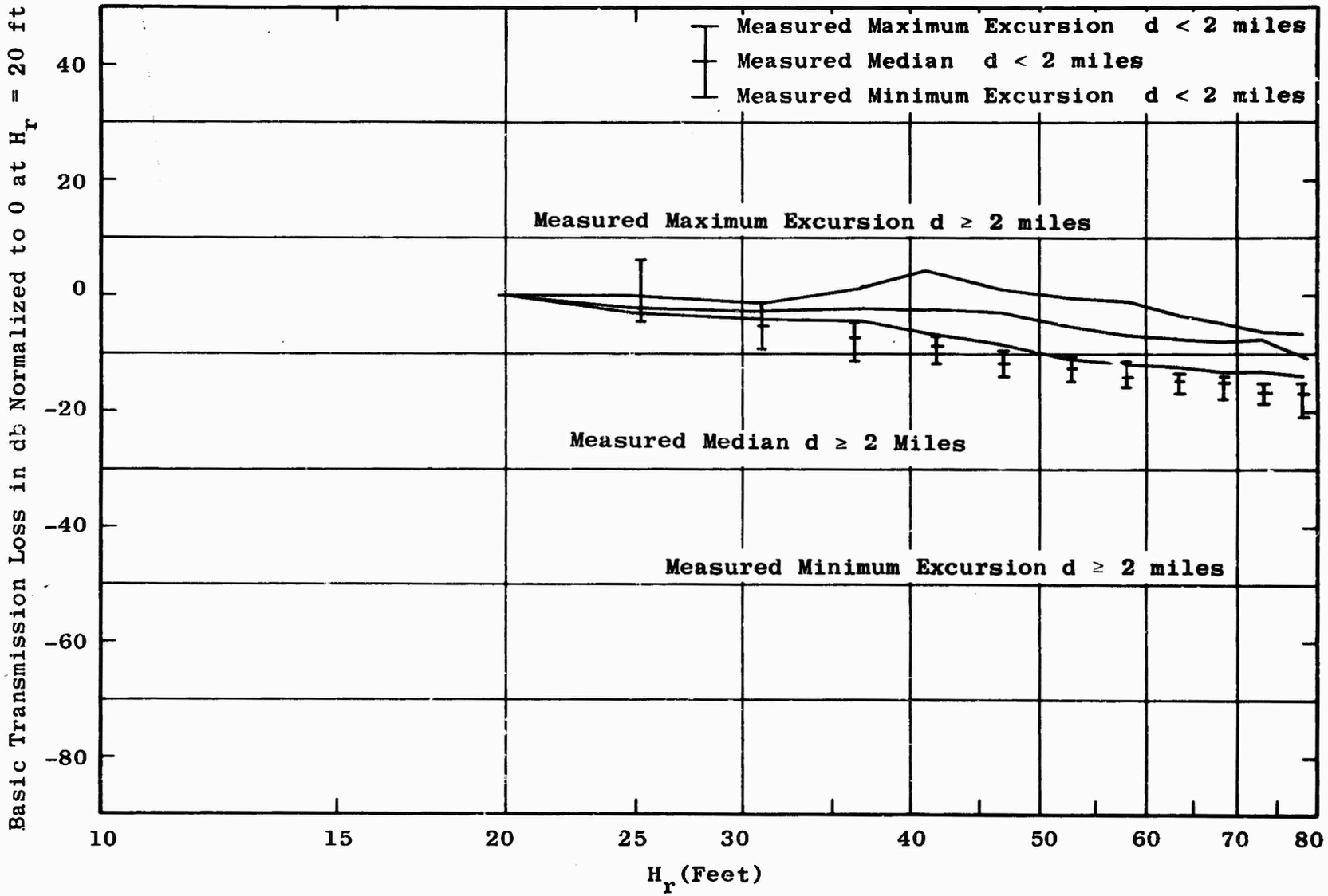

Figure 4.25T Comparison Between Measured Height Functions for d < 2 Miles and d ≥ 2 Miles
$L_b = F_A(50, 13, V, d, H_r)$

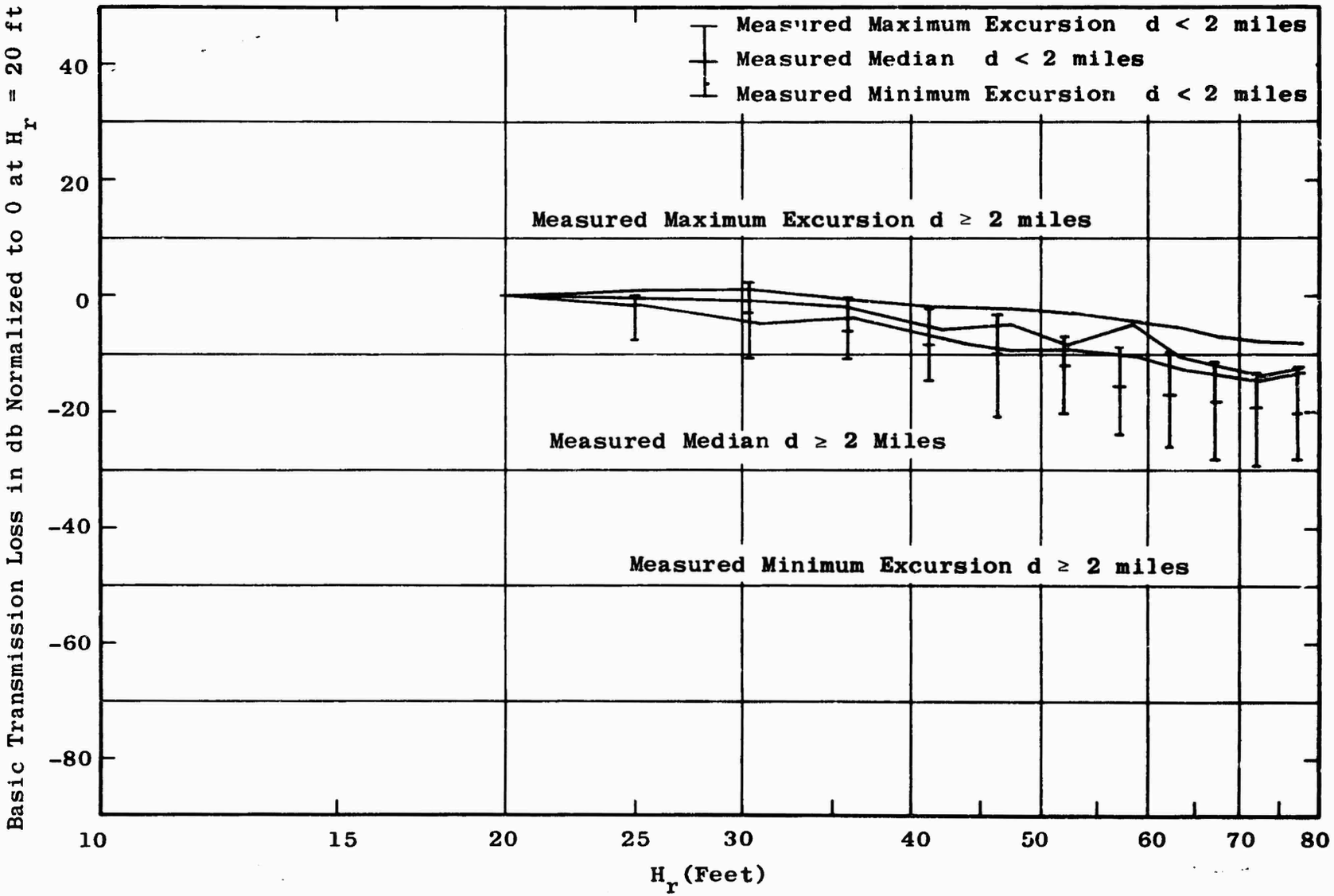

Figure 4.25U Comparison Between Measured Height Functions for d < 2 Miles and d ≥ 2 Miles
$L_b = F_A(100, 80, V, d, H_r)$

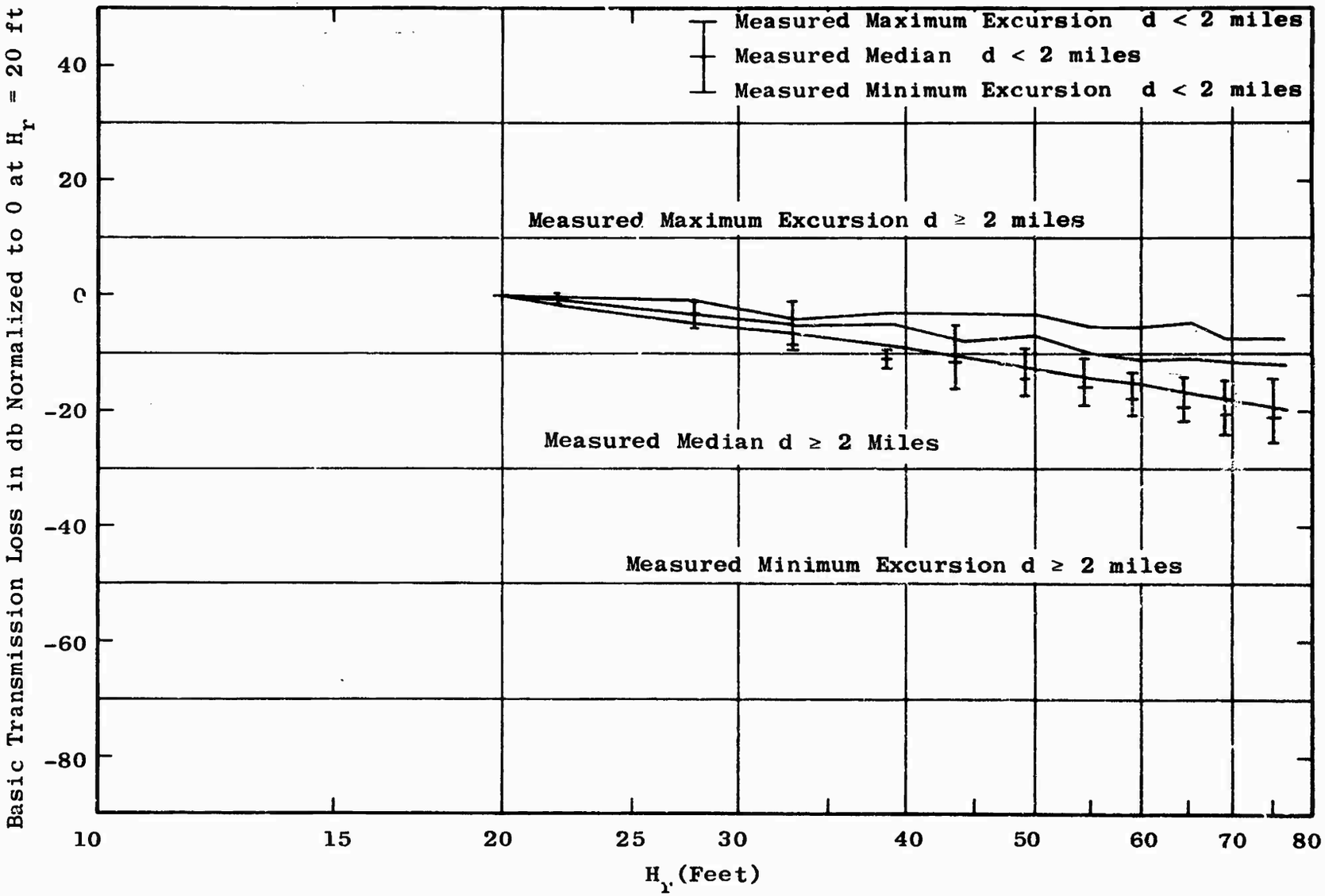

Figure 4.25V Comparison Between Measured Height Functions for d < 2 Miles and d ≥ 2 Miles
$L_b = F_A(100, 40, V, d, H_r)$

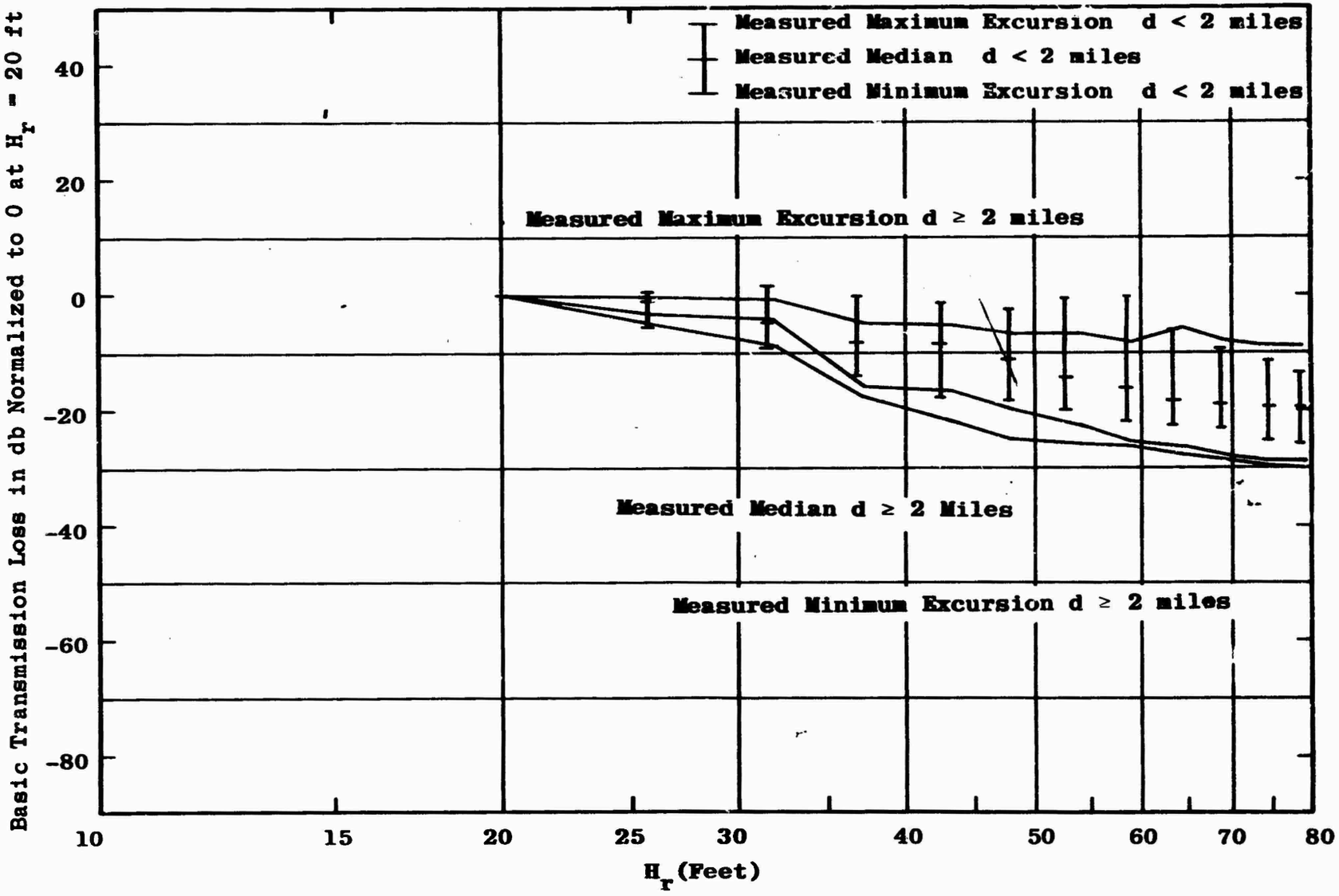

Figure 4.25W Comparison Between Measured Height Functions for d < 2 Miles and d ≥ 2 Miles
$L_b = F_A(100, 13, V, d, H_r)$

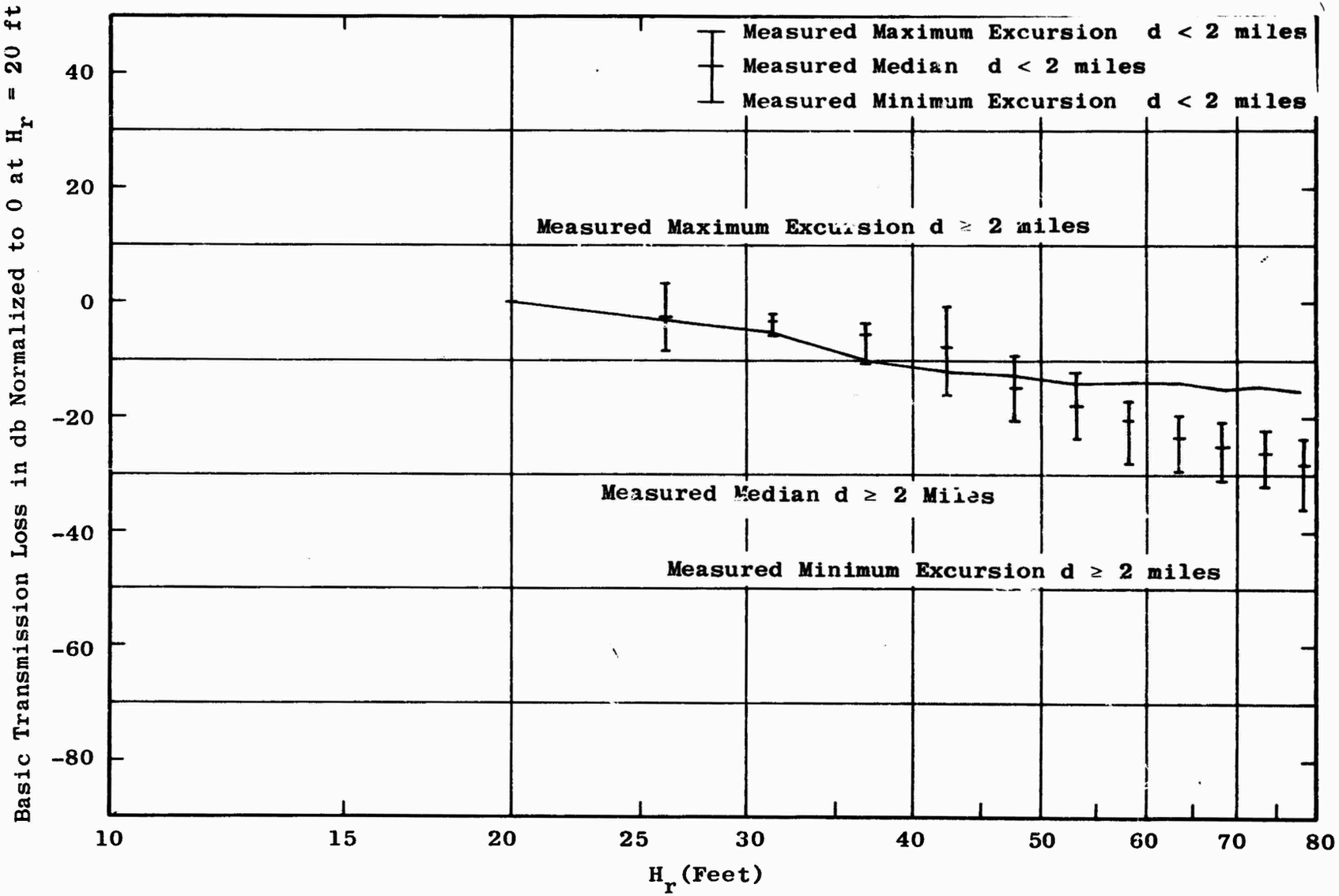

Figure 4.25X Comparison Between Measured Height Functions for d < 2 Miles and d ≥ 2 Miles
$L_b = F_A(250, 80, V, d, H_r)$

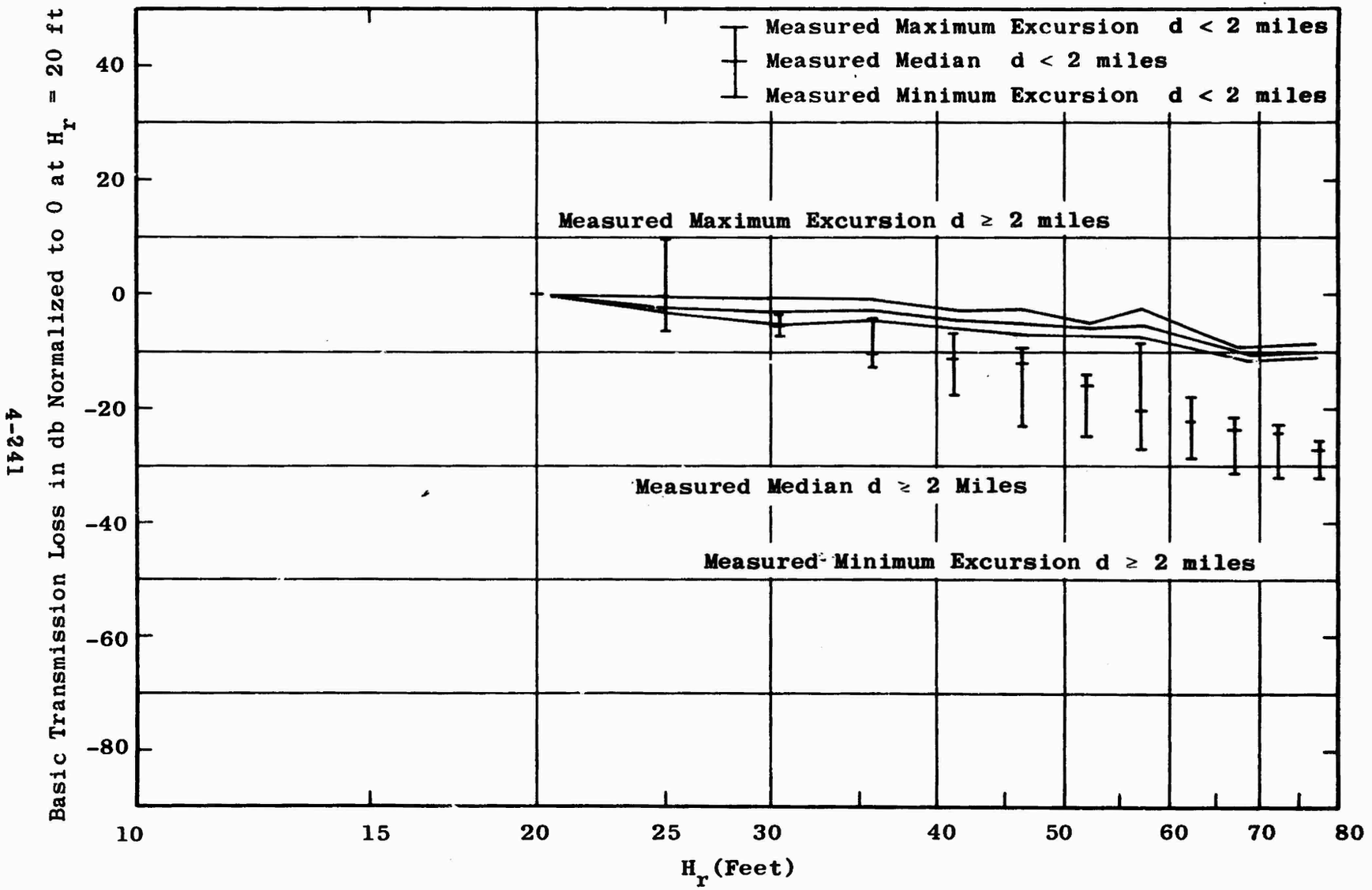

Figure 4.25AA Comparison Between Measured Height Functions for d < 2 Miles and d ≥ 2 Miles
$L_b = F_A(400, 80, V, d, H_r)$

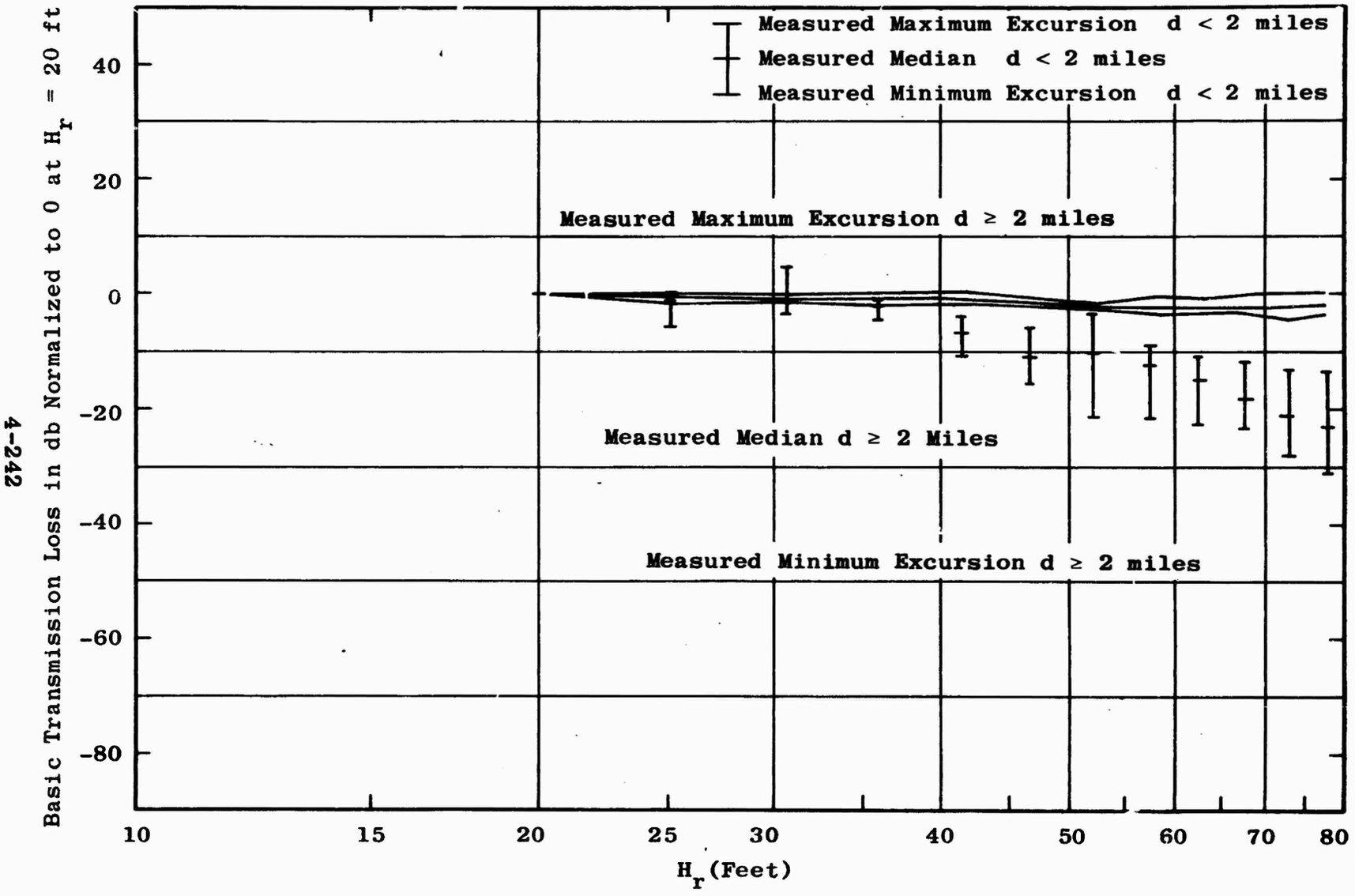

Figure 4.25BB Comparison Between Measured Height Functions for d < 2 Miles and d ≥ 2 Miles
$L_b = F_A(400, 40, V, d, H_r)$

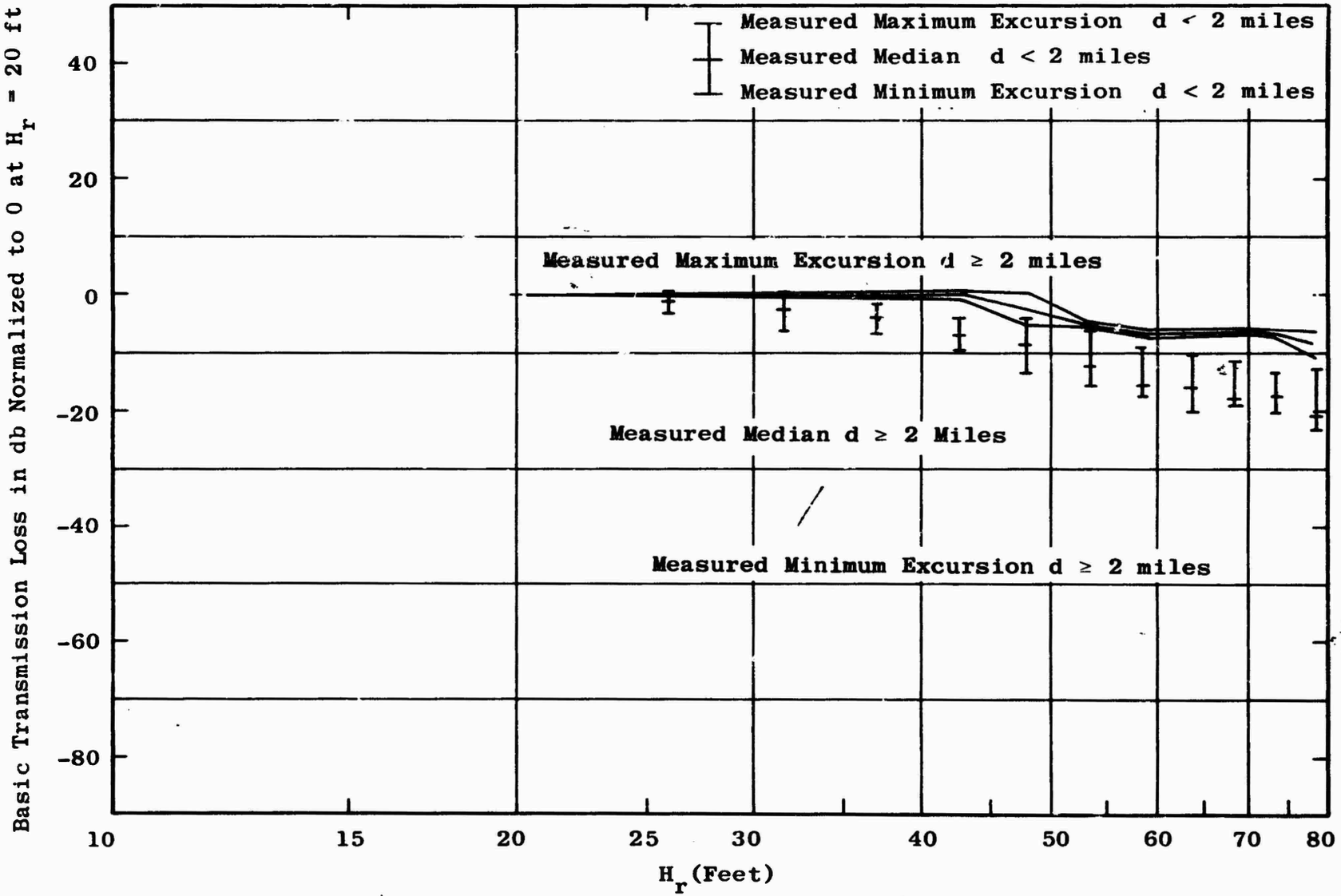

Figure 4.25CC Comparison Between Measured Height Functions for d < 2 Miles and d ≥ 2 Miles
$L_b = F_A(400, 13, V, d, H_r)$

4.3.3 Variability of L_b with Range

The vehicular measurements provide an insight into the relatively fine-grain details of field strength variability with distance in tropical vegetation. As a vehicle proceeds along a path cut through the vegetation, a fifth wheel mechanically drives a strip chart recorder which continuously records the widely varying measured field strength. Figures 4-26A through 4-26E provide samples of the data obtained in this way at the various test frequencies from 25.5 mc to 400 mc. The radials along which the vehicle moves have markers which indicate radial distance from the transmitter every 0.2 mile from 0.2 to 3 miles and every 0.5 mile thereafter. Each time the vehicle passes one of these distance markers, a calibration mark is made on the strip recording. Since the trails are never exact radials, the actual distance represented on the strip chart is always greater than the indicated radial distance.

A detailed analysis of the amplitude distribution within each 0.2-mile interval and each 0.5-mile interval has been made. The methods and results are described below. No other detailed analyses of this data have been performed as yet. However, a cursory examination of the data indicates very roughly the distance spacings between adjacent maxima and minima as shown below.

Frequency (mc)	Spacing (ft)
25.5	20
50.0	15
100.0	10
250.0	8
400.0	4

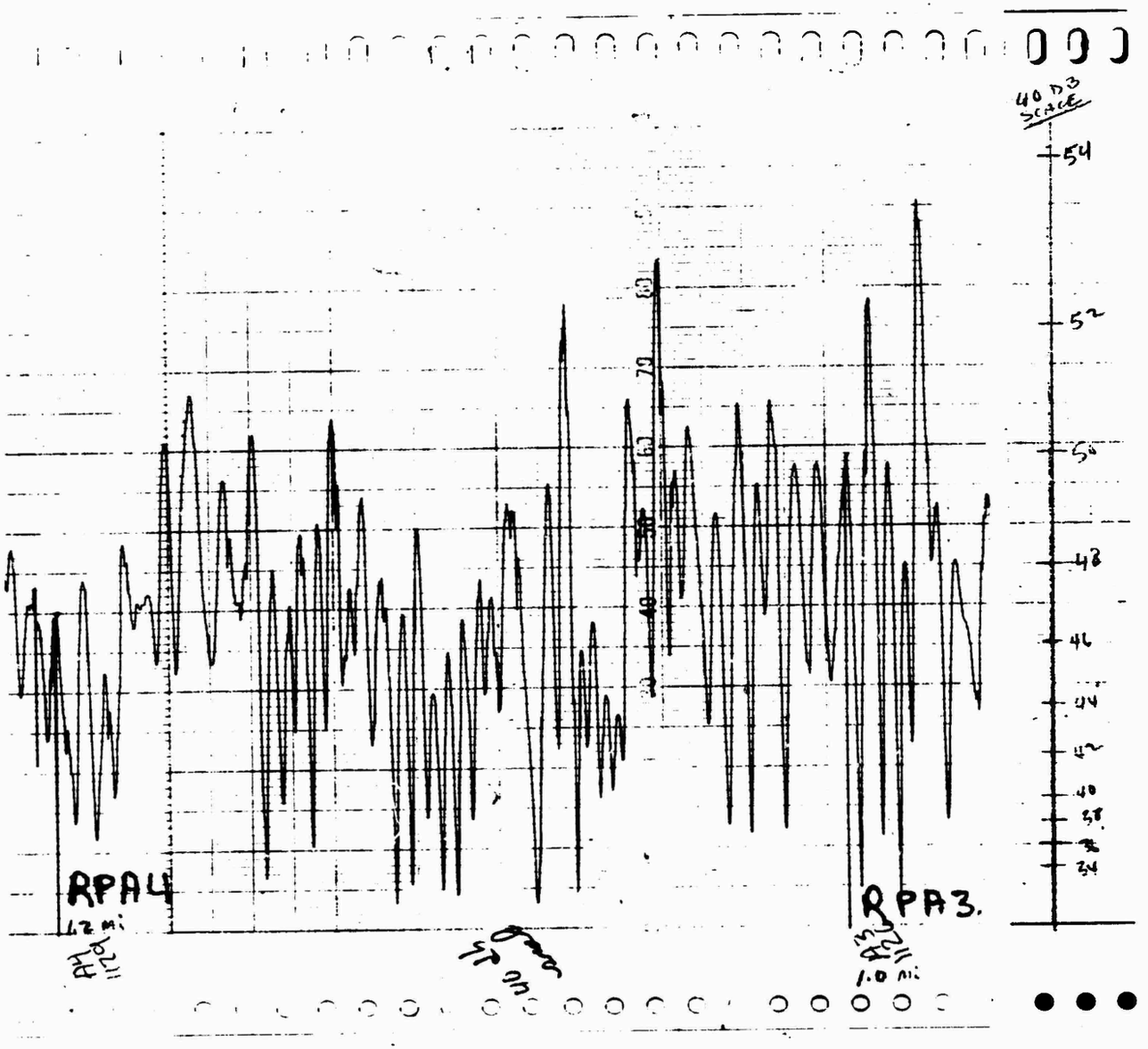

Figure 4.26A Example of Vehicular Raw Data
F_A(25.5, 40, V, 1.0-1.2, 7)

AR 5978

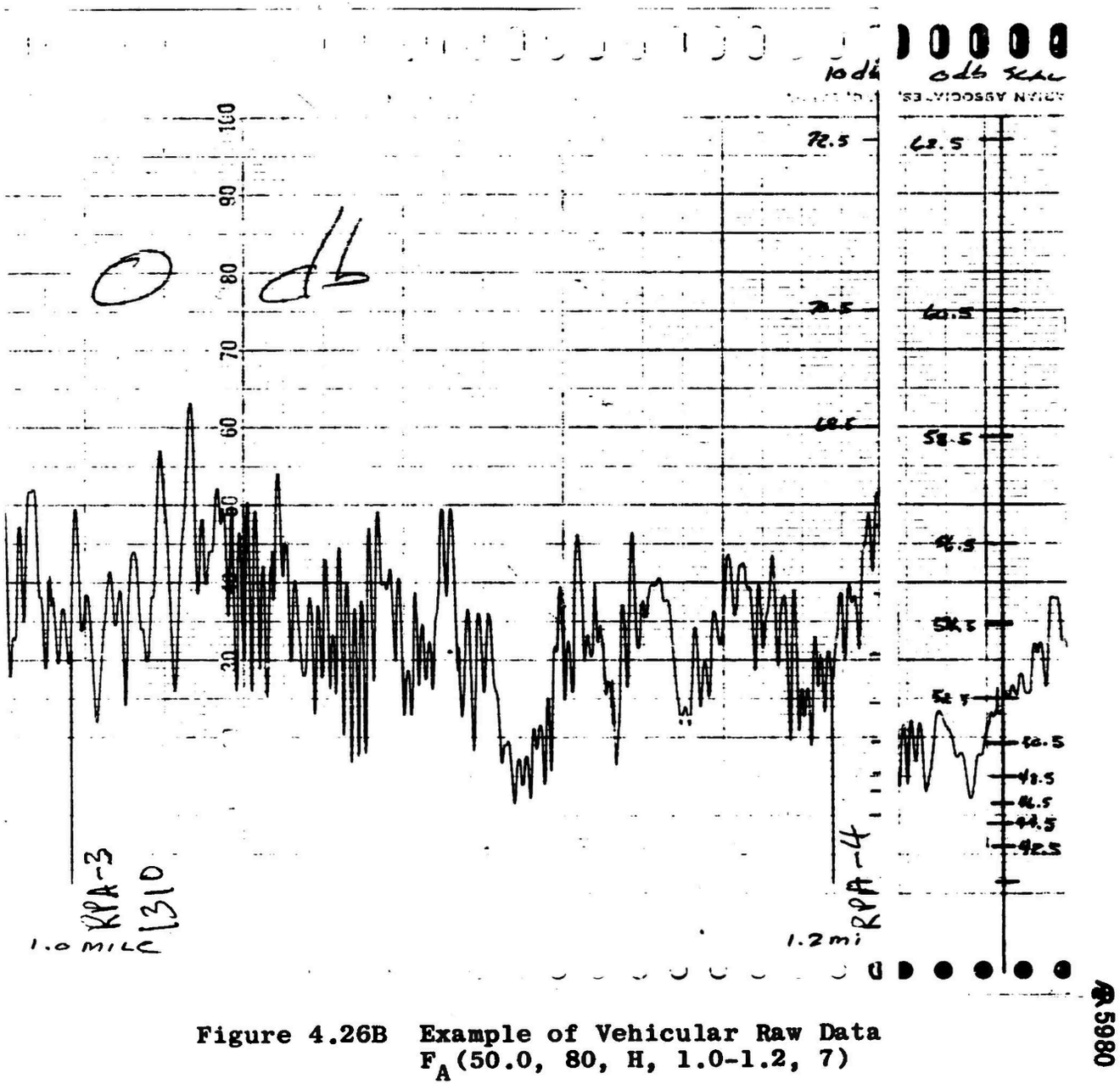

Figure 4.26B Example of Vehicular Raw Data
F_A(50.0, 80, H, 1.0-1.2, 7)

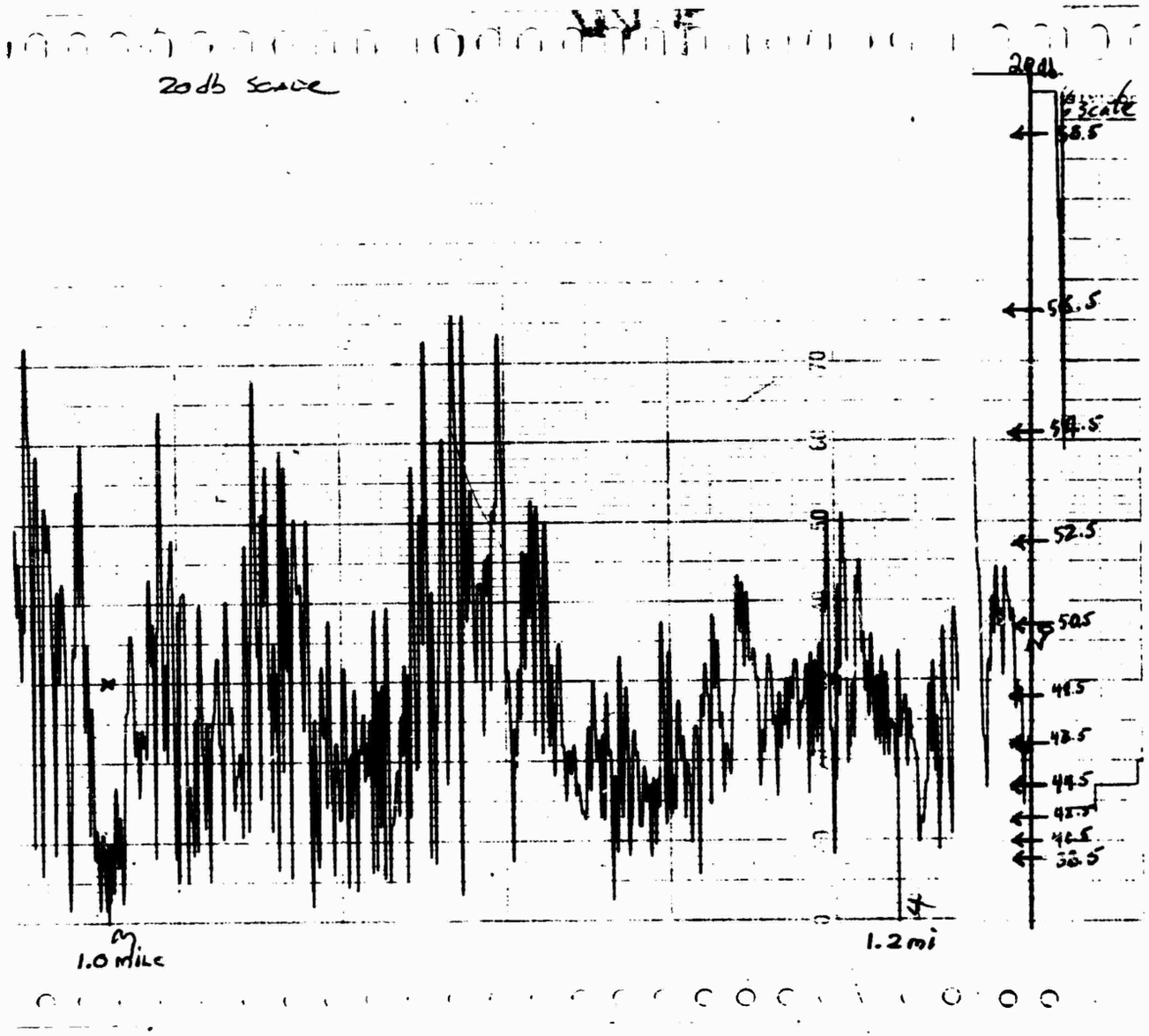

Figure 4.26C Example of Vehicular Raw Data
F_A(100, 40, H, 1.0-1.2, 7)

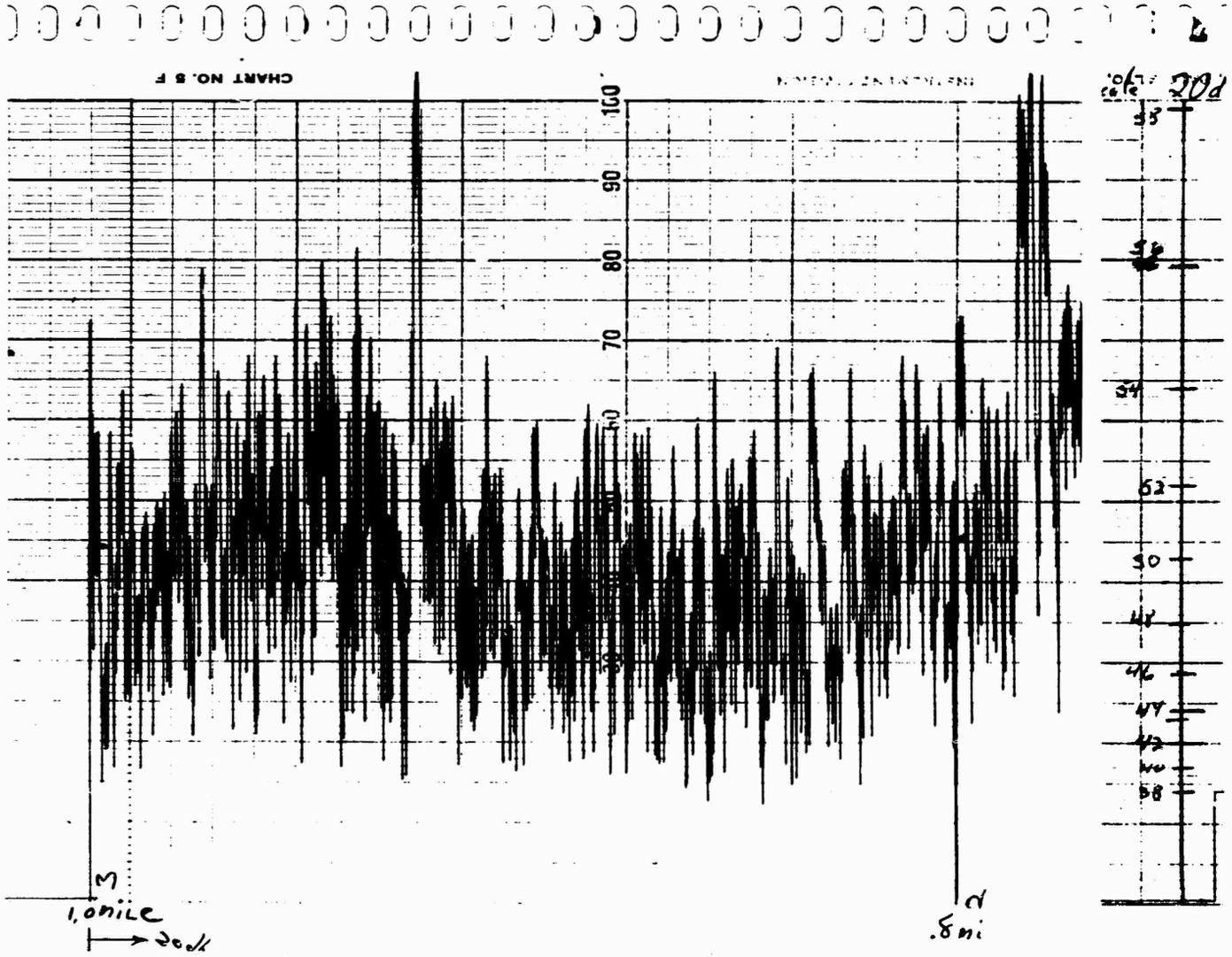

Figure 4.26D Example of Vehicular Raw Data
F_A(250, 80, V, 0.8-1.0, 7)

R 5981

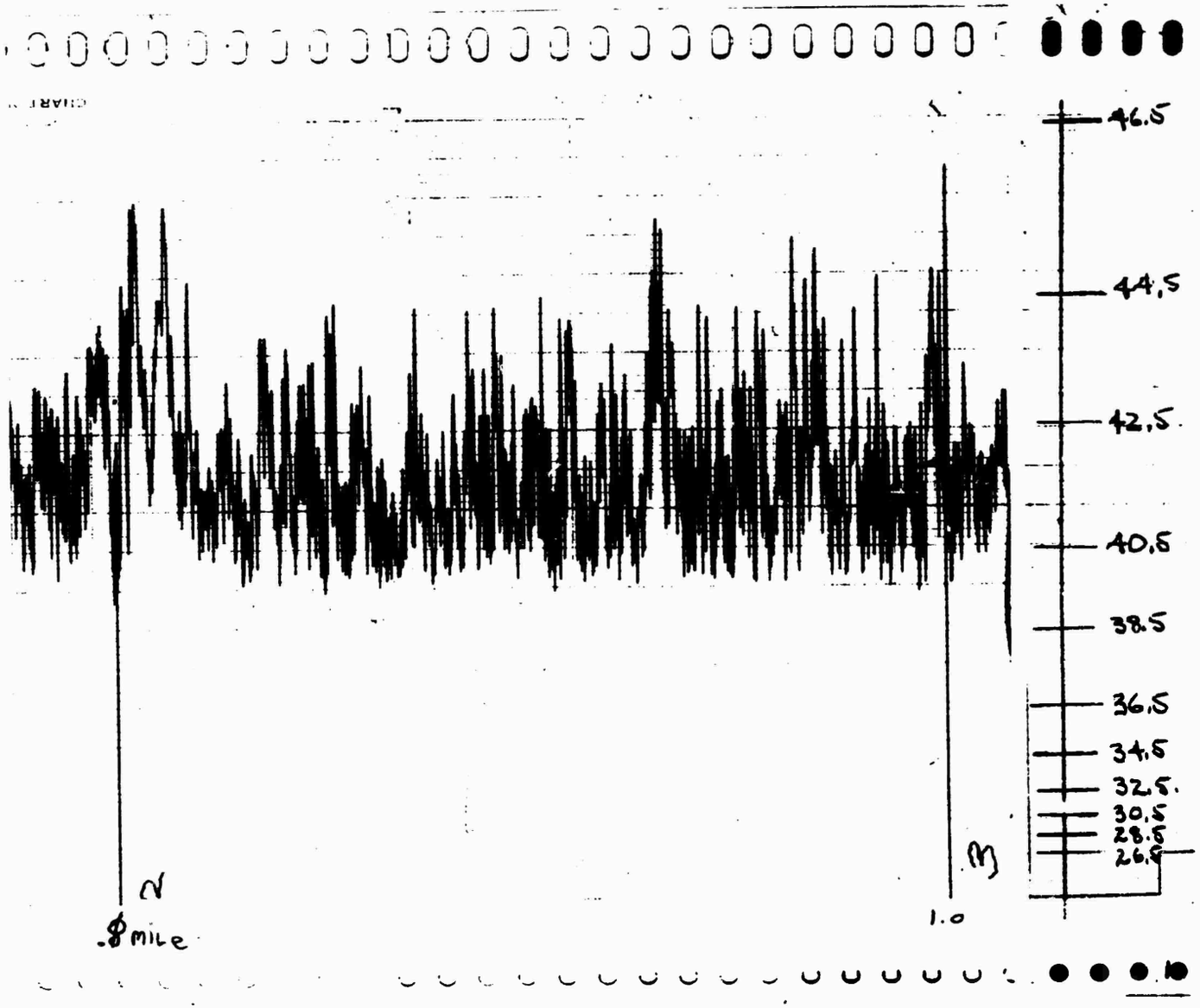

Figure 4.26E Example of Vehicular Raw Data
F_A(400, 40, H, 0.8-1.0, 7)

4.3.3.1 Data Analysis

The cumulative amplitude distribution for each 0.2- or 0.5-mile interval of data is obtained in the following way. A segment of the chart, such as the sample shown in Figure 4.27, has the ordinate (db) divided into 10 levels, each corresponding to a known db level. The abscissa of the chart, which represents distance along the trail, is divided into portions which lie between RPA (radial points on Trail A) points. RPA points are those predetermined points along the path whose radial distances from the transmitting antenna increase in 0.2-mile increments to 3 miles and by 0.5-mile increments beyond 3 miles.

Dividing distance over which each discrete preset level was exceeded by the total distance between adjacent RPA points yields a numerical ratio which corresponds to the probability that the particular db level is exceeded. An illustration of the calculation is given in Figure 4.27 and Table IV.

AR5975

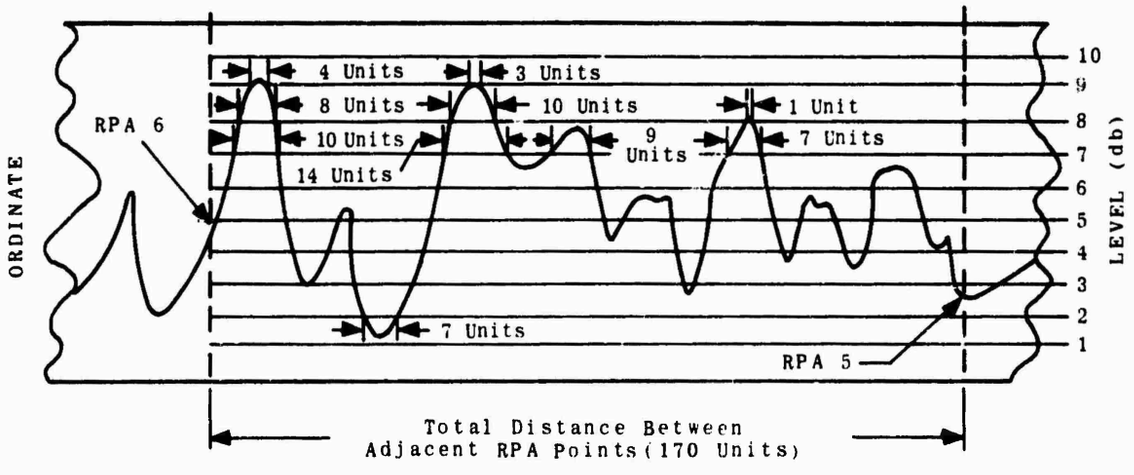

Figure 4.27 A Sample Strip Chart Analysis

Table IV

db Level	Distance db Level was Exceeded	Numerical Ratio	Percentage
10	0 = 0	0/170	0.0
9	4+3 = 7	7/170	4.1
8	8+10+1 = 19	19/170	11.2
7	10+14+9+7 = 40	40/170	23.5
6	12+37+12+10 = 71	71/170	41.7
5	15+3+39+11+15+8+12 = 103	103/170	60.6
4	18+5+58+18+12+20 = 131	131/170	77.0
3	22+10+61+59 = 152	152/170	89.4
2	170 - 7 = 163	163/170	95.8
1	170 = 170	170/170	100.0

The percentage probabilities which represent the amplitude distribution are given in the last column of Table IV.

A totalizer has been employed to reduce the large amount of vehicular data which is being collected in Thailand. A sketch of the machine is shown in Figure 4.28. As the strip chart passes through the machine at constant speed, 10 different clocks totalize the time each individual preset db level is exceeded and another time base clock runs continuously during the pass. Dividing each of the times on the 10 clocks by the total running time gives the numerical ratio, and thus the probability percentage is obtained.

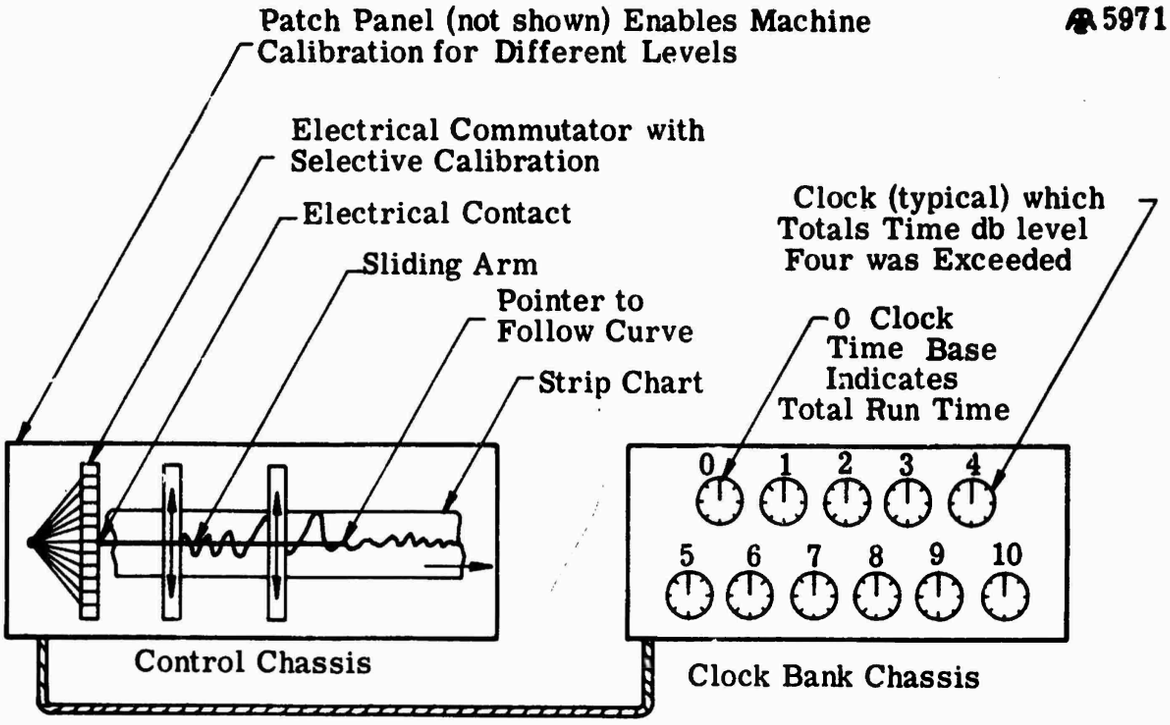

Figure 4.28 Totalizer Diagram

4.3.3.2 Summary of Vehicular Data Analysis Results

Figures 4.29A through 4.29N provide examples of the statistical distributions obtained from the analysis of vehicular data. Each distribution pertains to the signal amplitude or, correspondingly, the basic transmission loss experienced over the indicated trail segment. The amplitude distribution was obtained by using the totalizer described in the previous section.

The points plotted on Figures 4.29A through 4.29N represent the probabilities obtained from the totalizer. These points follow a straight line on arithmetic probability paper which implies a normal (Gaussian) probability distribution. There is often a deviation from normality at the ends of the distribution, but this fall-off is within the limits of experimental error. Since the analyzed chart segments are approximately 5 inches long, a total error of

from 1/16 to 1/8 inch in the totalizer result would create a 1.25 to 2.5 per cent error in the indicated probability.

Thus the analysis has shown that the random variations in transmission loss with distance are normally distributed over intervals of approximately 0.2 mile and 0.5 mile.

Figures 4.30 through 4.34 provide a summary of a detailed analysis of vehicular data for a range of 0.2 to 17 miles along Radial A at 880 kc, vertical polarization. The transmitting antenna was an 80-foot top-loaded vertical mast and the receiving antenna was a vehicle-mounted whip whose top was 7 feet above the ground. Figure 4.30 gives a plot of the median basic transmission loss as a function of radial distance along with the loss which was exceeded 90 per cent of the time and the loss which was exceeded for 10 per cent of the time. Figure 4.31 provides a plot of the standard deviation within each sampling interval as a function of radial distance from the transmitting antenna. Figure 4.32 is a comparison between the reduced vehicular data and the median field point data taken with the same 80-foot transmitting antenna and a 20-foot receiving antenna. Figure 4.33 gives a comparison between the reduced vehicular data and the theoretical smooth-earth basic transmission loss. Figure 4.34 gives a comparison between the reduced vehicular data and the theoretical smooth-earth basic transmission loss plus 9 db.

Figures 4.35 through 4.39 present a similar summary for one series of vehicular measurements made at 6 mc.

Figures 4.40 through 4.44 provide a summary of results for one series of vehicular measurements made at 12 mc.

At 25.5 mc, a number of different series of reduced vehicular measurements are given. Figures 4.45 through 4.48

pertain to vertical polarization and a transmitting antenna height of 40 feet. Figures 4.49 through 4.58 pertain to vertical polarization and a transmitting antenna height of 80 feet. Following sets pertain to horizontal polarization at 25.5 mc and transmitting antenna heights of 13, 40 and 80 feet.

At 25.5 mc comparisons between vehicular data and the Egli Model described in Section 4.2.2.4 have been made in Figures 4.48, 4.54, 4.62, 4.66 and 4.70. The comparison at 25.5 mc is not good, but the difference is consistent with the questions raised in Section 4.2.2.4 concerning the foliage factor at 25.5 mc. The comparisons between the Egli Model and vehicular data were better at the higher frequencies, as will be seen shortly.

Comparisons between vehicular data and the NBS model are also possible beginning at 25.5 mc. A sample of the comparison between vehicular data and the NBS model with the $G(\bar{H})$ functions is shown in Figure 4.57.

Samples of the comparison between vehicular data and the NBS model without the $G(\bar{H})$ functions appear in Figure 4.58.

Figure 4.55 compares vehicular data and the median of the computer-induced statistic, including the $G(\bar{H})$ functions, while Figure 4.56 provides the same comparison for the computer-induced statistic which excludes the $G(\bar{H})$ functions.

Figures 4-71 through 4-80 illustrate the analysis details for one series of vehicular data at 50 mc, vertical polarization.

For 100 mc, as was the case at 25.5 mc, the results from several series of vehicular data are presented.

Figures 4-81 through 4-84 pertain to vertical polarization and a transmitting antenna height of 13 feet. Figures 4-85 through 4-88 are for a transmitting height of 40 feet and Figures 4-89 through 4-98 pertain to a height of 80 feet.

Figures 4-99 through 4-114 are concerned with horizontal polarization at 100 mc and transmitting antenna heights of 13, 40 and 80 feet.

Figures 4-115 through 4-124 apply to one sample of vehicular data at 250 mc, vertical polarization.

The comparisons between field point data and vehicular data have consistently shown good correlation.

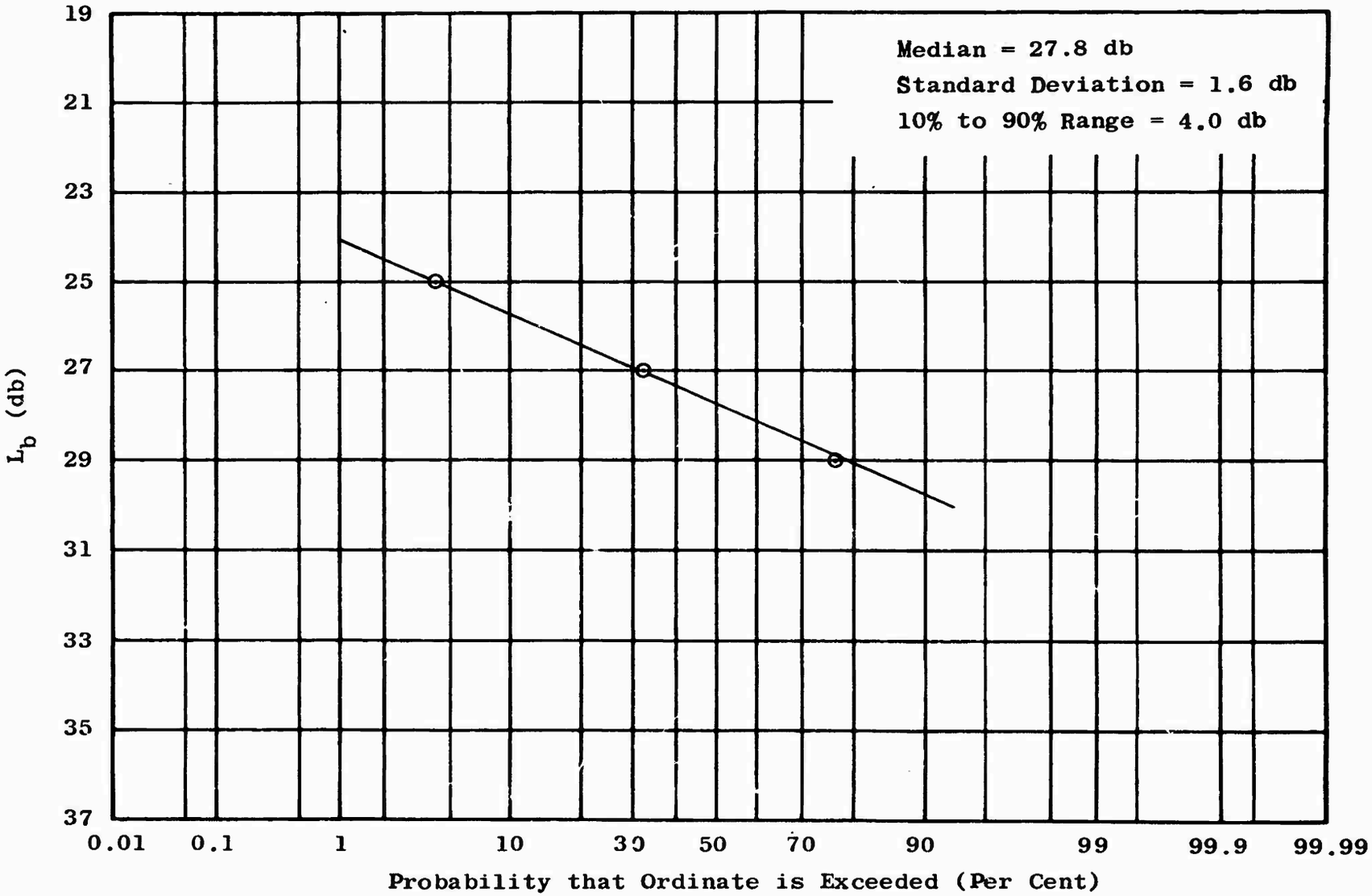

Figure 4.29A Statistical Distribution of L_b
$L_b = F_A(0.880, 80, V, 0.2\text{-}0.4, 7)$

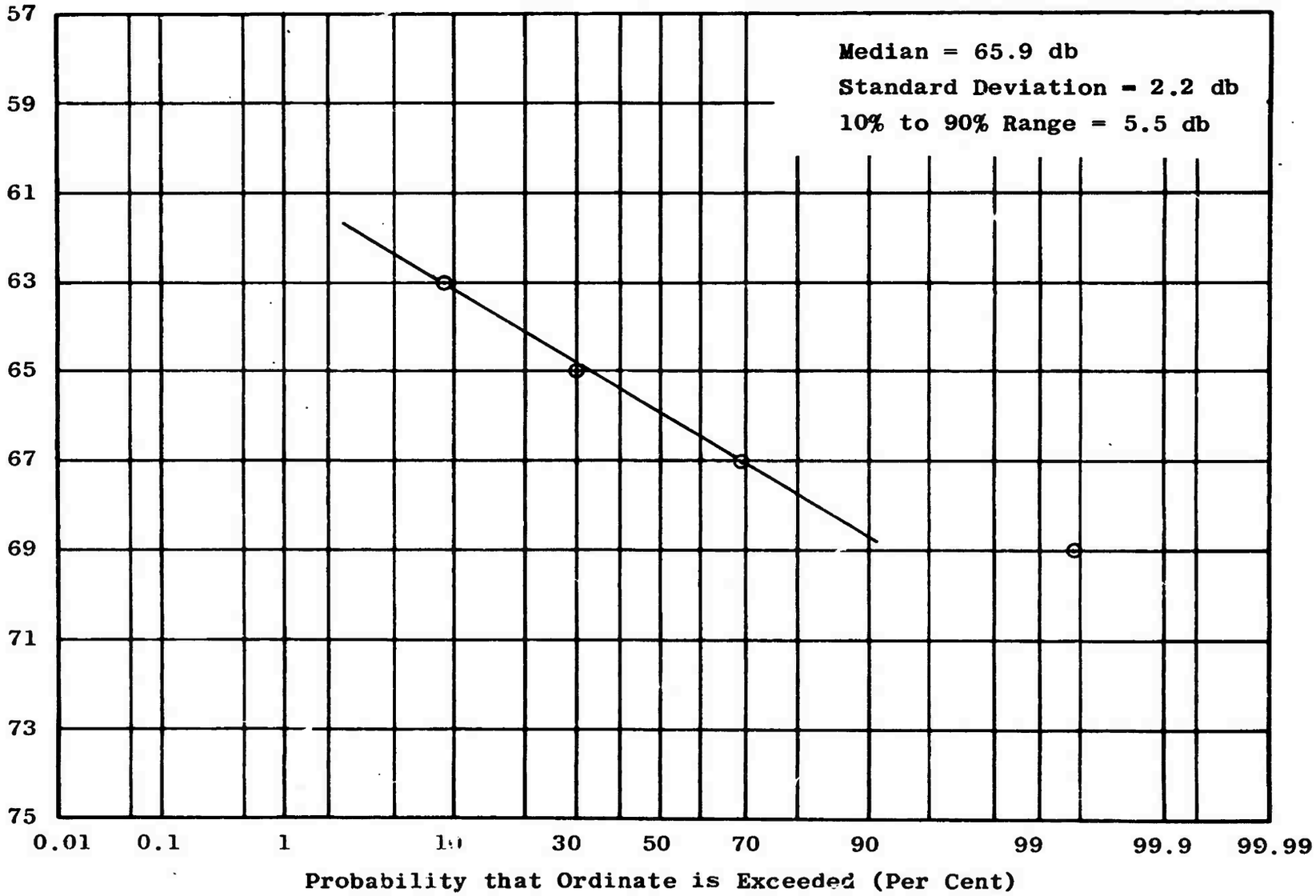

Figure 4.29B Statistical Distribution of L_b
$L_b = F_A(0.880, 80, V, 3.5\text{-}4.0, 7)$

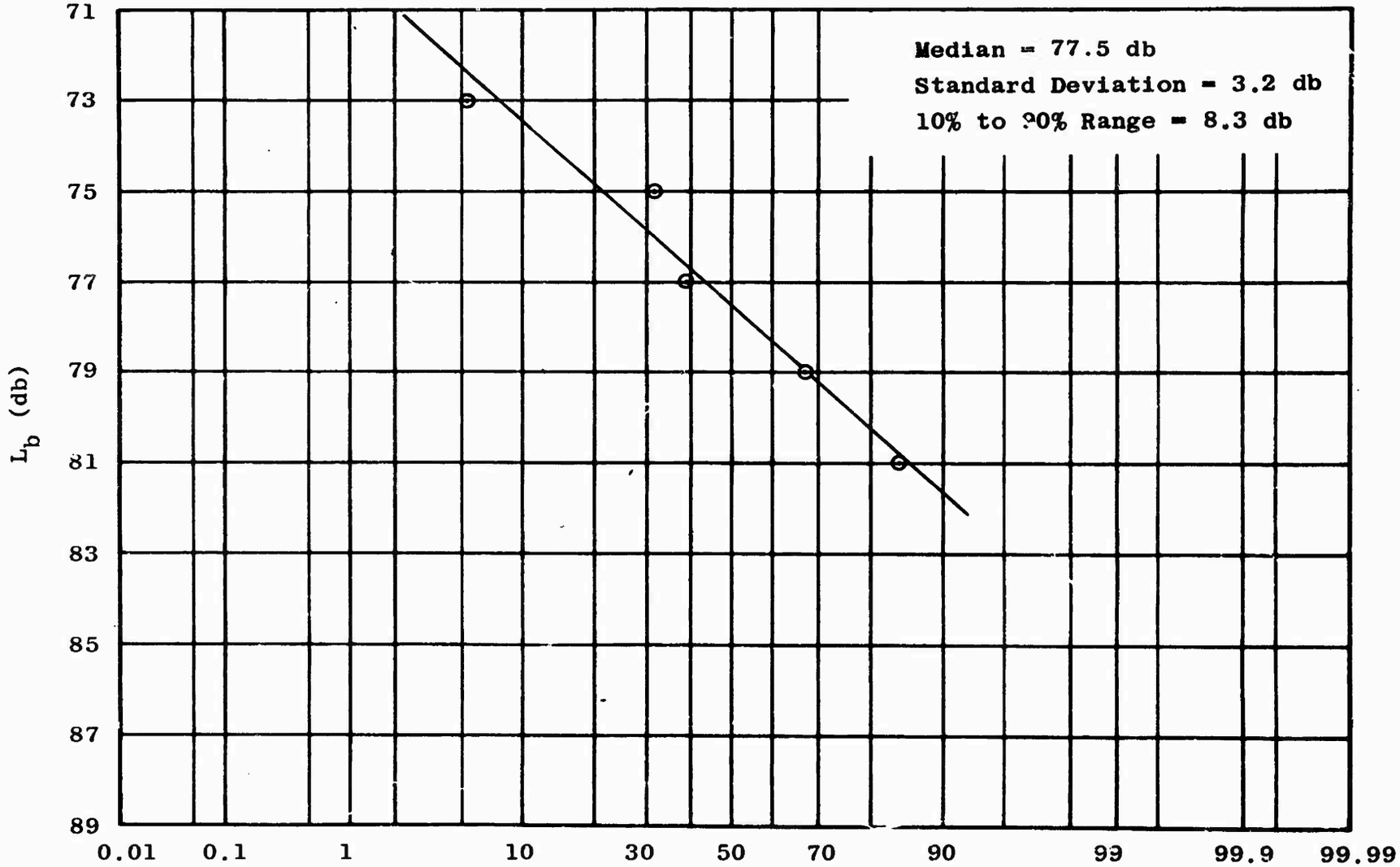

Figure 4.29C Statistical Distribution of L_b
$L_b = F_A(6.0, 40, V, 0.4\text{-}0.6, 7)$

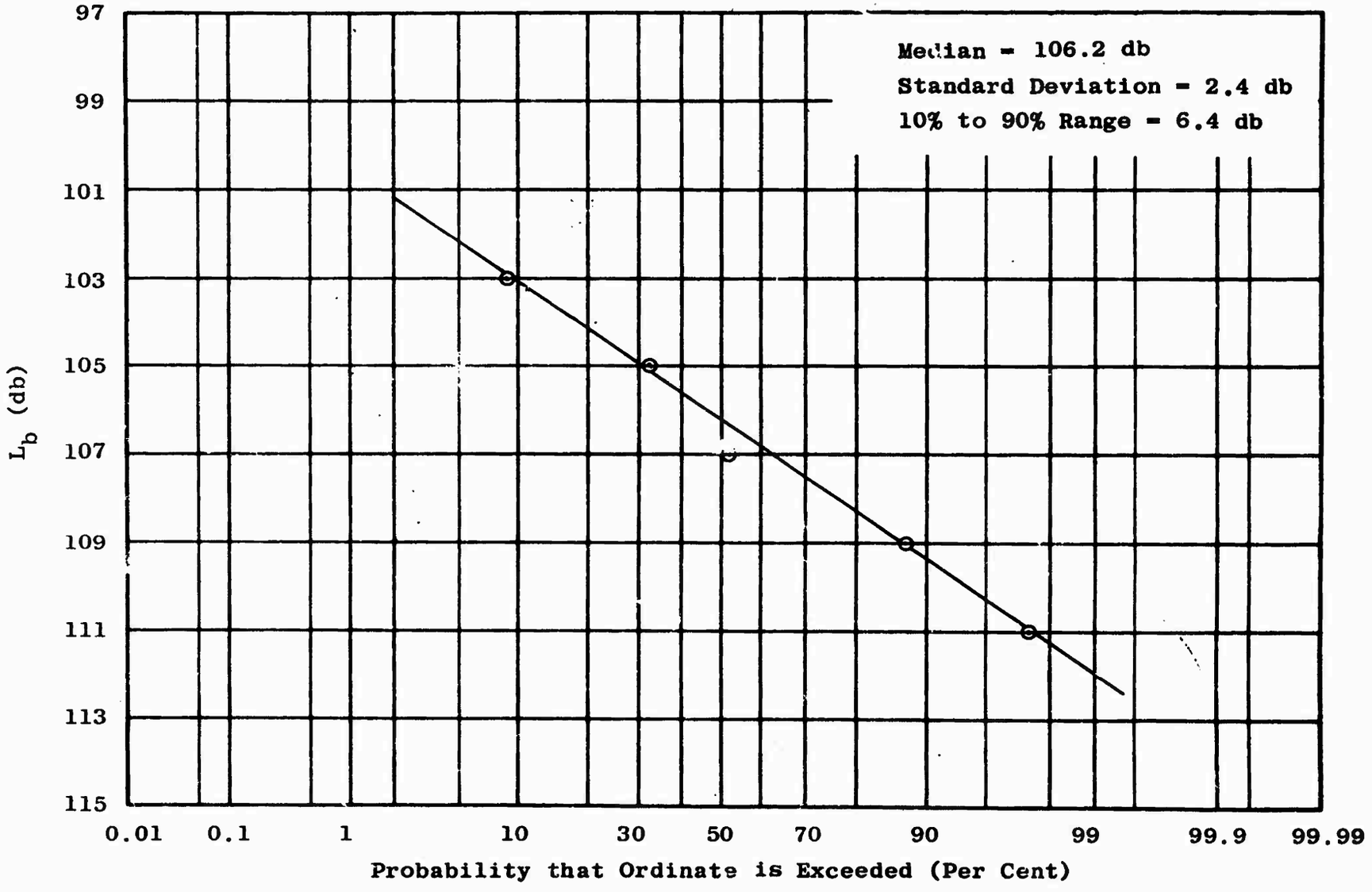

Figure 4.29D Statistical Distribution of L_b
$L_b = F_A(6.0, 40, V, 3.0\text{-}3.2, 7)$

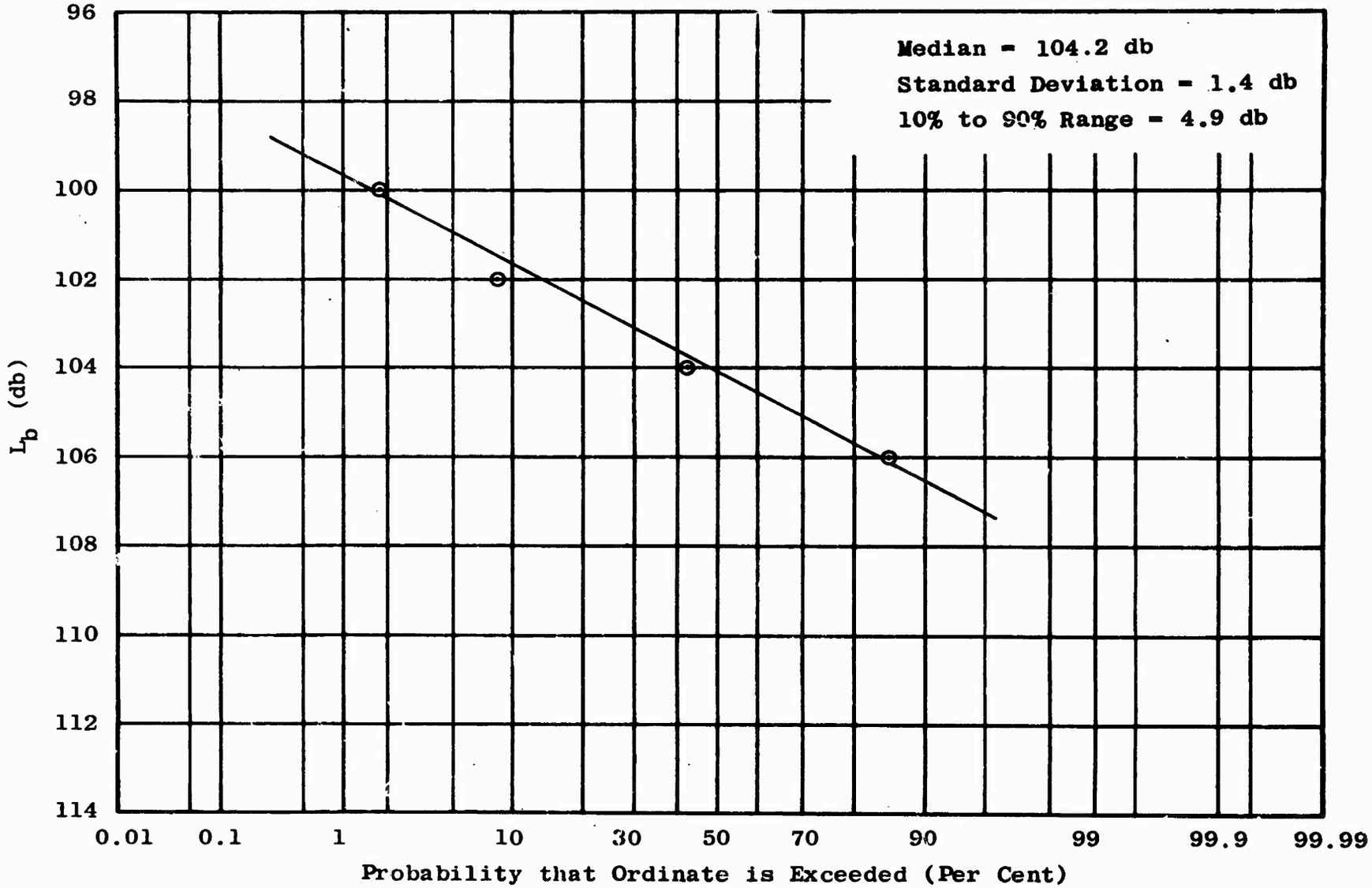

Figure 4.29E Statistical Distribution of L_b
$L_b = F_A(12.1, 21, V, 0.8\text{-}1.0, 7)$

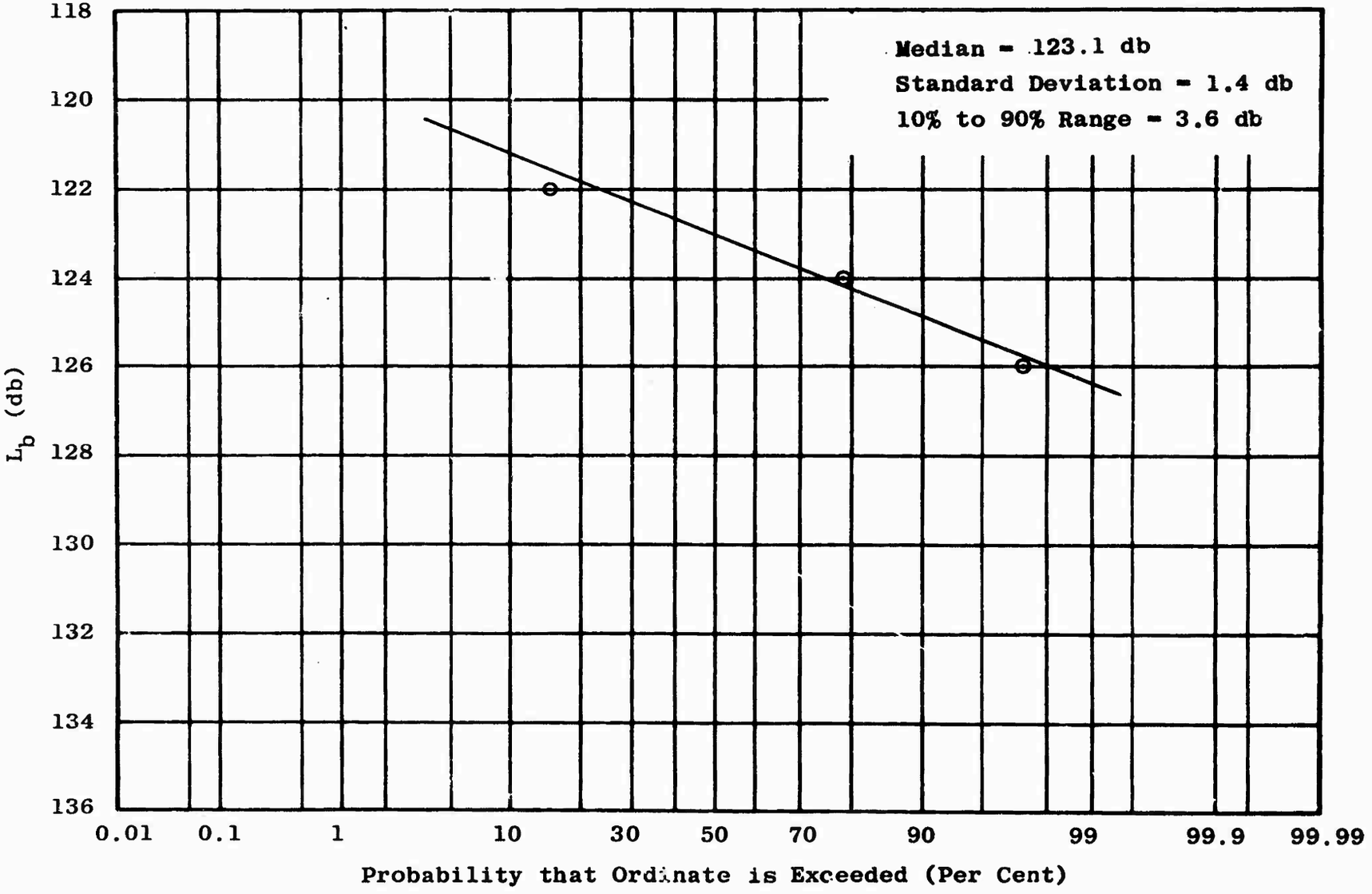

Figure 4.29F Statistical Distribution of L_b
$L_b = F_A(12.1, 21, V, 2.8\text{-}3.0, 7)$

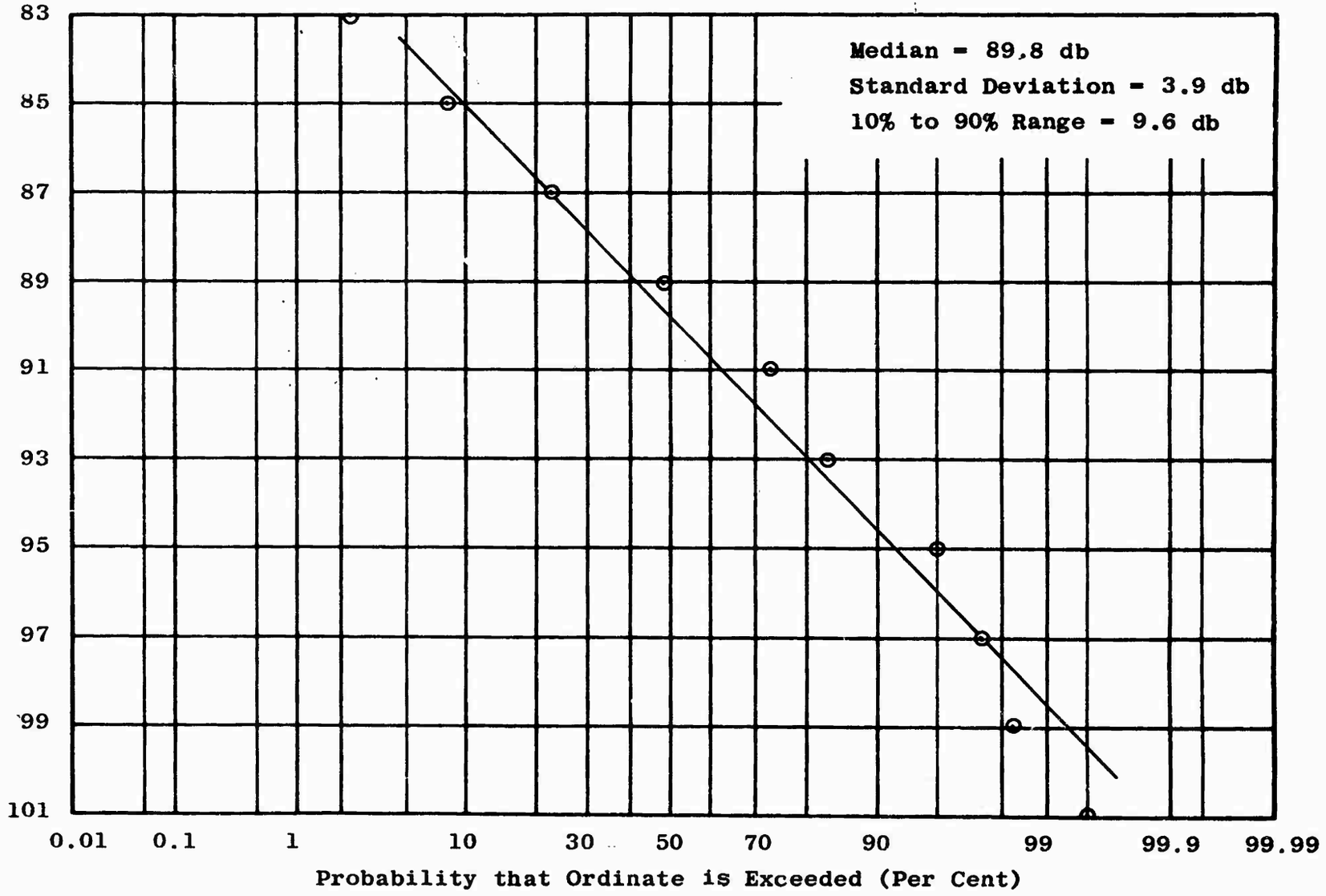

Figure 4.29G Statistical Distribution of L_b
$L_b = F_A(25.5, 80, V, 0.4\text{-}0.6 \text{ mi}, 7)$

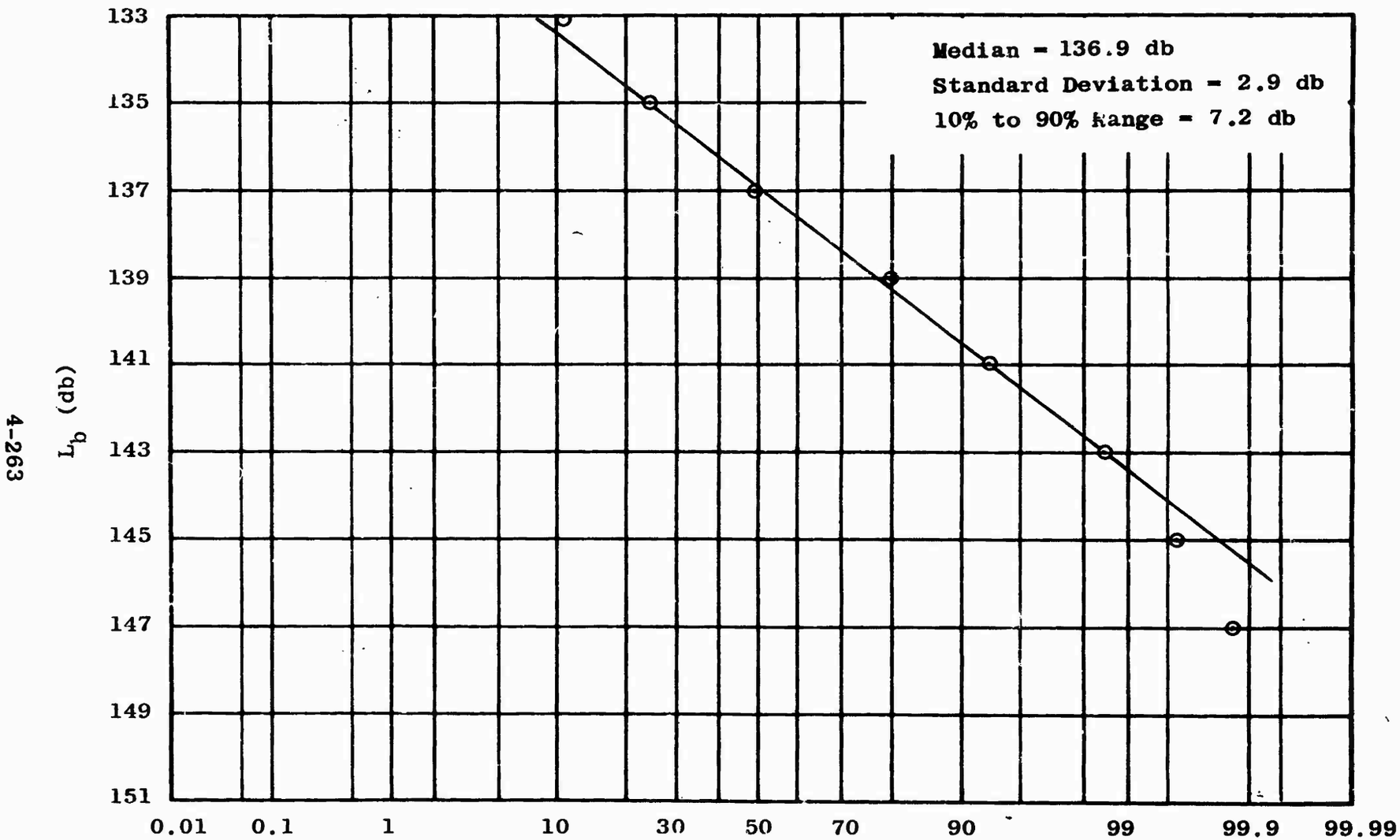

Figure 4.29H Statistical Distribution of L_b
$L_b = F_A(25.5, 80, V, 9.0\text{-}9.5, 7)$

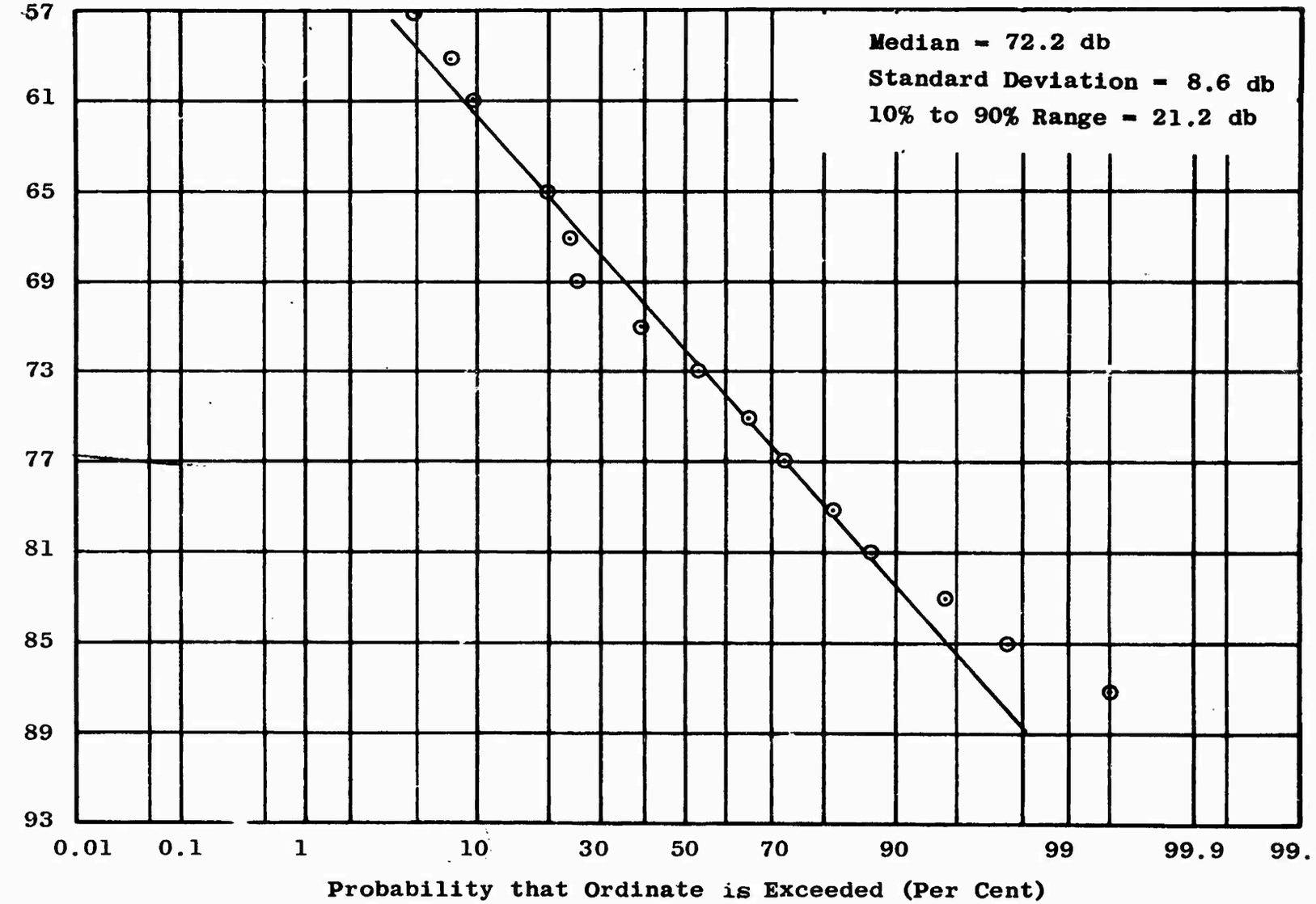

Figure 4.29I Statistical Distribution of L_b
$L_b = F_A(50, 80, V, 0.0\text{-}0.2, 7)$

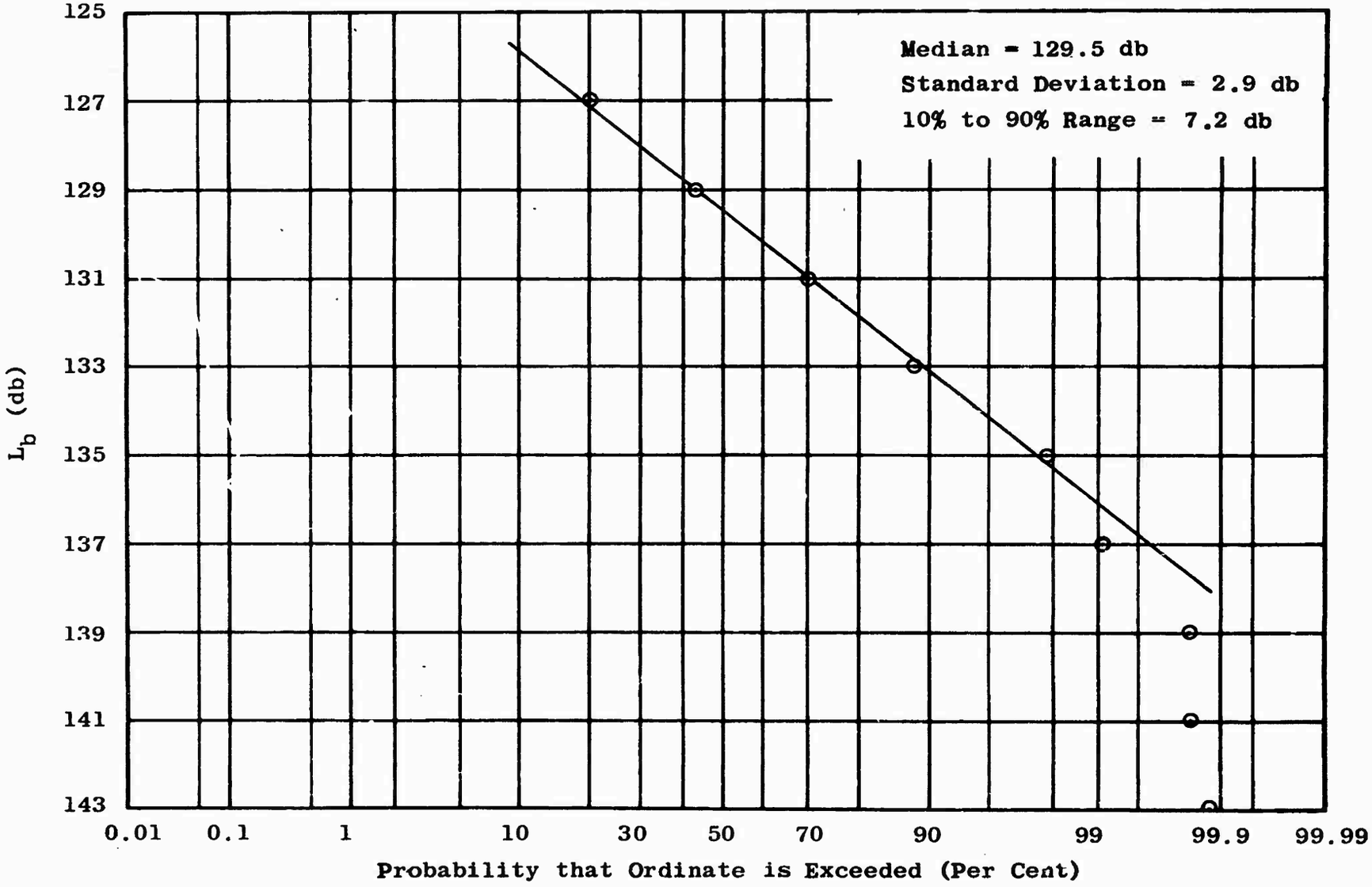

Figure 4.29J Statistical Distribution of L_b
$L_b = F_A(50, 80, V, 4.0\text{-}4.5, 7)$

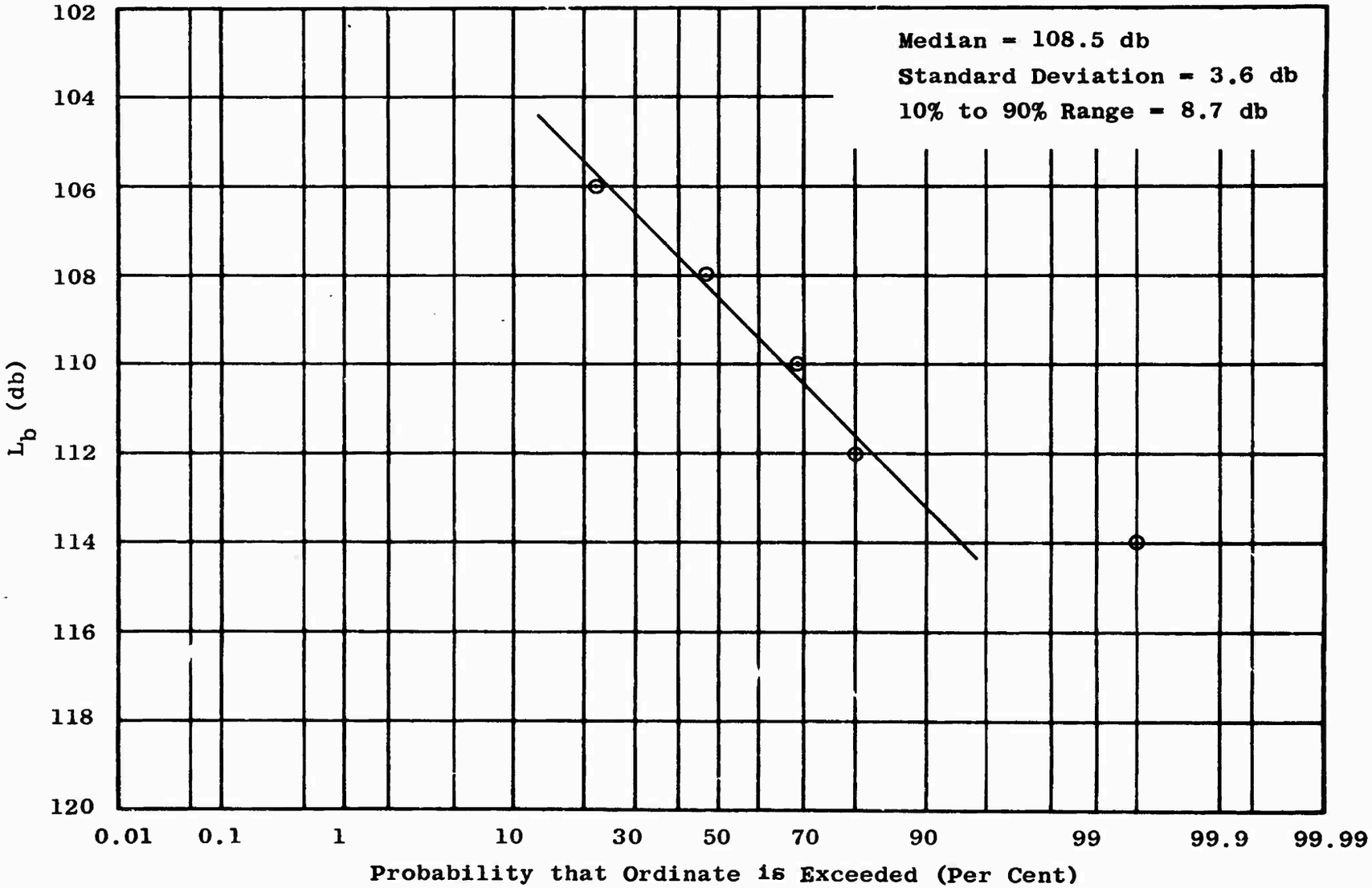

Figure 4.29K Statistical Distribution of L_b
$L_b = F_A(100, 80, V, 0.6\text{-}0.8, 7)$

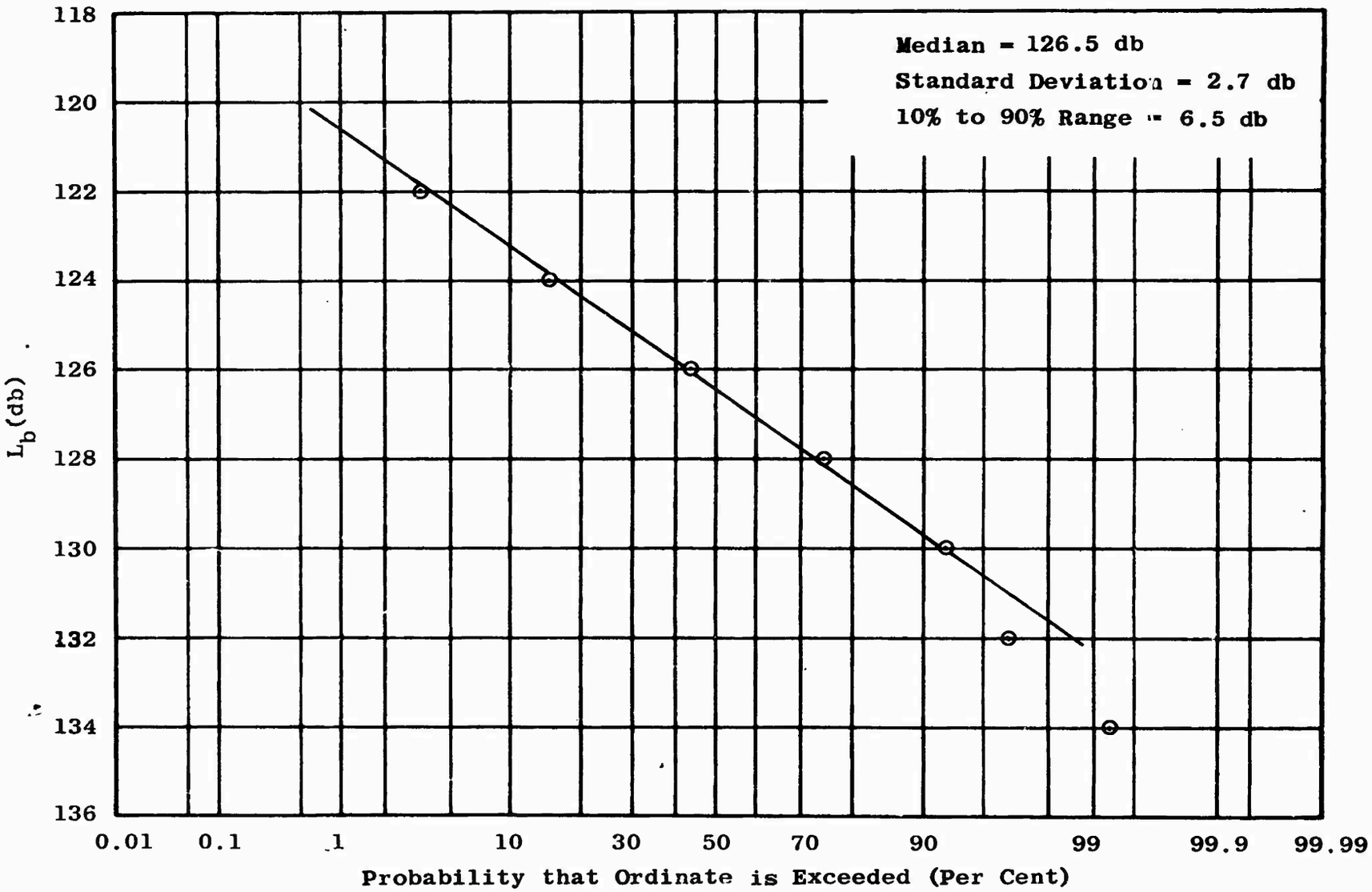

Figure 4.29L Statistical Distribution of L_b
$L_b = F_A(100, 80, V, 2.8\text{-}3.0, 7)$

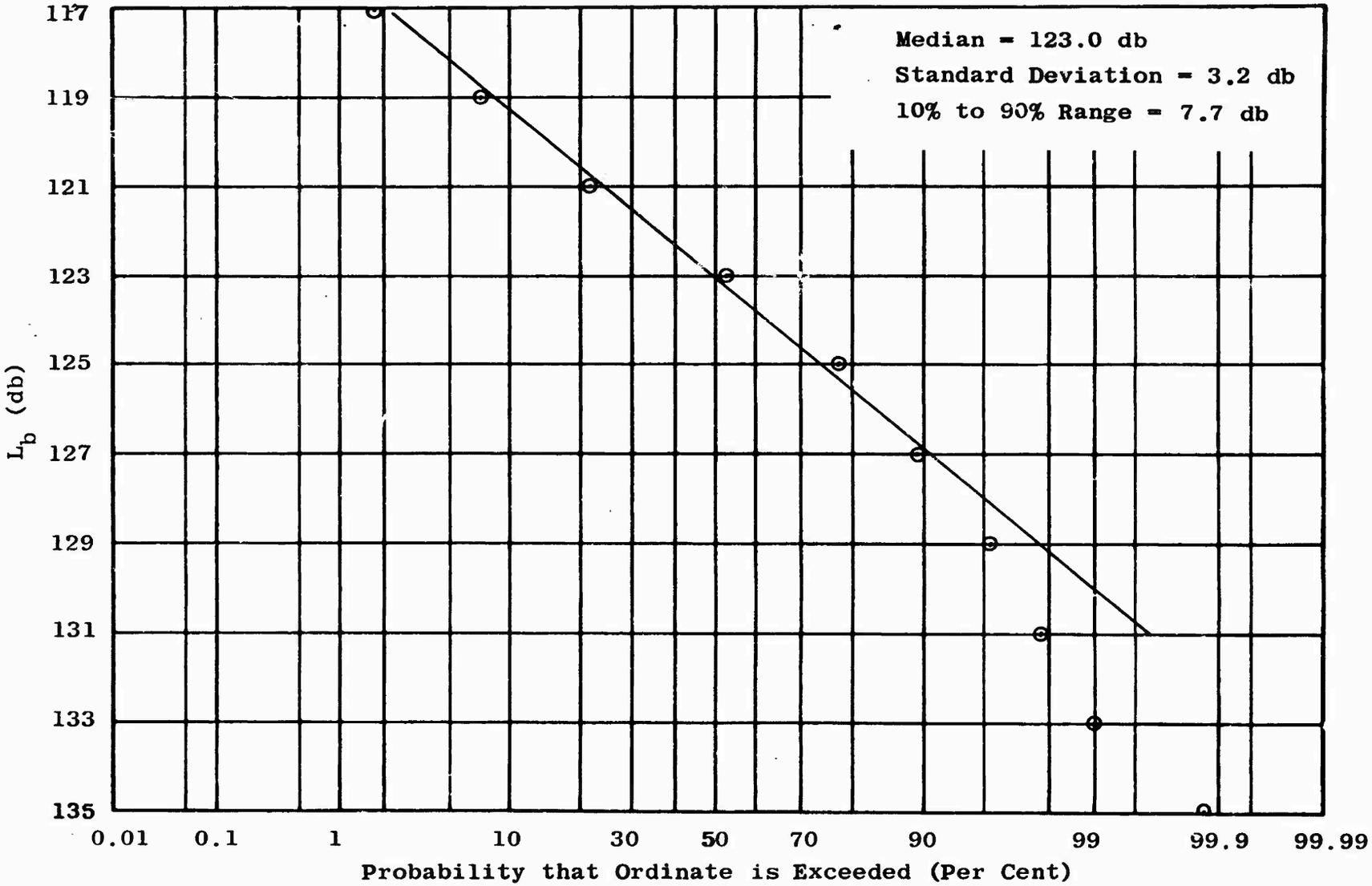

Figure 4.29M Statistical Distribution of L_b
$L_b = F_A(250, 80, V, 0.6\text{-}0.8, 7)$

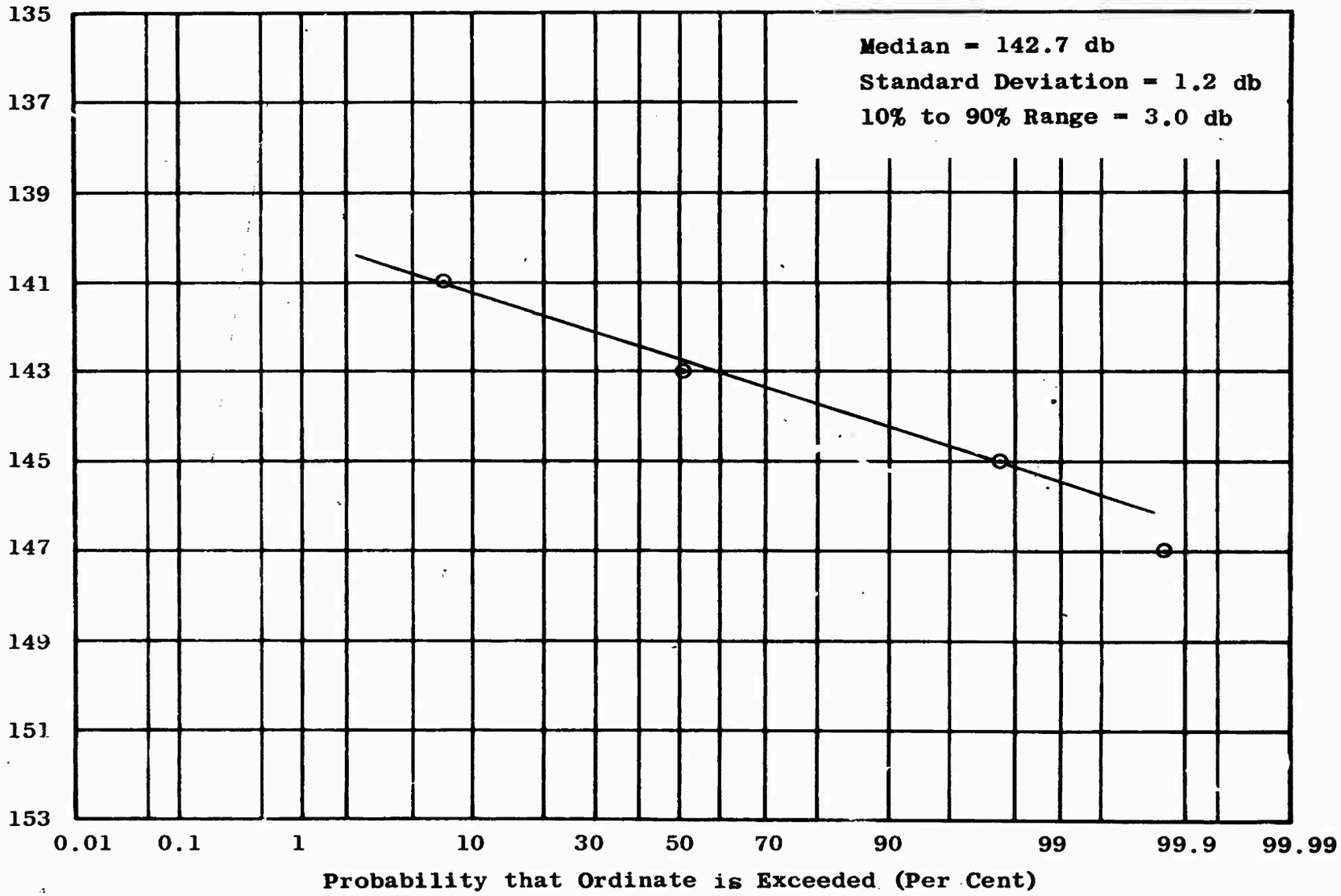

Figure 4.29N Statistical Distribution of L_b
$L_b = F_A(250, 80, V, 2.6\text{-}2.8, 7)$

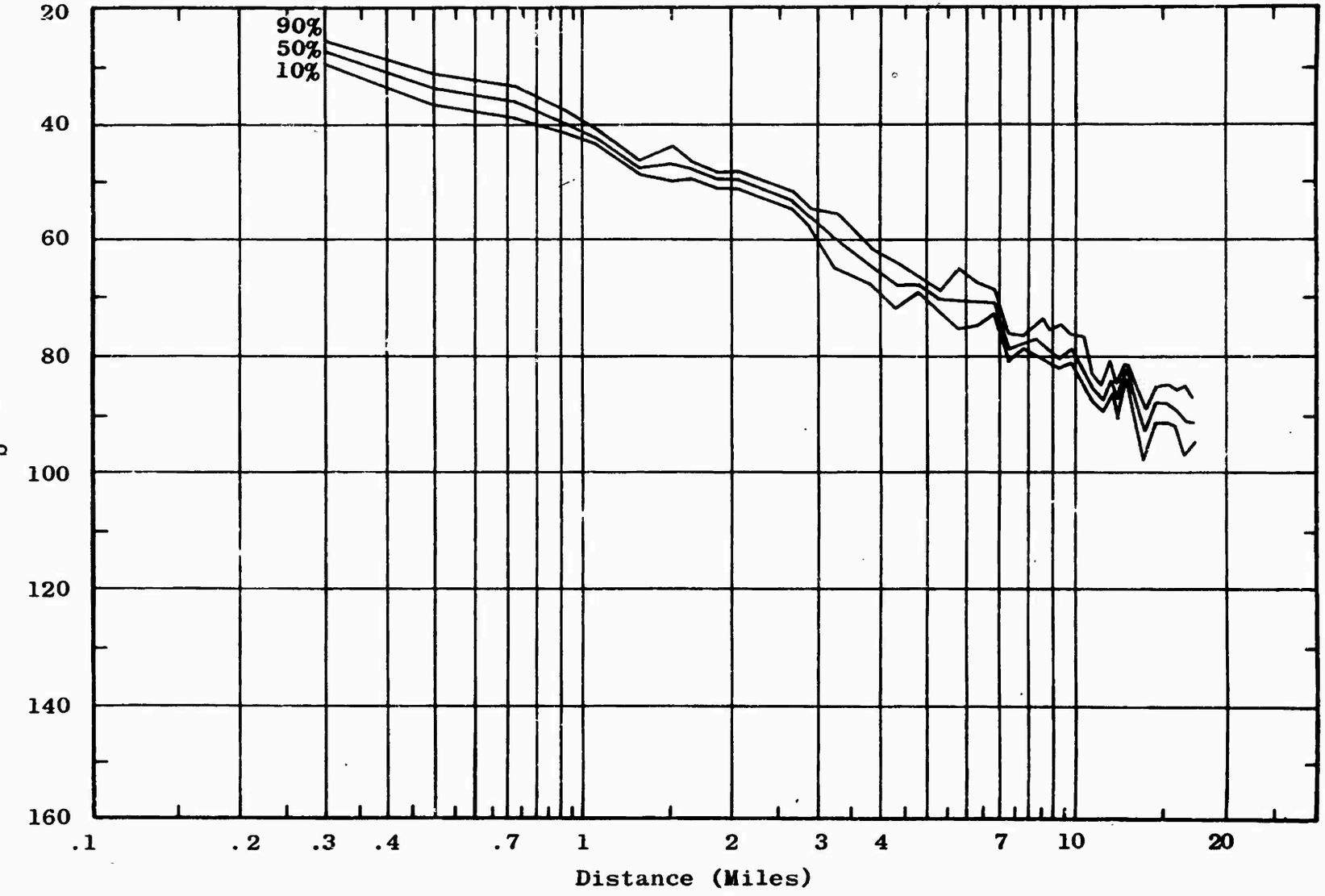

Figure 4.30 Reduced Vehicular Data
$L_b = F_A(0.880, 80, V, d, 7)$

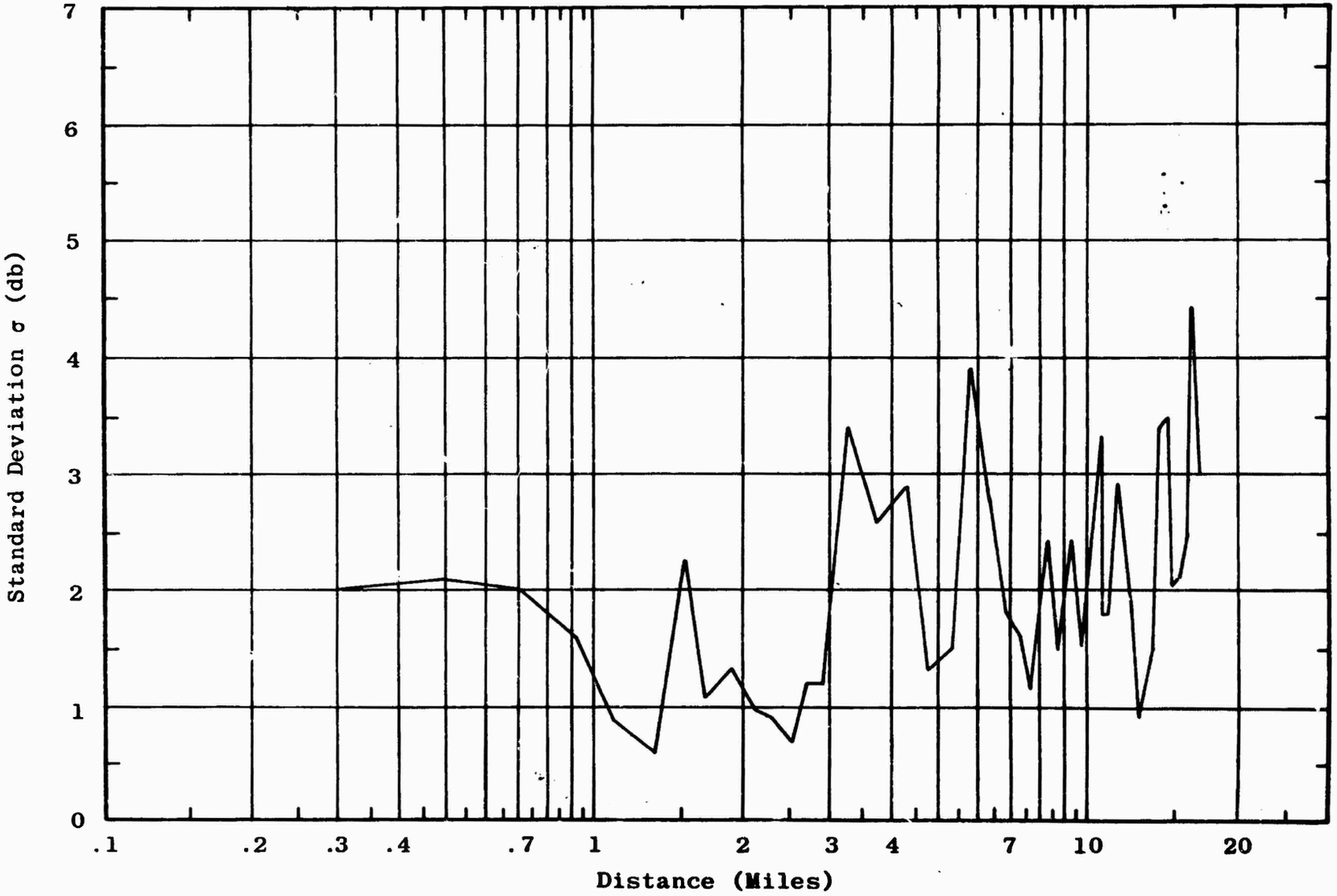

Figure 4.31 Standard Deviation of Vehicular Data
$L_b = F_A(0.880, 80, V, d, 7)$

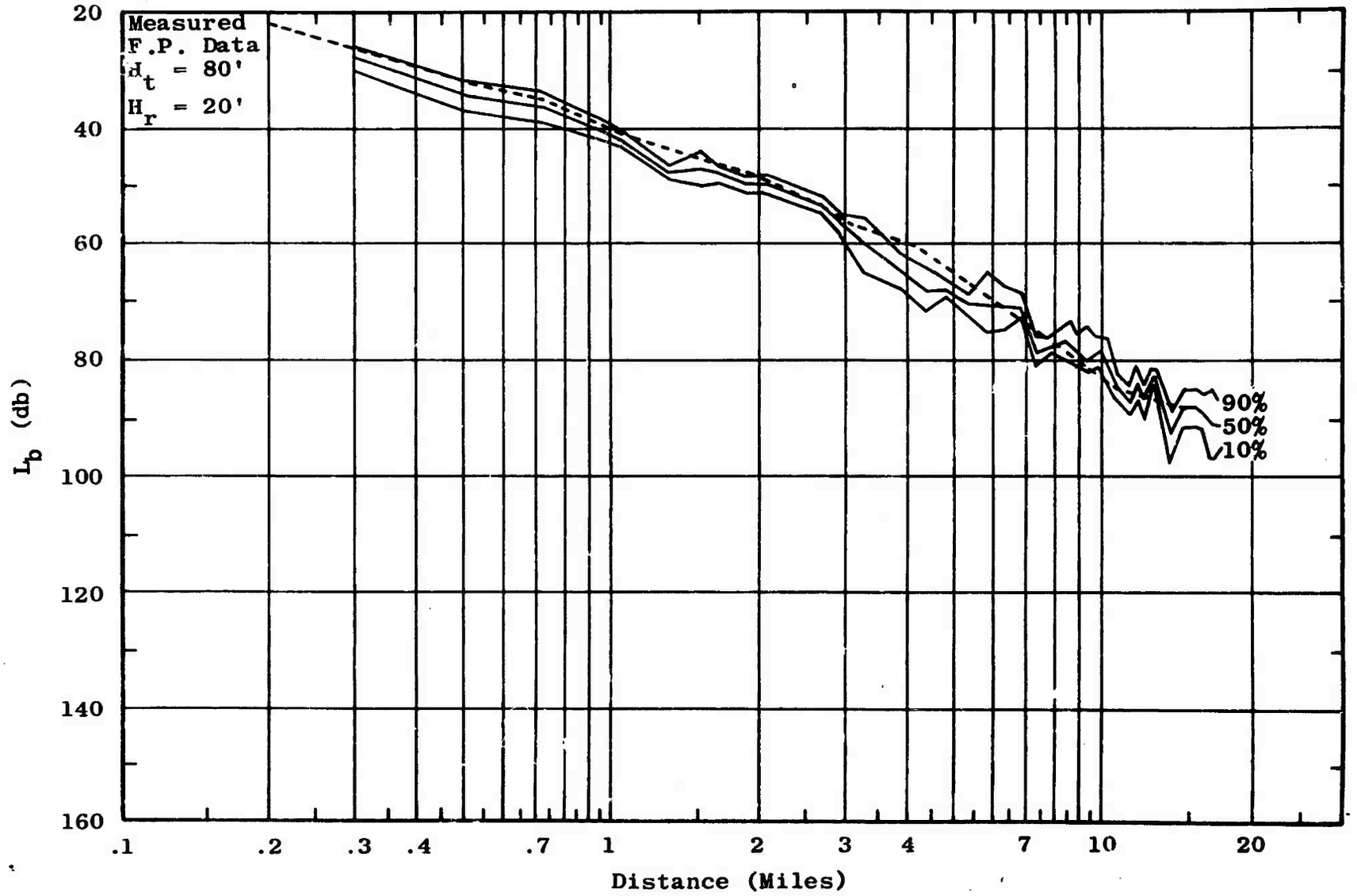

Figure 4.32 Comparison Between Vehicular Data and Measured F.P. Data
$L_b = F_A(0.880, 80, V, d, 7)$

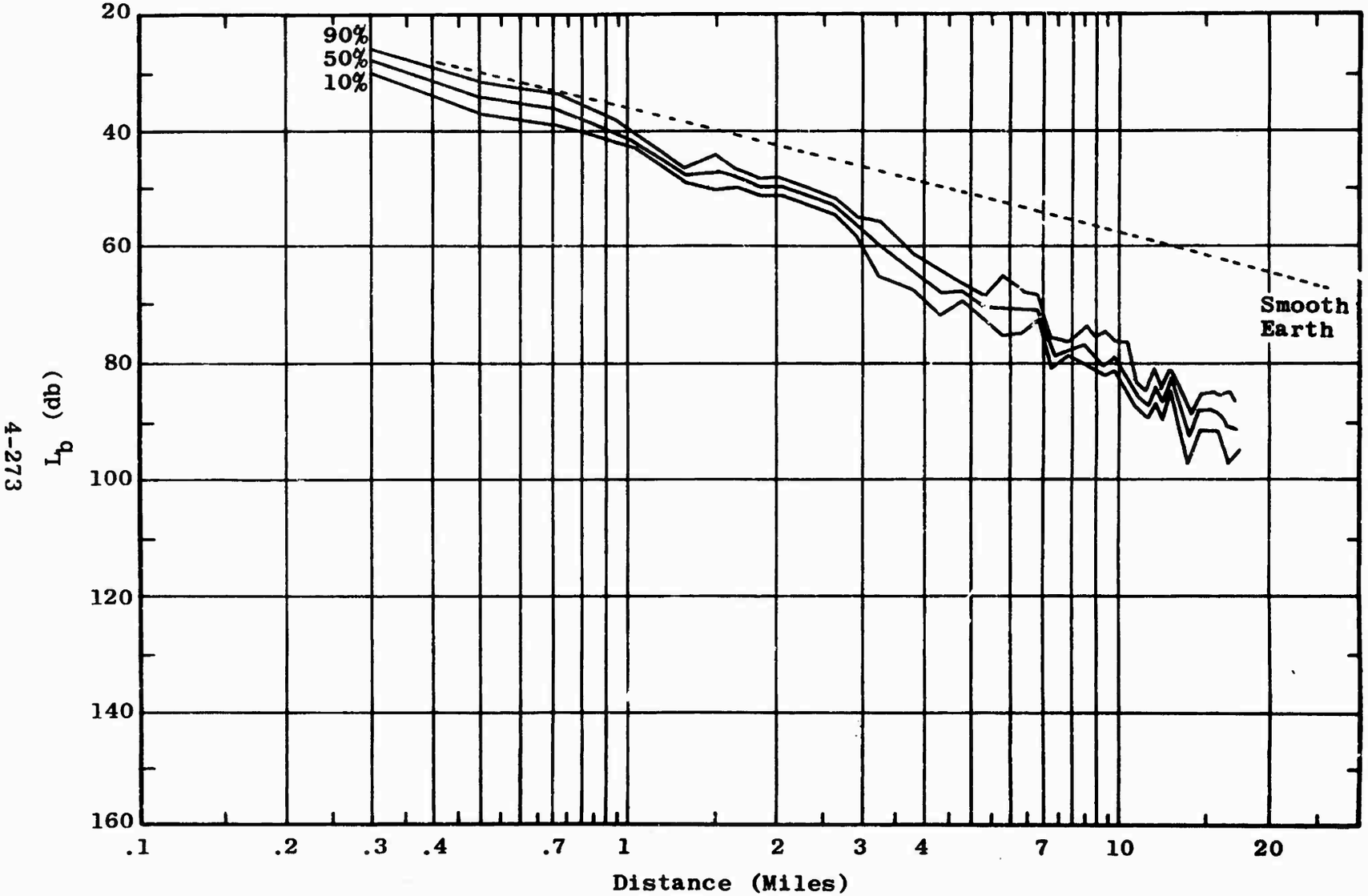

Figure 4.33 Comparison Between Vehicular Data and Theoretical Smooth-Earth Model
$L_b = F_A(0.880, 80, V, d, 7)$

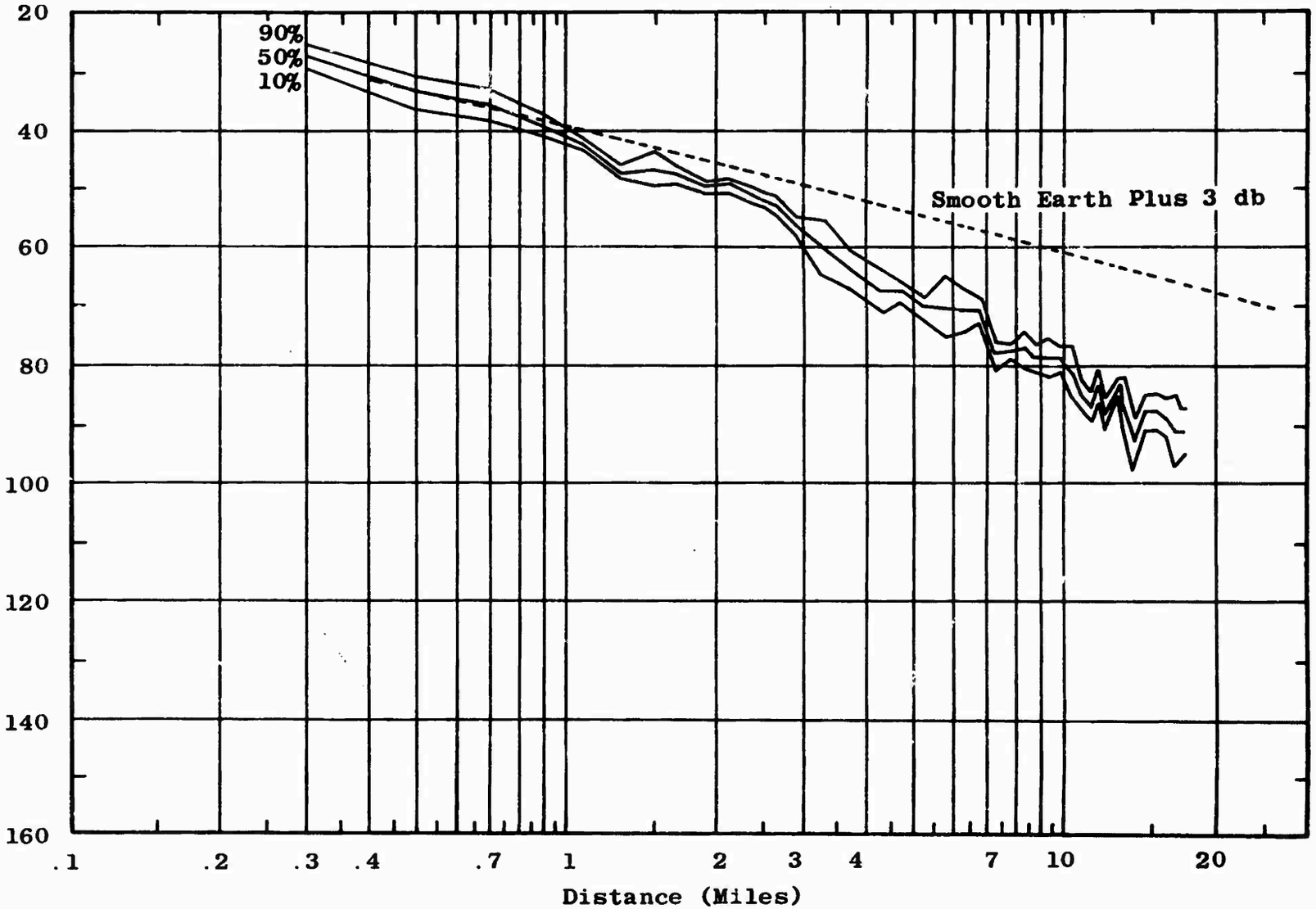

Figure 4.34 Comparison Between Vehicular Data and Theoretical Smooth-Earth Model Plus 9 db
$L_b = F_A(0.880, 80, V, d, 7)$

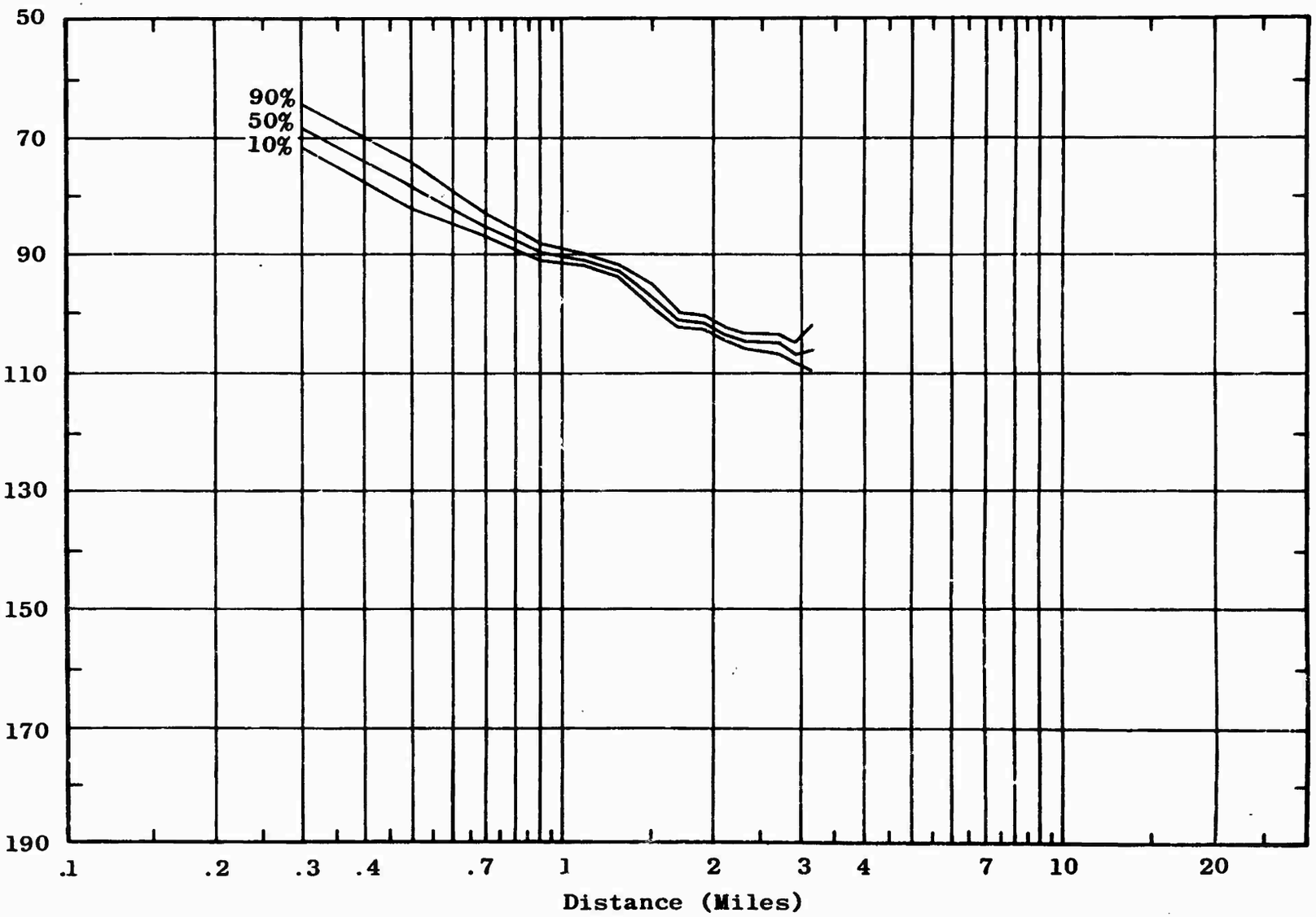

Figure 4.35 Reduced Vehicular Data
$L_b = F_A(6.0, 40, V, d, 7)$

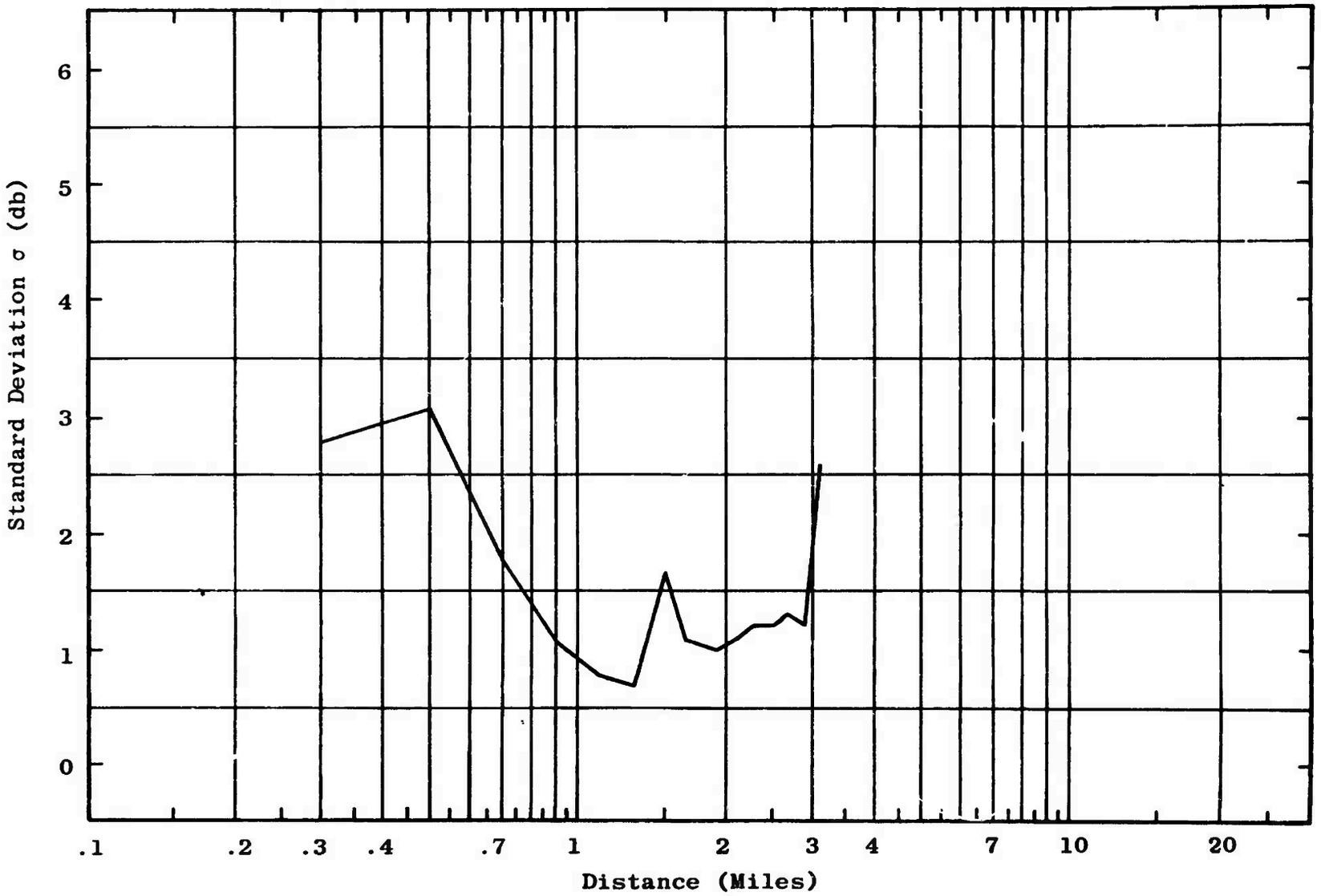

Figure 4.36 Standard Deviation of Vehicular Data
$L_b = F_A(6.0, 40; V, d, 7)$

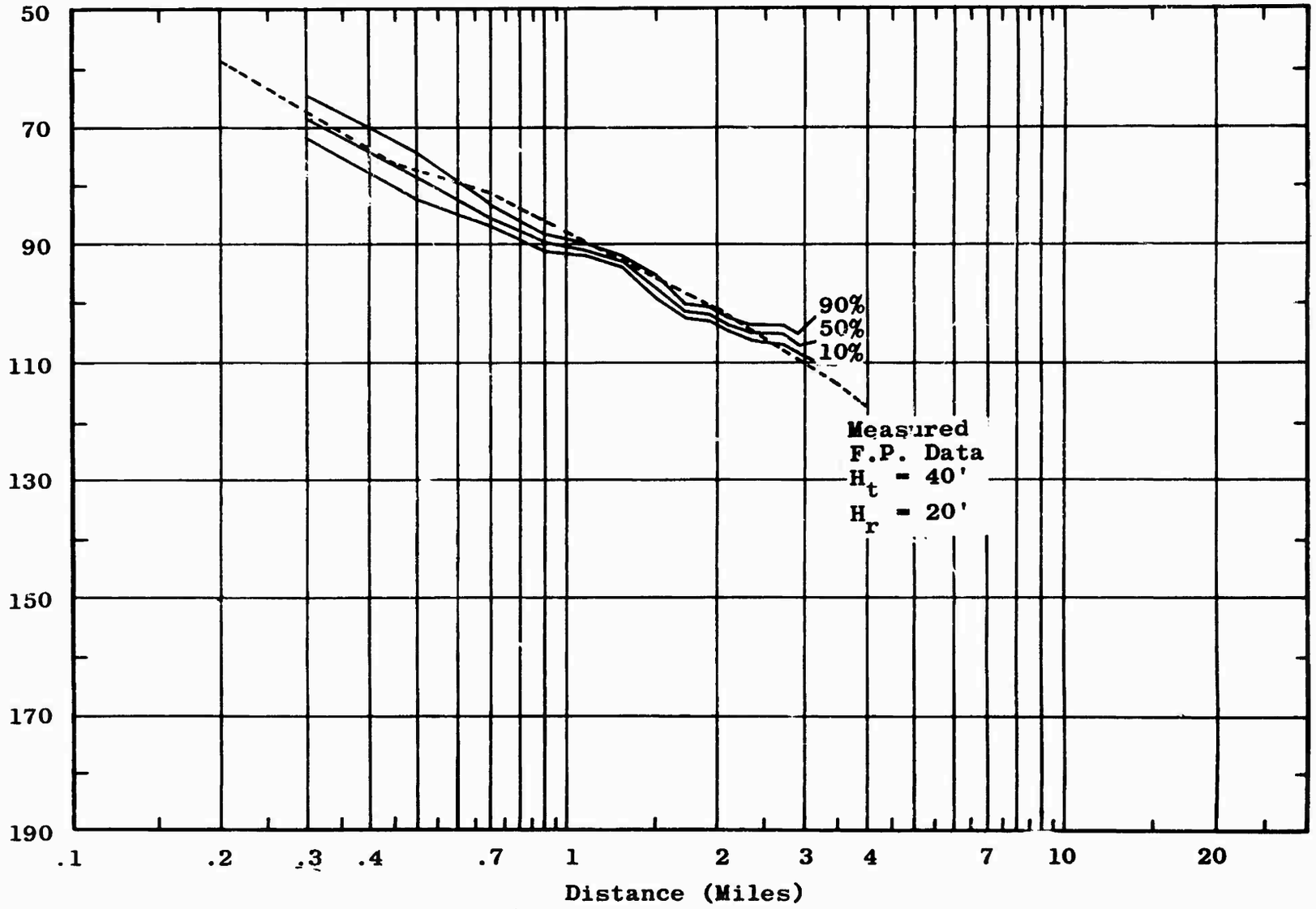

Figure 4.37 Comparison Between Vehicular Data and Measured F.P. Data
$L_b = F_A(6.0, 40, V, d, 7)$

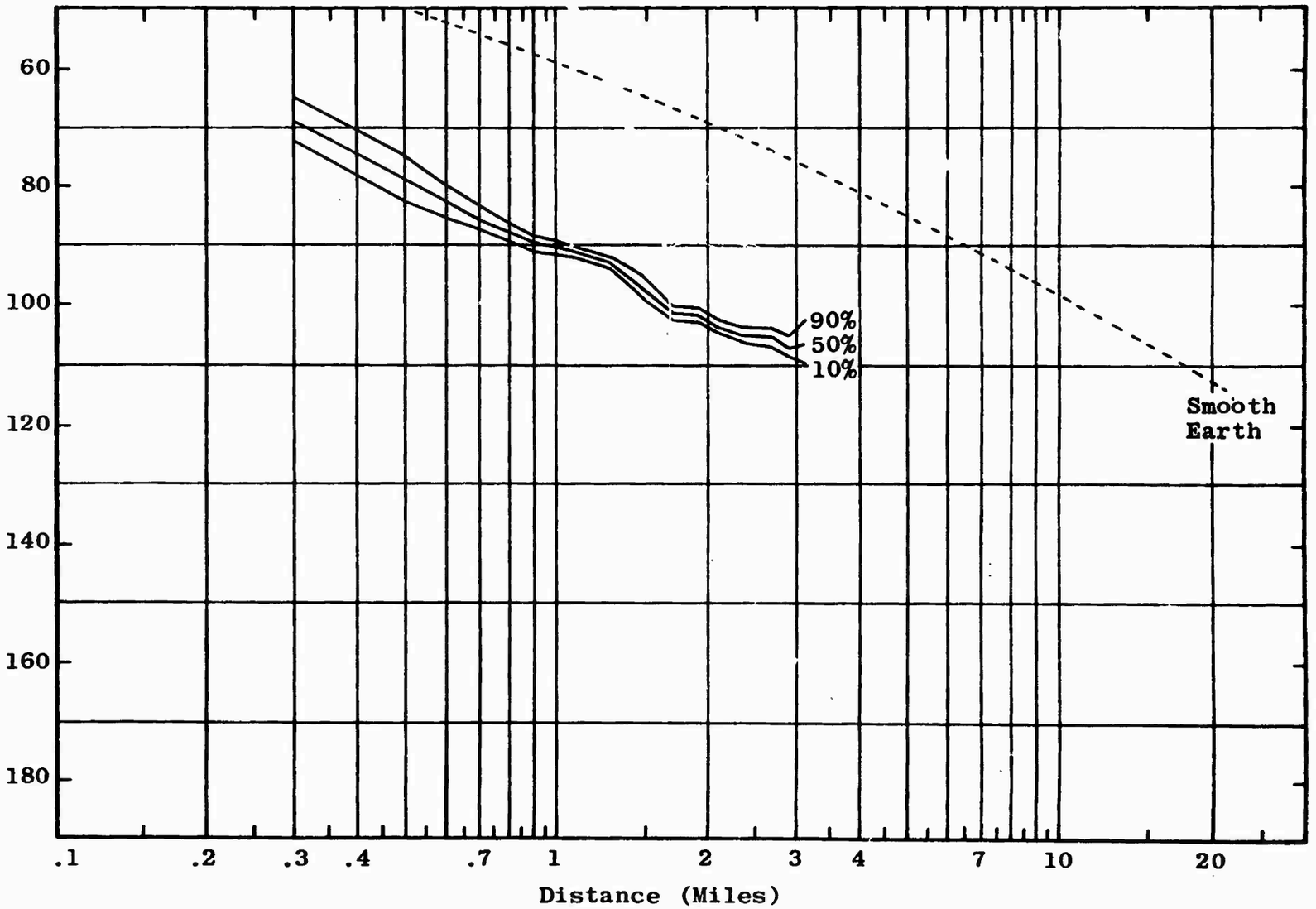

Figure 4.38 Comparison Between Vehicular Data and Theoretical Smooth-Earth Model
$L_b = F_A(6.0, 40, V, d, 7)$

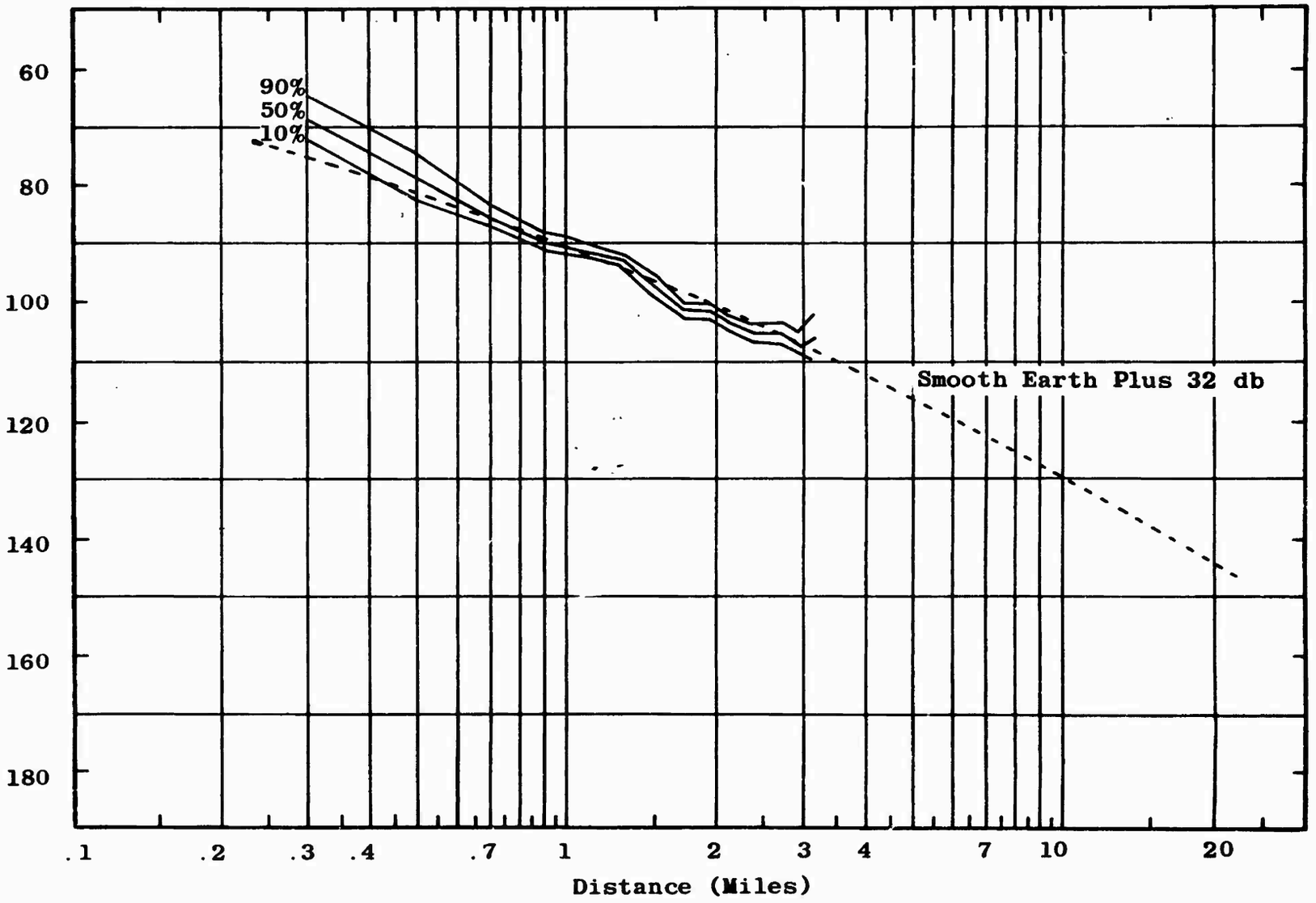

Figure 4.39 Comparison Between Vehicular Data and Theoretical Smooth-Earth Model Plus 30 db
$L_b = F_A(6.0, 40, V, d, 7)$

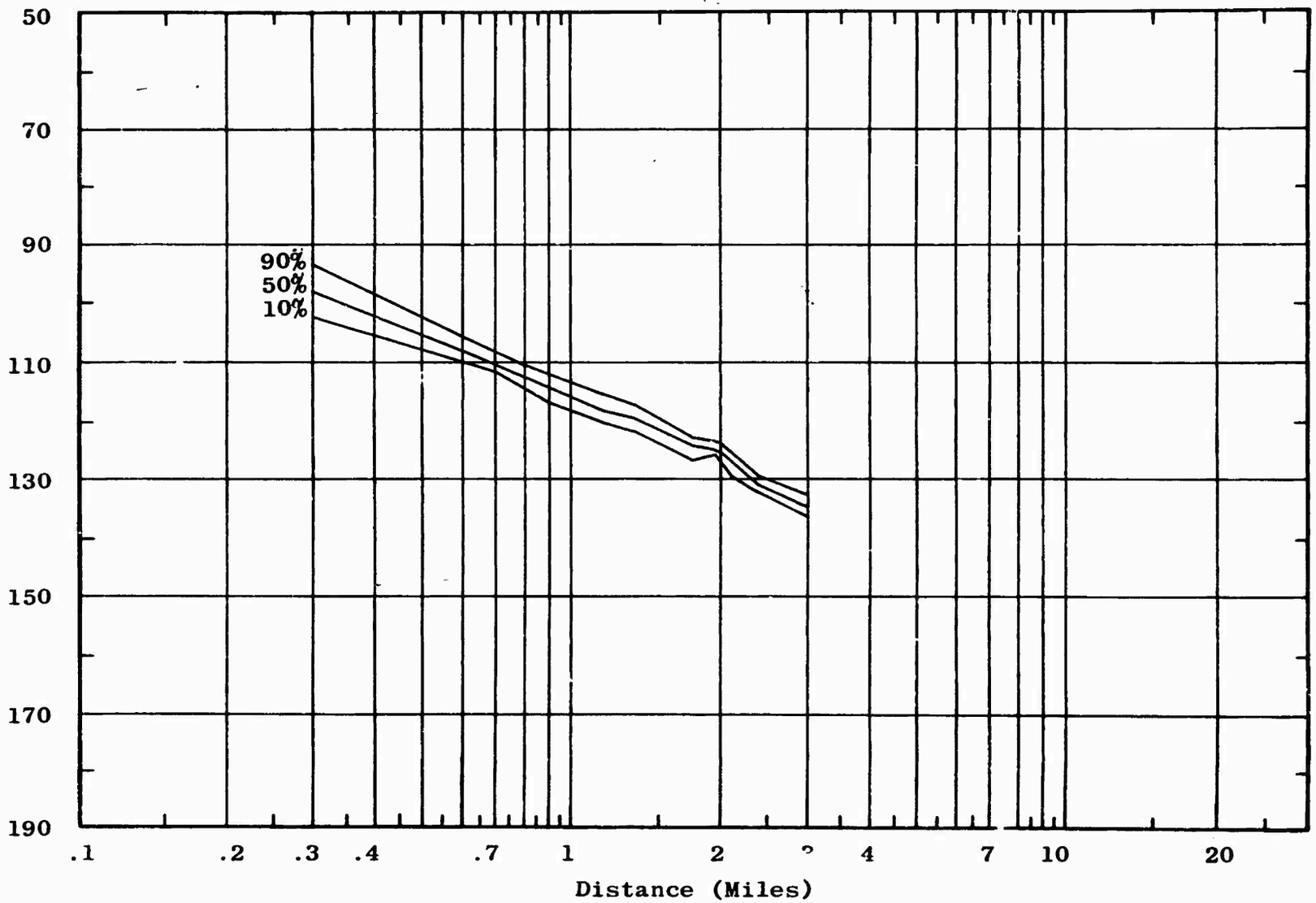

Figure 4.40 Reduced Vehicular Data
$L_b = F_A(12.1, 21, V, d, 7)$

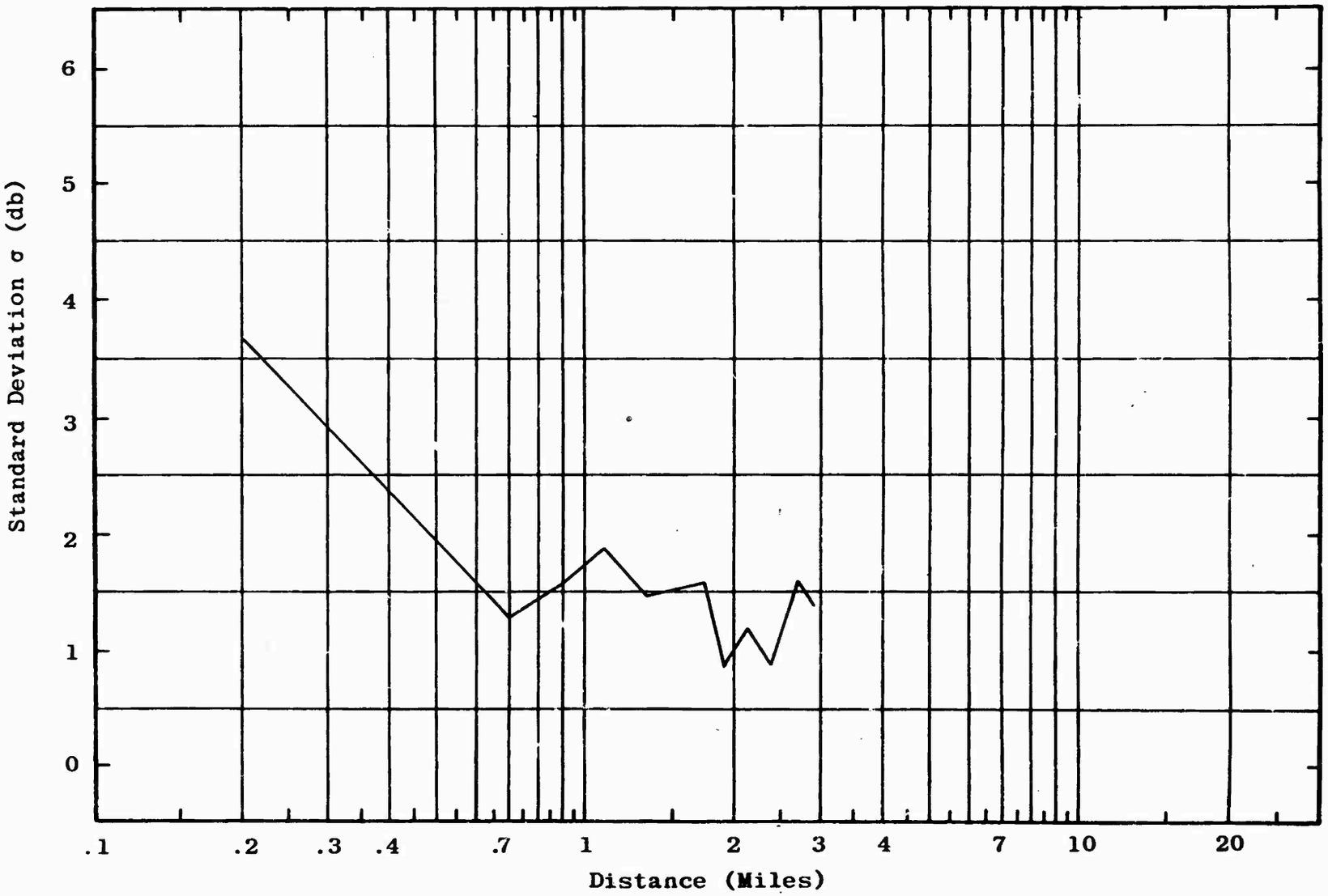

Figure 4.41 Standard Deviation of Vehicular Data
$L_b = F_A(12.1, 21, V, d, 7)$

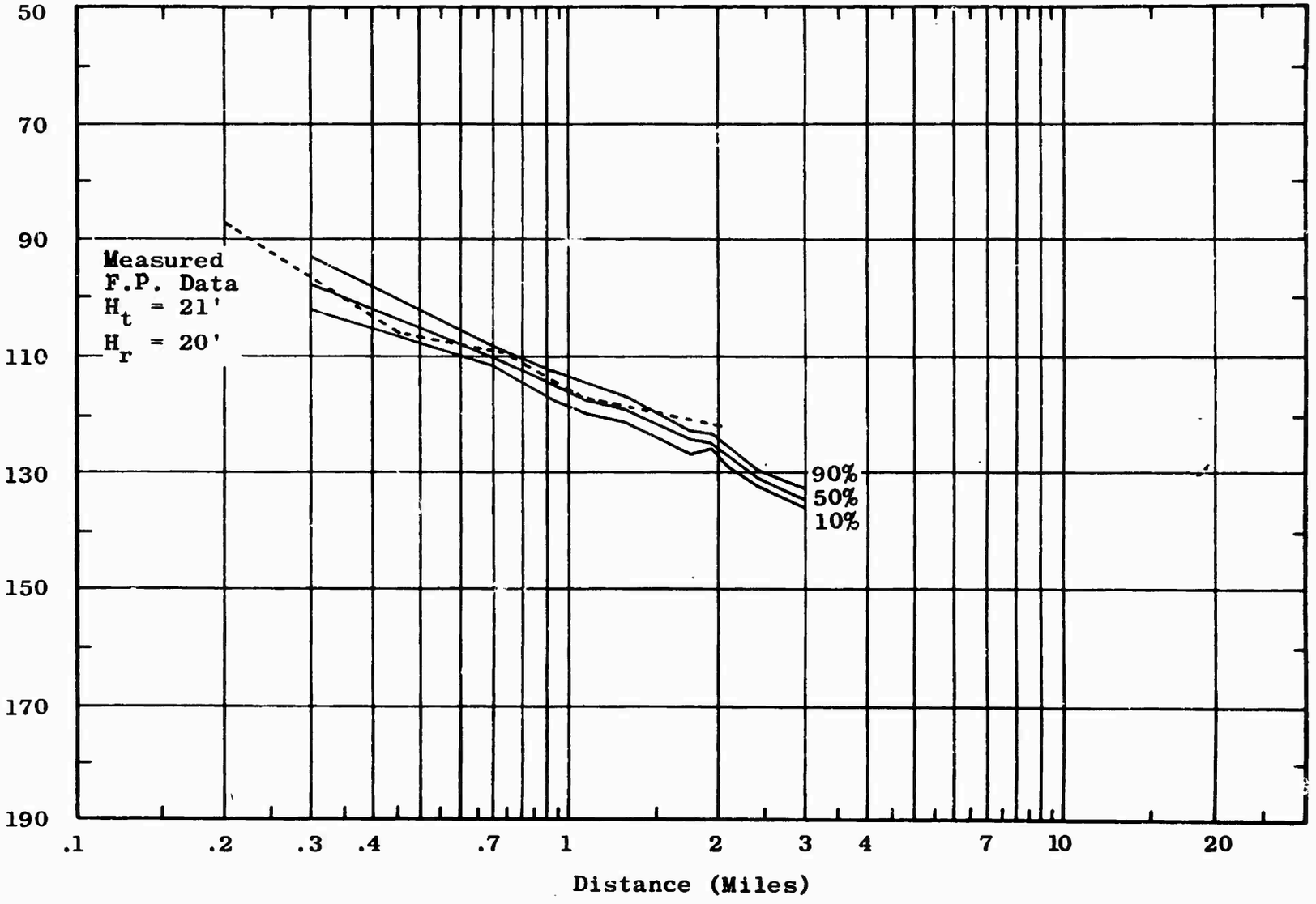

Figure 4.42 Comparison Between Vehicular Data and Measured F.P. Data
$L_b = F_A(12.1, 21, V, d, 7)$

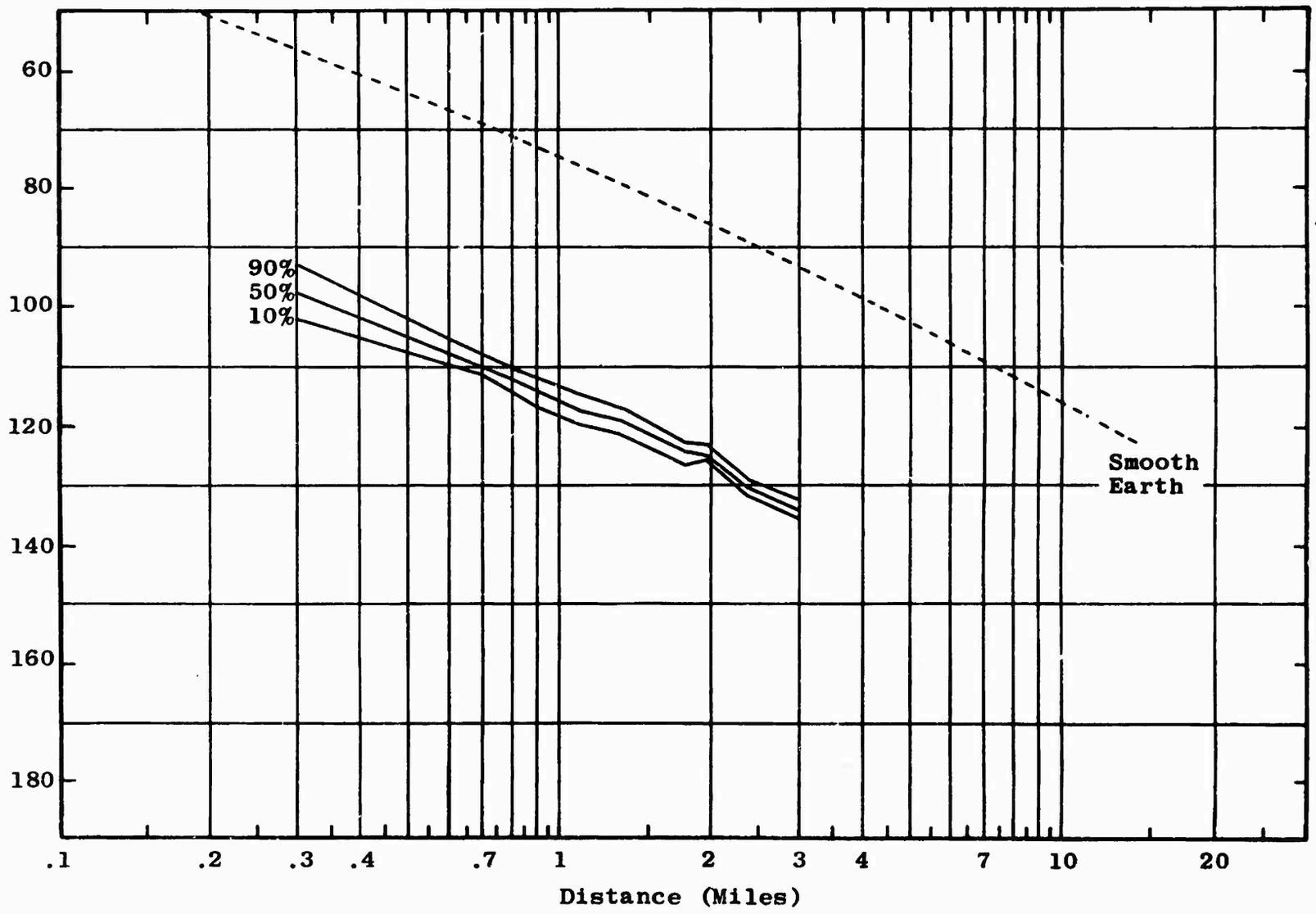

Figure 4.43 Comparison Between Vehicular Data and Theoretical Smooth-Earth Model
$L_b = F_A(12.1, 21, V, d, 7)$

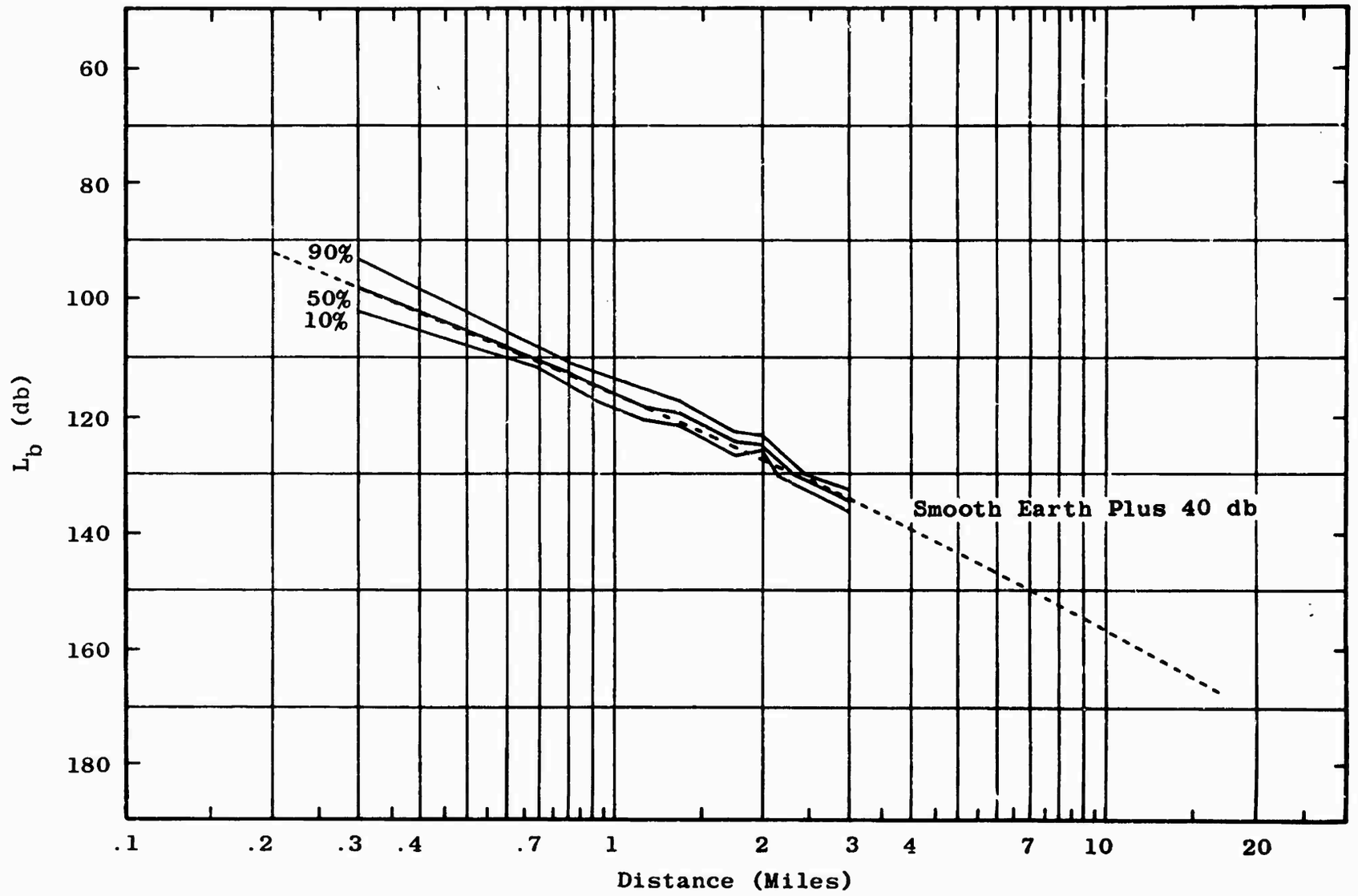

Figure 4.44 Comparison Between Vehicular Data and Theoretical Smooth-Earth Model Plus 17 db
$L_b = F_A(12.1, 21, V, d, 7)$

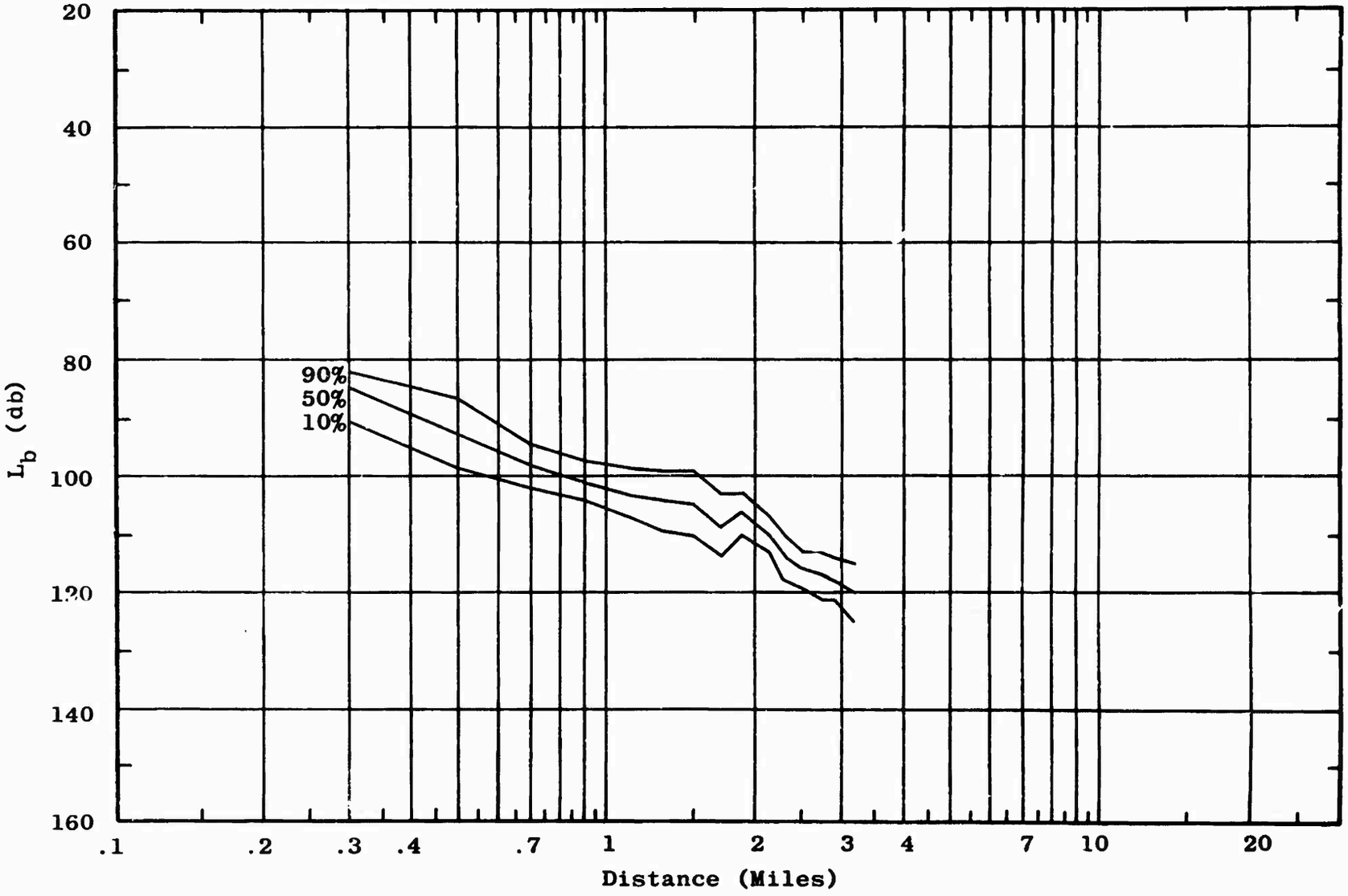

Figure 4.45 Reduced Vehicular Data
$L_b = F_A(25.5, 40, V, d, 7)$

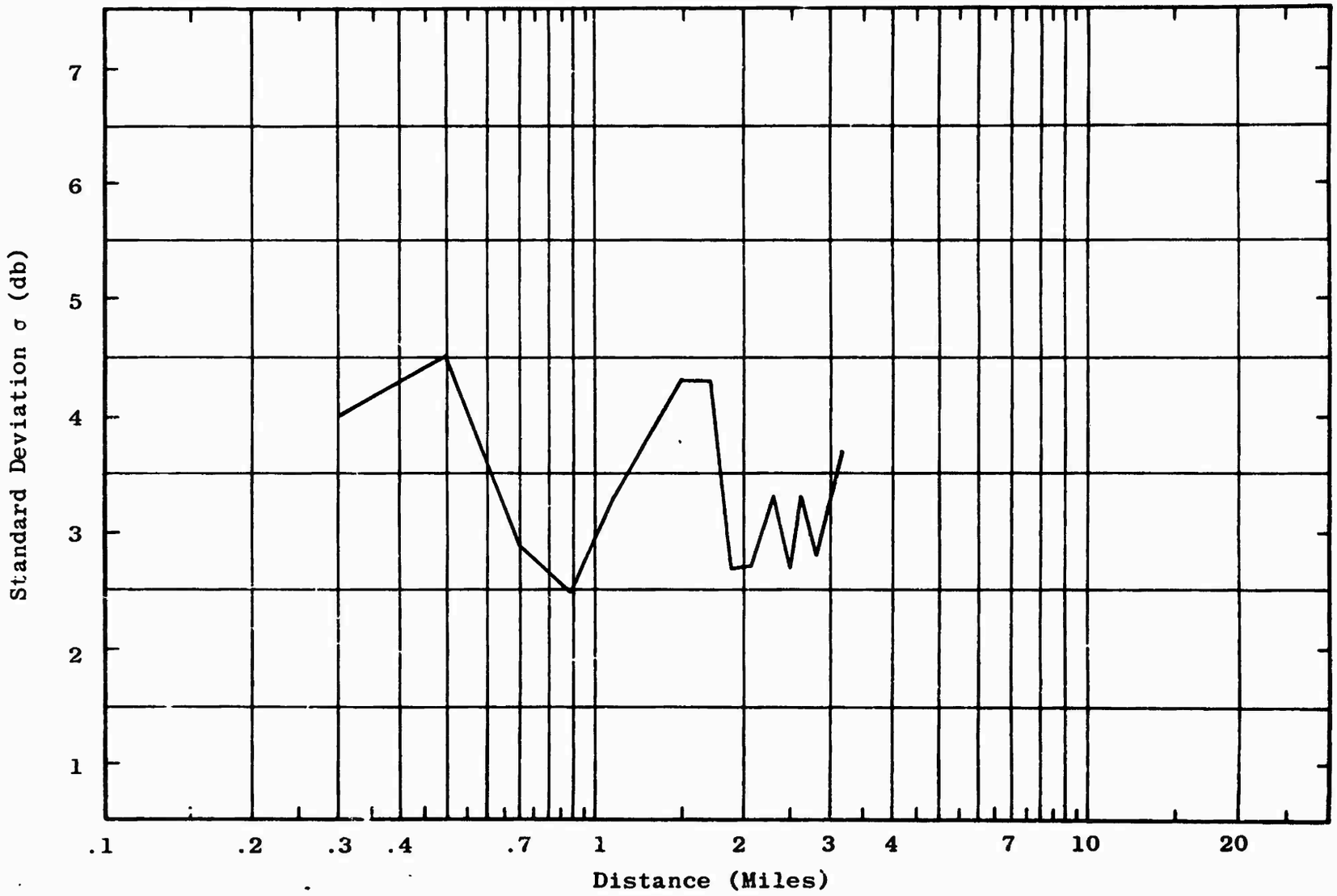

Figure 4.46 Standard Deviation of Vehicular Data
$L_b = F_A(25.5, 40, V, d, 7)$

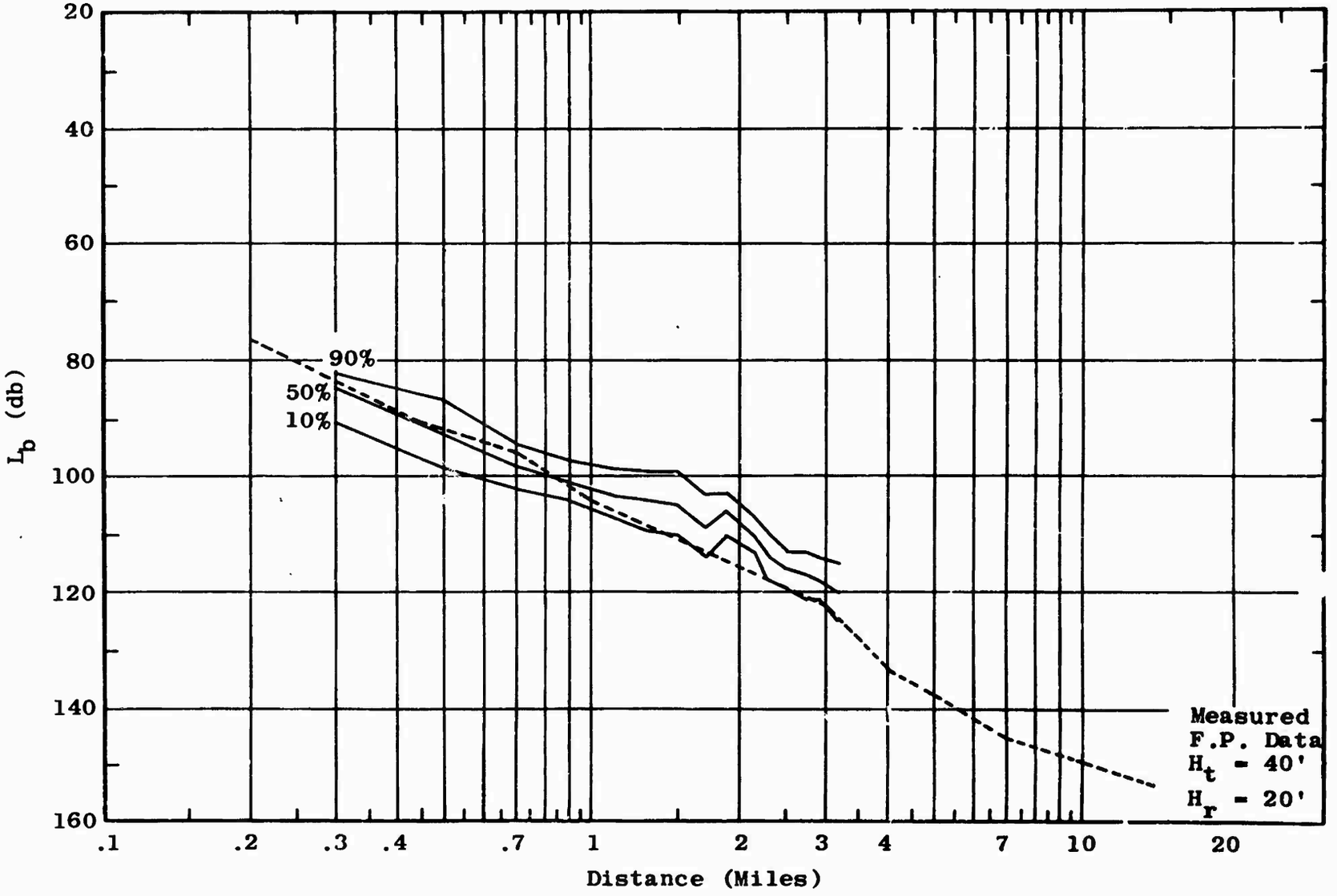

Figure 4.47 Comparison Between Vehicular Data and Measured F.P. Data
$L_b = F_A(25.5, 40, V, d, 7)$

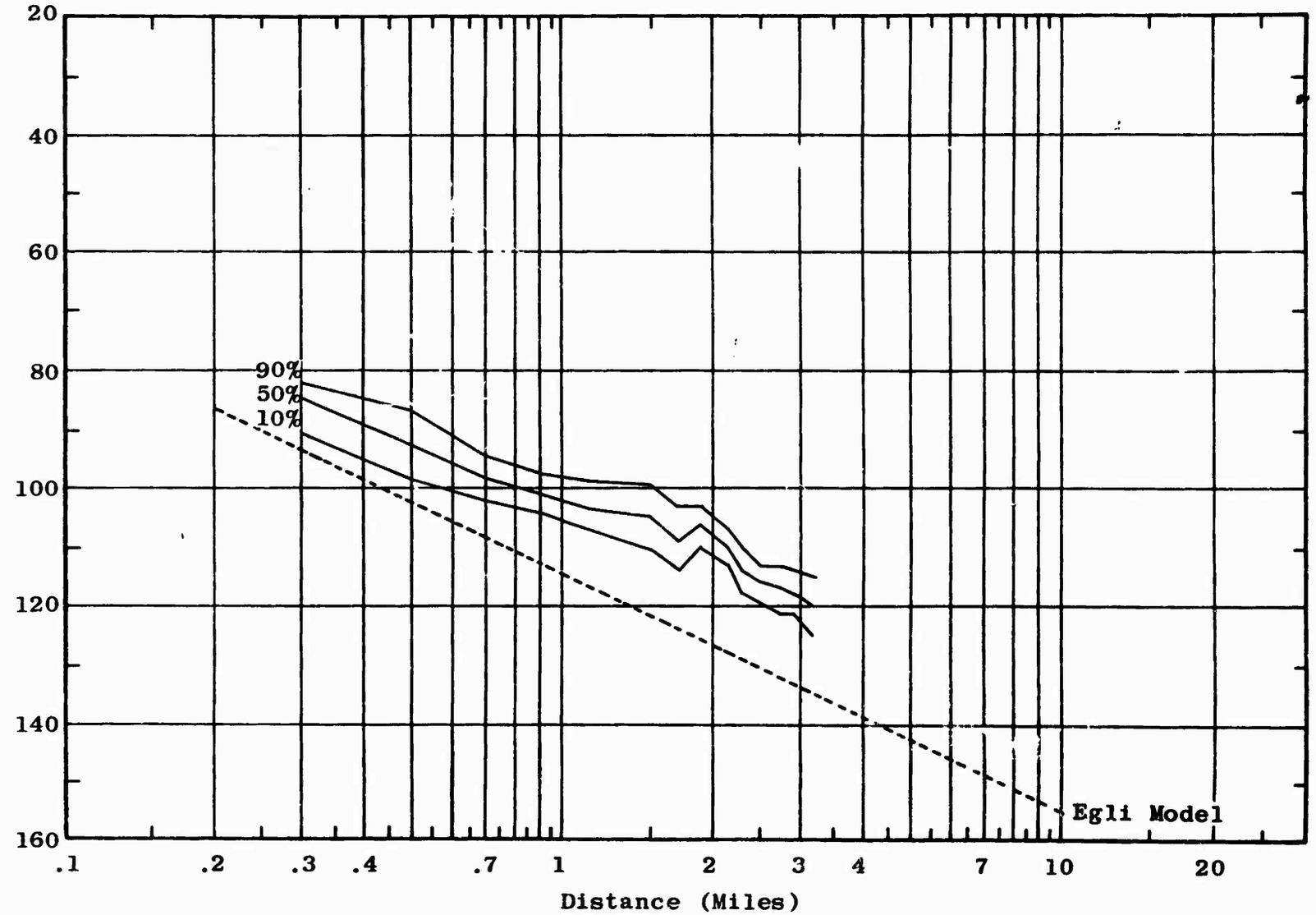

Figure 4.48 Comparison Between Vehicular Data and Egli Model
$L_b = F_A(25.5, 40, V, d, 7)$

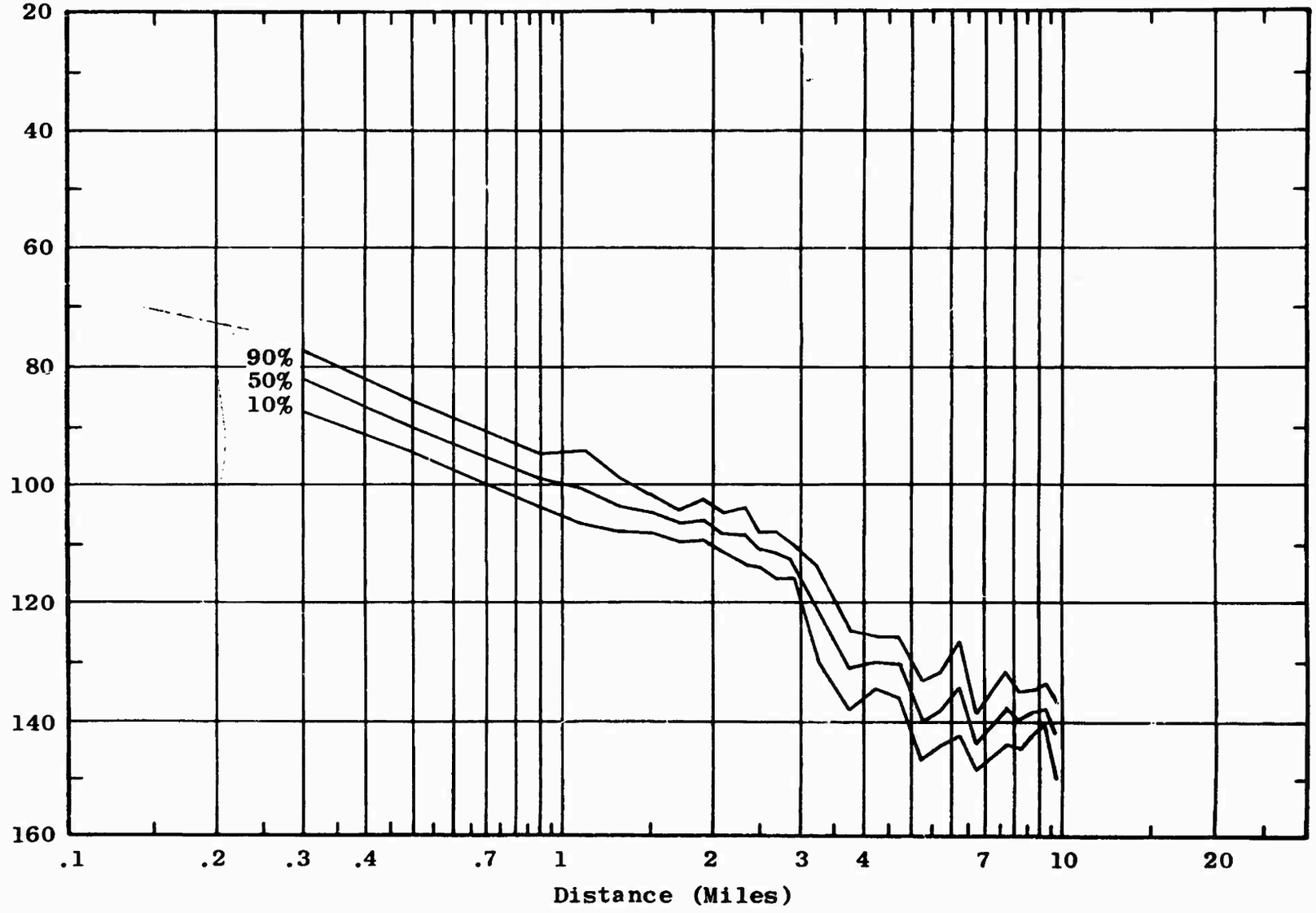

Figure 4.49 Reduced Vehicular Data
$L_b = F_A(25.5, 80, V, d, 7)$

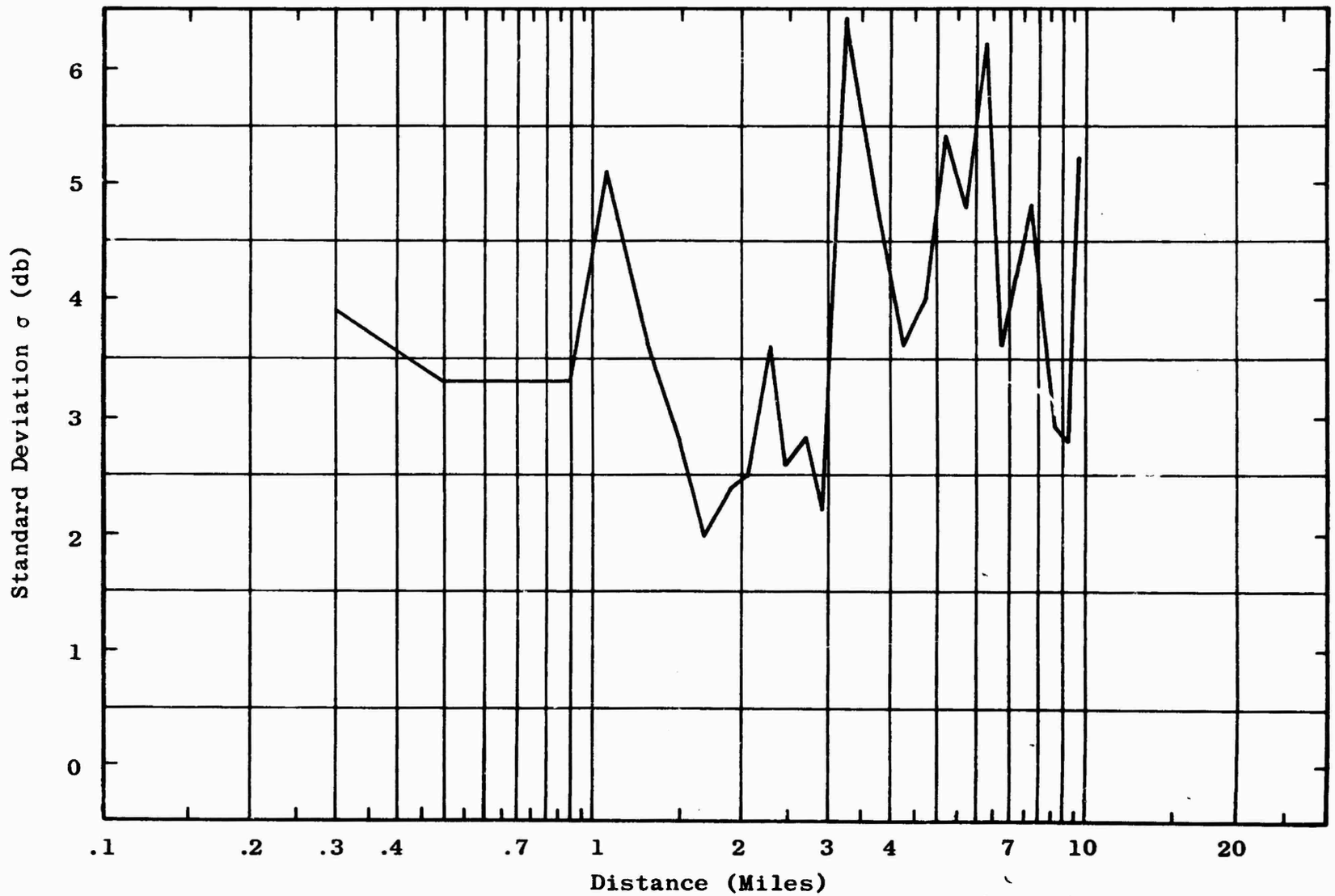

Figure 4.50 Standard Deviation of Vehicular Data
$L_b = F_A(25.5, 80, V, d, 7)$

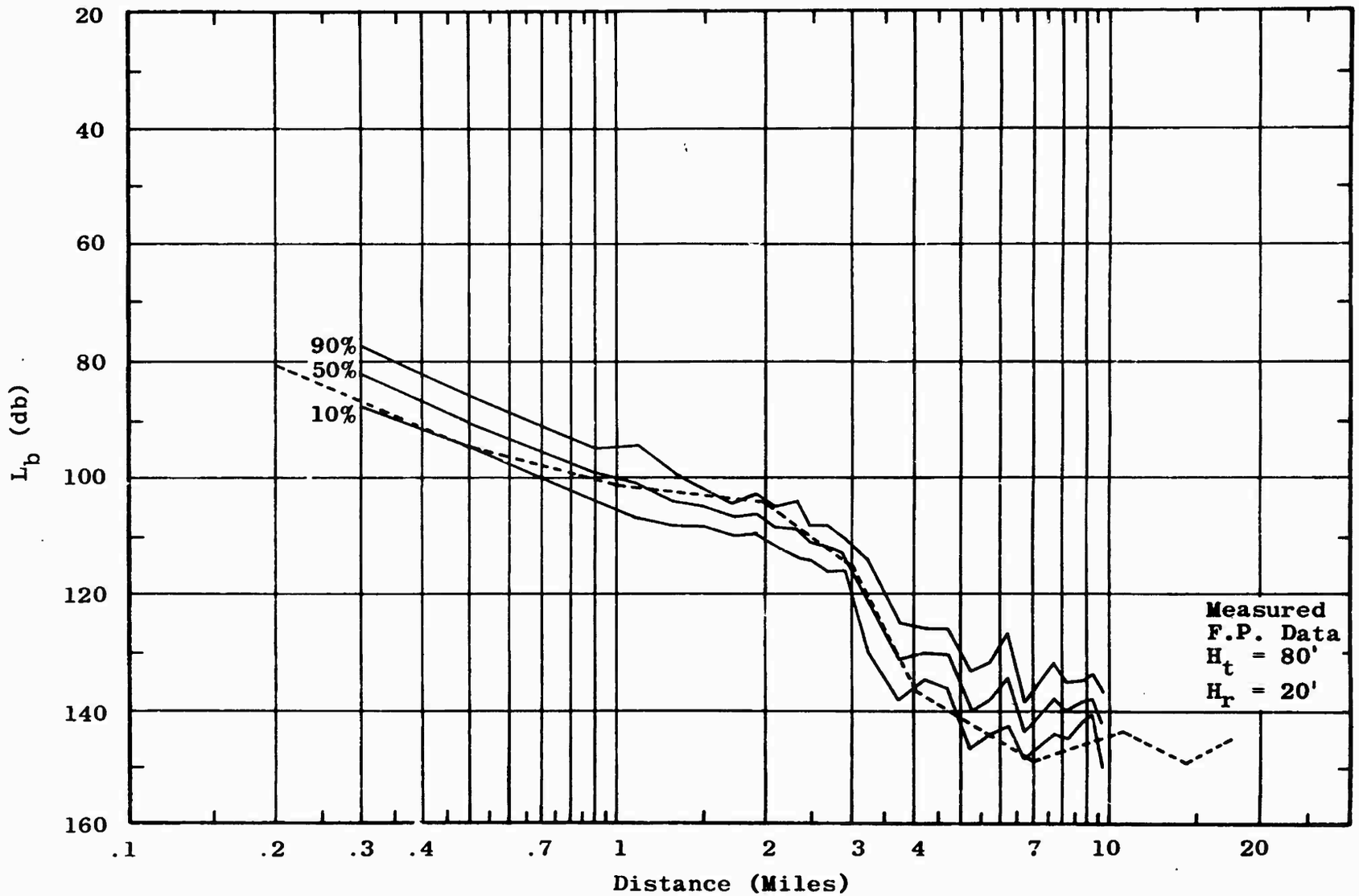

Figure 4.51 Comparison Between Vehicular Data and Measured F.P. Data
$L_b = F_A(25.5, 80, V, d, 7)$

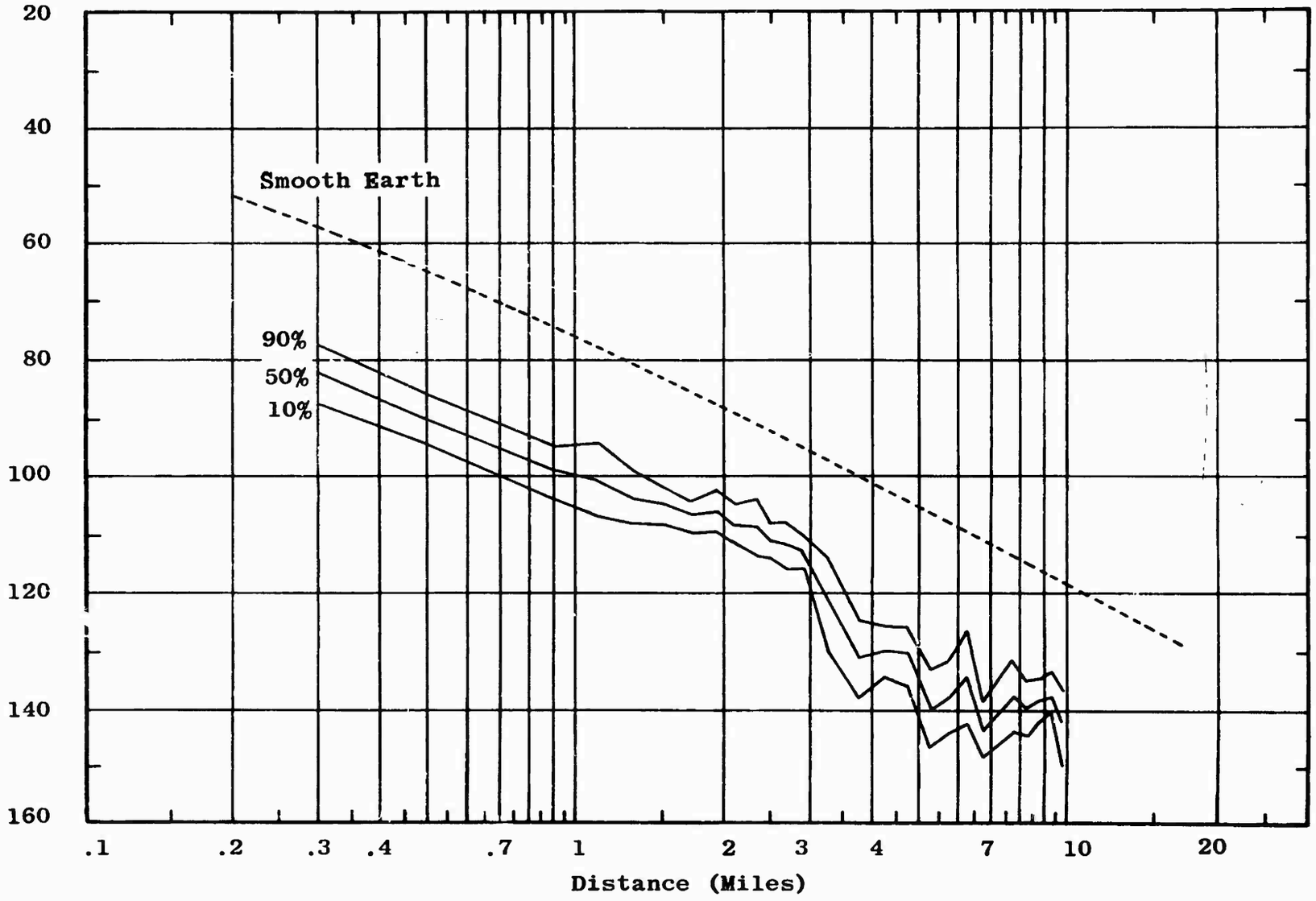

Figure 4.52 Comparison Between Vehicular Data and Theoretical Smooth-Earth Model
$L_b = F_A(25.5, 80, V, d, 7)$

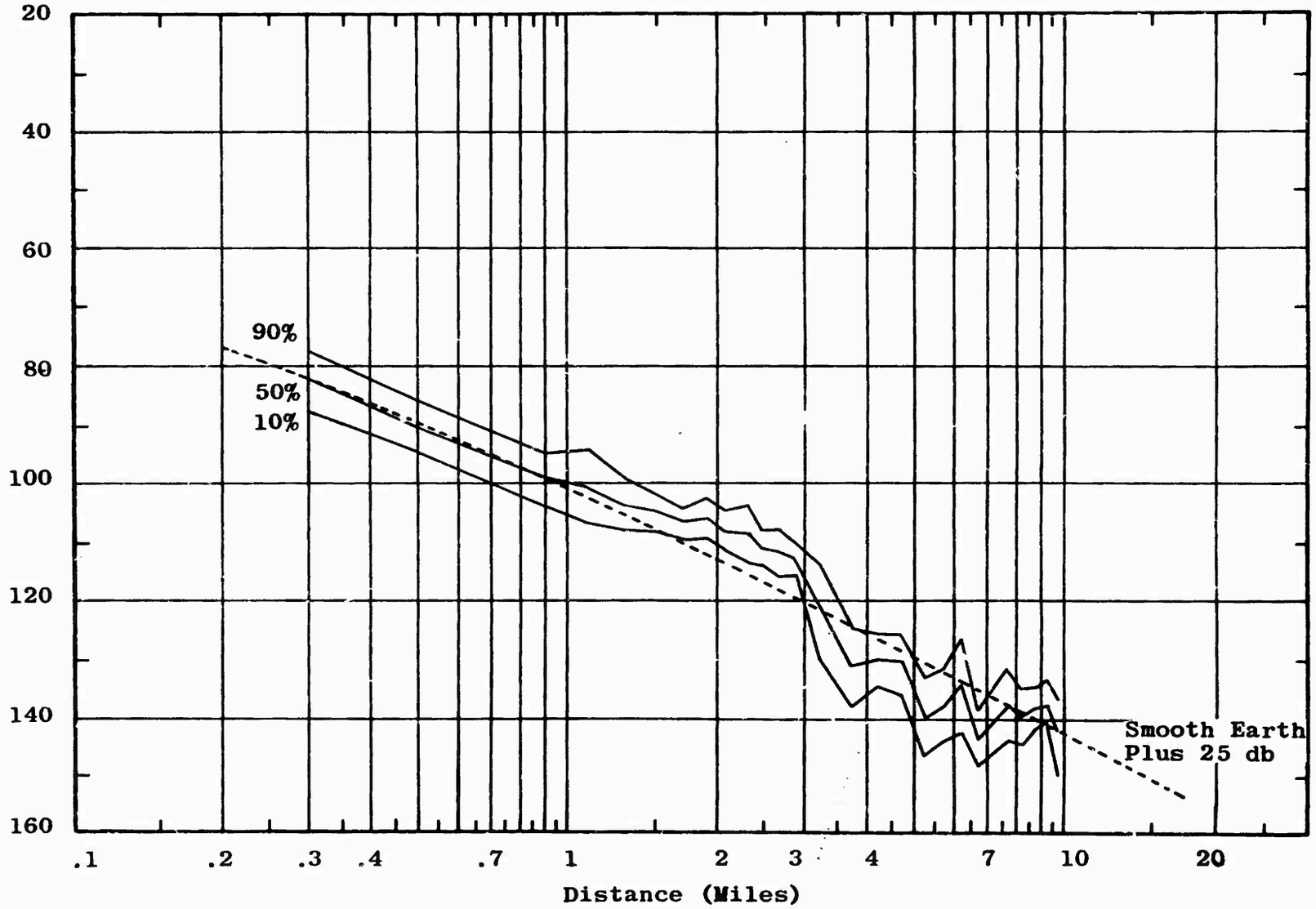

Figure 4.53 Comparison Between Vehicular Data and Theoretical Smooth-Earth Model Plus 25 db
$L_b = F_A(25.5, 80, V, d, 7)$

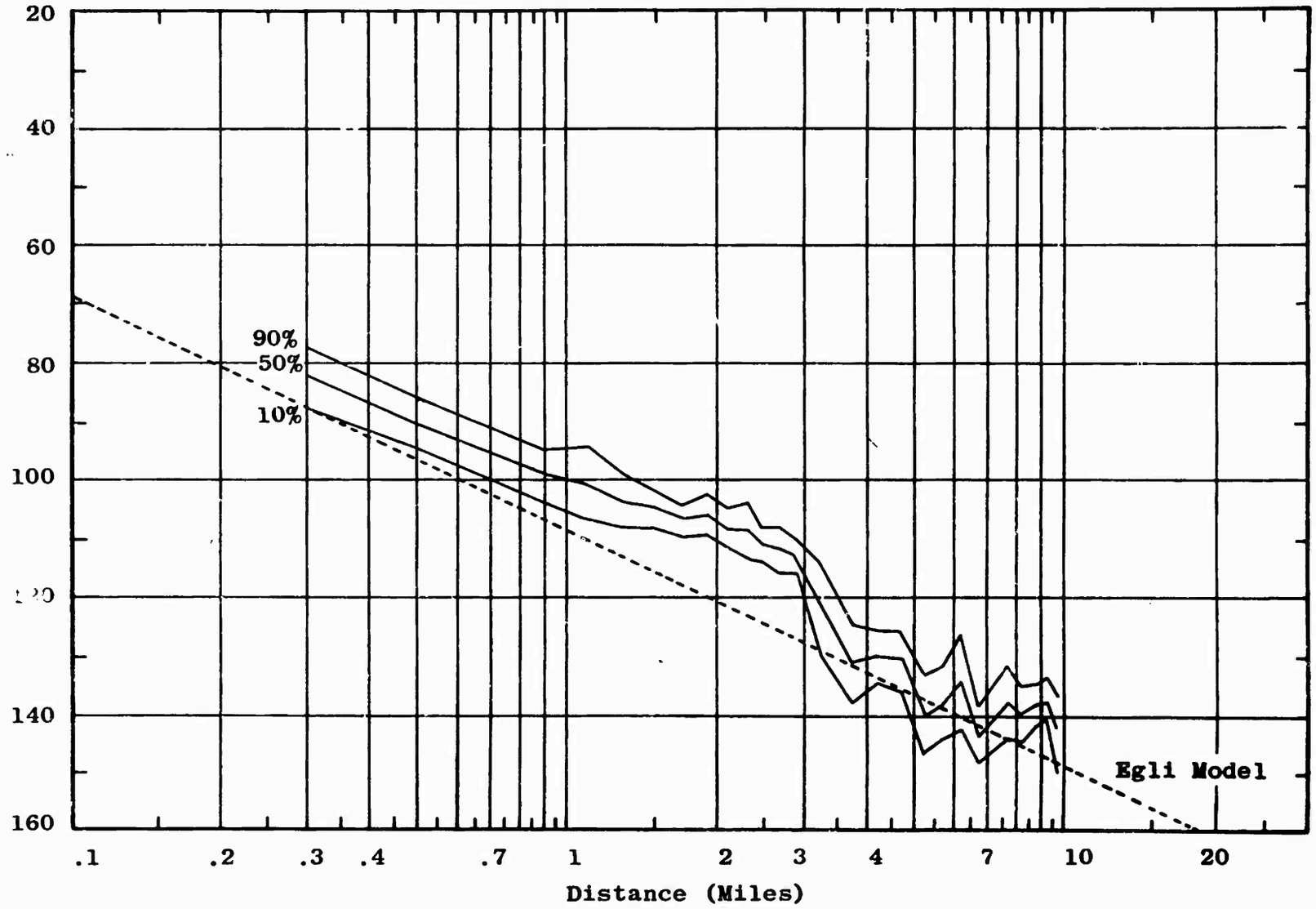

Figure 4.54 Comparison Between Vehicular Data and Egli Model
$L_b = F_A(25.5, 80, V, d, 7)$

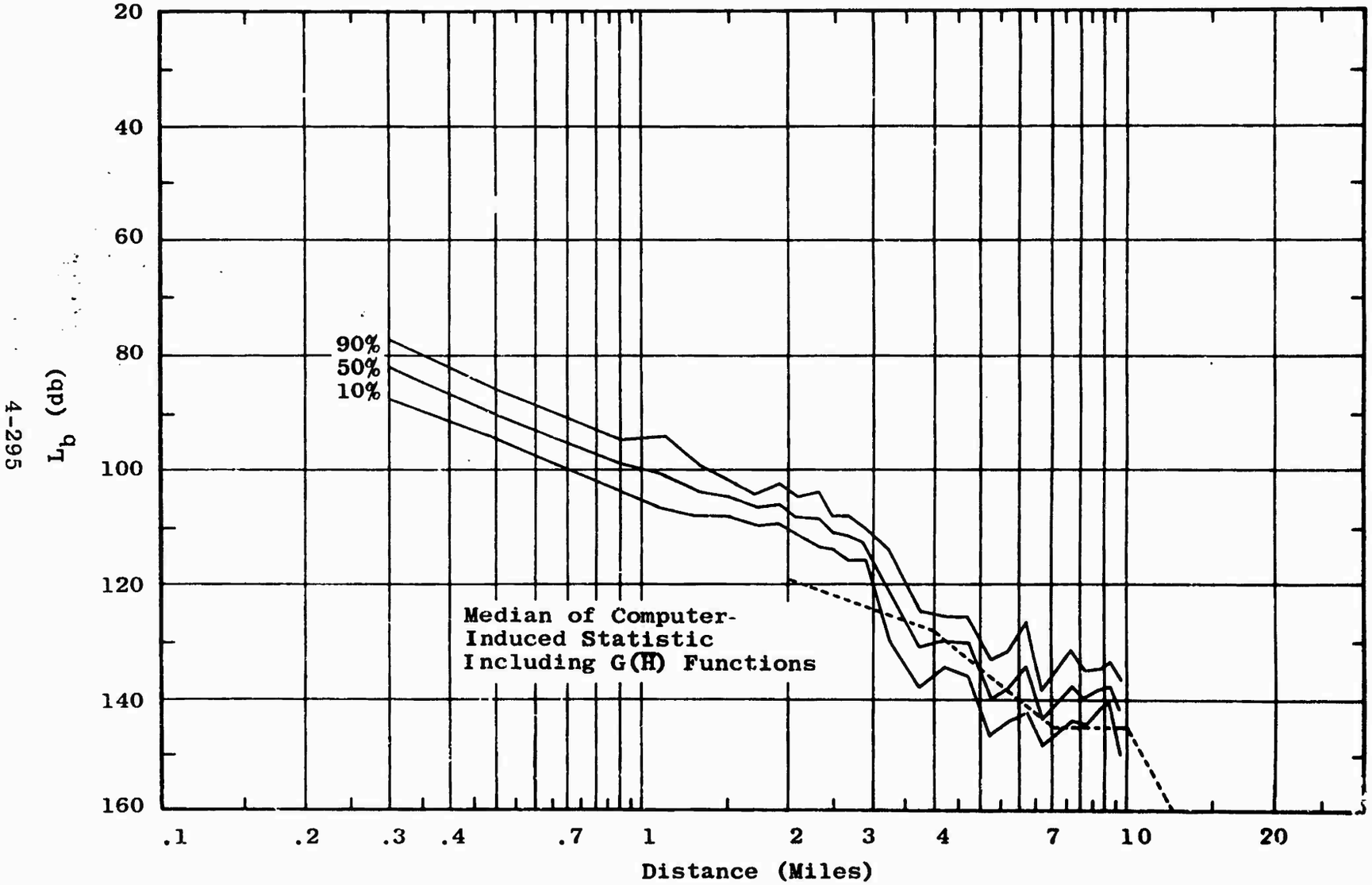

Figure 4.55 Comparison Between Vehicular Data and Median of Computer-Induced Statistic Including G(H) Functions
$L_b = F_A(25.5, 80, V, d, 7)$

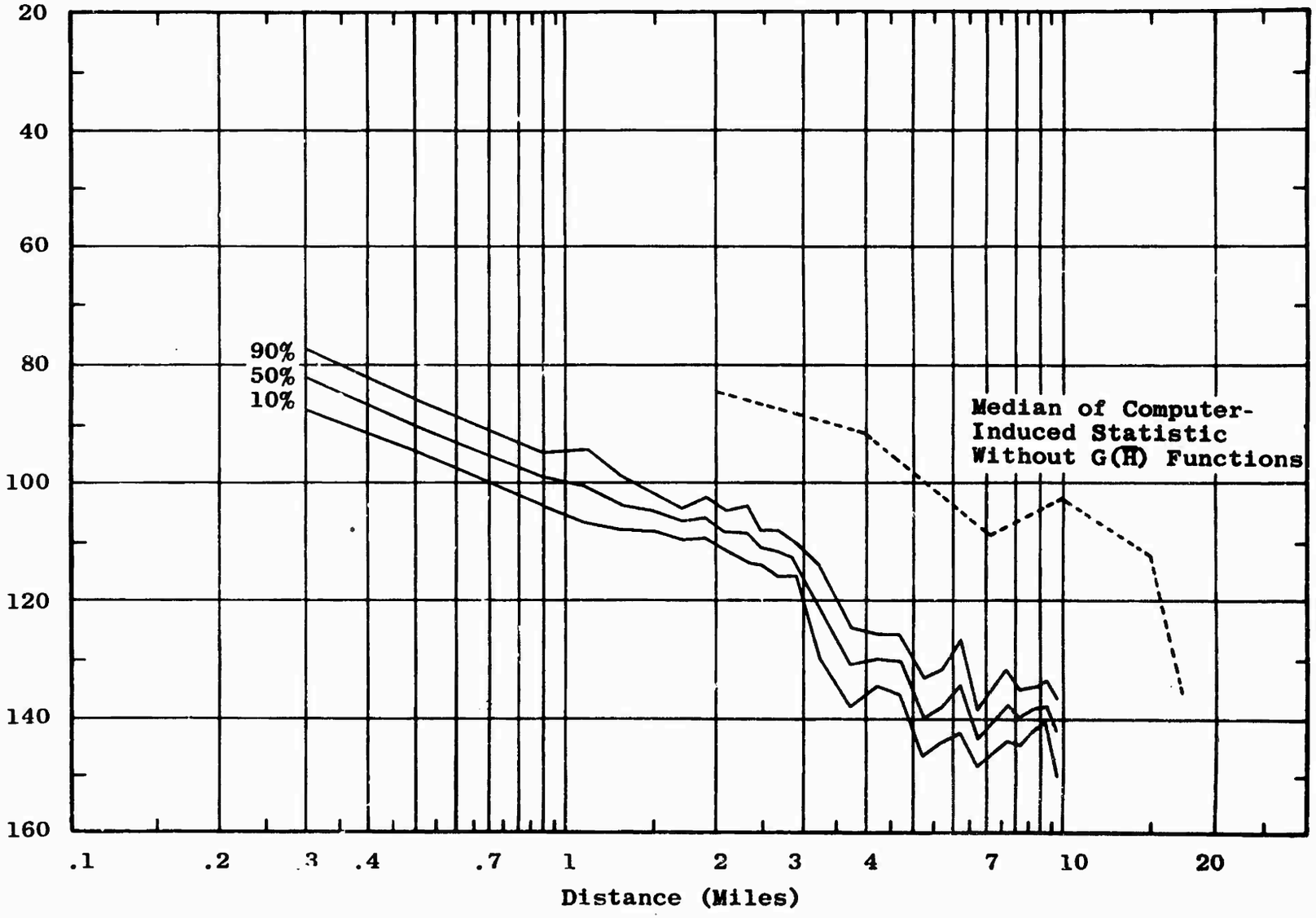

Figure 4.56 Comparison Between Vehicular Data and Median of Computer-Induced Statistic Without G(H) Functions
$L_b = F_A(25.5, 80, V, d, 7)$

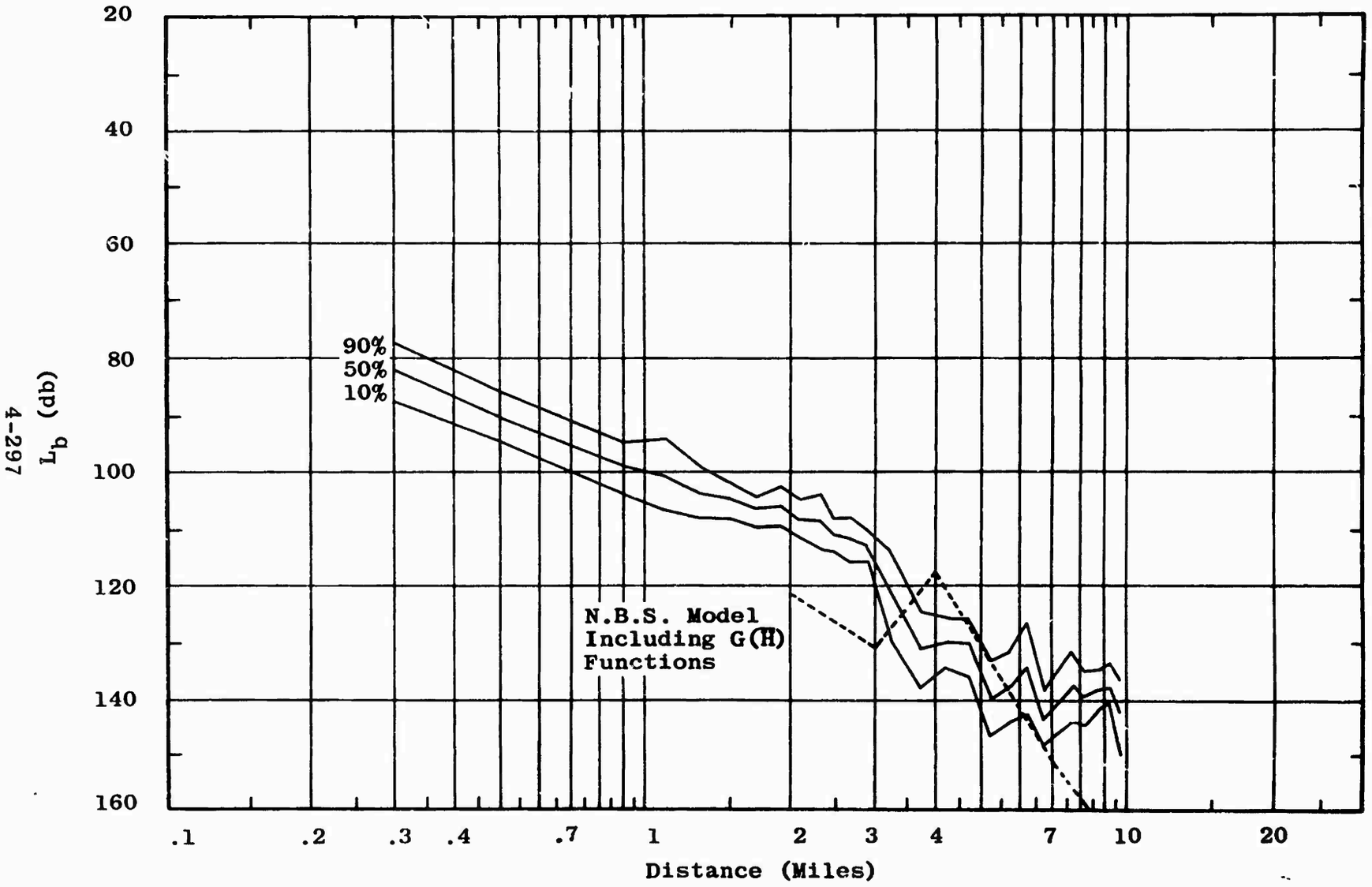

Figure 4.57 Comparison Between Vehicular Data and N.B.S. Model Including G(H) Functions
$L_b = F_A(25.5, 80, V, d, 7)$

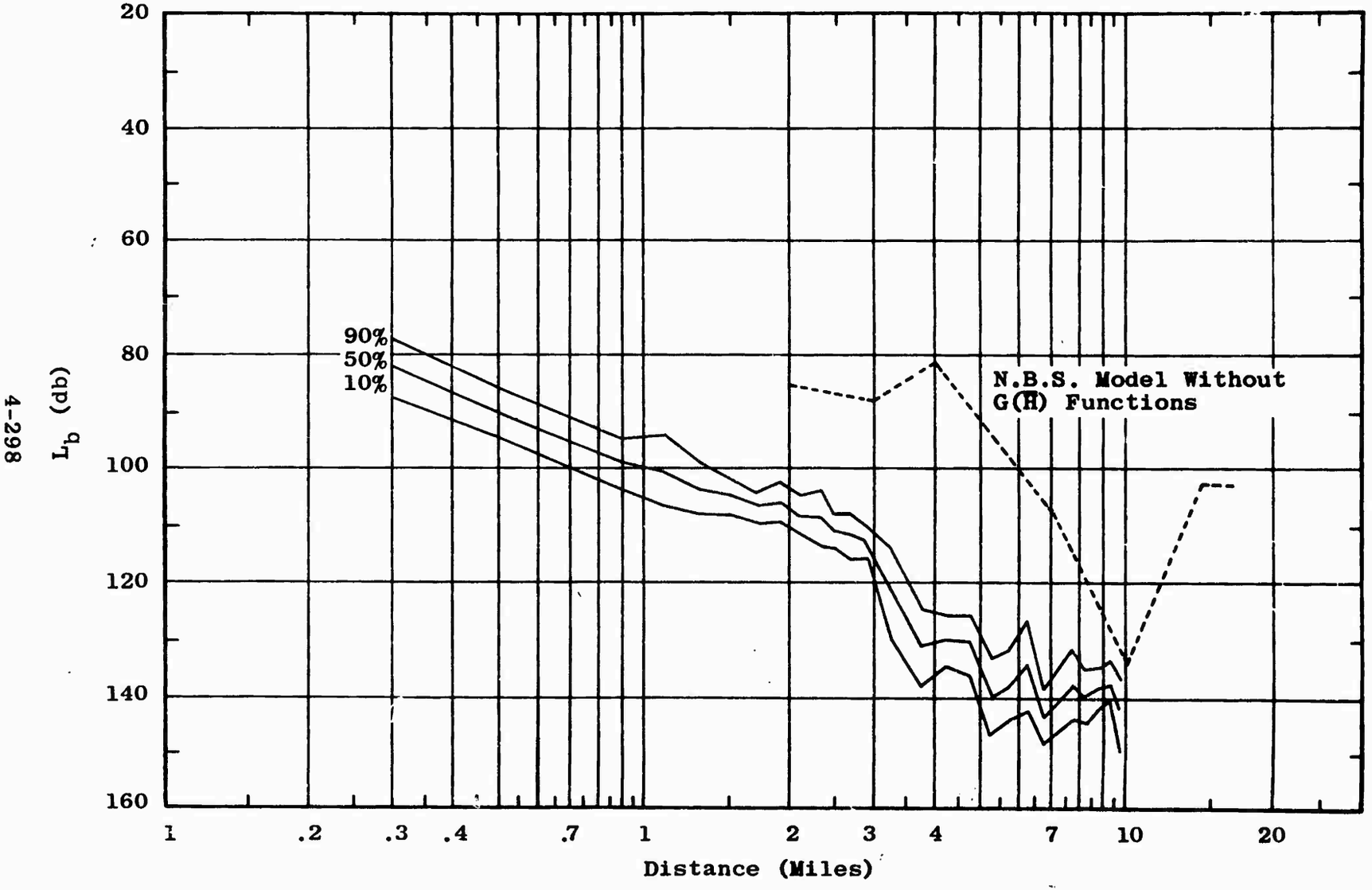

Figure 4.58 Comparison Between Vehicular Data and N.B.S. Model Without G(H) Functions
$L_b = F_A(25.5, 80, V, d, 7)$

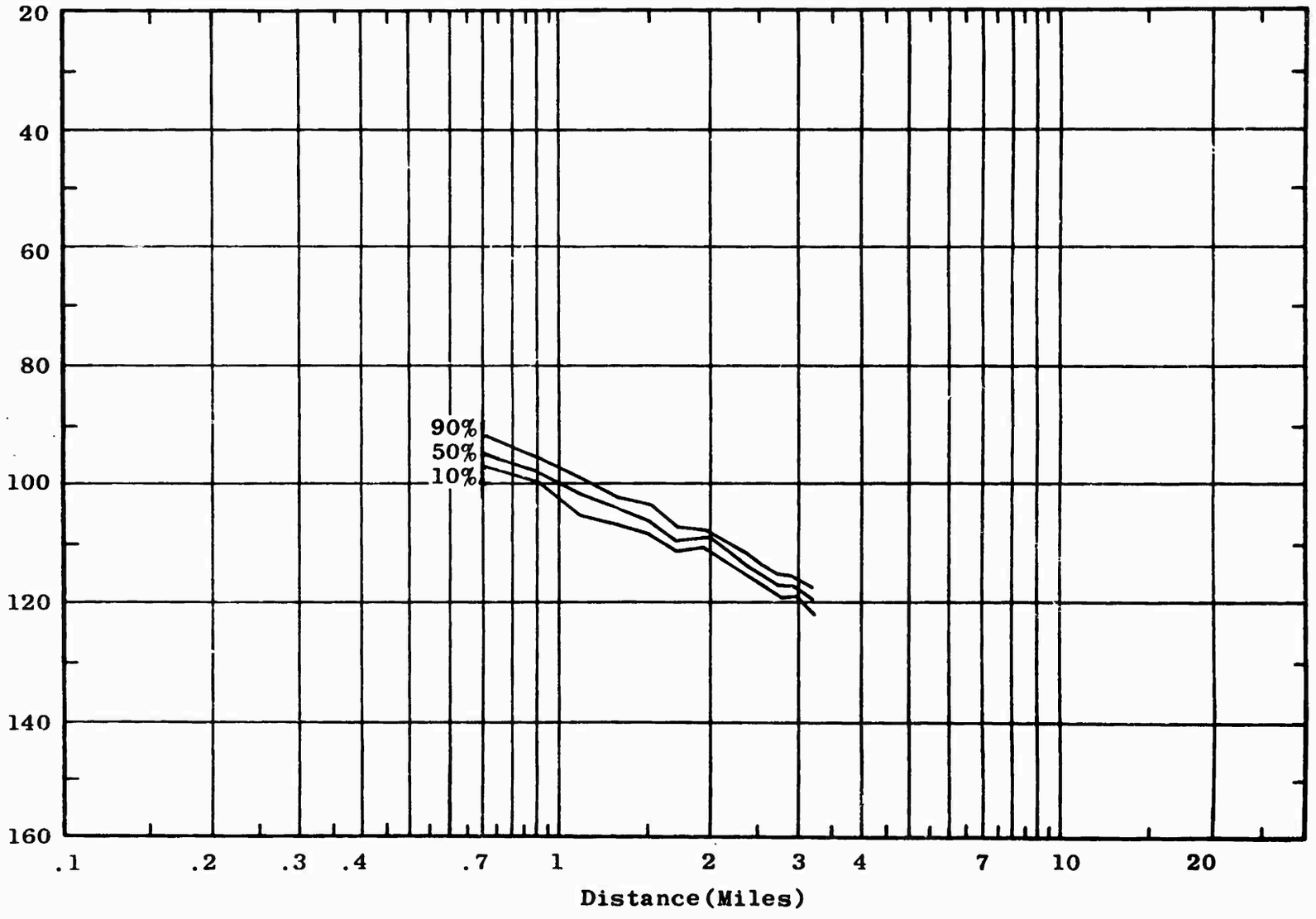

Figure 4.59 Reduced Vehicular Data
$L_b = F_A(25.5, 13, H, d, 7)$

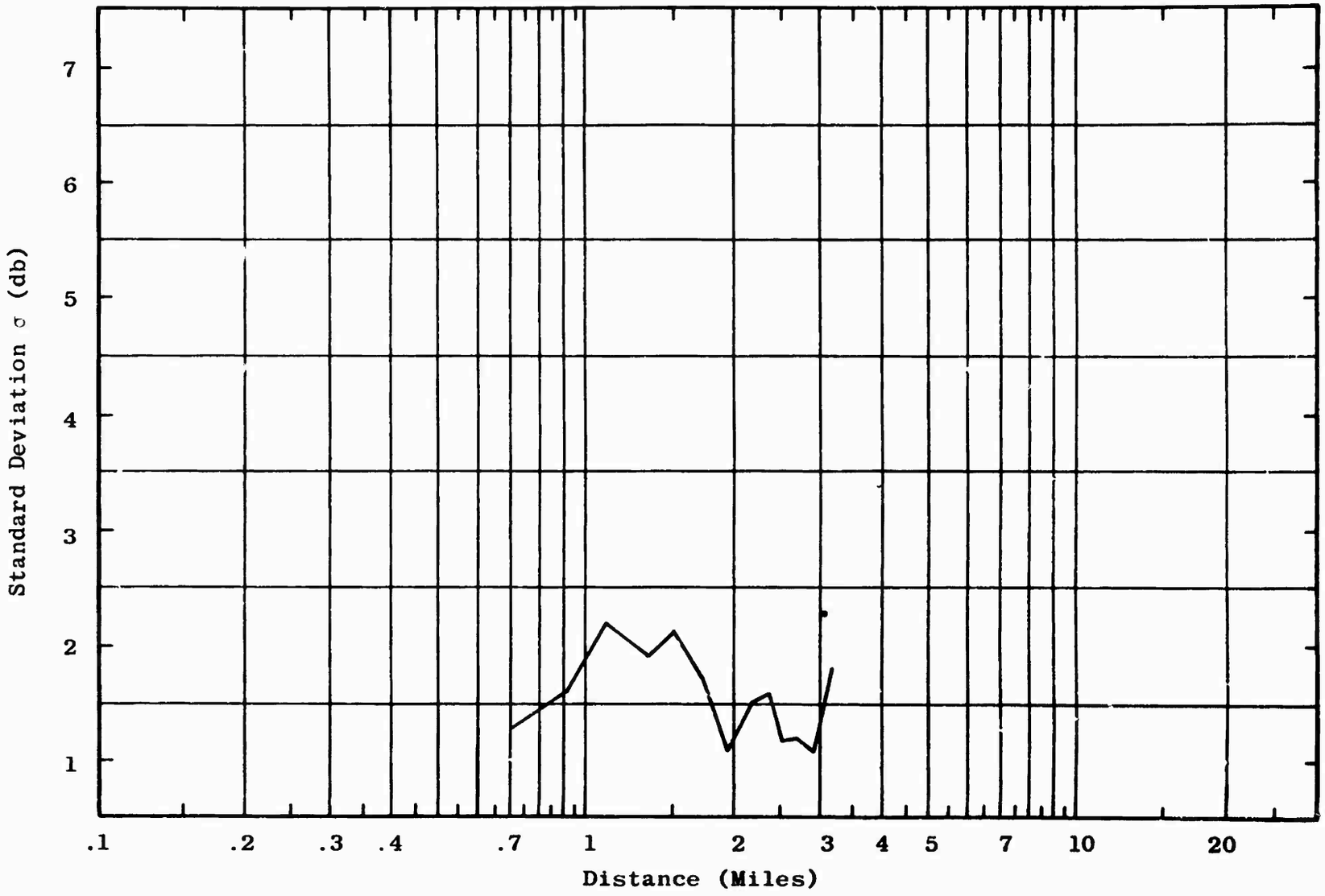

Figure 4.60 Standard Deviation of Vehicular Data
$L_b = F_A(25.5, 13, V, d\ 7)$

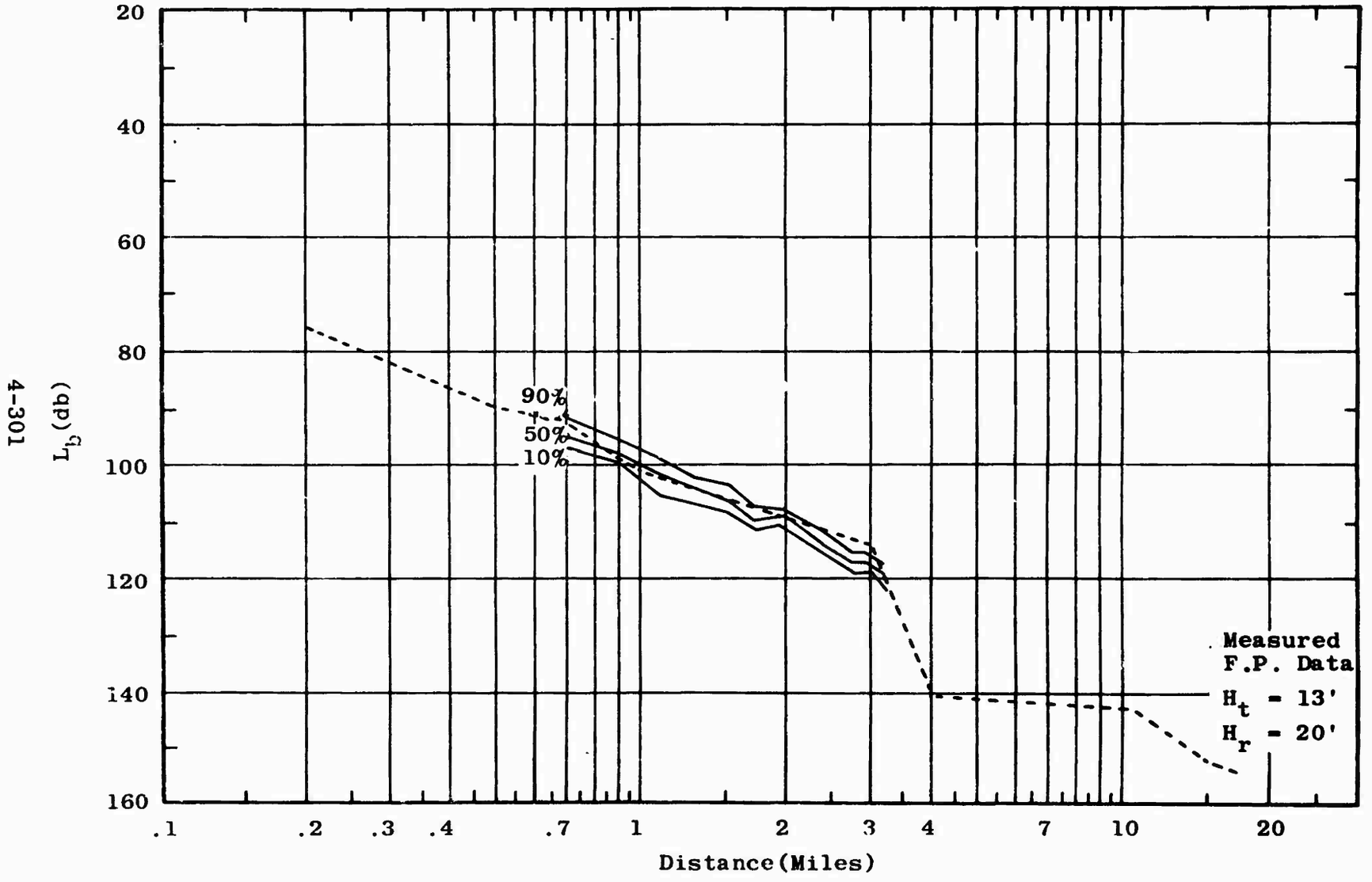

Figure 4.61 Comparison Between Vehicular Data and Measured F. P. Data
$L_b = F_A(25.5, 13, H, d, 7)$

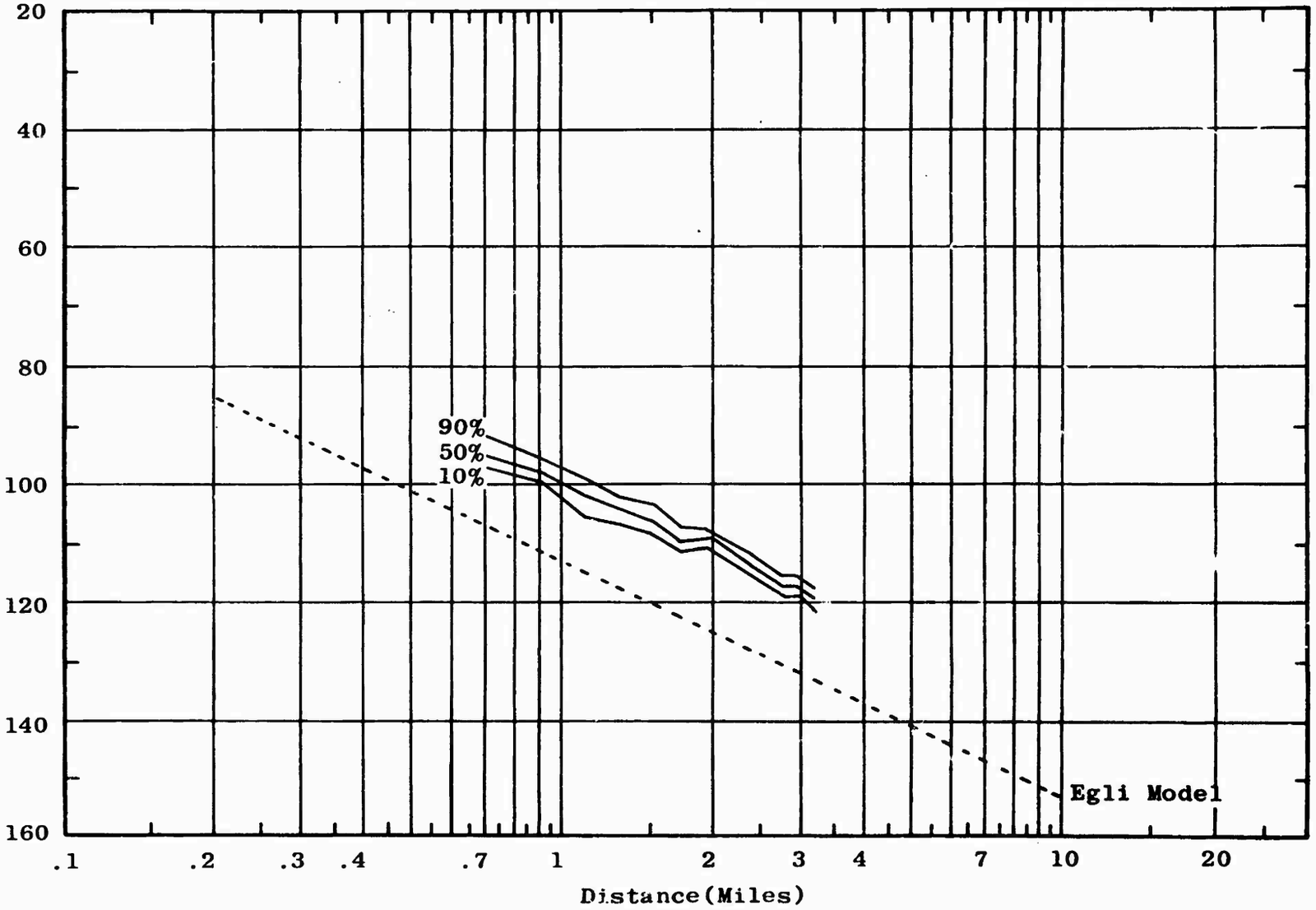

Figure 4.62 Comparison Between Vehicular Data and Egli Model
$L_b = F_A(25.5, 13, H, d, 7)$

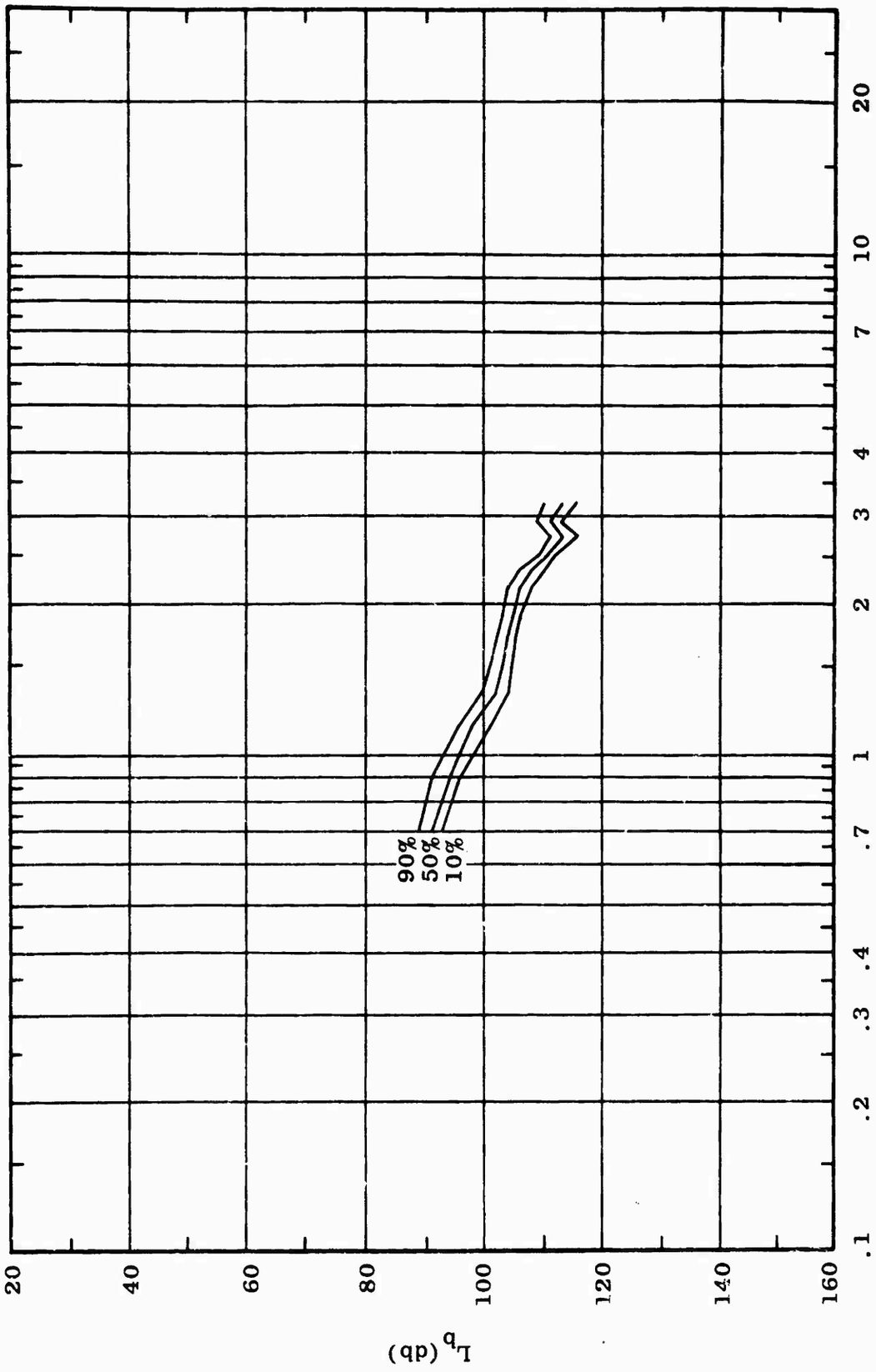

Figure 4.63 Reduced Vehicular Data
$L_b = F_A(25.5, 40, H, d, 7)$

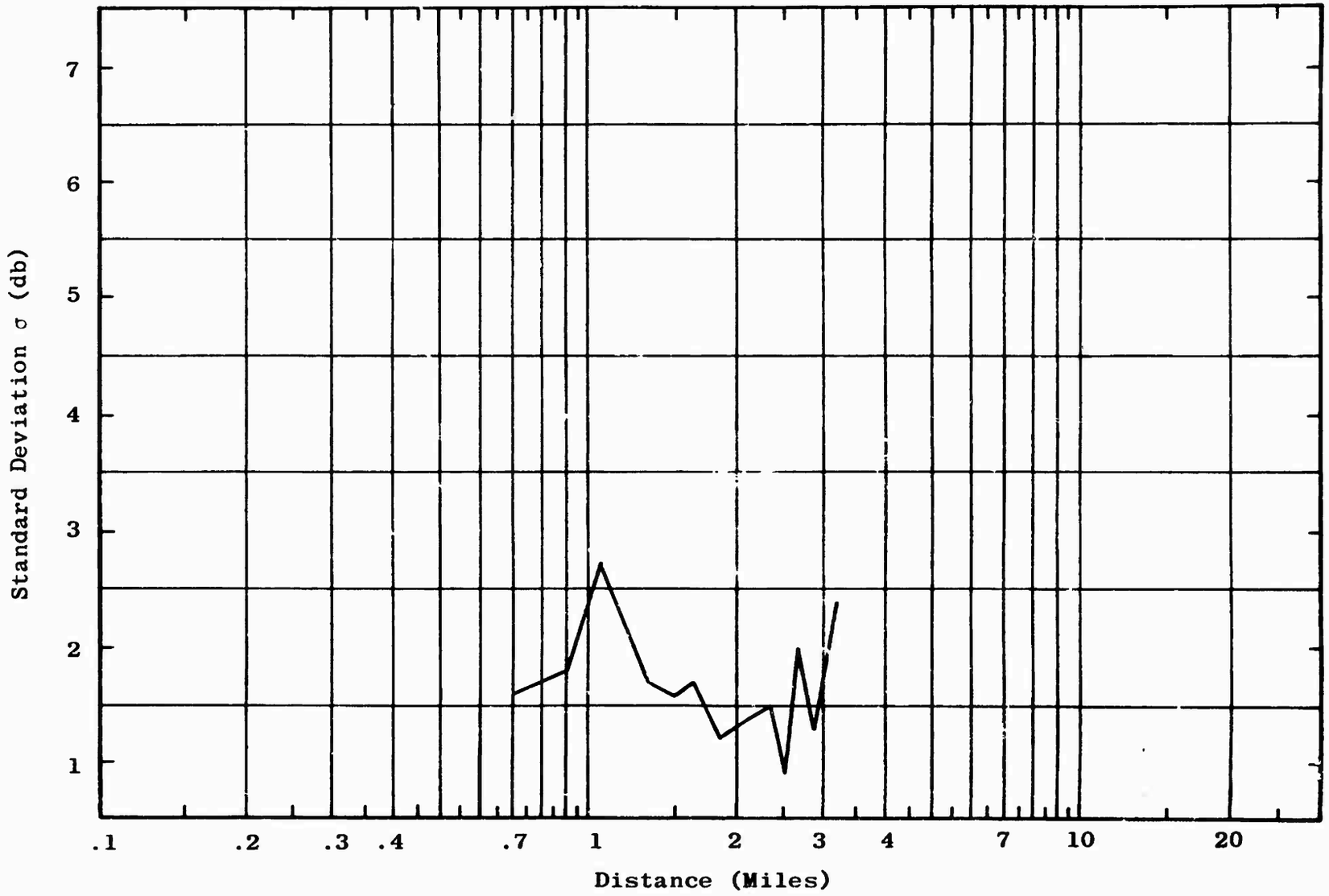

Figure 4.64 Standard Deviation of Vehicular Data
$L_b = F_A(25.5, 40, H, d, 7)$

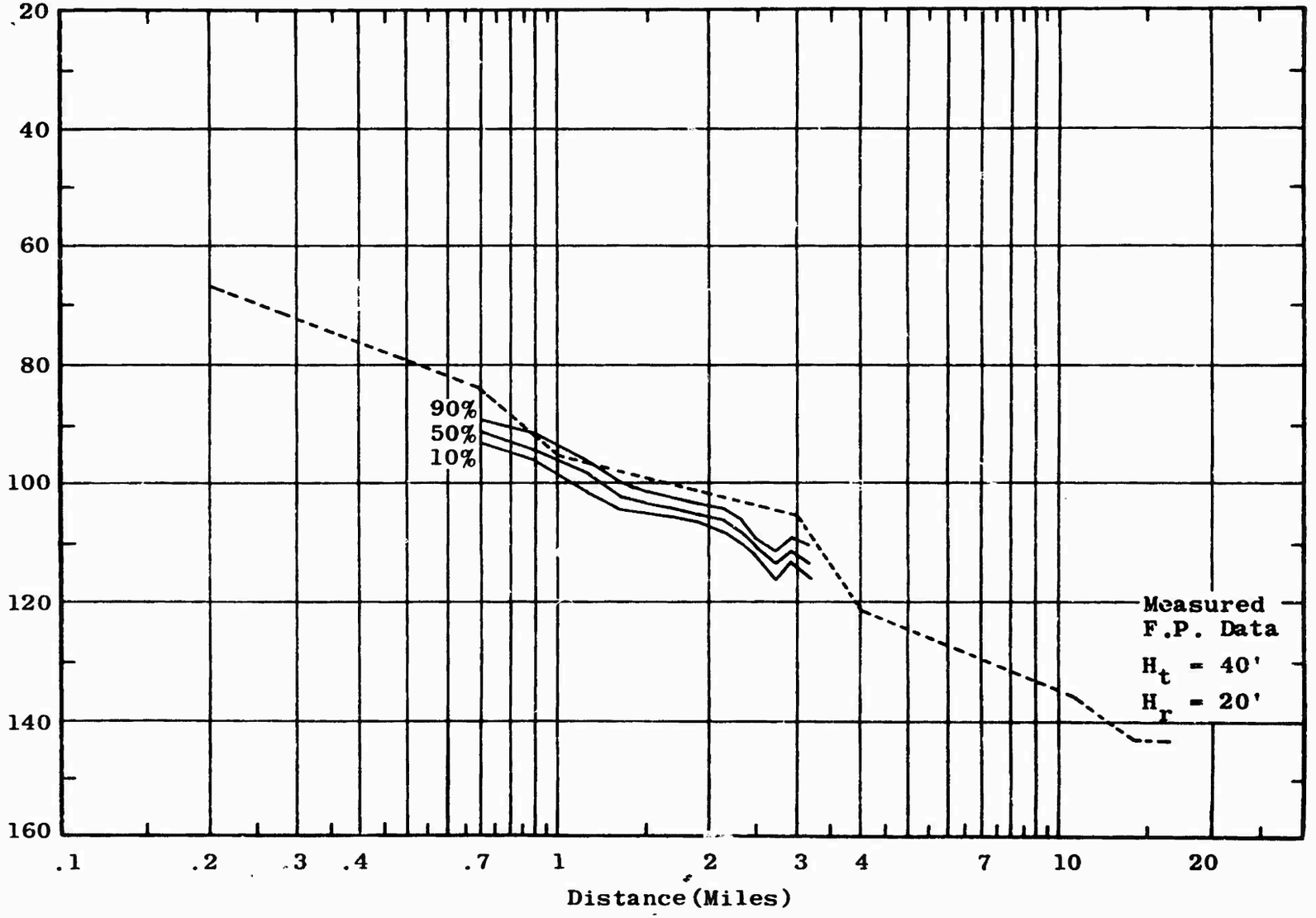

Figure 4.65 Comparison Between Vehicular Data and Measured F. P. Data
$L_b = F_A(25.5, 40, H, d, 7)$

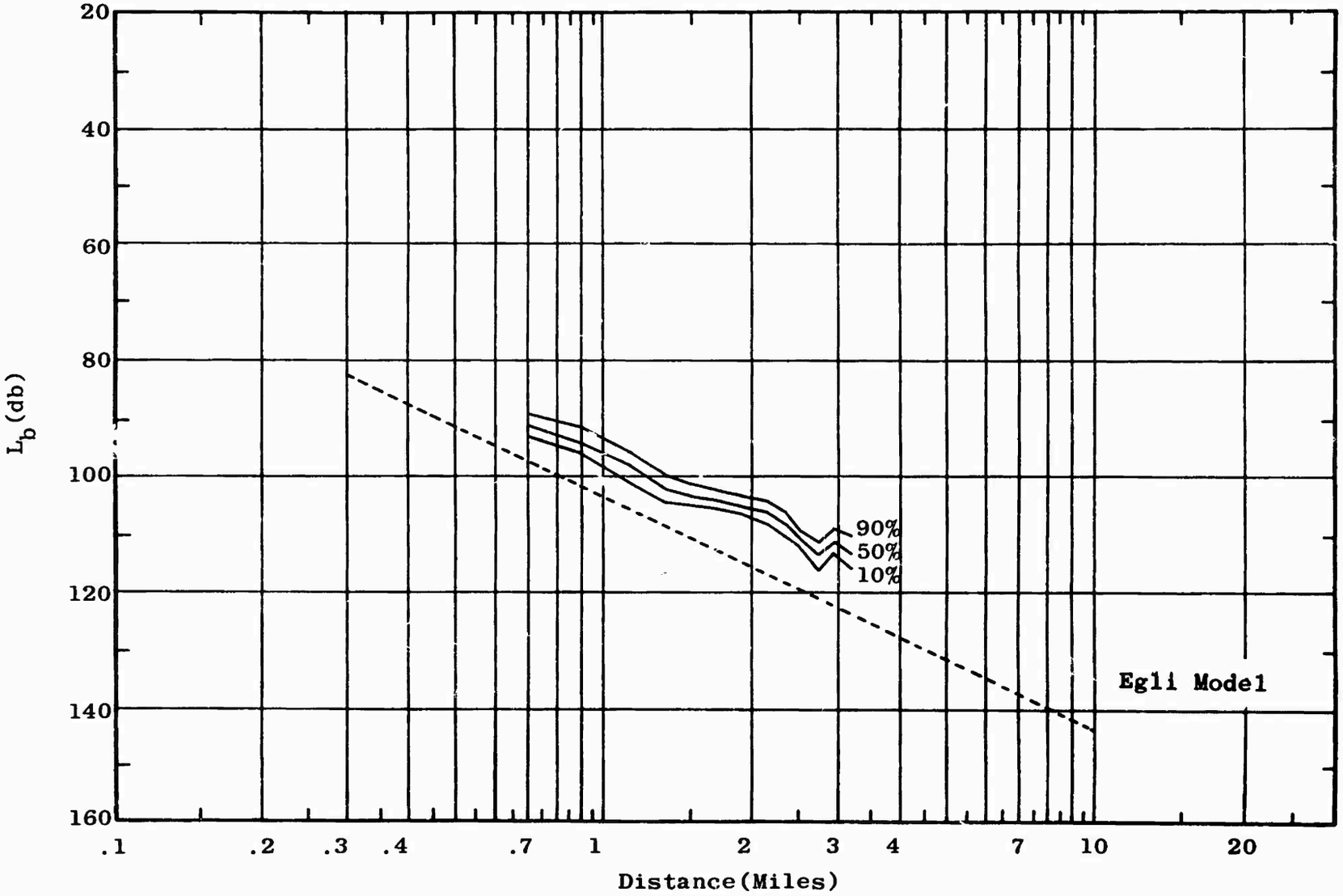

Figure 4.66 Comparison Between Vehicular Data and Egli Model
$L_b = F_A(25.5, 40, H, d, 7)$

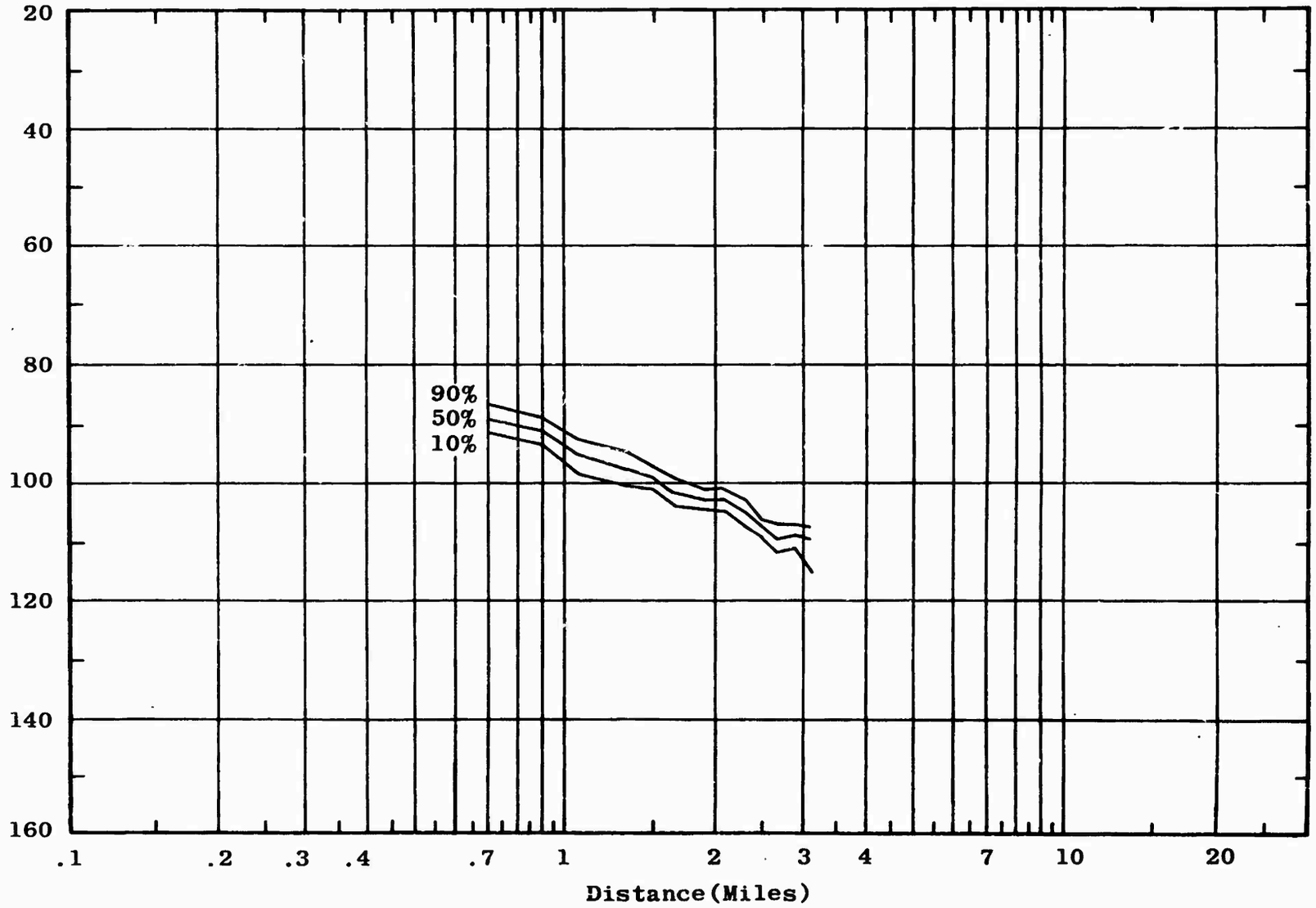

Figure 4.67 Reduced V hicular Data
$L_b = F_A(25.5, 80, H, d, 7)$

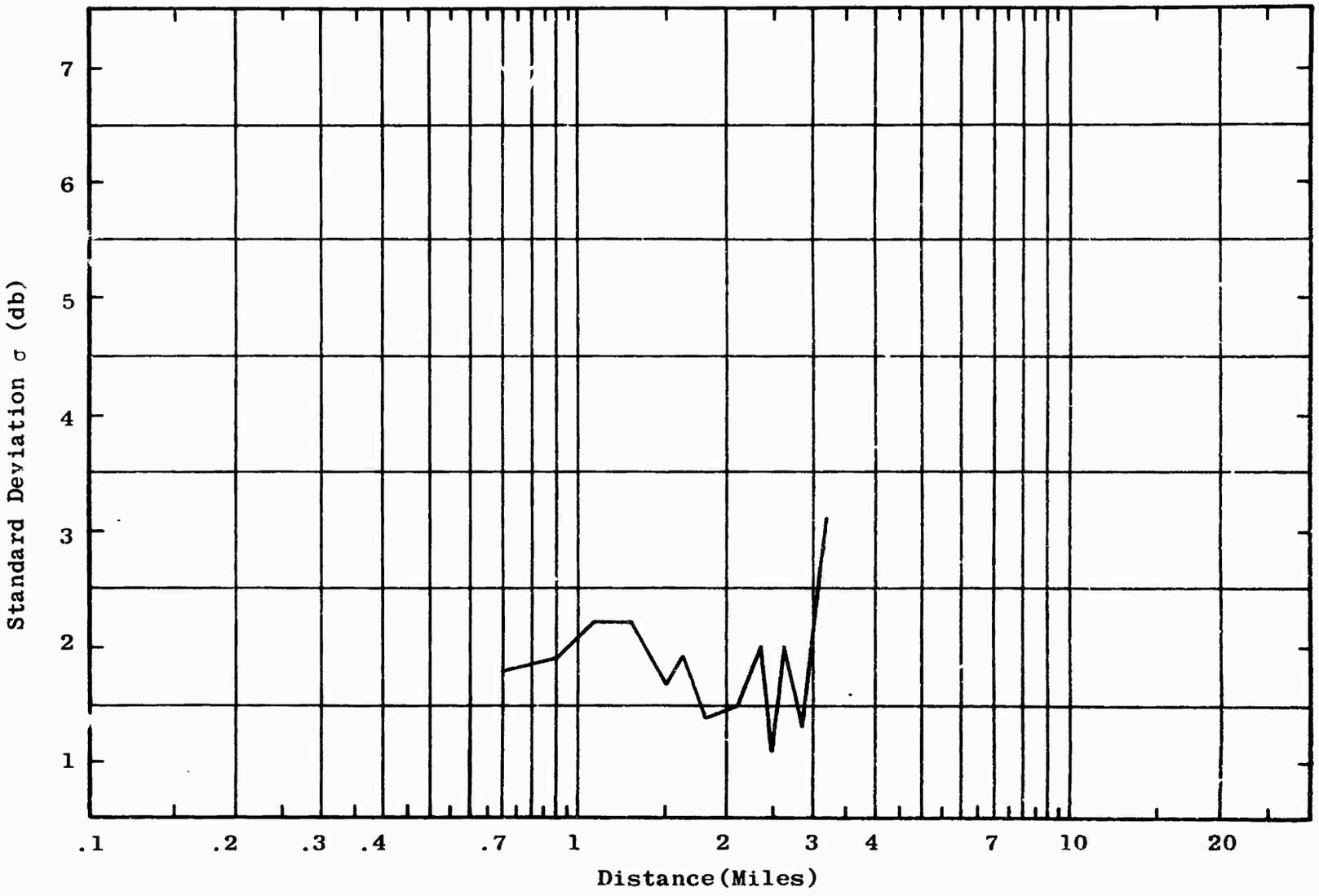

Figure 4.68 Standard Deviation of Vehicular Data
$L_b = F_A(25.5, 80, H, d, 7)$

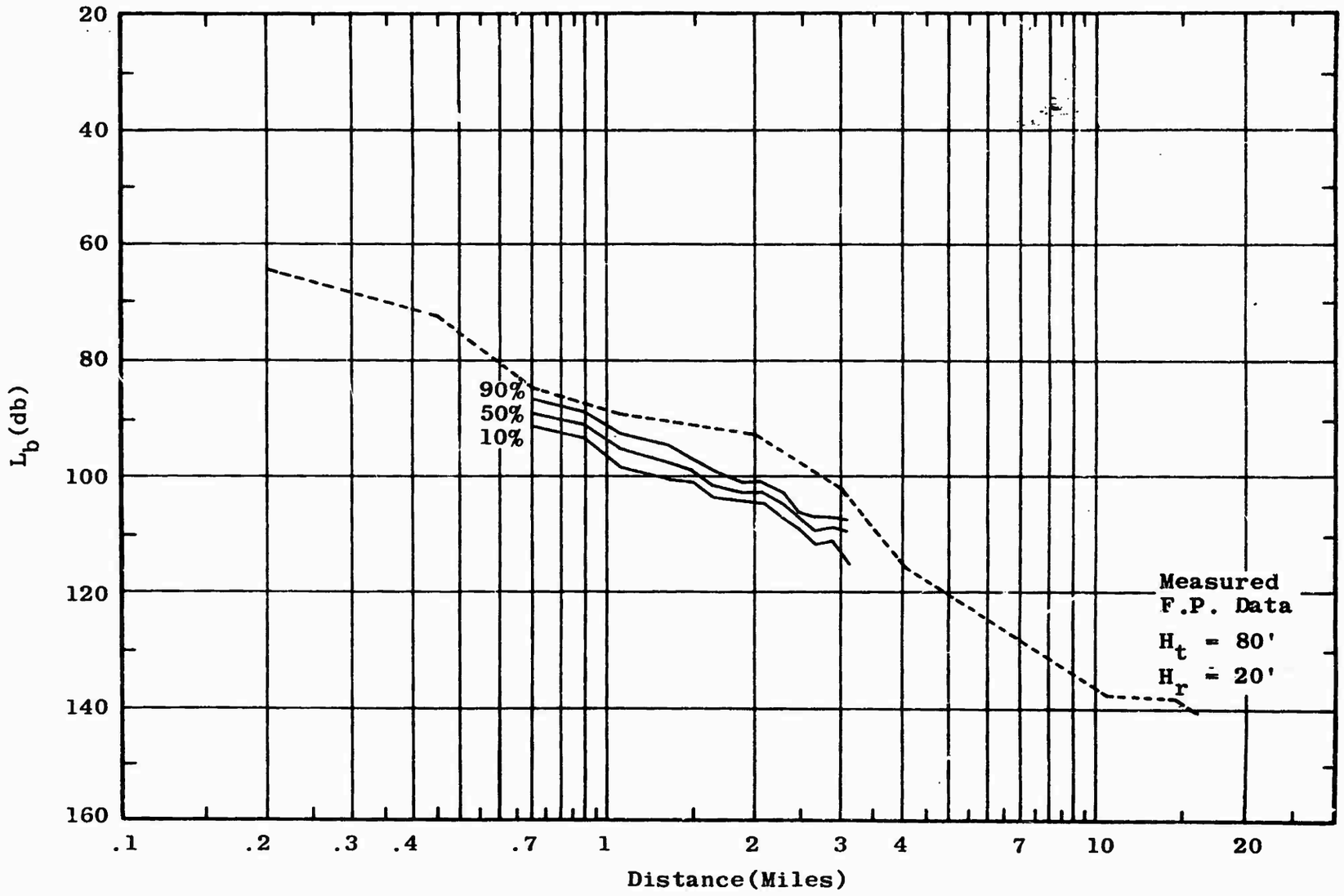

Figure 4.69 Comparison Between Vehicular Data and Measured F. P. Data
$L_b = F_A(25.5, 80, H, d, 7)$

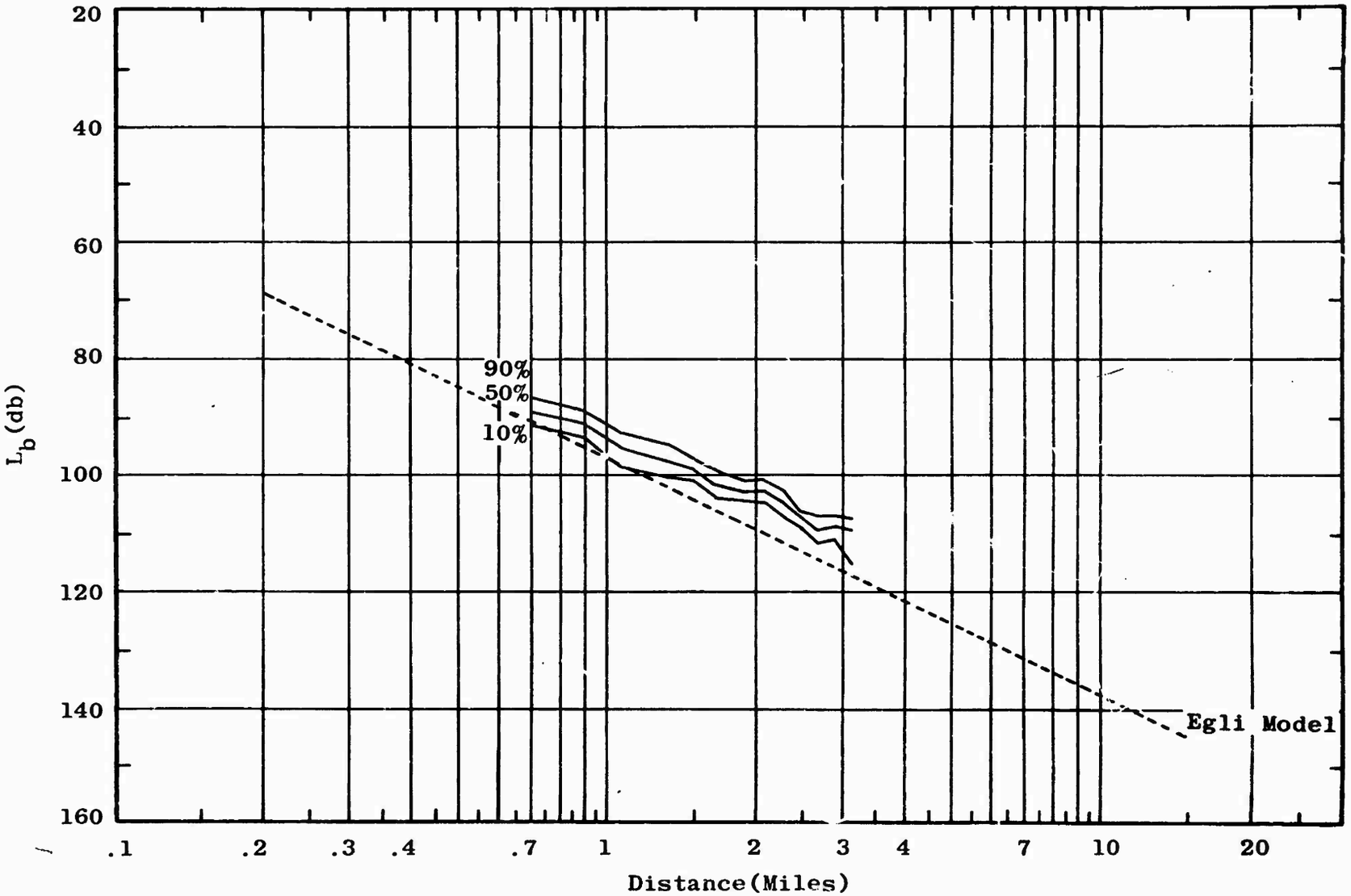

Figure 4.70 Comparison Between Vehicular Data and Egli Model
$L_b = F_A(25.5, 80, H, d, 7)$

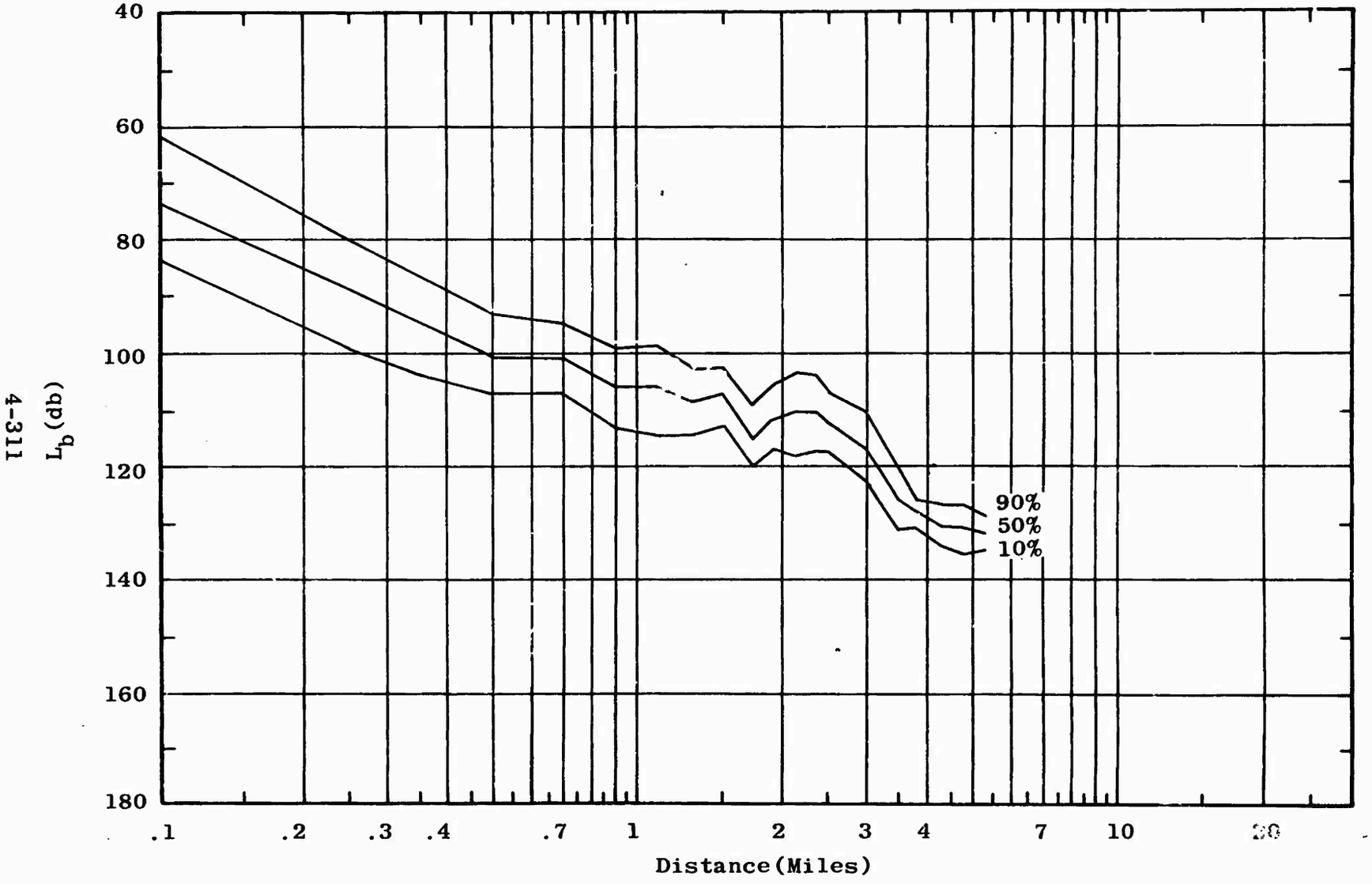

Figure 4.71 Reduced Vehicular Data
$L_b = F_A(50, 80, V, d, 7)$

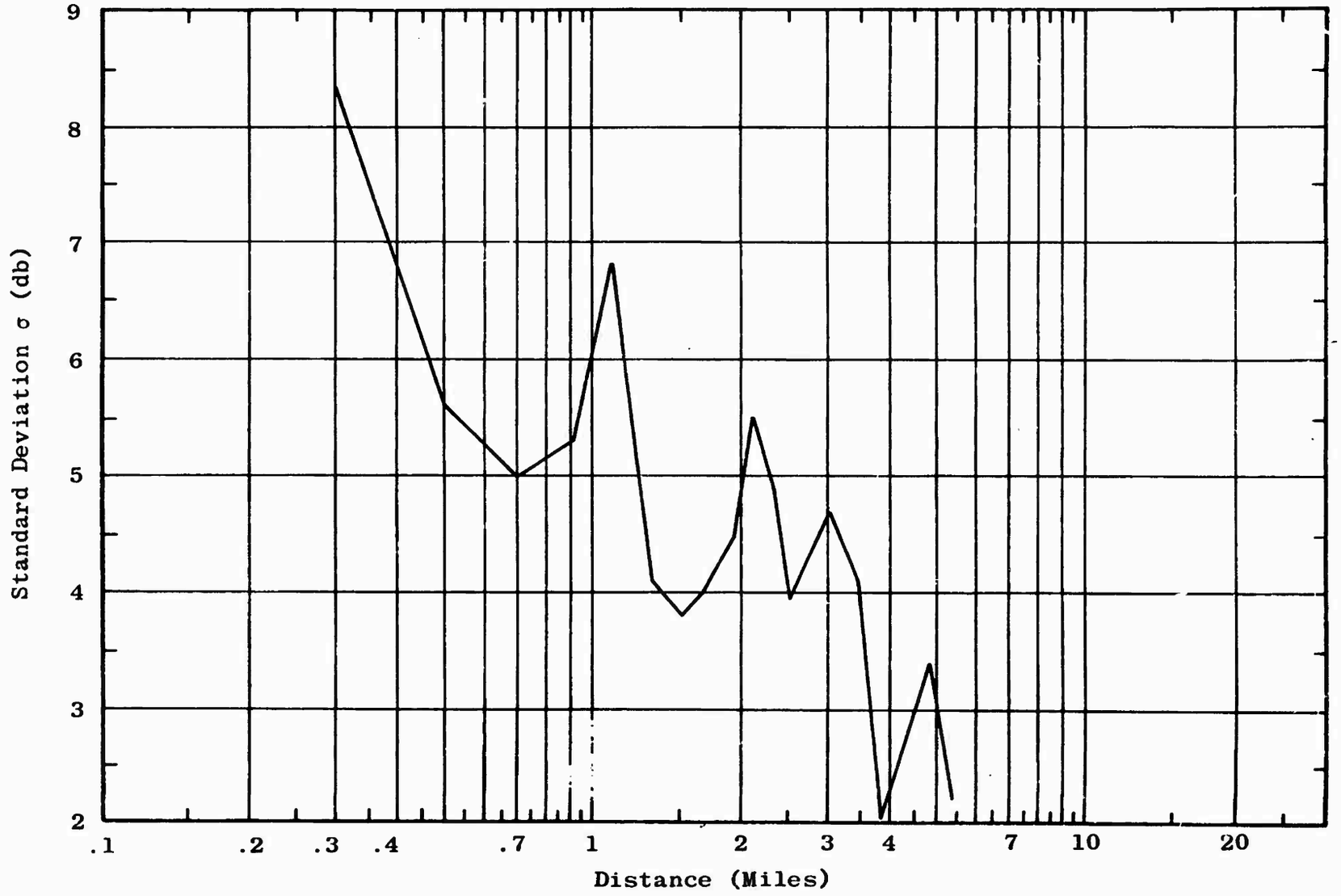

Figure 4.72 Standard Deviation of Vehicular Data
$L_b = F_A(50, 80, V, d, 7)$

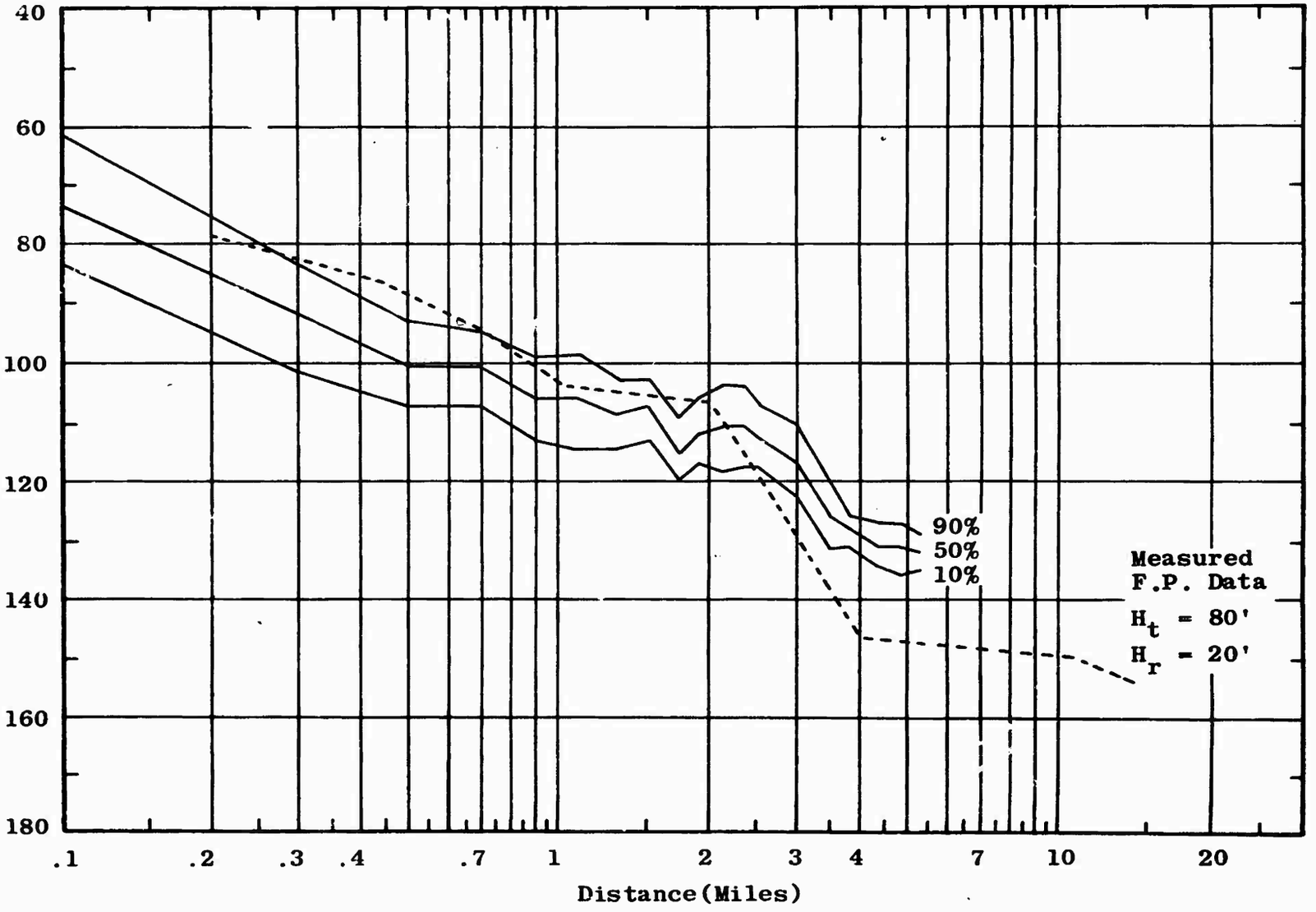

Figure 4.73 Comparison Between Vehicular Data and Measured F. P. Data
$L_b = F_A(50, 80, V, d, 7)$

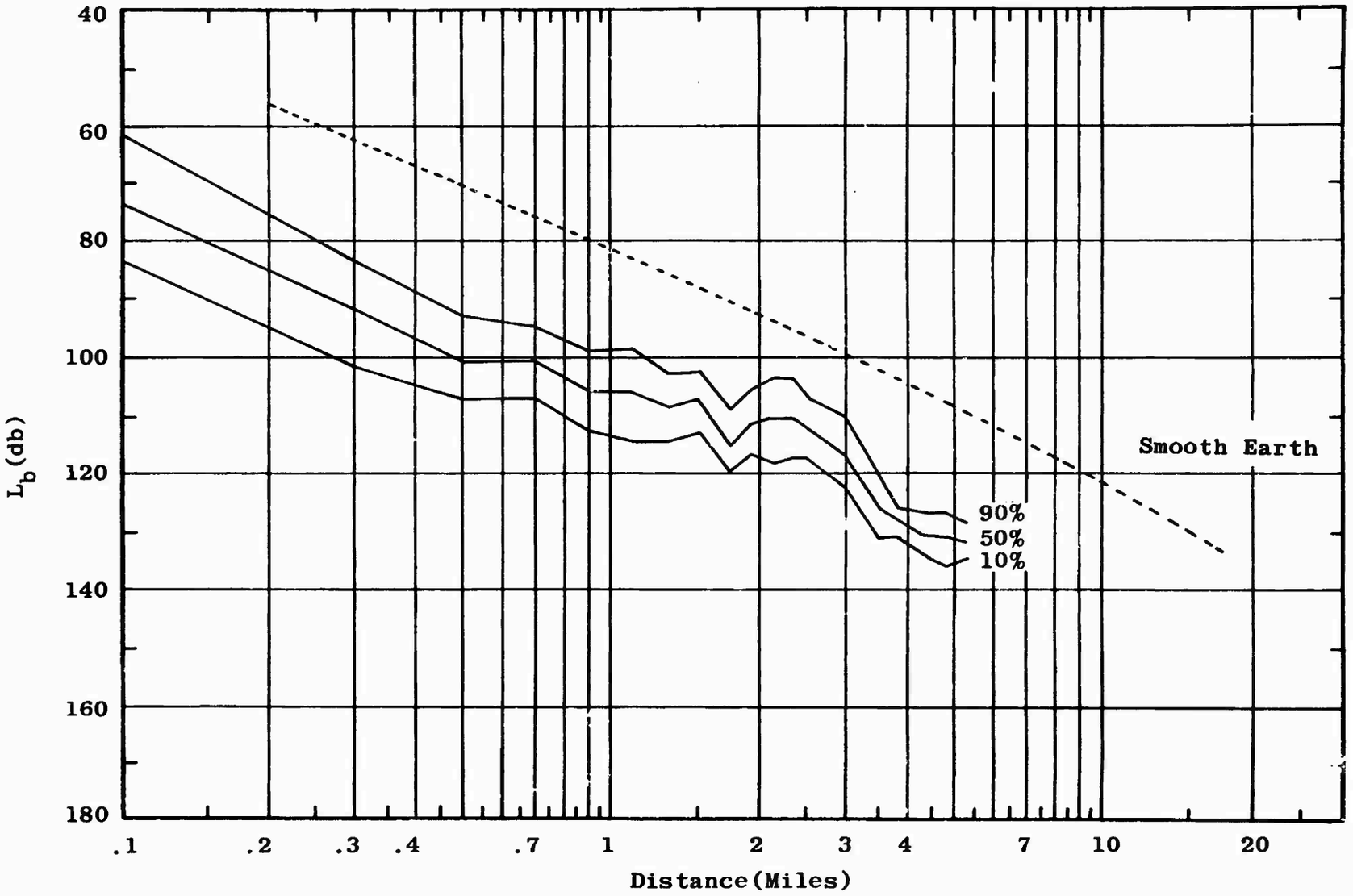

Figure 4.74 Comparison of Vehicular Data and Theoretical Smooth-Earth Model
$L_b = F_A(50, 80, V, d, 7)$

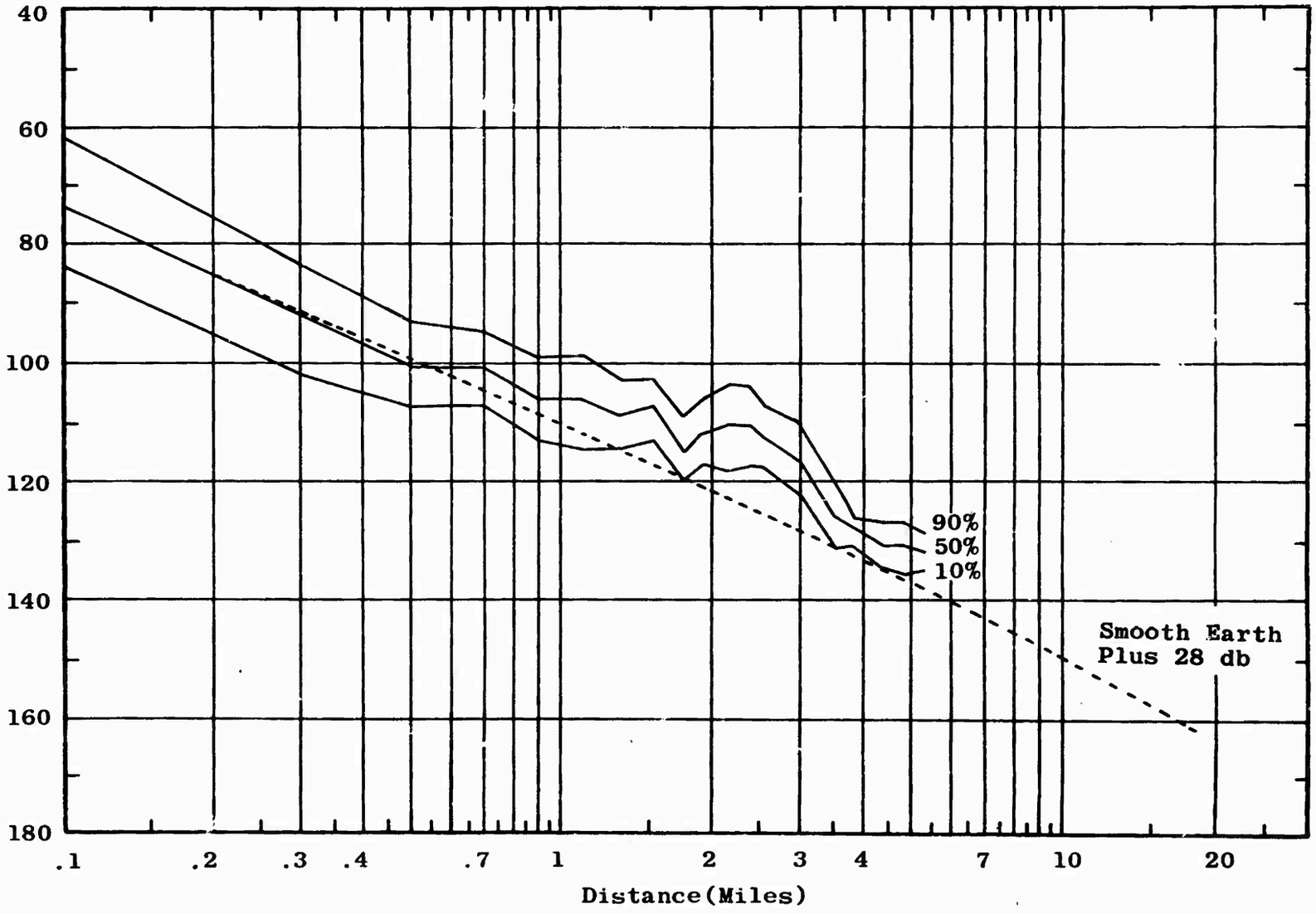

Figure 4.75 Comparison Between Vehicular Data and Theoretical Smooth-Earth Model Plus 28 db
$L_b = F_A(50, 80, V, d, 7)$

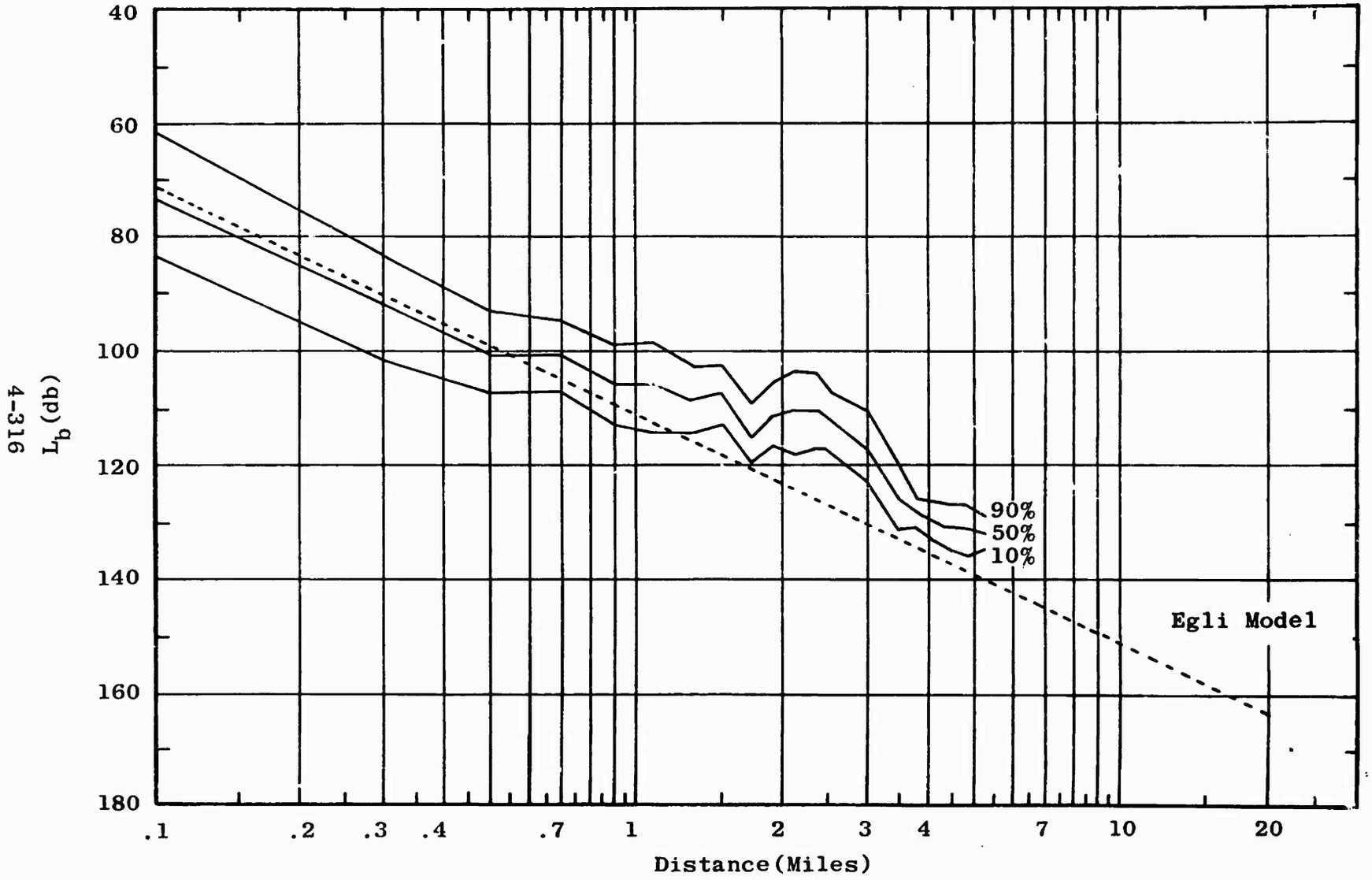

Figure 4.76 Comparison Between Vehicular Data and Egli Model
$L_b = F_A(50, 80, V, d, 7)$

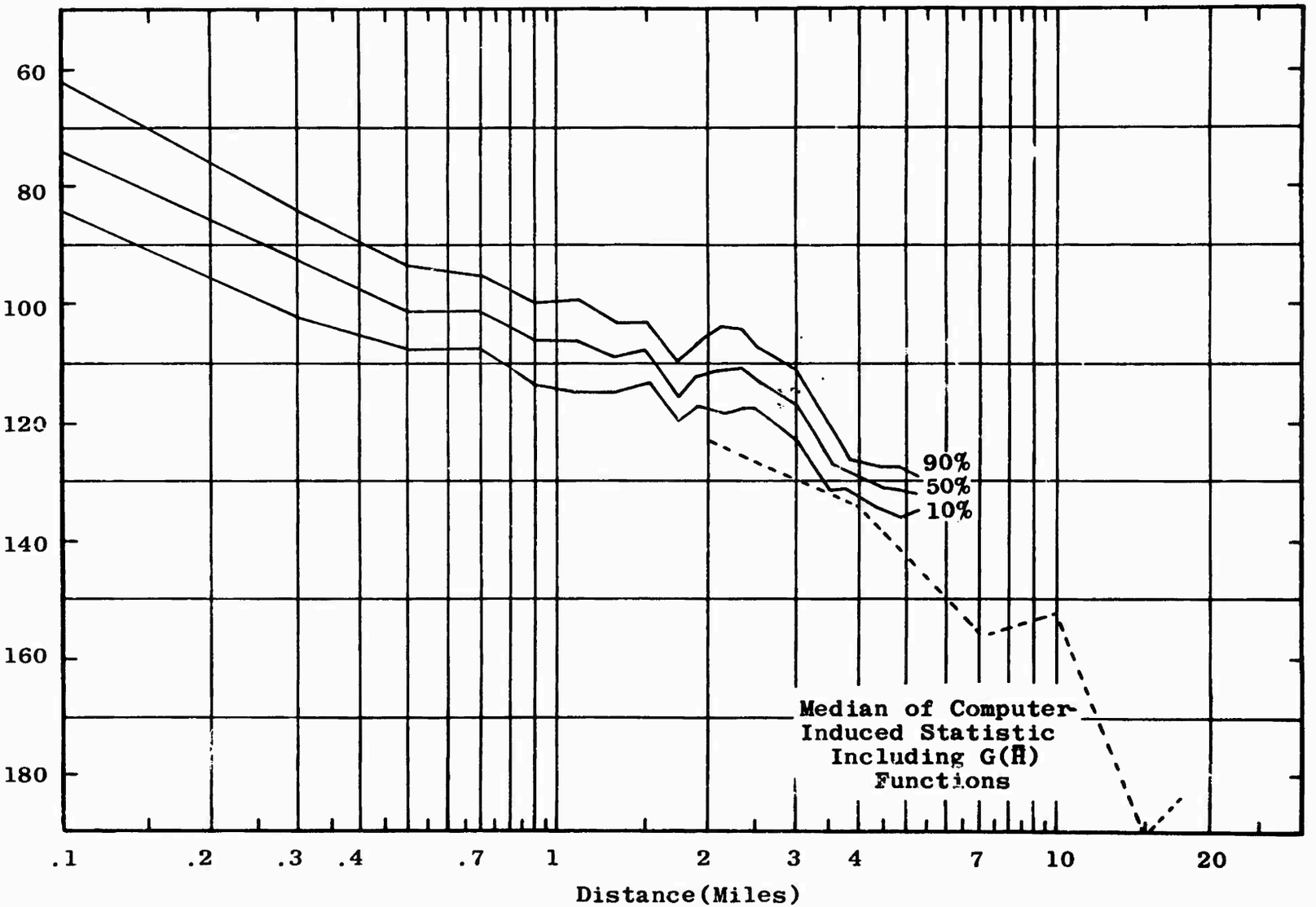

Figure 4.77 Comparison Between Vehicular Data and Median of Computer-Induced Statistic Including G(R) Functions
$L_b = F_A(50, 80, V, d, 7)$

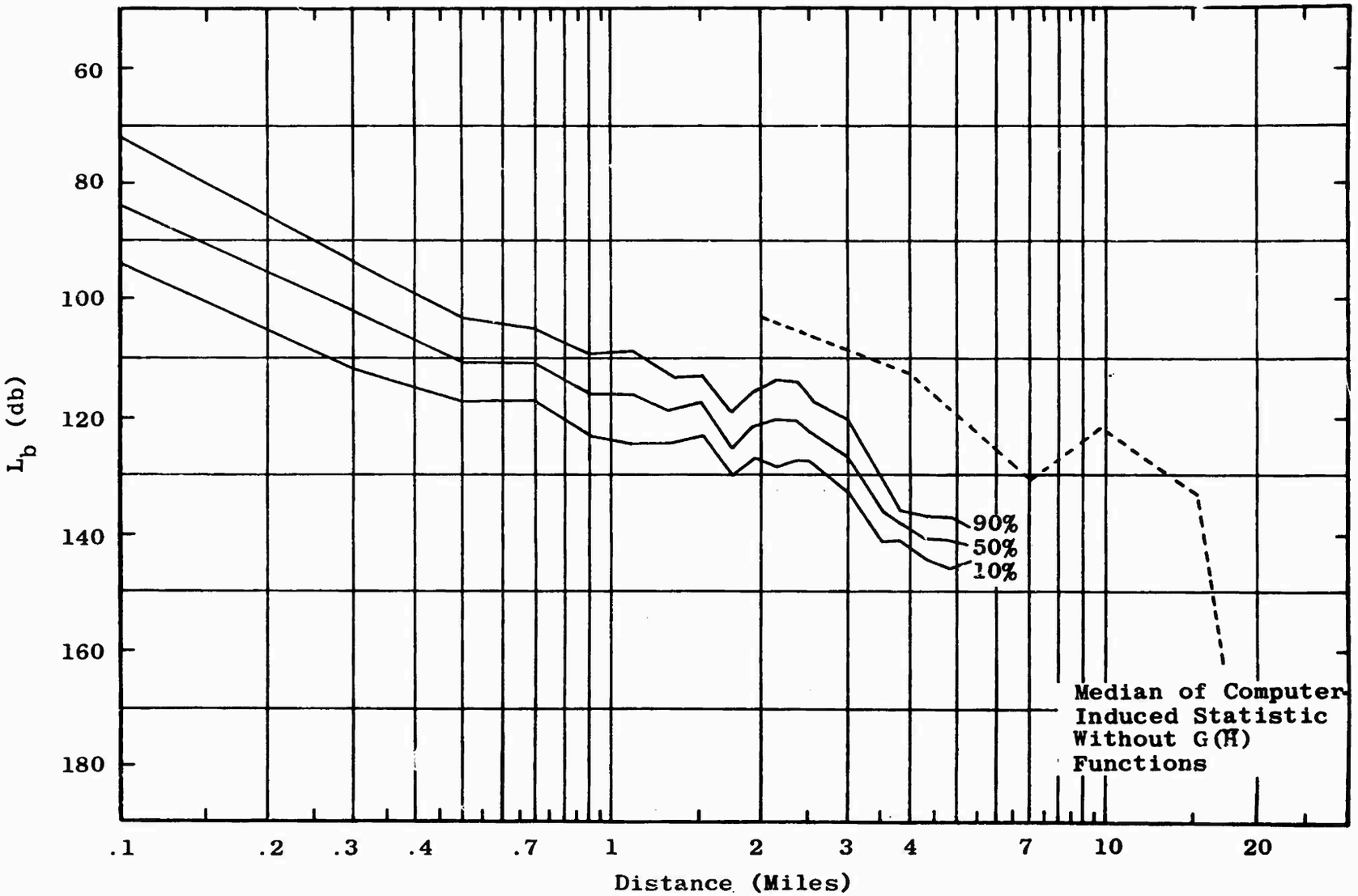

Figure 4.78 Comparison Between Vehicular Data and Median of Computer-Induced Statistic Without $G(\bar{H})$ Functions
$L_b = F_A(50, 80, V, d, 7)$

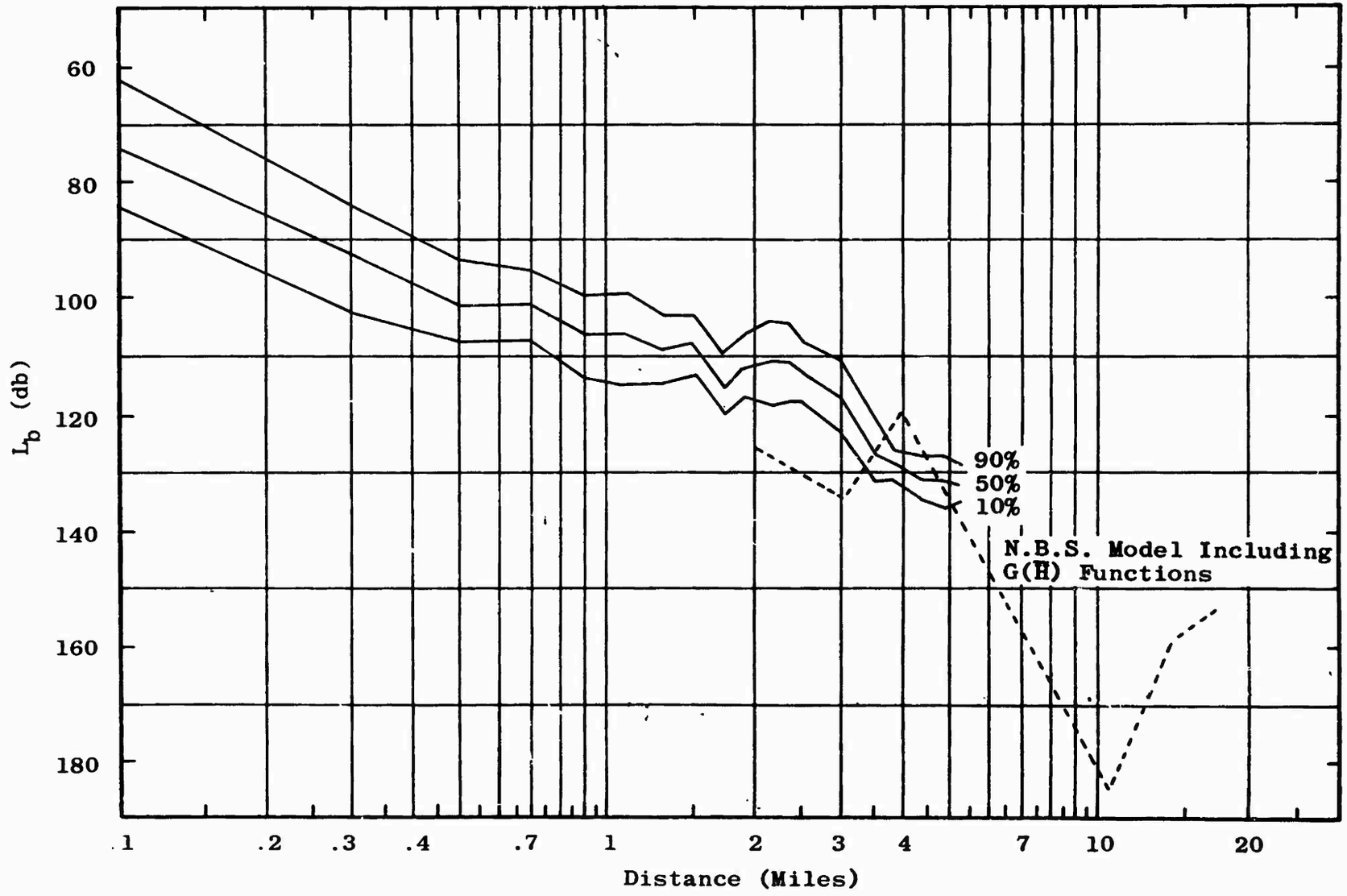

Figure 4.79 Comparison Between Vehicular Data and N.B.S. Model Including $G(\bar{H})$ Functions
$L_b = F_A(50, 80, V, d, 7)$

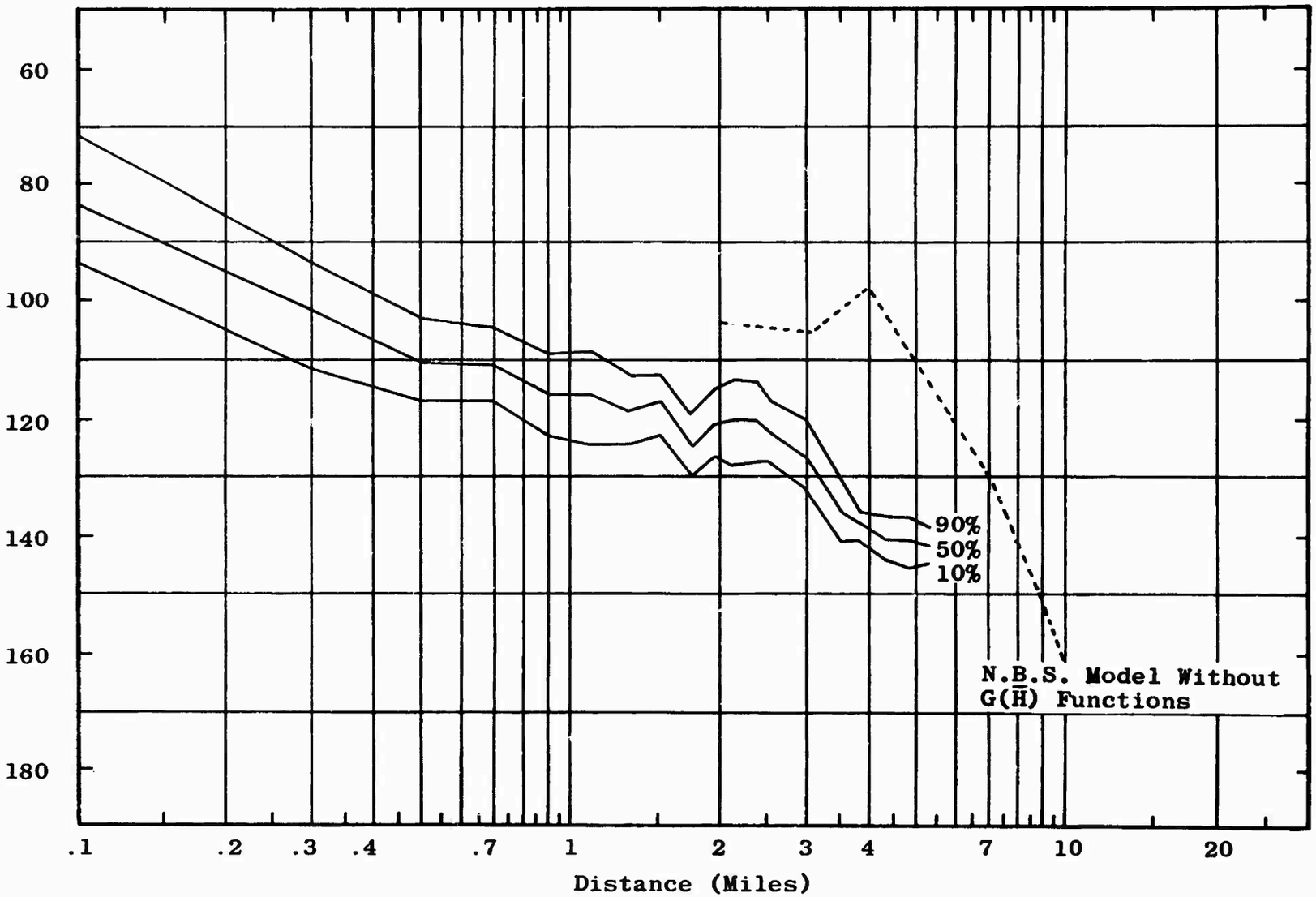

Figure 4.80 Comparison Between Vehicular Data and N.B.S. Model Without G($\bar{H}$) Functions
$L_b = F_A(50, 80, V, d, 7)$

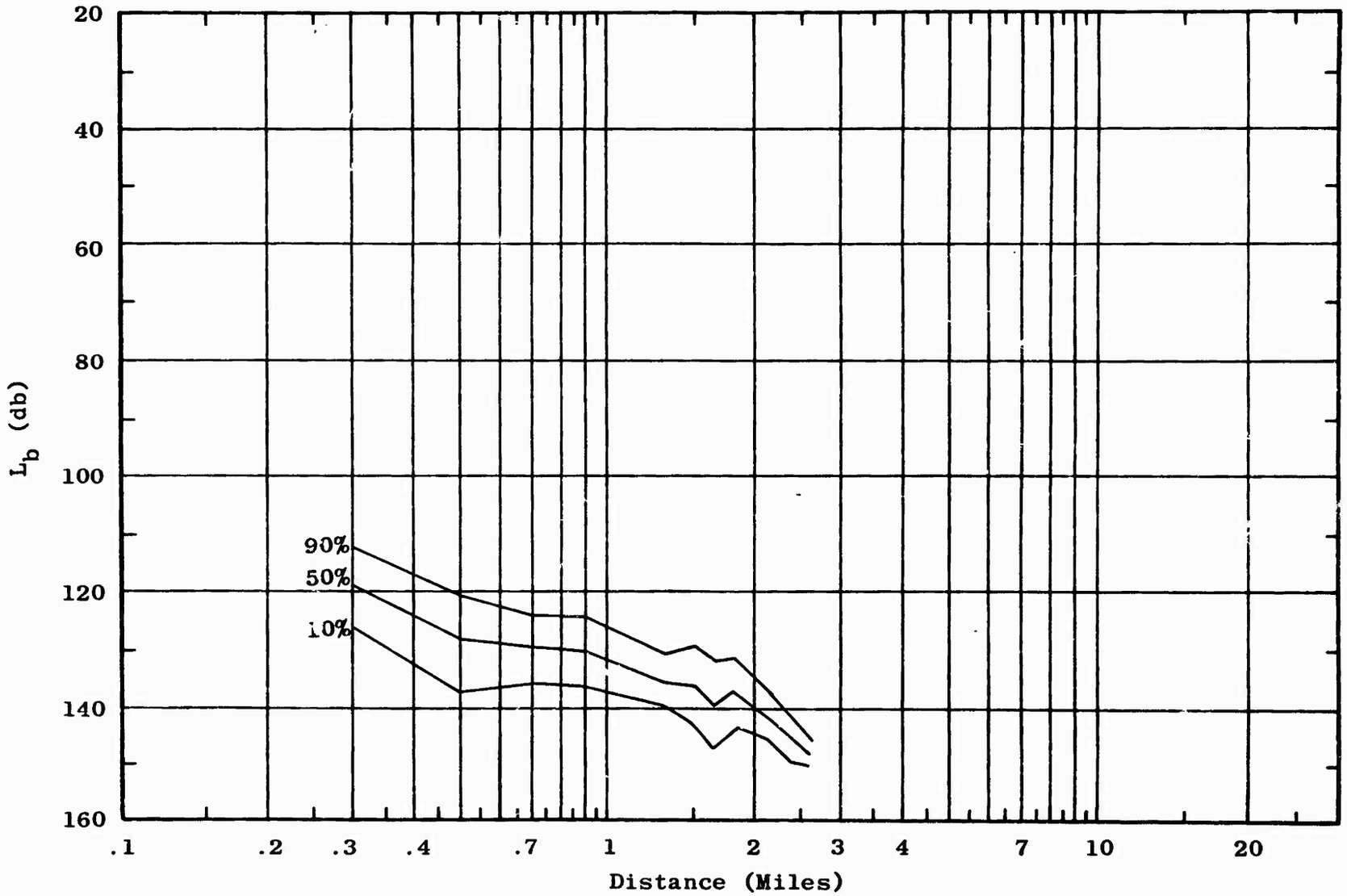

Figure 4.81 Reduced Vehicular Data
$L_b = F_A(100, 13, V, d, 7)$

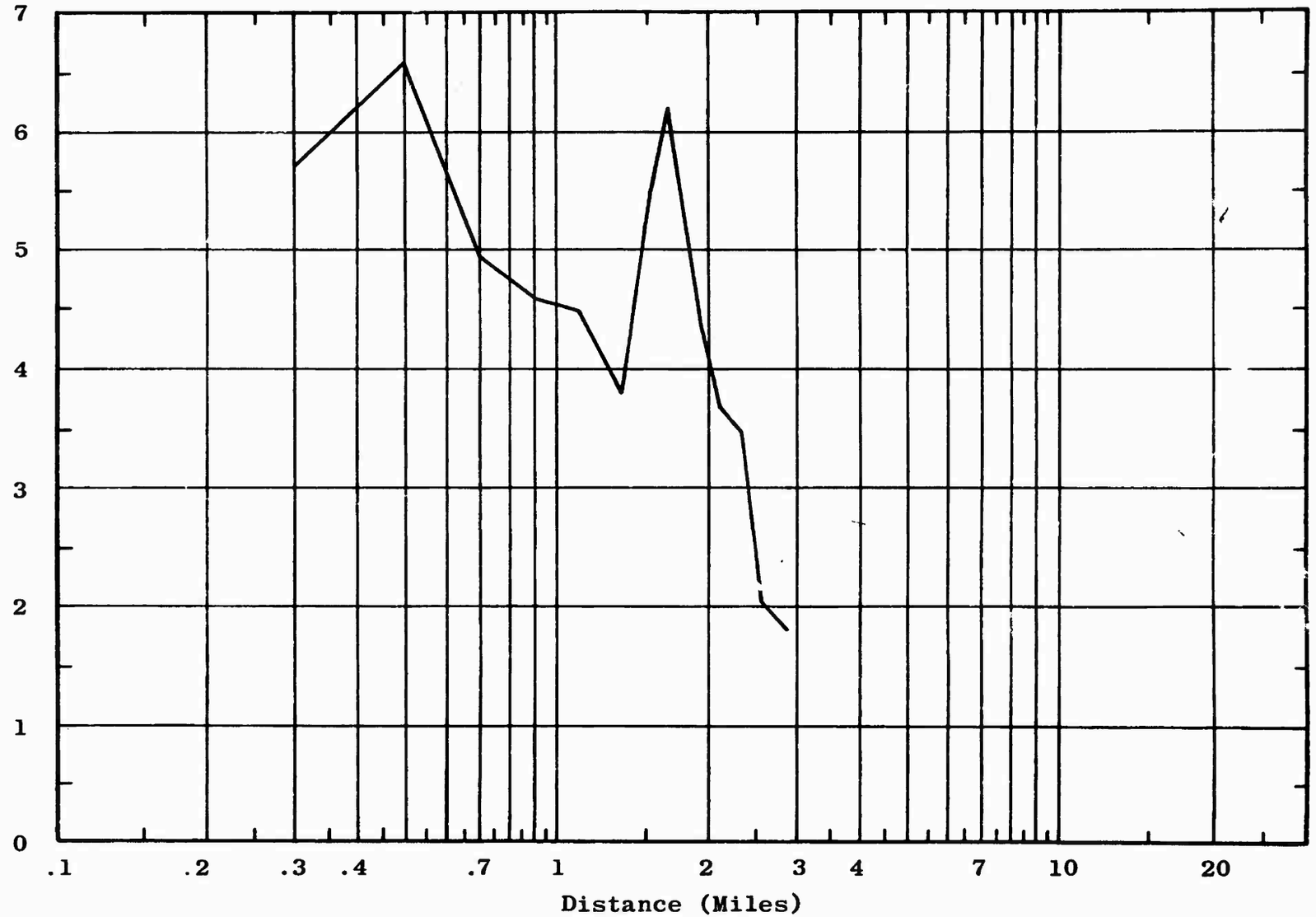

Figure 4.82 Standard Deviation of Vehicular Data
$L_b = F_A(100, 13, V, d, 7)$

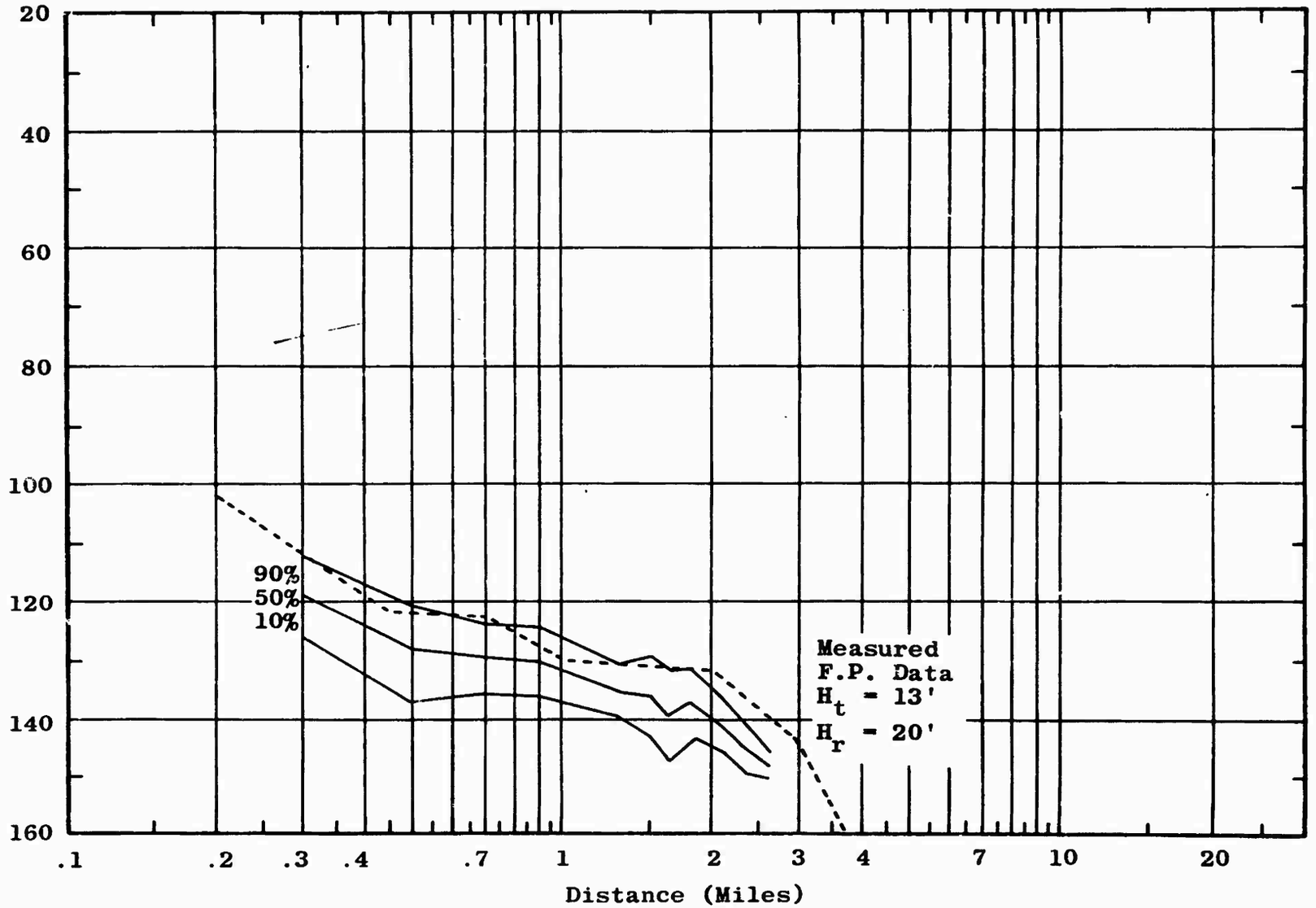

Figure 4.83 Comparison Between Vehicular Data and Measured F.P. Data
$L_b = F_A(100, 13, V, d, 7)$

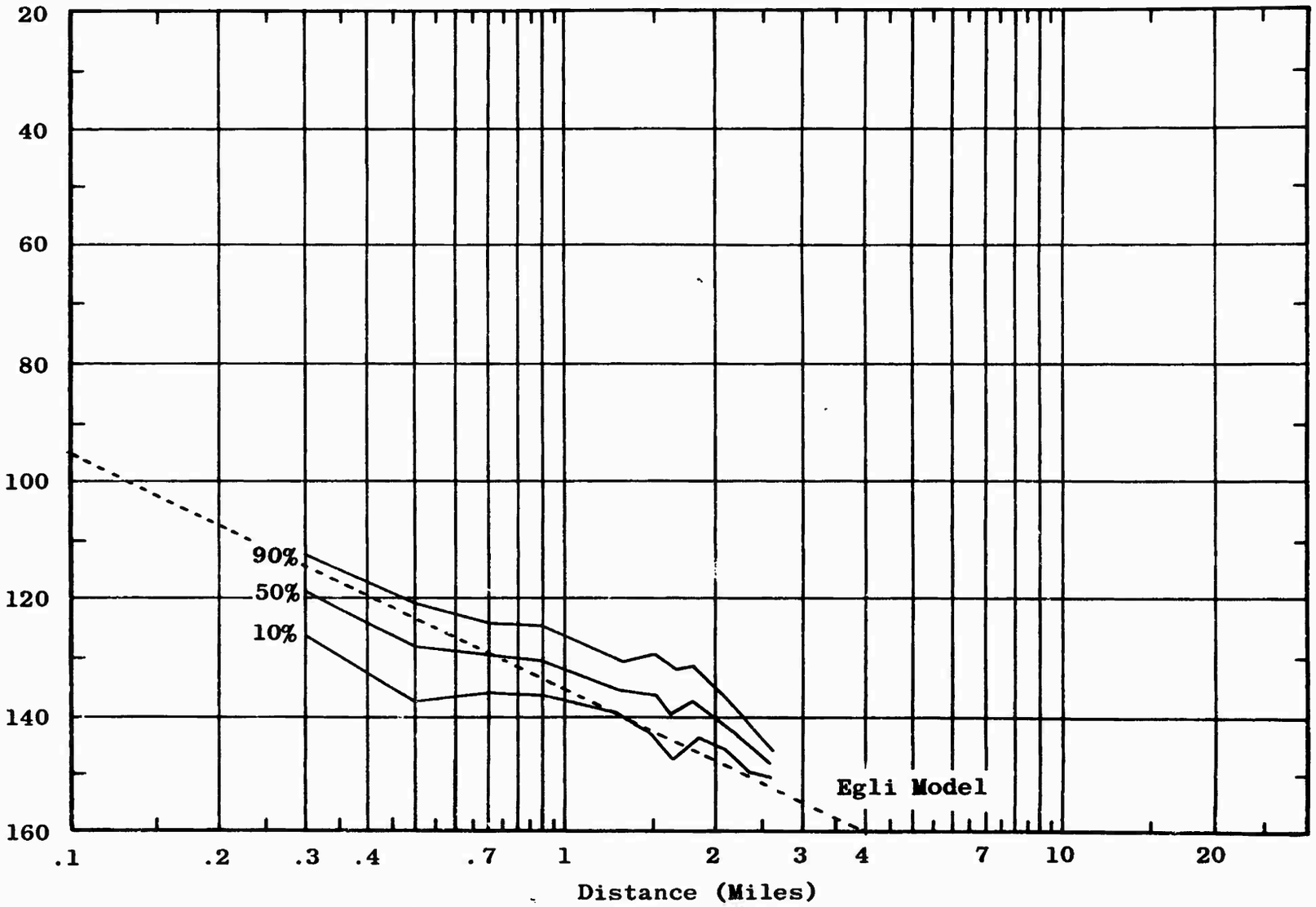

Figure 4.84 Comparison Between Vehicular Data and Egli Model
$L_b = F_A(100, 13, V, d, 7)$

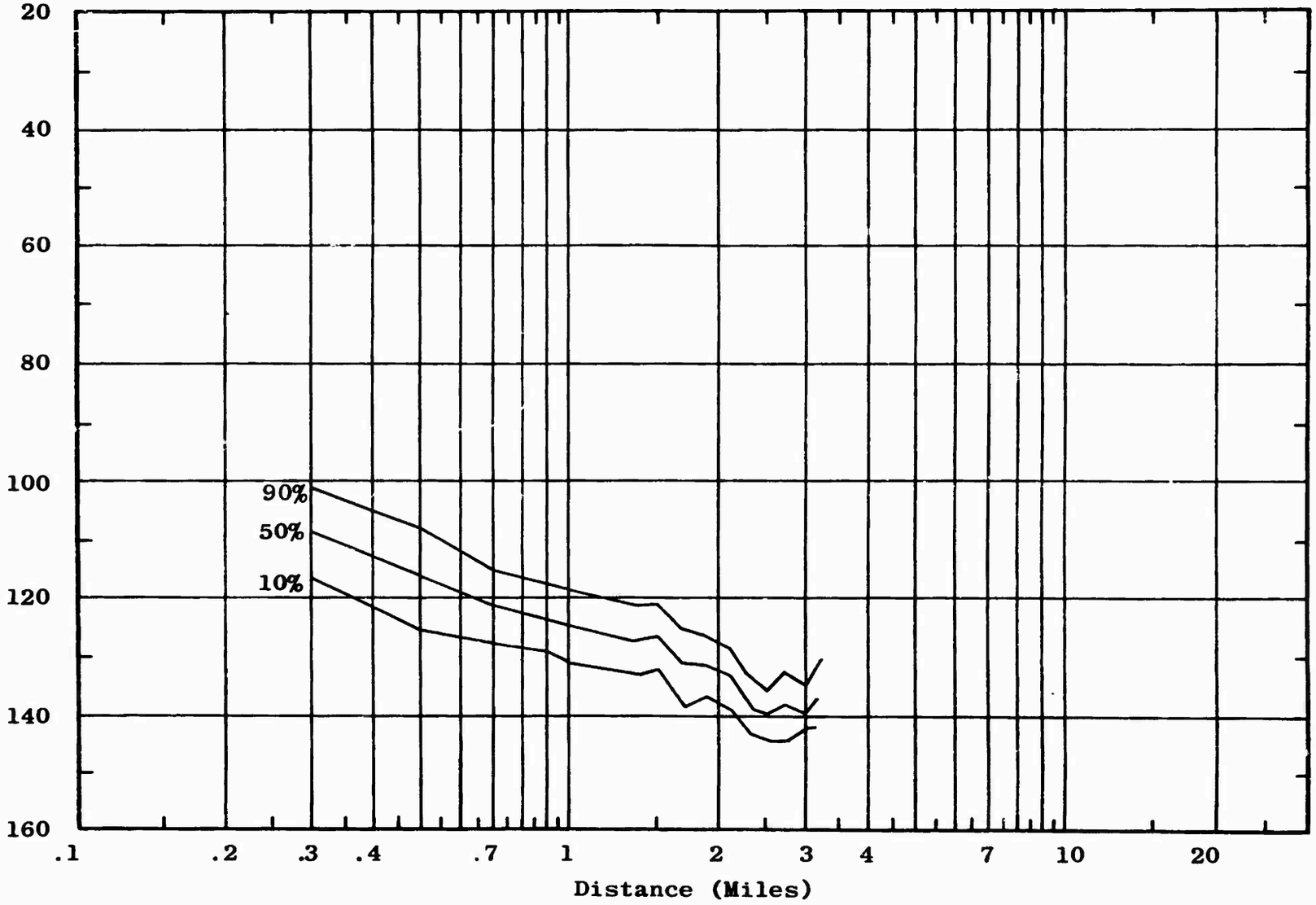

Figure 4.85 Reduced Vehicular Data
$L_b = F_A(100, 40, V, d, 7)$

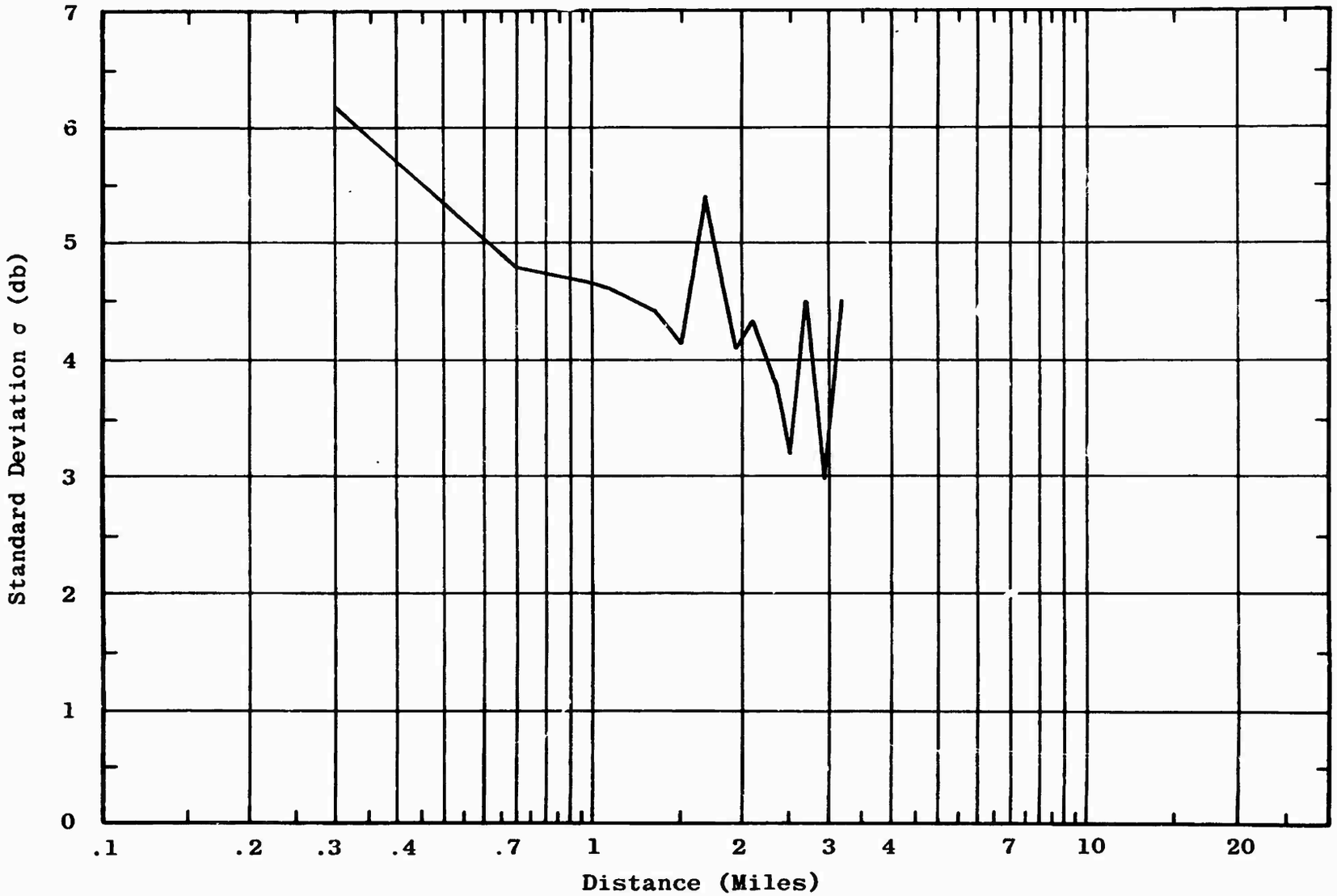

Figure 4.86 Standard Deviation of Vehicular Data
$L_b = F_A(100, 40, V, d, 7)$

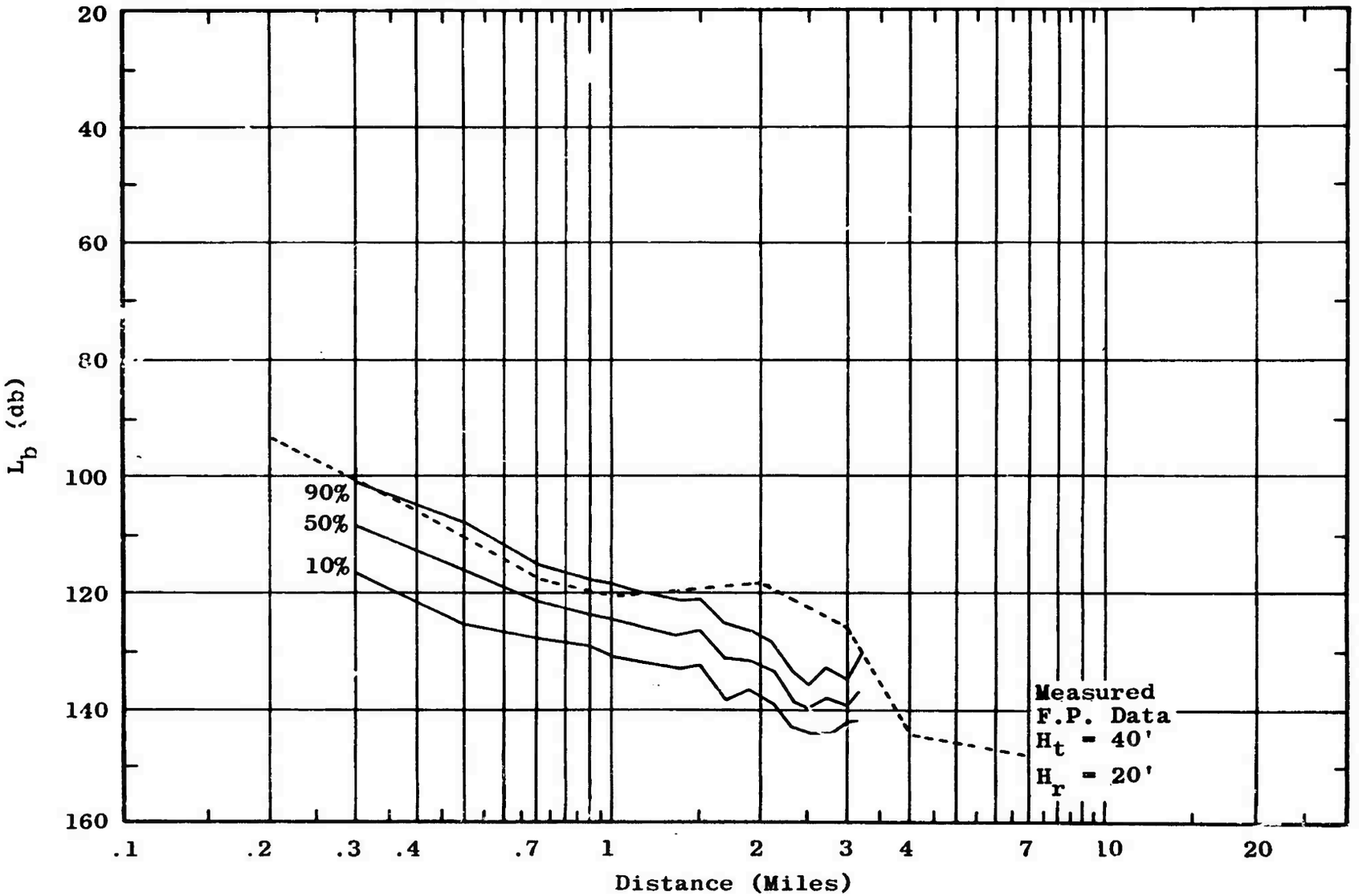

Figure 4.87 Comparison Between Vehicular Data and Measured F.P. Data
$L_b = F_A(100, 40, V, d, 7)$

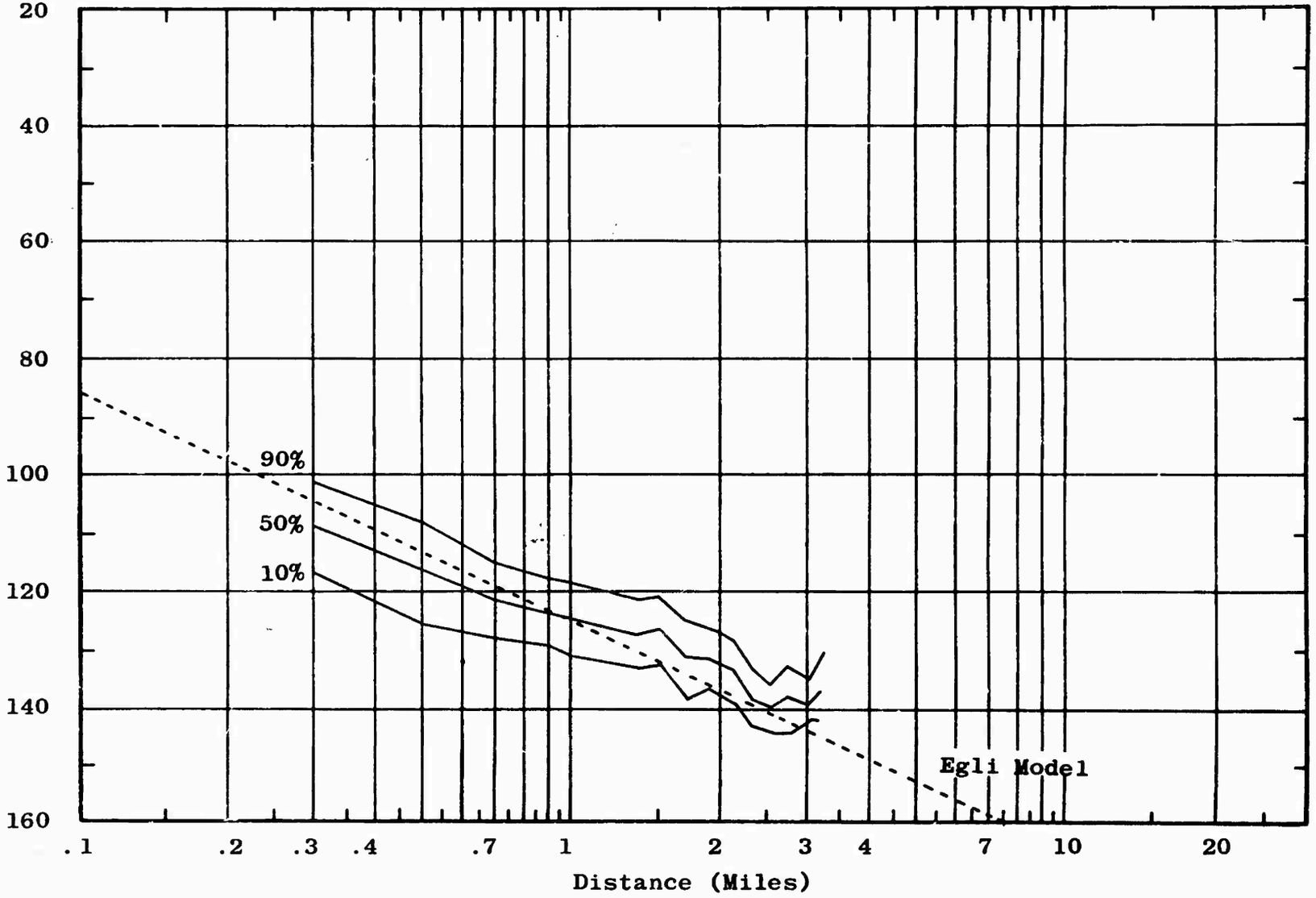

Figure 4.88 Comparison Between Vehicular Data and Egli Model
$L_b = F_A(100, 40, V, d, 7)$

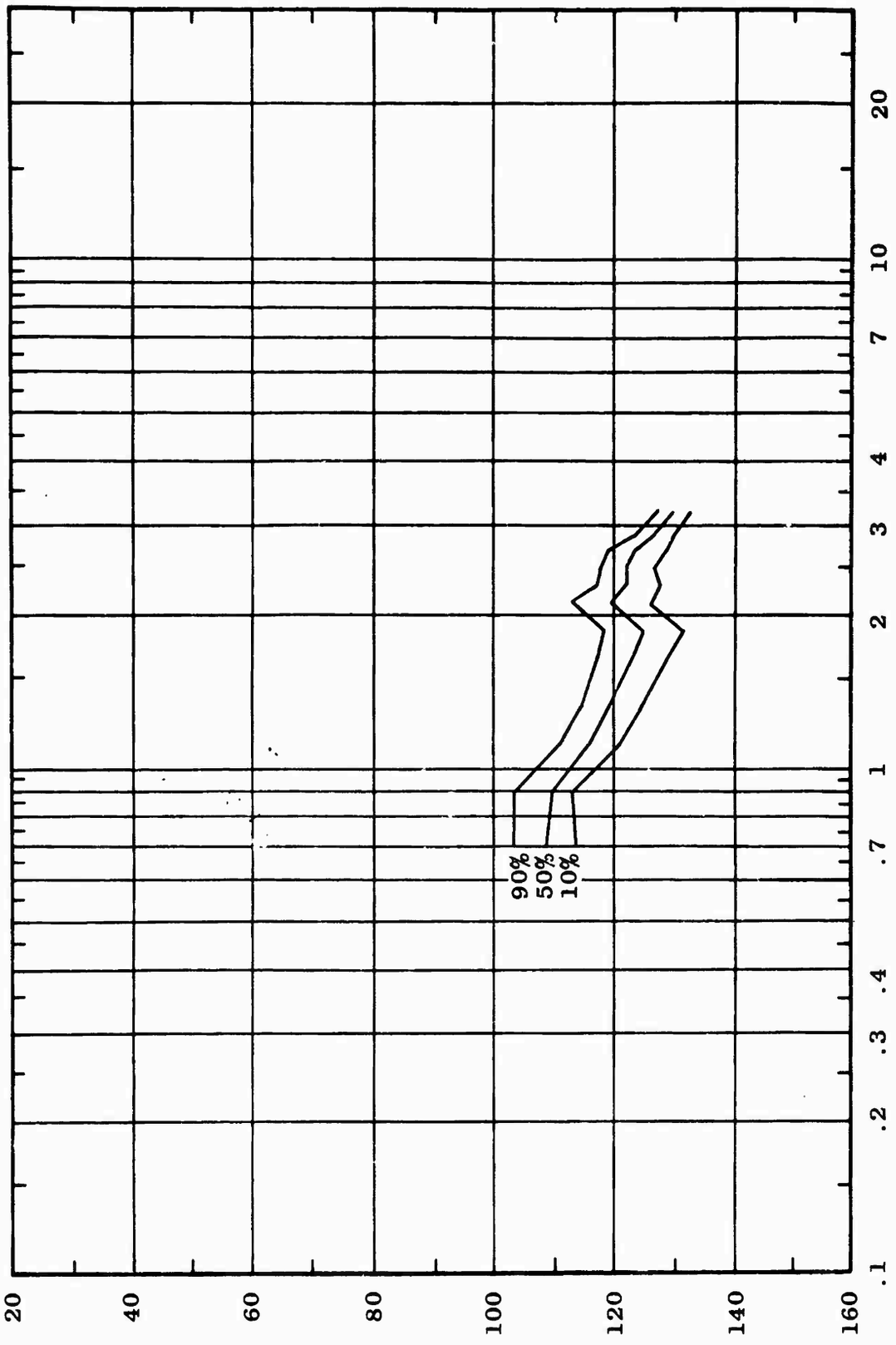

Figure 4.89 Reduced Vehicular Data
$L_b = F_A(100, 80, V, d, 7)$

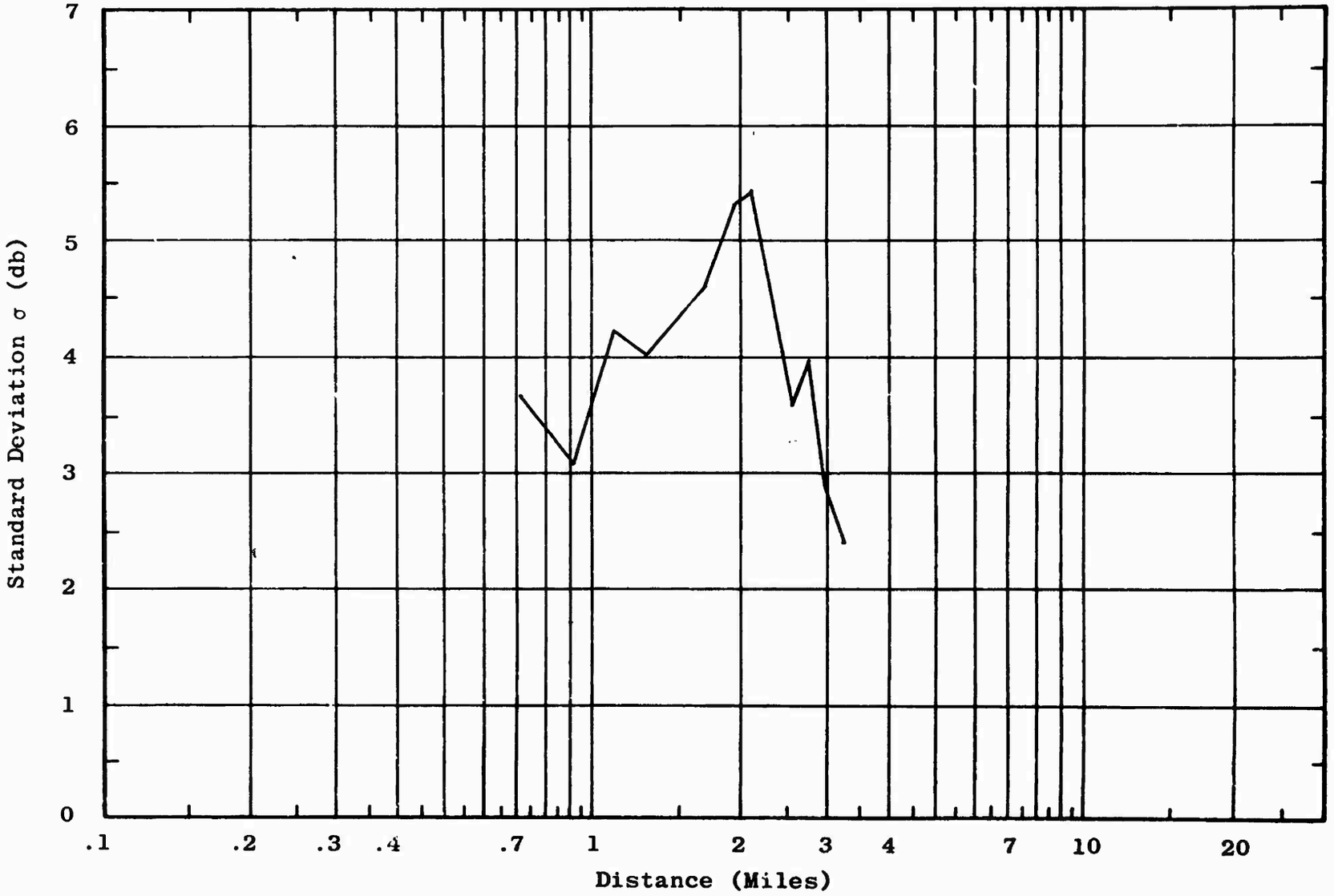

Figure 4.90 Standard Deviation of Vehicular Data
$L_b = F_A(100, 80, V, d, 7)$

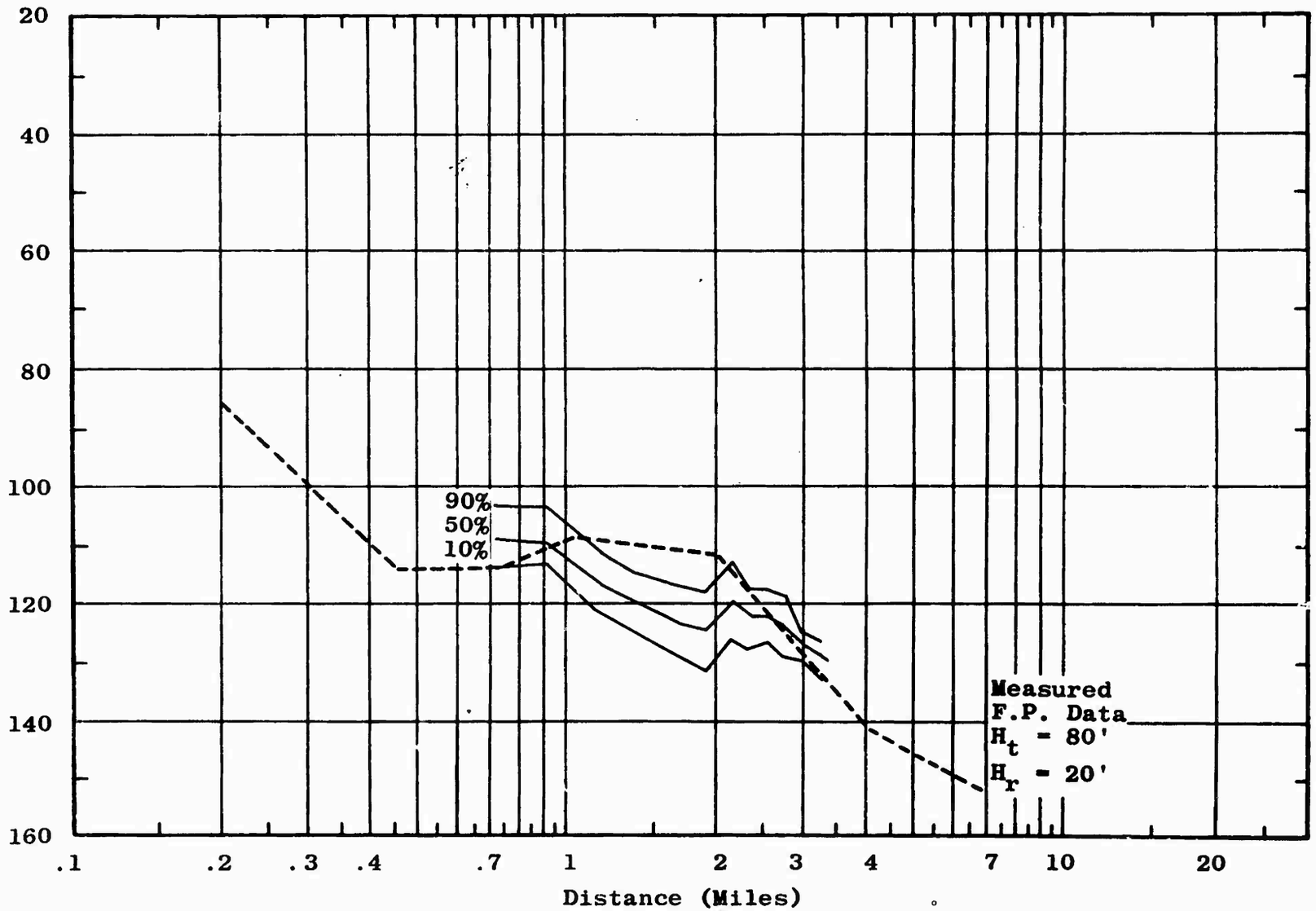

Figure 4.91 Comparison Between Vehicular Data and Measured F.P. Data
$L_b = F_A(100, 80, V, d, 7)$

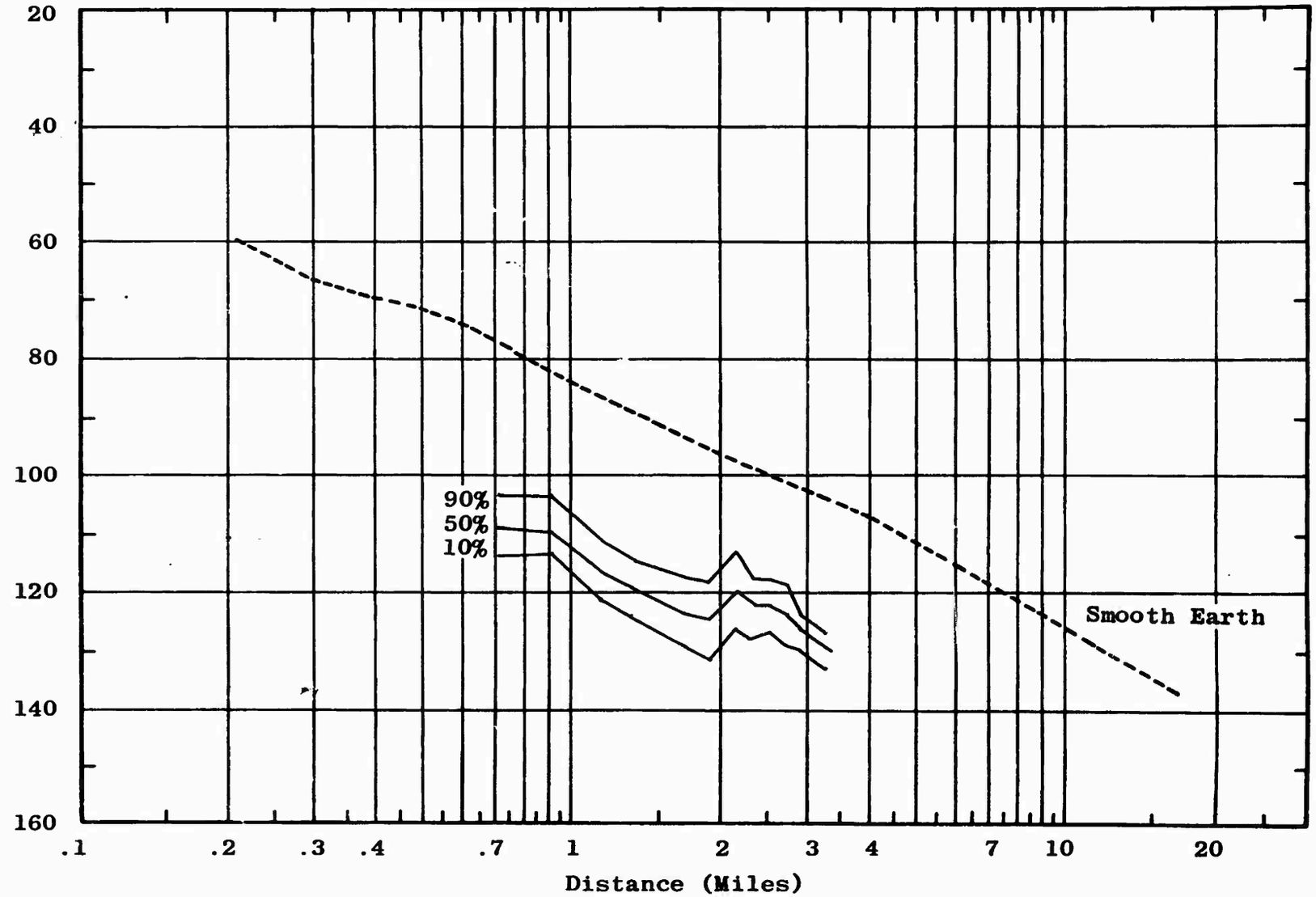

Figure 4.92 Comparison Between Vehicular Data and Theoretical Smooth-Earth Model
$L_b = F_A(100, 80, V, d, 7)$

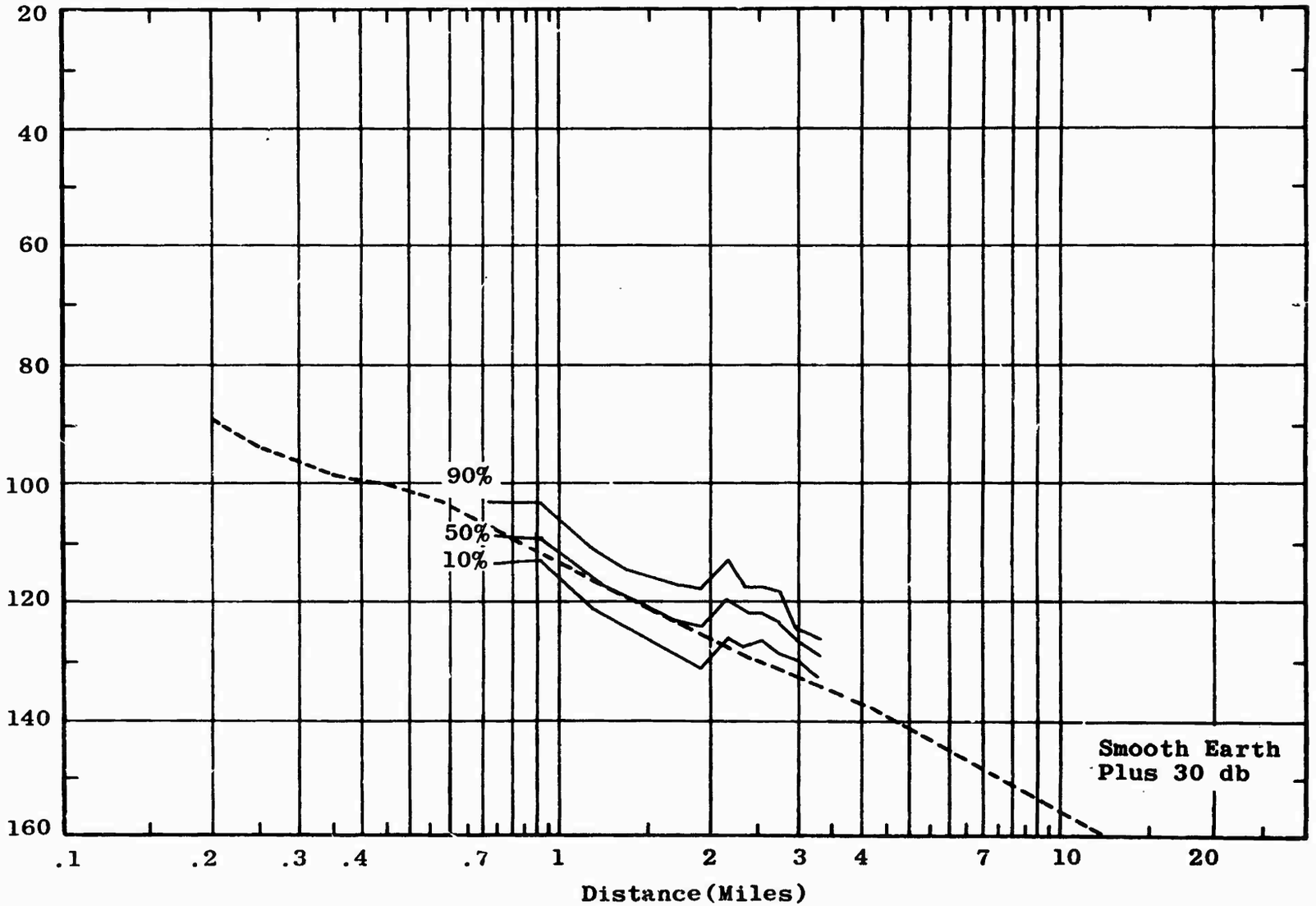

Figure 4.93 Comparison Between Vehicular Data and Theoretical Smooth-Earth Model Plus 30 db
$L_b = F_A(100, 80, V, d, 7)$

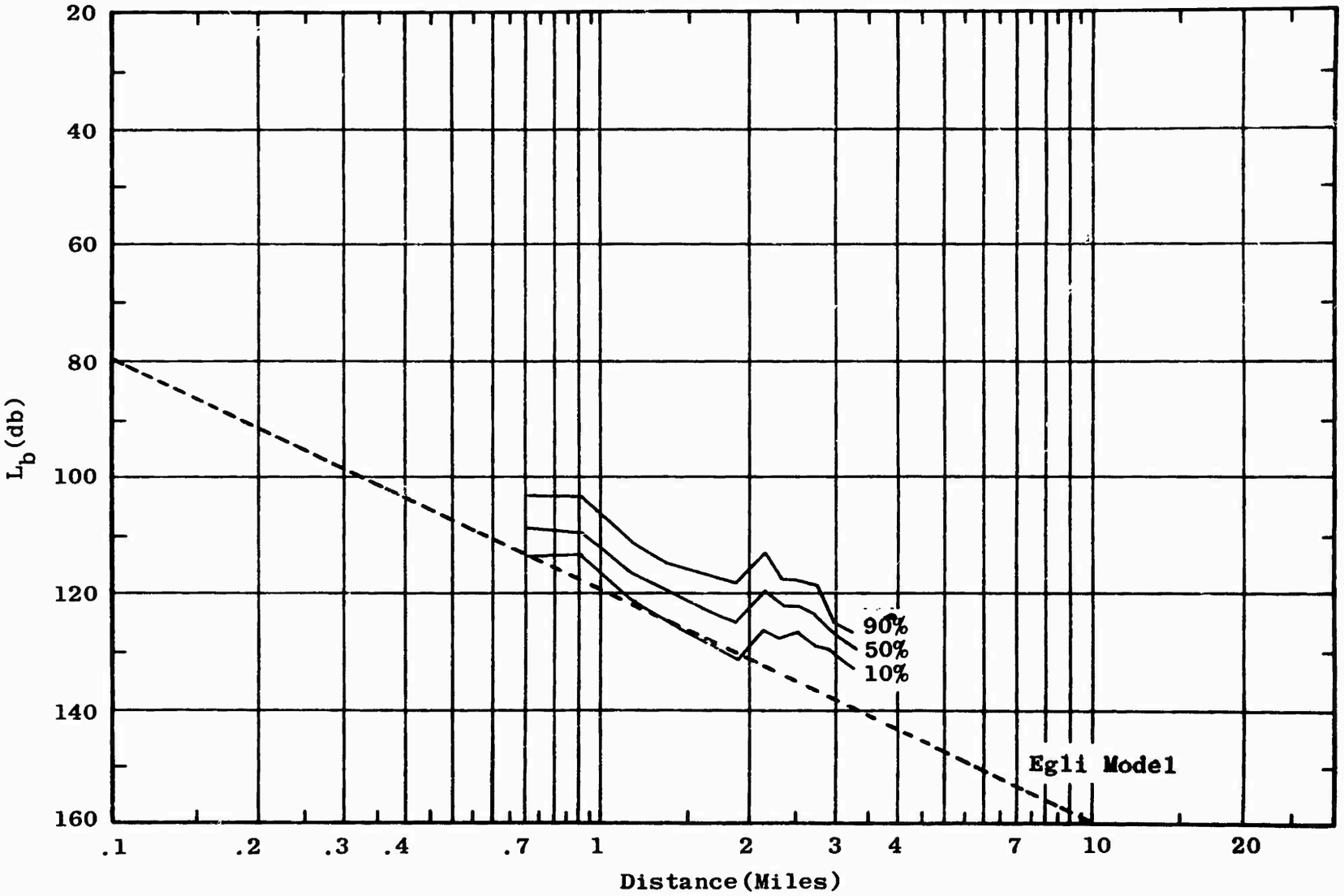

Figure 4.94 Comparison Between Vehicular Data and Egli Model
$L_b = F_A(100, 80, V, d, 7)$

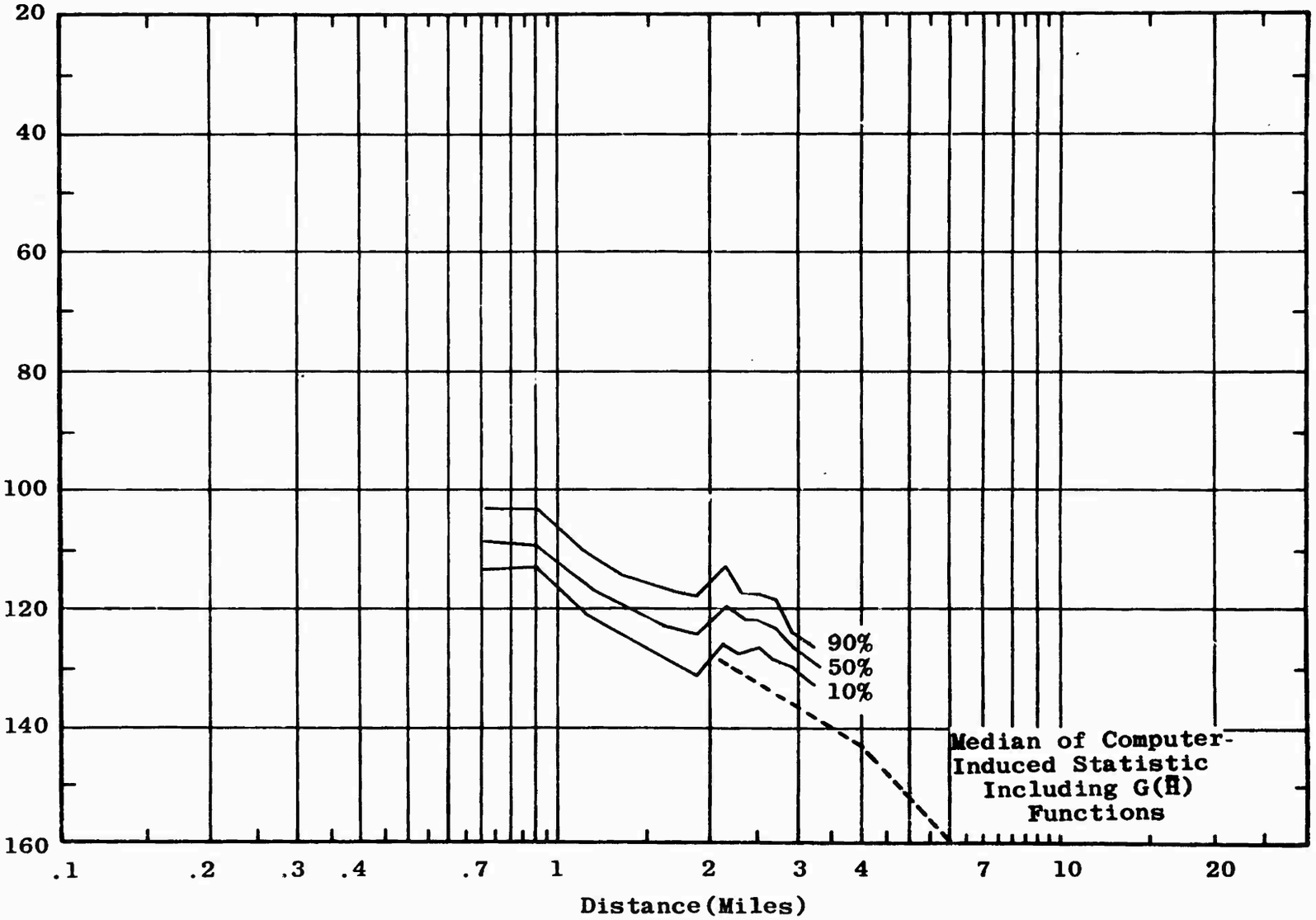

Figure 4.95 Comparison Between Vehicular Data and Median of Computer-Induced Statistic Including G(H) Functions
$L_b = F_A(100, 80, V, d, 7)$

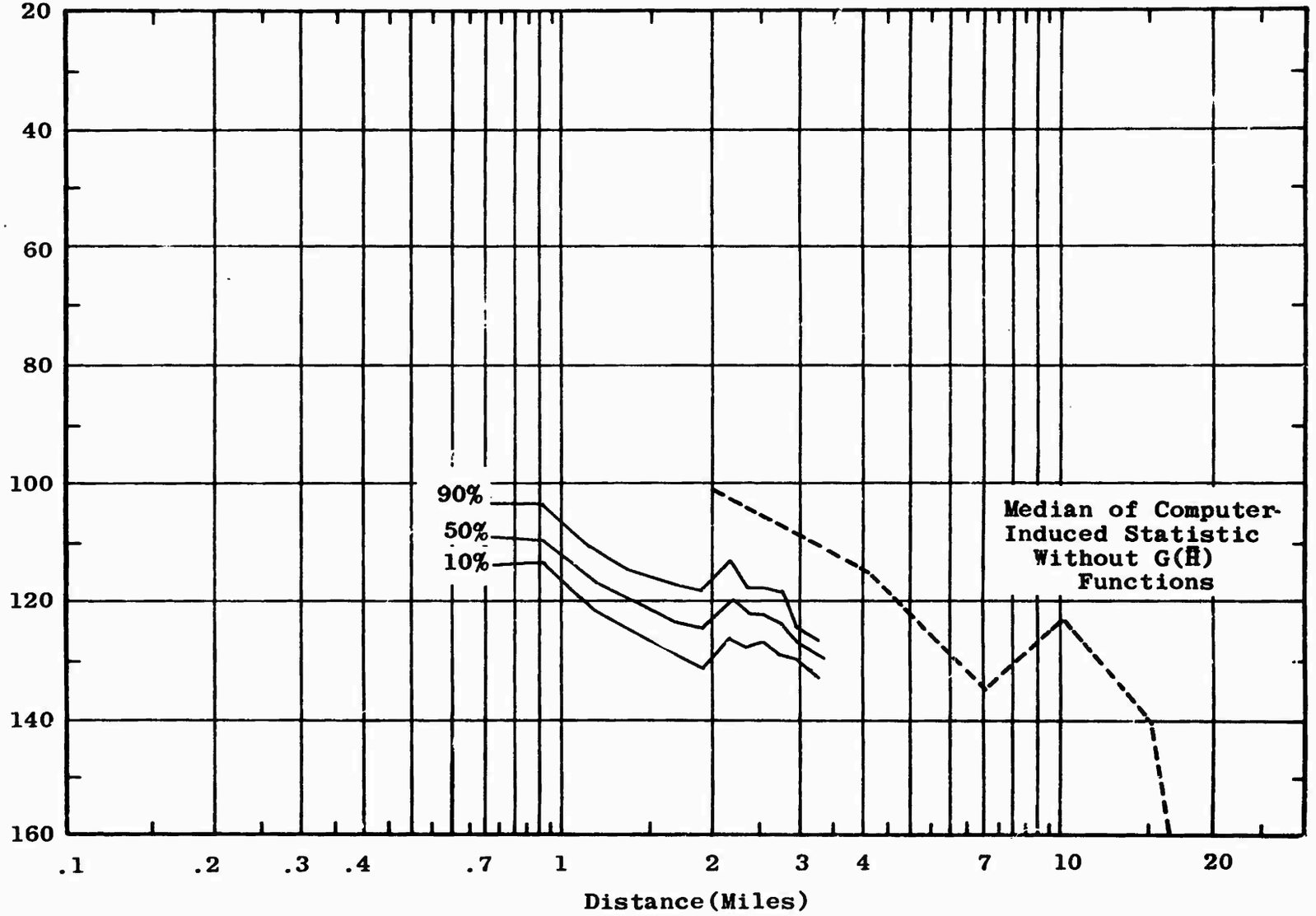

Figure 4.96 Comparison Between Vehicular Data and Median of Computer-Induced Statistic Without G(H̄) Functions
$L_b = F_A(100, 80, V, d, 7)$

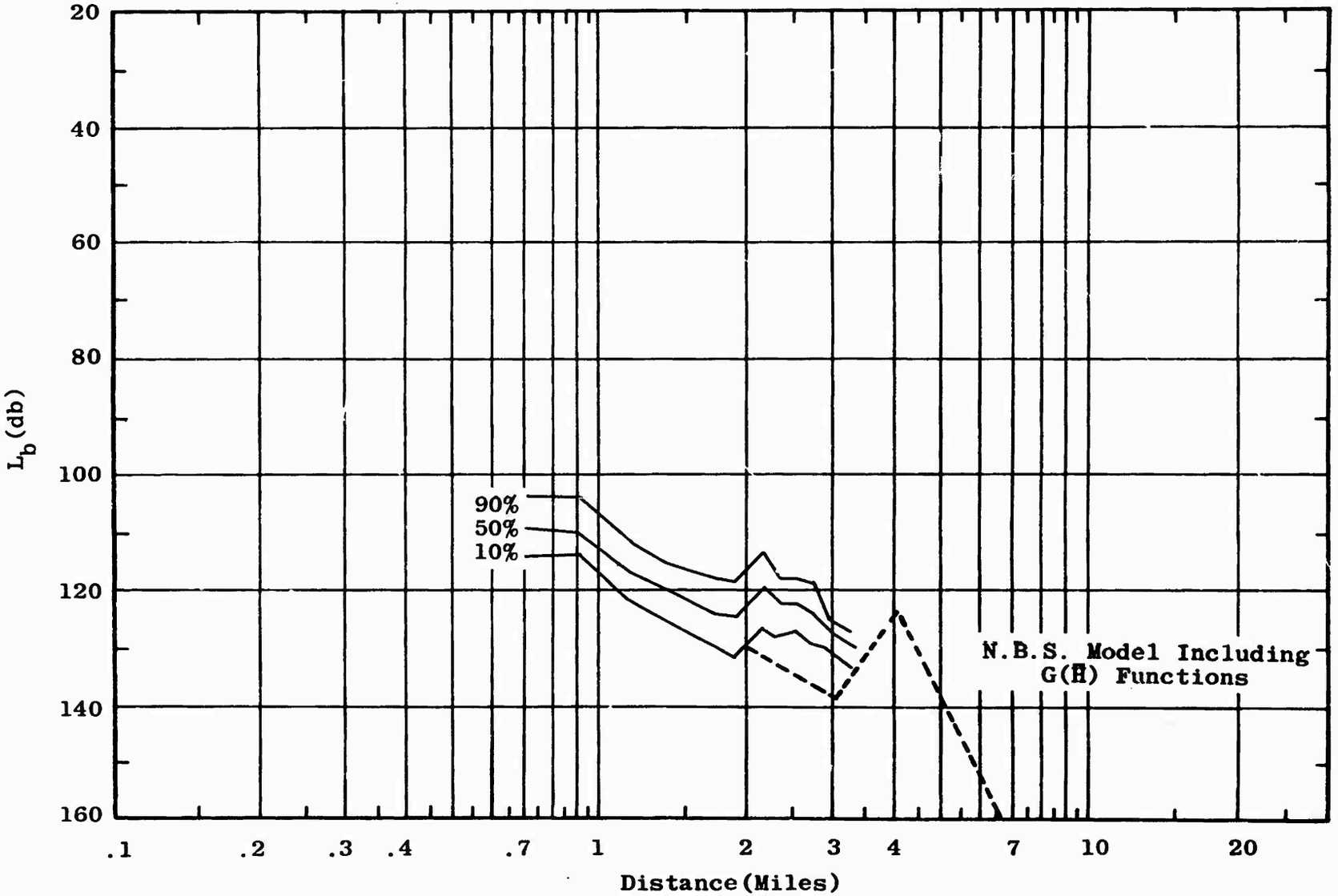

Figure 4.97 Comparison Between Vehicular Data and N.B.S. Model Including $G(\bar{H})$ Functions
$L_b = f_A(100, 80, V, d, 7)$

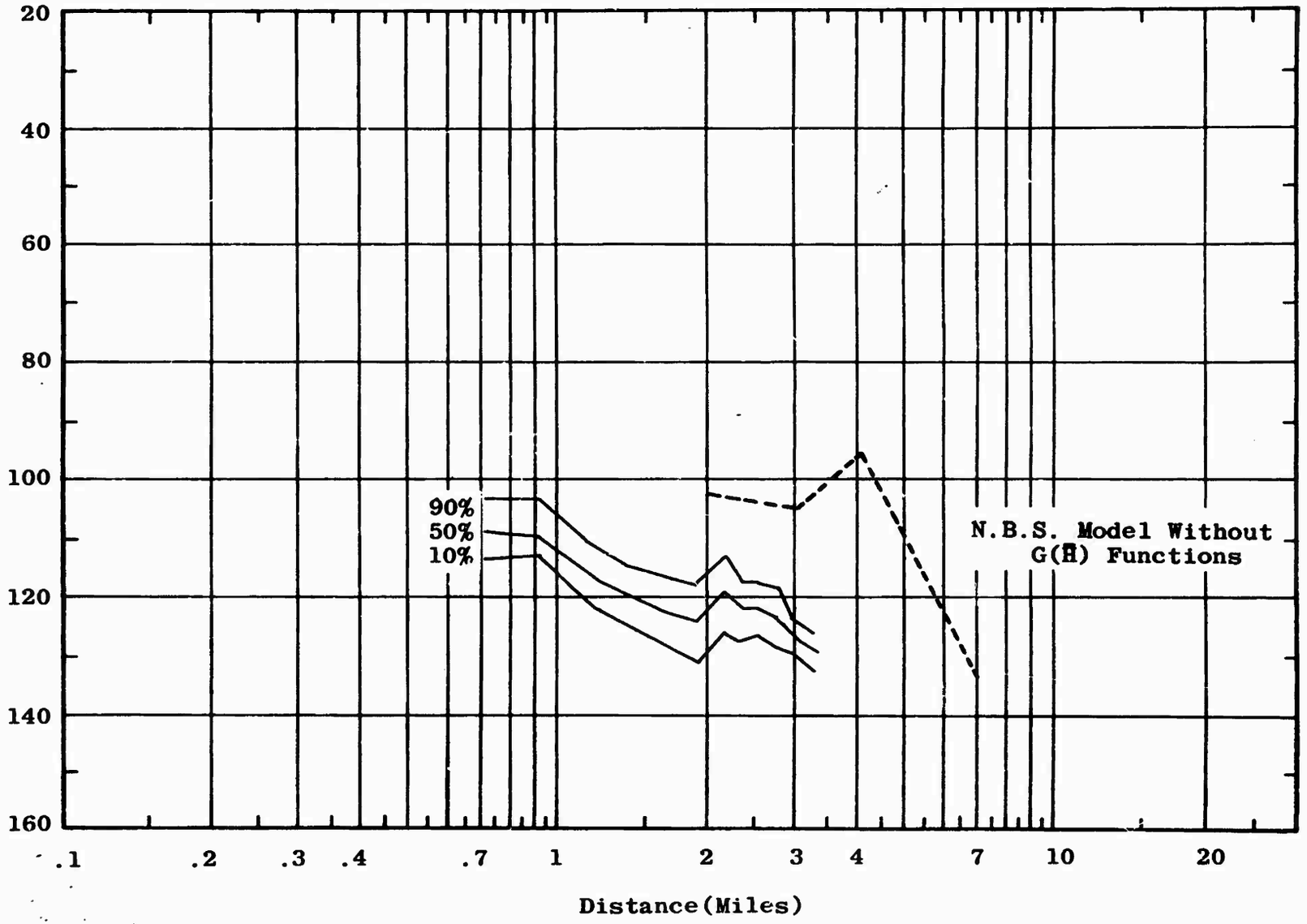

Figure 4.98 Comparison Between Vehicular Data and N.B.S. Model Without G(H̄) Functions
$L_b = F_A(100, 80, V, d, 7)$

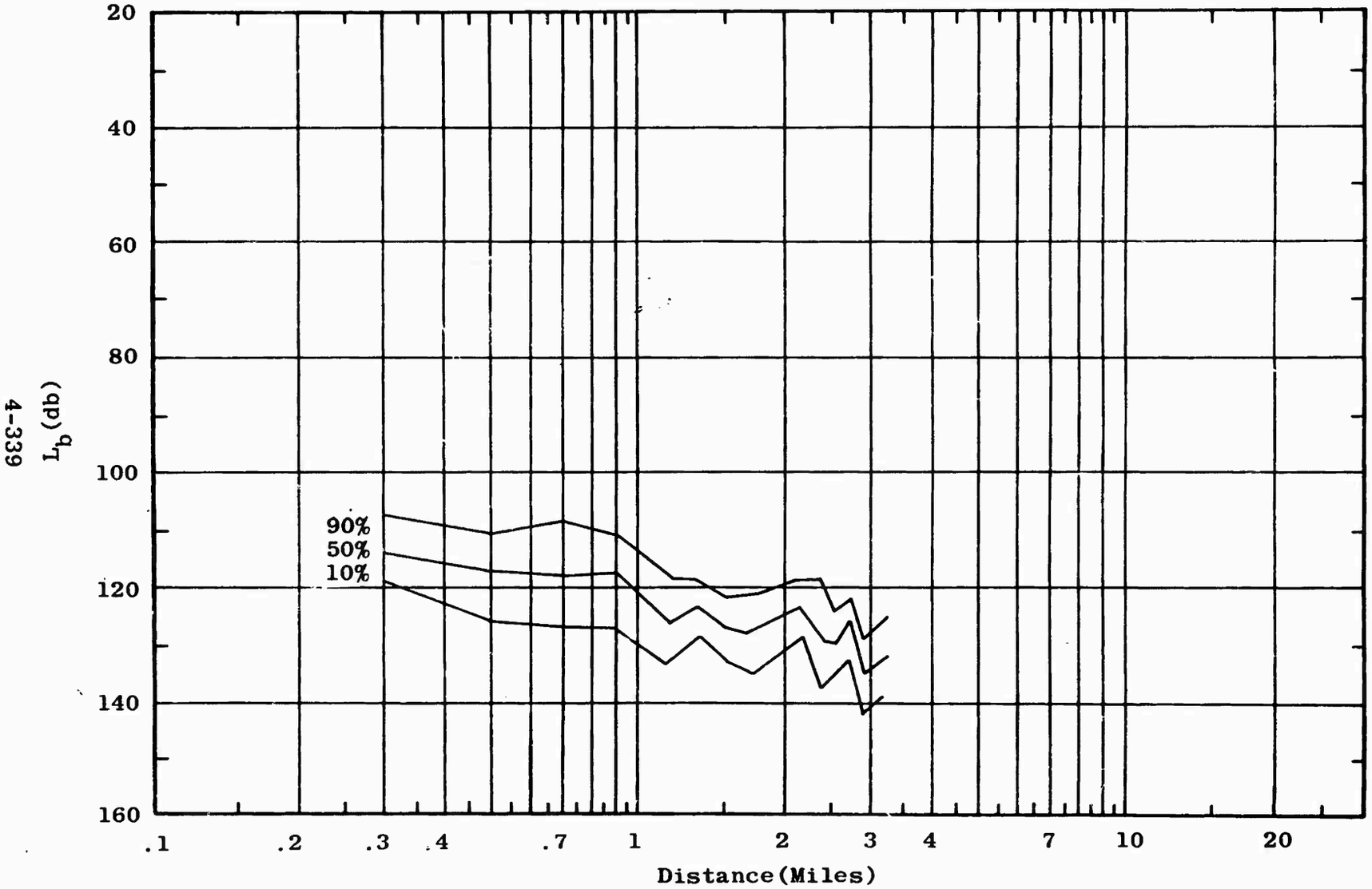

Figure 4.99 Reduced Vehicular Data
$L_b = F_A(100, 13, H, d, 7)$

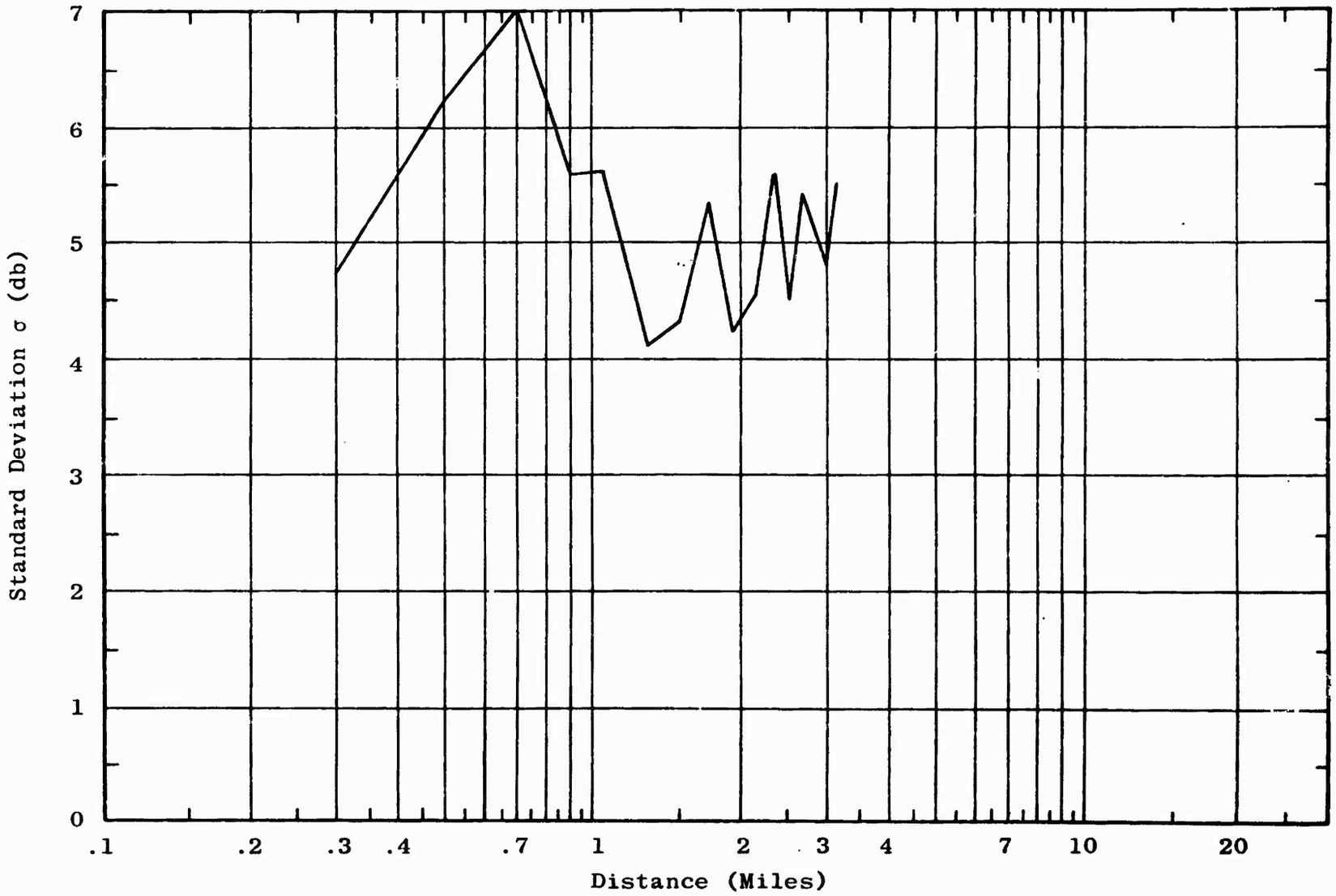

Figure 4.100 Standard Deviation of Vehicular Data
$L_b = F_A(100, 13, H, d, 7)$

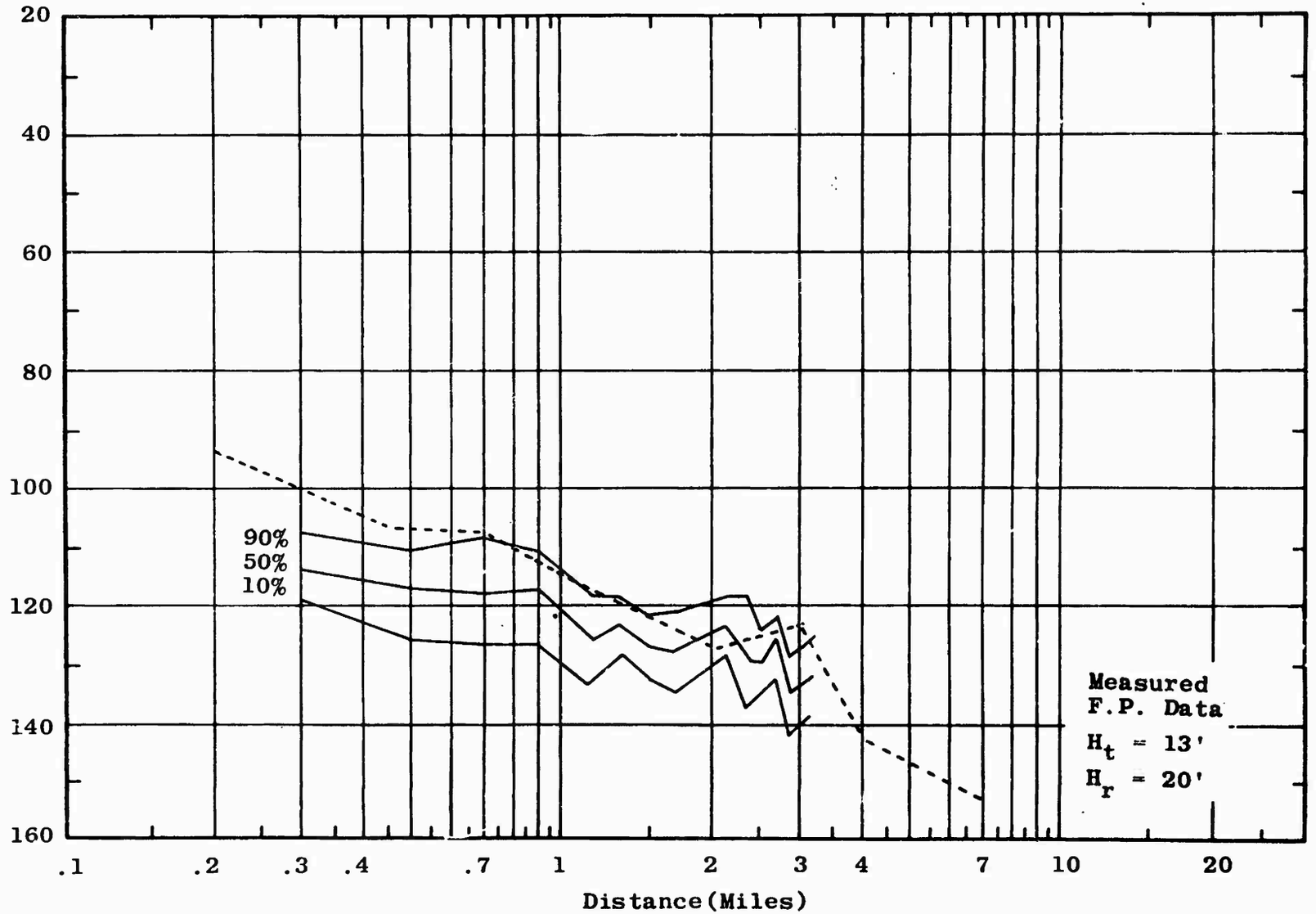

Figure 4.101 Comparison Between Vehicular Data and Measured F.P. Data
$L_b = F_A(100, 13, H, d, 7)$

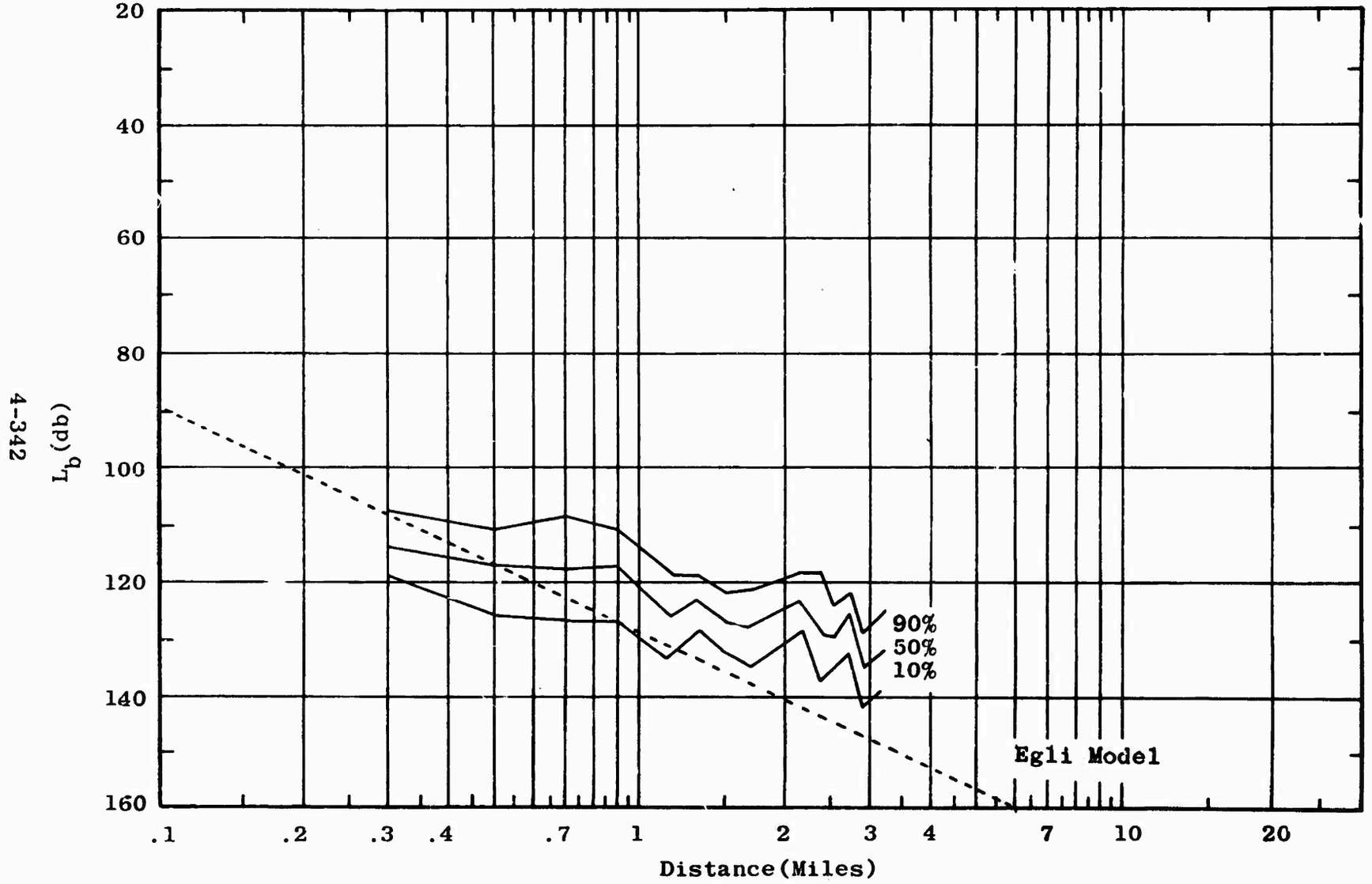

Figure 4.102 Comparison Between Vehicular Data and Egli Model
$L_b = F_A(100, 13, H, d, 7)$

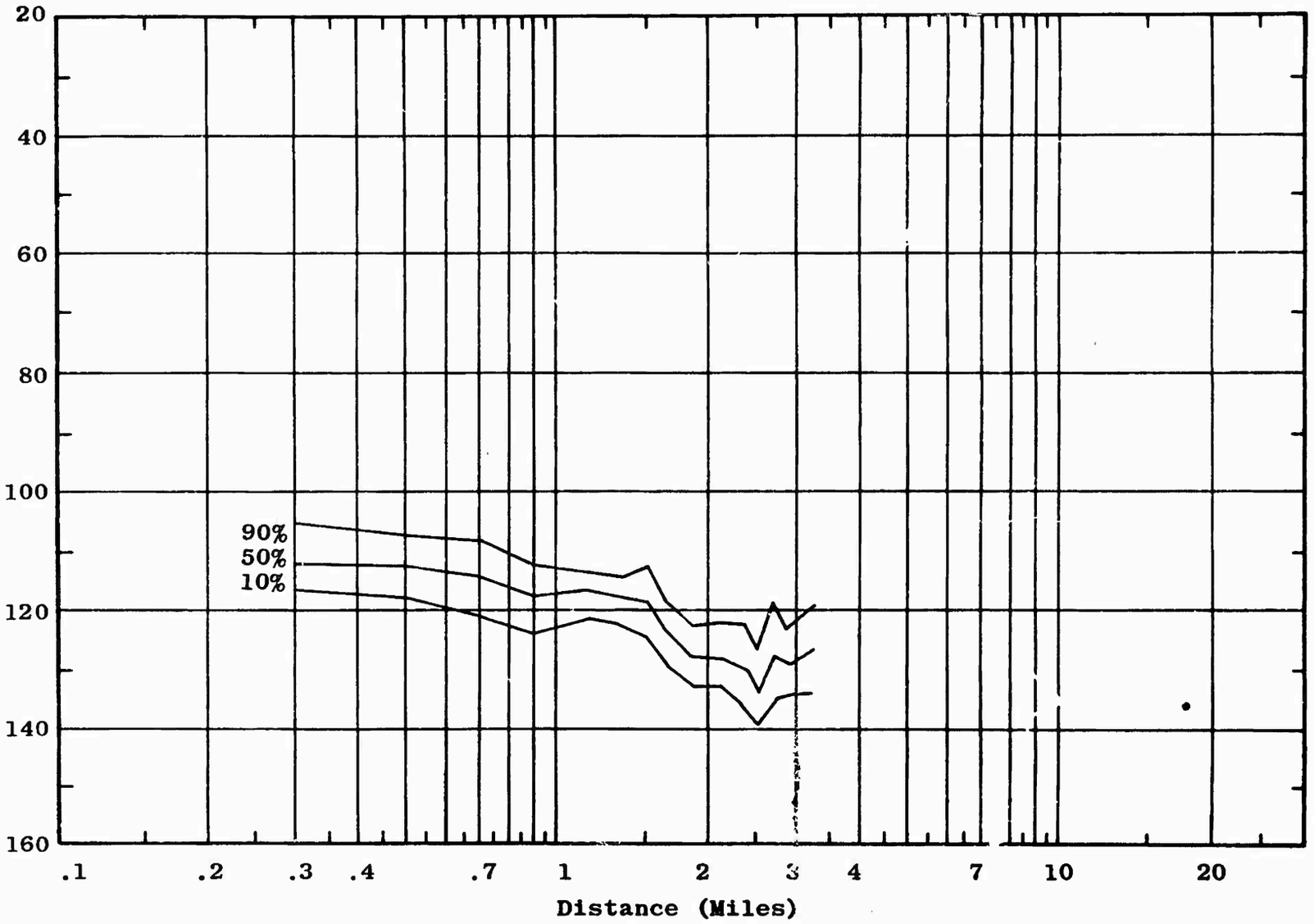

Figure 4.103 Reduced Vehicular Data
$L_b = F_A(100, 40, H, d, 7)$

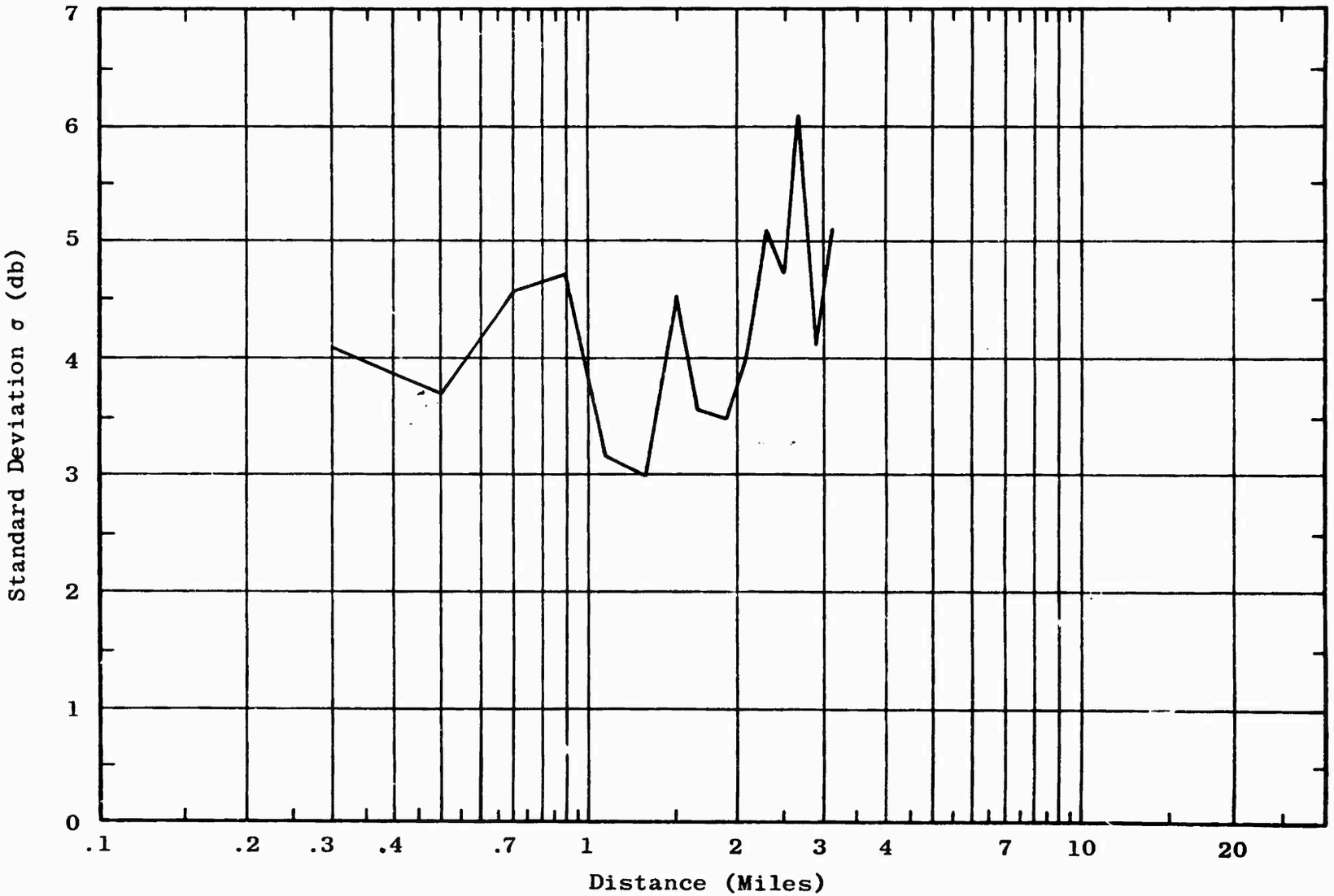

Figure 4.104 Standard Deviation of Vehicular Data
$L_b = F_A(100, 40, V, d, 7)$

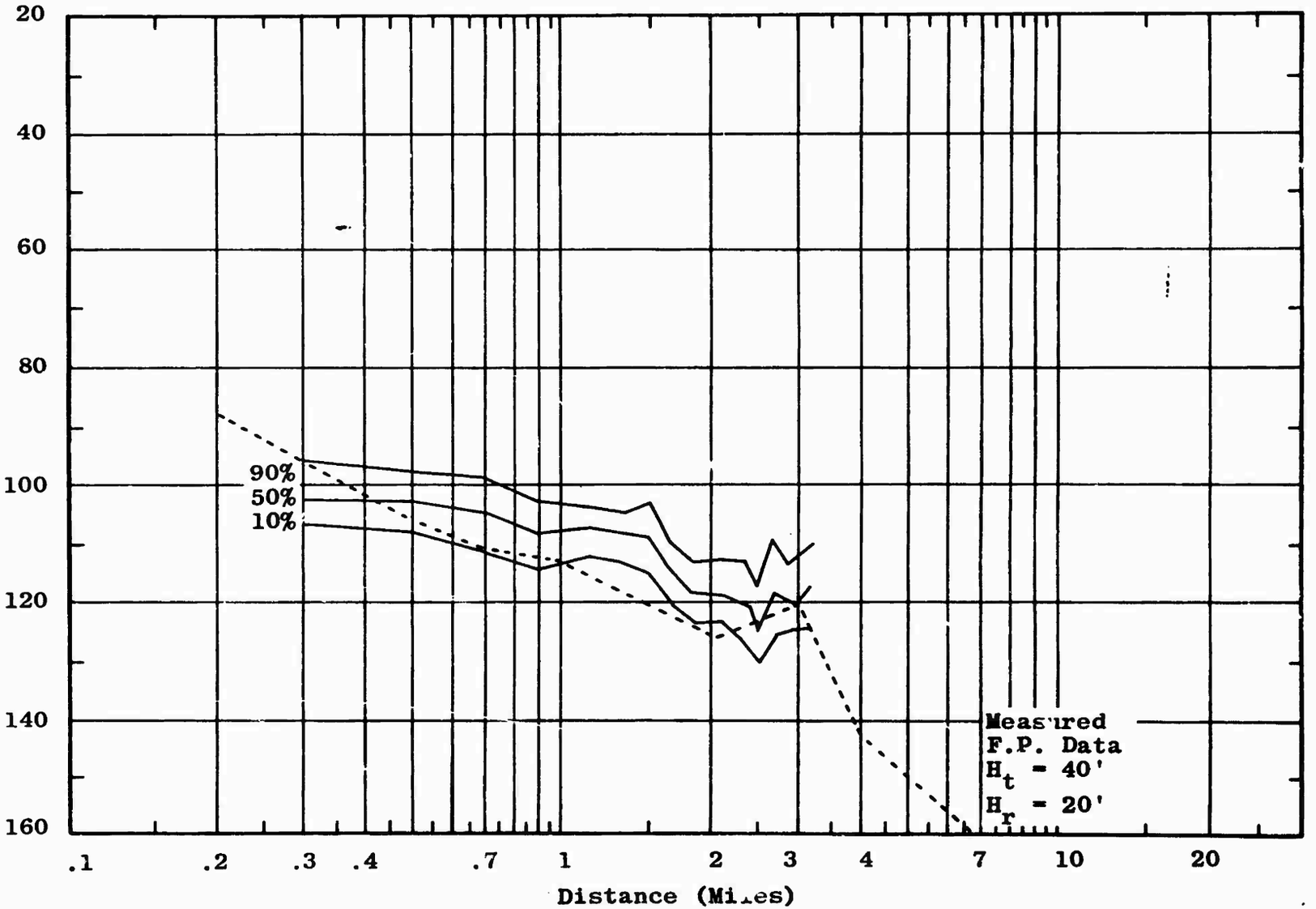

Figure 4.105 Comparison Between Vehicular Data and Measured F.P. Data
$L_b = F_A(100, 40, H, d, 7)$

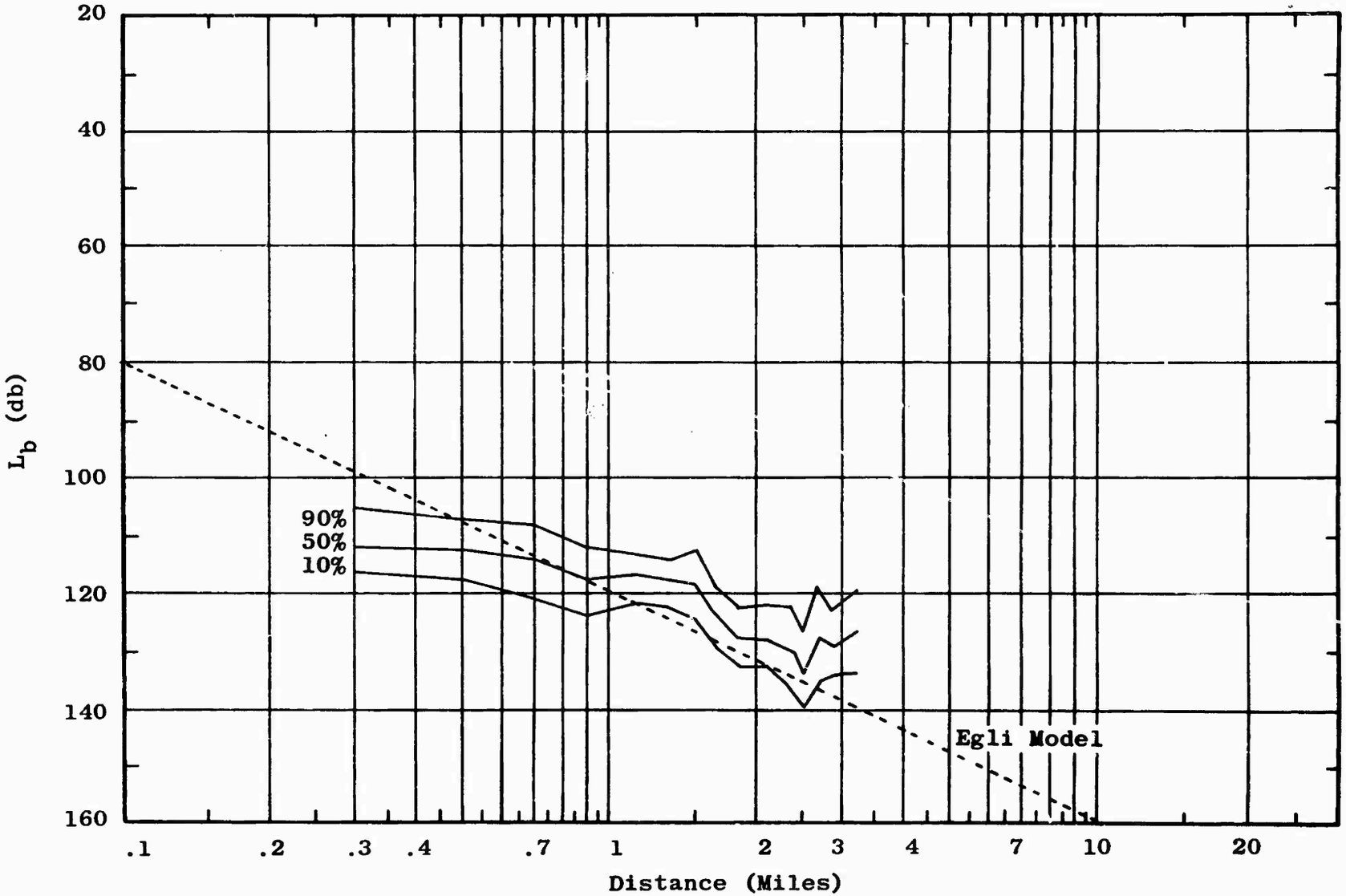

Figure 4.106 Comparison Between Vehicular Data and Egli Model
$L_b = F_A(100, 40, H, d, 7)$

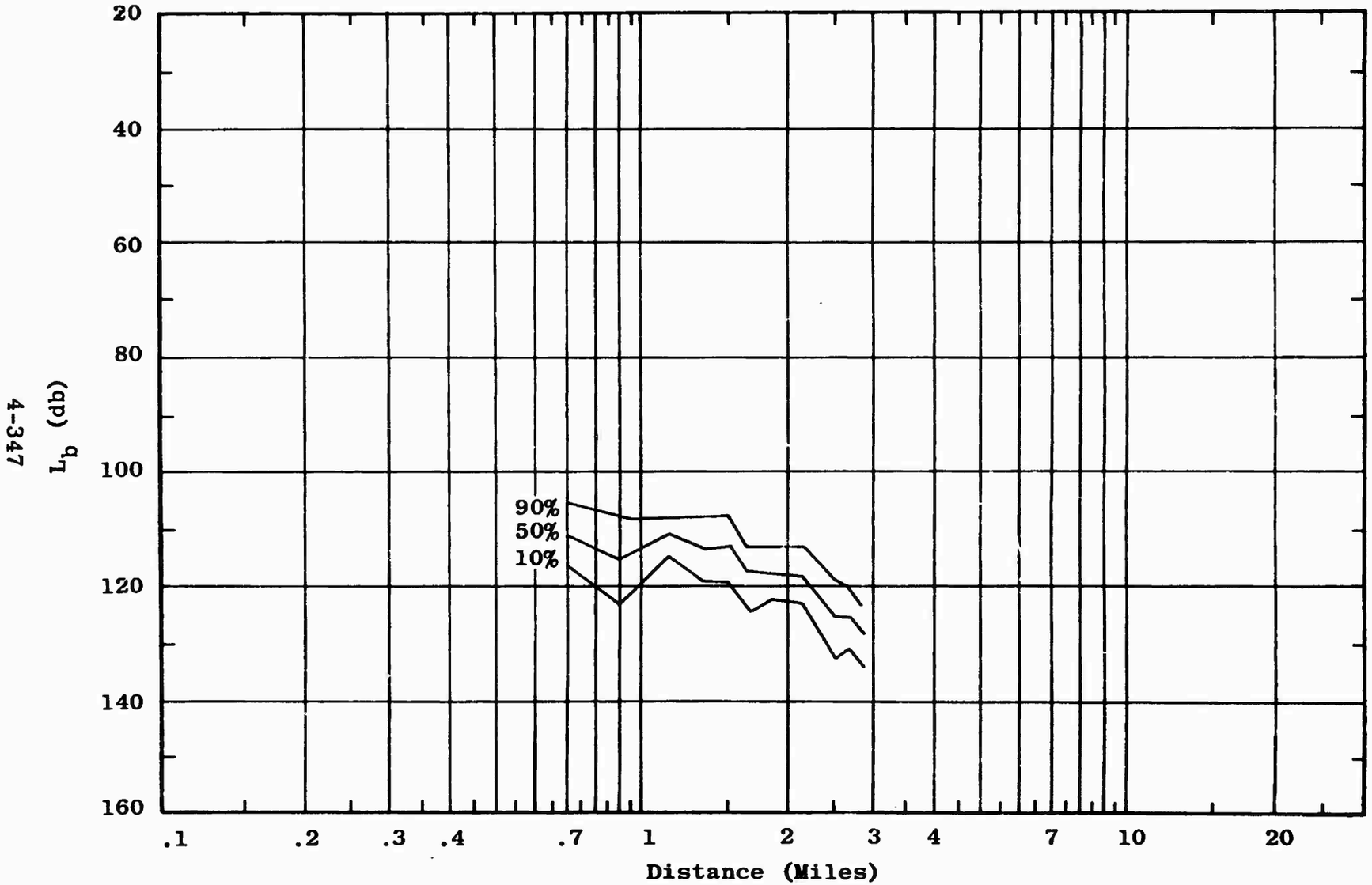

Figure 4.107 Reduced Vehicular Data
$L_b = F_A(100, 80, H, d, 7)$

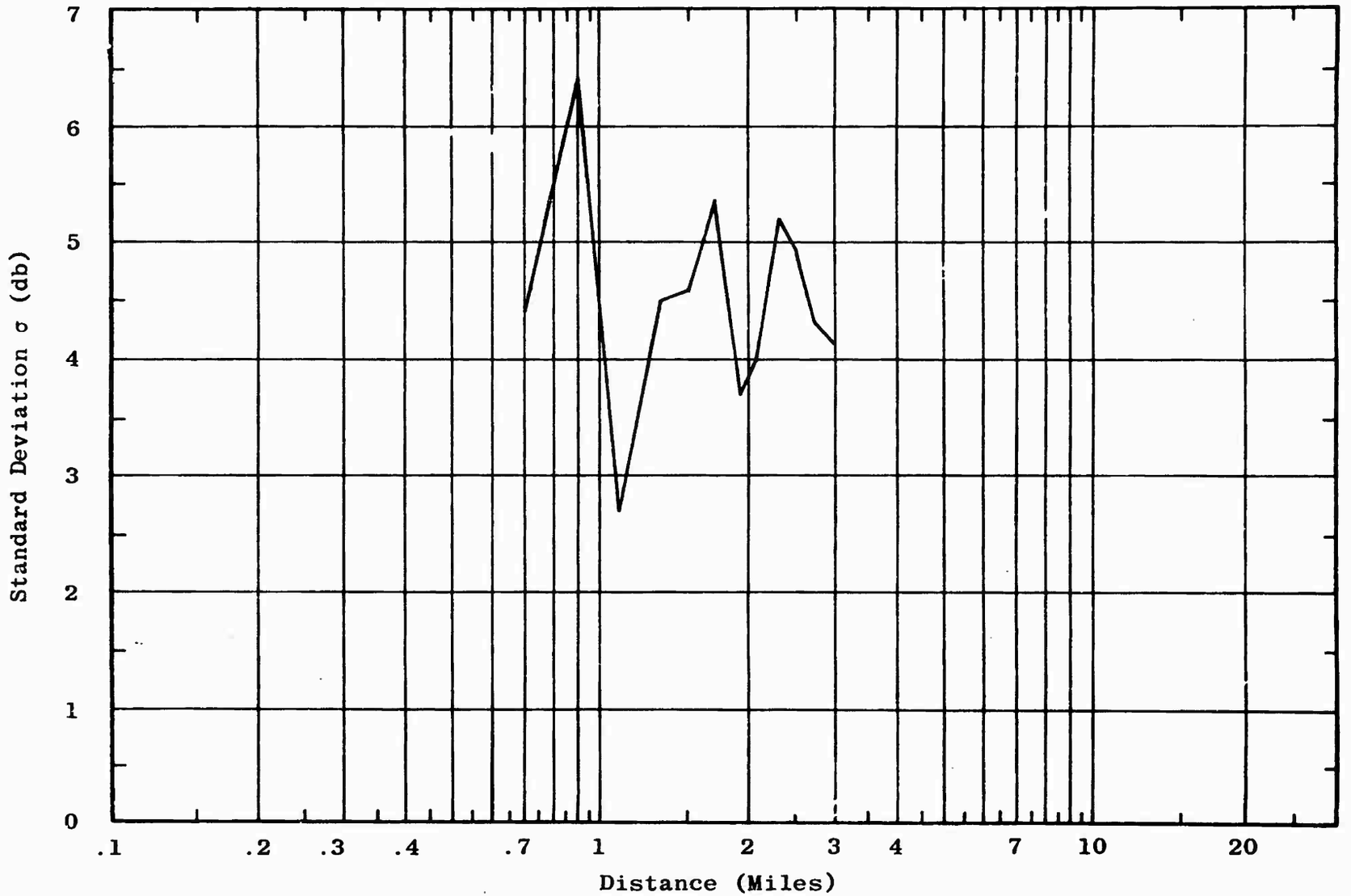

Figure 4.108 Standard Deviation of Vehicular Data
$L_b = F_A(100, 80, H, d, 7)$

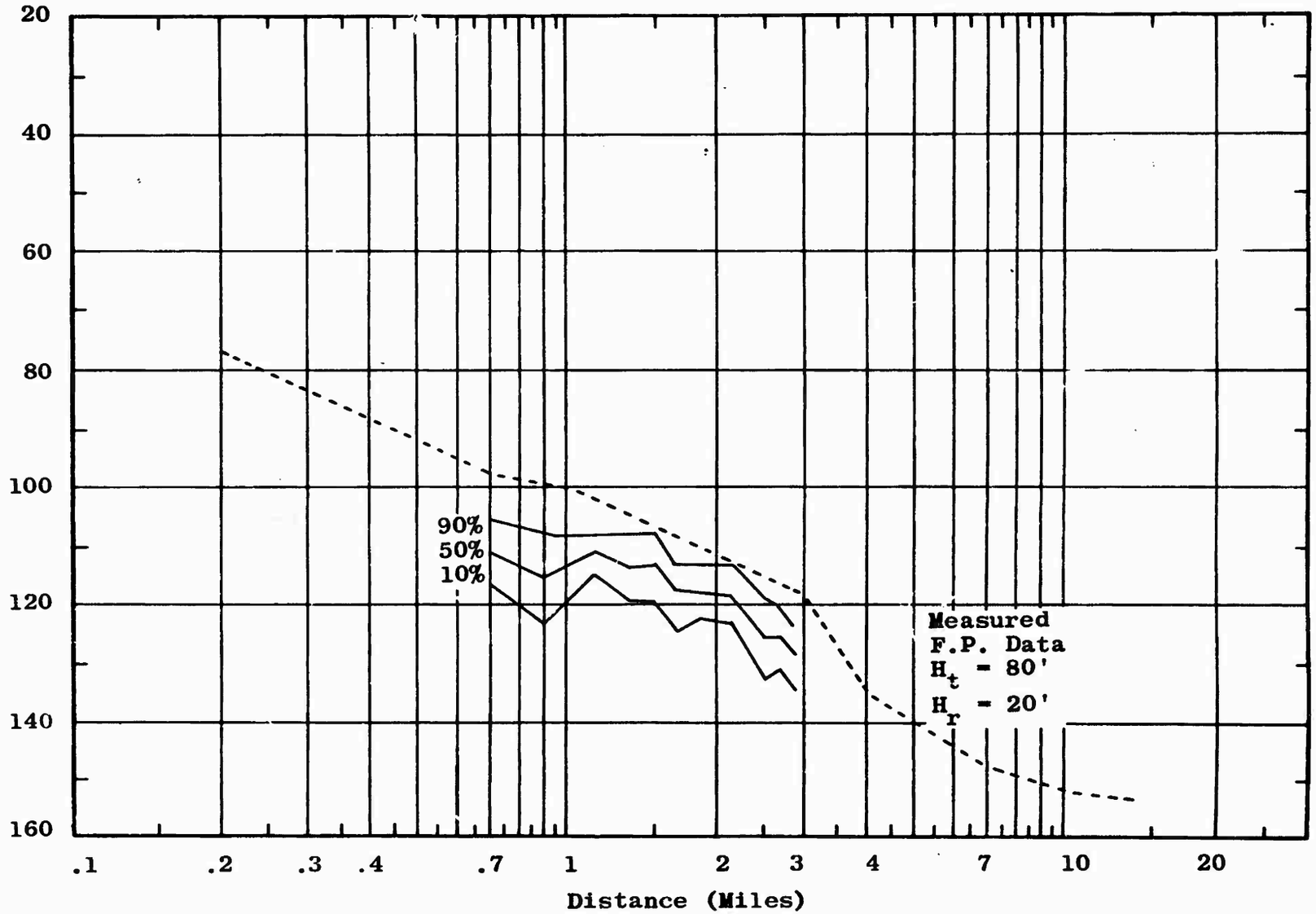

Figure 4.109 Comparison Between Vehicular Data and Measured F.P. Data
$L_b = F_A(100, 80, H, d, 7)$

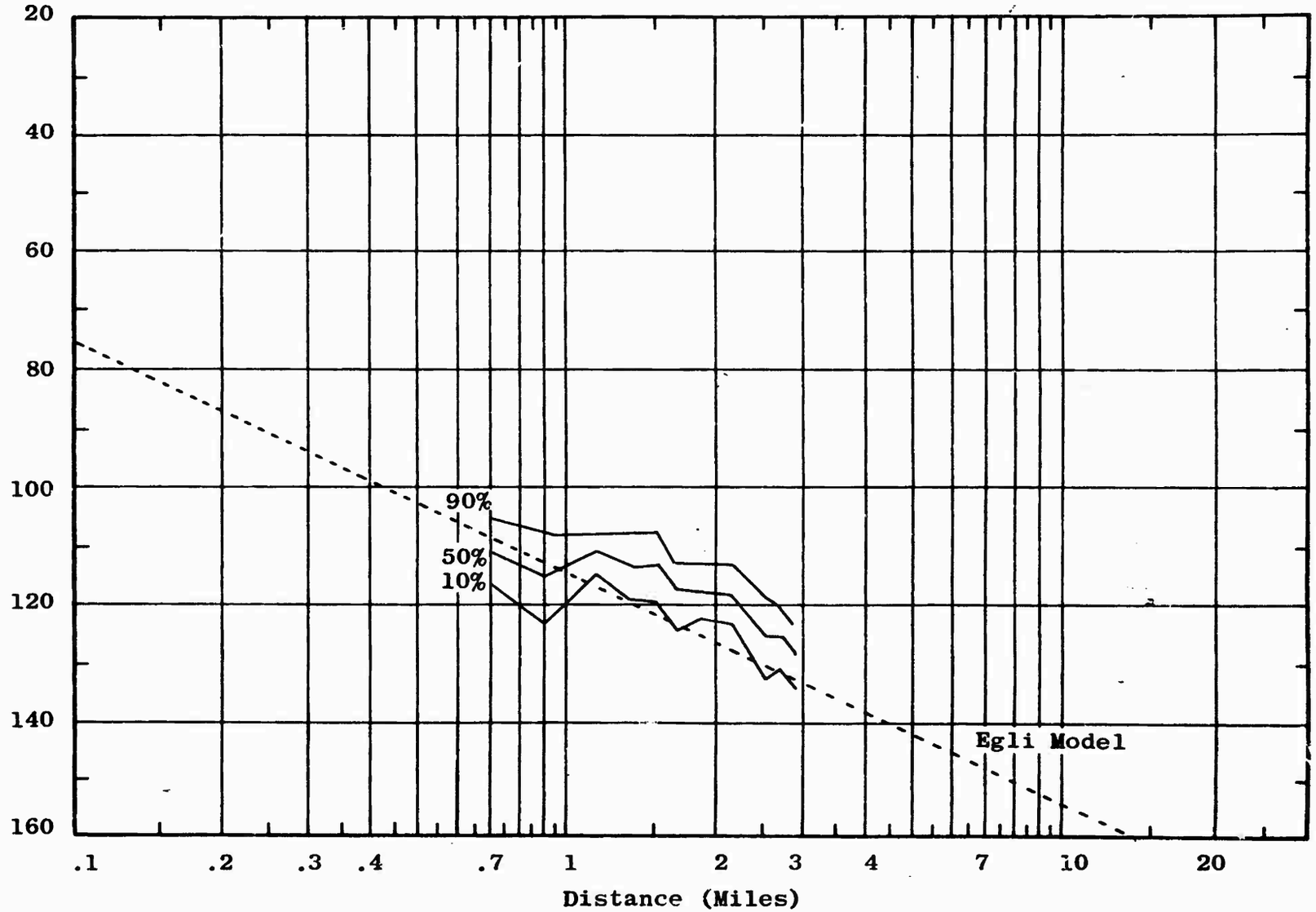

Figure 4.110 Comparison Between Vehicular Data and Egli Model
$L_b = F_A(100, 80, H, d, 7)$

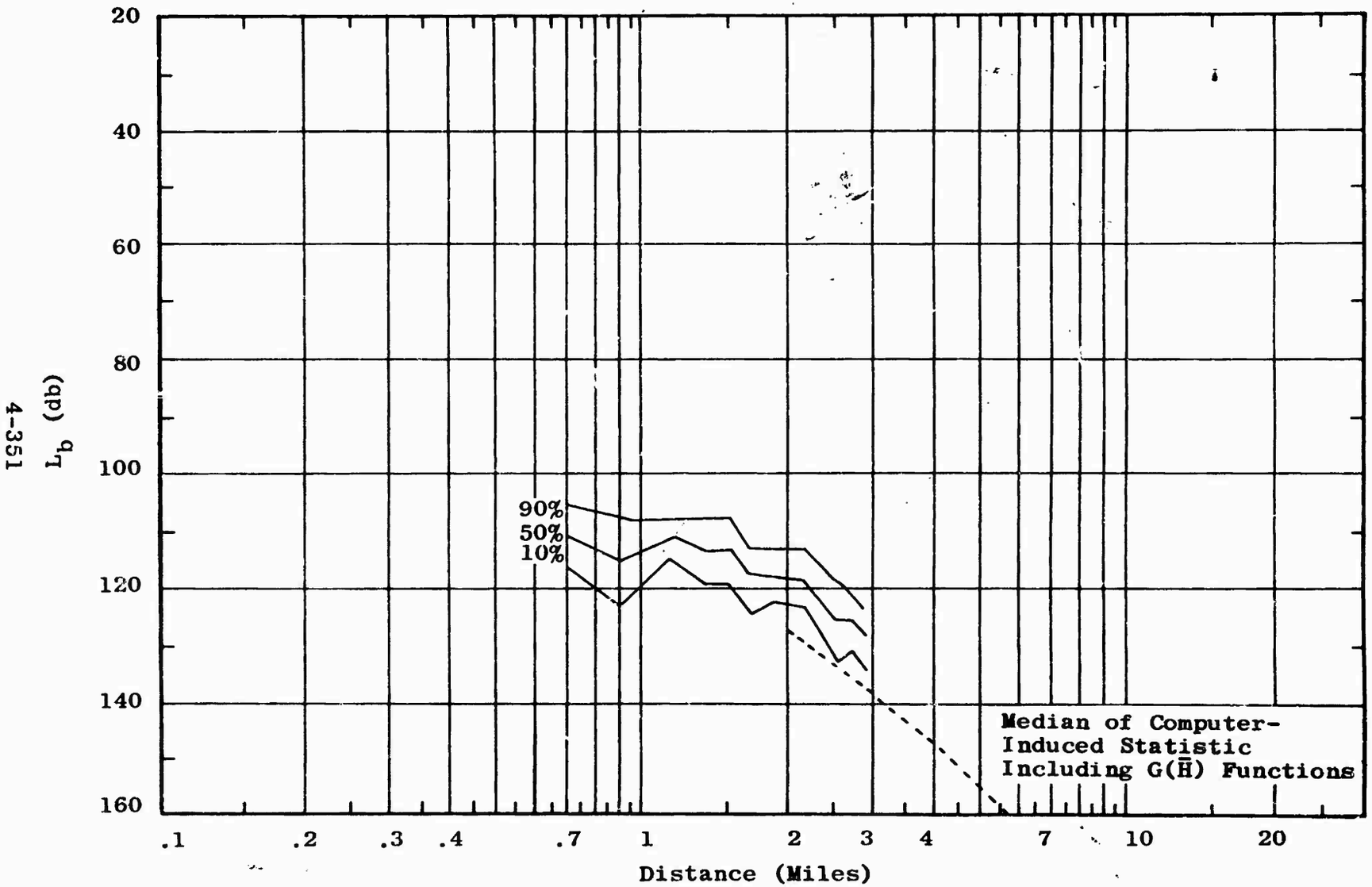

Figure 4.111 Comparison Between Vehicular Data and Computer-Induced Statistic Including G(H̄) Functions
$L_b = F_A(100, 80, H, d, 7)$

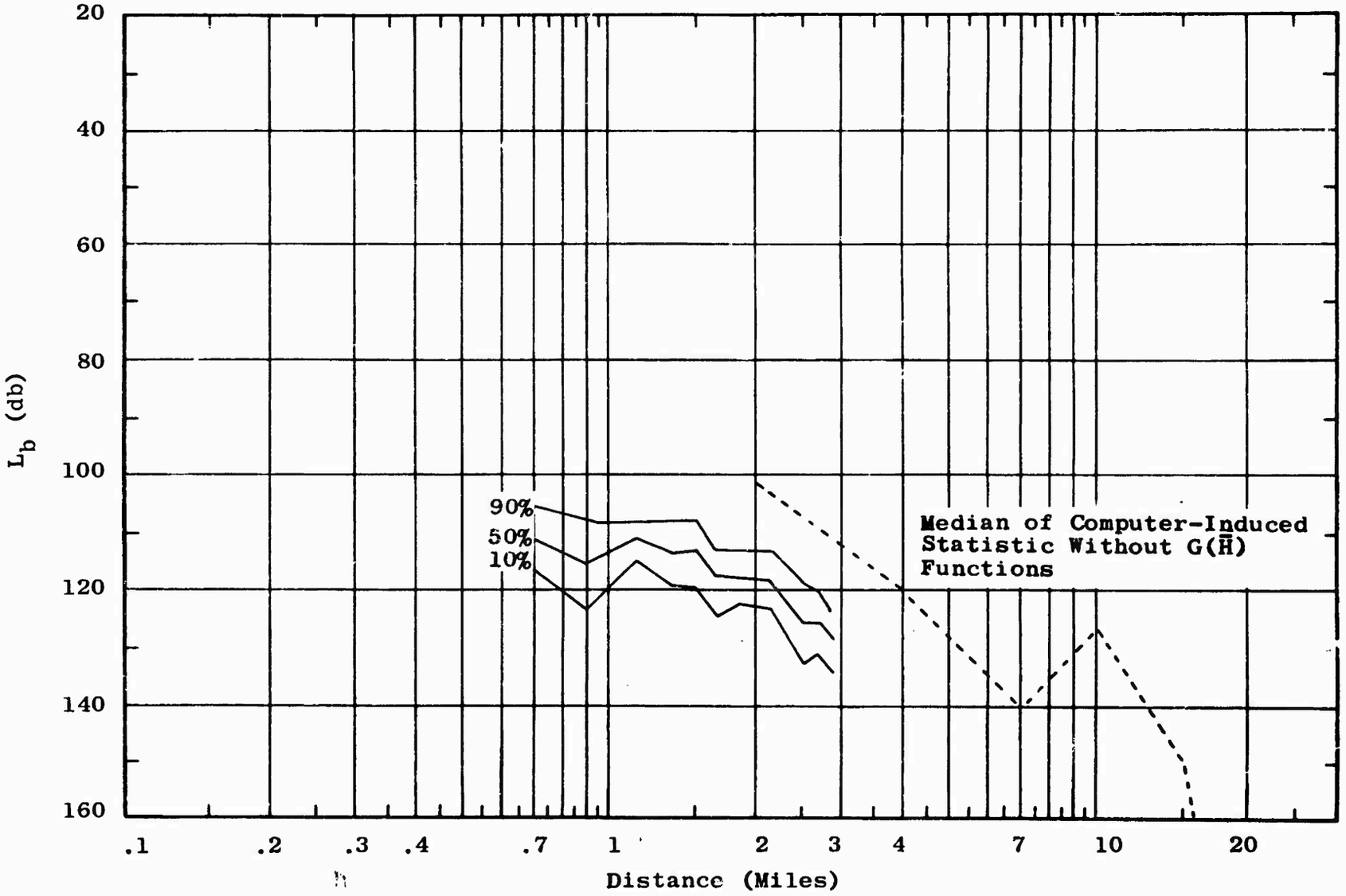

Figure 4.112 Comparison Between Vehicular Data and Computer-Induced Statistic Without G(H̄) Functions
$L_b = F_A(100, 80, H, d, 7)$

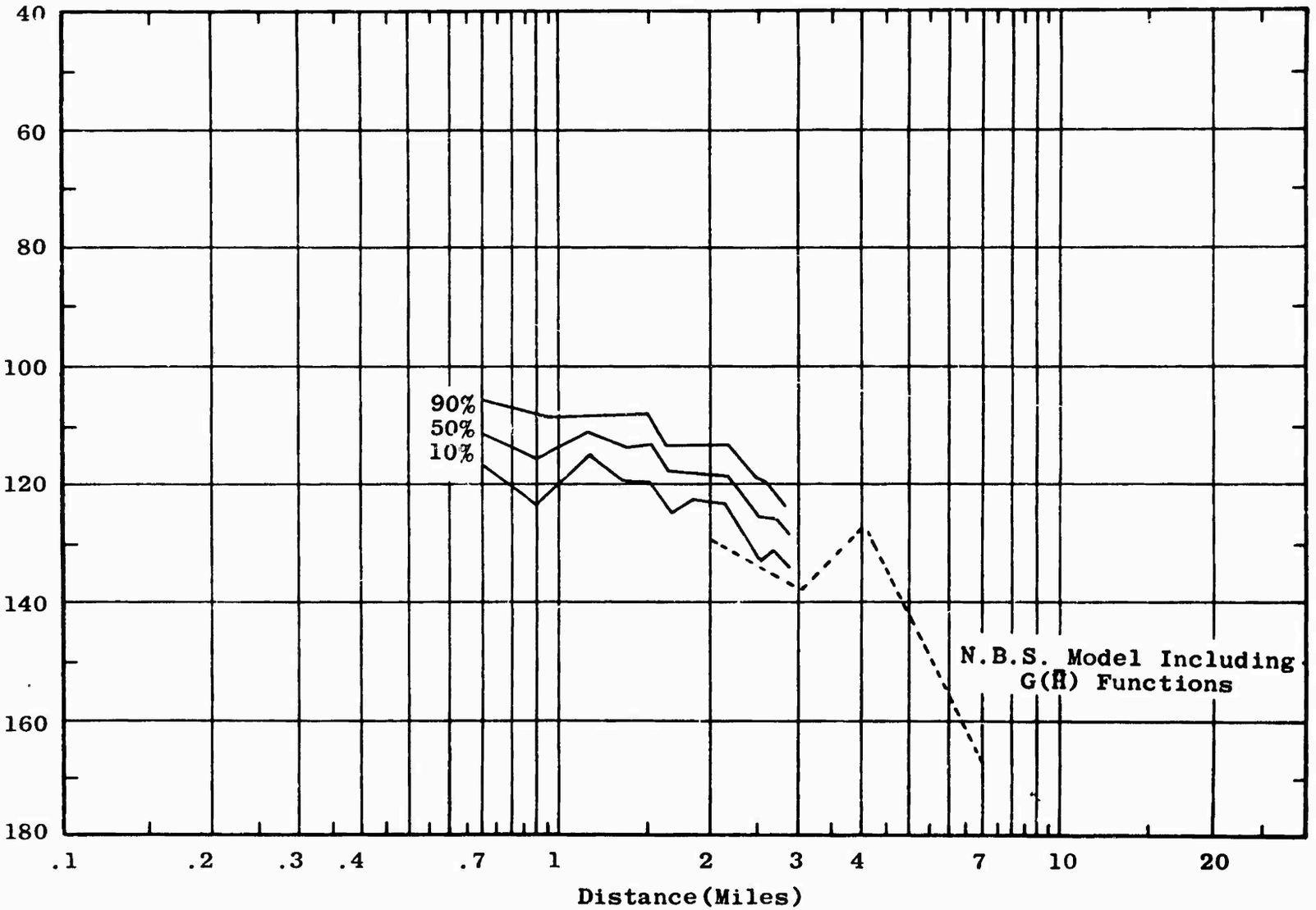

Figure 4.113 Comparison Between Vehicular Data and N.B.S. Model Including G(H) Functions
$L_b = F_A(100, 80, H, d, 7)$

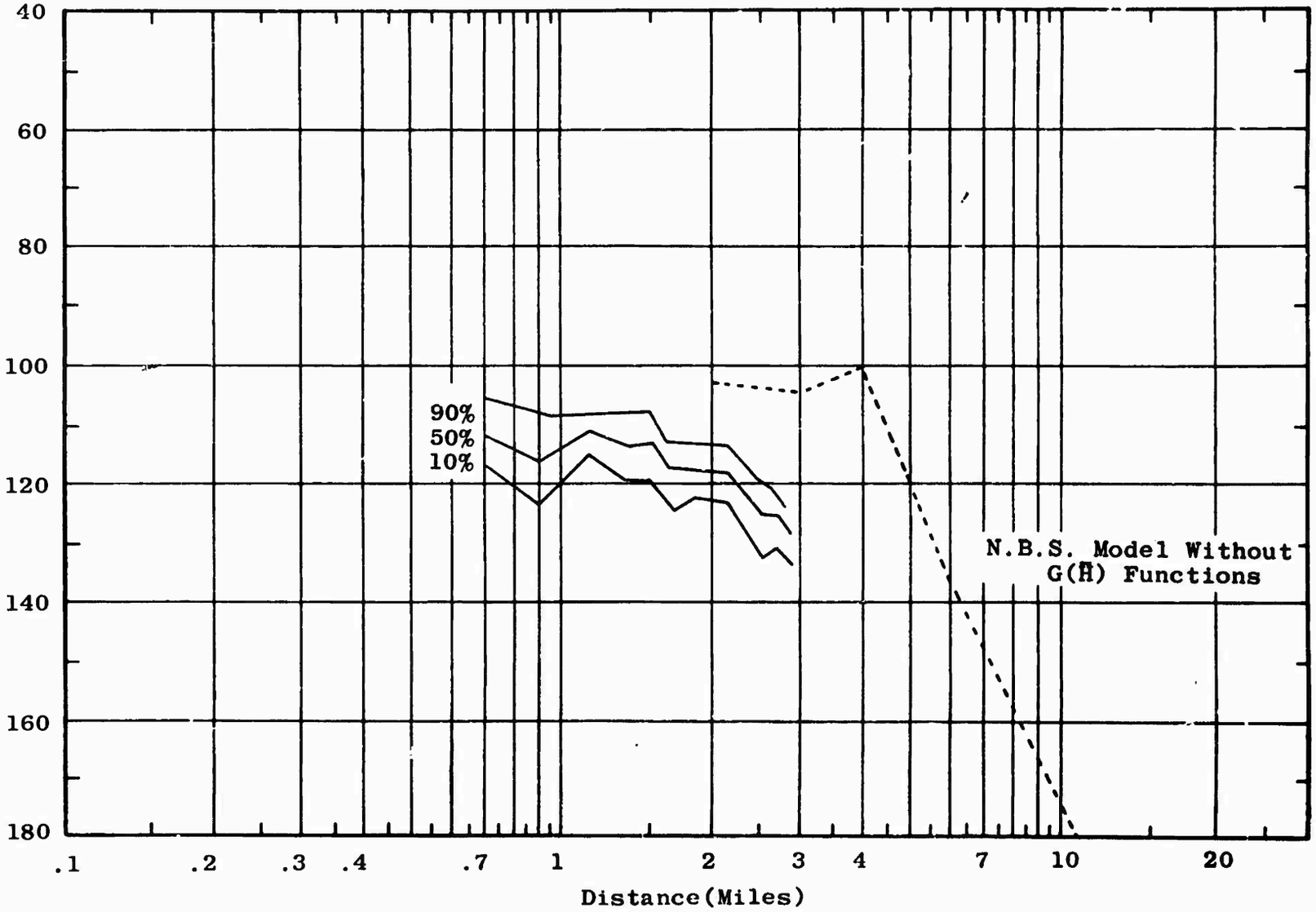

Figure 4.114 Comparison Between Vehicular Data and N.B.S. Model Without G(H̄) Functions
$L_b = F_A(100, 80, H, d, 7)$

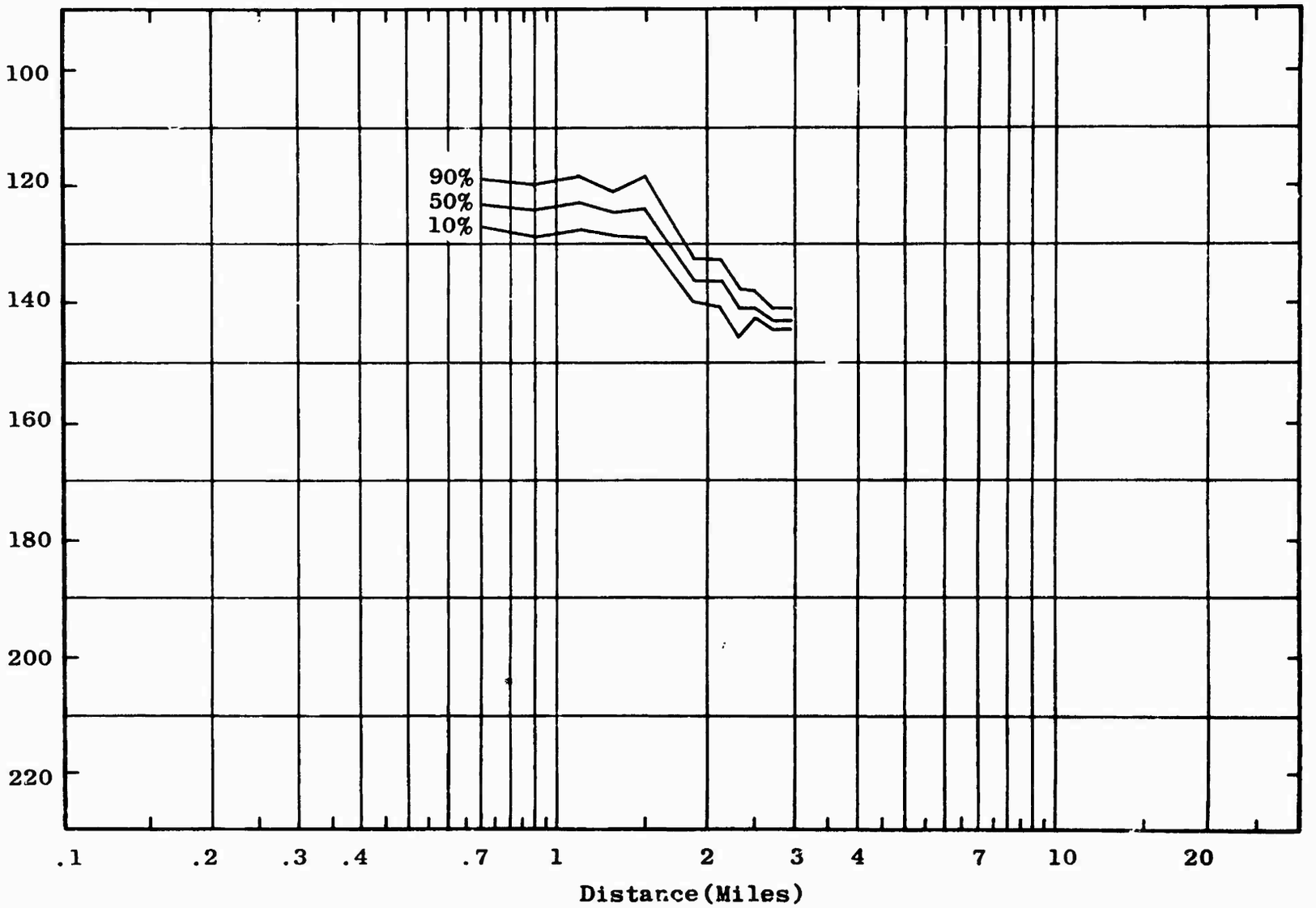

Figure 4.115 Reduced Vehicular Data
$L_b = F_A(250, 80, V, d, 7)$

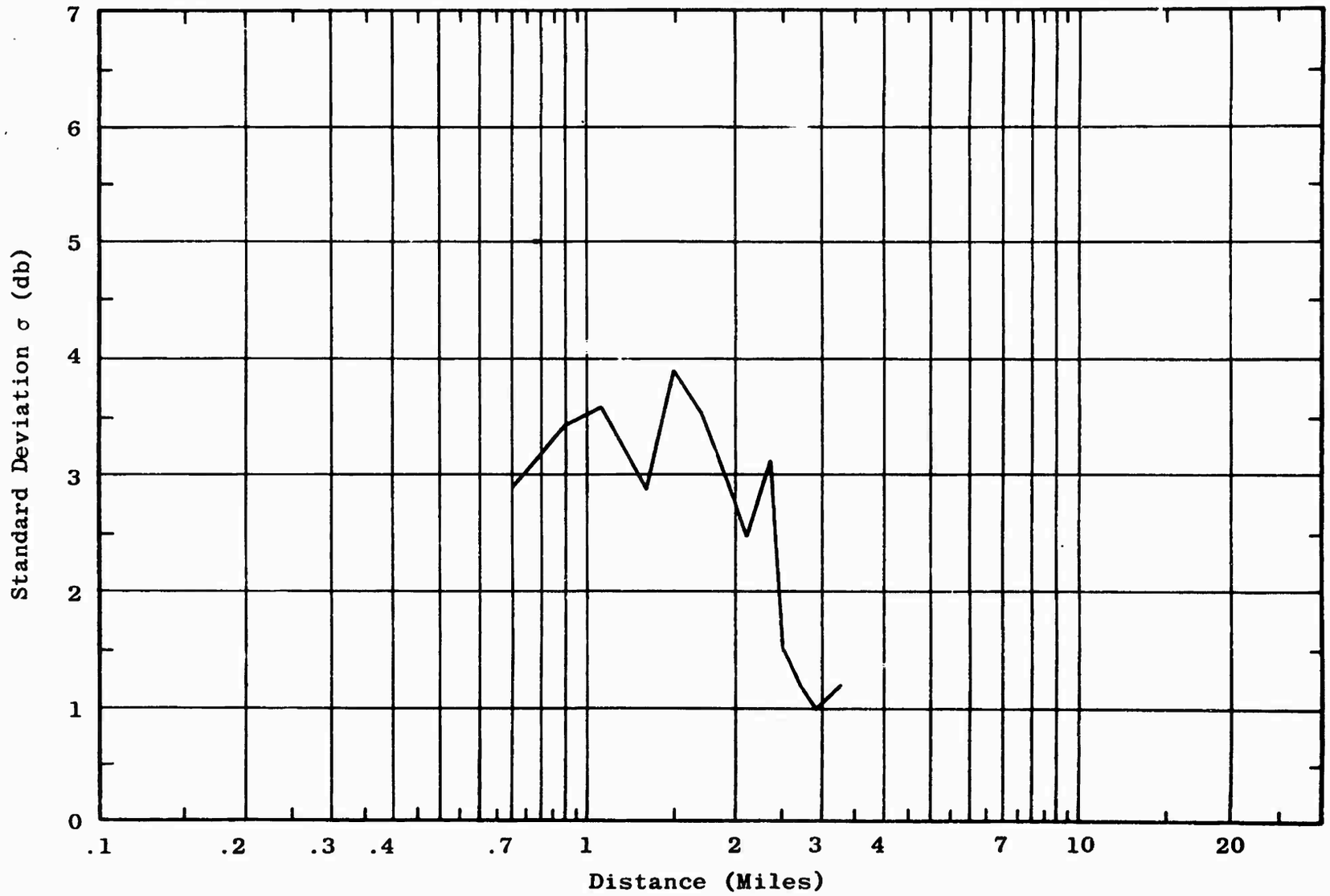

Figure 4.116 Standard Deviation of Vehicular Data
$L_b = F_A(250, 80, V, d, 7)$

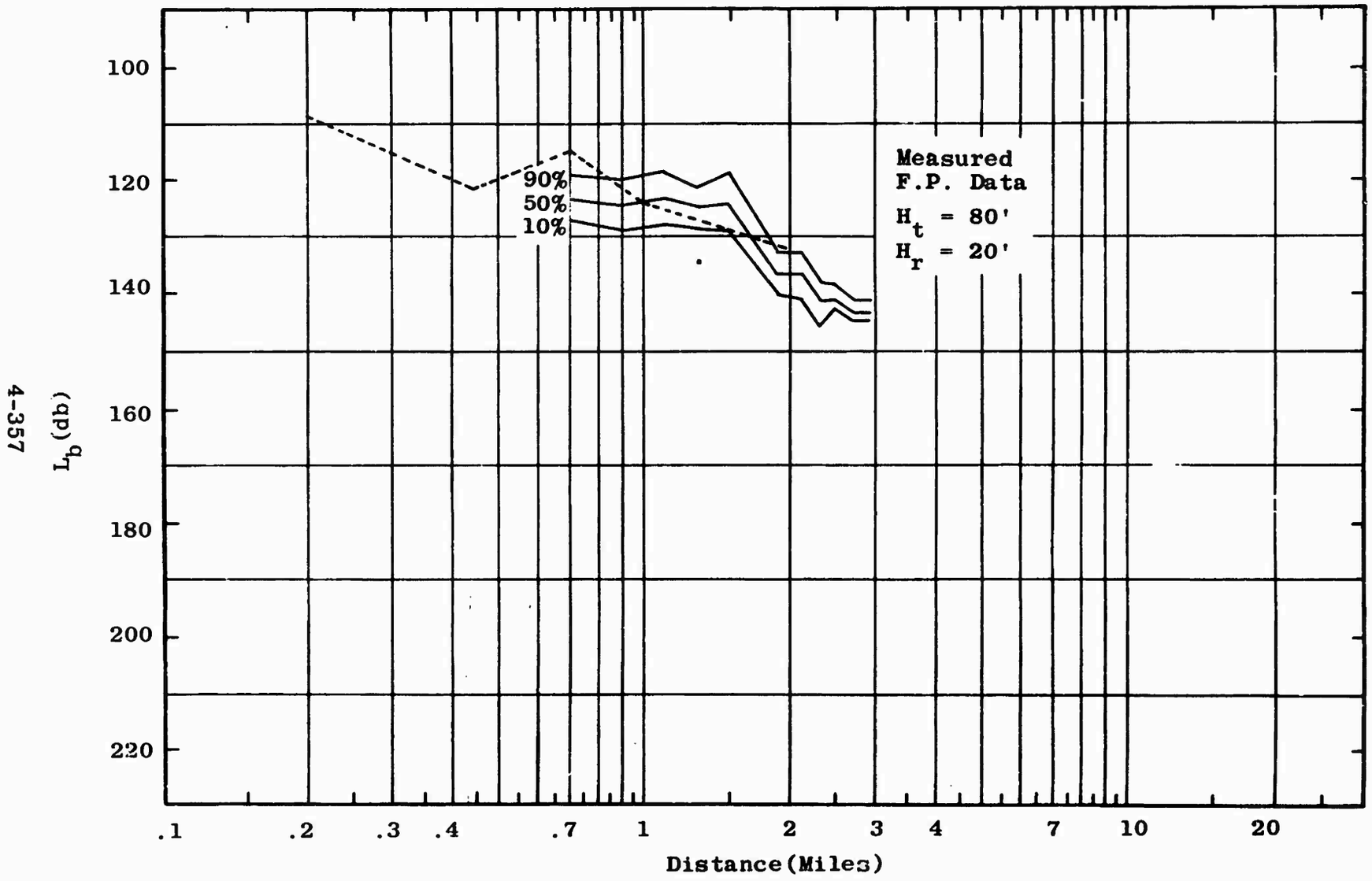

Figure 4.117 Comparison Between Vehicular Data and Measured F.P. Data
$L_b = F_A(250, 80, V, d, 7)$

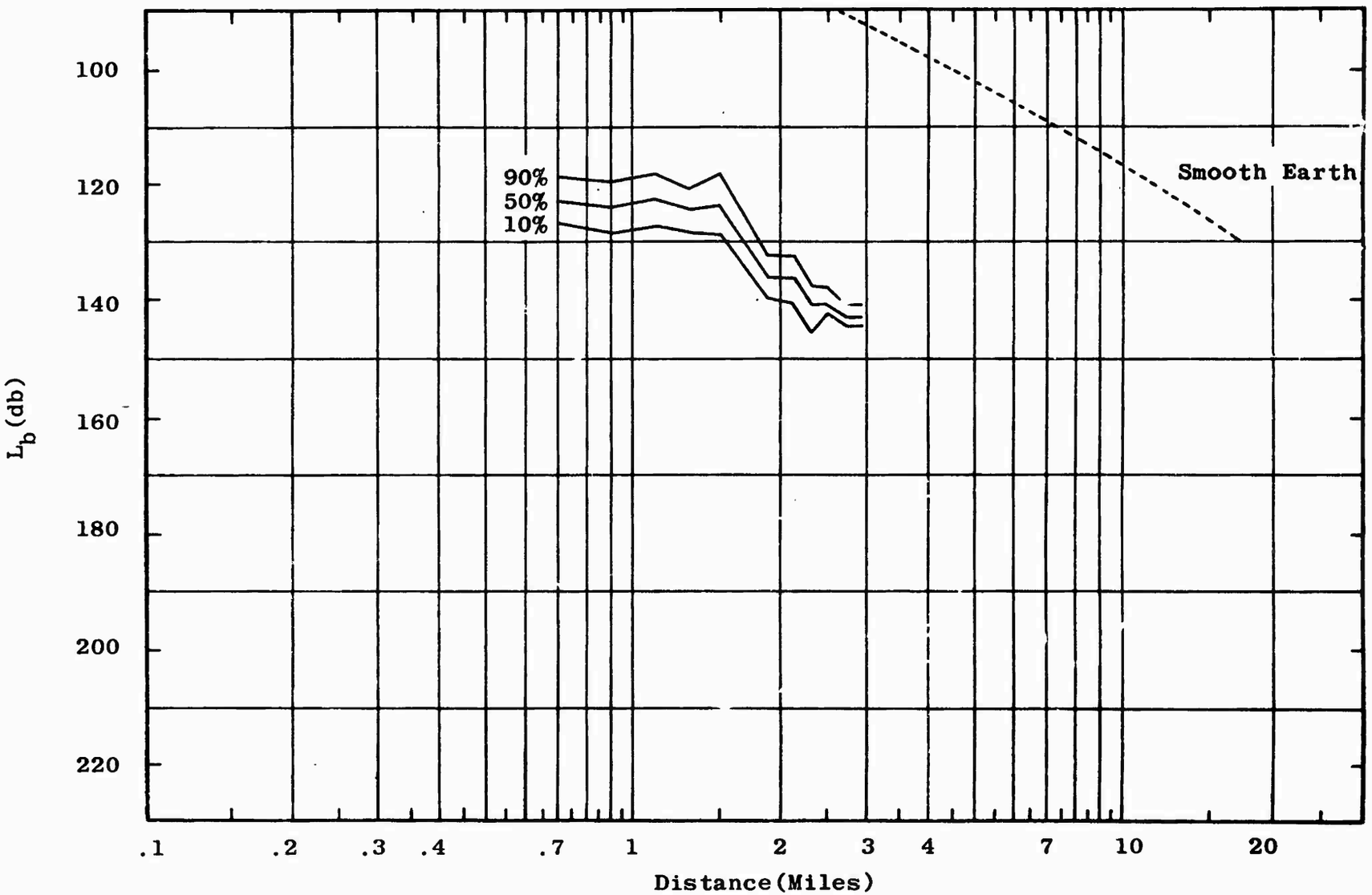

Figure 4.118 Comparison Between Vehicular Data and Theoretical Smooth-Earth Model
$L_b = F_A(250, 80, V, d, 7)$

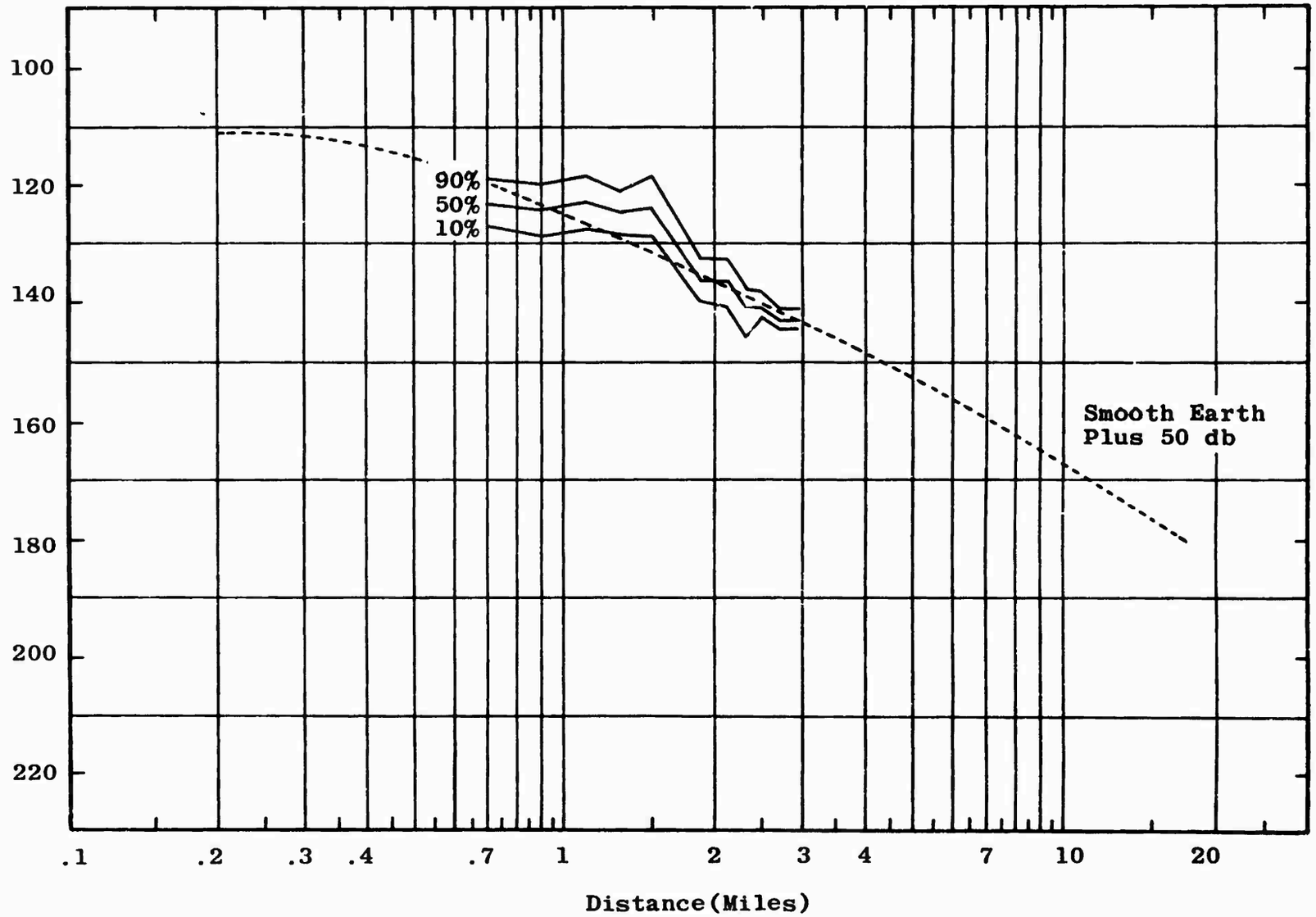

Figure 4.119 Comparison Between Vehicular Data and Theoretical Smooth-Earth Model Plus 50 db
$L_b = F_A(250, 80, V, d, 7)$

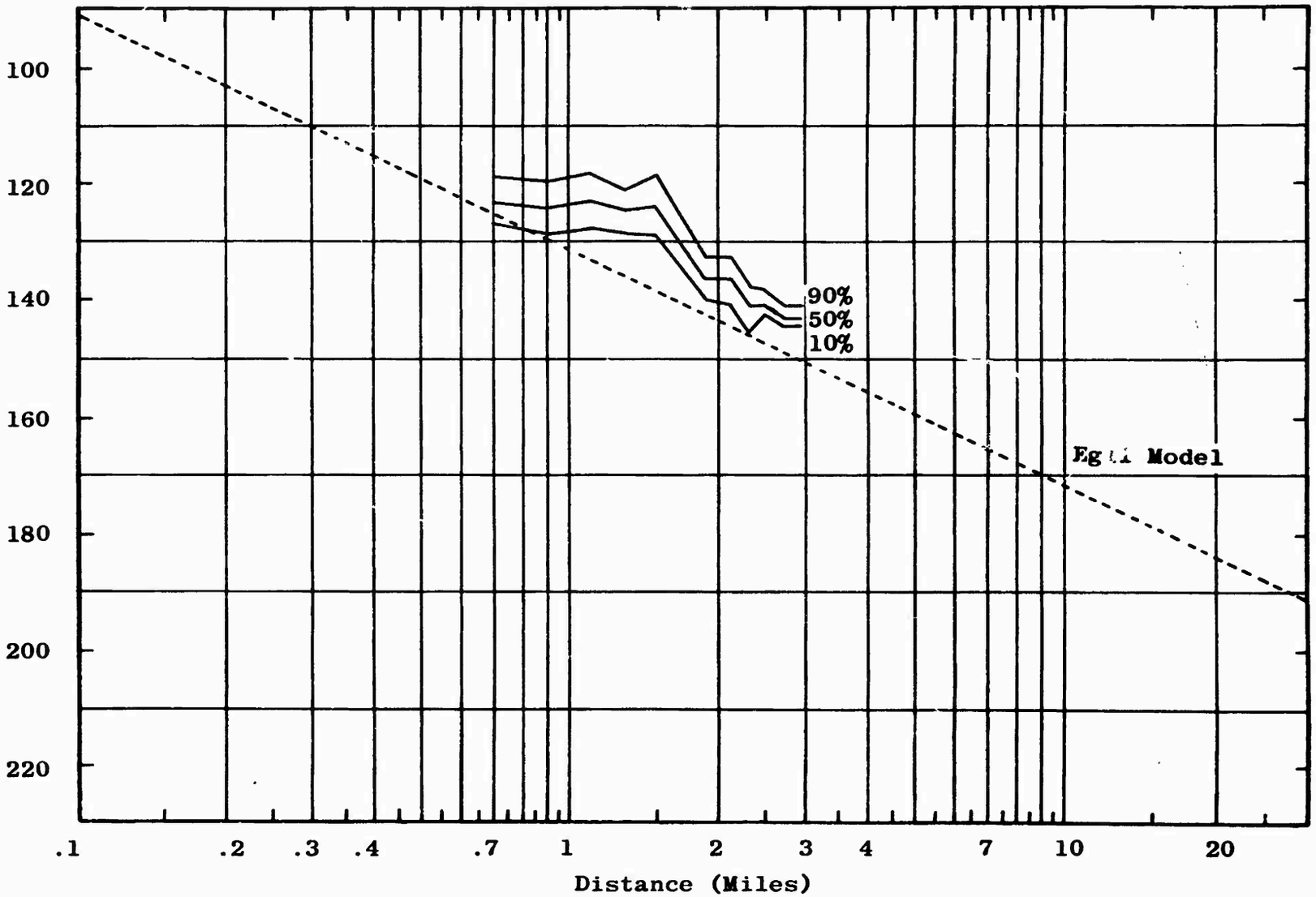

Figure 4.120 Comparison Between Vehicular Data and Egli Model
$L_b = F_A(250, 80, V, d, 7)$

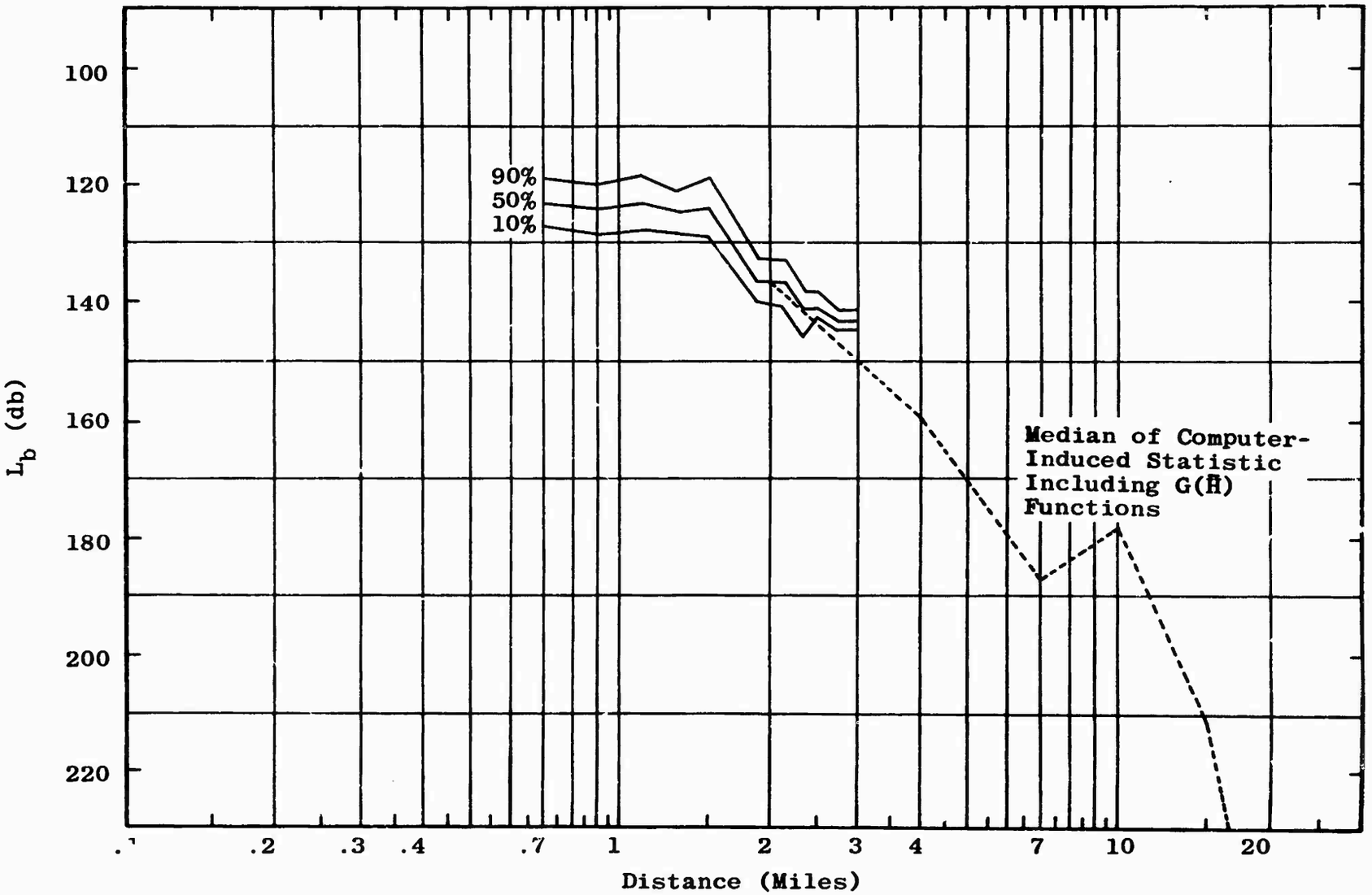

Figure 4.121 Comparison Between Vehicular Data and Median of Computer-Induced Statistic Including G(H̄) Functions
$L_b = F_A(250, 80, V, d, 7)$

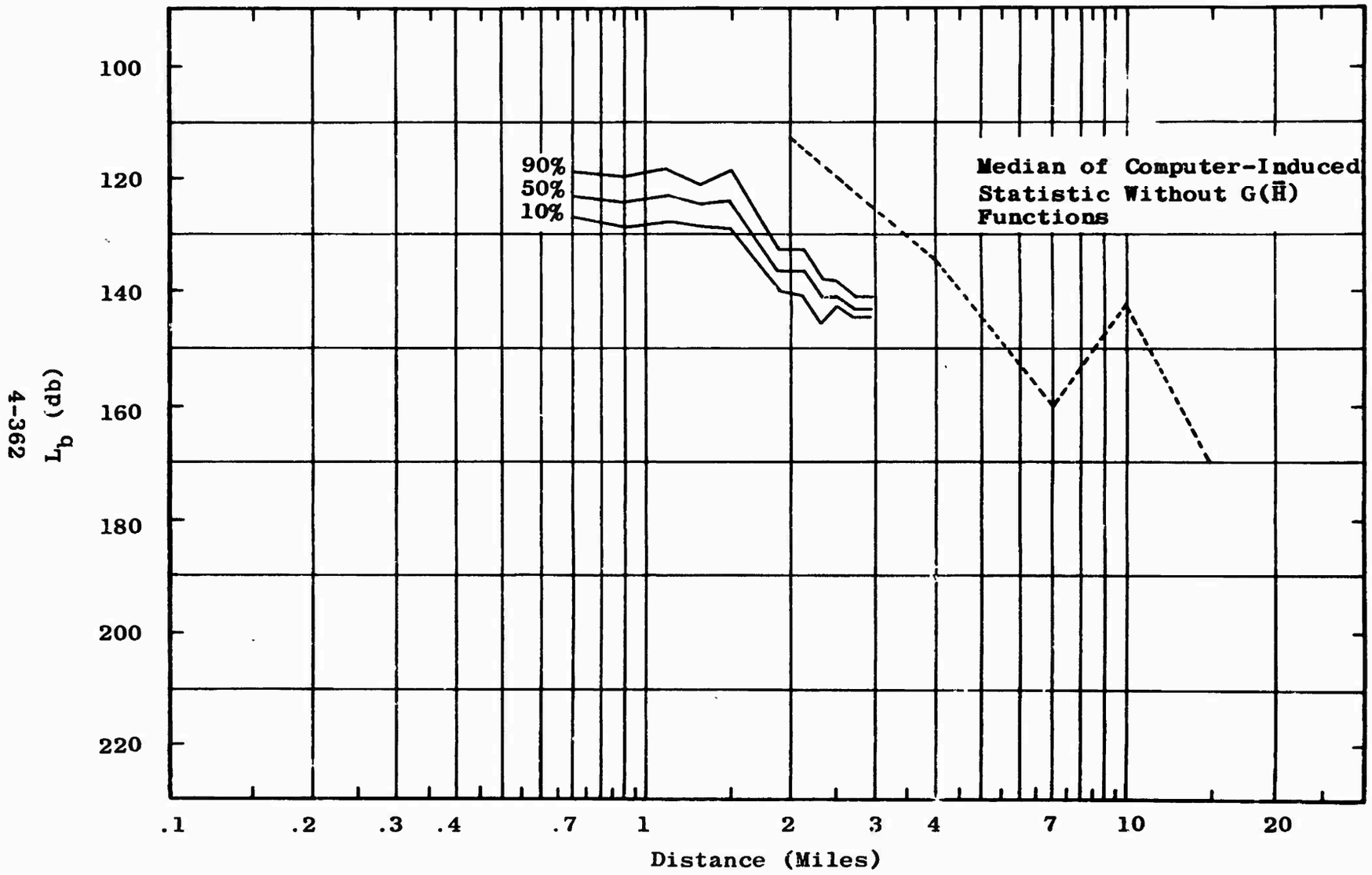

Figure 4.122 Comparison Between Vehicular Data and Median of Computer-Induced Statistic Without G($\bar{H}$) Functions
$L_b = F_A(250, 80, V, d, 7)$

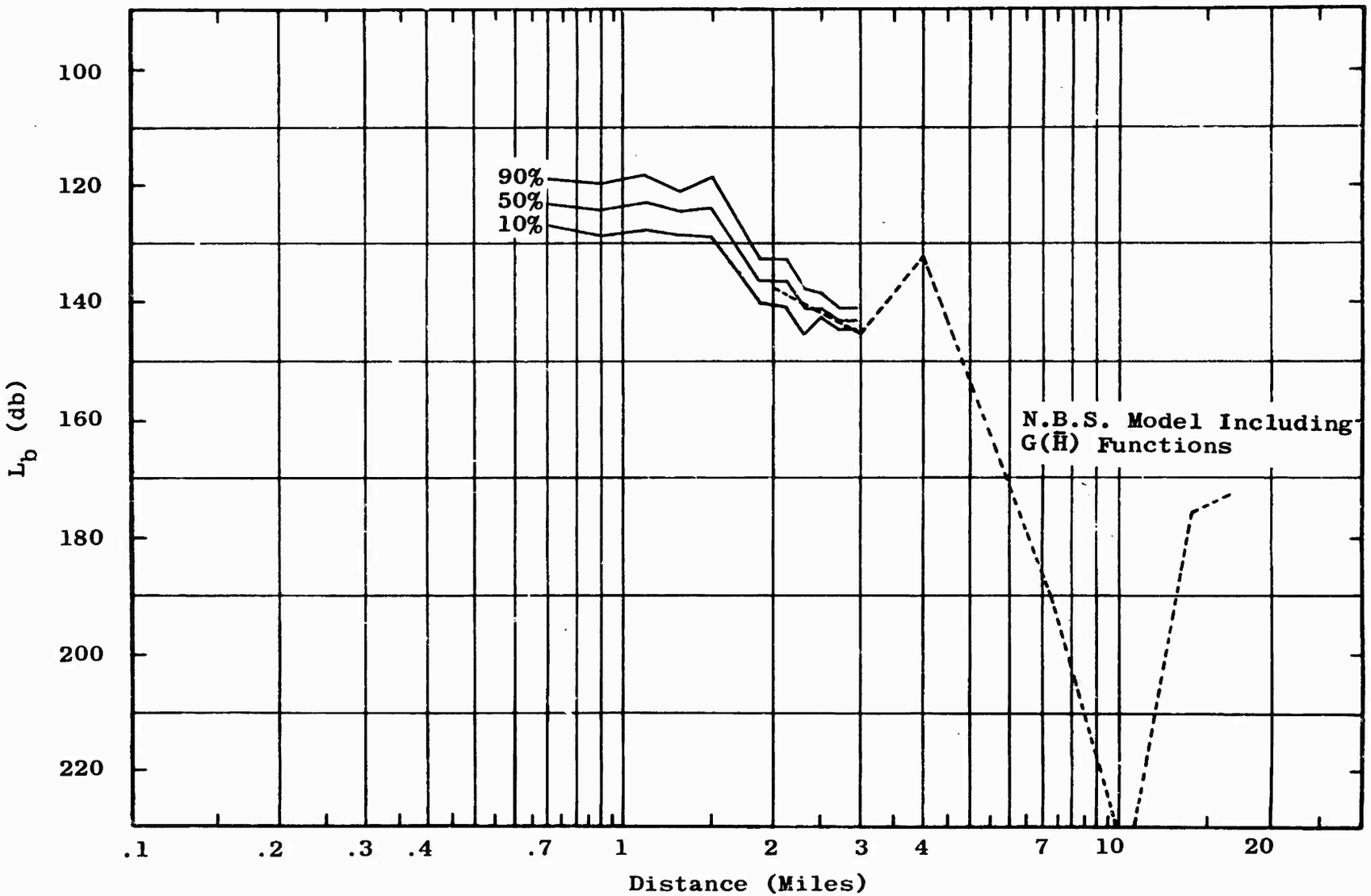

Figure 4.123 Comparison Between Vehicular Data and N.B.S. Model Including $G(\bar{H})$ Functions
$L_b = F_A(250, 80, V, d, 7)$

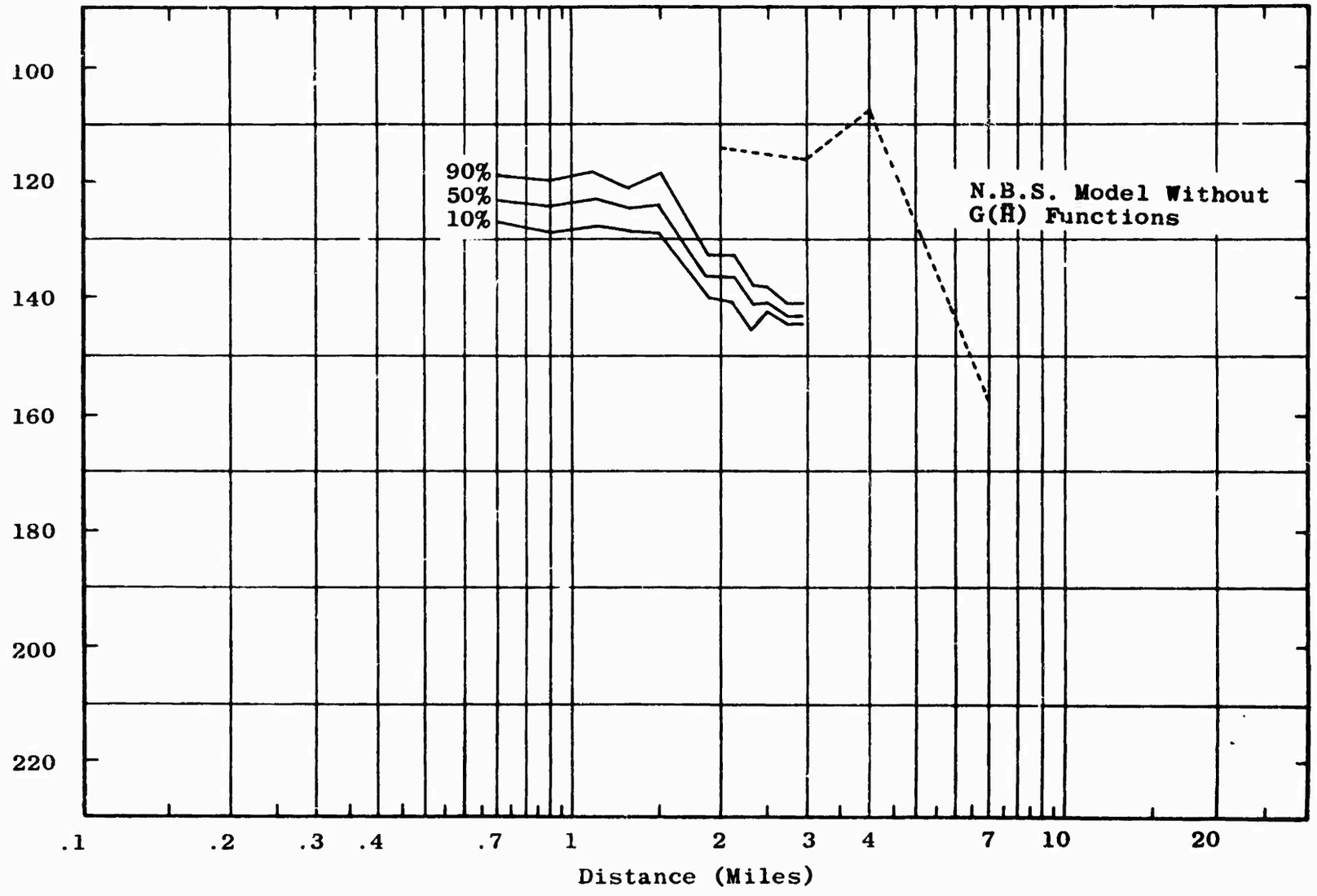

Figure 4.124 Comparison Between Vehicular Data and N.B.S. Model Without $G(\bar{H})$ Functions
$L_b = F_A(250, 80, V, d, 7)$

4.4 Other Factors Affecting L_b

4.4.1 Climatology

4.4.1.1 Analysis of Climatological Data

A considerable amount of climatological data has been collected and reduced for correlation with path loss data. The climatological factors of interest are rainfall, relative humidity, and ambient temperature. These factors are used in the determination of the refractive index, N_s, which in turn is used to determine the effective earth's radius factor, k. Figure 4.125 summarizes the climatological data collected from February 1964 through April 1965. The lower curve shows the total accumulated rainfall for each week of the test period. The two middle curves show the weekly average daytime humidity and temperature. Temperature and humidity readings were generally taken three times a day: in the morning, about noon, and in the late afternoon.

The top curve in Figure 4.125 gives the resulting weekly average effective earth's radius factor, k. The curve demonstrates that the changes in the average effective earth's radius factor are relatively small. The factor k varies from approximately 3/2 to almost 4/3, but never quite reaches the "standard atmosphere" of 4/3.

Data of the type shown in Figure 4.125 has been prepared for future correlation with measured path loss data.

4.4.1.2 Nomographs for Computation of N_s and k from Psychrometric Data

Following the adoption of Carrier's equation[5] to compute the partial water vapor pressure for given wet bulb, dry bulb, and ambient conditions, the equation was reduced to two practical nomographs to facilitate field computations.

---

5. Discussed in Section 3.2 of Semiannual Report Number 5

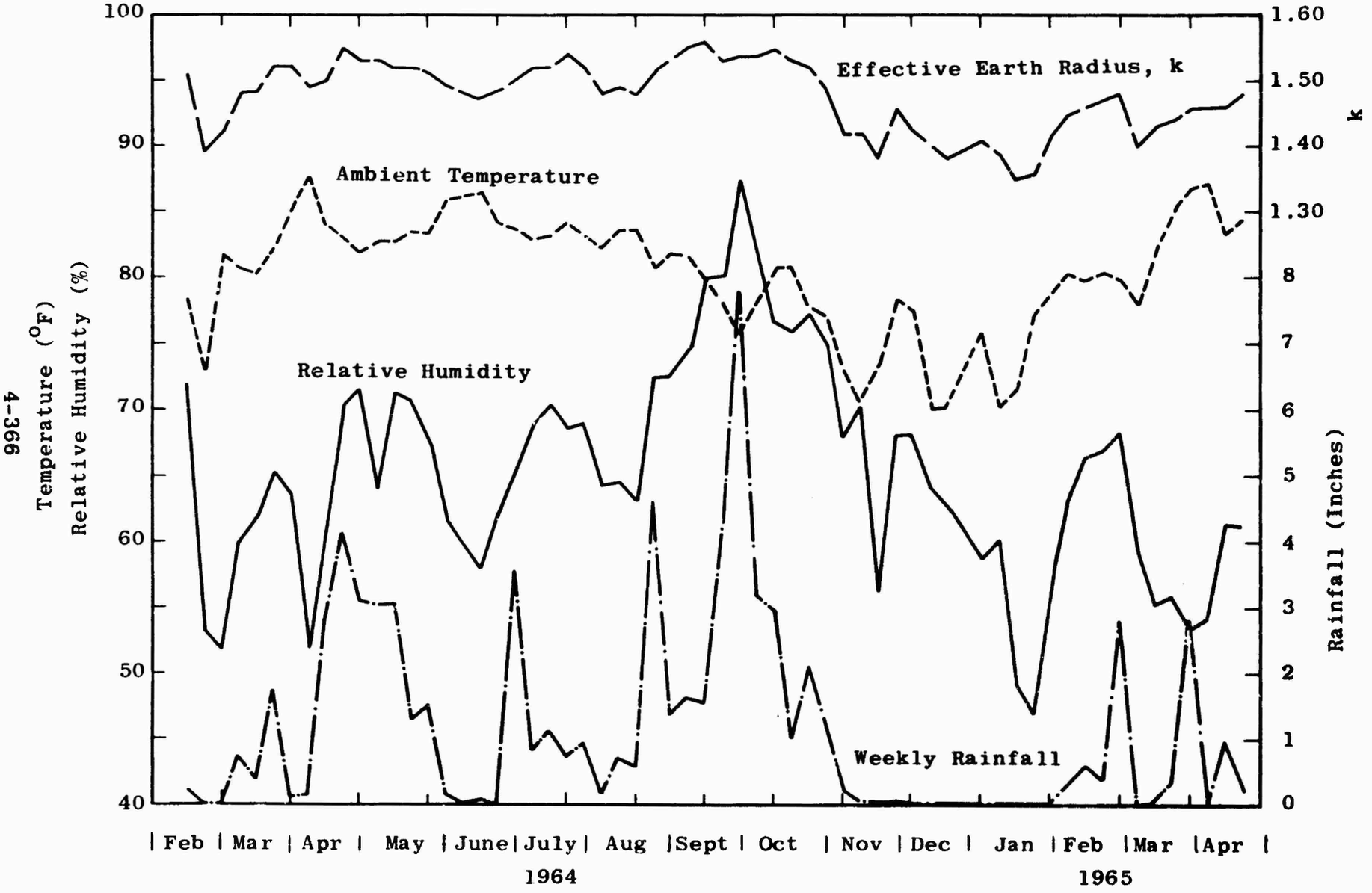

Figure 4.125 Climatological Data Summary

The basic parameters involved are wet and dry bulb temperatures, altitude of the measurement site, and the atmospheric pressure -- measured in terms of sea level pressure.

The first nomograph, Figure 4.126, permits computation of ambient pressure from the altitude of the measurement site and the pressure measurement, reduced to sea level reference. Wet bulb temperature and the difference between wet and dry bulb temperatures are used to compute partial pressure of water vapor, e, at the ambient conditions. Values derived from this nomograph which are used to complete the computations are the ambient pressure, P_a, (from Scale 3) and the partial pressure of water vapor, e, (from Scale 9).

In the second nomograph, Figure 4.127, the partial pressure of water vapor; e, the ambient pressure, P_a; and the dry bulb temperature are used to compute the radio refractive index, N_s. Since N_s is the only parameter involved, this nomograph is also used to compute k, the ratio of the effective earth radius to the actual radius.

All calibrated scales are marked in terms of the measured parameter, i.e., pressure factor in terms of altitude in feet or meters; measured pressure, P_a, in millimeters of mercury or millibars, referred to sea level pressure; saturation pressure at wet bulb temperature, P_g', in degrees Fahrenheit. Computed values are read in millimeters of mercury for all pressures. Unmarked scales, such as 4 and 7 on the first nomograph, and 3 and 5 on the second nomograph, are used as "turning points." These are marked temporarily with a pen or pencil in making computations.

The following steps are followed in making computations of N_s or k by Nomographs 1 and 2.

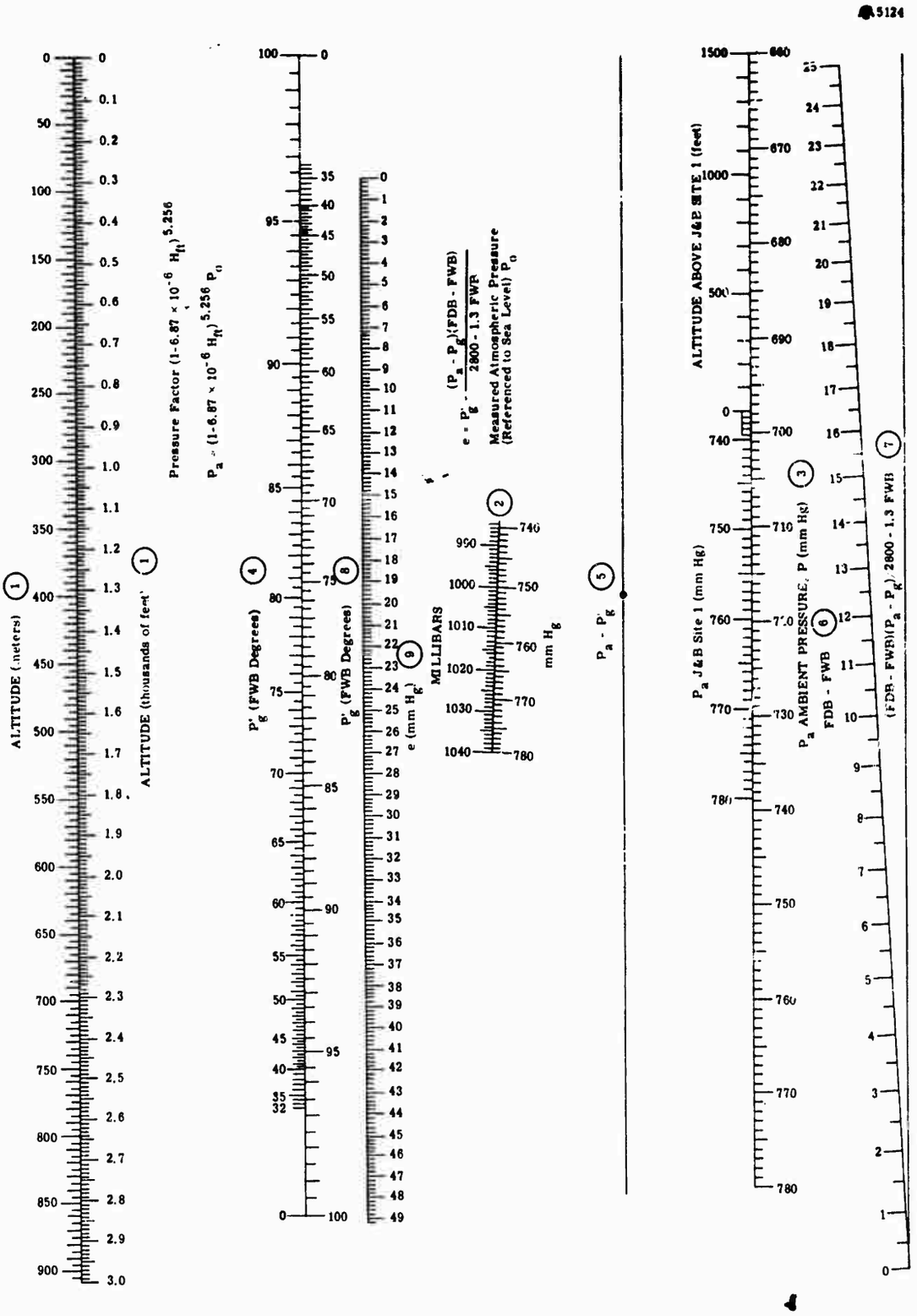

Figure 4.126 Nomograph 1. Computation of Partial Pressure of Water Vapor, e, from Psychrometric Data

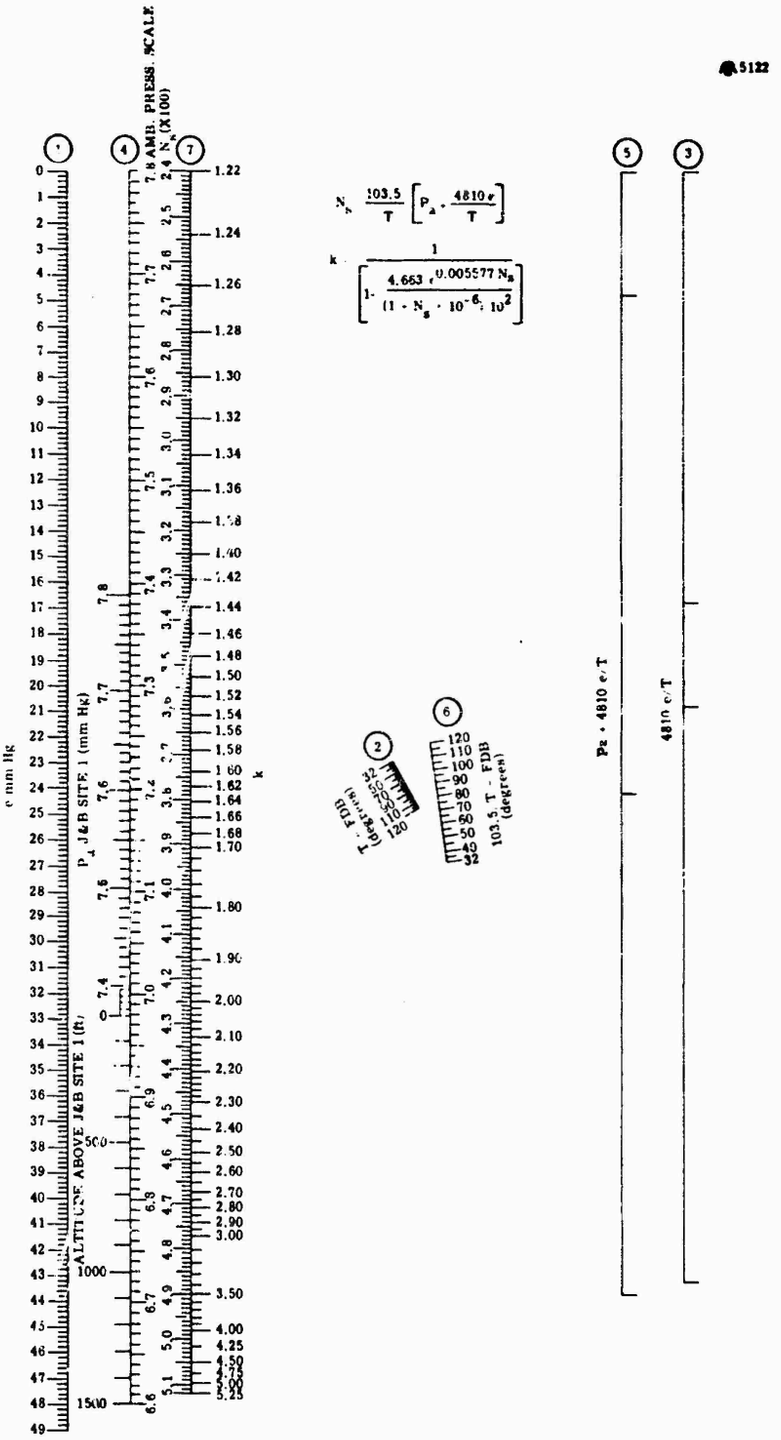

Figure 4.127 Nomograph 2. Computation of N_s and K from Partial Vapor Pressure, e, ($mm_S Hg$)

Nomograph 1

Step 1. Place a straight edge through the measured altitude (Scale 1) and the measured pressure (Scale 2). Mark and record the intersection of the extension of this line with Scale 3, ambient pressure.

Step 2. Place a straight edge through the ambient pressure on Scale 3 (Step 1) and the measured wet bulb temperature (Scale 4). Mark the intersection of this line with Scale 5.

Step 3. Place a straight edge between the marked point on Scale 5 (Step 2) and the difference between dry bulb temperature and wet bulb temperature (Scale 6) and mark the intersection of an extension of this line with Scale 7.

Step 4. Place a straight edge between the point of intersection on Scale 7 (Step 3) and the wet bulb temperature (Scale 8). Record the intersection of this line with Scale 9, e = mm Hg.

Nomograph 2

Step 5. Place a straight edge from the value of e = mm Hg (as determined in Step 4) on Scale 1 to the dry bulb temperature on Scale 2. Mark the intersection of the extension of this line with Scale 3.

Step 6. Place a straight edge between this point of intersection with Scale 3 (Step 5) and the measured pressure on Scale 1. This measured pressure will be the same reading used in Step 1. Mark the intersection of the extension of this line with Scale 5.

Step 7. Place a straight edge between the point of intersection on Scale 5 (Step 6) and the dry bulb temperature on Scale 6. The intersection of the extension of this line with Scale 7 gives either the "refractive index," N_s, or the "effective earth's radius," k.

Both Nomographs 1 and 2 have auxiliary scales on the ambient pressure scale. These scales refer to J & B Site 1 and are marked in millimeters of mercury, referred to sea level, measured at that site. In addition, there is an altitude scale in feet above J & B Site 1 which is used as a sliding scale to determine pressures above this site. This scale is to be used with the low-altitude wiresonde. Pressures may be corrected to the closest 25 feet by shifting the altitude measured to the ground pressure measurement and noting the corrected pressure. The use of this scale eliminates the need for Steps 1 and 2 and the need for the notation of P_a.

4.4.2 Tropical Vegetation

Among the various factors that influence the operating ranges of mobile and man-pack radio equipments in a natural tropical environment, those associated with the tropical vegetation, or "jungle," are perhaps the most difficult to deal with in a quantitative fashion. This difficulty stems from the fact that the interactions between the propagating waves and the vegetative elements are extremely complex in the spatial sense, and the situation cannot be resolved deterministically with mathematical rigor within the present state of the art. Even if the problem could be solved this way, it would require as input data such a considerable amount of detailed information about the physical

distribution of the vegetation, that the exact solution could not, therefore, be practically applied to the task of predicting radio path losses within a spectrum of actual conditions.

The problem is further complicated by the physical nature of the vegetation. Dealing with any problem in a scientific fashion, requires the ability to measure and count the phenomena so that they can be expressed in terms of numbers, and so that groups of related phenomena can be compared with one another on a numerical basis. This is not to suggest that the natural relations between phenomena must always be expressed in terms of numerical formulas, but it does mean that comparisons should attain to numerical expression, or numerical scaling, of the phenomena so as to be as stable and unequivocal as the numbers. This situation is particularly difficult to achieve with completeness with respect to a stand of vegetation.

Although many of the observable characteristics of a stand of vegetation in a given area are considerably influenced by the prevailing climatic and edaphic environments, the characteristics of the individuals in the stand are primarily hereditary in origin. For example, a certain type of tree is unique in the hereditary sense and all trees of this type can be depended upon to exhibit hereditary similarities. Likewise, trees of different heredities will exhibit different characteristics. Consequently, many of the important concepts of vegetation that have been developed in the field of botany have concentrated on the hereditary attributes of vegetation phenomena. Such an approach is taxonomical in nature and the scientific usefulness of these concepts is greatly dependent on the investigator's ability to observe through the visual sense and to interpret

the phenomena in the light of his prior knowledge and experience with the subject. This is the essence of the descriptive approach to science, and the field of botany is well noted for its refinement of this art. But the application of this approach always depends to some extent on the investigator's personal understanding of the vegetation with which he works and is, therefore, unavoidably subjective in nature. While such methods are no less valid, and important scientific contributions have been obtained this way, such methods do not lend themselves particularly well to the concepts of quantification, or scaling, in terms of numbers.

On the other hand, there are many attributes of a stand of vegetation that can be described in terms of units of measure, or numbers. The heights of the trees, the number of trees per unit of area, or the diameters of the trees at some standardized height are examples of such attributes. When an attribute is measured, or scaled, a parameter is produced. It, therefore, appears that the collection of attributes of a stand of vegetation can be thought of in terms of two broad classes: those attributes which can be parameterized with relative ease, such as tree heights; and those for which suitable parameters cannot be easily found, such as floristic character. It also seems clear that the first class of attributes, being dimensional in nature, is associated with the dimensional properties of the stand, whereas the second class is identified with the abstract and subjective features of the stand. Since the dimensional properties of vegetation vary randomly from place to place, and from season to season, the parameterized attributes of the stand are, therefore, statistical in nature.

One of the objectives of this project is to determine the quantitative influence of tropical vegetation on radio wave propagation. To this end, the fundamental techniques of statistical correlation are employed to measure the interdependence, or interrelationship, between two sets of empirical data, and to develop prediction procedures for other similar environments. One set of data is obtained from the propagation measurements while the other set of data consists of a collection of the physical parameters of the vegetation in which the measurements were made. From the philosophical point of view, it is perhaps important to recognize that both sets of data are statistical in nature and, with the introduction of statistical concepts, the answers thus obtained cannot be regarded as certainties, and agreement between measured and predicted values can be expected only in the sense of ensemble averages. However, with respect to the practical aspects of radio communications, this distinction as to methods of approach is unimportant.

The first step to be taken to correlate these two sets of data is to analyze the propagation data so as to separate out a set of propagation parameters, or factors, that can be associated with the existence of vegetation in the propagation path. Such factors may be referred to as "foliage factors." This part of the problem has been previously discussed in Section 4.2.2.4 and a set of such factors is presented in Figure 4.17. The remaining part of this section presents data resulting from physical measurements of the vegetation in the Thailand test area.

4.4.2.1 Vegetation Measurements

A model of tropical vegetation employed to attempt to

determine the effects on such vegetation on radio wave propagation is conceived as being a layer of space above a ground surface with a random distribution of vegetative material which has the electrical properties of lossy dielectrics. The principal effects of the vegetation on radio wave propagation are to attenuate the wave through absorption and to scatter the wave front. The degree of these effects is, therefore, related to the dimensional properties of the distribution of the material and to the electrical properties of the material in the model space. Accordingly, ignoring the electrical properties of the material for the time being, the primary purpose of the vegetation measurements is to obtain as much dimensional information about the vegetation as is possible by practical methods of physical measurements.

The data thus obtained is regarded as a collection of individual sets of data, each of which is statistical in nature, and which is related to a different attribute of the model. A determination can be made of the vegetation parameters best suited to the problem of path loss predictions in vegetated environments by analyzing the interrelationships between these sets and correlating with the foliage factor derived from the propagation data.

This, of course, implies that at least two different data samples from two different types of vegetation, along with corresponding propagation data, will be needed to establish two points on any useful correlation measure. But the vegetation in the Thailand test area must be considered as homogenous from the point of view of its dimensional properties and from the fact that the test area is exposed to the same type of climatic conditions, namely "wet-dry tropical." Therefore, the Thailand measurements can provide only one sample in the vegetation sample space. To provide another

sample requires moving the experiments to a vegetated area in another kind of tropical region.

The data presented in Figures 4.128 through 4.157 was obtained from nine sample plots in the Thailand test area; the plots being selected from the radial sector where propagation measurements were made. The vegetation measurements were made by the Environmental Research Section of MRDC, under the supervision of Lt. Col. W. R. Scheible. With the exception of Figures 4.146 through 4.155, the data appearing in the graphs was prepared by this group. A summary of the vegetation measurements in the Jansky & Bailey test area in the Korat Plateau of Thailand appears below.

Plot No.	Plot Area (Meters^2)	Trees/Acre	Basal Area Feet^2/Acre	Median Ht. (Meters)
1	400	354	55.9	8.6
2	400	364	45.7	5.5
3	400	314	68.0	12.0
4	400	475	74.2	8.5
5	600	337	109.0	14.0
6	400	354	175.0	11.0
7	400	405	130.0	10.0
8	400	334	165.0	11.0
9	600	458	175.0	10.0
Avg.		377	110.9	10.1

This data will be found useful for comparing the dimensional properties of vegetated areas in other geographical areas with the Thailand test area, which is classified as a wet-dry, or Savanna, climatic region.[1]

1. Encyclopedia Britannica, World Atlas 1963, Plate 21.

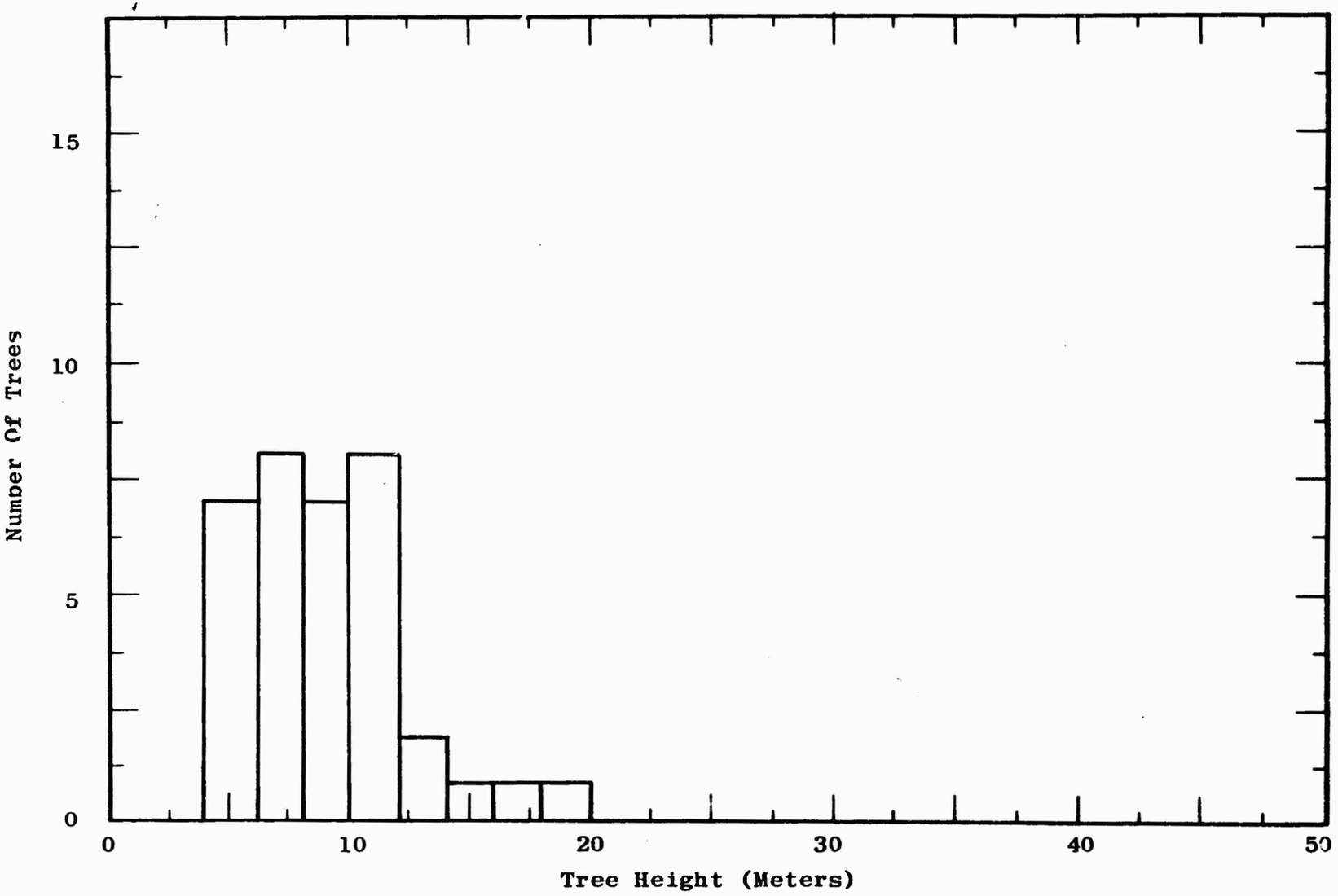

Figure 4.128 Frequency Distribution Of Tree Heights In Plot #1

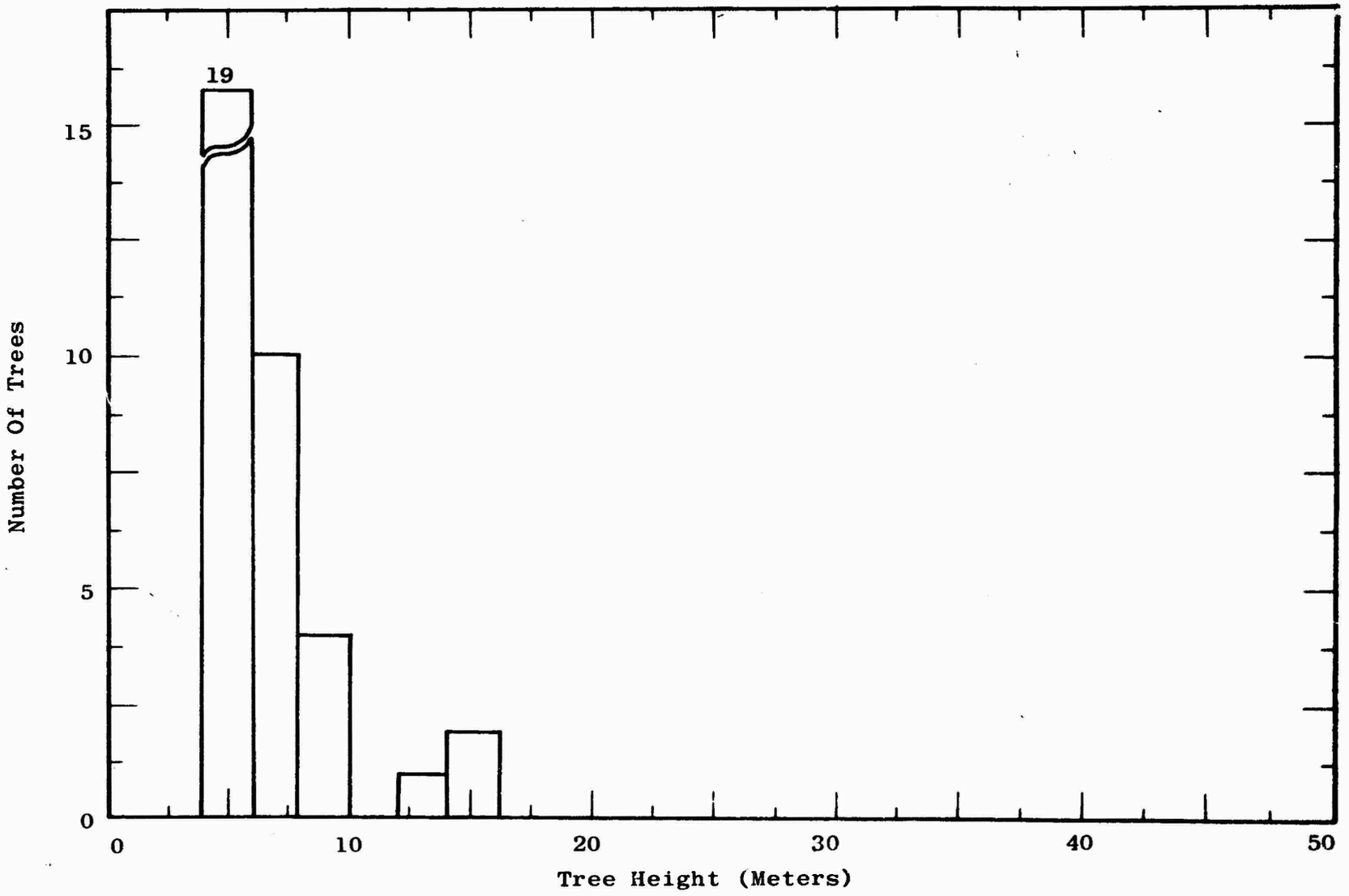

Figure 4.129 Frequency Distribution Of Tree Heights In Plot #2

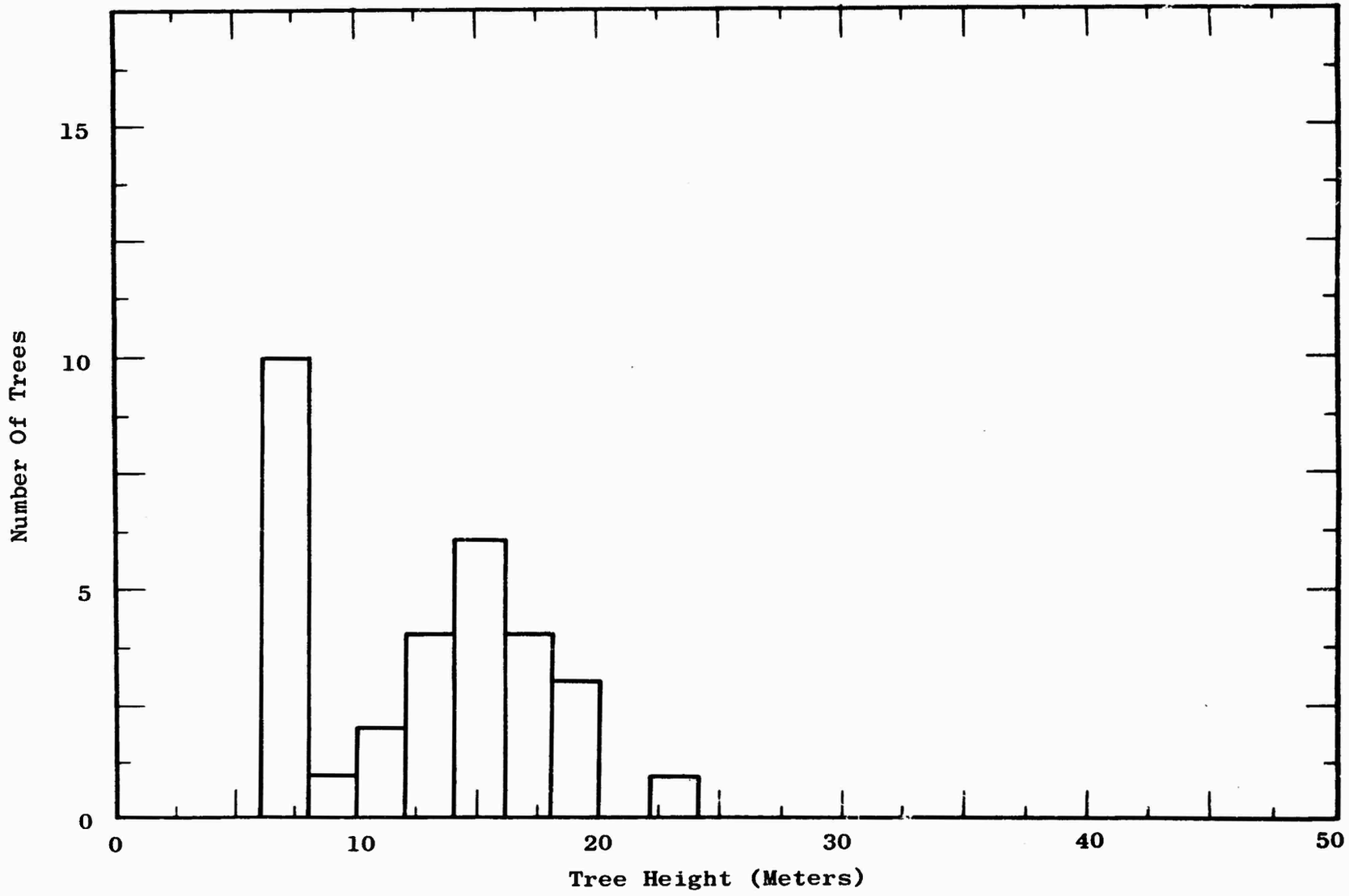

Figure 4.130 Frequency Distribution Of Tree Heights In Plot #3

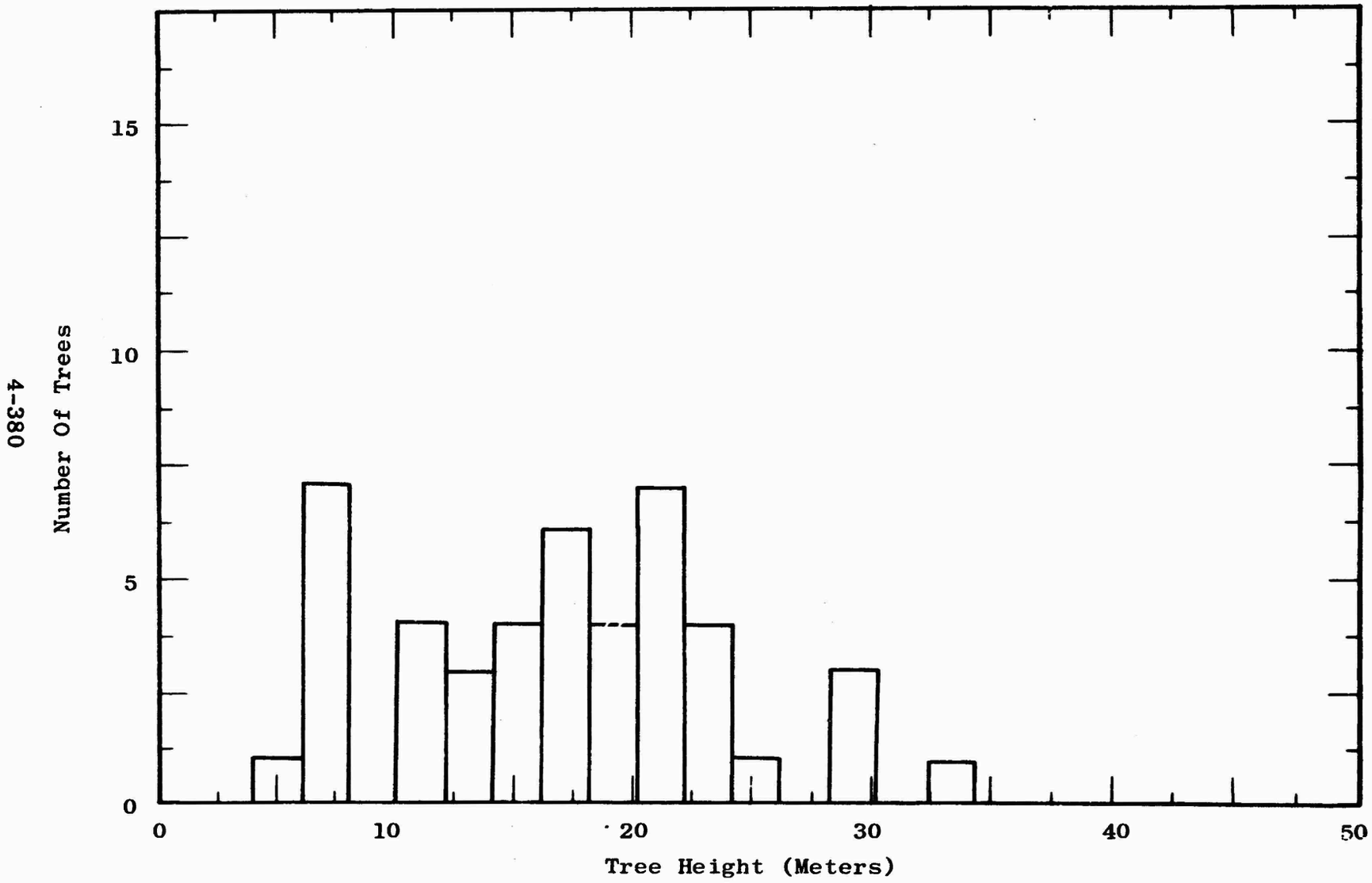

Figure 4.131 Frequency Distribution Of Tree Heights In Plot #5

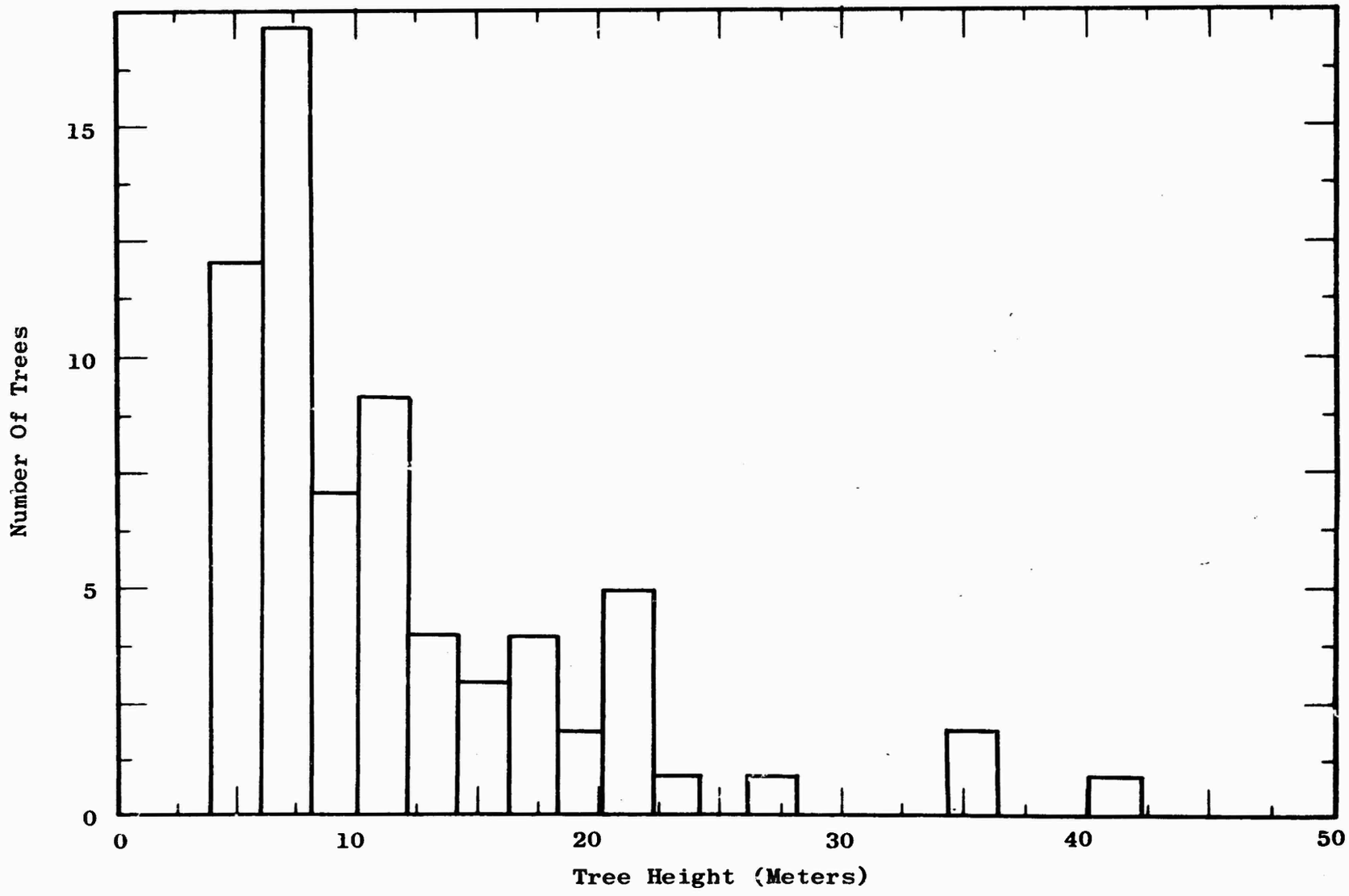

Figure 4.132 Frequency Distribution Of Tree Heights In Plot #5.5

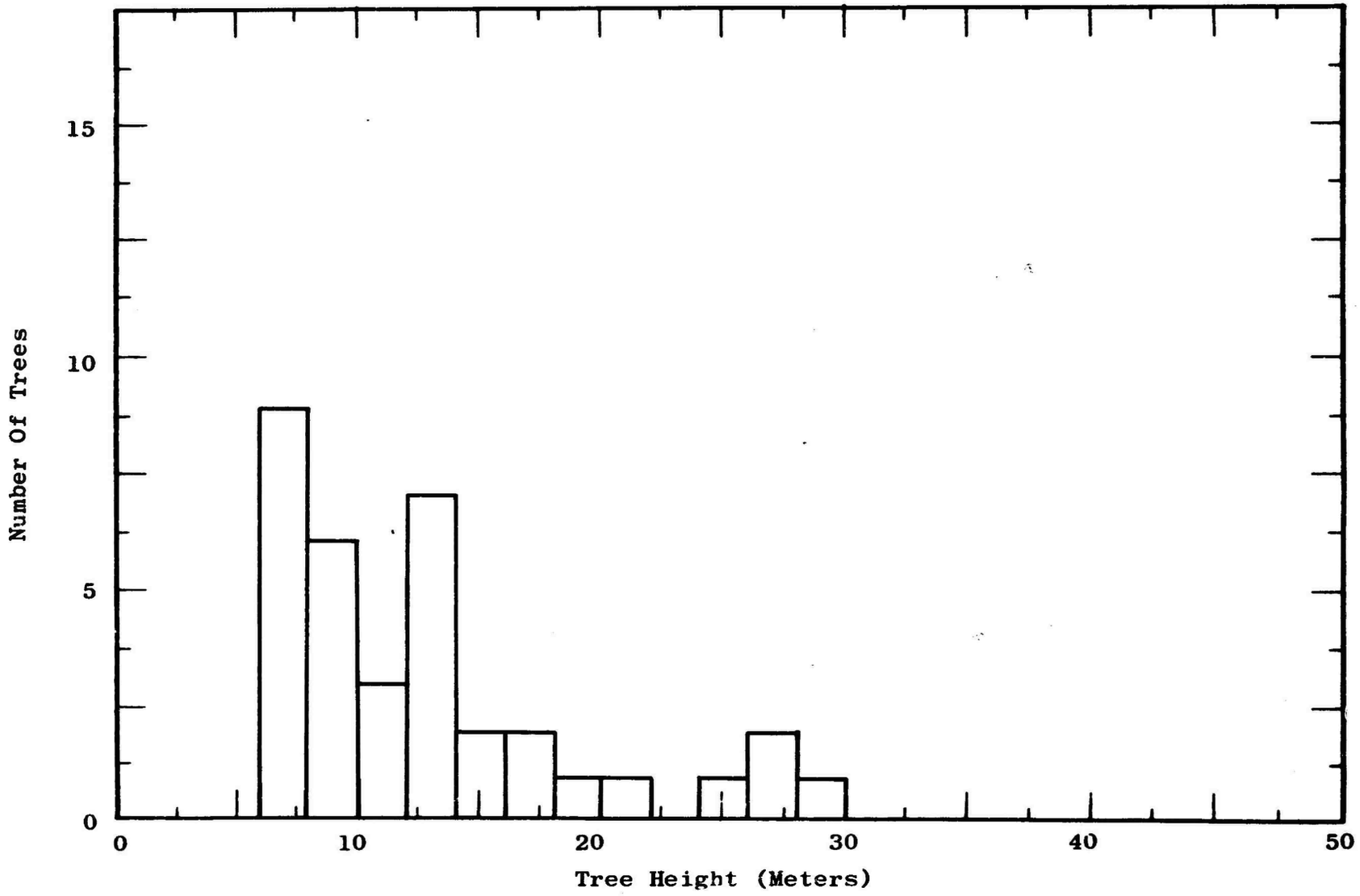

Figure 4.133 Frequency Distribution Of Tree Heights In Plot #6

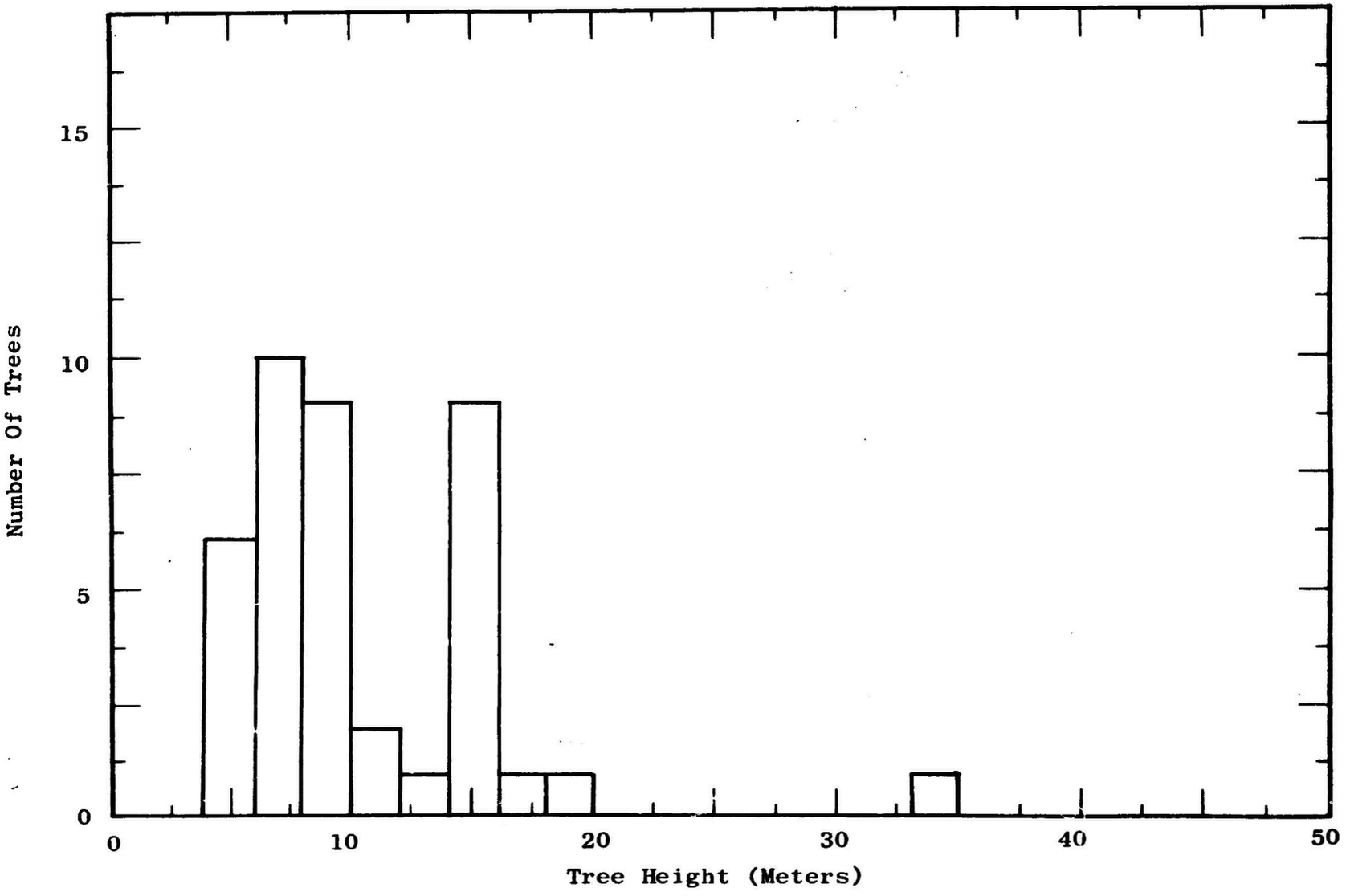

Figure 4.134 Frequency Distribution Of Tree Heights In Plot #7

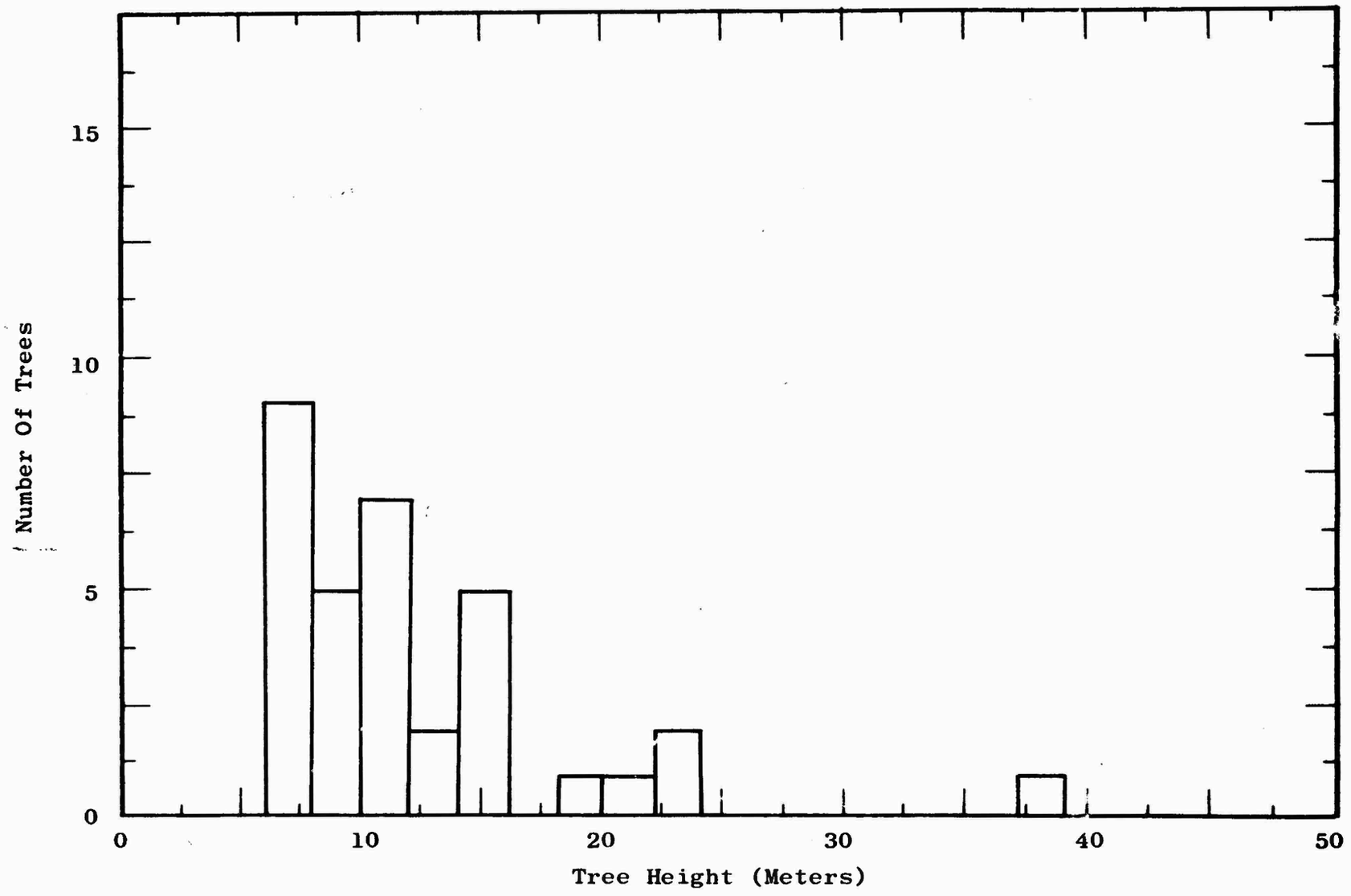

Figure 4.135 Frequency Distribution Of Tree Heights In Plot #8

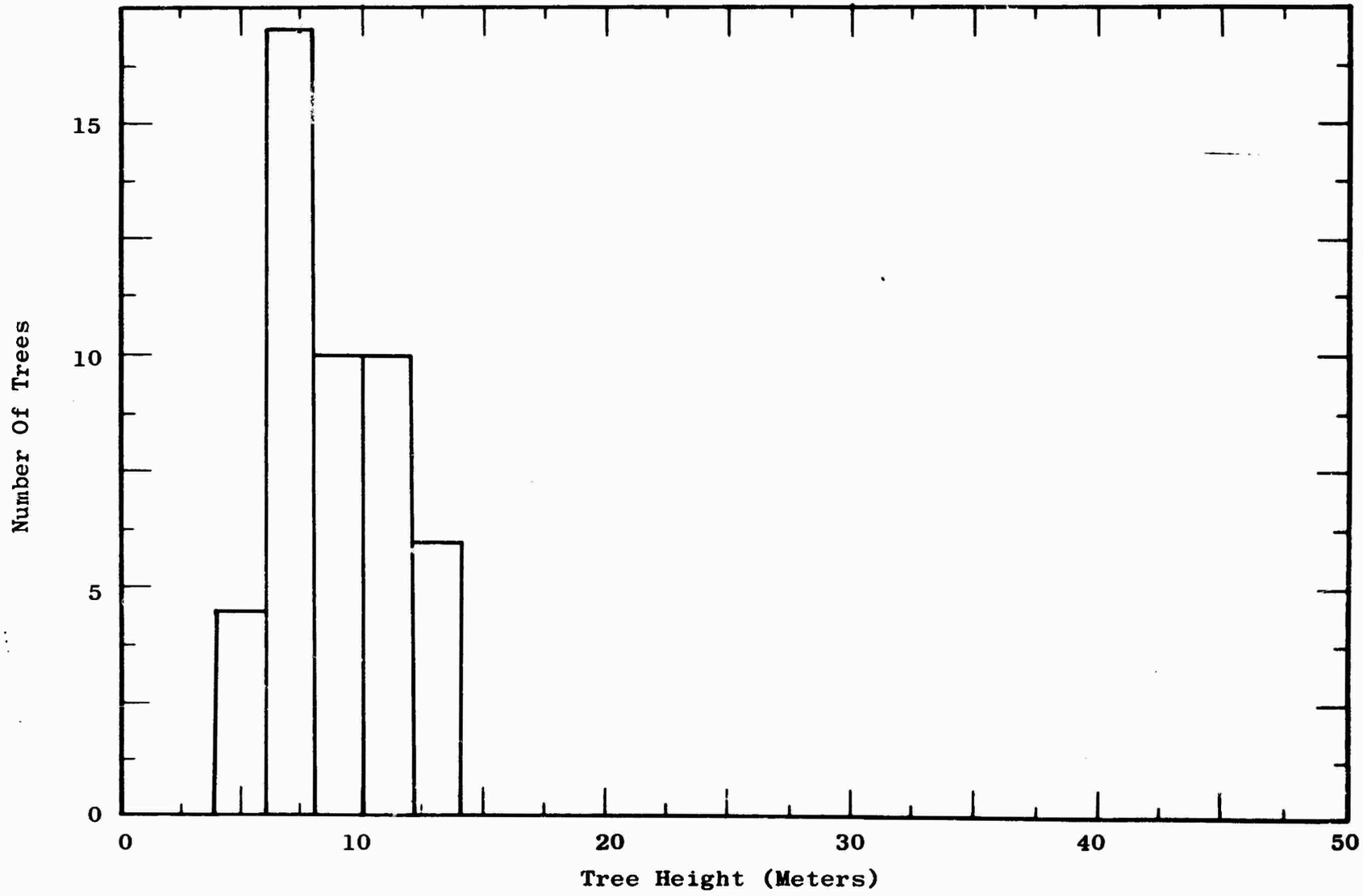

Figure 4.136 Frequency Distribution Of Tree Heights In Plot #9

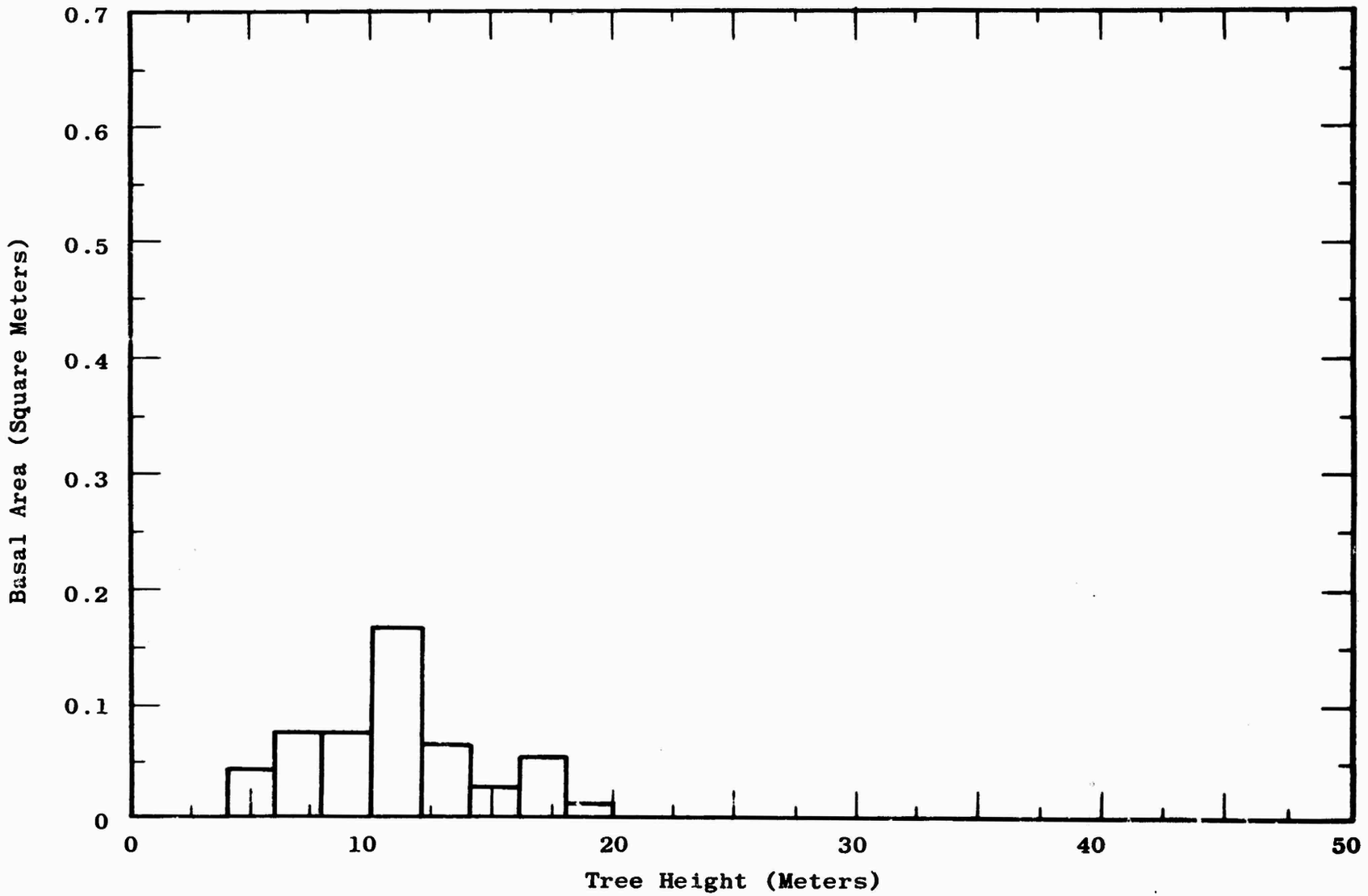

Figure 4.137 Basal Area vs Tree Height In Plot #1

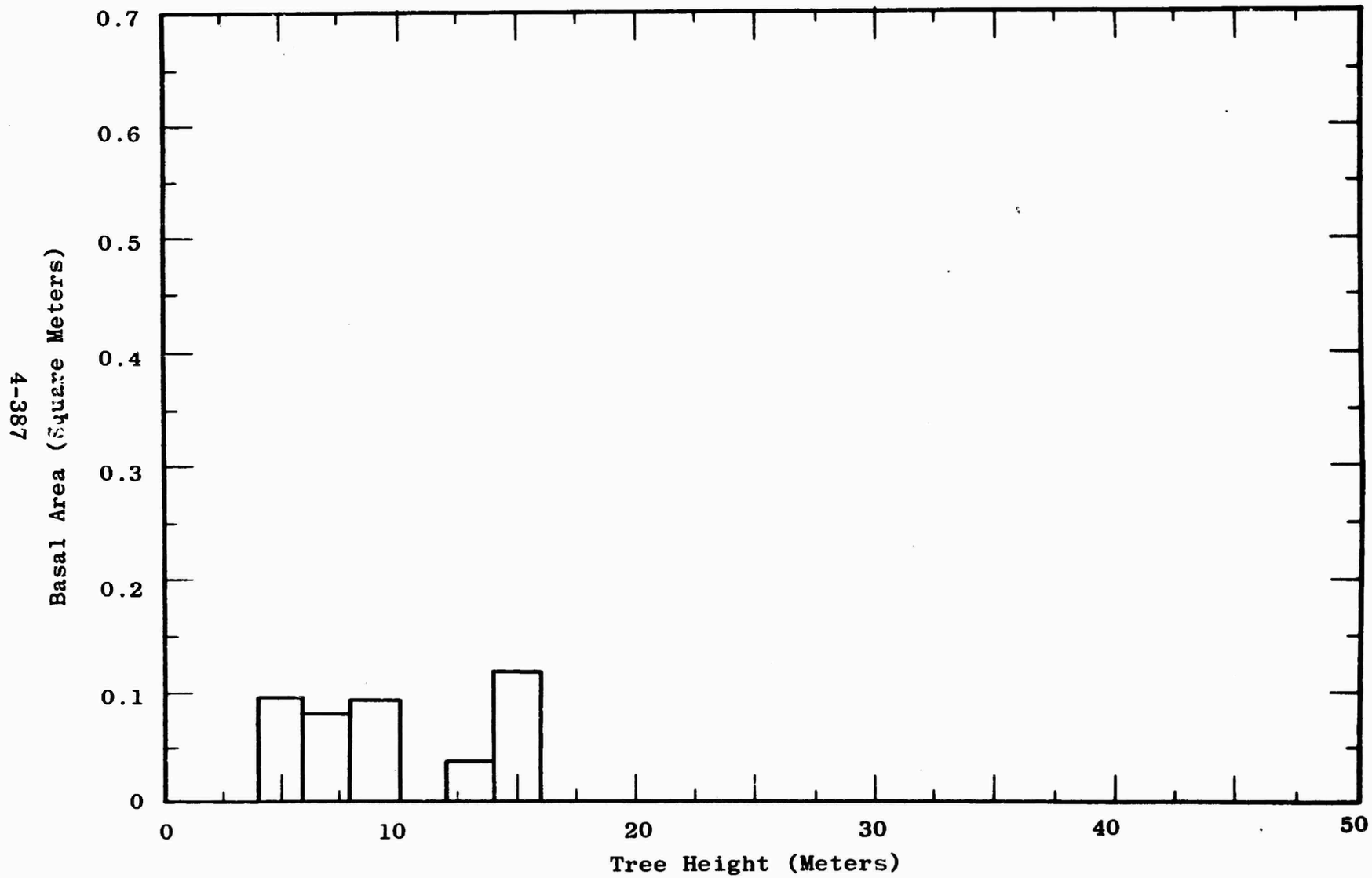

Figure 4.138 Basal Area vs Tree Height In Plot #2

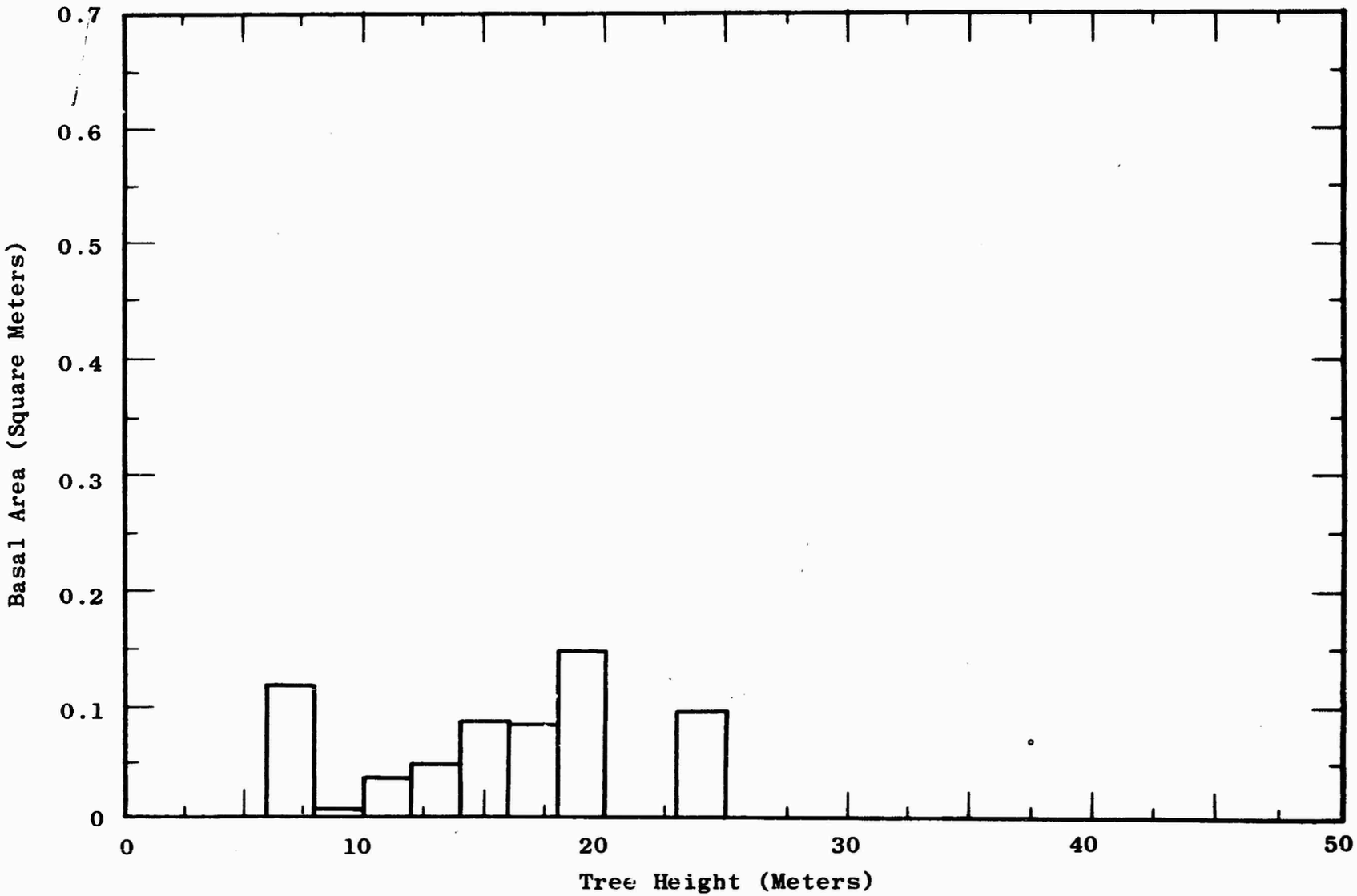

Figure 4.139 Basal Area vs Tree Height In Plot #3

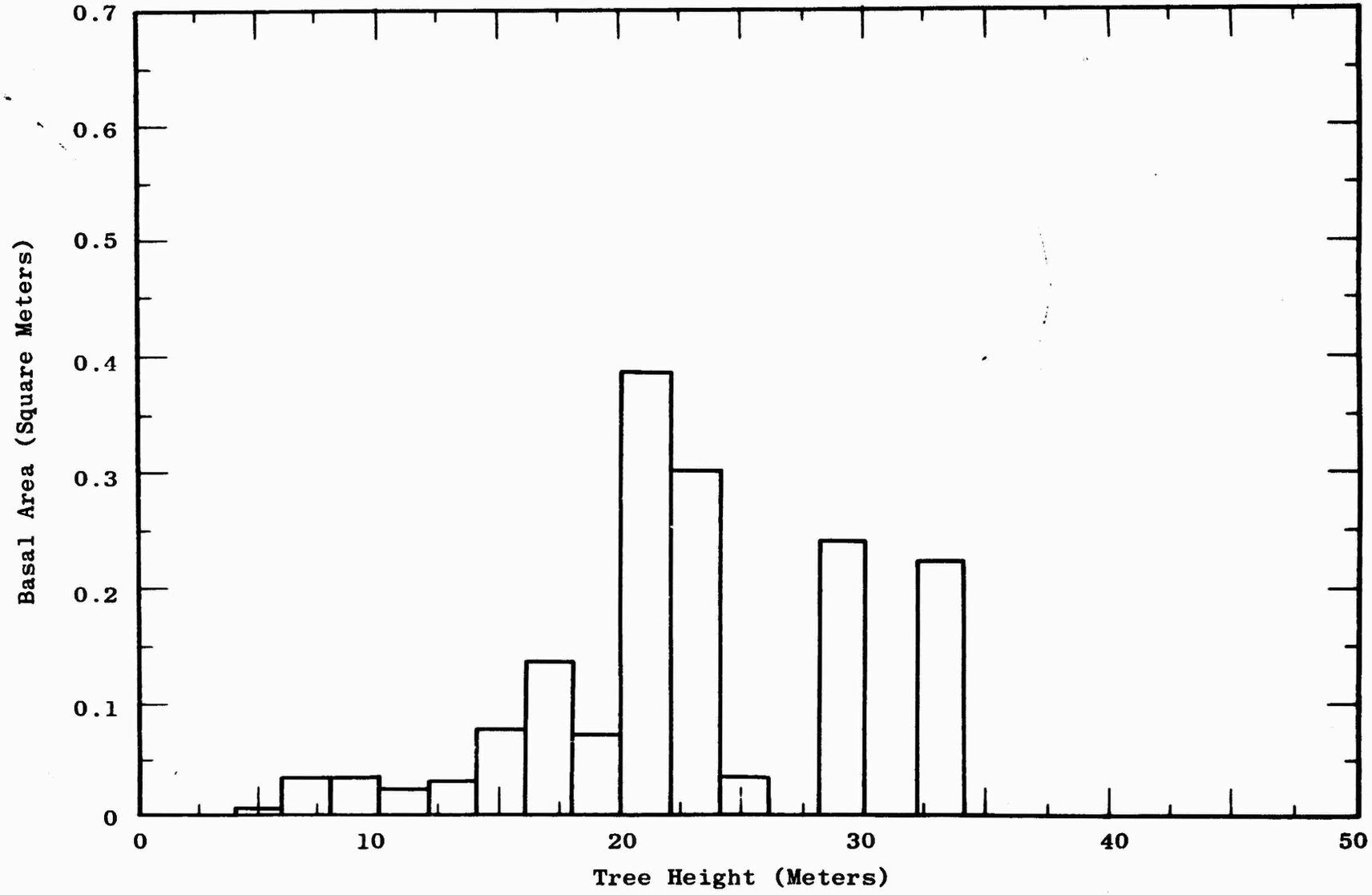

Figure 4.140 Basal Area vs Tree Height In Plot #5

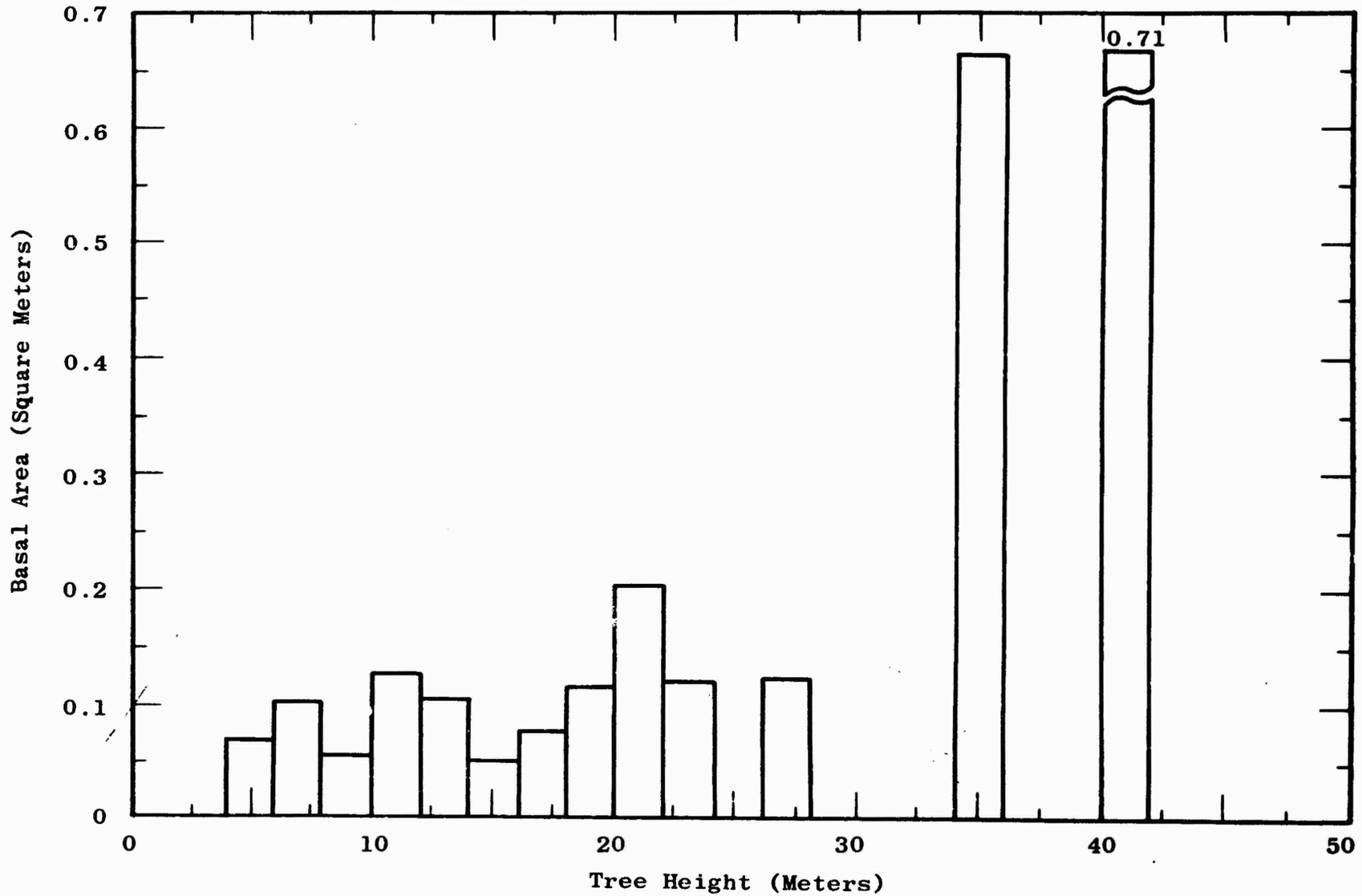

Figure 4.141 Basal Area vs Tree Height In Plot #5.5

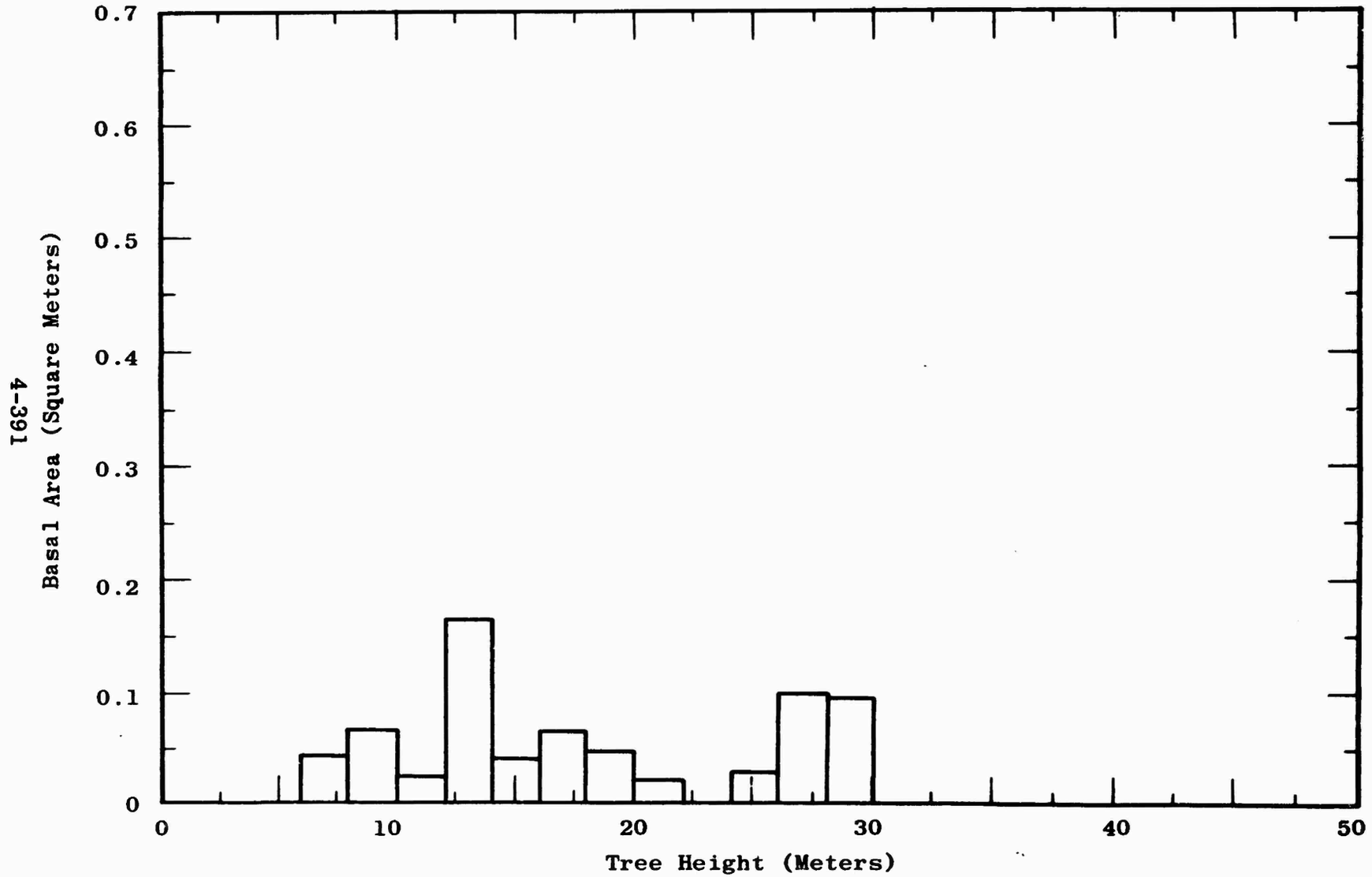

Figure 4.142 Basal Area vs Tree Height In Plot #6

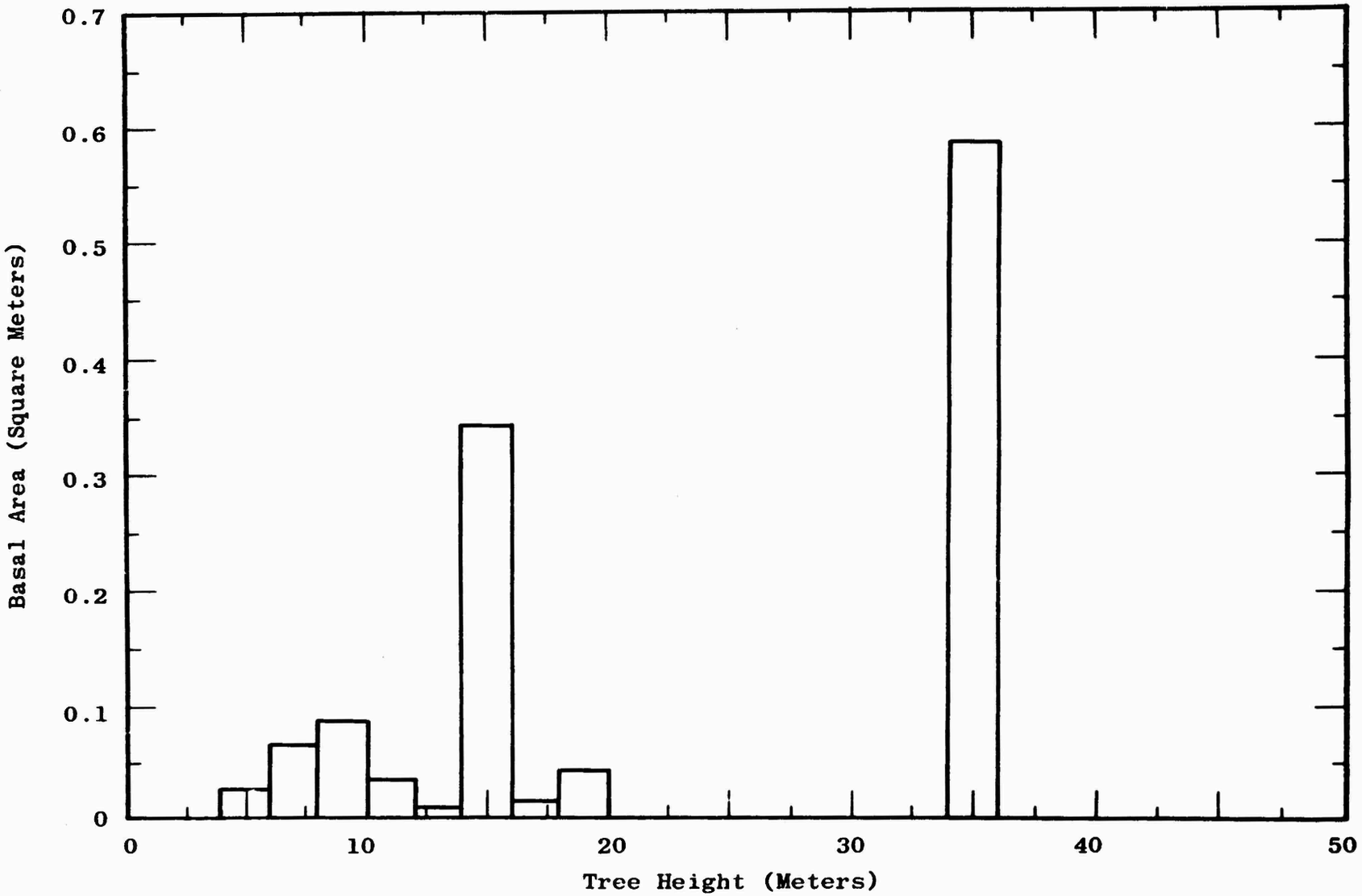

Figure 4.143 Basal Area vs Tree Height In Plot #7

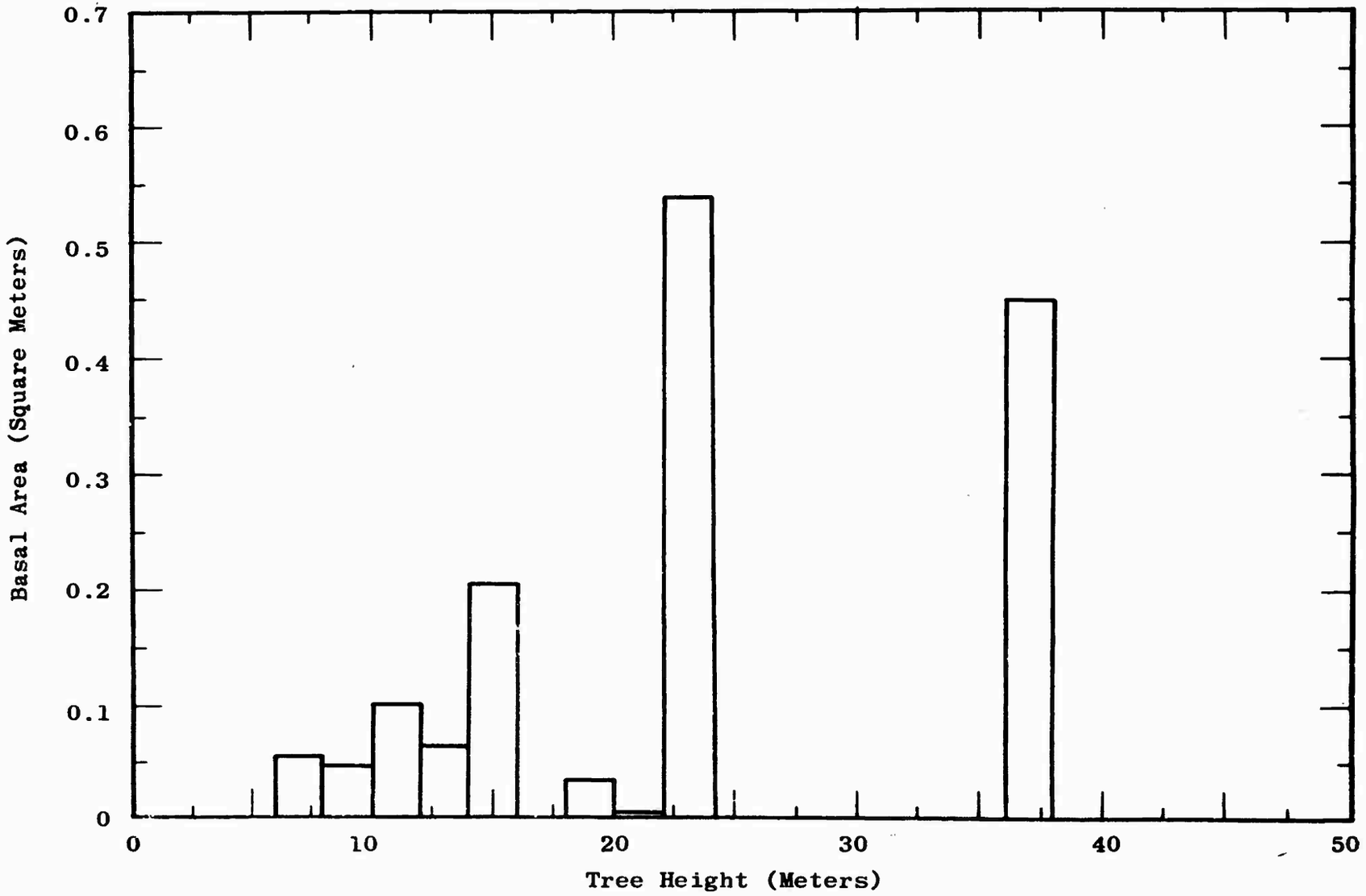

Figure 4.144 Basal Area vs Tree Height In Plot #8

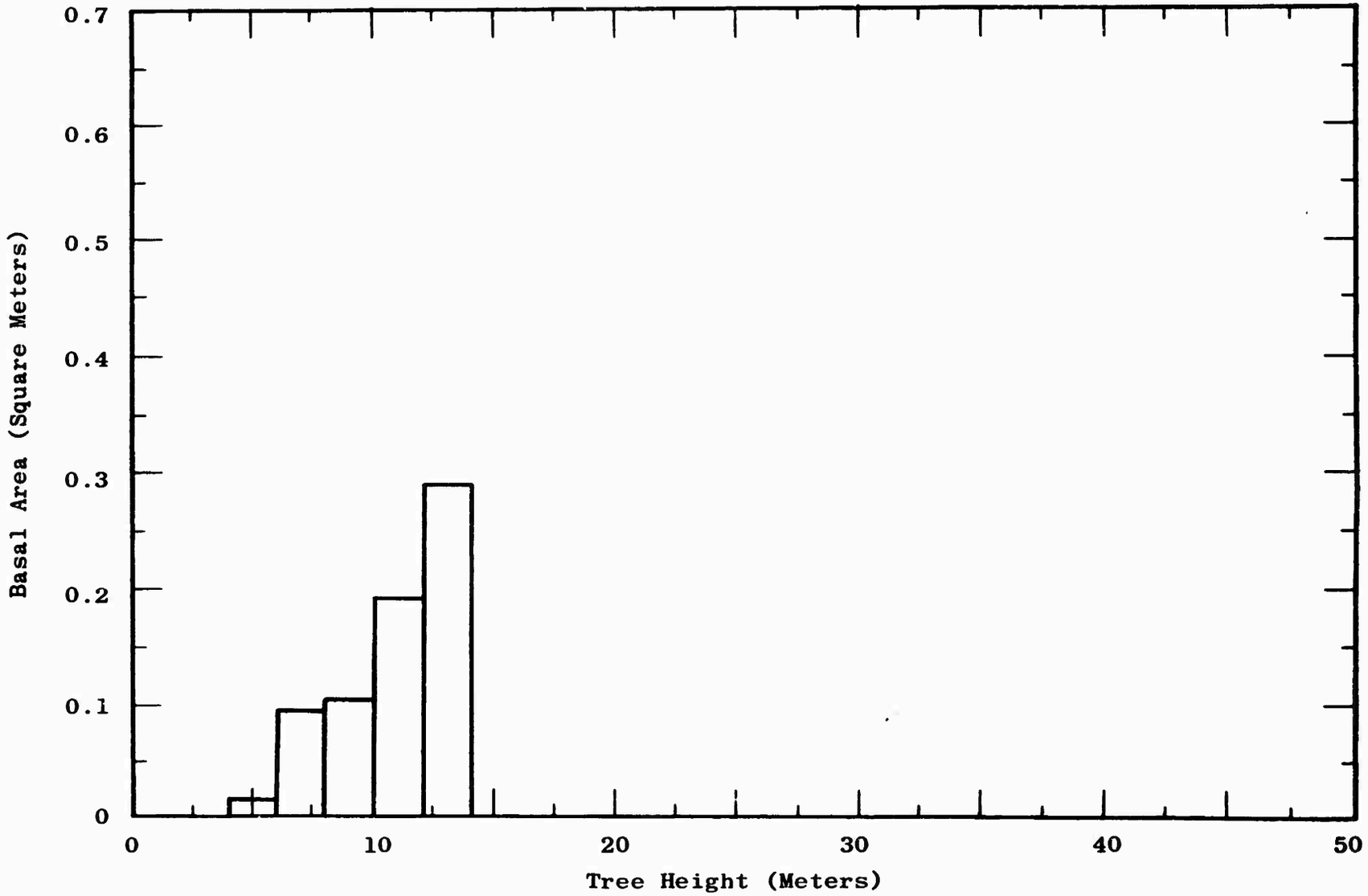

Figure 4.145 Basal Area vs Tree Height In Plot #9

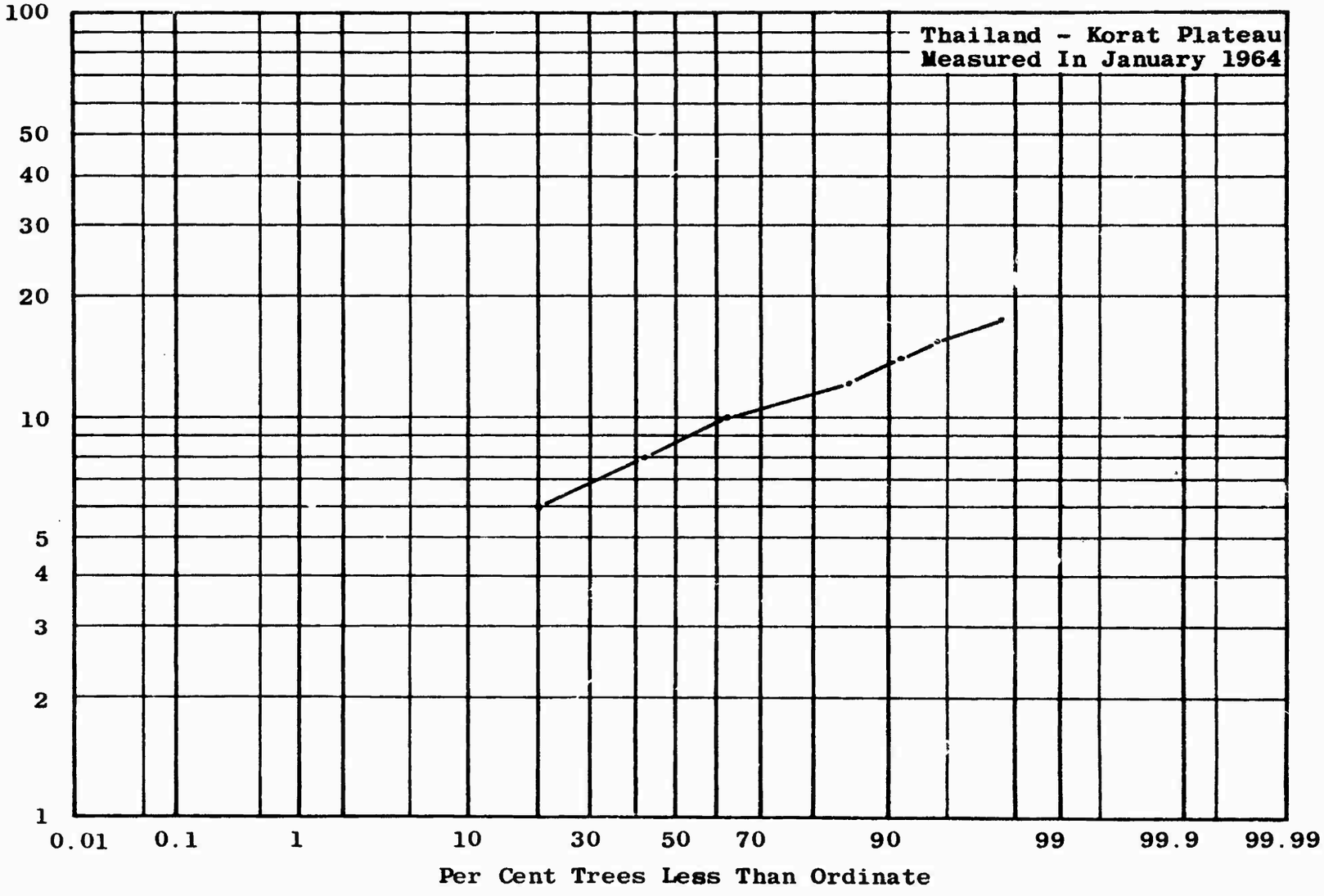

Figure 4.146 Distribution Of Tree Heights In Plot #1

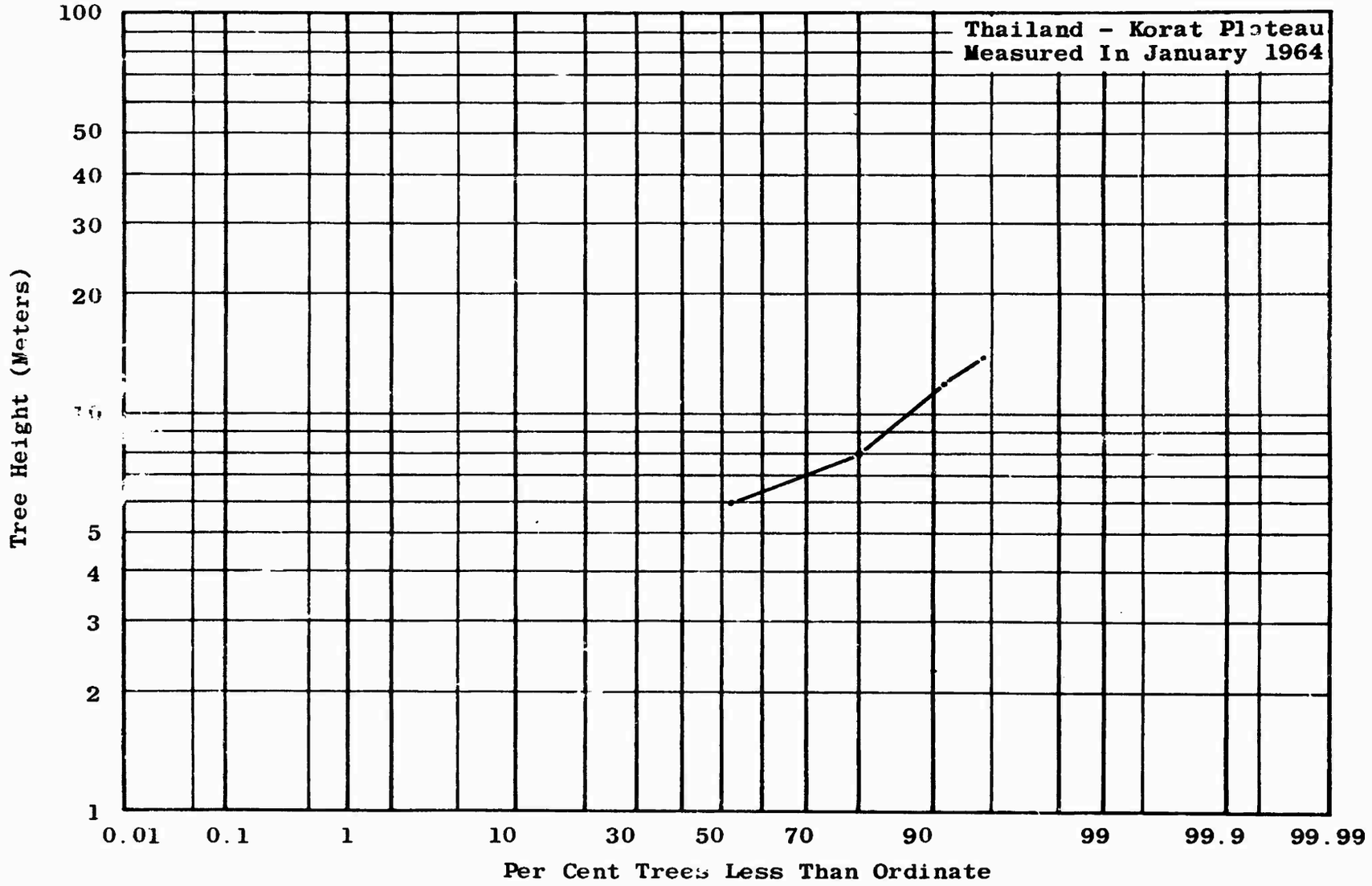

Figure 4.147 Distribution Of Tree Heights In Plot #2

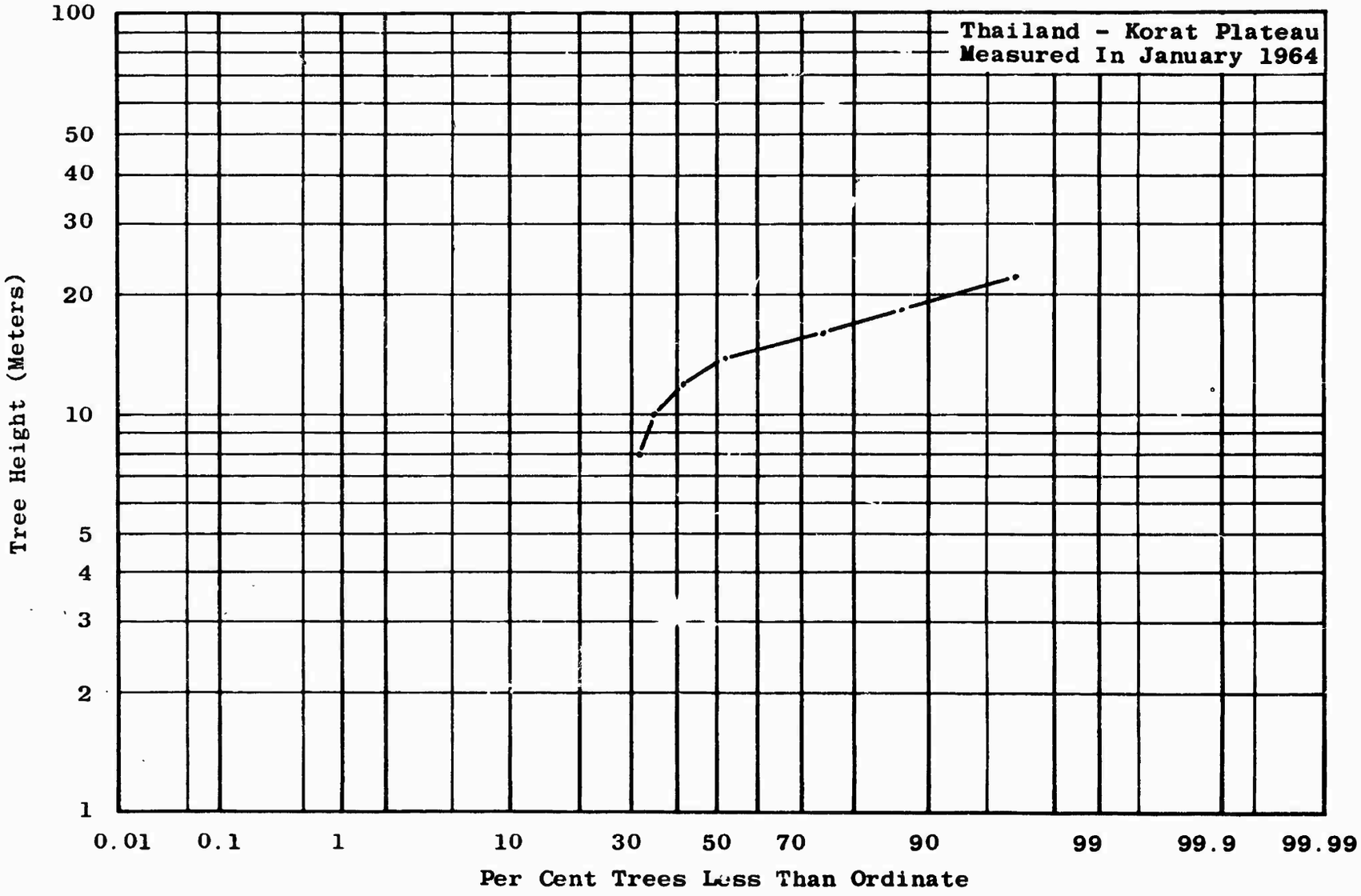

Figure 4.143 Distribution Of Tree Heights In Plot #3

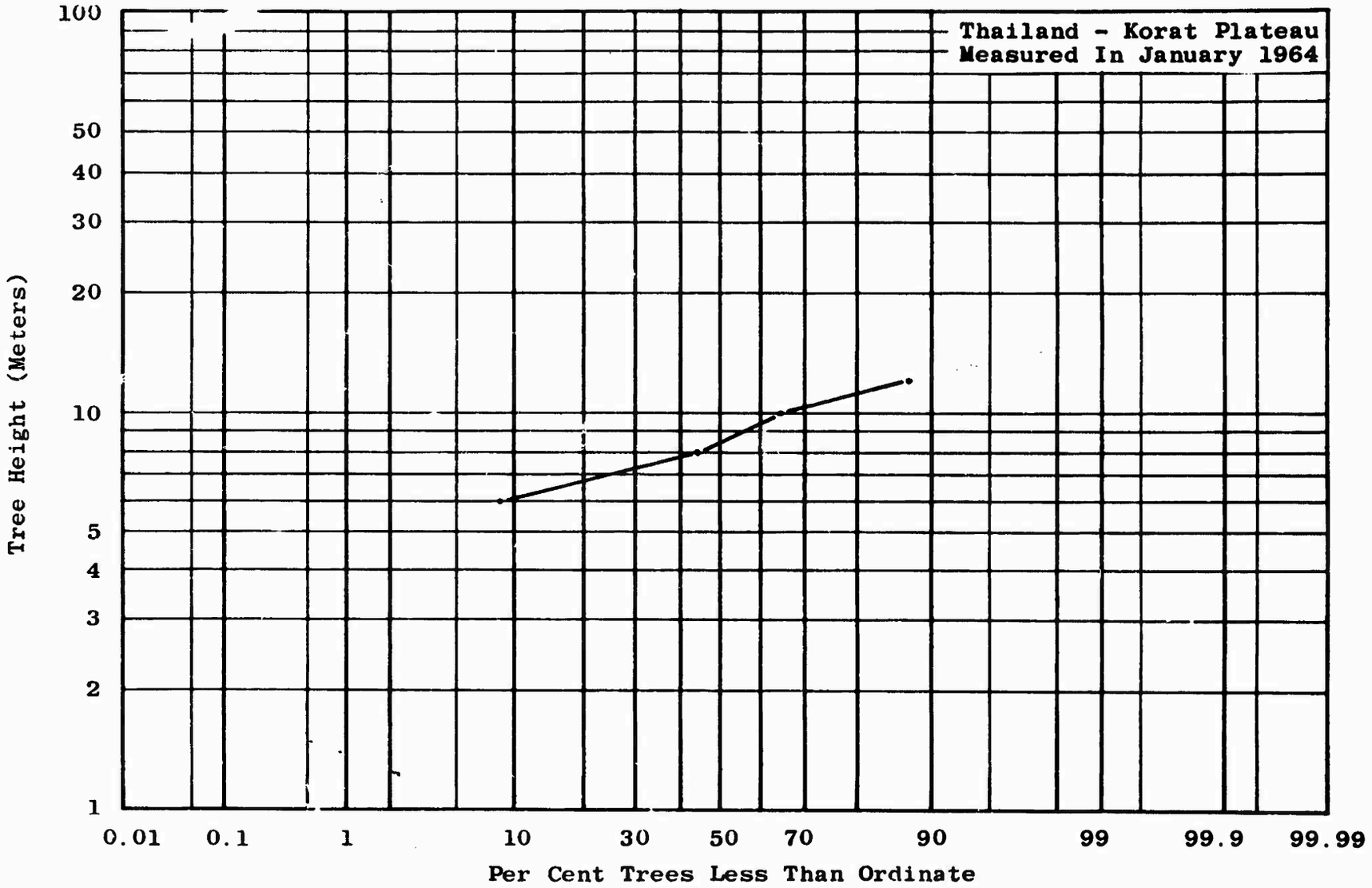

Figure 4.149 Distribution Of Tree Heights In Plot #5

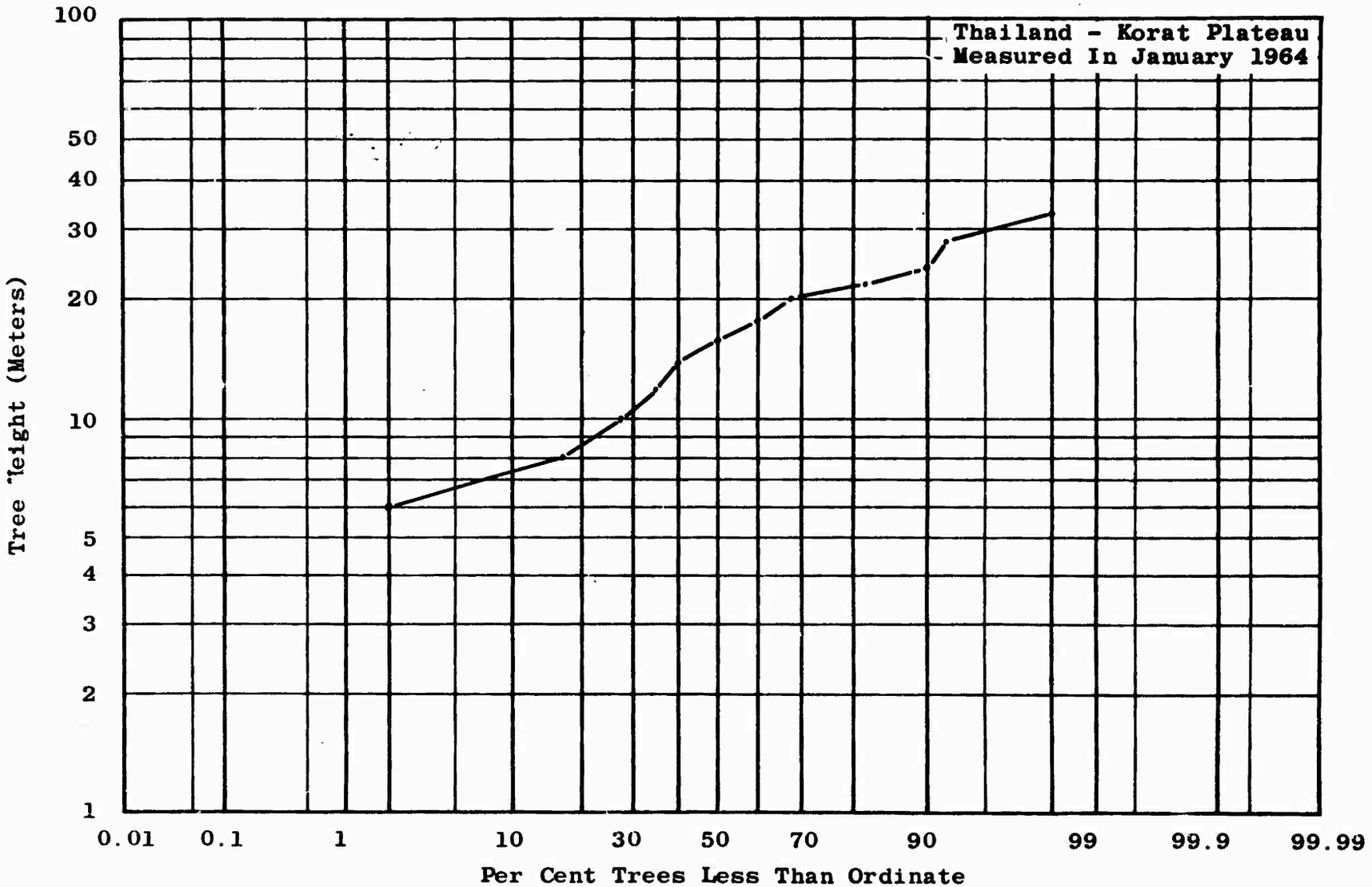

Figure 4.150 Distribution Of Tree Heights In Plot #5.5

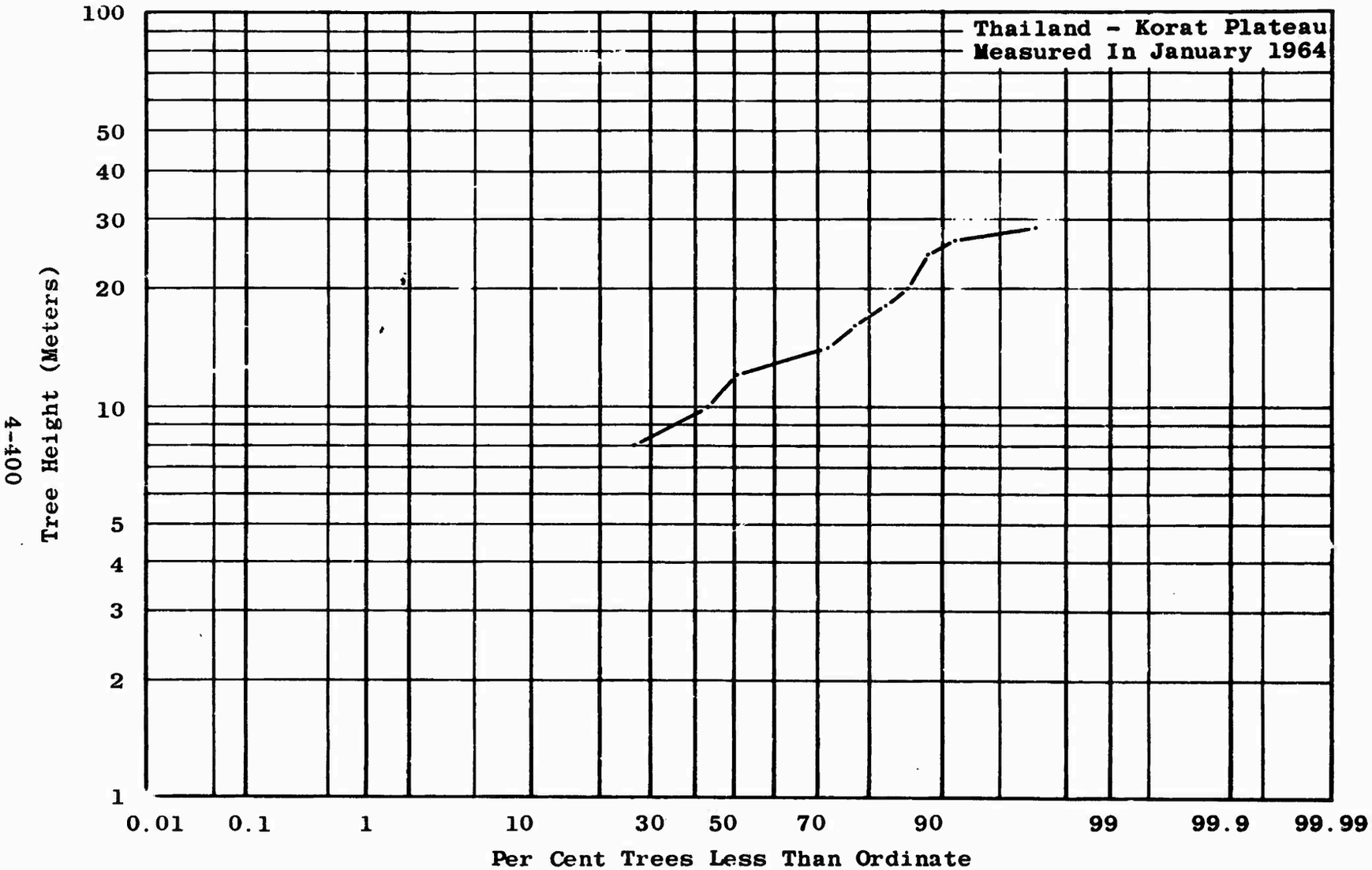

Figure 4.151 Distribution Of Tree Heights In Plot #6

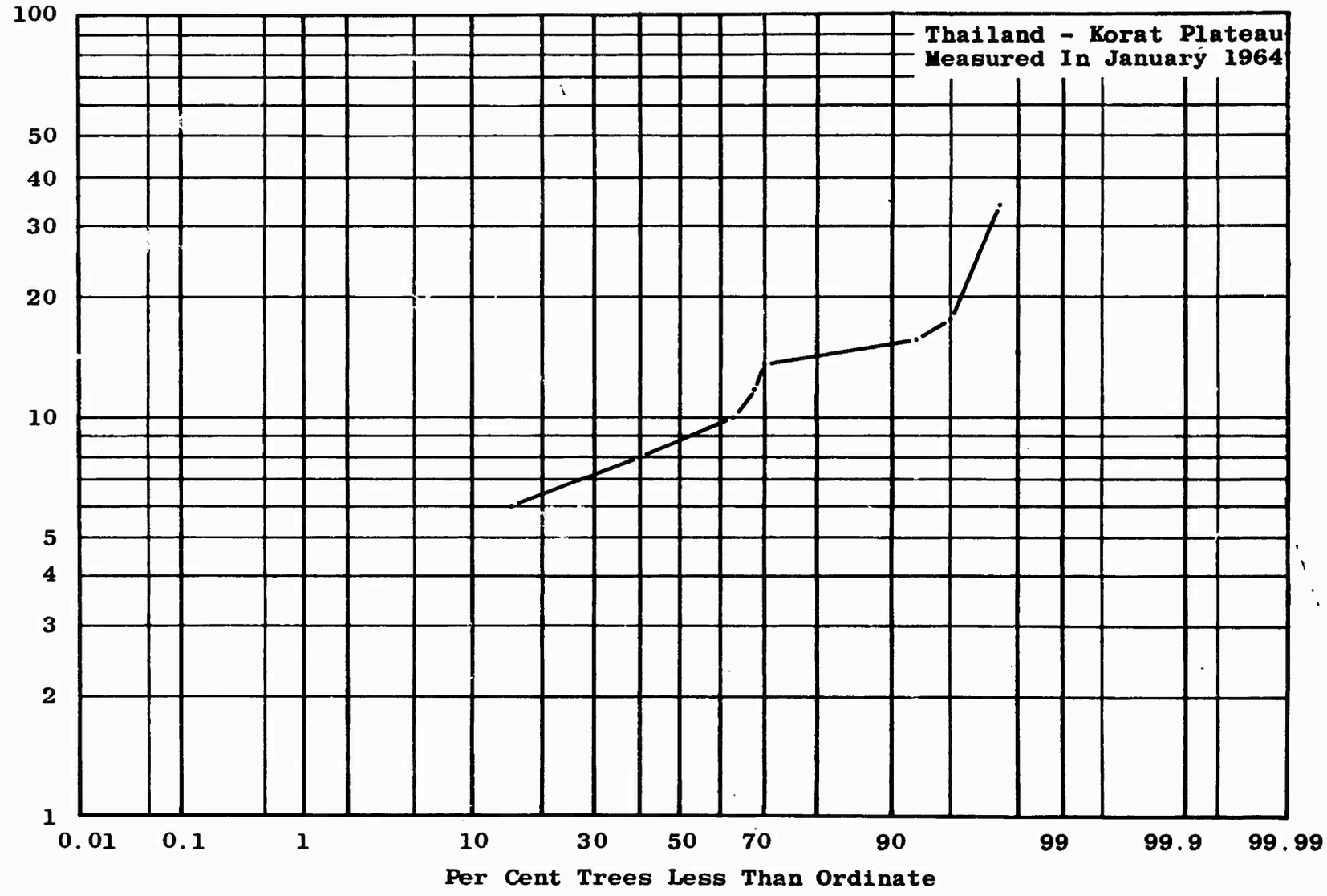

Figure 4.152 Distribution Of Tree Heights In Plot #7

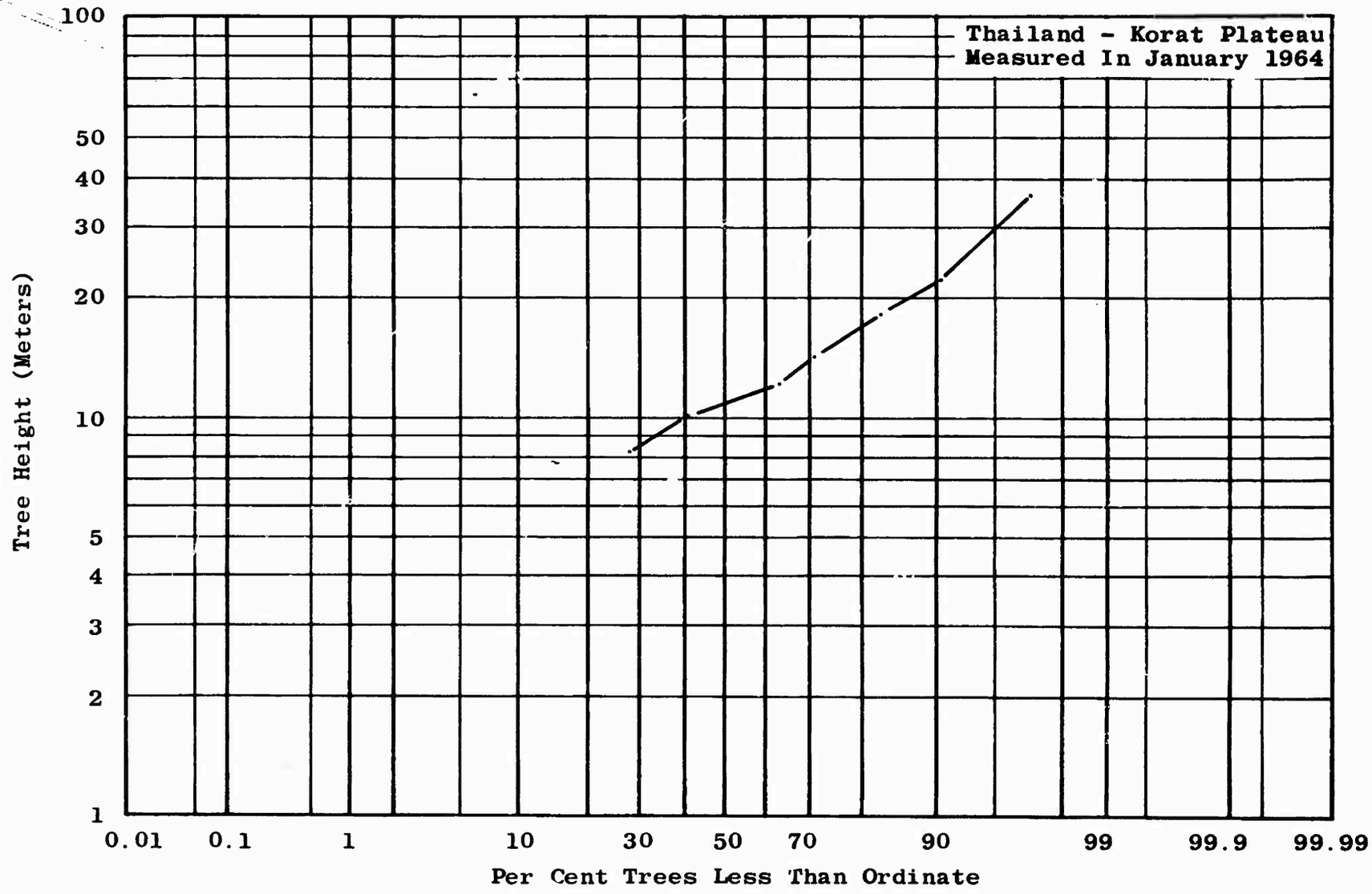

Figure 4.153 Distribution Of Tree Heights In Plot #8

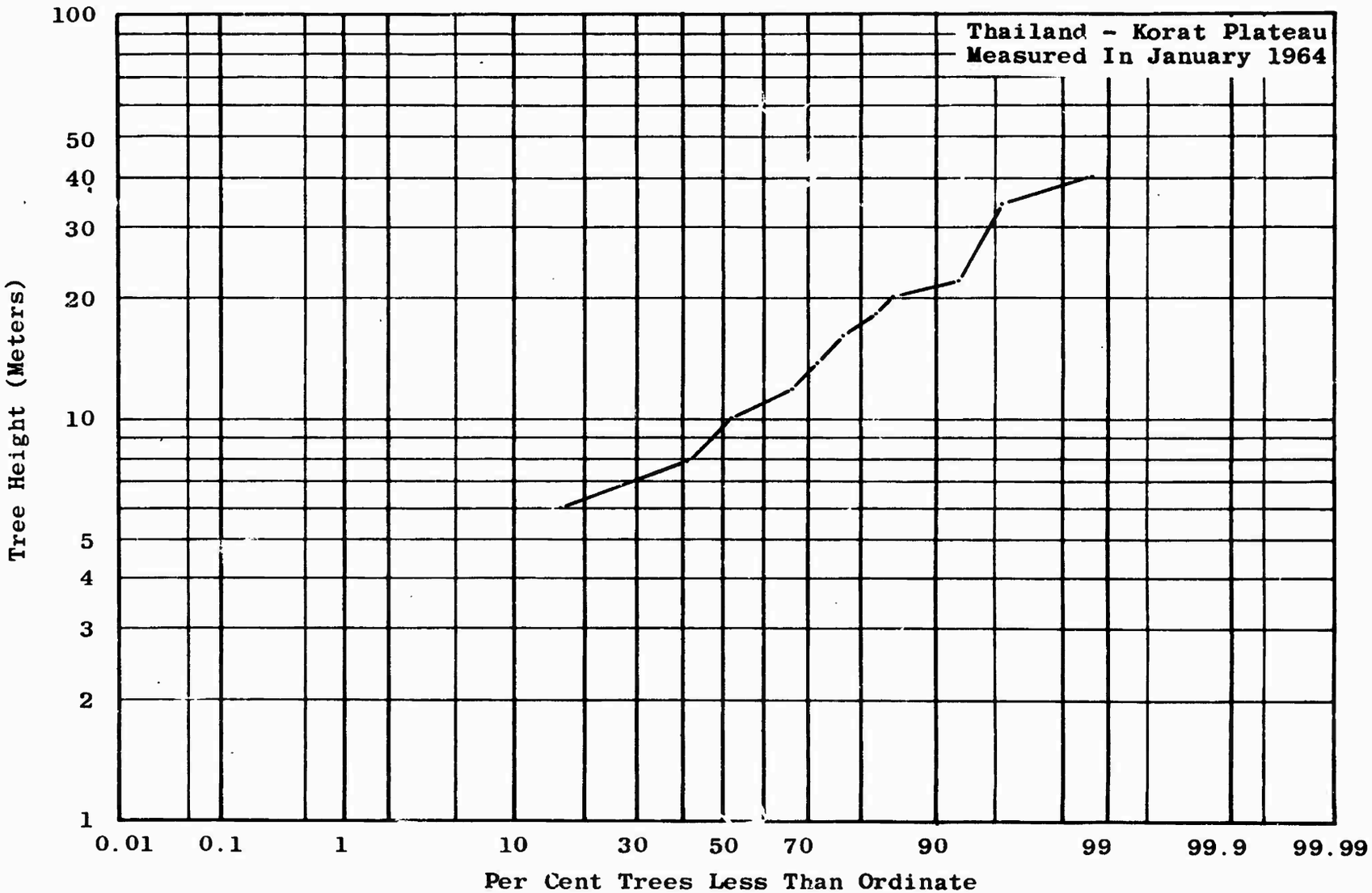

Figure 4.154 Distribution Of Tree Heights In Plot #9

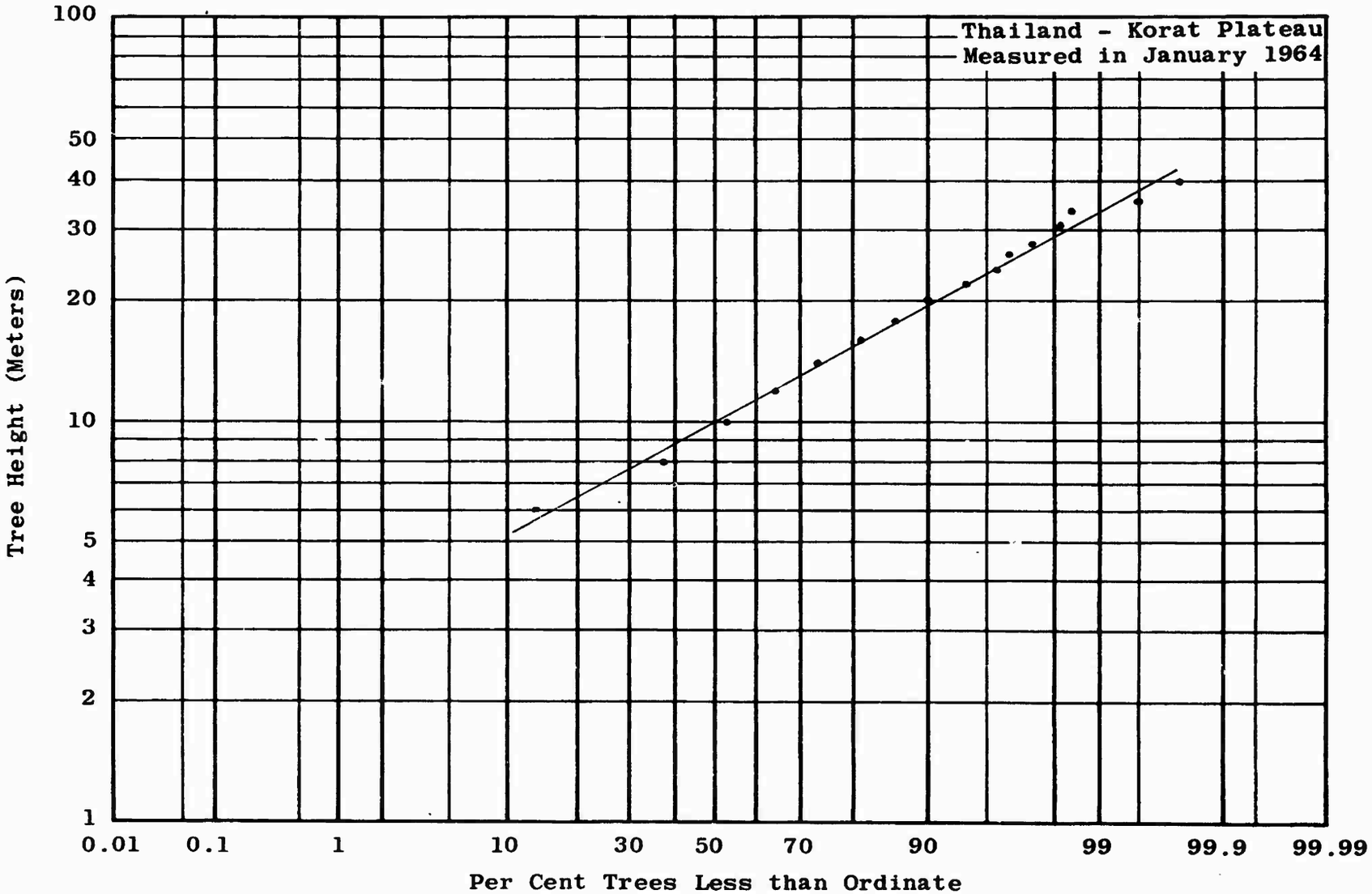

Figure 4.155 Composite Distribution of Tree Heights from All Plots

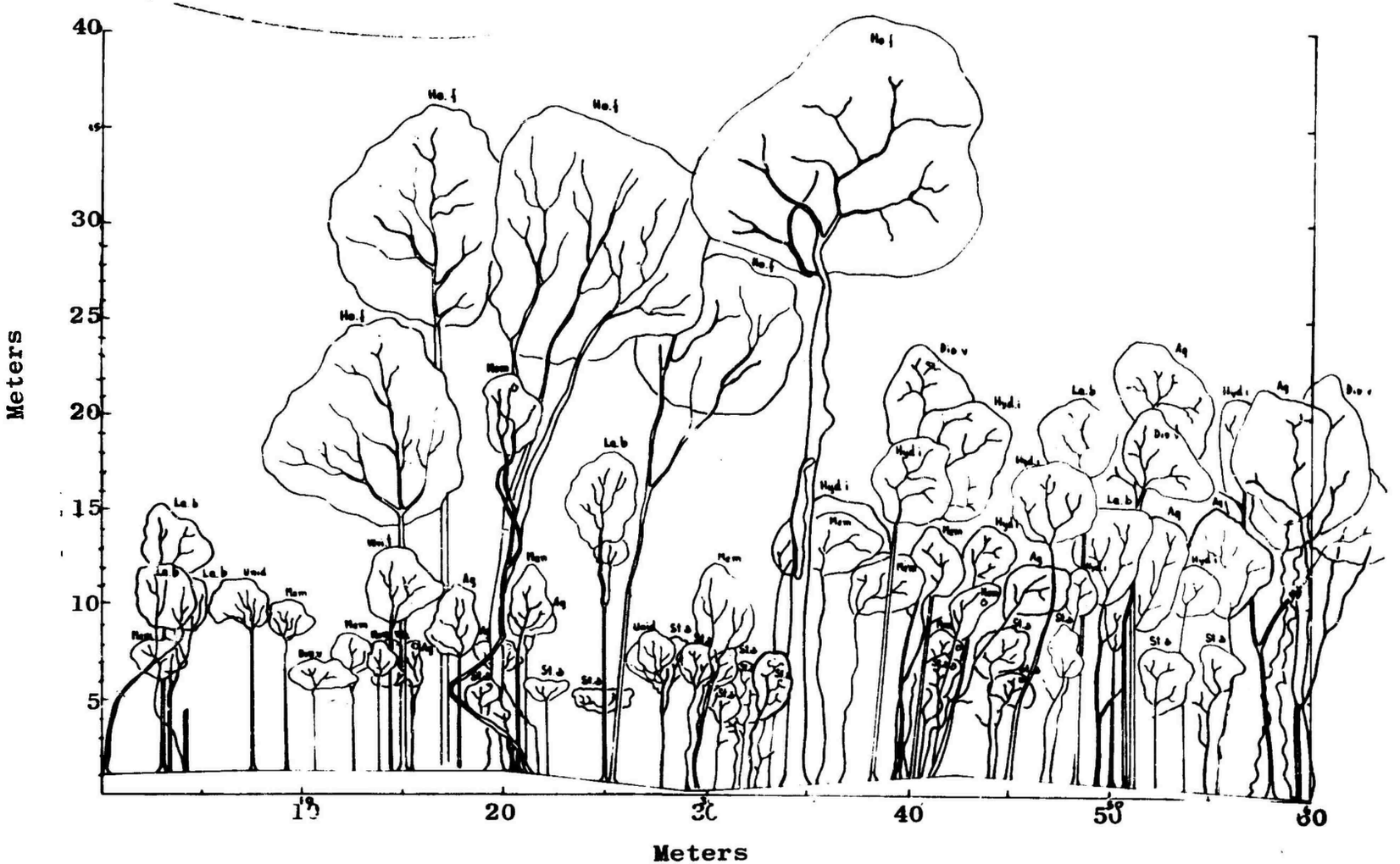

Figure 4.156 Floristic Profile for Plot #9

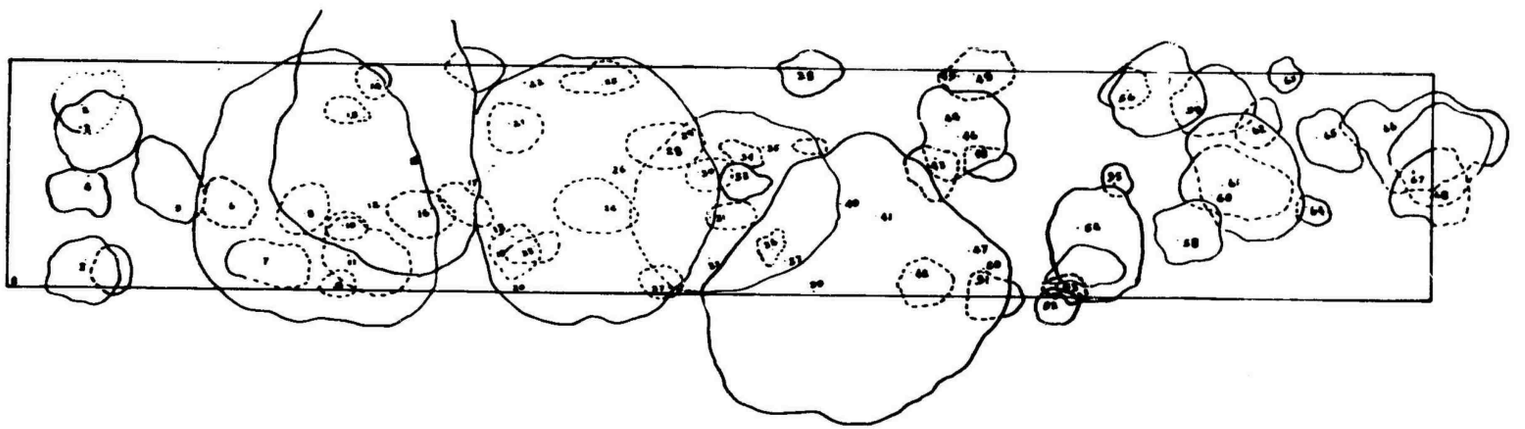

Figure 4.157 Floristic Profile, Plan View, Plot #9

4.4.3 Polarization

The effect of polarization on propagation loss is summarized in the comparisons in Figures 4.158 through 4.162. Figure 4.158 compares basic transmission loss for horizontal and vertical polarizations at 25.5 mc. Three combinations of antenna heights are given. The bottom curve corresponds to the relatively low antenna heights of 13 feet for transmitting and 20 feet for receiving. At these heights both antennas are well immersed in the foliage and, as Figure 4.158 shows, there is significantly greater loss for the vertical polarization. The middle curve of Figure 4.158 corresponds to transmitting and receiving antenna heights of 40 feet. At this height, the two antennas are on a level with the average tree height. The loss is still greater for vertical polarization, but the margin is much smaller. The top curve corresponds to transmitting and receiving antenna heights of 80 feet. In this case, the two antennas are well above the average tree height although there are a relatively small number of trees that tower above the average tree ceiling and attain a height of 80 feet or more. As the top curve shows, the advantage of horizontal polarization begins to disappear at the high antenna elevations. However, some horizontal polarization advantage remains at the highest antenna elevations at 25.5 mc.

Figure 4.159 shows a similar comparison at 50 mc. For the low antenna heights, the loss is greater for vertical polarization, as was the case at 25.5 mc. At 50 mc, however, the margin of advantage begins to decrease. For the higher antenna elevations, the advantage of horizontal polarization begins to disappear. Figures 4.160 through 4.162 show similar comparisons for 100, 250 and 400 mc, respectively. At 400 mc the advantage of horizontal polarization has disappeared, even at the lowest antenna heights. On the average, the results at 100 mc and above appear to be consistent with the trends seen at 25.5 and 50 mc.

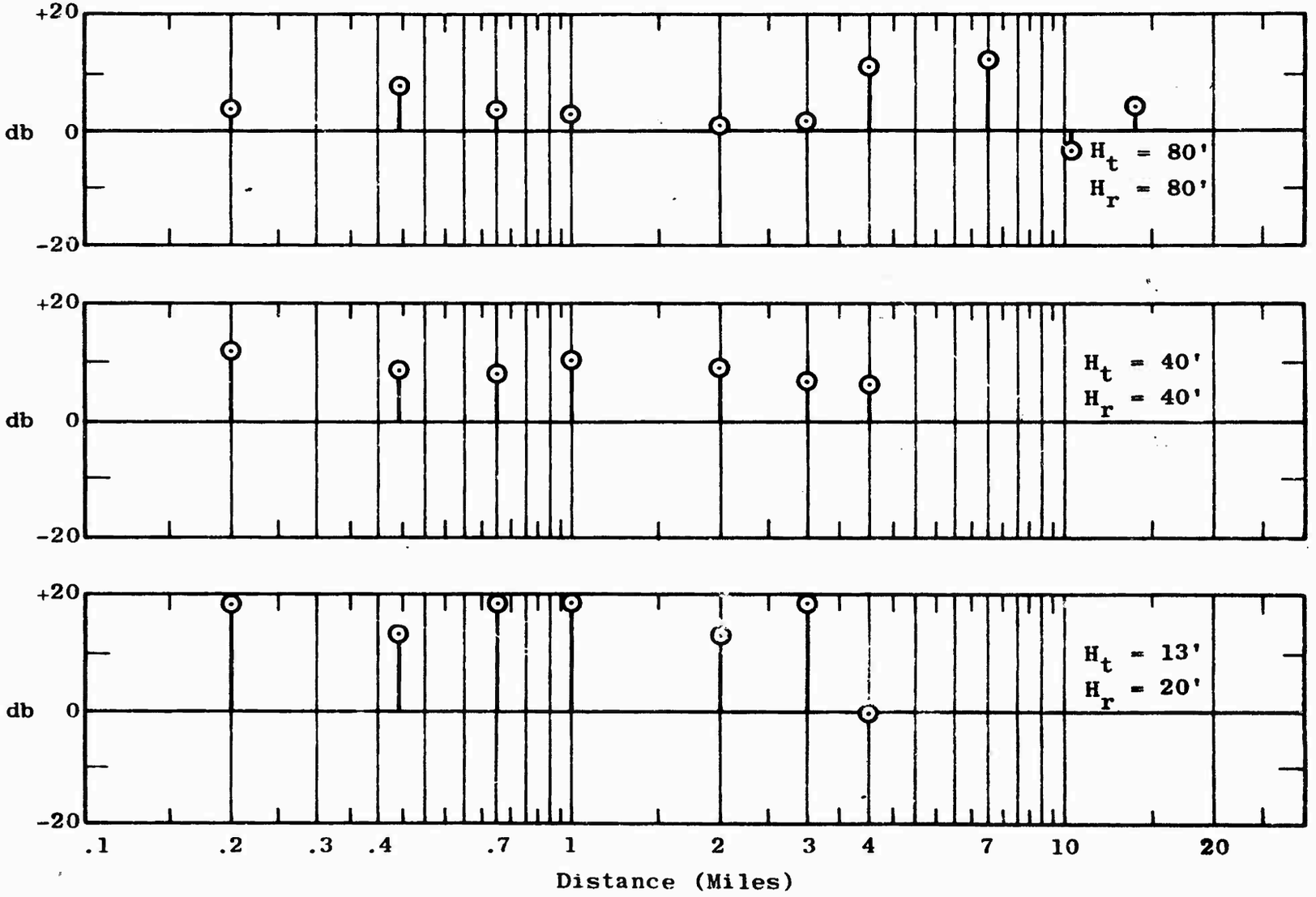

Figure 4.158 L_b for Vertical Polarization Minus L_b for Horizontal Polarization at 25.5 mc

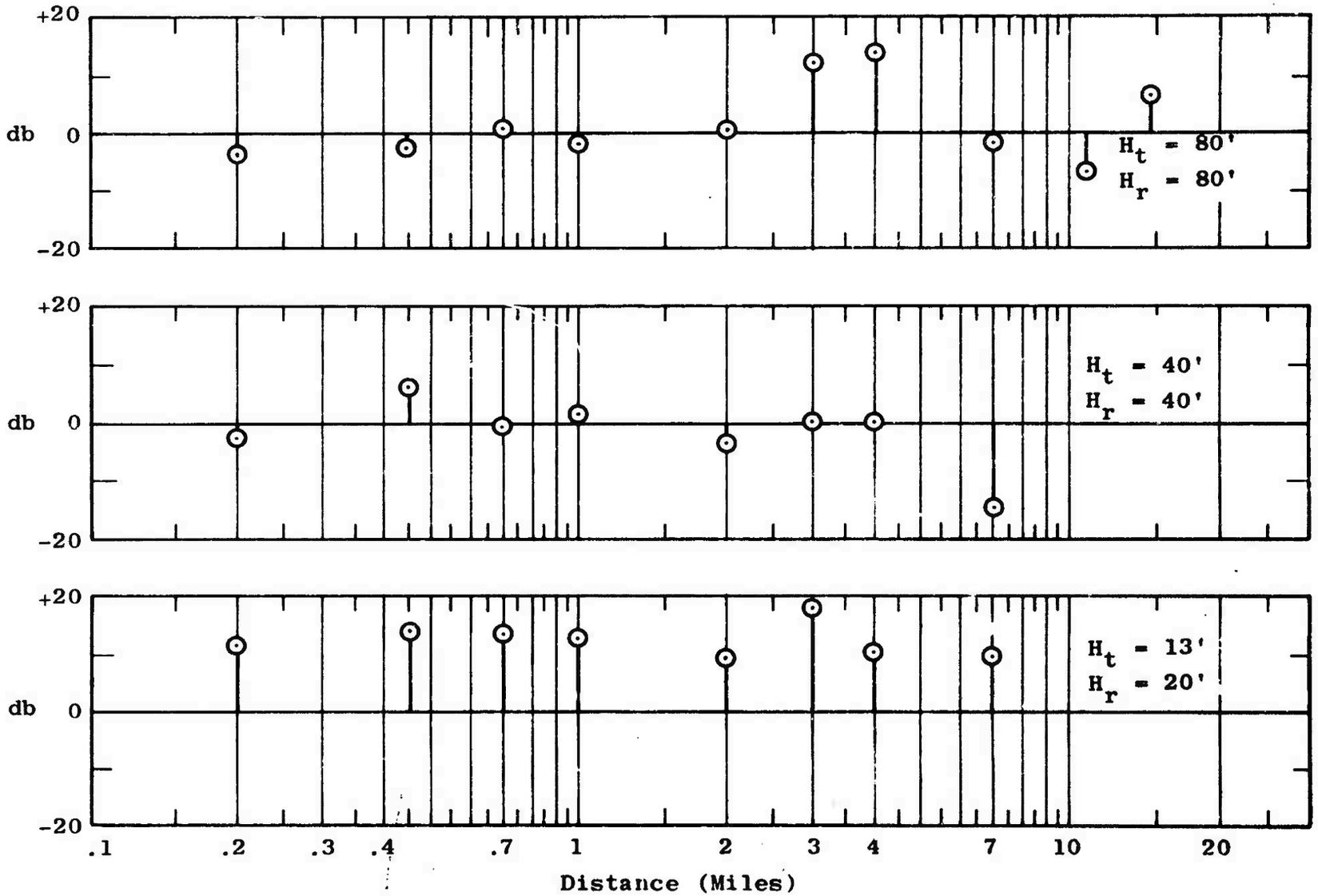

Figure 4.159 L_b for Vertical Polarization Minus L_b for Horizontal Polarization at 50 mc

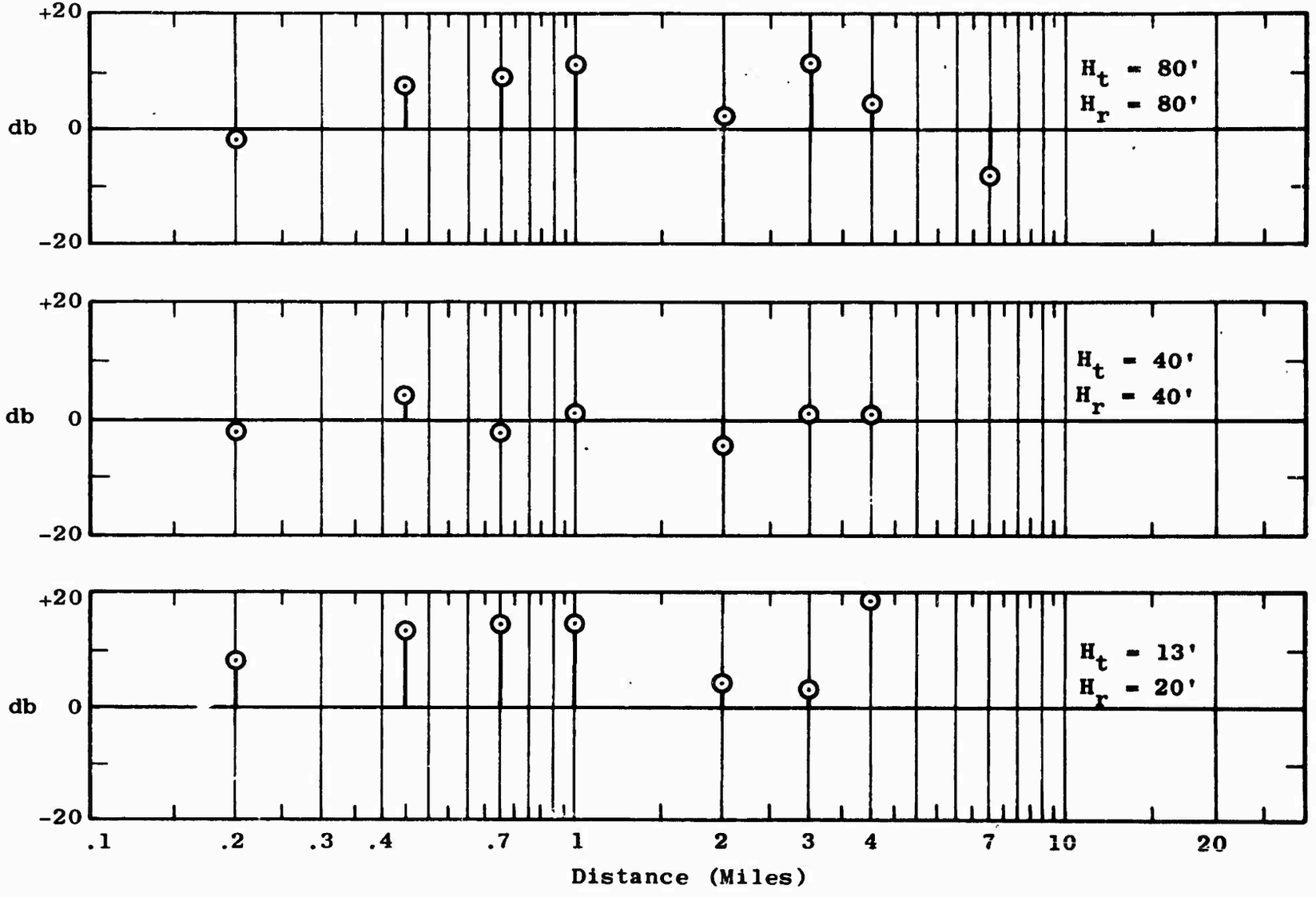

Figure 4.160 L_b for Vertical Polarization Minus L_b for Horizontal Polarization at 100 mc

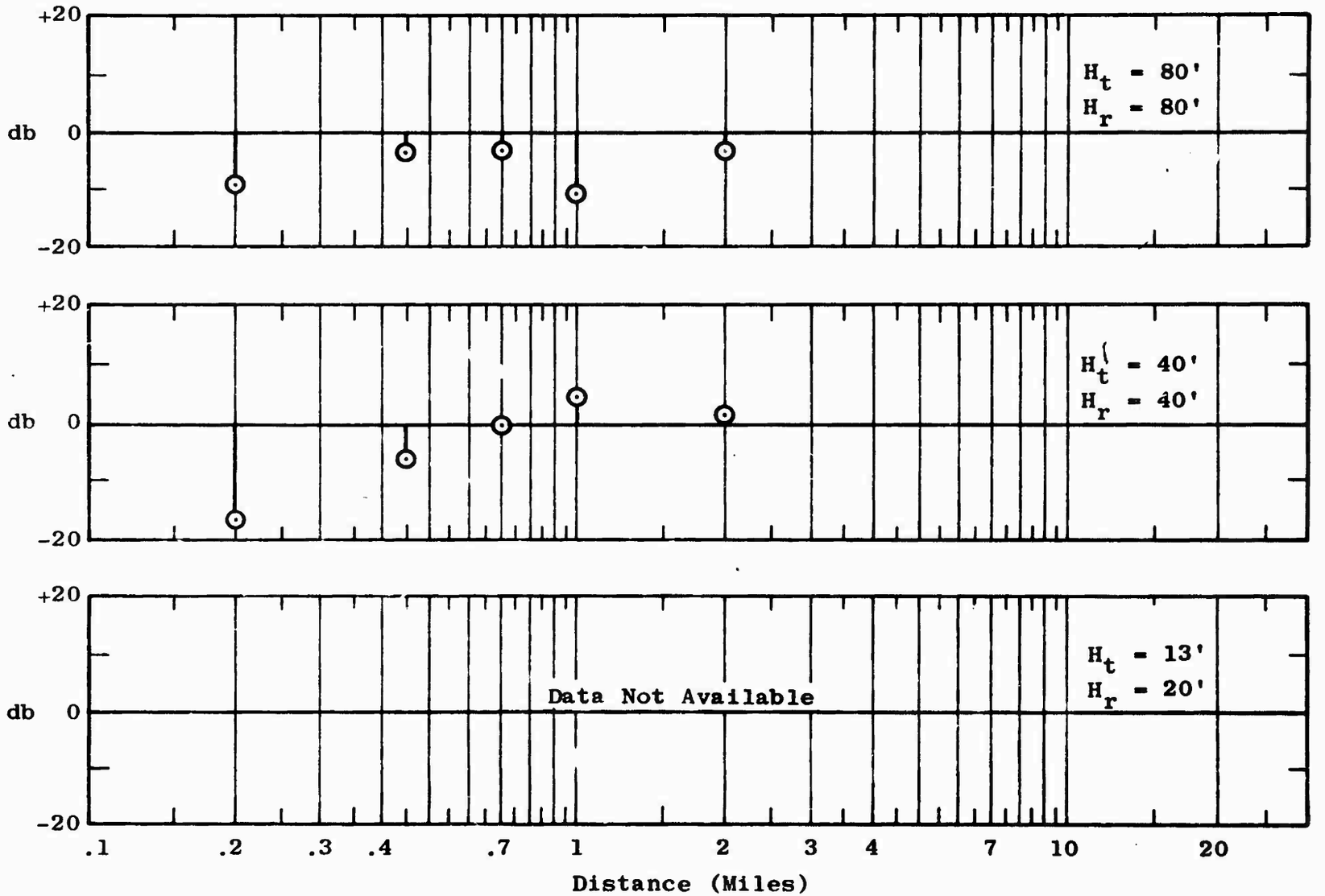

Figure 4.161 L_b for Vertical Polarization Minus L_b for Horizontal Polarization at 250 mc

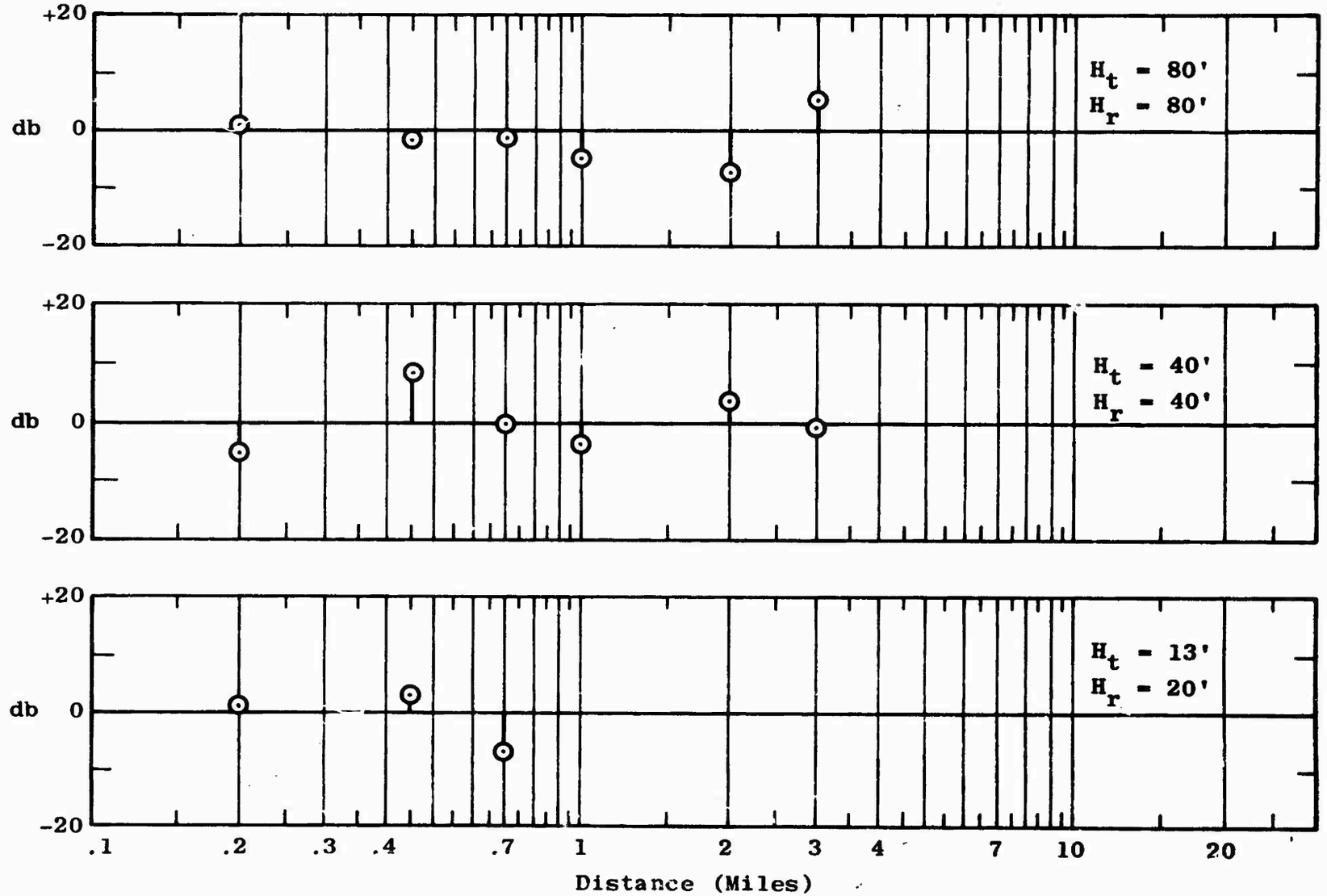

Figure 4.162 L_b for Vertical Polarization Minus L_b for Horizontal Polarization at 400 mc

4.5 Radio Noise Measurements

The experimental program in Thailand includes measurements of radio noise in the vegetated test area, using the same equipment used for the field strength measurements. These measurements are made at all test frequencies below 50 mc and are intended to serve three purposes. First, the measurements are sometimes needed to correct the field strength readings at certain test frequencies when the field strength level begins to approach the noise level. Second, the measurements are used to examine the possibility that the presence of the vegetation might affect the radio noise level as a function of receiving antenna height in the vegetation. Third, the collection of noise data will serve the ultimate purpose of characterizing the noise environment of the Thailand area in relation to other areas where similar measurements have been made, or may be made in the future.

Before discussing some of the results of the noise measurements in Thailand, it will perhaps be helpful to review some of the general principles involved with respect to atmospheric noise. When communications equipment is operated at frequencies of less than about 50 mc, atmospheric noise determines the minimum allowable signal level for a given grade of service. For higher frequencies, thermal noise associated with the receiving equipment becomes the dictating factor.

The interference potential of atmospheric noise is a function of not only its average level, but also of its detailed characteristics. Due to the complex nature of the atmospheric noise wave form, the detailed characteristics are best described by a statistical process, such as the amplitude distribution function. This is simply a plot of instantaneous noise level vs the probability (based on per cent of

time) that the level is exceeded.

Early investigators concluded that atmospheric noise behaved exactly as thermal noise, whose amplitude distribution functions obey the Rayleigh law. As a consequence, the interfering potential was thought to be fully assessed by specifying the RMS, average, and peak values of the noise pulses. However, recent work has established that the typical atmospheric noise wave form does not completely follow a Rayleigh distribution but instead deviates and eventually becomes log-normal at the low probability end of the distribution. The Rayleigh portion of the distribution is represented by the straight-line segment for probabilities between about 70 per cent and 100 per cent. The curved center portion of the plot is neither Rayleigh nor log-normal, but represents a smooth transition between the two. The Rayleigh distribution results from the fact that the low-amplitude components of the wave form are composed of random overlapping events, each containing a small portion of the total energy. As the levels increase in amplitude, less and less random overlapping occurs until the extreme low end of the amplitude distribution function is composed of widely spaced, discrete components.

The National Bureau of Standards, through the use of a measurement system capable of responding to and recording the instantaneous noise envelope, has accumulated numerous amplitude distributions at various locations throughout the world. The shape of the distribution did not change significantly from one location to another, although the RMS level varies over a wide range. This uniformity of shape of the distribution as a function of time and location has led to the feasibility of accurately predicting the distribution when a few of the measured statistical parameters in the time domain are known.

The amplitude distribution function, RMS, peak, and average values all vary with the bandwidth of the measuring device. Therefore, in order to use noise data in a bandwidth different from that of the device used to gather the data, a transformation of the measured values must be made. Theoretical work relating the amplitude distribution function to bandwidth has been carried out at the National Bureau of Standards and preliminary results show good agreement with measured data for the Rayleigh portion of t. ? curve, but break down for the remainder of the curve. Further work is being conducted in an attempt to accurately transform the entire distribution.

However, the empirical relationships between the peak, RMS, and average values of atmospheric noise and bandwidth have been experimentally determined and used for many years. When the peak, average, and RMS voltages are plotted vs bandwidth of the measuring instrument on a log-log graph, the plots are approximately straight lines at different slopes. The relation of the line slopes to one another indicates that the peak, average, and RMS voltage levels all vary approximately as the square root of the bandwidth. Due to the slight variations in the structure of atmospheric noise as a function of time and locations, the slopes of the lines will vary over a small range, depending upon the particular sample. Thus, to convert noise level data from one bandwidth to another, it is only necessary to multiply the level by the square root of the ratio of bandwidths and this procedure will be used in this work.

Generally speaking, the variations in atmospheric noise levels within a given geographical region are much greater and more dynamic in the time and frequency domains than in the spatial domain. The methods of instrumentation to comprehensively study noise behavior, therefore, must be

capable of responding to and recording wide and rapidly varying levels as a function of time. Also, the time span and amount of data required for analysis are both quite large. In this regard, the Thailand noise measurements cannot be considered as a comprehensive study of noise behavior. Rather, these measurements were designed to serve a limited set of specific objectives, as described previously in this section. However, the noise measurements thus far obtained do afford some insight into the behavior of radio noise in the test area, and the results of these measurements are discussed in the next section.

4.5.1 Results of Noise Measurements

Noise levels were measured by the Empire Devices NF-105 field strength meter with the function selector switch in the "peak" position. A brief description of the noise detection circuitry of this instrument is given in the next section of this report. However, from a study of this circuitry, it would appear that the true peaks of the noise wave form are not really measured by this instrument, and that there is some uncertainty in the relation between measurements made in the "peak" and "carrier" positions. This uncertainty is related to the statistics of the noise wave form and cannot be resolved with measurements from this instrument alone. However, past noise readings on this instrument indicate that the "peak" position readings averaged 10 db higher than those for the "carrier" position.

To measure the change in noise level with receiving antenna height, the initial measurement procedure was devised to continuously measure and record the noise field as the antenna was varied from about 10 to 80 feet in height. In addition, the noise level was sampled and recorded as a function of time (1-minute duration) at a fixed receiving antenna

height. These measurements were carried out for all test frequencies at which field strength measurements were also made.

When sufficient data became available from the above measurements, a preliminary analysis was carried out in an attempt to determine the change in noise level caused by the vegetation as a function of antenna height. Results of the analysis showed the variation with height to be a random fluctuation, unlike the relatively smooth relationship that is exhibited by CW signal measurements. Figure 4.163 illustrates these fluctuations for a few sample cases.

Typical fluctuation of the noise over a 1-minute period was approximately 4 or 5 db. Observation of Figure 4.163 shows about the same degree of fluctuation. Thus, it is reasonable to assume that the variation of the noise level with antenna height as shown in Figure 4.163 is attributable to "short-term" variability of the noise rather than to the effects of the vegetation. The character of this data suggests that the effects of the vegetation on noise levels will be difficult to separate from short-term variability of the data unless the vegetation effects are quite significant as a function of antenna height.

In an attempt to obtain data in a form which would allow the time variations and variations due to vegetation to be separated, the measurement procedure described above was modified. Rather than continuously measuring noise as a function of antenna height only, three discrete antenna elevations were selected and the noise was sampled as a function of time at each of these pre-selected levels. The heights selected were roughly 10, 42 and 80 feet. The median value of noise at each antenna level was recorded as well as the total variation with time.

Samples were accumulated over a three-month period and the over-all median value at each antenna height was

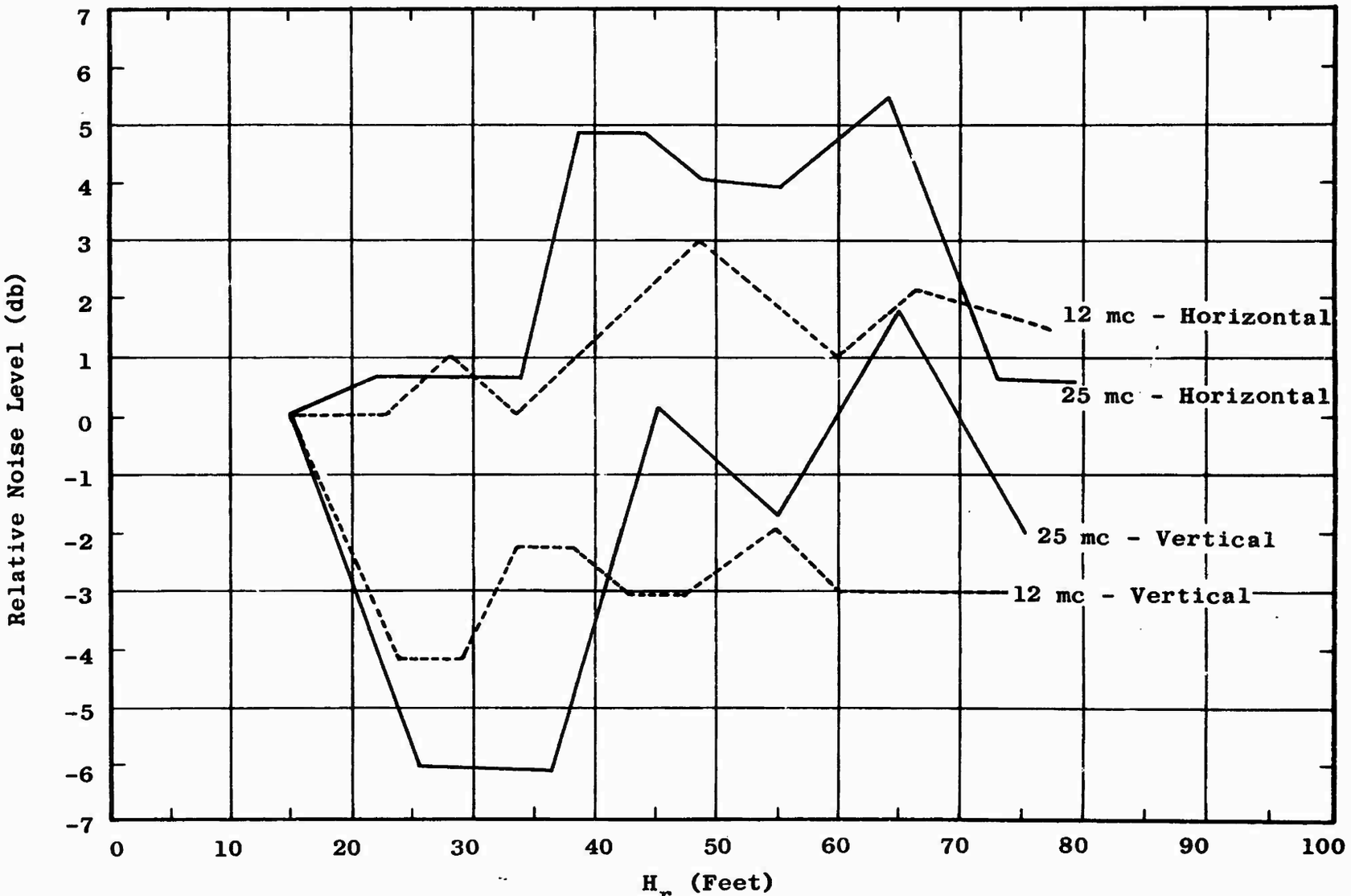

Figure 4.163 Variation of Recorded Noise Level With Antenna Height

determined. This data is shown plotted vs frequency in Figure 4.164 for horizontal polarization. Vertical polarization is plotted in Figure 4.165. The threshold level of the measurement system is shown in each plot. This threshold level is simply the level below which atmospheric noise cannot be detected due to the presence of "set" noise and to the losses in the measuring antenna system. Shown plotted with the measured data are two curves representing noise grades of 40 and 80 which are typical of the noise level variations in Southeast Asia.[6]

It should be noted that the CCIR curves represent RMS noise levels while the measured data is more indicative of peak values. If a 10-db difference is attributed to the ratio between peak and RMS, then the measured data would follow roughly the contour presented by a noise grade of 80.

The noise data below 12 mc is proving to be more difficult to analyze than was anticipated. There are some indications in the data of possible contamination by noise locally induced in the measuring system from other auxiliary equipment, and this matter requires further investigation before the data can be reported.

4.5.2 Noise Measuring Instrumentation

The radio noise measurements are made by means of an NF-105 Empire Devices field strength meter. The second-detector characteristics of this instrument are determined by the position of a "function switch," having a position marked "Peak" and a position marked "Carrier." This switch alters the coupling network between the meter detector and pulse stretcher, as shown in the following diagram.

---

6. International Radio Consultive Committee, Documents of the VIIIth Plenary Assembly, Vol. 1, Warsaw, 1956, p. 352.

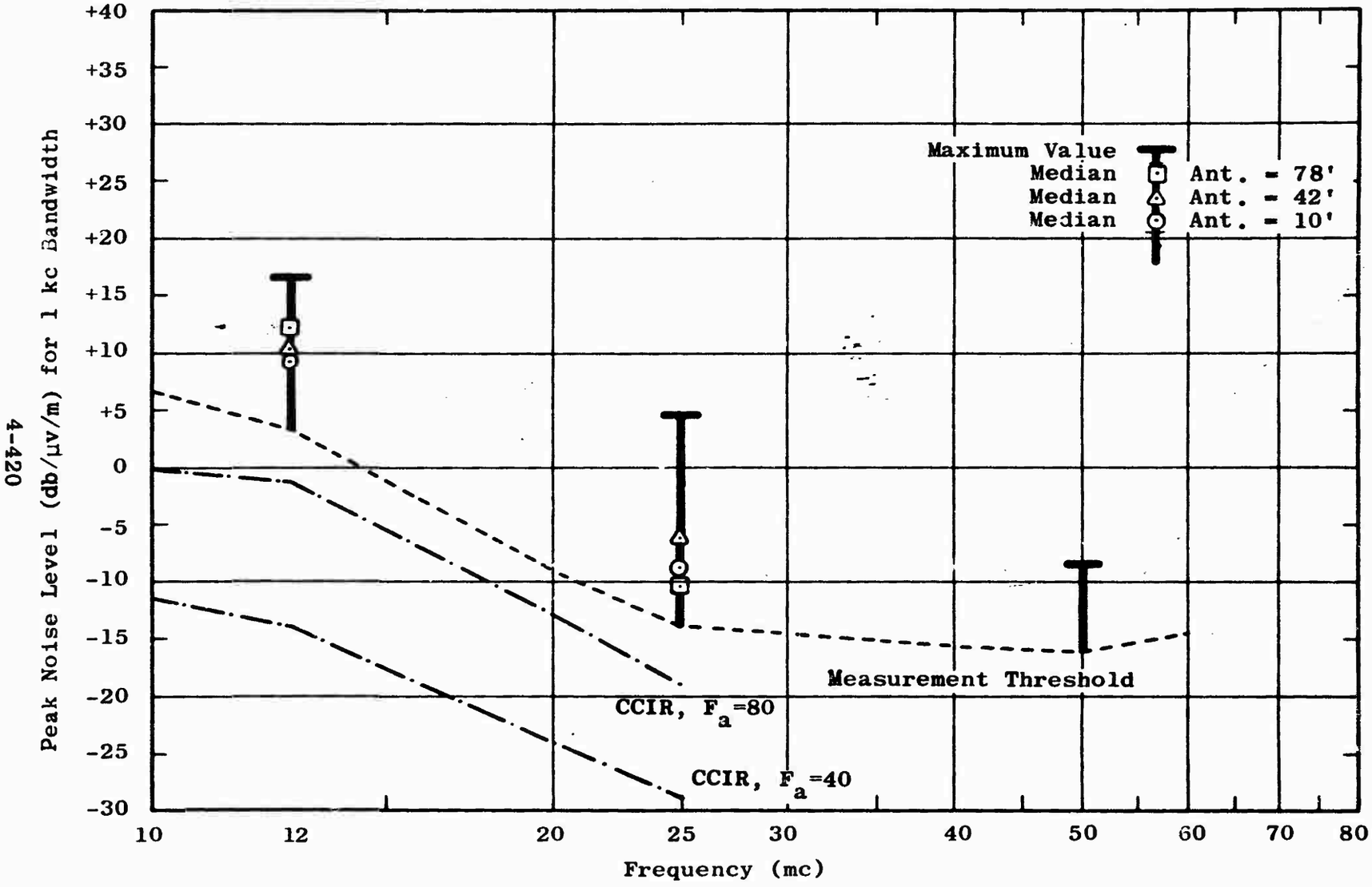

Figure 4.164 Combined Median Noise Levels for Nov., Dec., and Jan. For Horizontal Polarization

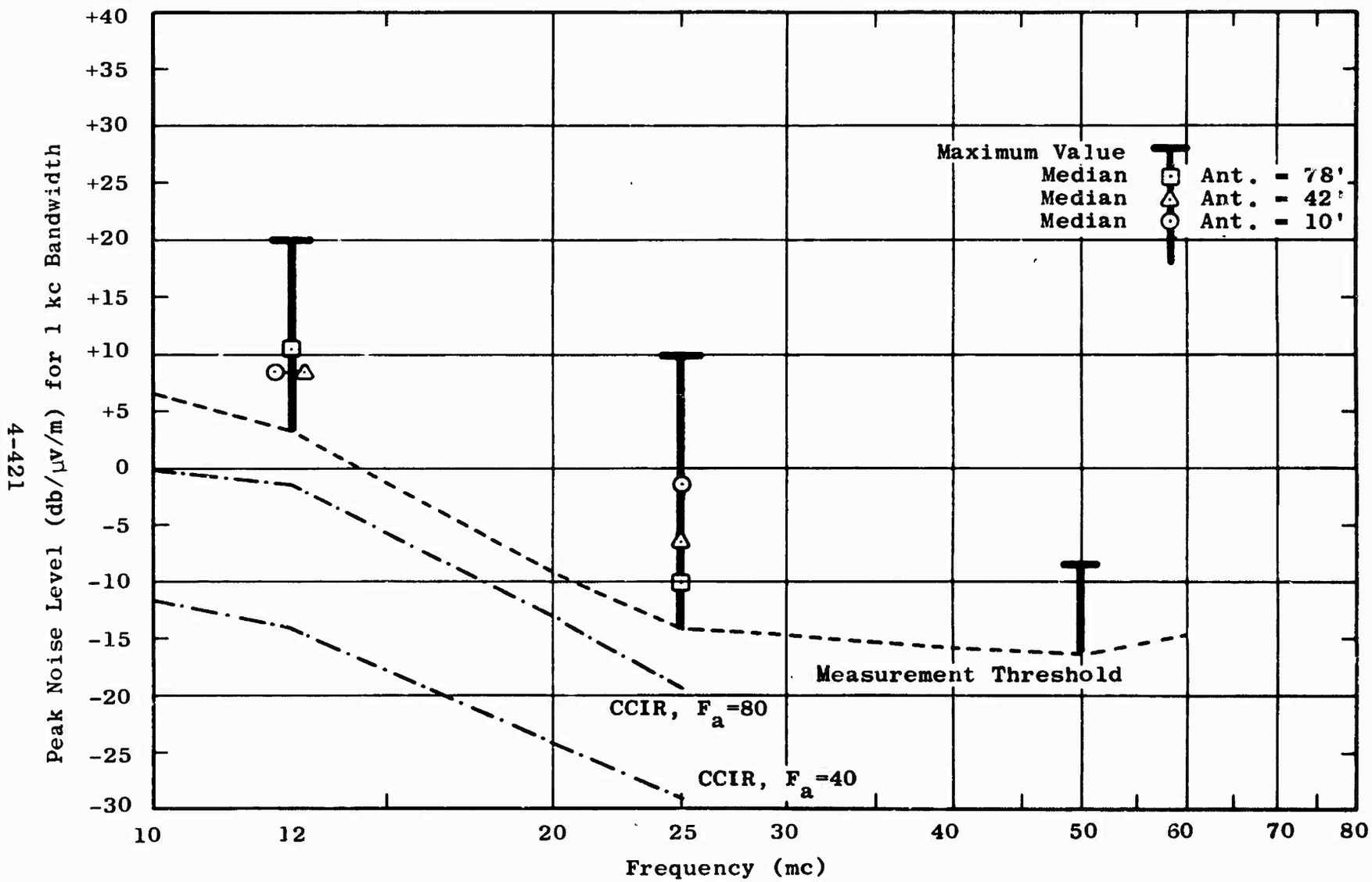

Figure 4.164 Combined Median Noise Levels for Nov., Dec., and Jan. for Vertical Polarization

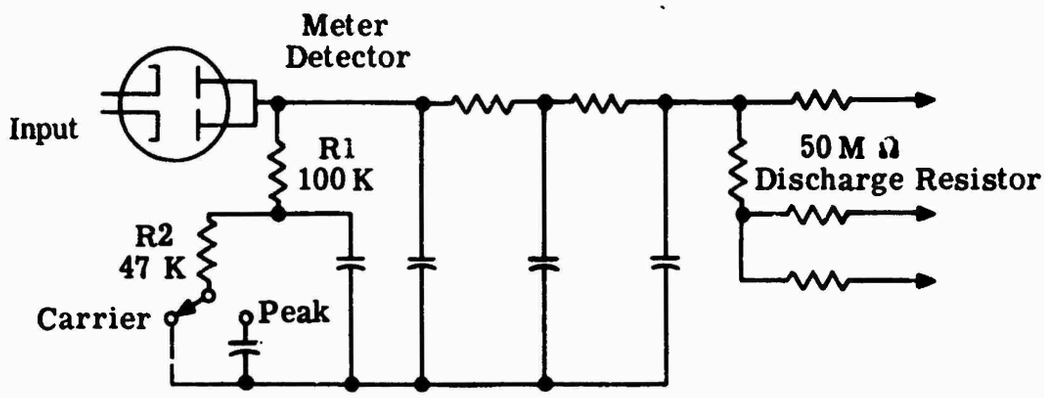

The meter detector circuit can be operated as a peak or average detector. The circuit operates as an average detector when the switch shown in the schematic is in the "carrier" position. For peak detection, the "peak" switch position is used.

The input voltage for the detector circuit is provided by a cathode follower whose characteristic output impedance is low. Since the input impedance of the two sections of the detector is also low, the resulting charge time is extremely short.

In the "peak" position, the discharge time is made long by using a discharge resistance of 50 megohms. This discharge time is further increased by applying the 50-megohm resistor in the grid circuit of one-half a double triode with negative feedback so that it operates as a resistance "magnifier" or pulse stretcher.

In the carrier position, the 50-megohm discharge resistor is effectively shunted by R1 and R2 to a value of approximately 150 K ohms. Thus, the discharge time is sufficiently shortened to permit

indication of average rather than peak values.

When noise wave forms are being detected, it can be seen that the output will depend upon the statistical distributions of the wave form in time and amplitude. Therefore, under these conditions, the circuits measure neither peak nor average values exactly. However, observation of numerous noise measurements indicates that the difference between the peak readings and the carrier readings is typically of the order of 10 db.

4.6 Use of Propagation Data for Communication Calculations

The purpose of this section is to discuss methods of applying the results of this report to communications calculations for vegetated environments similar to Thailand. The AN/PRC-10 radio set was chosen as an example. A sample calculation of its expected range under these environmental conditions was carried out.

The following inequality must be satisfied before there can be satisfactory communication

$$P_t - C_t + G_t - L_b + G_r - C_r \geq P_r \qquad (7)$$

where

P_t = transmitter power in dbm

C_t = total coupling loss from transmitter to transmitting antenna

G_t = effective transmitting antenna gain

L_b = basic transmission loss

G_r = effective receiving antenna gain

C_r = total coupling loss from receiving antenna to receiver

P_r = power in dbm required at input of receiver to provide desired grade of service

If external noise is limiting,

$$P_r = S/N + F_a + R \tag{8}$$

where

S/N = signal-to-noise ratio required at receiver input

F_a = noise power (dbm) from receiving antenna

R = reliability margin

If receiver sensitivity is limiting,

$$P_r = S/N + P_o + R \tag{9}$$

where

P_o = minimum detectable input signal in dbm.

Inequality 7 can be rearranged to yield

$$(P_t - P_r) - (C_t + C_r) + (G_t + G_r) - L_b \geq 0 \tag{10}$$

as the condition for satisfactory communication.

It is convenient to define the term

$$M = (P_t - P_r) - (C_t + C_r) + (G_t + G_r) - L_b \tag{11}$$

where M will be called the communication margin. If $M \geq 0$, communication is possible with the desired reliability; if $M < 0$, communication is not possible with the desired reliability.

In general, each of the terms in equation 11 will be uncertain to some extent. For example, the exact power output will depend in large measure upon battery age. The factors C_t and C_r may vary from set to set of the same type. The antenna gain factors are subject to variation, depending upon the proximity of the antennas to foliage, and L_b can vary in a random manner from one location to the next, as has been demonstrated in previous sections of this report.

Thus, the communication margin, M, becomes a statistic. The probability that $M \geq 0$ is the probability that communication can take place. The distance which corresponds to a probability of P per cent that $M \geq 0$ is defined as the communication range associated with a confidence level of P per cent. The median communication range is the distance for which there is a 50 per cent probability that $M \geq 0$.

Two questions arise: (1) What statistics should be associated with each of the factors on the right of equation 11? and (2) knowing the statistics which are associated with each of the factors on the right of equation 11, how is the statistical distribution of the communication margin, M, determined?

Considering the second question first, assume that m_i (as i runs from 1 to 7) is the mean value of each of the random variables (P_t, P_r, G_t, G_r, C_t, C_r and L_b) to be summed in equation 11. Further, assume that σ_i (as i again runs from 1 to 7) is the standard deviation of the seven random variables to be summed in equation 11. Then the mean value, m, of the communication margin, M, is

$$m = \sum_{i=1}^{7} m_i \tag{12}$$

and the standard deviation, σ, of the communication margin, M, is

$$\sigma = \sum_{i=1}^{7} \sigma_i^2 \tag{13}$$

The mean value, standard deviation and type of distribution completely define the desired statistic. The mean

value and standard deviation can always be determined from equations 12 and 13. This leaves the question as to what type of statistical distribution results from the summation of the seven factors which go into the communication margin. With a normal distribution for each of the seven factors, the resulting communication margin is normally distributed with the mean and standard deviation presented above.

Usually, but not always, the distributions which must be used may be satisfactorily approximated by normal distributions. Variables with any arbitrary statistical distribution may be combined by convolution. The only requirement for practical application is that the distributions be adequately known, either in analytic or tabular form.

The convolution is performed in the following manner. Assume that X_1, X_2, ... X_7 represent the seven independent random variables which are to be added in equation 11 to obtain the communication margin, M. Their statistical frequency distributions will be written as $f_1(X)$, $f_2(X)$, ... $f_7(X)$, and their cumulative probability distributions expressed as $F_1(X)$, $F_2(X)$, ... $F_7(X)$. Either the frequency distribution or the cumulative distribution uniquely defines the statistical distribution since they are related by the equation

$$f(X) = \frac{dF(X)}{dX} \tag{14}$$

Either the frequency distribution, f(X), or the cumulative distribution, F(X), of the variable M must be determined. The communication margin, M, is given by the notation just adopted as

$$M = \sum_{i=1}^{7} X_i \tag{15}$$

The frequency distribution $f_{1,2}(X)$ of the sum of X_1 and X_2 is given by

$$f_{1,2}(X) = \int_{-\infty}^{\infty} f_1(X - \tau)\, f_2(\tau)\, d(\tau) \qquad (16)$$

Applying equation 16 six times will yield the required frequency distribution for the communication margin, M. Equivalently, the convolution process, as given in equation 16 may be applied to the cumulative distribution, thus

$$F_{1,2}(X) = \int_{-\infty}^{\infty} F_1(X - \tau)\, d\left[F_2(\tau)\right] \qquad (17)$$

In this way, the statistical distribution representing the communication margin can be obtained for any situation of interest. In general, the assumption of normality for each contributing factor is sufficient, and the result is a normal distribution whose mean and standard deviation are given simply by equations 12 and 13.

As to the first important question about what statistics should be associated with each of the factors which go into the determination of the communication margin, M, the largest statistical uncertainty is almost always found in L_b, the basic transmission loss. Attention will be focused upon the L_b factor in the remainder of this section.

This report presents two possible sources of L_b statistics which can be of immediate use. The first source is the modified Egli model, which is discussed in Section 4.2.2.4. Based on the results appearing in Section 4.2.2.4, the median L_b for 25.5 mc and above is given by

$$L_b = 116.57 + 20 \log f - 20 \log (h_1 h_2) + 40 \log d + F.F. \qquad (18)$$

where

f = frequency in megacycles

h_1, h_2 = transmitting and receiving antenna heights in feet, respectively

d = separation distance in miles

F.F. = foliage factor (Figure 4.17) for both horizontal and vertical polarizations.

L_b can be assumed to be normally distributed with a standard deviation, σ_ℓ, as follows.

$$\sigma_\ell = 5.7 \log f - 2.6 \qquad (19)$$

Alternatively, the vehicular data in Section 4.3.3.2 can be used. The section presents the medians and standard deviations for the normally distributed L_b for a large number of sample distance intervals.

The following sample problem provides an example of the use of the above data in conjunction with the communication margin to determine possible communication ranges. The AN/PRC-10 man-pack set will be used as an example. The AN/PRC-10 has been the object of intensive measurement as a part of the Department of Defense Spectrum Signature Program. The following characteristics will be assumed at 50 mc, based on information provided by measurements on the AN/PRC-10.[7]

---

7. The following related reports, submitted October 1963 to the U. S. Army Electronic Proving Ground, Fort Huachuca, Arizona, under Contract No. DA 36-039 SC-80928, by the Jansky & Bailey Research and Engineering Division of Atlantic Research Corporation, and Frederick Research Corporation: "U. S. Army RFCP Spectrum Signature Program, Radio Set AN/PRC-10 (Ser. No. 732), SS-315.1 (F), Test Sample 1 of 3 Sample Lot," "U. S. Army RFCP Spectrum Signature Program, Radio Set AN/PRC-10 (Ser. No. 9099), SS-315.2 (F), Test Sample 2 of 3 Sample Lot," and U. S. Army Spectrum Signature Program, Radio Set AN/PRC-10 (Ser. No. 639), SS-315.3 (F), Test Sample 3 of 3 Sample Lot."

Factor	Median	Standard Deviation	Distribution
P_t	25 dbm	2 db	Normal
P_r	-115 dbm	2 db	Normal
C_t	2 db	1/2 db	Normal
C_r	2 db	1/2 db	Normal
G_t	3 db	1 db	Normal
G_r	3 db	1 db	Normal

Equations 18 and 19 will be used to obtain the mean, m, and the standard deviation, σ, for L_b, assuming antenna heights of 7 feet and vertical polarization at each end. Thus from equation 18

$$L_b(\text{mean}) = 133 + 40 \log d \text{ (db)} \tag{20}$$

and from equation 19

$$\sigma_\ell = 6.1 \text{ db} \tag{21}$$

The mean value of the communication margin, M, is given by using equation 12 as follows:

$$M \text{ (mean)} = 25 \text{ dbm} + 115 \text{ dbm} - 2 \text{ db} - 2 \text{ db} + 3 \text{ db} + 3 \text{ db} - 133 - 40 \log d \tag{22}$$

or

$$M(\text{mean}) + 17 - 40 \log d \tag{23}$$

The mean effective range is the point at which M (mean) = 0. In this case it is the distance at which

$$40 \log d = 17 \tag{24}$$

or

$$d = 2.6 \text{ miles} \tag{25}$$

The standard deviation for the communication margin, M, is given by equation 13 as follows:

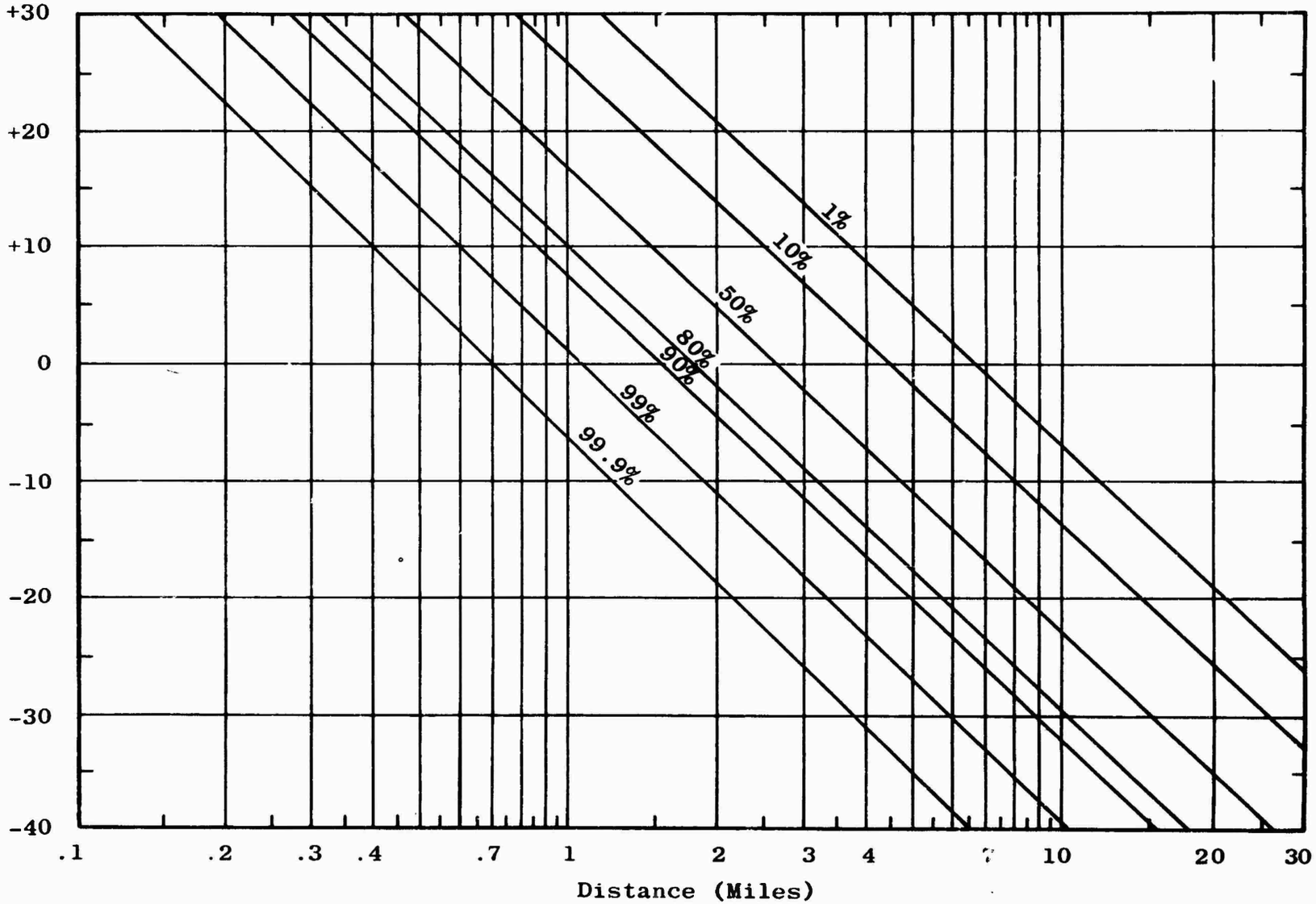

Figure 4.166 Communication Margin as a Function of Confidence Level

$$\sigma^2 = 2^2 + 2^2 + (1/2)^2 + (1/2)^2 + (1)^2 + (1)^2 + (6.1)^2 \quad (26)$$

$$\sigma = 6.9 \text{ db} \quad (27)$$

Using the fact that the communication margin, M, is normally distributed with a mean value of 17 - 40 log d and a standard deviation of 6.9 db, it is possible to plot the family of curves shown in Figure 4.166. Each curve of the family has a certain probability associated with it. That probability is defined as the confidence level.

The communication margin at any confidence level is related to the median communication margin as follows:

$$M\ (P\%) = M\ (\text{median}) - C\ (P\%) \quad (28)$$

where

M (P%) = the communication margin at a P% confidence level

M (median) = the median (i.e., 50%) confidence level

C (P%) = an adjustment factor, given in Figure 4.167.

In the case of a normal distribution, M (median) is equal to M (mean). The distance at which a given confidence level curve crosses zero on Figure 4.166 is the range that will be attainable at the indicated confidence level. The results from Figure 4.166 can be replotted as shown in Figure 4.168. Figure 4.168 shows that for the AN/PRC-10 used in this sample problem, there is a 90 per cent confidence level of obtaining a range of 1.5 miles, but only a 10 per cent confidence level of obtaining a range of 4.5 miles.

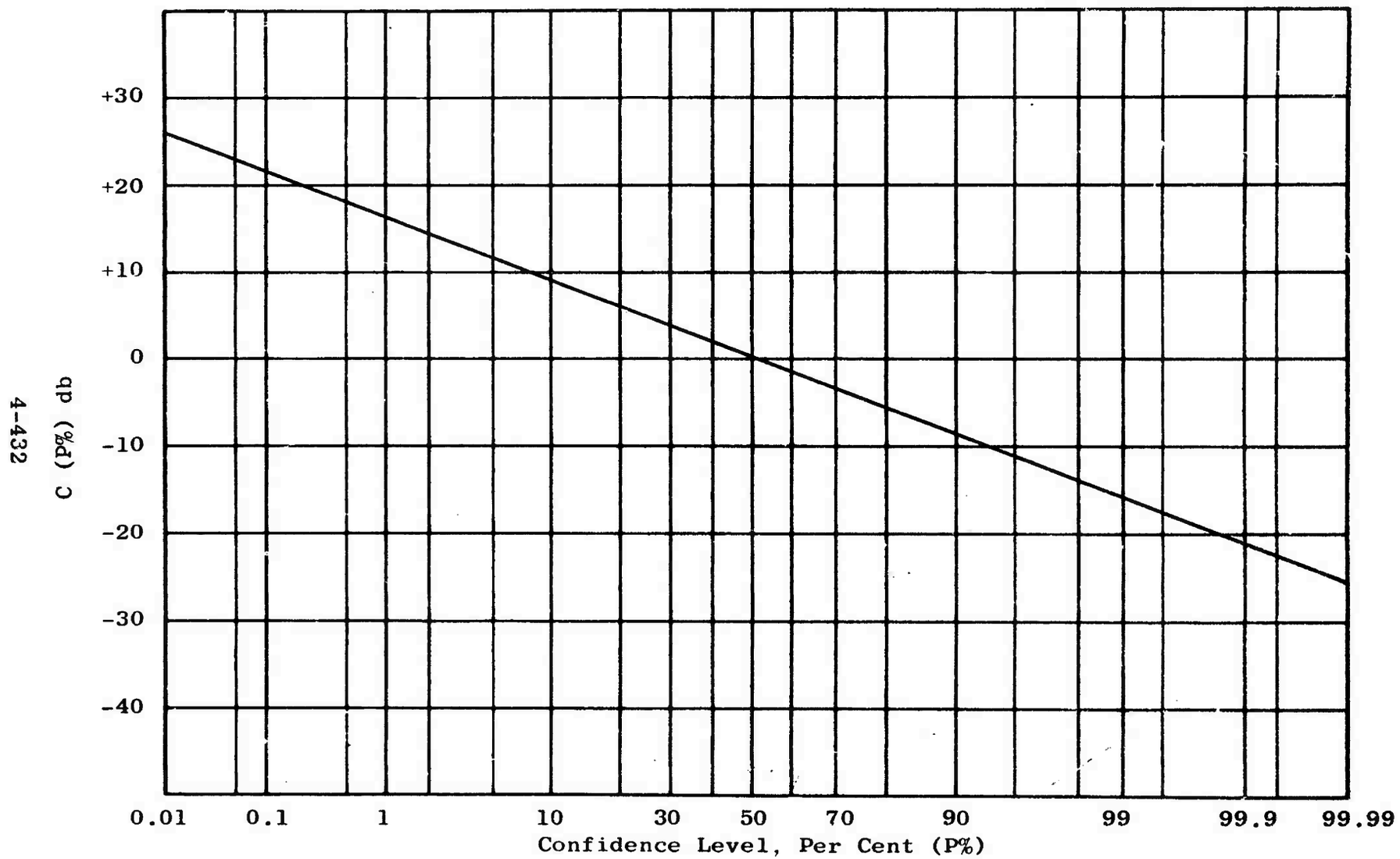

Figure 4.167 Factor to Convert M (Median) to M (P%)

Figure 4.168 Communication Range as a Function of Confidence Level

5. MEASUREMENTS ABOVE 425 MC

The propagation measurement program in Thailand has been extended to cover the frequency range from 0.4 to 10 gc. These measurements consist chiefly of measurements of line-of-sight transmissions over an obstacle, refractive index measurements along the line-of-sight path, and measurements of short-range transmissions directly through foliage. The purpose of these measurements is to obtain and analyze basic propagation data which will be useful in the design and evaluation of ground-based surveillance and intrusion detection systems as well as of communications systems. The instrumentation systems for these tests are described in Semiannual Report Number 5.

The basic measurement equipment was received at the Principal Laboratories early in this report period. Spare parts and miscellaneous maintenance equipment were also procured. All equipment was tested individually for compliance with the manufacturer's specifications and several items had to be returned to suppliers for repairs. The equipment was also interconnected and operated in the various test and calibration system configurations to check the over-all performance and procedures.

Since the antennas used for the short-range measurements in the foliage must be capable of being elevated above ground level, remote antenna positioning for azimuth, elevation and polarization was necessary. A remote azimuth positioning mechanism was fabricated to be used as the mounting base for the Ant-Lab antenna positioner. This base provides for the azimuthal movement and the Ant-Lab positioner provides for the elevation and polarization adjustments. A servo-indicator system was incorporated to provide remote position readout as well as remote position control. A

framework assembly, supporting the positioner and antenna, was constructed and provisions were made for raising this assembly on a tower using a geared hoist.

5.1 Measurement Site Selection

As noted in the field test plan for the extended frequency measurements, two different foliated areas in Thailand are required for these measurements. One of these, designated Area A, has been selected in the vicinity of the site being used for the 100-kc to 425-mc tests. Jansky & Bailey personnel, assisted by members of the MRDC staff, devoted considerable time to the selection of a suitable location for Area B. Aerial and surface surveys were conducted over large areas of southeastern Thailand before the final selection was made of a location near Sattahip. The area chosen is on land under control of the Thai Navy and negotiations were started through MRDC to obtain permission for the use of this location. The vegetation in this area differs considerably from that in the Pak Chong region. It is extremely dense and green. The growth is primarily bamboo, about 20 to 30 feet high, with heavy underbrush.

Additional surveys were also made in Area A to establish a suitable line-of-sight path with a well-defined, foliated obstacle near mid-path.

The location of Areas A and B are shown in Figure 5.1. Figures 5.2 and 5.3 show the line-of-sight paths within the two areas.

5.2 Field Measurements

The first series of measurements is presently under way in Area A. The path selected has rising terrain at each extremity, thus providing for variation in the heights of

the transmitting and receiving antennas. Field personnel had to clear away considerable foliage in the vicinity of the antennas to provide an unobstructed antenna foreground. Two wooden towers approximately 40 feet high were erected for the antennas at the transmitting end of the path.

The hill at the receiver end is very steep and only short antenna towers are required to provide adequate Fresnel zone clearance. Nine antenna support platforms were constructed at the receiving end. An area at the top of the receiver hill was cleared to provide a helicopter landing area. The steepness of the hill makes helicopter transportation of equipment virtually essential. Additional portable equipment shelters and camp-type living quarters were erected at each end of the path. Antenna calibration towers were erected in the clearing of the main test site for use in calibrating and making pattern measurements of the transmitting and receiving antennas.

An engineer from the Principal Laboratories was assigned to Thailand in June to advise and work with the field team during the initial phases of the measurement program. All equipment was moved from Bangkok to the test site and complete operational checkouts were made. Calibration checks and comparisons were conducted on all attenuators, power meters and field intensity meters. Antenna gain and pattern measurements were made on all the discone, dish, and horn antennas. Throughout this process emphasis was placed on establishing standard procedures for these calibrations in addition to obtaining calibration data.

A short series of line-of-sight measurements was made. These measurements were essentially of a preliminary nature, primarily intended to establish the proper standard procedures for measuring radiated power at the transmitting

antenna and received power at the receiving antenna. In addition, data recording procedures were reviewed and established. A similar series of short-range tests is planned to establish efficient operational techniques and to obtain approximate foliage attenuation values which can be used as a guide in finalizing the short-range test procedures.

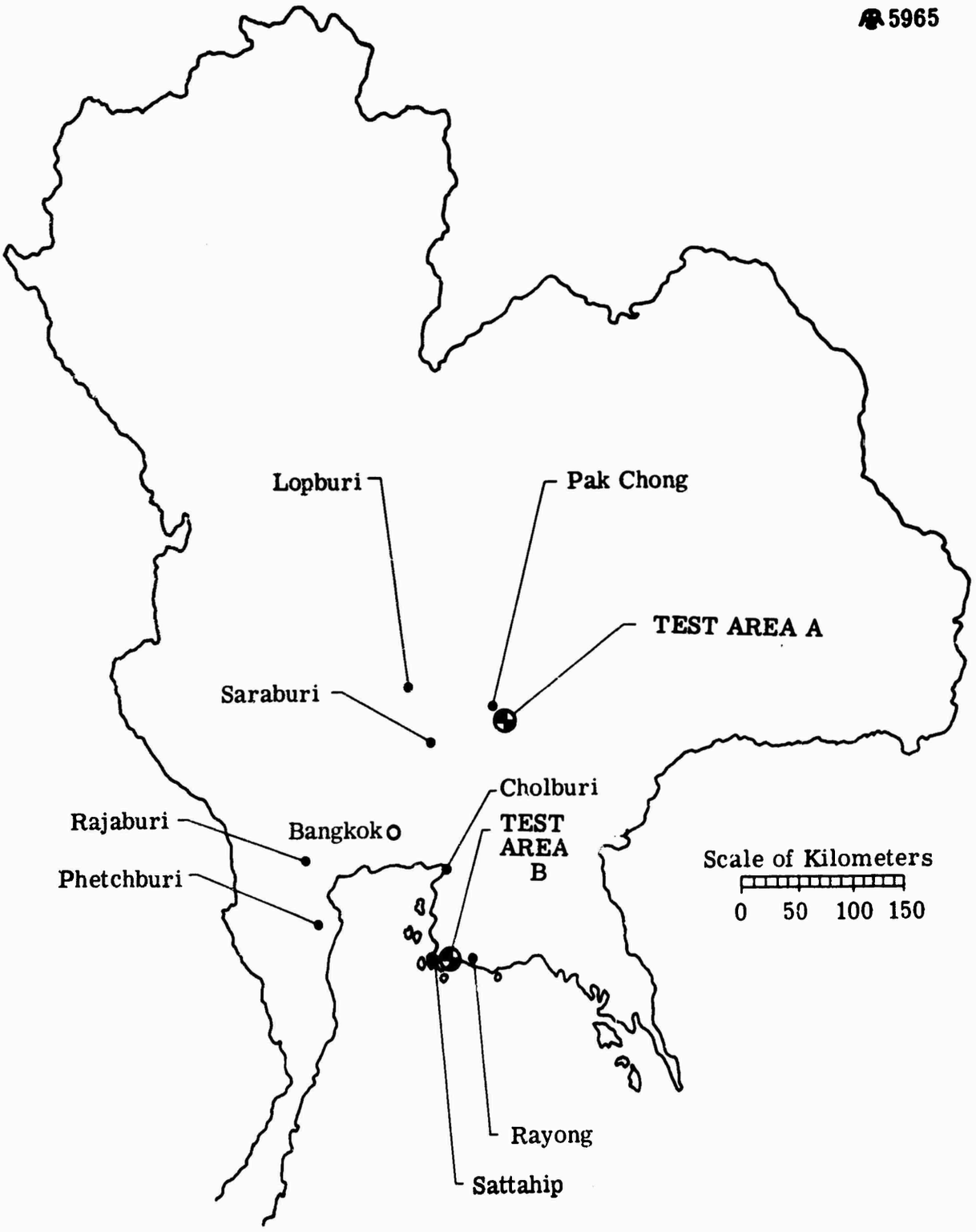

Figure 5.1 Test Areas for Measurements Above 425 Mc

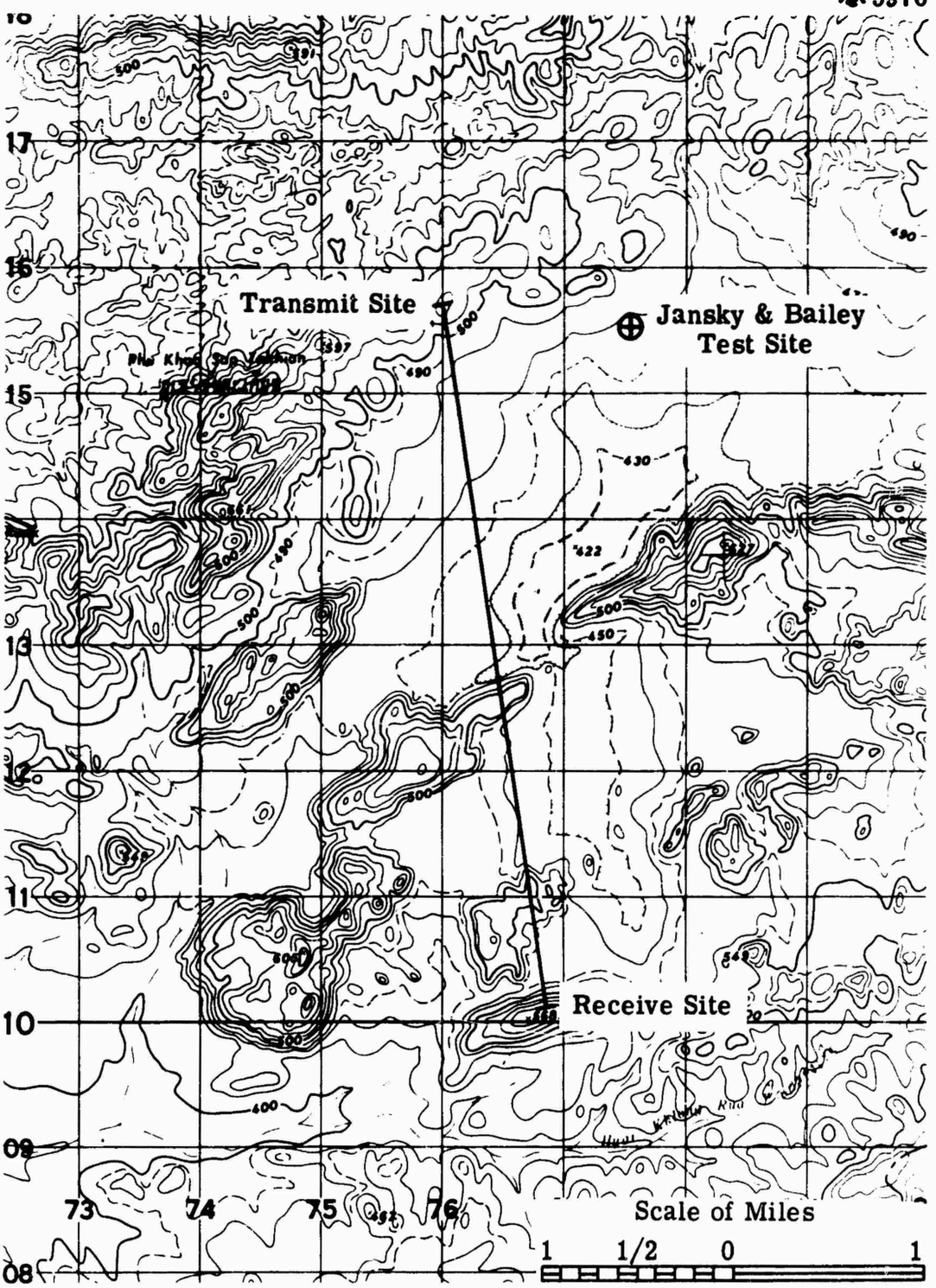

Figure 5.2 Area A for Measurements Above 425 Mc
Line-of-Sight Test Path

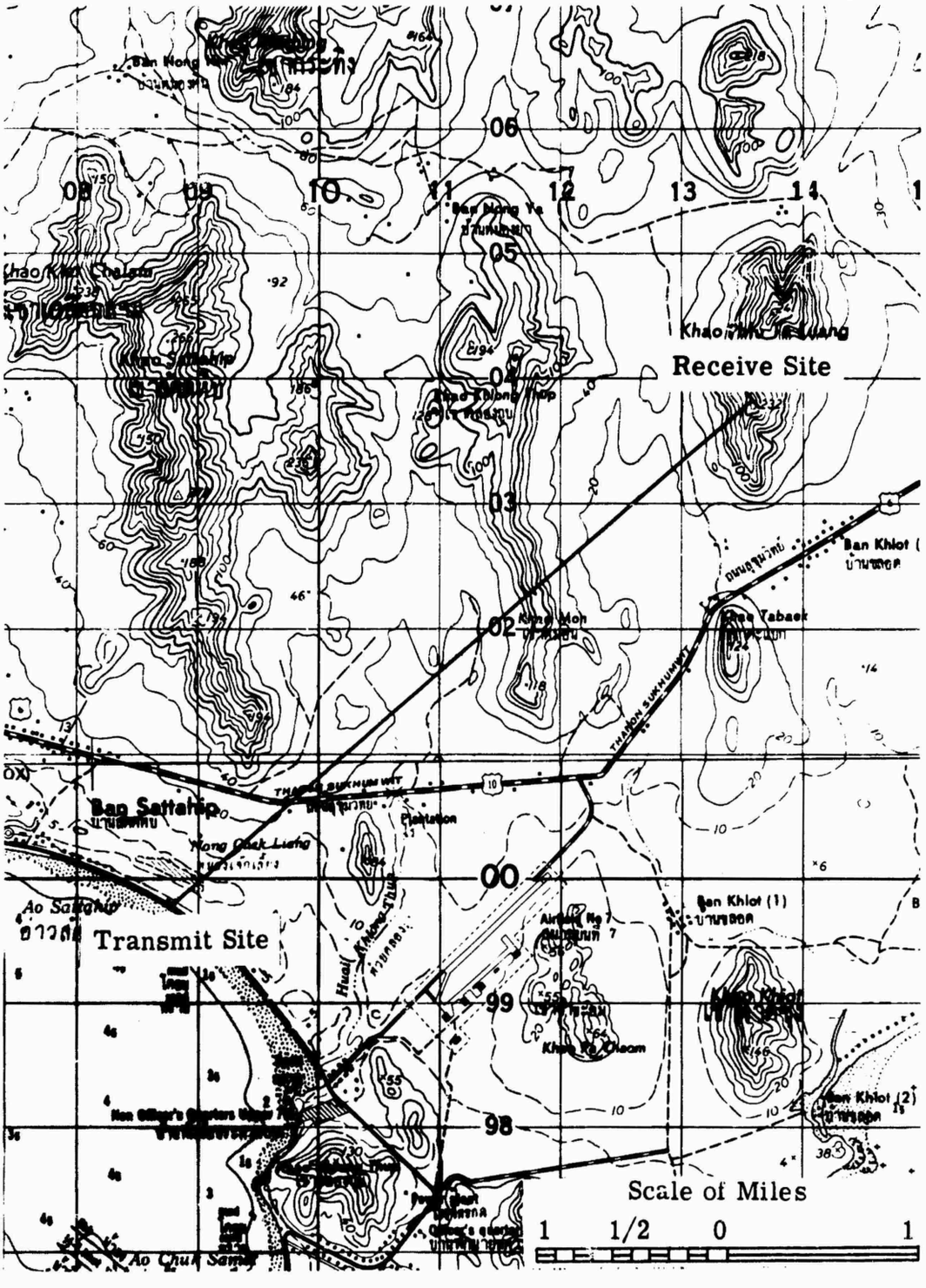

Figure 5.3 Area B for Measurements Above 425 Mc Line-of-Sight Test Path

6. TECHNICAL FILM REPORTS

The second SEACORE film, titled "Defense Communications Research in Thailand," was completed during this period. This film was produced with both English and Thai language sound tracks, the Thai text having been submitted to ARPA for approval prior to printing. All copies of this film are currently in the process of being delivered to the Government, thus completing this task under the propagation research program.

7. MEETINGS AND CONFERENCES

11-12 January 1965. The Project Director visited the Rolligon Corporation, Houston, Texas, with the Contracting Officer's Technical Representative, USAEL. The purpose of this visit was to review the results of the preliminary tests of the Rolligon in Thailand, and to discuss various modifications to increase the stability and cross-country speed of this special vehicle. The Rolligon Corporation demonstrated three versions on rough and muddy ground. All three versions exhibited increased stability, but the version with a two-bag trailer proved to be the most stable.

4 March 1965. Representatives of the Stanford Research Institute and Jansky & Bailey attended a conference conducted by Messrs. Robert Kulinyi and Howard Kitts of USAEL. The purpose of the conference, which was held at Fort Monmouth, was to discuss the technical feasibility of carrying out three-dimentional antenna pattern measurements of the transmitting antennas being used by Jansky & Bailey at its transmitting site in Thailand. These measurements would be made by SRI, using their XELDOP system. The fundamentals of a feasible technical plan were developed during this conference and are currently being being further refined by USAEL.

19 May 1965. Mr. George Hagn of Stanford Research Institute met with project personnel at the Atlantic Research Principal Laboratories to discuss the application of the J & B path loss data to the work Mr. Hagn is doing to develop methods for predicting mean effective ranges for mobile radio equipments. The latter half of this conference was attended by Messrs. Robert Kulinyi and Howard Kitts and Major Alexander Sidon of USAEL.

24 May 1965. The Project Director presented a briefing on the tropical propagation research program for Major General Benjamin Pochyla, Commanding General of the U. S. Army Electronic Proving Ground, and members of his staff at Fort Huachuca, Arizona. This briefing included a showing of the "Defense Communications Research in Thailand" film.

28 May 1965. The Project Director met with Colonel William D. Tigertt, Director, Walter Reed Army Institute of Research, and Dr. David P. Jacobus, Chief of the Institute's Department of Medicinal Chemistry, to discuss possible preventives for the particular strain (or strains) of malaria that has become evident in the J & B test area as well as in other areas in Thailand. During this conference a basic plan was established for close cooperation between J & B personnel and Army medical personnel in Thailand. This cooperation would include providing the medical personnel with blood samples, etc., from J & B personnel contracting this strain of malaria. Slides of these samples would be returned to Walter Reed for further study.

8 June 1965. The Project Director and the Project Engineer of the Propagation group met with representatives of USAEL and the Defense Research Corporation (California) at Fort Monmouth, New Jersey, to discuss Jansky & Bailey's providing DRC with copies of unreduced Thailand field data. Basic arrangements were made for DRC representatives to visit the Jansky & Bailey facility in Alexandria, Virginia, to select the units of data they wanted.

10-11 June 1965. The Project Director and the Project Engineer of the Propagation group attended the National Bureau of Standards conference on radio wave propagation over irregular terrain at Boulder, Colorado. Members

of the CRPL staff presented several excellent discussions, and the conference provided an opportunity to become acquainted with the considerable research work now being done in the area of radio propagation at CRPL.

16-17 June 1965. Two representatives of the Defense Research Corporation met with members of the J & B staff at Alexandria, Virginia, to review the basic Thailand field data. As a result of this conference some 1200 sheets of the field data were selected for reproduction and transmission to DRC.

8. PROJECT PERSONNEL

The success of any research project such as this depends on the technical contributions of many dedicated people, working both behind the scenes and in the forefront. In this regard, credit is due all the engineers and technicians who make up the project teams. Particularly, credit is due Mr. Neil J. Schairer, who heads the instrumentation team; Mr. Charles B. Sykes, who heads the field measurement activities in Thailand; and Mr. Kenneth G. Heisler, who heads the data reduction and analysis team at the Principal Laboratories.

With respect to the technical writing and preparation of this report, special credit is due Mr. Heisler and members of his team: Mr. J. P. Kallenborn, Mr. Standish Marriott, and Mr. W. P. Seneker.

Additionally, the following people contributed to the program effort during the interval covered by this report:

P. A. Anti	Field Engineer
R. W. Ayers	Field Technician
W. A. Backus	Engineer
S. L. Bailey	Vice President, Atlantic Research Corporation
R. F. Bass	Field Engineer
K. E. Bodle	Field Technician
F. I. Clevenger	Technician
C. O. Conway	Field Technician
S. R. Courtney	Technician
H. R. Cozzens	Field Administrator, Thailand
R. H. Dawson	Field Technician
T. J. Deebel	Field Technician
L. L. Engel	Technician
J. J. Grant, IV	Assistant Project Engineer, Thailand

C. E. Greeley	Mechanical Design Engineer
R. W. Gross	Assistant Project Engineer, Thailand
E. J. Knowles	Data Technician
C. R. Kocherhans	Field Technician
R. E. Linehan	Machinist
G. V. Lucha	Assistant Project Engineer, Thailand
F. T. Mitchell, Jr.	Division Director
W. B. Munson	Engineer
J. D. O'Neal	Mechanical Engineer
E. O. Parham	Field Technician
L. V. Pellettier	Assistant to Project Director
D. C. Ports	Manager, E & C Development Department
J. E. Pratt	Field Technician
Dr. H. R. Reed	Propagation Consultant
L. L. Reiser	Technician
A. M. Richardson	Machinist
R. G. Robertson	Field Engineer
W. C. Roehr, Jr.	Field Engineer
L. G. Sturgill	Project Director
D. L. Trafton	Engineer
R. L. Weddle	Technician
K. E. Zasowski	Field Technician

Appendix A

SMOOTH-EARTH HEIGHT FUNCTIONS

Height functions for beyond-the-horizon transmission under smooth-earth conditions are given by Norton[3] as follows: Transmitting and receiving of antenna heights are measured in terms of a numerical antenna height, q_1 and q_2. These numerical antenna heights are functions of frequency, polarization, ground constants, and the actual antenna heights. Either q_1 or q_2 may be calculated as follows:

For vertical polarization

$$q = \frac{2\pi h}{\lambda} \left(\frac{\text{Cos}^2\ b''}{x\ \text{Cos}\ b'}\right)^{\frac{1}{2}} \tag{1}$$

where

h = antenna height

λ = wavelengths in same units as h

$$x = 60\sigma\lambda \tag{2}$$

where

σ = earth conductivity in mho-m/sq m

λ = wavelengths in meters

$$\text{Tan}\ b' = \frac{\epsilon_r - 1}{x} \tag{3}$$

where

ϵ_r = relative permittivity of ground

$$\text{Tan}\ b'' = \frac{\epsilon_r}{x} \tag{4}$$

$$b = 2b'' - b' \tag{5}$$

---

3. K A. Norton, "The Calculation of Ground-Wave Field Intensity Over a Finitely Conducting Spherical Earth," Proc. IRE, pp 623-639, December 1941.

For horizontal polarization

$$q = \frac{2\pi h}{\lambda} \left(\frac{x}{\cos b'}\right)^{\frac{1}{2}} \qquad (6)$$

where

h = antenna height
λ = wavelength in same units as h
x = quantity defined by equation 2
b' = angle defined by equation 3

The height functions denoted as $f(q_1)$ and $f(q_2)$ are essentially unity for values of q_1 or q_2 up to approximately 0.1. This means that there is no height variation as q_1 or q_2 ranges over values below 0.1.

For values of q_1 or q_2 greater than approximately 10, $f(q_1)$ and $f(q_2)$ are equal to q_1 and q_2, respectively. Since $f(q_1)$ and $f(q_2)$ are equal to q_1 and q_2, and q_1 and q_2 are directly proportional to h_1 and h_2 (as equations 1 and 6 show), the height effect is directly proportional to antenna height for q values greater than 10.

For values of q_1 and q_2 between 0.1 and 10, the dependence of $f(q_1)$ and $f(q_2)$ on height gradually changes from no dependence at all to direct dependence. The rate of change from one state to the other depends upon the angle b given by equation 5 which, in turn, depends upon frequency and the ground constants.

The height functions represented by $f(q_1)$ and $f(q_2)$ have been plotted in Figures A.1 and A.2 for the frequencies of interest in this report. Ground constants of 0.03 mhos per meter for ground conductivity and 15 for relative permittivity were used.

Figure A.1 gives the height function for vertical polarization and Figure A.2 gives the height function for horizontal polarization.

Figure A.1 indicates that there should be no height effect for frequencies of 12 mc and below for vertical polarization on a smooth-earth basis. In Section 4.3.2.2.1 it was noted that the measured data indicated a height effect at 12 mc. Figure A.2 indicates a height effect at every frequency for horizontal polarization. This is consistent with the measured results in that a height effect was noted at every frequency measured for horizontal polarization as noted in Section 4.3.2.2.1.

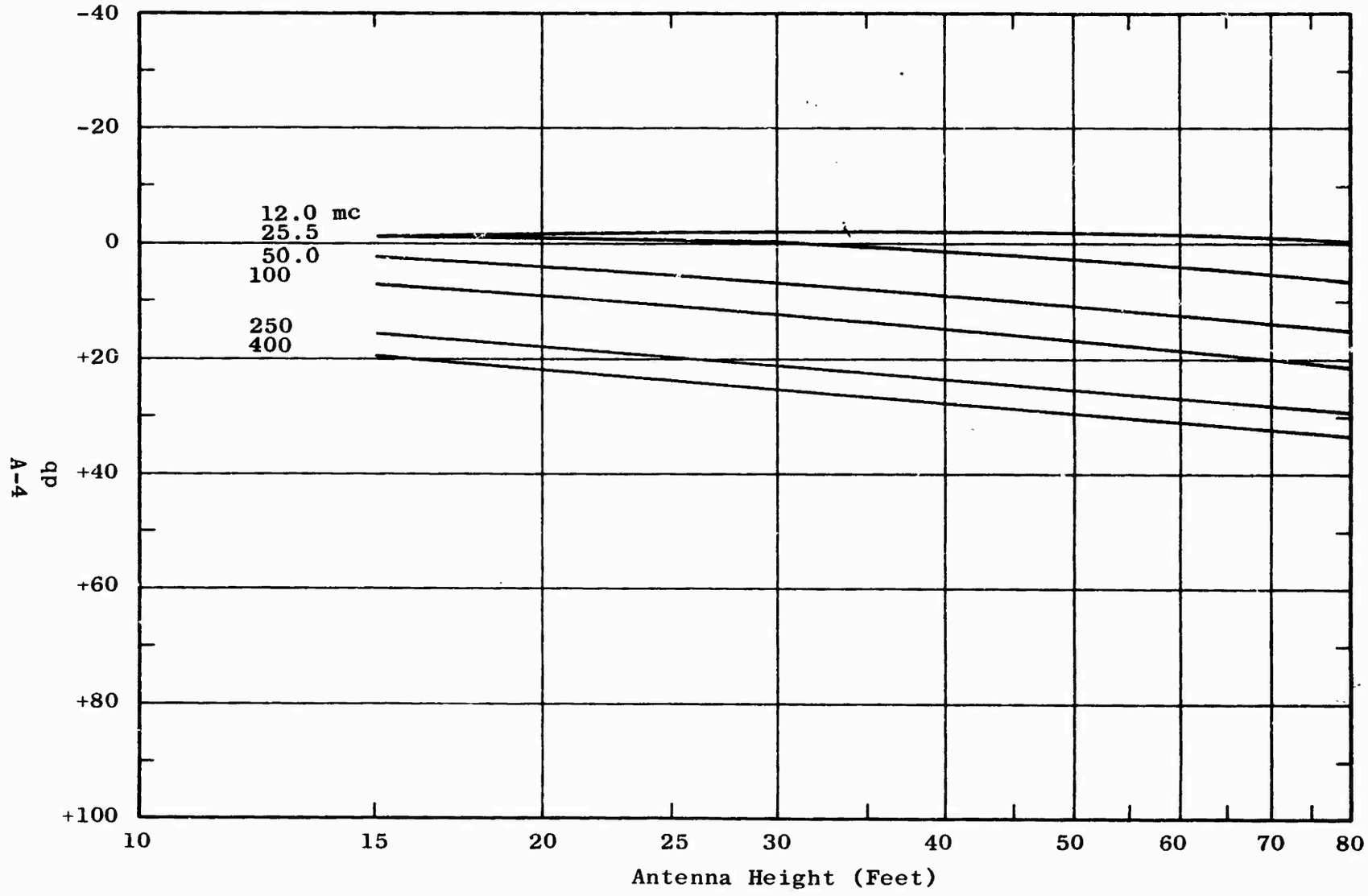

Figure A.1 Theoretical Smooth-Earth Height Functions, Vertical Polarization

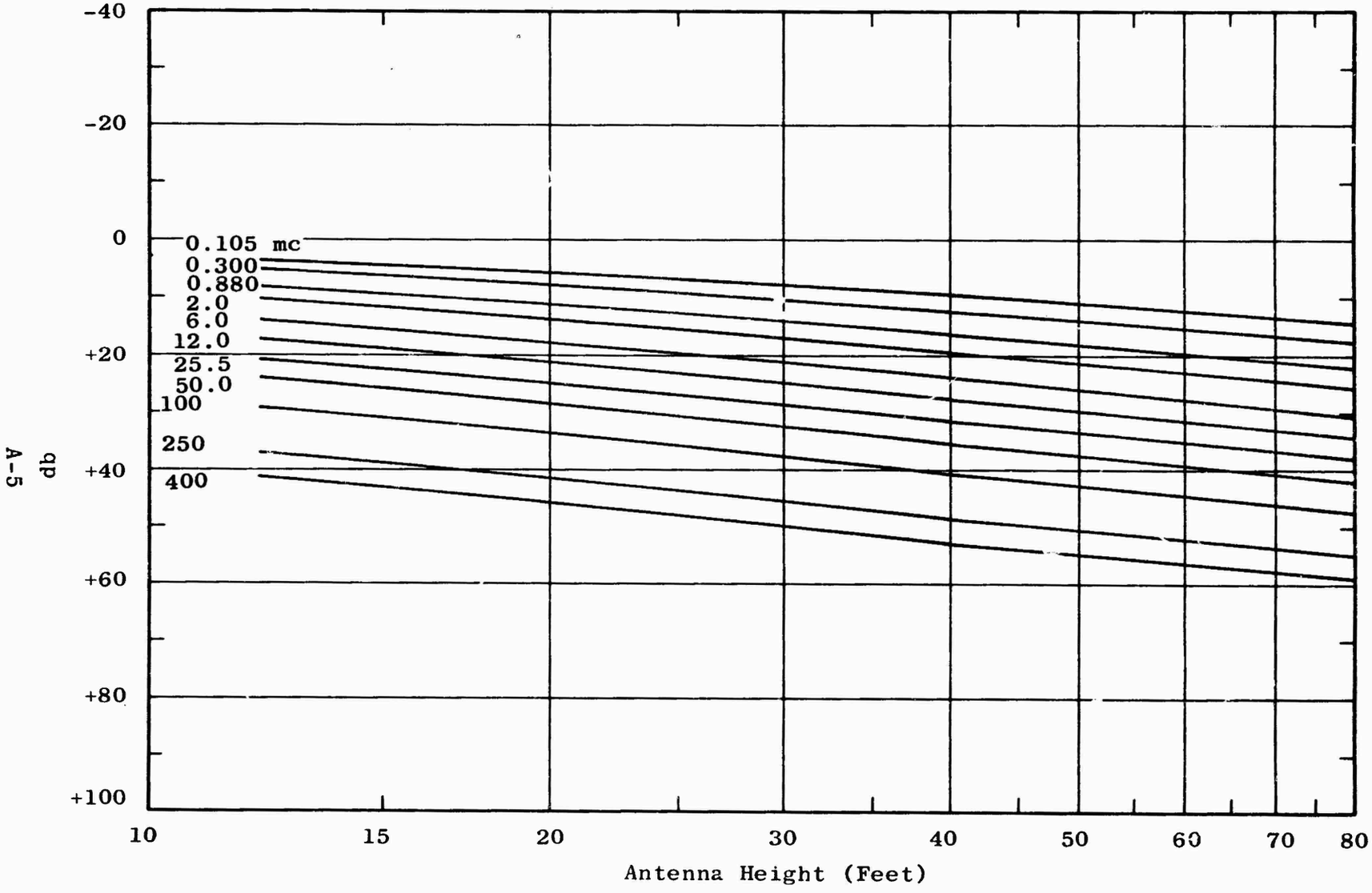

Figure A.2 Theoretical Smooth-Earth Height Functions, Horizontal Polarization

APPENDIX B

FIELD MEASUREMENT NOTES

Fig. No.	Measurement Parameters		Measurement Number	Date of Measurement
3.10	$L_b = F_A$ (25.5, V, 21,	0.2, H_r)	W-109	12/14/64
		0.45	P-61	9/26/64
		0.7	W-62	11/4/64
		1.0	P-80	11/5/64
		2.0	J-71	9/6/64
		3.0	W-57	9/17/64
		4.0	L-70	9/16/64
3.11	$L_b = F_A$ (25.5, V, 40,	0.2, H_r)	W-10	7/23/64
		0.45	L-12	7/22/64
		0.7	L-11	7/22/64
		1.0	L-6	7/22/64
		2.0	W-7	7/23/64
		3.0	W-55	9/17/64
		4.0	P-33	7/16/64
		7.0	P-35	7/16/64
		10.5	L-32	8/10/64
		14.0	W-23	8/10/64
3.12	$L_b = F_A$ (25.5, H, 13,	0.2, H_r)	P-48	9/1/64
		0.45	P-60	9/26/64
		0.7	L-46	9/3/64
		1.0	L-50	9/3/64
		2.0	J-61	9/2/64
		3.0	L-54	9/3/64
		4.0	L-68	9/16/64
		7.0	W-86	12/6/64
		10.5	W-92	12/7/64
		14.0	W-96	12/7/64
		17.0	W-99	12/8/64
3.13	$L_b = F_A$ (50, V, 13,	0.2, H_r)	L-40	8/29/64
		0.45	J-52	8/30/64
		0.7	J-56	8/30/64
		1.0	L-44	8/29/64
		2.0	J-57	8/30/64
		3.0	T-32	8/31/64
		4.0	T-33	8/31/64
		7.0	W-90	12/6/64
		10.5	W-93	12/7/64
		14.0	W-98	12/7/64

Fig. No.	Measurement Parameters	Measurement Number	Date of Measurement
3.14	$L_b = F_A$ (50, H, 13, 0.2, H_r)	P-49	9/1/64
	0.45	P-54	9/1/64
	0.7	L-47	9/3/64
	1.0	L-51	9/3/64
	2.0	J-63	9/2/64
	3.0	L-56	9/3/64
	4.0	L-73	9/16/64
	7.0	W-89	12/6/64
	10.5	W-94	12/7/64
	14.0	W-97	12/7/64
	17.0	W-100	12/8/64
3.15	$L_b = F_A$ (50, H, 80, 0.2, H_r)	B-31	6/30/64
	0.45	B-34	6/30/64
	0.7	B-53	7/2/64
	1.0	B-40	7/1/64
	2.0	B-43	7/1/64
	3.0	B-46	7/1/64
	4.0	B-49	7/2/64
	7.0	S-135A	7/9/64
	14.0	S-136D	7/10/64
3.16	$L_b = F_A$ (100, H, 13, 0.2, H_r)	L-41	8/29/64
	0.45	J-53	8/30/64
	0.7	J-54	8/30/64
	1.0	L-42	8/29/64
	2.0	J-64	9/2/64
	3.0	L-57	9/3/64
	4.0	T-35	8/3/64
	7.0	W-88	12/6/64
3.17	$L_b = F_A$ (250, V, 13, 0.2, H_r)	L-65	9/13/64
	0.45	W-45A	9/10/64
	0.7	W-41	9/8/64
	1.0	P-82	11/5/64
	2.0	W-49	9/14/64
	3.0	W-54	9/17/64
3.18	$L_b = F_A$ (250, V, 40, 0.2, H_r)	L-66	9/13/64
	0.45	T-72	12/13/64
	0.7	W-40	9/8/64
	1.0	J-82	9/7/64
	2.0	W-47	9/14/64
	3.0	W-56	9/17/64
3.19	$L_b = F_A$ (250, H, 40, 0.2, H_r)	L-18	8/7/64
	0.45	L-19	8/7/64
	0.7	P-43	8/8/64
	1.0	P-44	8/8/64
	2.0	W-10	12/4/64
	3.0	L-26	8/8/64

Fig. No.	Measurement Parameters	Measurement Number	Date of Measurement
3.20	$L_b = F_A$ (250, H, 80, 0.2, H_r)	L-62	9/13/64
	0.45	T-73	12/13/64
	0.7	L-89	11/3/64
	1.0	L-8	7/22/64
	2.0	W-101	12/14/64
	3.0	W-4	7/23/64
	4.0	P-32	7/15/64
3.21	$L_b = F_A$ (400, V, 13, 0.2, H_r)	P-57	9/26/64
	0.45	W-32	9/5/64
	0.7	W-61	11/4/64
	1.0	J-76	9/7/64
	2.0	J-75	9/6/64
	3.0	J-66	9/6/64
3.22	$L_b = F_A$ (400, V, 80, 0.2, H_r)	P-13	5/11/64
	0.45	P-14	5/11/64
	0.7	P-16	5/12/64
	1.0	P-17	5/12/64
	2.0	B-9	4/24/64
	3.0	S-131	5/22/64
3.23	$L_b = F_A$ (400, H, 13, 0.2, H_r)	P-56	9/26/64
	0.45	W-33	9/5/64
	0.7	W-38	9/5/64
	1.0	P-81	11/5/64
	2.0	J-74	9/6/64
	3.0	J-67	9/6/64
3.24	$L_b = F_A$ (400, H, 40, 0.2, H_r)	W-29	9/5/64
	0.45	W-34	9/5/64
	0.7	W-63	11/4/64
	1.0	J-78	9/7/64
	2.0	J-73	9/6/64
	3.0	J-68	9/6/64
3.25	$L_b = F_A$ (400, H, 80, 0.2, H_r)	W-28	9/5/64
	0.45	W-35	9/5/64
	0.7	T-78	12/13/64
	1.0	P-79	11/5/64
	2.0	W-105	12/14/64
	3.0	J-69	9/6/64

Fig. No.	Measurement Parameters	Measurement Number	Date of Measurement
3.26	$L_b = F_B$ (25.5, V, 21, 0.2, H_r)	L-76	10/8/64
	0.4	P-70	10/14/64
	0.6	L-88	10/15/64
	1.0	P-83	11/5/64
	2.0	L-162	12/16/64
	3.0	J-98	11/11/64
	4.3	L-161	12/16/64
	6.7	L-159	12/15/64
	19.0	L-141	12/12/64
3.27	$L_b = F_B$ (25.5, V, 40, 0.2, H_r)	W-64	11/15/64
	0.4	L-102	11/19/64
	0.6	P-115	11/22/64
	1.0	P-118	11/25/64
	2.0	J-89	11/9/64
	3.0	B-62	11/13/64
	4.3	P-136	11/29/64
	6.7	L-157	12/15/64
	10.5	J-120	10/12/64
	14.2	J-129	12/11/64
	19.0	L-151	12/12/64
3.28	$L_b = F_B$ (25.5, V, 80, 0.2, H_r)	W-64A	11/15/64
	0.4	L-103	11/19/64
	0.6	P-114	11/22/64
	1.0	W-85	11/24/64
	2.0	J-90	11/9/64
	3.0	J-97	11/11/64
	4.3	P-137	11/29/64
	6.7	L-158	12/15/64
	10.5	J-122	12/10/64
	14.2	J-128	12/11/64
	19.0	L-150	12/12/64
3.29	$L_b = F_B$ (25.5 H, 13, 0.2, H_r)	W-68	11/15/64
	0.4	L-100	11/19/64
	0.6	L-107	11/23/64
	1.0	W-77	11/24/64
	2.0	J-91	11/9/64
	3.0	P-106	11/10/64
	4.3	P-145	11/29/64
	6.7	L-160	12/15/64
	10.5	J-113	12/10/64
	14.2	L-137	12/11/64
	19.0	L-140	12/12/64

Fig. No.	Measurement Parameters	Measurement Number	Date of Measurement
3.30	$L_L = F_B$ (25.5, H, 40, 0.2, H_r)	W-58	10/6/64
	0.4	P-69	10/14/64
	0.6	L-87	10/15/64
	1.0	P-84	11/5/64
	2.0	P-92	11/8/64
	3.0	P-111	11/10/64
	4.3	P-140	11/29/64
	6.7	L-156	12/15/64
	10.5	J-119	12/10/64
	14.2	L-134	12/11/64
	19.0	L-147	12/12/64
3.31	$L_b = F_B$ (25.5, H, 80, 0.2, H_r)	W-67	11/15/64
	0.4	L-101	11/19/64
	0.6	L-105	11/23/64
	1.0	W-82	11/24/64
	2.0	J-86	11/9/64
	3.0	J-94	11/11/64
	4.3	P-139	11/29/64
	6.7	T-54	12/2/64
	10.5	J-118	12/10/64
	14.2	L-133	12/11/64
	19.0	L-146	12/12/64
3.32	$L_b = F_B$ (50, V, 13, 0.2, H_r)	L-80	11/16/64
	0.4	W-123	11/18/64
	0.6	L-166	11/23/64
	1.0	B-59	11/24/64
	2.0	P-87	11/9/64
	3.0	P-108	11/10/64
	4.3	T-37	11/30/64
	6.7	T-67	12/3/64
	10.5	J-112	12/10/64
	14.2	L-135	12/11/64
3.33	$L_b = F_B$ (50, V, 40, 0.2, H_r)	L-93	11/16/64
	0.4	J-110	11/18/64
	0.6	L-167	12/16/64
	1.0	W-79	11/24/64
	2.0	J-84	11/9/64
	3.0	J-93	11/11/64
	4.3	P-143	11/29/64
	6.7	T-66	12/3/64
	10.5	J-115	12/10/64

Fig. No.	Measurement Parameters	Measurement Number	Date of Measurement
3.34	$L_b = F_b$ (50, V, 80, 0.2, H_r)	W-71	11/15/64
	0.4	J-109	11/18/64
	0.6	L-106	11/23/64
	1.0	W-78	11/24/64
	2.0	J-85	11/9/64
	3.0	J-92	11/11/64
	4.3	P-144	11/29/64
	6.7	T-65	12/3/64
	10.5	J-114	12/10/64
	14.2	L-131	12/11/64
	19.0	L-142	12/12/64
3.35	$L_b = F_B$ (50, H, 13, 0.2, H_r)	L-79	10/13/64
	0.4	P-153	12/17/64
	0.6	P-72	10/18/64
	1.0	B-60	10/21/64
	2.0	T-43	11/30/64
	3.0	P-107	11/10/64
	4.3	T-38	11/30/64
	6.7	T-68	12/3/64
	10.5	J-111	12/10/64
	14.2	L-136	12/11/64
	19.0	L-138	12/12/64
3.36	$L_b = F_B$ (50, H, 40, 0.2, H_r)	L-95	11/16/64
	0.4	J-108	11/18/64
	0.6	L-109	11/23/64
	1.0	W-81	11/24/64
	2.0	J-87	11/9/64
	3.0	J-96	11/11/64
	4.3	P-141	11/29/64
	6.7	T-64	12/3/64
	10.5	J-117	12/10/64
	14.2	J-132	12/11/64
	19.0	L-145	12/12/64
3.37	$L_b = F_B$ (50, H, 80, 0.2, H_r)	L-94	11/16/64
	0.4	J-143	12/17/64
	0.6	L-108	11/23/64
	1.0	W-80	11/24/64
	2.0	J-88	11/9/64
	3.0	J-95	11/11/64
	4.3	P-142	11/29/64
	6.7	T-63	12/3/64
	10.5	J-116	12/10/64
	14.2	J-131	12/11/64
	19.0	L-144	12/12/64

Fig. No.	Measurement Parameters	Measurement Number	Date of Measurement
3.38	$L_b = F_B$ (100, V, 13, 0.2, H_r)	L-78	10/13/64
	0.4	P-155	12/1/64
	0.6	L-165	12/16/64
	1.0	P-125	11/25/64
	2.0	P-90	11/7/64
	3.0	P-110	11/10/64
	4.3	P-146	11/29/64
3.39	$L_b = F_B$ (100, V, 80, 0.2, H_r)	W-70	11/15/64
	0.4	J-106	11/18/64
	0.6	L-111	11/23/64
	1.0	W-84	11/24/64
	2.0	P-100	11/8/64
	3.0	B-64	11/13/64
	4.3	P-132	11/27/64
3.40	$L_b = F_B$ (100, V, 80, 0.2, H_r)	W-69	11/15/64
	0.4	J-105	11/18/64
	0.6	L-110	11/23/64
	1.0	W-83	11/24/64
	2.0	P-100	11/8/64
	3.0	B-63	11/13/64
	4.3	P-133	11/27/64
	6.7	T-59	12/2/64
	10.5	J-125	12/10/64
	14.2	J-130	12/11/64
	19.0	L-152	12/12/64
3.41	$L_b = F_B$ (100, H, 13, 0.2, H_r)	L-77	10/13/64
	0.4	P-154	12/1/64
	0.6	P-73	10/18/64
	1.0	P-76	10/21/64
	2.0	P-89	11/7/64
	3.0	P-109	11/10/64
	4.3	P-147	11/29/64
3.42	$L_b = F_B$ (100, H, 40, 0.2, H_r)	W-65	11/15/64
	0.4	J-134	12/13/64
	0.6	L-113	11/23/64
	1.0	P-117	11/25/64
	2.0	P-98	11/8/64
	3.0	B-66	11/13/64
	4.3	P-130	11/27/64
	6.7	T-58	12/2/64
	19.0	L-149	12/12/64

Fig. No.	Measurement Parameters	Measurement Number	Date of Measurement
3.43	$L_b = F_B$ (100, H, 80, 0.2, H_r)	W-66	11/15/64
	0.4	J-103	11/18/64
	0.6	L-112	11/23/64
	1.0	P-116	11/25/64
	2.0	P-99	11/8/64
	3.0	B-65	11/13/64
	4.3	P-131	11/27/64
	6.7	T-57	12/2/64
	10.5	J-123	12/10/64
	14.2	J-127	12/11/64
	19.0	L-148	12/12/64
3.44	$L_b = F_B$ (250, V, 13, 0.2, H_r)	L-75	10/8/64
	0.4	P-151	12/1/64
	0.6	L-164	12/16/64
	1.0	B-58	10/21/64
	2.0	P-85	11/7/64
3.45	$L_b = F_B$ (250, V, 40, 0.2, H_r)	B-69	11/17/64
	0.4	J-136	12/17/64
	0.6	L-115	11/23/64
	1.0	P-120	11/25/64
	2.0	P-96	11/8/64
	3.0	L-128	11/26/64
3.46	$L_b = F_B$ (250, V, 80, 0.2, H_r)	B-70	11/17/64
	0.4	J-135	12/17/64
	0.6	L-114	11/23/64
	1.0	P-119	11/25/64
	2.0	P-97	11/8/64
	3.0	L-127	11/26/64
	4.3	P-129	11/27/64
	6.7	T-52	12/2/64
3.47	$L_b = F_B$ (250, H, 13, 0.2, H_r)	L-74	10/8/64
	0.4	P-65	10/14/64
	0.6	L-163	12/16/64
	1.0	B-57	10/21/64
	2.0	P-93	11/8/64
3.48	$L_b = F_B$ (250, H, 40, 0.2, H_r)	B-68	11/17/64
	0.4	J-138	12/17/64
	0.6	L-117	11/23/64
	1.0	P-122	11/25/64
	2.0	P-94	11/8/64
	3.0	L-130	11/26/64

Fig. No.	Measurement Parameters		Measurement Number	Date of Measurement
3.49	$L_b = F_B$ (250, H, 80,	0.2, H_r)	B-67	11/17/64
		0.4	J-137	12/17/64
		0.6	L-116	11/23/64
		1.0	P-121	11/25/64
		2.0	P-95	11/8/64
		3.0	L-129	11/26/64
		4.3	P-127	11/27/64
3.50	$L_b = F_B$ (400, V, 13,	0.2, H_r)	W-60	10/6/64
		0.4	P-67	10/14/64
		0.6	L-84	10/15/64
		1.0	P-78	10/21/64
		2.0	T-46	11/30/64
3.51	$L_b = F_B$ (400, V, 40,	0.2, H_r)	P-160	12/19/64
		0.4	J-142	12/17/64
		0.6	L-119	11/23/64
		1.0	W-76	11/24/64
		2.0	P-104	11/8/64
3.52	$L_b = F_B$ (400, V, 80,	0.2, H_r)	P-158	12/19/64
		0.4	J-141	12/17/64
		0.6	L-118	11/23/64
		1.0	W-75	11/24/64
		2.0	P-105	11/8/64
		3.0	L-122	11/26/64
		4.3	P-135	11/29/64
3.53	$L_b = F_B$ (400, H, 13,	0.2, H_r)	W-59	10/6/64
		0.4	P-149	12/1/64
		0.6	L-83	10/15/64
		1.0	P-77	10/21/64
		2.0	P-91	11/8/64
3.54	$L_b = F_B$ (400, H, 40,	0.2, H_r)	P-157	12/19/64
		0.4	J-140	12/17/64
		0.6	L-121	11/23/64
		1.0	W-73	11/24/64
		2.0	P-102	11/8/64
		3.0	L-125	11/26/64
3.55	$L_b = F_B$ (400, H, 80,	0.2, H_r)	P-156	12/19/64
		0.4	J-139	12/17/64
		0.6	L-120	11/23/64
		1.0	W-74	11/24/64
		2.0	P-103	11/8/64
		3.0	L-124	11/26/64
		4.3	P-134	11/29/64

REFERENCES

1. K. A. Norton, P. L. Rice, L. E. Volger, "The Use of Angular Distance in Estimating Transmission Loss and Fading Range for Propagation Through a Turbulent Atmosphere Over Irregular Terrain," Proc. IRE, October 1955.

2. NBS Technical Note 101, Transmission Loss Predictions for Tropospheric Communication Circuits," May 7, 1965.

3. K. A. Norton, "The Calculation of Ground-Wave Field Intensity Over a Finitely Conducting Spherical Earth," Proc. IRE, December 1941.

4. J. J. Egli, "Radio Propagation Above 40 mc Over Irregular Terrain," Proc. IRE, October 1957.

5. Jansky & Bailey Research and Engineering Division, Atlantic Research Corporation, "Tropical Propagation Research, Semiannual Report No. 5," Section 3.2, Contract DA 36-039 SC-90889.

6. International Radio Consultive Committee, Documents of the VIIIth Plenary Assembly, Vol. 1, Warsaw, 1956.

7. The following related reports, submitted October 1963 to the U. S. Army Electronic Proving Ground, Fort Huachuca, Arizona, under Contract No. DA 36-039 SC-80928, by the Jansky & Bailey Research and Engineering Division of Atlantic Research Corporation and Frederick Research Corporation: "U. S. Army RFCP Spectrum Signature Program, Radio Set AN/PRC-10 (Ser. No. 732), SS-315.1 (F), Test Sample 1 of 3 Sample Lot," "U. S. Army RFCP Spectrum Signature Program, Radio Set AN/PRC-10 (Ser. No. 9099), SS-315.2 (F), Test Sample 2 of 3 Sample Lot," and U. S. Army Spectrum Signature Program, Radio Set AN/PRC-10 (Ser. No. 639), SS-315.3 (F), Test Sample 3 of 3 Sample Lot."

UNCLASSIFIED

Security Classification

DOCUMENT CONTROL DATA - R&D

(Security classification of title, body of abstract and indexing annotation must be entered when the overall report is classified)

1 ORIGINATING ACTIVITY (Corporate author) Atlantic Research Corporation Jansky & Bailey Division	2a REPORT SECURITY CLASSIFICATION 2b GROUP

3 REPORT TITLE

Tropical Propagation Research (U)

4 DESCRIPTIVE NOTES (Type of report and inclusive dates)

Semi-Annual Report #6 1 January 1965 - 30 June 1965

5 AUTHOR(S) (Last name, first name, initial)

L. G. Sturgill and Staff

6 REPORT DATE	7a TOTAL NO. OF PAGES	7b. NO. OF REFS
July 1965	528	7

8a CONTRACT OR GRANT NO. DA 36-039 SC-90889 b. PROJECT NO. AMC Code #5621-11-919-01-13 c. AMC Sub Task #1P620501 A 4480113 d pertaining to ARPA Order #371	9a. ORIGINATOR'S REPORT NUMBER(S) 9b. OTHER REPORT NO(S) (Any other numbers that may be assigned this report)

10. AVAILABILITY/LIMITATION NOTICES

Qualified requesters may obtain copies of this report from DDC. DDC release to CFSTI not authorized.

11 SUPPLEMENTARY NOTES	12. SPONSORING MILITARY ACTIVITY
Report on experimental studies of RF propagation in Tropical vegetated environments.	U. S. ARMY ELECTRONICS COMMAND FORT MONMOUTH, N. J.

13 ABSTRACT This sixth semi-annual report presents results of work accomplished during the period 1 January 1965 to 30 June 1965 under a program on radio propagation research in tropical vegetated environments. The objectives of this program are to collect and analyze basic propagation data, together with basic environmental data, needed to improve the design and operation of radio communications in such environments.

The field measurements on this program are being carried out in Thailand in a specially selected area of tropical vegetated terrain about 30 miles in diameter. Measurements of transmission loss are conducted in the frequency range of 100 kc to 10 gc, with antenna heights, polarizations, and transmission ranges as the primary measurement variables. Basic environmental data, such as range profiles, vegetation characteristics, and weather data are also collected and through the technique of statistical correlation, are used to identify the quantitative effects of the environment on propagation path loss.

This report continues, as has been the case with previous reports, with the reporting of new data reduced directly from the field measurements. This data is presented in graphic form in terms of basic transmission loss. However, the major portion of this report is devoted to the detailed analysis of a relatively large quantity of the field data. The block of measured data selected for analysis consists of all the data thus far obtained from one sector of the test area, designated as Radial A, and includes an analysis of data presented in Semi-annual Reports 4 and 5 as well.

DD FORM 1 JAN 64 1473

UNCLASSIFIED

Security Classification

UNCLASSIFIED

Security Classification

14. KEY WORDS	LINK A		LINK B		LINK C	
	ROLE	WT	ROLE	WT	ROLE	WT
Propagation	8, 10	4				
Techniques	10	4				
Tropical Environment	8, 10	4				
SEA - Southeast Asia		4				
Thailand - SEA				4		
Path Loss			8, 7	4		
Climatology - Rainfall, Temperature, Barometric Pressure			8,7	4		
Antenna Height			8, 7	4, 3		
Transmission Distance			8,7	4,3		

INSTRUCTIONS

1. ORIGINATING ACTIVITY: Enter the name and address of the contractor, subcontractor, grantee, Department of Defense activity or other organization *(corporate author)* issuing the report.

2*a*. REPORT SECURITY CLASSIFICATION: Enter the overall security classification of the report. Indicate whether "Restricted Data" is included. Marking is to be in accordance with appropriate security regulations.

2*b*. GROUP: Automatic downgrading is specified in DoD Directive 5200.10 and Armed Forces Industrial Manual. Enter the group number. Also, when applicable, show that optional markings have been used for Group 3 and Group 4 as authorized.

3. REPORT TITLE: Enter the complete report title in all capital letters. Titles in all cases should be unclassified. If a meaningful title cannot be selected without classification, show title classification in all capitals in parenthesis immediately following the title.

4. DESCRIPTIVE NOTES: If appropriate, enter the type of report, e.g., interim, progress, summary, annual, or final. Give the inclusive dates when a specific reporting period is covered.

5. AUTHOR(S): Enter the name(s) of author(s) as shown on or in the report. Enter last name, first name, middle initial. If military, show rank and branch of service. The name of the principal author is an absolute minimum requirement.

6. REPORT DATE: Enter the date of the report as day, month, year; or month, year. If more than one date appears on the report, use date of publication.

7*a*. TOTAL NUMBER OF PAGES: The total page count should follow normal pagination procedures, i.e., enter the number of pages containing information.

7*b*. NUMBER OF REFERENCES: Enter the total number of references cited in the report.

8*a*. CONTRACT OR GRANT NUMBER: If appropriate, enter the applicable number of the contract or grant under which the report was written.

8*b*, 8*c*, & 8*d*. PROJECT NUMBER: Enter the appropriate military department identification, such as project number, subproject number, system numbers, task number, etc.

9*a*. ORIGINATOR'S REPORT NUMBER(S): Enter the official report number by which the document will be identified and controlled by the originating activity. This number must be unique to this report.

9*b*. OTHER REPORT NUMBER(S): If the report has been assigned any other report numbers *(either by the originator or by the sponsor)*, also enter this number(s).

10. AVAILABILITY/LIMITATION NOTICES: Enter any limitations on further dissemination of the report, other than those imposed by security classification, using standard statements such as:

(1) "Qualified requesters may obtain copies of this report from DDC."

(2) "Foreign announcement and dissemination of this report by DDC is not authorized."

(3) "U. S. Government agencies may obtain copies of this report directly from DDC. Other qualified DDC users shall request through _____."

(4) "U. S. military agencies may obtain copies of this report directly from DDC. Other qualified users shall request through _____."

(5) "All distribution of this report is controlled. Qualified DDC users shall request through _____."

If the report has been furnished to the Office of Technical Services, Department of Commerce, for sale to the public, indicate this fact and enter the price, if known.

11. SUPPLEMENTARY NOTES: Use for additional explanatory notes.

12. SPONSORING MILITARY ACTIVITY: Enter the name of the departmental project office or laboratory sponsoring *(paying for)* the research and development. Include address.

13. ABSTRACT: Enter an abstract giving a brief and factual summary of the document indicative of the report, even though it may also appear elsewhere in the body of the technical report. If additional space is required, a continuation sheet shall be attached.

It is highly desirable that the abstract of classified reports be unclassified. Each paragraph of the abstract shall end with an indication of the military security classification of the information in the paragraph, represented as *(TS)*, *(S)*, *(C)*, or *(U)*.

There is no limitation on the length of the abstract. However, the suggested length is from 150 to 225 words.

14. KEY WORDS: Key words are technically meaningful terms or short phrases that characterize a report and may be used as index entries for cataloging the report. Key words must be selected so that no security classification is required. Identifiers, such as equipment model designation, trade name, military project code name, geographic location, may be used as key words but will be followed by an indication of technical context. The assignment of links, rules, and weights is optional.

UNCLASSIFIED

Security Classification

SUPPLEMENTARY

INFORMATION

AD-474 377 Atlantic Research Corp., Alexandria, Va. Jansky and Bailey Research and Engineering Div. Semiannual rept. no. 6, 1 Jan-30 Jun 65. 3 Jun 65 Contract DA-36-039-SC-90889	No Foreign without approval of Army Electronics Command, Fort Monmouth, N. J.	No limitation	USAEC ltr, 14 Mar 69